Methodology for environmental impact evaluation – 2-D vs 3-D case study

Task A-1

ERC Review Meeting
Tucson, AZ
February 23rd - 24th,2006

Ajay Somani, Sarah Jane White, Duane Boning,
Philip Gschwend and Rafael Reif
Massachusetts Institute of Technology, Cambridge MA

Objectives of Project

- Develop methodology to analyze environmental impacts for new process technologies
- Construct a corresponding database which is more transparent than previous LCA studies
- Identify critical unit processes that need to be designed with environmental considerations in addition to performance and cost

Description of Approach / Methodology

- Identify boundaries for analysis (wafer fabrication)
- Define functional unit for comparison (e.g., # of transistors)
- Generate environmental footprint for fabrication of a standard IC functional unit with chemical/material specificity
- Compare alternative fabrication technologies with respect to performance, cost and environmental footprint
- Identify critical unit processes which have performance, cost, or environmental issues
- Design new unit process approaches to improve performance, cost AND environmental issues

MIT's 3-D Process Flow

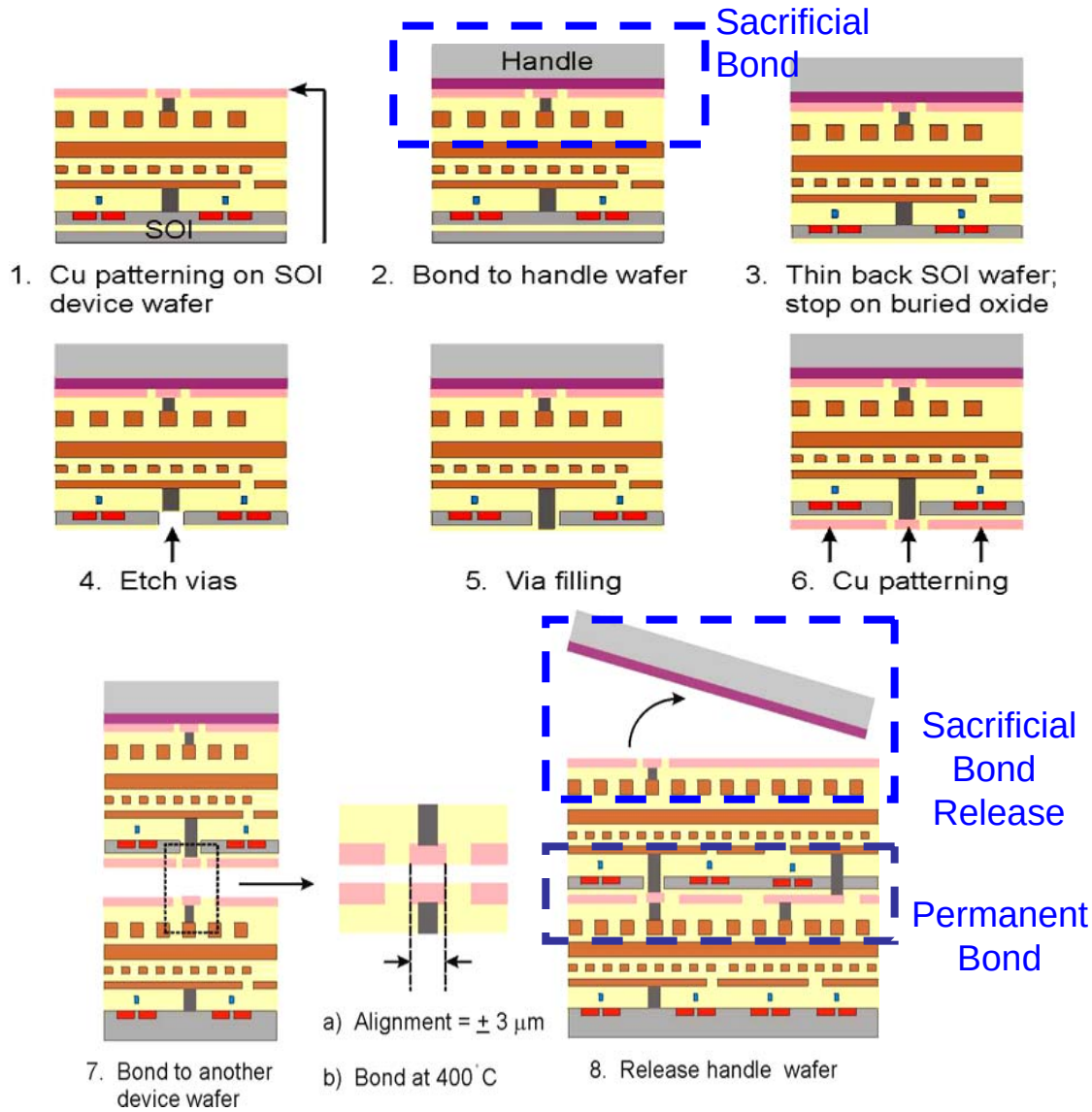

Case Study: 2-D vs. 3-D

- Functional unit is quite a challenge in comparing 2D vs 3D technologies
  - Integrating cross functionality in case of 3D
  - No meaning of Si real estate
  - No real product available (so far)
  - Need to define functional unit depending on what is currently integrated for SoC (System on Chip)
  - 1 Logic + 1 Cache (high-speed SRAM) + 1 DRAM memory
  - Packaging has to be considered in this option

- Standard 2D IC energy inventory is known[1,2]; but full environmental footprint remains to be done

- New/additional 3-D unit processes were identified
  - Grinding has been estimated using oxide CMP, not exactly new to CMOS but not very common
  - Bonding was another new process has been estimated like annealing (with pressure term as another additional energy consumption)
  - Handle wafer bonding and releasing is new to IC technology, there is no standard process developed yet for this technology so still in design phase and can be designed as environmentally benign

[1] Murphy et al., Environ. Sci.& Tech., Vol. 37(23), pp 5373-5382
[2] Boyd et al., presentation at MRS 2005

2-D vs. 3-D in Terms of Processes

Unit operation	2D process flow (for one wafer)	Additional 3D processes in flow
Photo/stepper/ashing	25	1
Dry Etch	13	2
Wet etch/Clean	31/14	3/4
CVD	11	1
CMP	14	2
Sputtering Al	1 (0.5 µm for metal 1)	2 (20 µm)
Sputtering Ta/Cu	6	1
Electrodeposition Cu	6	1
Bonding	0	2
Grinding	0	1

First-Order **Energy** Comparison 2-D vs. MIT's 3-D Process Flow

- Sputtering twice 20 micron Al for release layer involves a large energy consumption
- Bonding and Grinding are new processes that need to be evaluated
- Besides these, other processes add only incrementally to full process flow; so initially ignored
- Grinding can be estimated using CMP; it takes a bit longer to thin wafer, but energy usage must be similar
- Bonding can be estimated using a typical high-vacuum process with thermal budget of 300 ^{o}C for half an hour

Handle Wafer: Function and Issues

- Use of a handle wafer may play an important role for 3D IC fab'
- Handle wafer bonding and release is one process for which no standard process data exist
- This presents a unique opportunity for DFE (Designing for Environment) white still accounting for performance and cost.
- This process, unlike other processes, does not influence any process upstream or downstream for our particular study
- Function
  - For thin-first approaches, handle wafer is mechanical support
  - It also provides repeatability of stacking
- Issues
  - Withstand grinding for 600 microns
  - Withstand wet etch-back of Si (TMAH)
  - Should etch selectively to other bonding layer (in our case Cu-Cu)
  - Bonding and release thermal budget is limited by back-end
  - Release with ease

Handle Wafer Options

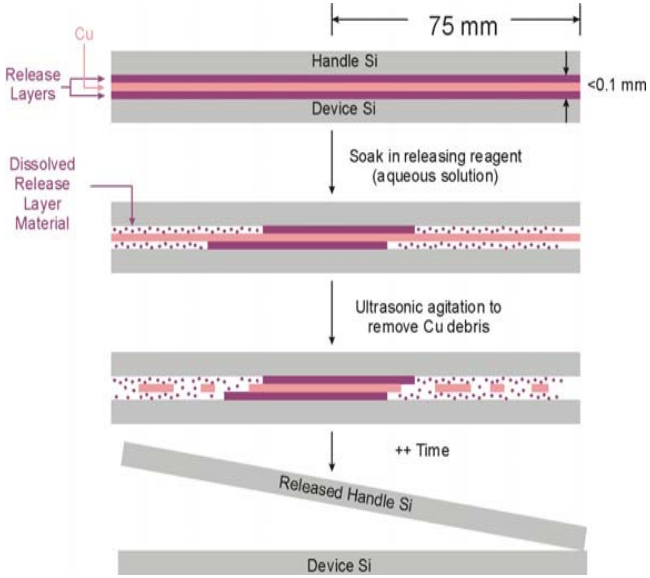

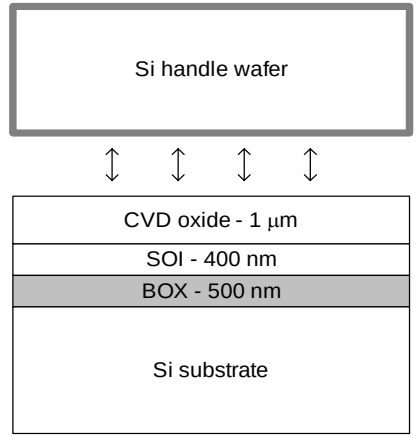

Top wafer is bonded to handle wafer (CVD-to-thermal oxides bonding).

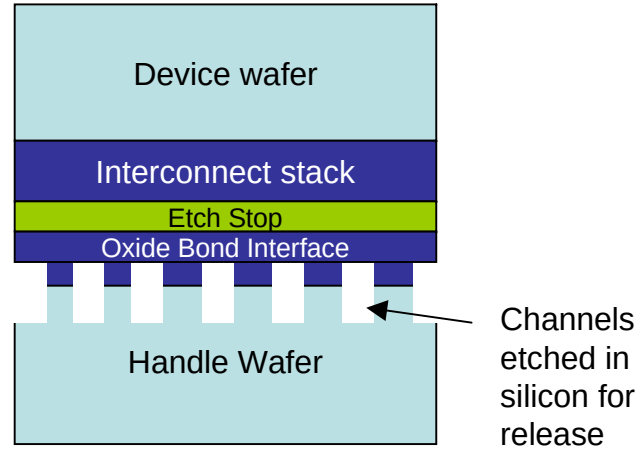

Al release layer[1]

- Described in MIT 3-D IC
- Requires 20 µm Al (twice) on each handle and device wafer
- Cu-Cu bonding, use Ta
- Yield is still an issue ~ for die level, works fine

Smart cut release[2]

- H_2 implant @ 150KeV
- High energy and expensive
- Use oxide-oxide bonding
- Thermal energy required to release
- Yield is good

Oxide release structures

- Similar oxide-oxide bonding
- Channels etched in handle wafer for release
- Nitride used as etch stop
- 49% HF used for release
- Yield is good but still to prove layer transfer – work in progress

[1] Fan et al., Electrochem. Solid State Lett., 2, 534 (1999)
[2] Tan et al., SOI Conference 2005

Comparison of Handle Wafer Options

Overall comparison	Al release	Smart cut	Oxide release
Yield (performance)	10% - depends on Cu-Cu bonding and mass transfer of acid	80% - work with oxide bond subjected to CMP oxide	80% subjected to functionality – as layer transfer is yet to be proven
Cost -additional	Cost for depositing Al on Si wafer which means 1.2 X	Cost for H_2 implantation which is 10 X	Oxidation, etch along with one CMP which means 1.2X
Environmental - additional	Illustrated very briefly in table below.		

Environmental comparison for additional steps	Al release	Smart cut	Oxide release
Energy	50-100 KWH primarily Al sputtering	20-40 KWH primarily H_2 implant	10-20 KWH oxidation, CMP, Photo and etch
Water	Primarily PCW for cooling Al dep./ Wet etch requires DI water	PCW for implantation, CMP and annealing	PCW for oxidation, etching and CMP, DI water for wet etch in 49% HF
Chemical (inputs)	Al, HCl, Ta, Cu	H2, SiH2Cl2, O2, CMP slurry, piranha	SiH2Cl2, O2, CMP slurry, NH4, HF, piranha, photoresist
Chemical (outputs)	$AlCl_3$, HCl	Oxide CMP waste, oxide dep. exhaust	Oxide CMP waste, oxide and nitride dep. exhaust, HF, SIF4

- Overall comparisons of different handle wafer options are considered in table above
  - Performance here primarily is denoted by yield
  - Cost are estimates and they are expressed in terms of one Si wafer cost
  - Additional means processes required for that handle wafer option
- Environmental comparison of different handle wafer options in qualitative way has been illustrated in table below
  - Energy has been guess estimated based on which processes are energy intensive in that option
  - Water usage – process cooling water (PCW), de-ionized (DI) water for cleaning
  - Chemical Inputs depending upon process and similarly probable outputs were listed
  - Contrast manufacturing fluxes with estimates of natural fluxes (e.g., Ta)

Global Cycle of Tantalum: contrast natural and industrial fluxes

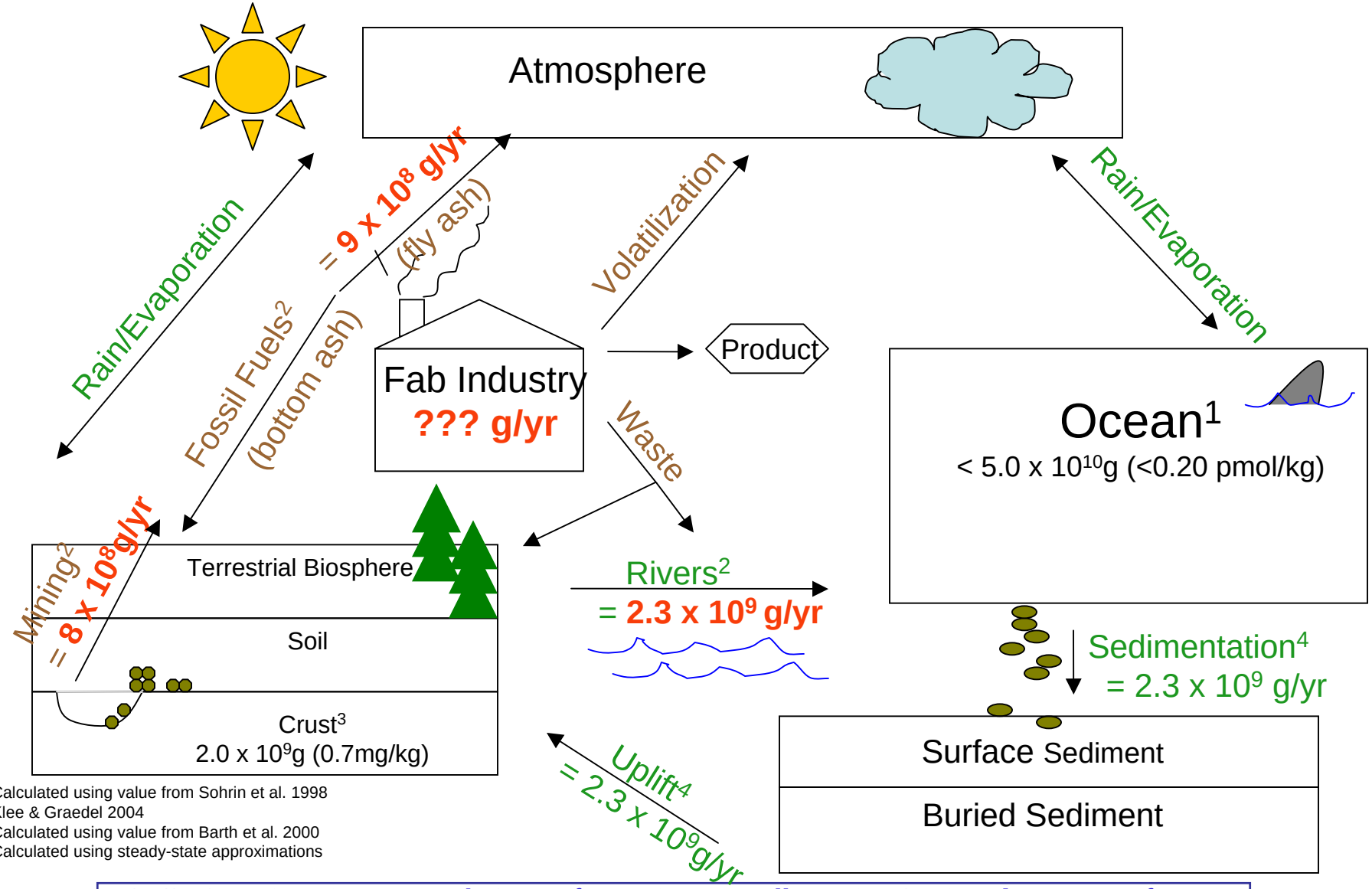

[1]Calculated using value from Sohrin et al. 1998
[2]Klee & Graedel 2004
[3]Calculated using value from Barth et al. 2000
[4]Calculated using steady-state approximations

Conclusion and Future Work

- Methodology for environmental evaluation has been established
  - Establish environmental footprint (energy and specific material uses) for standard flow
  - Compare it with new/additional significant processes
- MIT 3D technology serving as case study from energy standpoint
  - Will consider similar technology comparisons for other environmental axes such as air emissions of specific compounds
- Identified handle wafer as critical process in 3D IC
- Comparing different options for handle wafer on three axes: performance, cost and environment

Solventless Low k Dielectrics (Task 425.001: ERC EBSM)

Tom Casserly[+], Kelvin Chan[+], April Ross[+]*
and Karen Gleason
Department of Chemical Engineering
Massachusetts Institute of Technology

**now at Applied Materials*
[+]SRC Fellowships

Evolution of Low-k Dielectrics

Either increasing fragile porous low k materials must be integrated

or

A robust sacrificial layer must be integrated which can form air in the final step
(sacrificial layer = 100% porogen)

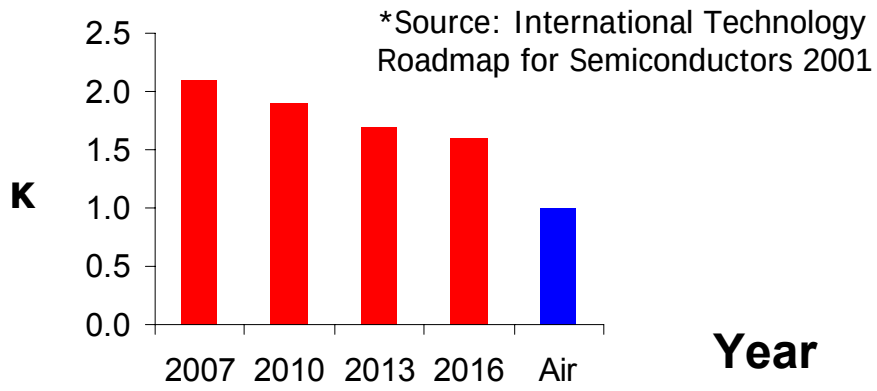

"Let's face it. The air gap is a pretty crazy idea. Rather than filling the space between interconnecting wires with anything that would increase line-to-line capacitance and RC delay, just go straight for the best performing low-k dielectric of all: Air. More unusual things have happened. Like effectively taking sandpaper to your device — later perfected into the state-of-the-art technology of CMP."

Laura Peters, Senior Editor -- 1/1/2005, Semiconductor International

Early air gap work:

- **Havemann and Jeng (TI), US Patent 5461003, 1995.**
- **Anand *et al., IEEE*, 1997.**

OSG Mechanical Properties

"For solids in which all atoms are able to form two or more bonds, the percolation of rigidity occurs at an average connectivity number of 2.4"*

* J. Phillips, *J. Non-Cryst. Solids* **34**, 153 (1979)

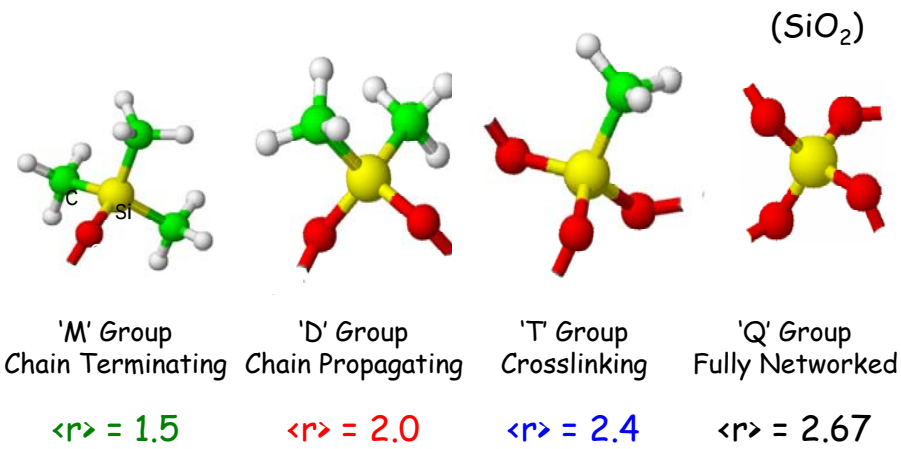

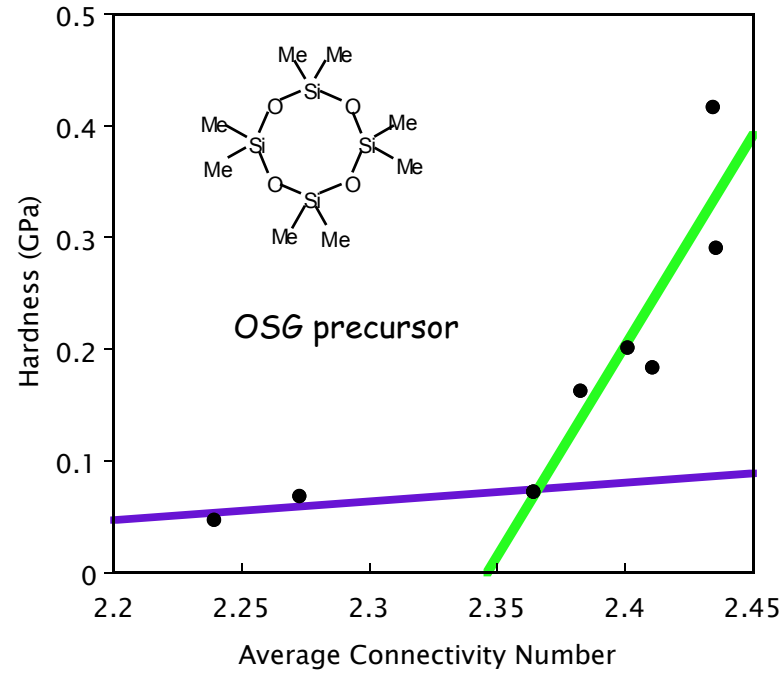

Ross AD and Gleason KK, J. Appl. Phys. 97, 113707 (2005)

100% T groups gives a matrix just at the percolation threshold

Density Functional Theory for OSG Precursors

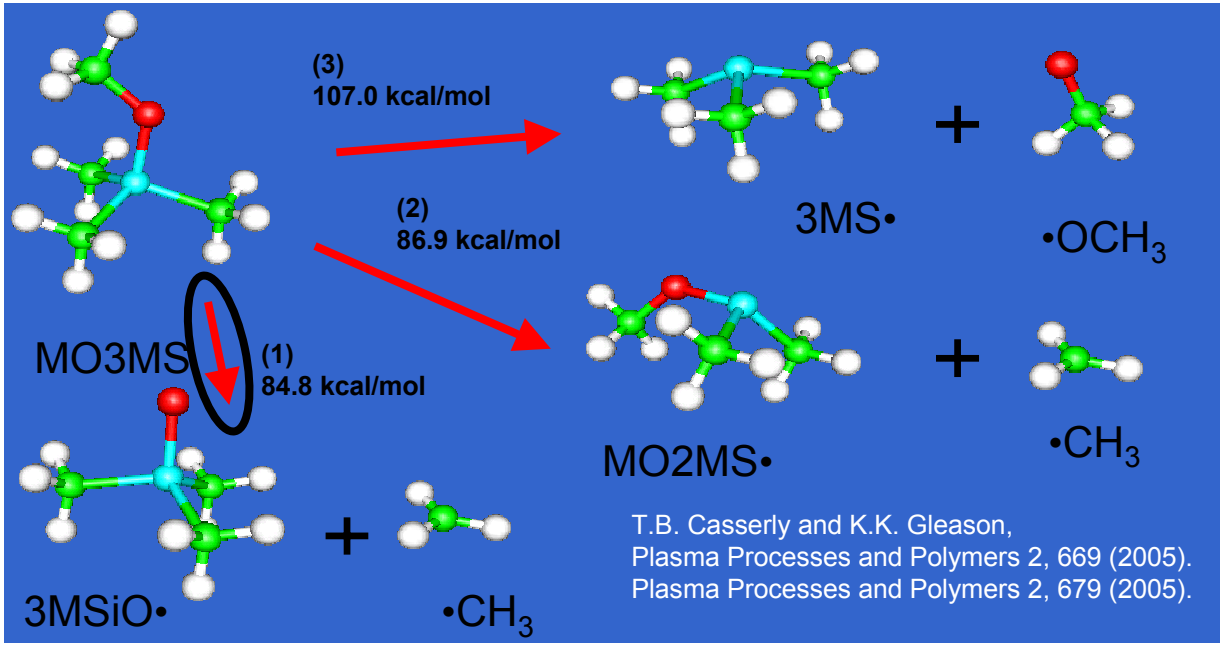

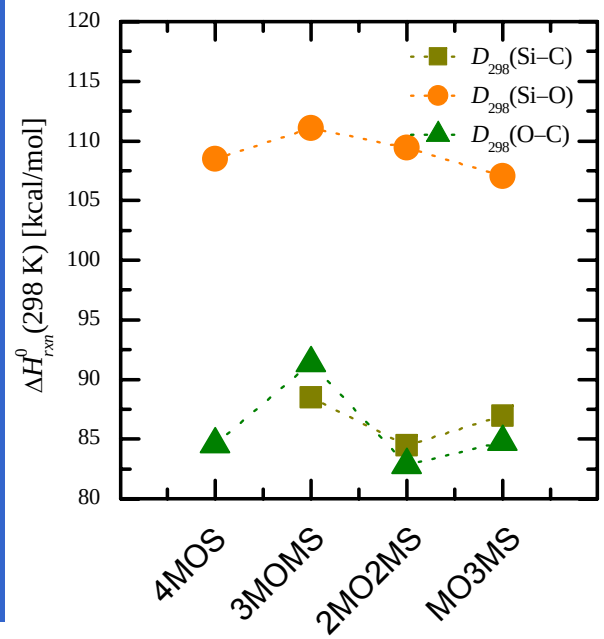

- Si-O bond is strongest (likely preserved)
- Si-C and O-C bonds have similar bond strengths
  - No selectivity
  - Likely loss of Si-C bonding
- Expectations
  - MO3MS – M
  - 2MO2MS – D
  - 3MOMS – T

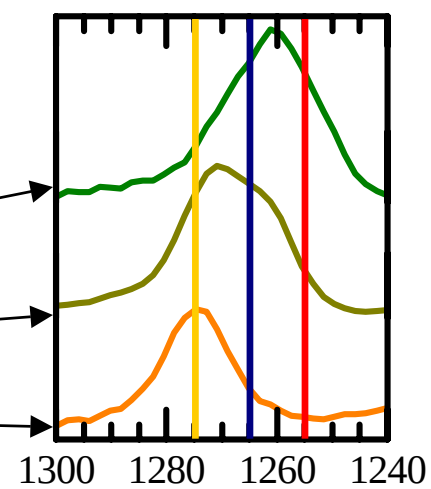

FTIR from low power PECVD films

DFT predicts even stronger selectivity to T group with addition of H_2 to 3MOMS

Air-Gap Fabrication

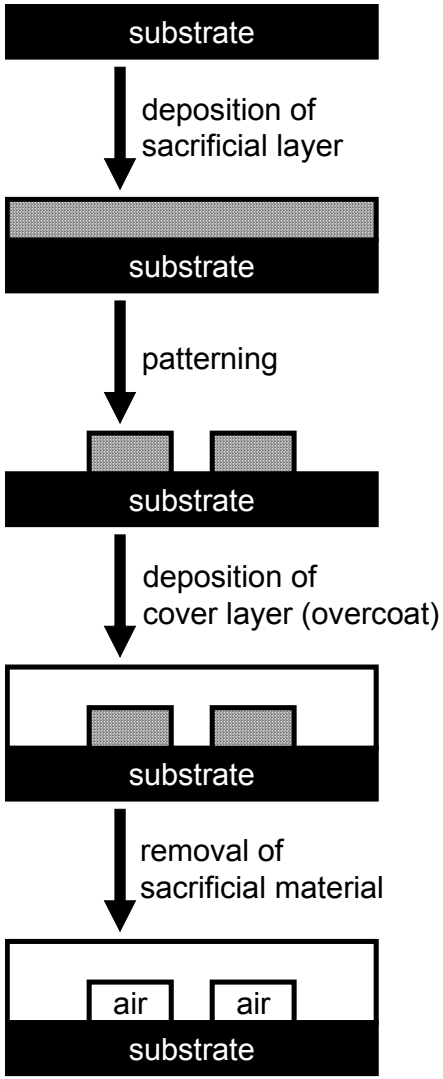

- **Ordinary Sacrificial Materials**
  - Require physical contact with etchant/solvent for selective removal
  - Surface-tension problems for wet processes
- **Self-Decomposing Sacrificial Materials**
  - Requires no agent for removal
  - Dry removal process (heat, UV, e-beam)
  - Allow fabrication of closed-cavity structures
- **CVD sacrificial layers**
  - evolutionary from CVD silicon dioxide and from OSG low k materials
  - environmentally attractive

CVD for Sacrificial Polymers

Plasma Enhanced

- nonselective chemistry
- uncontrolled crosslinking which gives rise to char formation: unsuitable for sacrifical layers

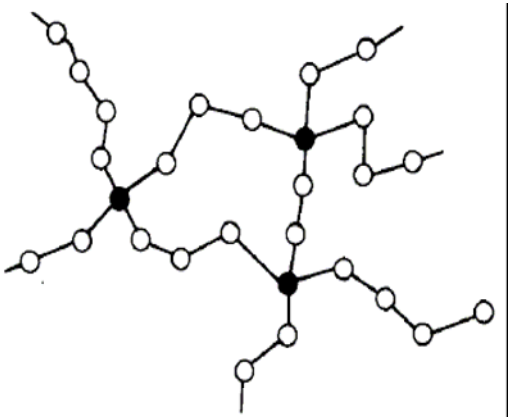

Initiated

- selective bond scission
- systematic compositional variation using feed gas
- controlled cross-linking
  - increases solvent stability (insolubility, lack of swelling)
  - increased thermal stability
  - increased mechanical strength
  - designed to prevent char formation

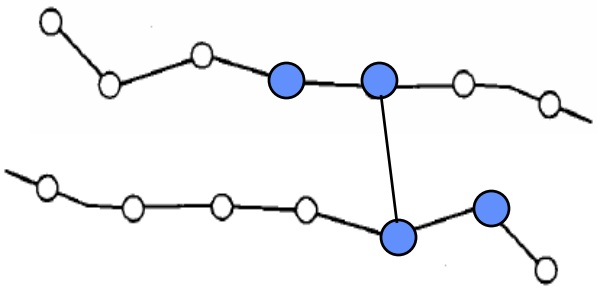

iCVD process characteristics:

- low energy input (<10 watts for 200 mm wafer)
- low-temperature process (substrate at ~ room temperature)
- no ion bombardment or UV irradiation (no plasma)
- All-dry process, no worker exposure to solvents

CVD Sacrificial Layer Chemistry

monomer

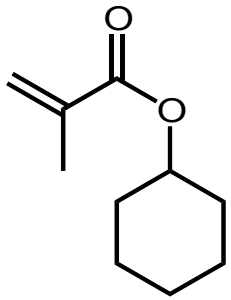

cyclohexyl methacrylate (CHMA)

Stable under normal temperatures and pressures.

Hazardous Decomposition Products: carbon monoxide, carbon dioxide.

Hazardous Polymerization: Will not occur.

Potential Health Effects: Causes eye and skin irritation.

Carcinogenicity: Not listed by ACGIH, IARC, NIOSH, NTP, or OSHA.

crosslinker

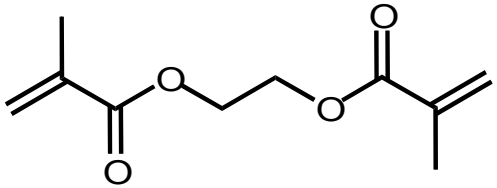

ethylene glycol dimethacrylate (EGDMA)

Stable under normal temperatures and pressures.

Irritating to respiratory system.

LD50/LC50: Oral, mouse: LD50 = 2 gm/kg; Oral, rat: LD50 = 3300 mg/kg.

Carcinogenicity: Not listed by ACGIH, IARC, NIOSH, NTP, or OSHA

initiator

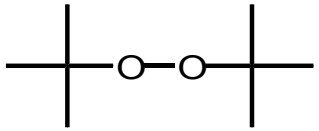

tert-butyl peroxide

Stability : Explosive if heated, subjected to shock, or treated with reducing agents. Highly flammable. Refrigerate.

IPR-RAT LD50 3.210 g/kg : ORL-RAT LD50 > 25 g/kg

Carcinogenicity: Not listed by ACGIH, IARC, NIOSH, NTP, or OSHA

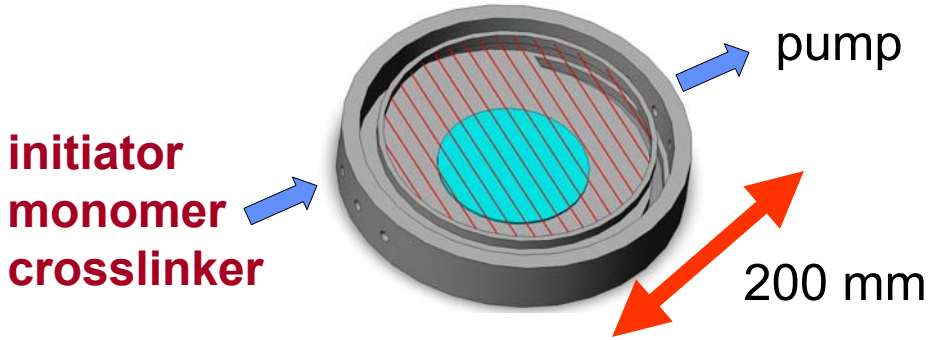

Cross-link Density (FTIR & XPS)

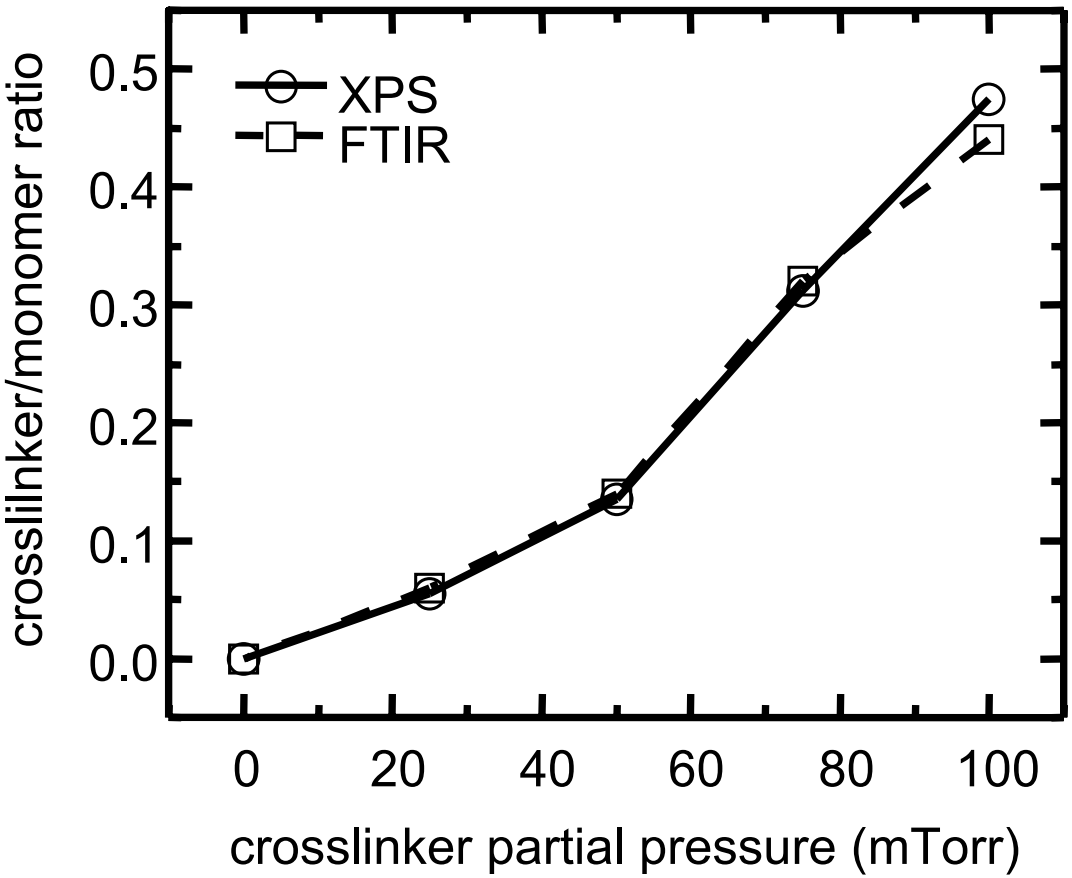

two independent methods confirm systematic control over crosslink incorporation in the film

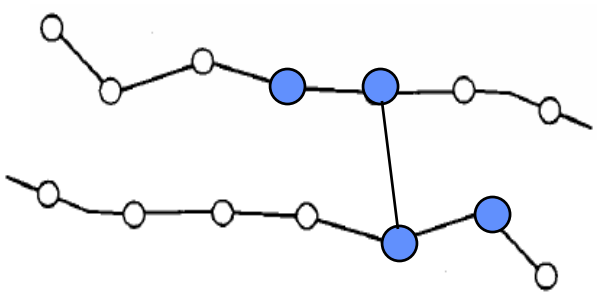

- degree of crosslinking can be systematically adjusted
- impossible to spin cast insoluble crosslinked material

Control using Surface Concentration

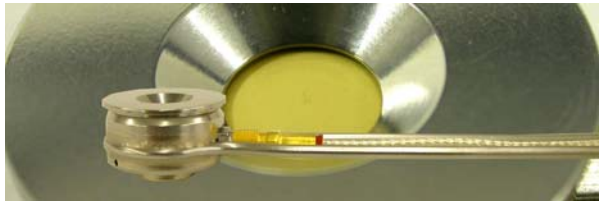

Quartz Crystal Microbalance (QCM) measures surface concentration of monomer, [M], in the absence of reaction

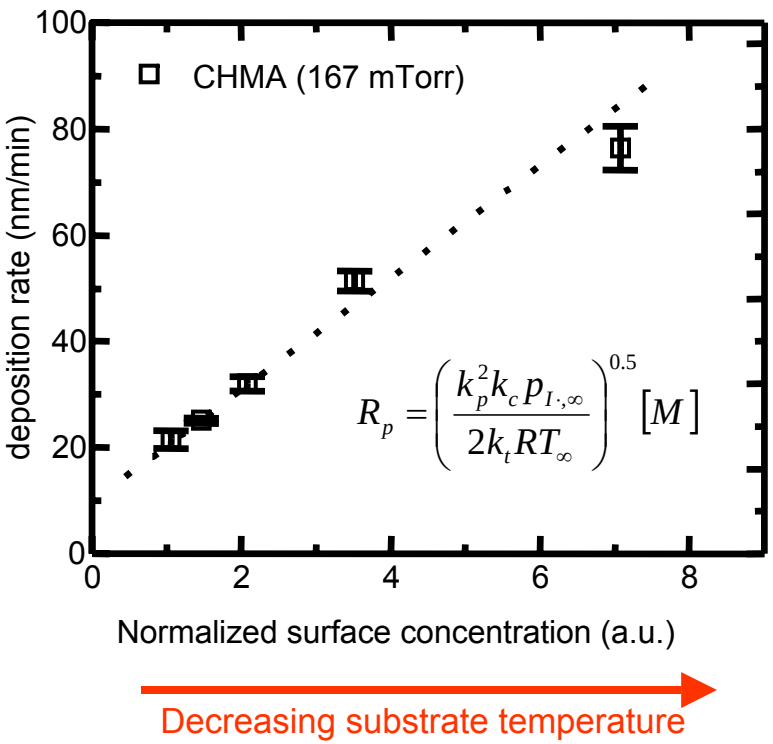

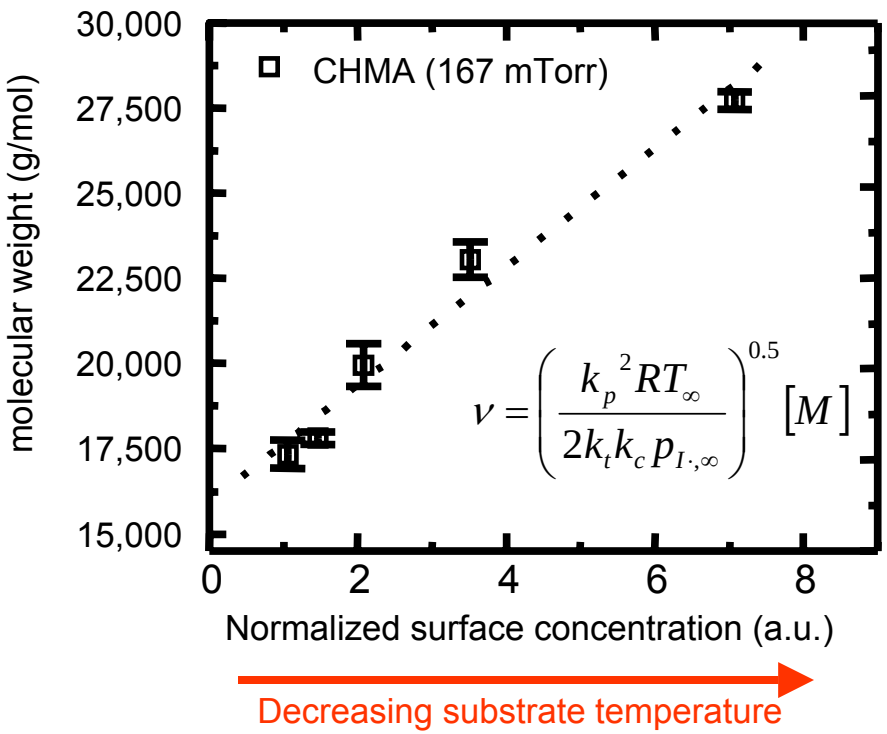

Film Properties

- Does not dissolve in any commonly used solvents: photoresist can be removed by dissolution instead of ashing.
- Decomposition > 99.7% by thickness (VASE). Crosslinking via the dimethacrylate monomer is key.
- Onset temperature of decomp. ~ 270 °C (ITS)
- Good adhesion to substrate and photoresist
- High etch rate in oxygen RIE (0.35 µm/min). Eliminates the need for a hard mask, an economic and environmental improvement over previously-reported spin-on sacrificial materials

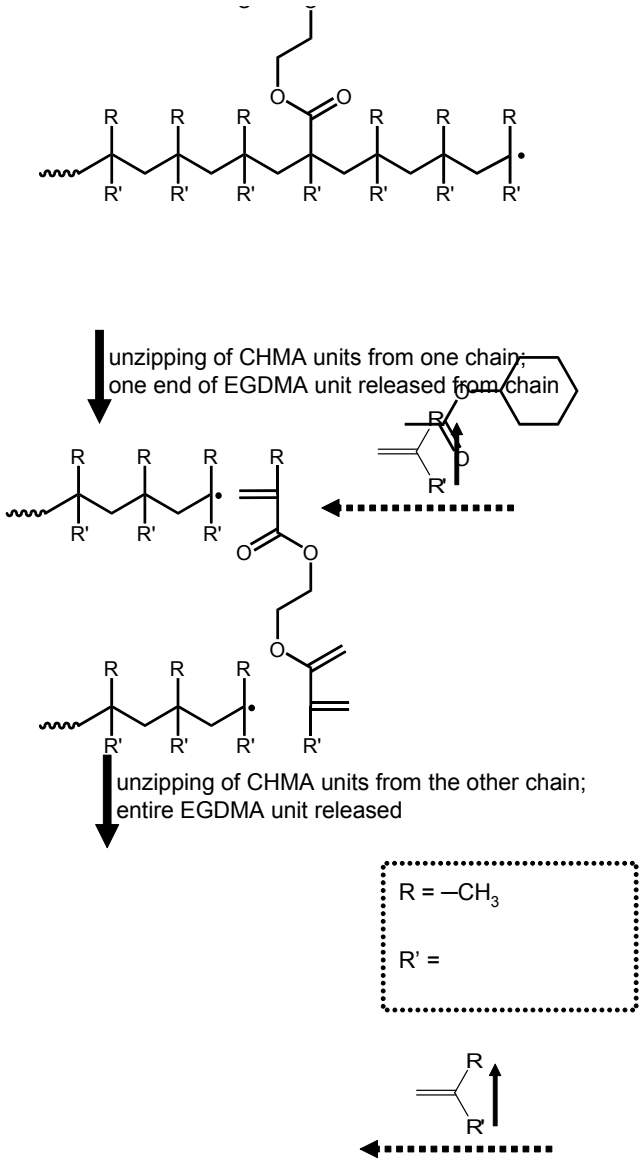

Fabrication

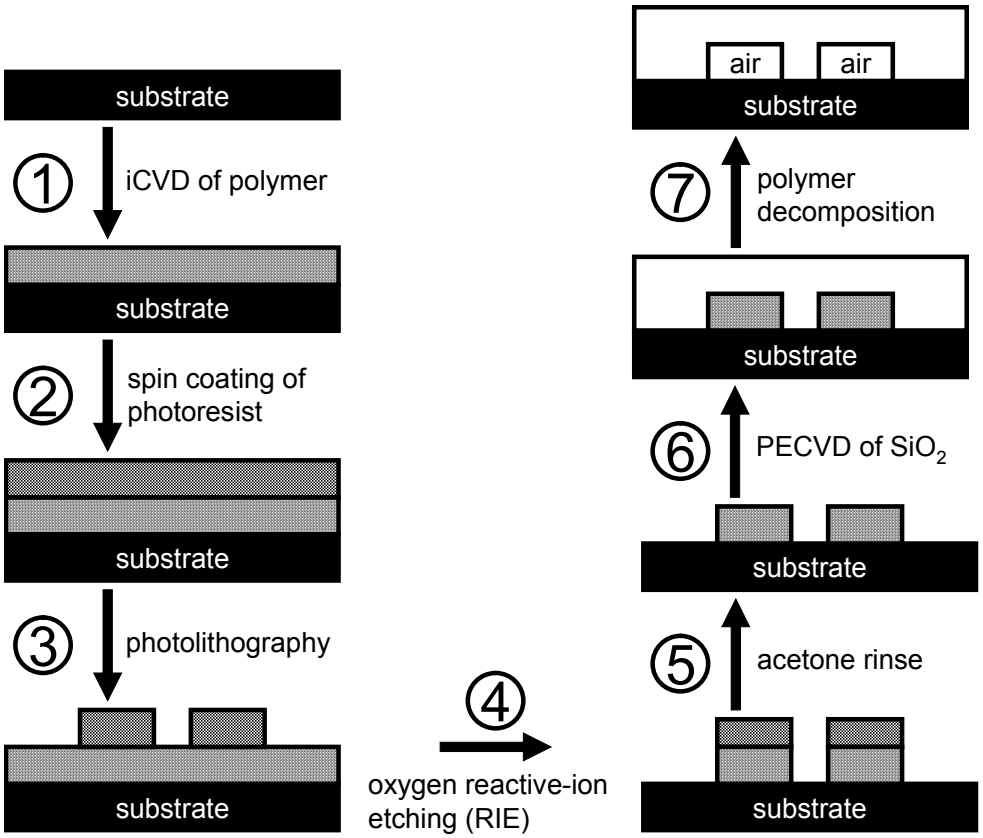

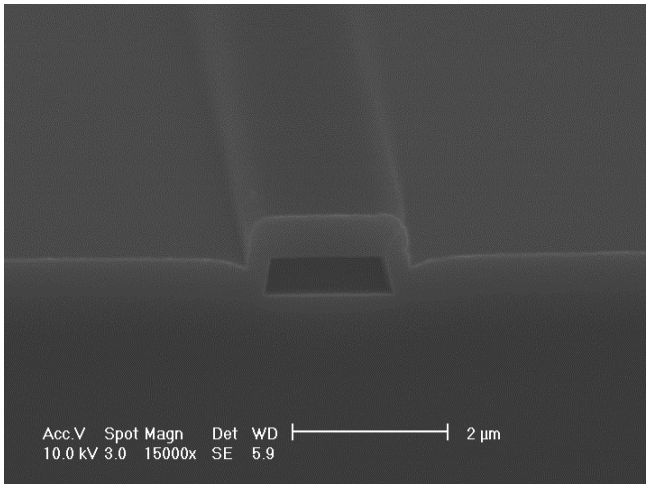

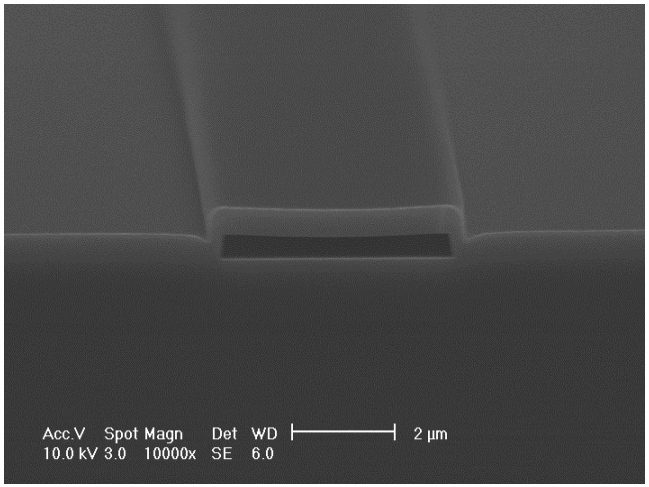

With better lithography, smaller feature sizes can be fabricated.

- **no hardmask**
- **RIE resist strip**

Conclusions

- Local bonding environments in OSG films determine mechanical strength: all "T" groups represents a percolation of rigidity limit.
- Density functional theory (DFT) calculations for new precursors predict the likelyhood of formation of local bonding environments in OSG films.
- iCVD sacrificial layers represent a evolutionary and environmentally friendly strategy for the integration of air gaps.
  - controllable crosslinking which cleanly degrades
  - no hardmask required for fabrication

Environmentally Benign Precursors for Pore Sealing and Repair of Porous Low-k Films

W. Shannan O'Shaughnessy, Karen K. Gleason

Department of Chemical Engineering
Massachusetts Institute of Technology, Cambridge, MA 02139

Sri Satyanarayana, Eric Busch
Sematech Project Advisors

Goals and Approach

- Goals
  - Utilize environmentally benign precursors and process to deposit hermetic sealant for porous low-k films
  - Requirements:
    - Dielectric constant ~2.3
    - Adhesive to substrate
    - Block subsequent ALD metal precursors from invading porous layer
- Approach
  - Baseline data on parylene thermal CVD process originally developed at RPI (molecular caulking)
  - Novel CVD strategy to improve adhesion of the pore sealing layer to the porous organosilicate glass (OSG) low k
    - chemical similarity of new monomer, V_3D_3, to OSG layer is expected to enhance adhesion
    - large cyclic structure is expected to produce pore sealing
    - potential to covalently tether the new monomer to the OSG

Parylene for Pore Sealing

Gorham Process

~30 Å parylene deposited on substrate with porous dielectric

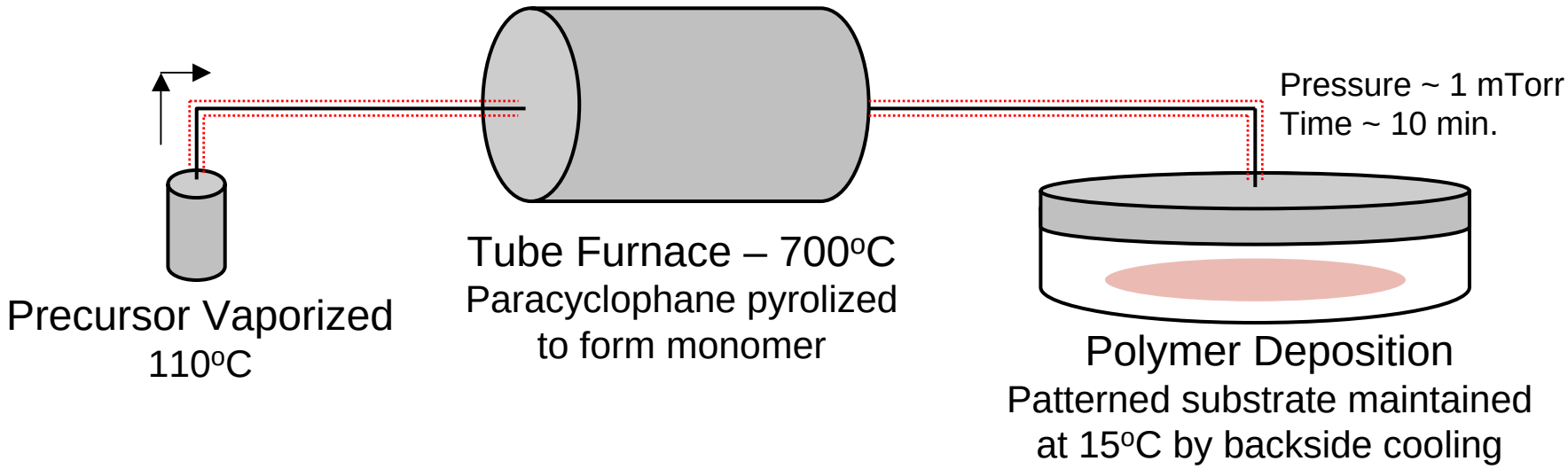

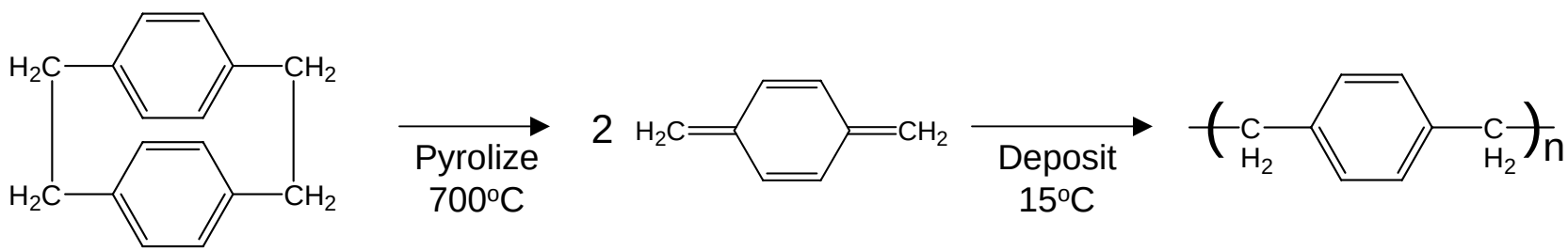

[2,2] paracyclophane
or di-para-xylylene

Para-xylylene
(monomer)

Poly(paraxylylene)
(Parylene)

Novel Organosilicon Pore Sealing Material

Monomer

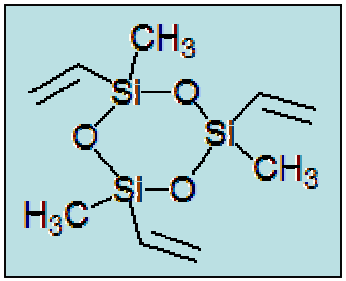

Trivinyl-Trimethyl-Cyclotrisiloxane (V_3D_3)

Initiator

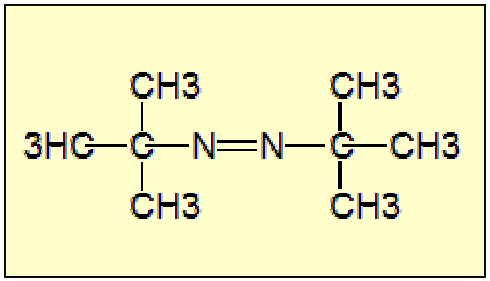

Azo-t-Butane

- Deposition in 1-D flow "pancake" reactor
- Initiator broken down by heated filament
- Conditions:
  - Pressure = 250 mTorr
  - Filament Temperature = 500°C
  - Stage Temperature = 80°C
  - Total Gas Flowrate = 18 sccm
  - Precursor : Initiator Ratio = 5:1

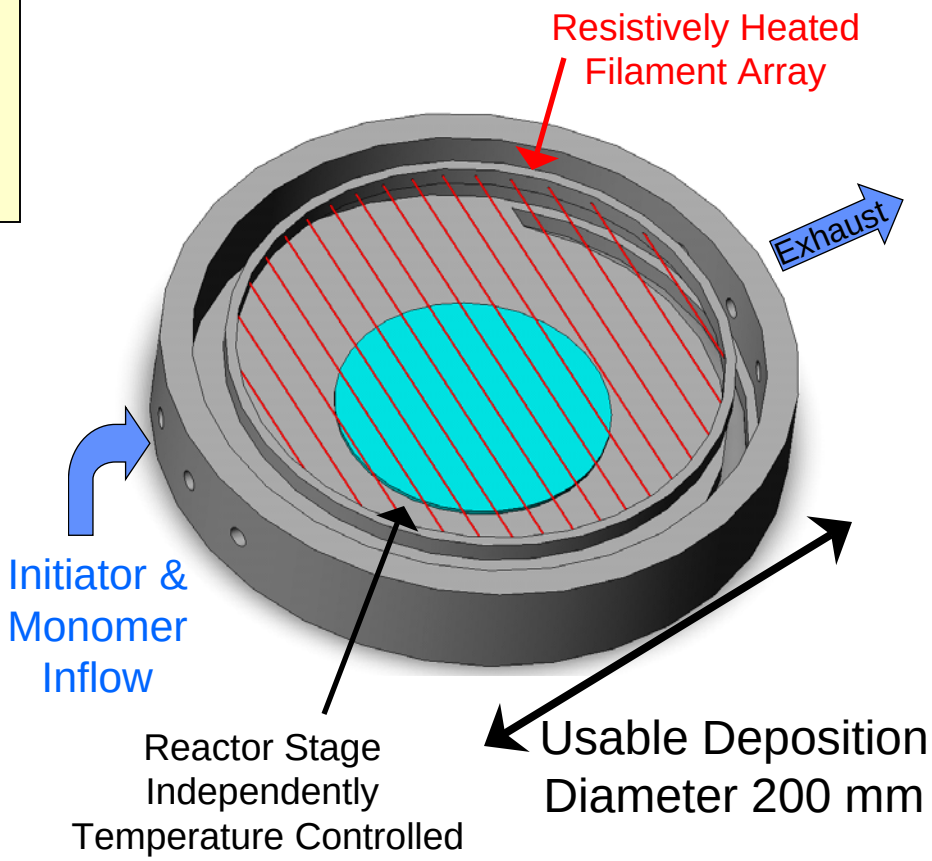

no plasma

Potential Organosilicon Structure

for related D_3 monomer

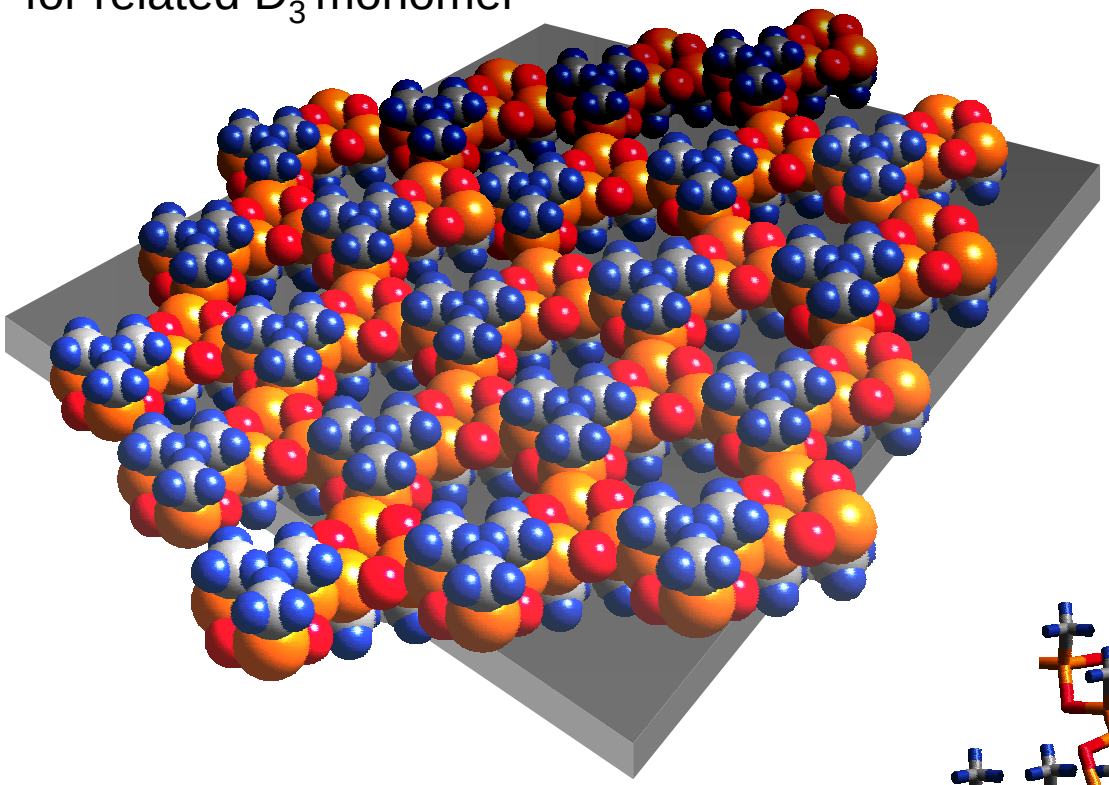

minimum film thickness ~ 10Å

monomer units "tiled" into film

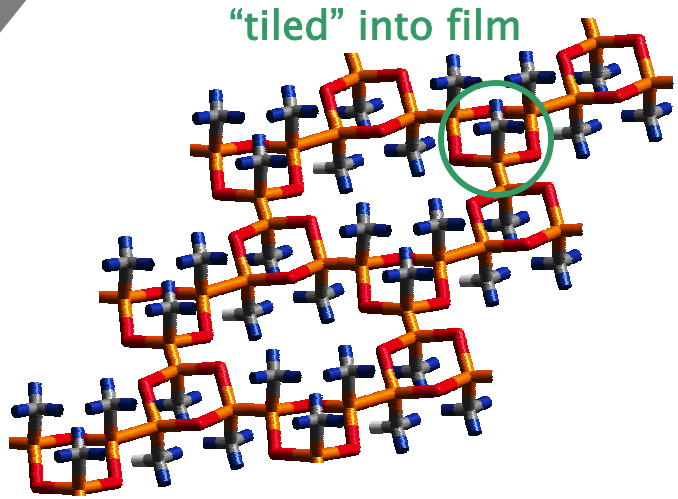

Novel Monomer may deposit with preferential orientation to more effectively seal pores in low k dielectric

V_3D_3 Material Physical Properties

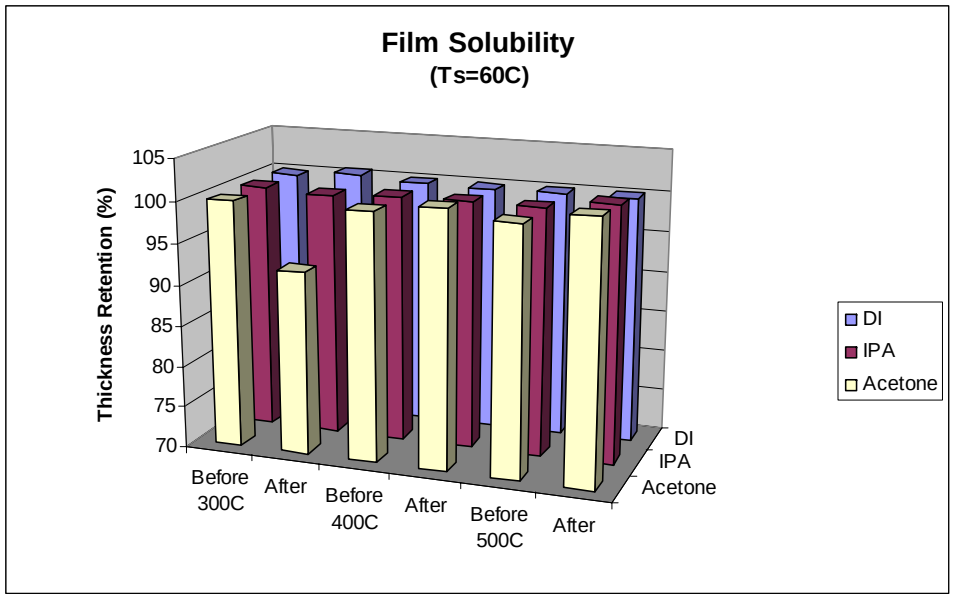

- Insoluble in all tested solvents
  - Water, IPA, Acetone, DMSO, DMAC, DMF
  - Insolubility beneficial for subsequent processing steps
- Low Dielectric Constant
  - Multiple samples tested with values 2.3 – 2.5
- Highest possible adhesion rating on silicon substrates
  - ASTM Tape Test D3359-02
  - No change in adhesion after boiling in DI

AFM of V3D3 Film

<u>RMS Roughness</u> 3.7 Å
(bare substrate ~1.5 Å

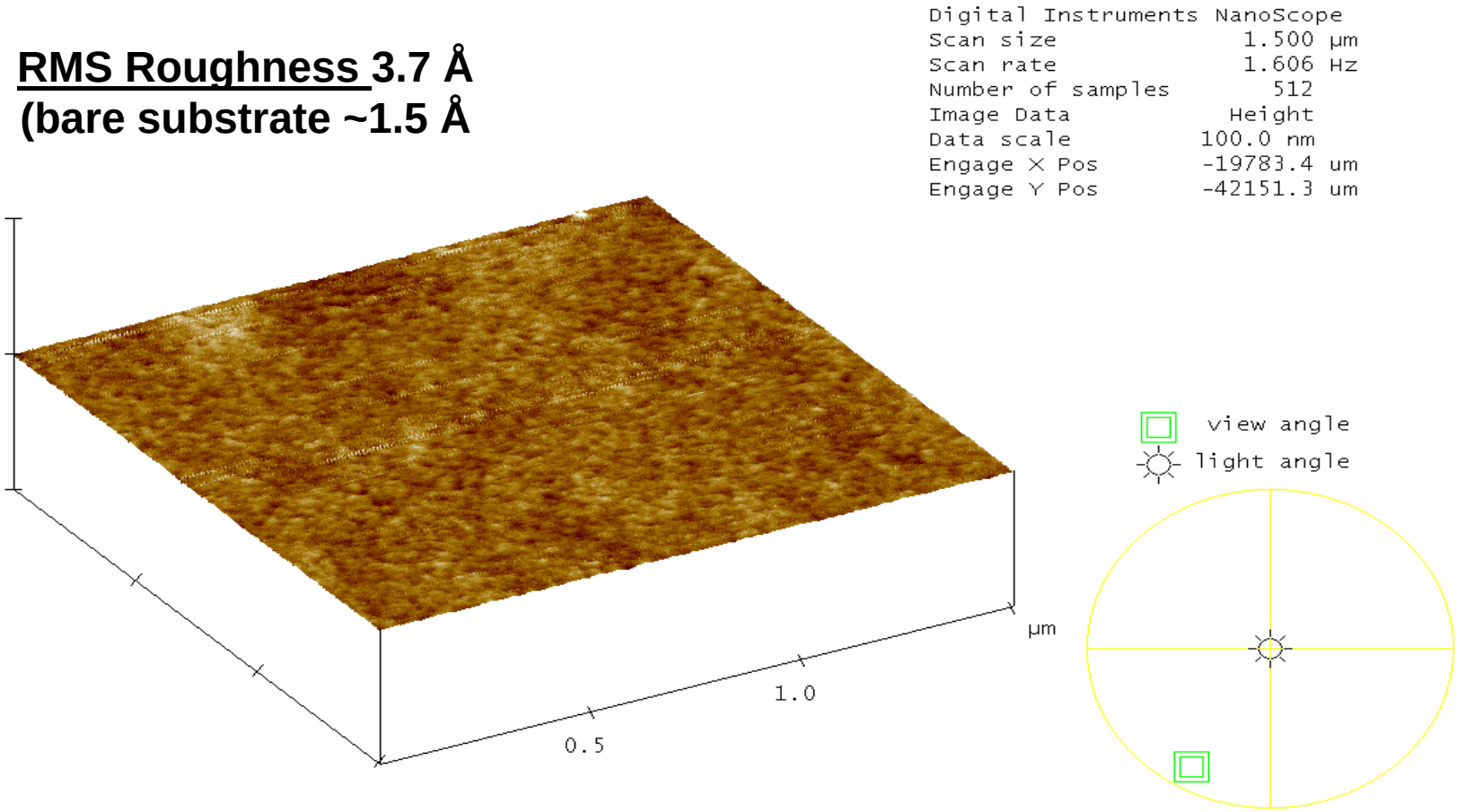

- **Very smooth coatings obtained at optimized conditions**
- **Minimizes required polishing prior to subsequent processing**

AFM of V3D3 Film

Low peak to peak roughness in addition to overall RMS roughness

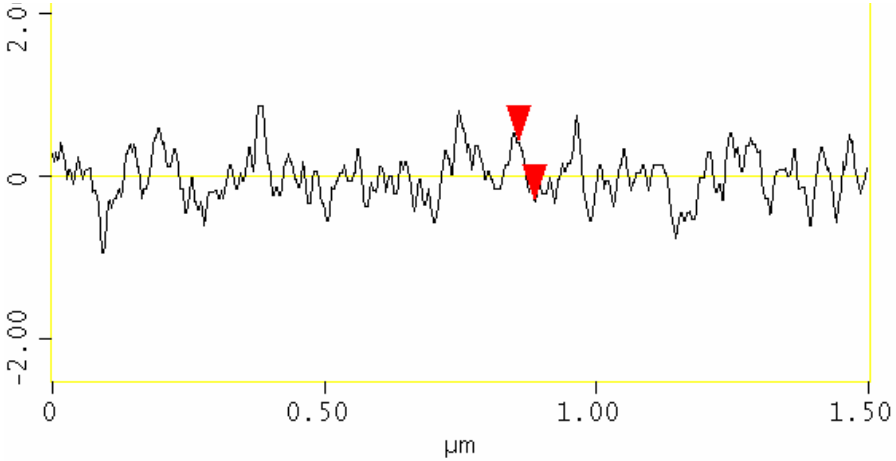

L	29.297 nm
RMS	0.239 nm
lc	DC
Ra(lc)	0.059 nm
Rmax	0.240 nm
Rz	0.175 nm
Rz Cnt	4
Radius	290.19 nm
Sigma	0.113 nm

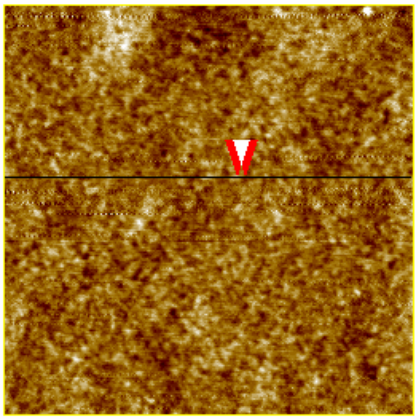

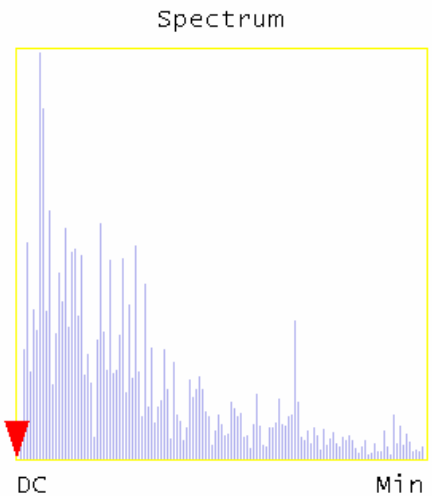

Surface distance	29.319 nm
Horiz distance(L)	29.297 nm
Vert distance	0.719 nm
Angle	1.405 °
Surface distance	
Horiz distance	
Vert distance	
Angle	
Surface distance	
Horiz distance	
Vert distance	
Angle	
Spectral period	DC
Spectral freq	0 /µm
Spectral RMS amp	0 nm

4gr21110.002

Cursor: fixed Zoom: 2:1 Cen line: Off Offset: Off

Cross-section SEM images after M1 trench processing

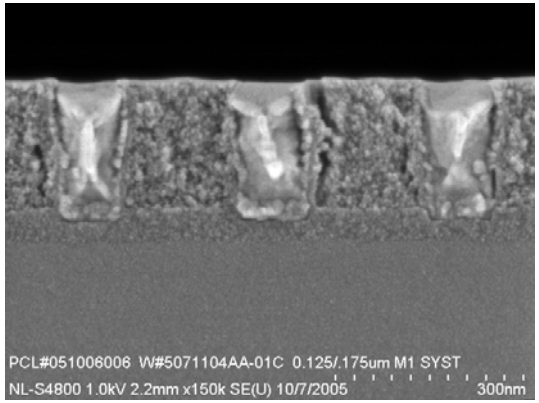

V_3D_3

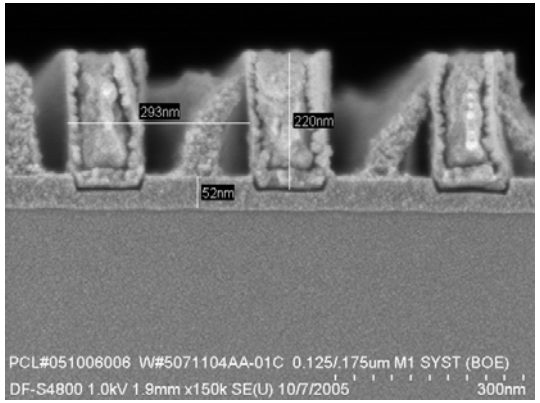

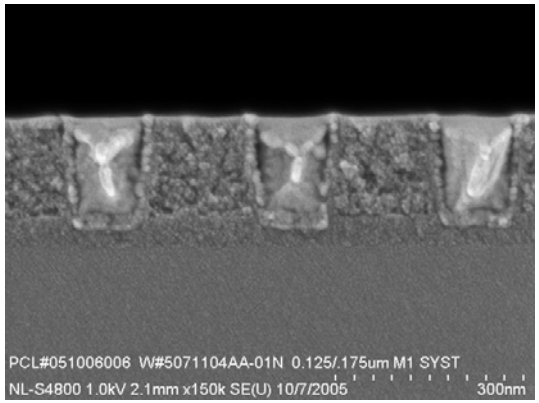

parylene

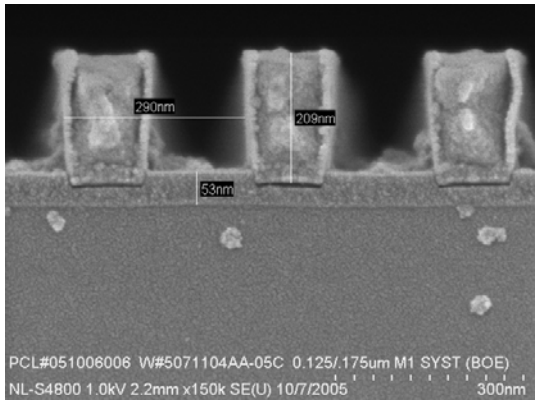

- **Ambiguous Results**
  - **Coating may be pealing away from metalization**
  - **Need electrical testing to confirm or discount**

TEM of Pore Sealed Dielectric Stack Cross-Sections

- Parylene baseline process
  - Metal particles present at base of porous layer
  - Incomplete pore sealing
- V3D3 sealed sample
  - Some metal still apparent at interface
  - Improved vs parylene
  - Require further analysis to determine if electrical properties improved

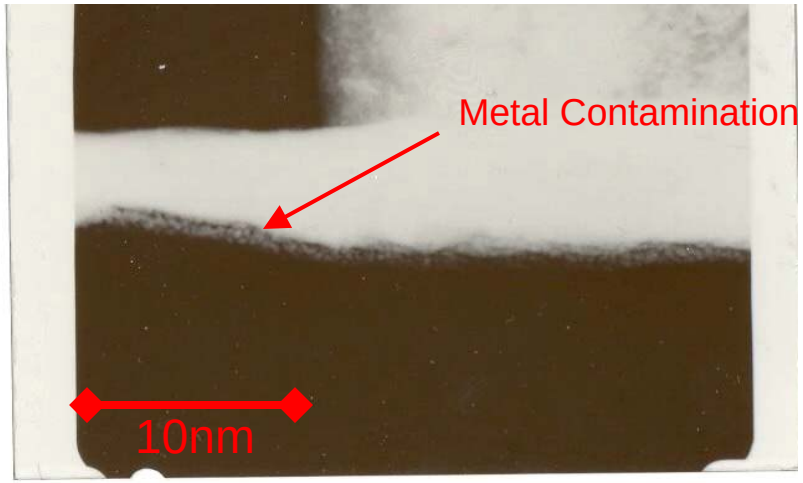

Parylene Sealed Sample

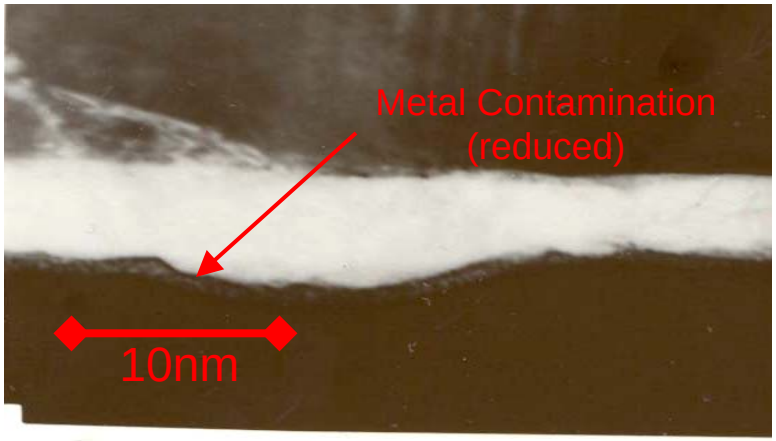

V_3D_3 Sealed Sample

Electrical Data

- Electrical testing of V3D3 coating vs. parylene coating shows improved pore sealing
  - Decreased capacitance
  - Increased Resistance
- Future testing of blanket wafers to confirm

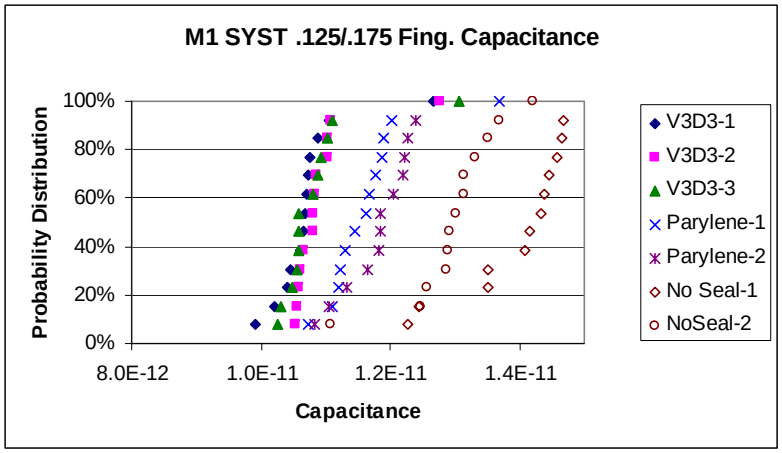

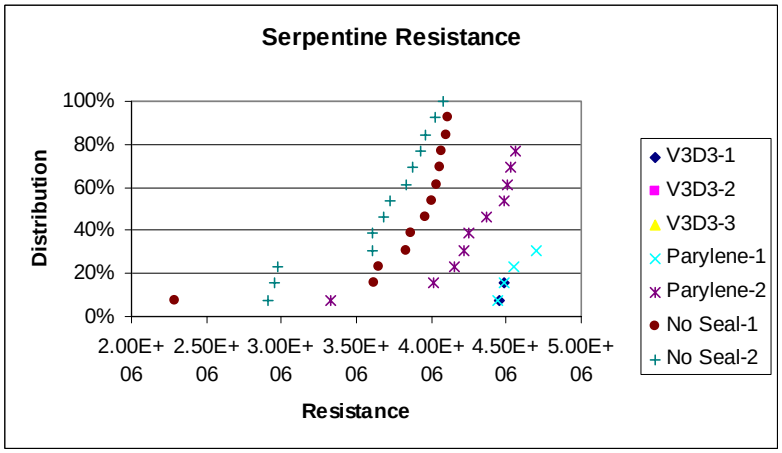

Conclusions & Future Work

- Conclusions:
  - V3D3 polymer shows promise as environmentally benign pore sealing material
    - Low dielectric constant
    - Smooth
    - Adhesive to silicon
    - Decreased metal encroachment into porous layer & improved electrical properties vs. parylene
- Future Work
  - Further electrical testing to confirm pore sealing properties
    - Deposit on blanket porous low-k wafers for electrical impedence testing
  - Asses preferential depositional properties on silicon vs. copper
    - Avoid increased resistance due to blocked vias
  - Improve thermal stability
    - Films stable to 350°C, move to 400°C

Progress in Modeling and Optimization of Multilevel Copper Metallization

Hong Cai – Ph.D. Candidate, MSE
Prof. Duane Boning, EECS

Microsystems Technology Laboratories
Massachusetts Institute of Technology

Thrust A: Back-End Processing
Subtasks A4-1 and A6-3

ERC Annual Review, February 2006

Project Objectives & ESH Impact

- Performance of copper CMP depends strongly on pre-CMP topography. We want to model both electroplating and CMP in order to identify problem areas on the chip, optimize the integrated plating/polishing process, and define design rules.
- Co-optimization of electroplating/polishing module can save time, energy and chemicals.
- Characterization, modeling and optimization of new pads and slurries can reduce waste and improve performance.
- Abrasive-free polishing (AFP) must overcome problem of lack of clearing of large areas due to plating thickness variation. Optimized chip-scale plating is needed for adoption of AFP with the resulting elimination of solid abrasives in CMP wastes.

ESH Metrics

- Yield improvements of several % by identification of problem topography on chip
- Circuit performance of ~5-10% through model-based dummy fill may be possible

	Usage Reduction			Emission Reduction			
Goals/Possibilities	Energy	Water	Chemicals	PFCs	VOCs	HAPs	Other Hazardous Wastes
Plating optimization	10%	10%	10%	N/A	N/A	N/A	10% reduction
Integrated plating/ polishing optimum	10%	10%	10%	N/A	N/A	N/A	10% reduction
Replace abrasive-slurries with AFP	comparable	50% reduction in rinse & clean	comparable	N/A	N/A	N/A	No solid particles in polishing effluent stream

Joint Optimization of Process/ESH Performance

Manufacturing Performance
- **Ability to planarize chip**
- Yield (wafer edge)
- Uniformity
- Cost
- …

A4-1 Modeling of pattern dependent effects

ESH Performance
- Slurry, pad, & water consumption
- Slurry solid waste output
- Slurry effluent waste
- …

Joint Optimization of Process/ESH Performance
- Minimize film thickness, plating/CMP time, consumables/effluent

A6-3 Coupled plating and planarization

Process Alternatives
- Abrasive free polishing (AFP) to eliminate solid slurry waste, while achieving high performance
- Electrochemical-mechanical planarization (ECMP)

Overall Methodology

- Motivation: performance & yield loss, pattern induced Cu thickness variation
- Goal: chip-scale prediction of Interconnect topography for any layouts

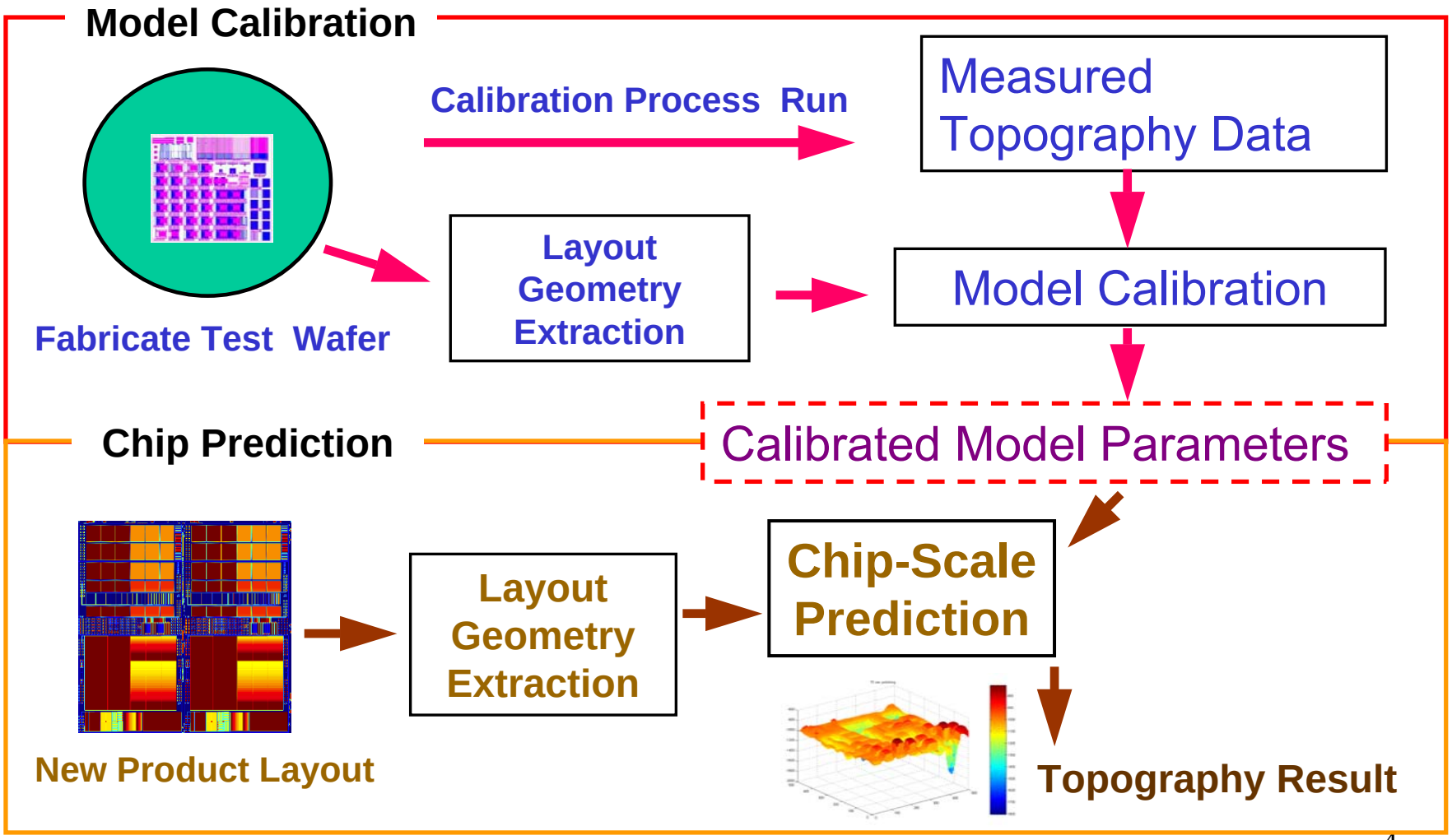

Review: Tae's Electroplating Model

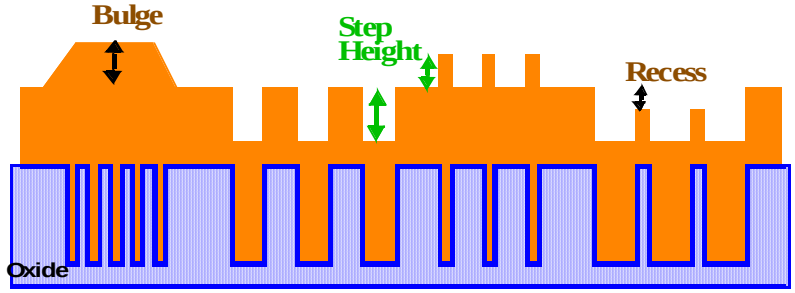

- Tae's Electroplating Model
  - Step height and array height are fitted by separate semi-empirical response surface models as a function of underlying layout parameters for conventional and super-filling electroplating processes.
  - Additional field thickness variation is modeled by considering the so-called average "surface area" computed over a region of size *P* on the chip. This parameter is conceptually based on a total "exposed" surface area accounting for sidewalls as well as the tops and bottoms of features.
- Problems
  - No direct physical relation between the models of step height and array height. Thus, the formulae are valid for a fixed nominal thickness.
  - Over-fitting problem (Each formula need several fitted parameters.)
  - Line width and line space are not generalized underlying layout parameters.
  - No clear physical meanings for the so-called average "surface area".
  - Field thickness is not a solid variable for a random layout.

[1] Tae Park, Tamba Tugbawa, Duane Boning, Chidi Chidambaram, Chris Borst and Gregg Shin, Journal of The Electrochemical Society, 2004, Vol. 151, No. 6, pp. C418–C430

Review: Hong's Non-Time-Step Model

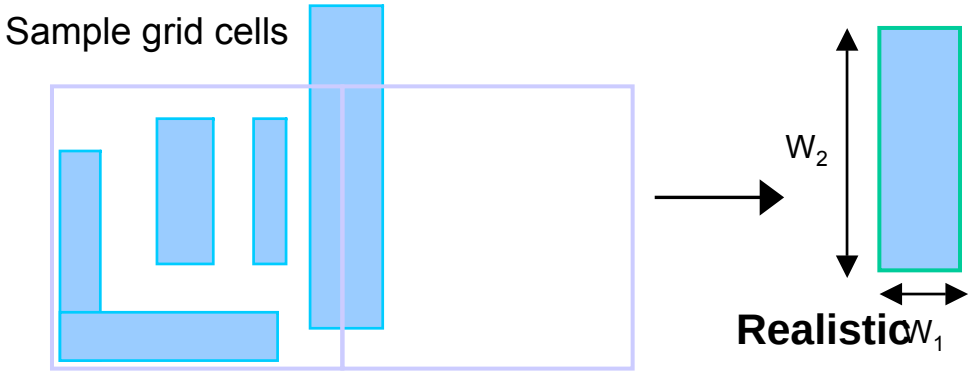

Layout extractor is used to compute layout parameters in each cell across the whole chip

All features in a cell are treated as rectangular objects with W_1 and W_2 (here, $W_2 > W_1$)

- Effective Width is calculated as:

$$\frac{1}{W_{eff}} = \frac{1}{W_{1avg}} + \frac{1}{W_{2avg}}$$

  - W_{1avg}: Average of all W_1's
  - W_{2avg}: Average of all W_2's (derived from perimeter of all objects)
  - D_{cell}: Copper pattern density
  - ***Weff*** captures 2D geometry information in each cell

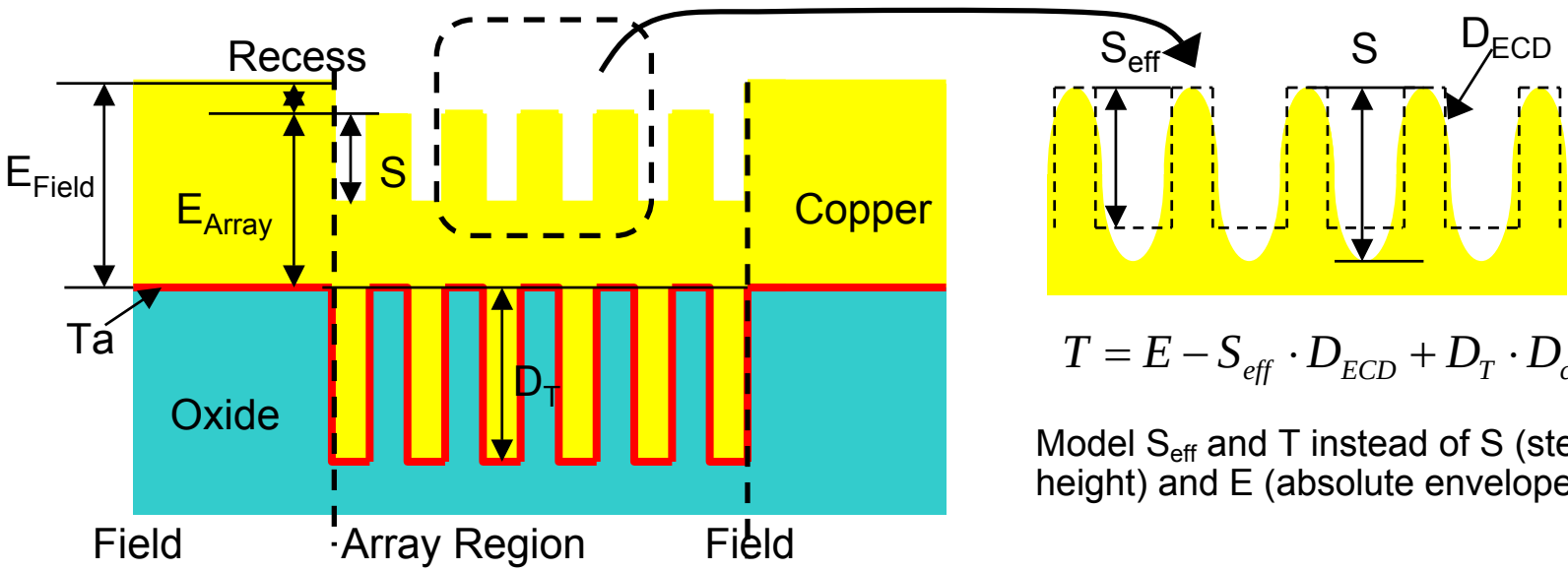

$$T = E - S_{eff} \cdot D_{ECD} + D_T \cdot D_{cell}$$

Model S_{eff} and T instead of S (step-height) and E (absolute envelope)

[2] Hong Cai, Tae Park, and Duane Boning, ERC Annual Retreat 2004, Stanford, CA

Review: Hong's Non-Time-Step Model

- Hong's Electroplating Model
  - Model effective step-height and average copper thickness instead of step height, array height and average field thickness in Tae's model.
  - Effective step height and average copper thickness are fitted by separate semi-empirical response surface models as a function of underlying layout parameters, effective line width and layout pattern density.
  - Long-range electroplating effect is attributed to copper ion depletion effect, which is decide by the deposited copper amount in the surrounding area.

$$T = T_{nom} \cdot F_{con}$$

$$F_{con} = (F_{dep})^{-\alpha}$$

$$F_{dep} = f(T, ECD\ Depletion\ Length)$$

α and ECD Depletion Length are model parameters for copper depletion effect

- Cons and Pros
  - Only need to model 2 variable instead of 3 variables.
  - No physical link between step-height and average copper thickness, over-fitting still is a problem.
  - Effective line width is more robust for random layout and incorporates some 2-dimensional information.
  - Clear physical meanings for copper ion depletion effect and explain the long-range pattern dependence successfully.
  - Average copper thickness is a solid variable for a random layout .

[2] Hong Cai, Tae Park, and Duane Boning, ERC Annual Retreat 2004, Stanford, CA

Time-Step Model: Objective and Strategy

- Objective
  - Build a time-step electroplating model which can simulate the chip-scale post-electroplating topography with different nominal deposition thickness.
  - Keep the computation efficiency of Tae's and Hong's model and physically link the step-height and array height (or average copper thickness) models, thus solve the over-fitting problem.
  - Follow the part of copper ion depletion effects in Hong's Model to explain the long-range pattern dependence.
  - Comparable model accuracy although step height and array height (or average copper thickness) have to be simulated at the same time.
  - Extendable for multi-level copper metallization and any random layout.
- Strategy
  - Directly model the copper film growth on the top, the bottom and the side wall of the patterned features by using the fundamental layout parameters (no effective line width). Other variables, such as (effective) step-height, array height and average copper thickness could be easily derived.
  - Use straight line segments to simplify the details of the topography.
  - The growth rate on the top, the bottom and the sidewall is determined by the surface coverage of the organic additives in the electroplating liquid and the effective local copper ion concentration.
  - The effective local ion concentration could be derived by incorporating copper ion depletion effect.

Time-Step Model: Feature-scale Models

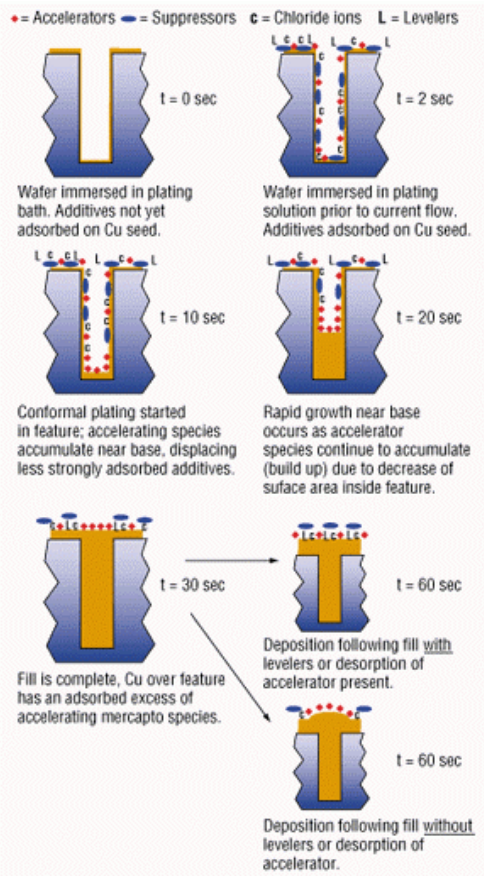

Figure 6. Illustration of additive adsorption behavior during plating fill. A mechanism for the establishment and propagation of bottom-up fill is suggested.

[3] Jon Reid, Steve Mayer, Eliot Broad, etc. Solid State Technology, July, 2000

West and Cale

Surface kinetics of the accelerator

$$\frac{d(A\theta_{acc})}{dt} = k_1 A(\theta_{acc} - \theta_{acc,eq})$$

$$\frac{d\theta_{acc}}{dt} = \frac{i\Omega}{nF} k_2 \kappa \theta_{acc} - k_1 A(\theta_{acc} - \theta_{acc,eq})$$

Surface kinetics of the suppressor

$$\frac{d\theta_{\sup}}{dt} = -k_3(\theta_{\sup} - K(1-\theta_{\sup}))$$

$$K = 30\exp\left(-7\sqrt{\theta_{acc}}\right)$$

Local current density

$$i = \mathrm{I}(1-\theta_{\sup})$$

Moffat

Local interface current density

$$i = i_0\left(1 - \frac{i}{i_L}\right)\exp\left(-\frac{\alpha F}{RT}\eta\right)$$

$$i(\theta) = (0.4726\theta + 0.0374)\exp\left(-\frac{(0.5+0.25\theta)F}{RT}\eta\right)$$

Growth rate

$$v(\theta) = A + B\theta$$

$$\frac{d\theta}{dt} = \frac{i\Omega}{2F}\kappa\theta$$

Time-Step Model: Implementation

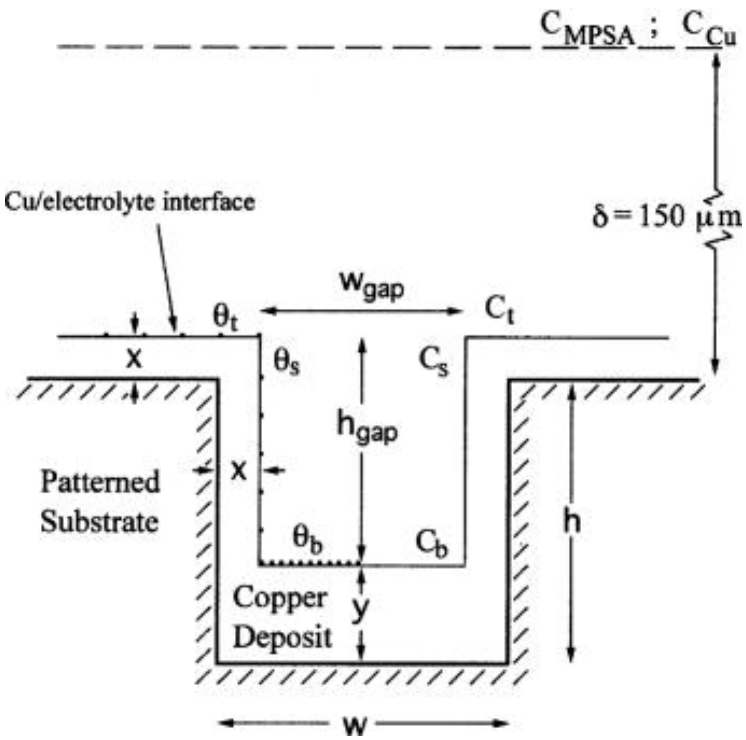

A Schematic of the Approximate Geometry for a Simple Model

[4] D. Josell, D. Wheeler, W. H. Huber, and etc. J.E.S. , 2001, Vol. 148, No. 12, pp. C418–C430

A Simple Geometrical Model :

- Based on CEAC Model
- Straight Vertical and Horizontal Lines
- Local Growth Rate
- Horizontal and Vertical Displacement

Growth rate

$$v = A\left(1 - \theta_{\sup} + k\theta_{acc}\right)F_1 F_2$$

F_1: Inner-feature depletion factor
F_2: Inter-feature depletion factor

Coverage of accelerator and suppressor on the top, side and bottom of the trench is calculated by the method used by Cale

Assumption:

- Ignore additive depletion
- Consider Cu ion inner-feature and inter-feature depletion effect
- Accelerator dominant
- Straight approximate geometry
- Ignore negative step height

Time-Step Model: Flowchart

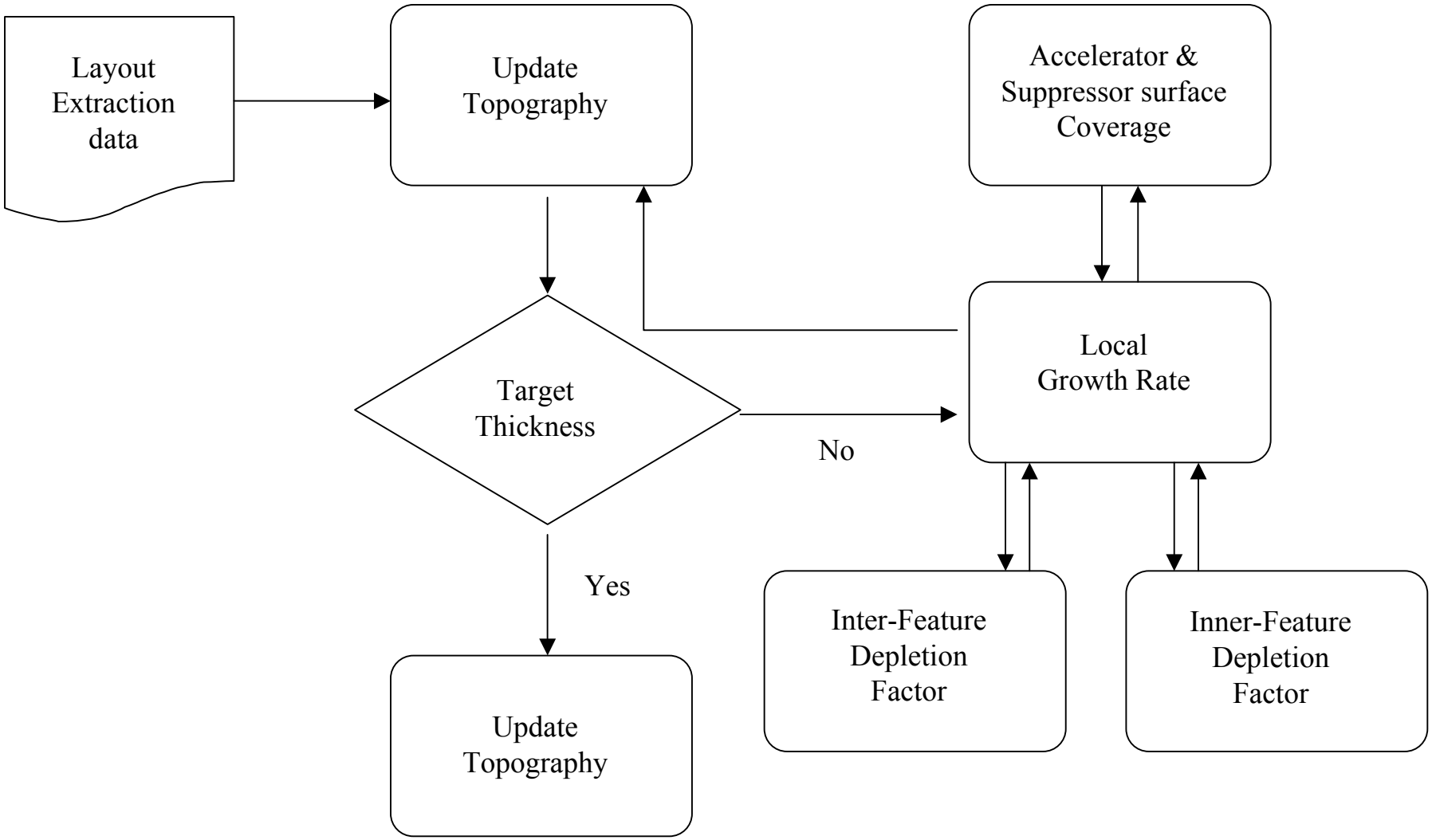

Time-Step Model: Simulation Results

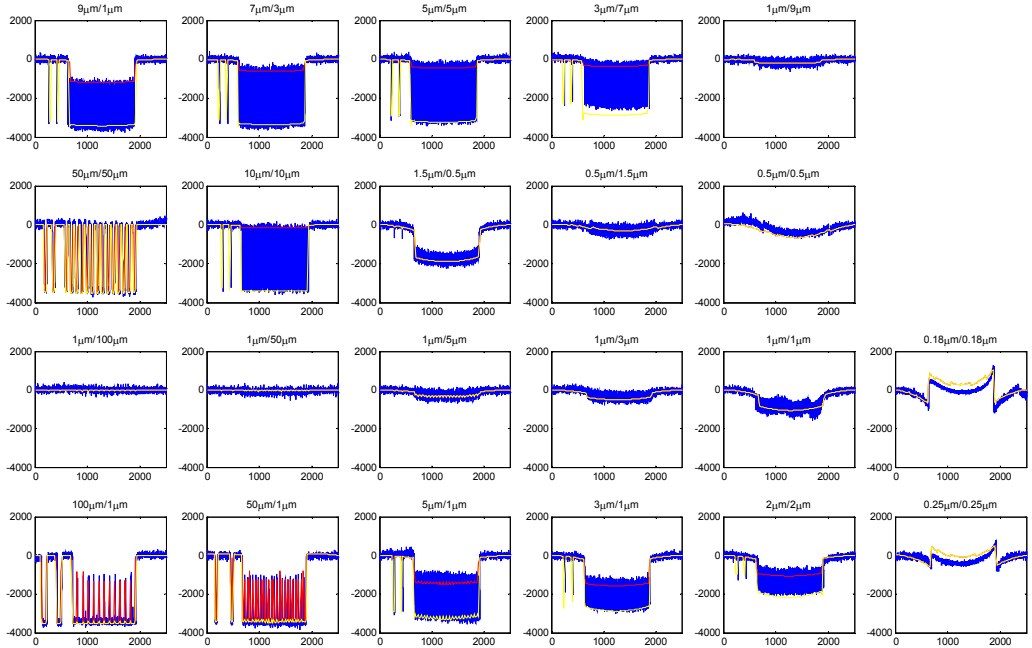

High-resolution profiler scans in patterned areas (blue) and the corresponding simulation topography (yellow for lower area and red for upper area in aach grid).

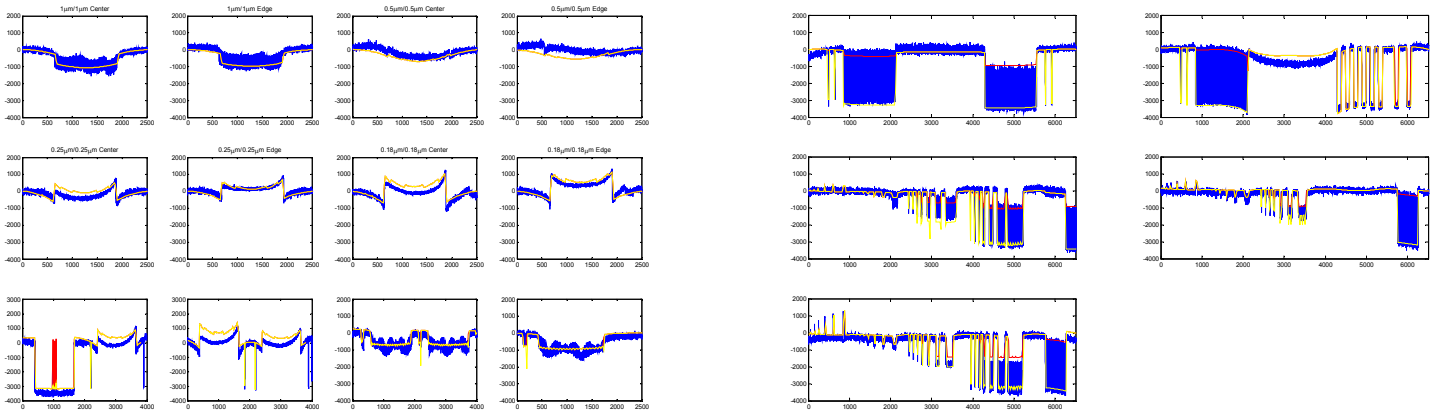

Time-Step Model: Simulation Results

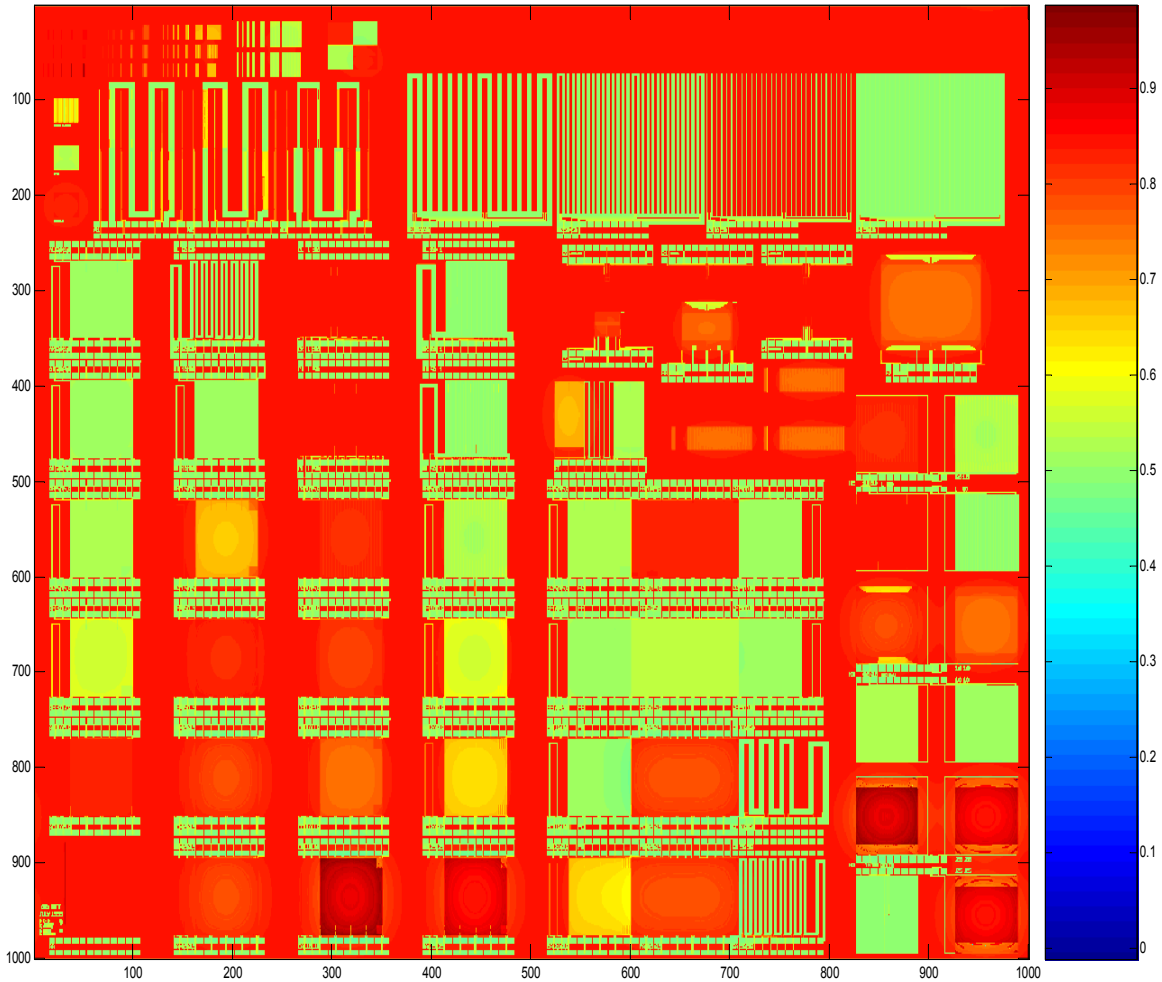

Chip-scale Topography Simulation (Thickness in µm)

Industrial Collaborations & Technology Transfer

- Praesagus, Inc. – layout interface data, oxide thickness, HRP and e-test
- Magna Chip, Inc. – experiments, measurement, financial support
- Neopad – CMP pad experiments
- Philips Analytical – copper thickness measurement

Future Plans

- Finalize the time-step electroplating model and extend the model in multi-level copper metallization case.
- Improve the physics-base CMP model and generalize it in the multi-level copper metallization.
- Integrate the time-step electroplating and CMP models.
- Develop optimization methods for coupled plating/CMP process optimization that minimize process thickness, process time, and consumable usage.

Conclusions

- A physics-based time-step copper electroplating model is developed to accurately simulate the post-electroplating topographical evolution.
- With a limited set of parameters, the simulation errors of envelope and step-height could be reduced to 10-20 nm.
- The new framework could be seamlessly integrated with our chip-scale CMP model and extended to multi-level copper metallization case.

Modeling and Physical Understanding of STI CMP Process

Daniel Truque – Ph.D. Candidate, EECS
Xiaolin Xie – Ph.D. Candidate, Physics
Prof. Duane Boning, EECS

Microsystems Technology Laboratories
Massachusetts Institute of Technology

Thrust A: Back-End Processing
Subtasks A-4-1

ERC Annual Review, February 2005

Project Objective

- Physical understanding of STI CMP process
- Improve die-level CMP model
- Better control and optimize STI CMP

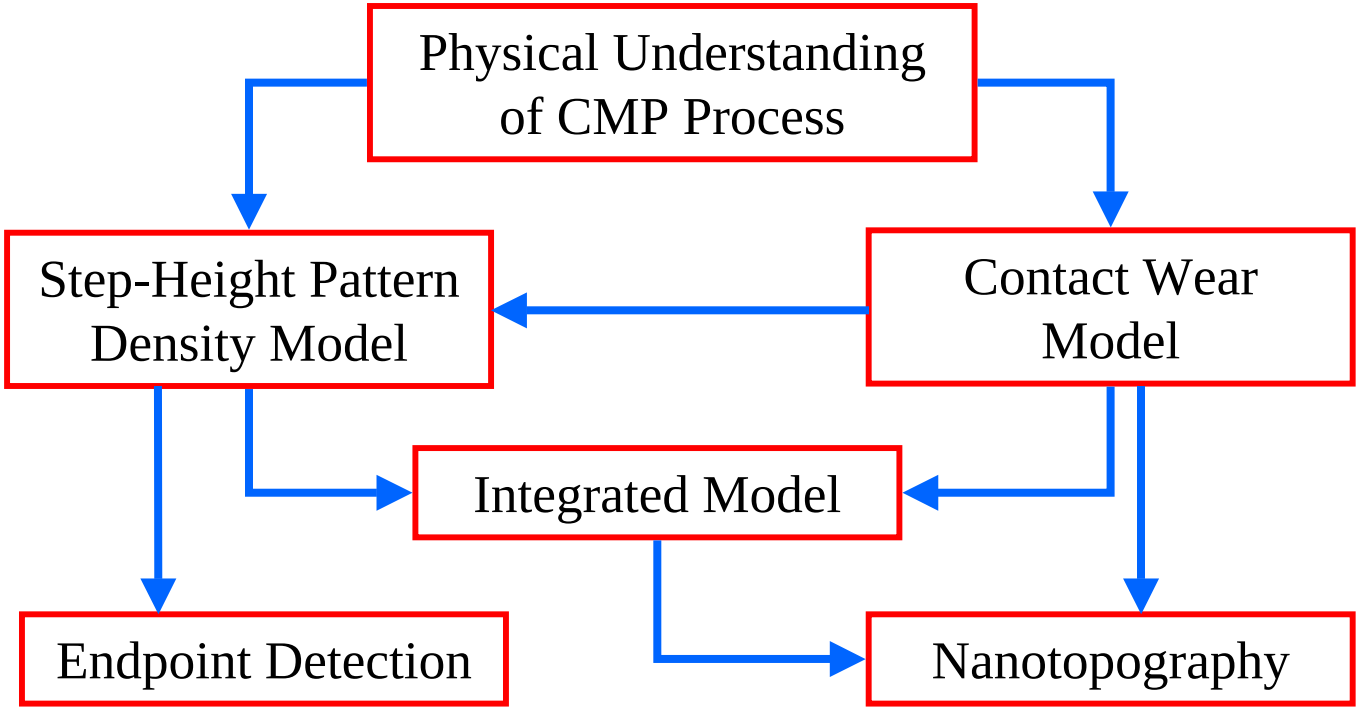

Optimization of Process/ESH Performance

A4-1 Modeling of pattern dependent effects

Manufacturing Performance
- **Ability to planarize chip**
- Yield (wafer edge)
- Uniformity
- Cost
- …

ESH Performance
- Slurry, pad, & water consumption
- Slurry solid waste output
- Slurry effluent waste
- …

Joint Optimization of Process/ESH Performance
- Minimize film thickness, CMP time, consumables/effluent

Roadmap of Research on STI CMP

- Recent Work
  - Simulation of wafer edge roll-off effect
  - Modeling and simulation of endpoint detection of STI CMP *(with Sandia, Rohm & Haas, IMEC)*
  - Nanotopography impact study *(with Infineon, Siltronic)*
  - Pad planarization performance modeling *(with JSR)*

- In Progress
  - Data analysis of nanotopography experiment on patterned wafers *(with Infineon, Siltronics)*
  - Physical understanding and modeling of ceria-based slurry and modeling of endpoint signal *(with Rohm & Haas, IMEC)*
  - Study the relationship between pad properties and CMP performance
  - Model improvement

Edge Roll-Off Effect

CMP tool setup

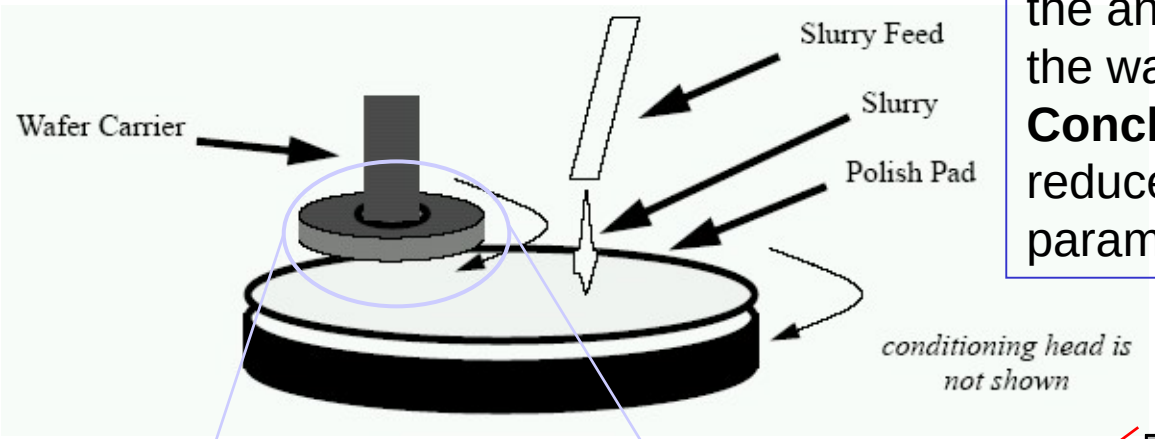

Problem: Edge roll-off effect refers to the anomaly polishing near the edge of the wafer caused by tool structure.
Conclusion: Edge roll-off could be reduced with good combination of tool parameters and improve *yield*.

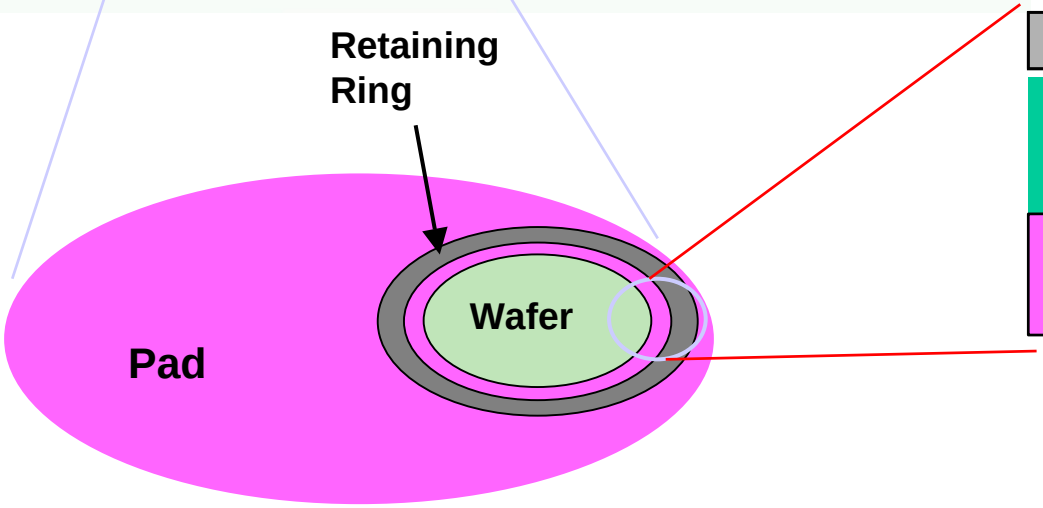

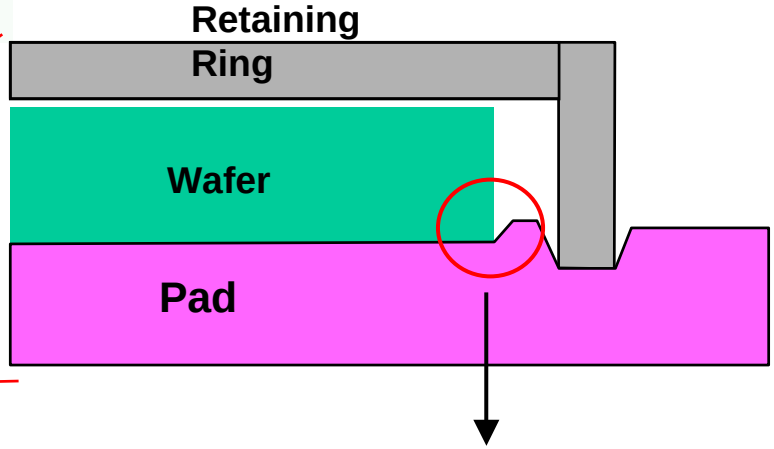

Nonuniform pressure concentrations cause excess or insufficient polishing

Model of CMP with Ceria-Based Slurry

- An empirical model for ceria slurry

$$K = K(t)\frac{\gamma + 1/\rho}{\gamma + 1}$$

  - K(t) is determined by blanket polishing experiment
  - γ is a model parameter, which adjusts the pattern density contribution

Fitting Error of 126 Å

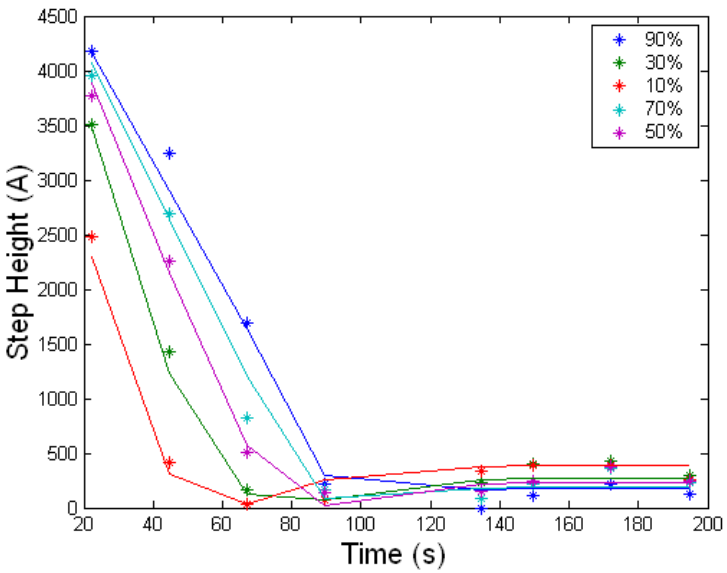

Fitting Error of 157 Å

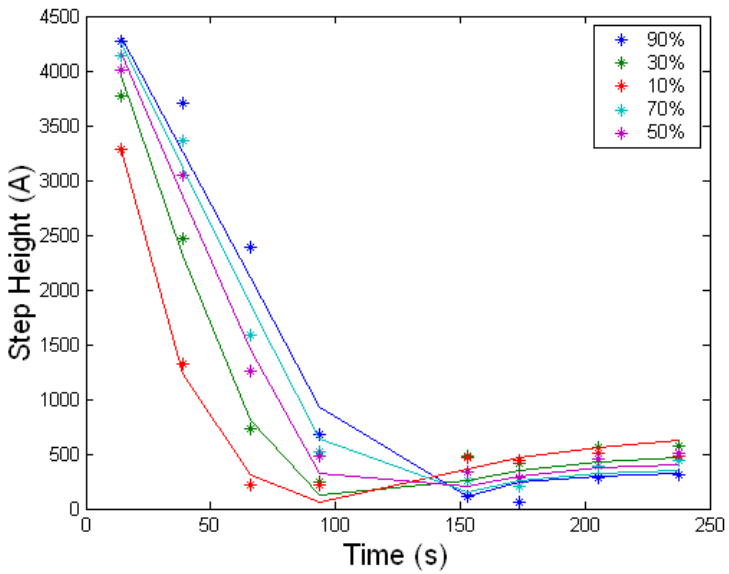

Simulation of Endpoint Signal

Measured EPD Signal | **Predicted Friction**

Process 1

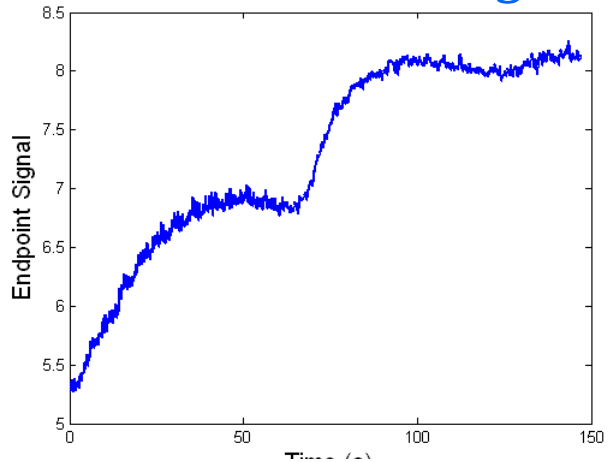

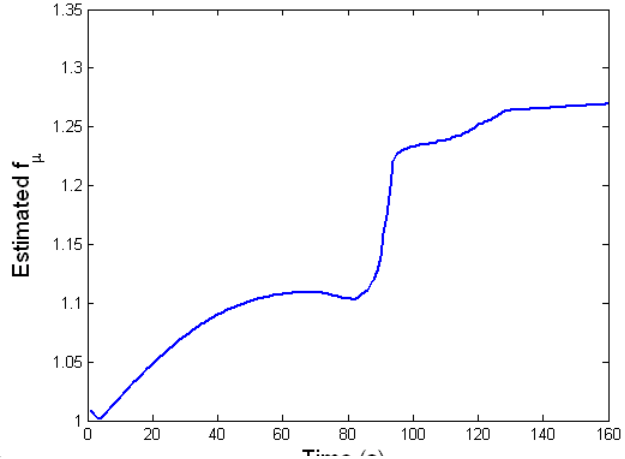

Process 2

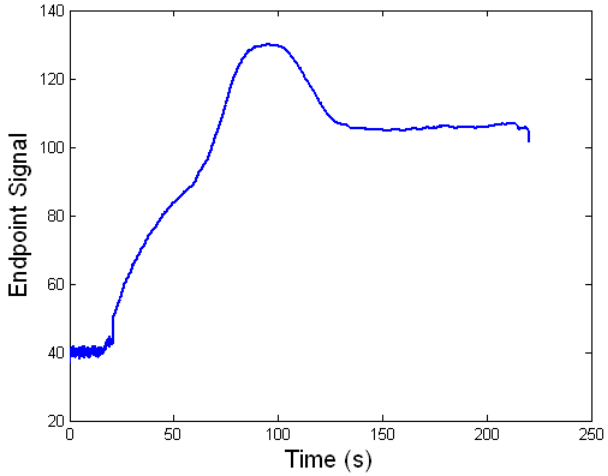

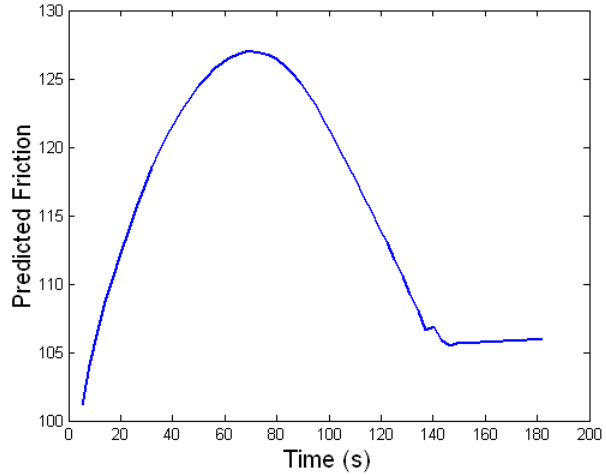

Identify Nanotopography Impact

- A blanket CMP DOE using 4 CMP processes, 3 wafer finishes, and 2 polishing stages
- Compute the correlation between material removal map and nanotopography map for each case

Processes Stopped in Oxide

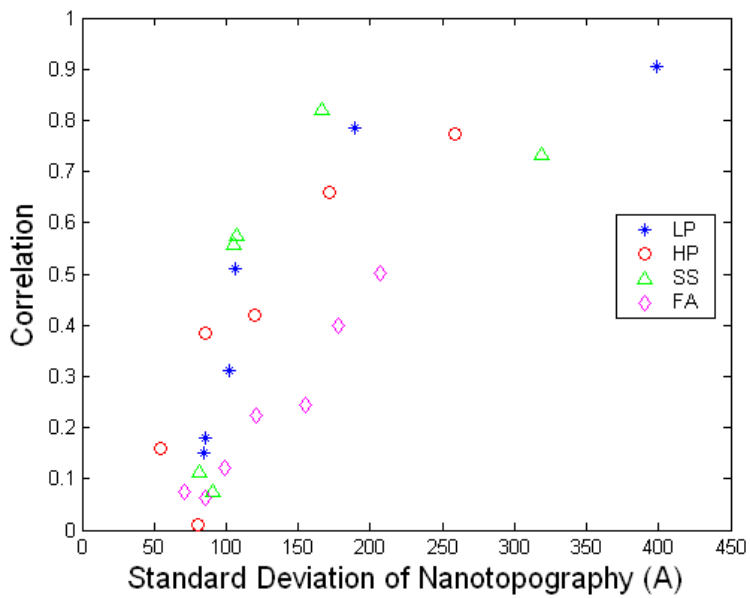

Processes Stopped in Nitride

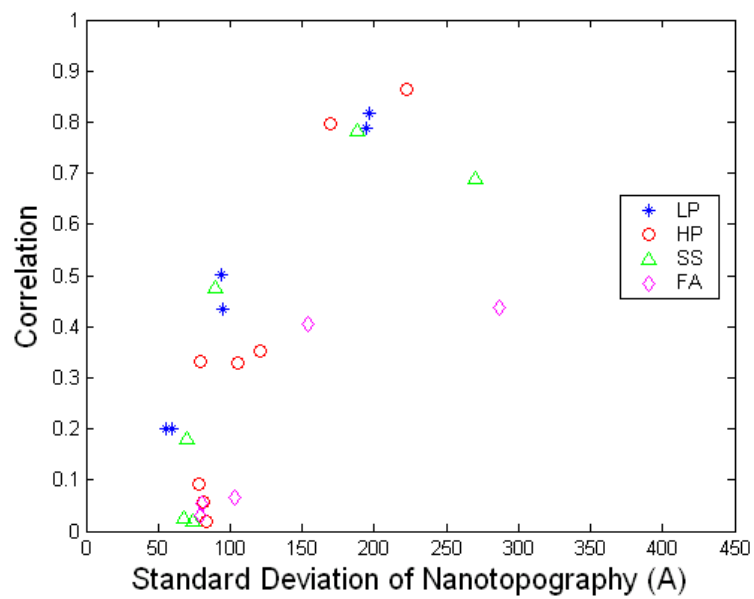

Modeling of Nanotopography Impact

- Contact wear model is used to model the nanotopography impact
- Modeling works well for all processes except the fix-abrasive process
- Nanotopography impact is less significant for smoother initial wafer surface

Filtered AR Map

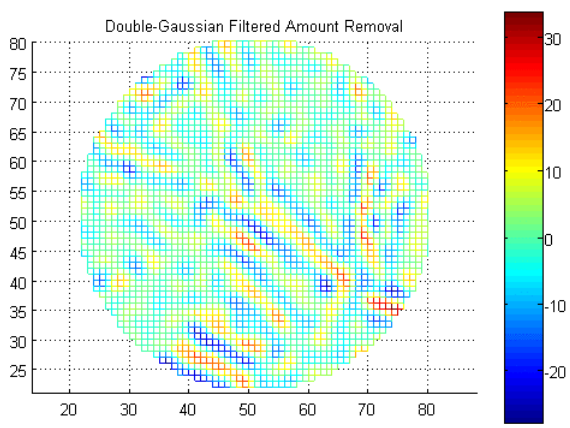

Predicted AR Map

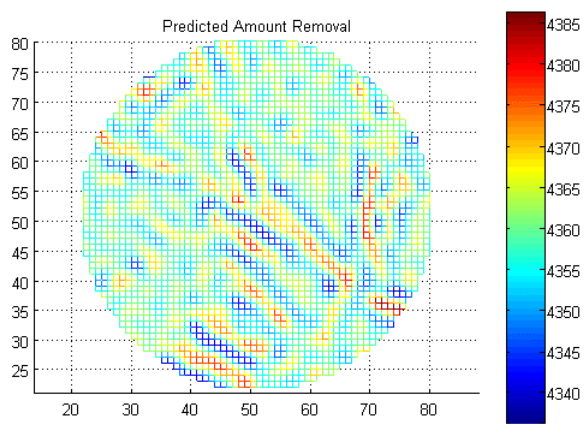

Cross-section Comparisoin

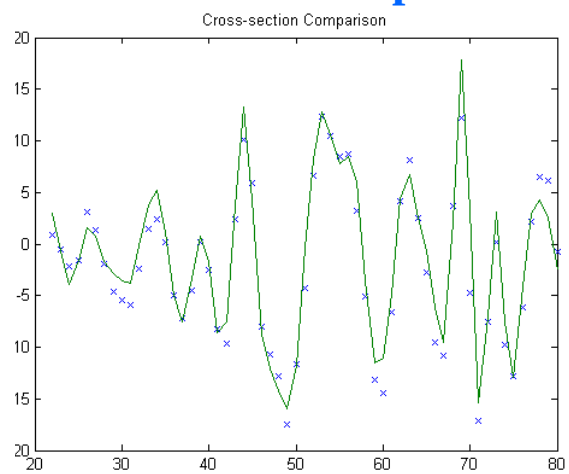

Pad Planarization Performance Modeling

- **Goal --** Understand how pad parameters, such as stiffness, pore size and distribution, relate to pad performance as captured by the model parameters
- **Observations**
  - Conventional pad polishes faster
    - but at the expense of possible overpolishing in lower pattern density areas
  - JSR pad exhibits lower pattern dependency
    - a smaller spread in the times required to planarize 10% to 90% structures

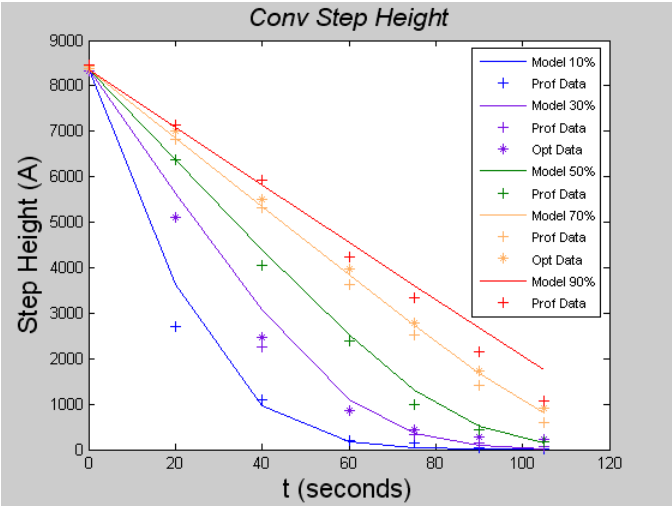

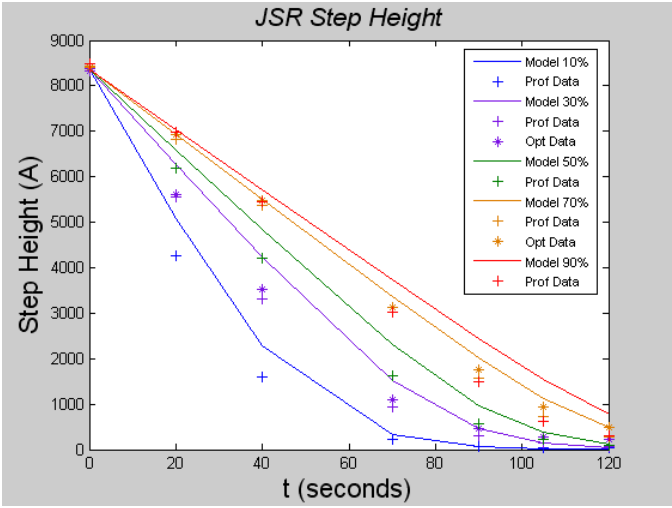

Future Plans

- Data analysis of nanotopography experiment on patterned wafers
- Physical understanding and modeling of ceria-based slurry
- Modeling of friction endpoint signal
- Develop a DOE to study the relationship between the model parameters (*K, PL, hc*) to pad parameters (pore size, density, etc)

Industrial Collaborations

- Rohm & Haas Materials
- IMEC
- Siltronic AG
- Infineon Technologies
- JSR
- NSF/SRC ERC for Environmentally Benign Semiconductor Manufacturing

Conclusions

- Edge roll-off could be reduced with good combination of tool parameters
- Nanotopography impacts identified in blanket wafer experiment and is modeled reasonably well by contact wear model
- Friction model is improved and in reasonable agreement with experiment data of CMP processes using ceria-based model

Characterizing Copper – Hydrogen Peroxide Film Growth and Dissolution Kinetics for Application in Multi-Step Chemical Mechanical Planarization Models

(Subtask A-4-2)

D. DeNardis, D. Rosales – Yeomans, and A. Philipossian

(University. of Arizona, Tucson, AZ, USA)

L. Borucki

(Intelligent Planar, Mesa, AZ, USA)

Copper CMP

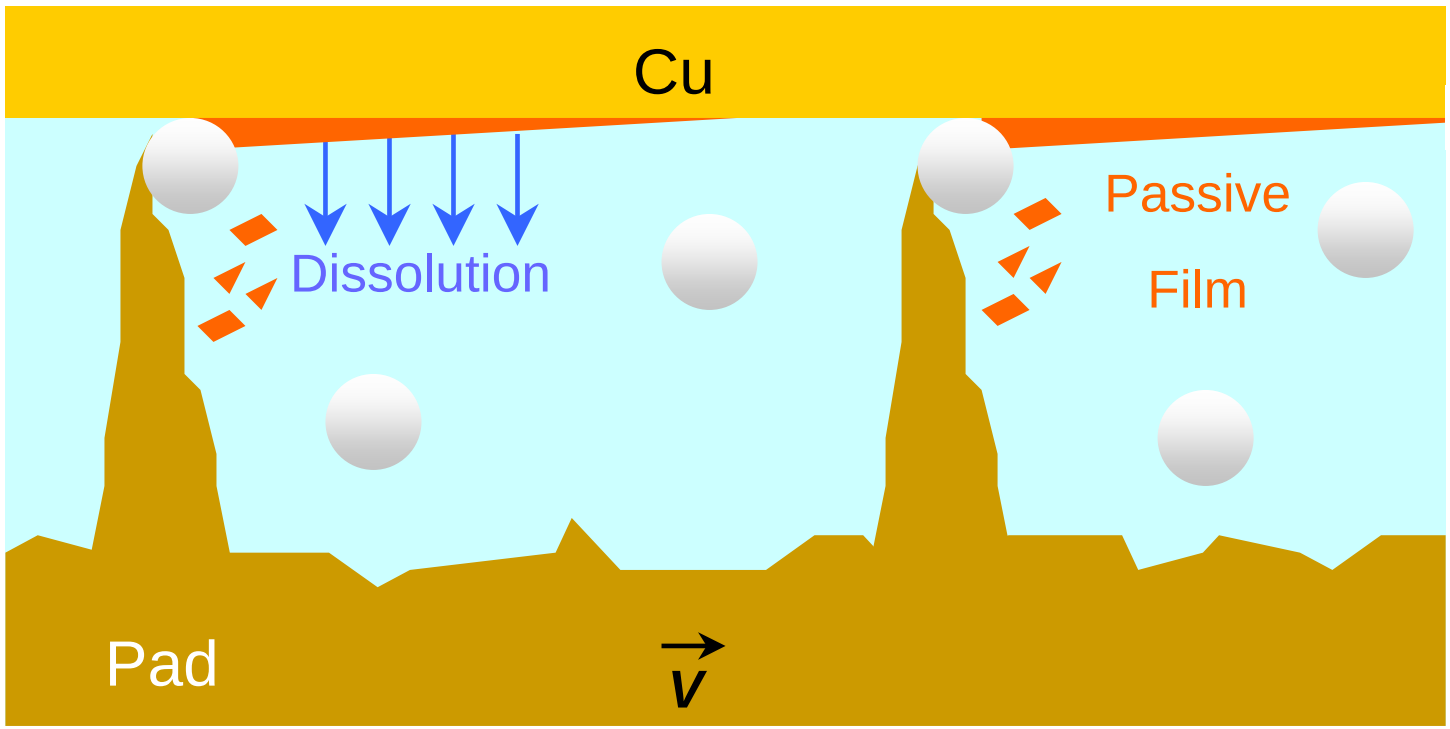

Two – Step Removal Mechanism:

$$Cu + OX \xrightarrow{k_1} CuOX^* \xrightarrow{k_2} CuOX$$

** Indicates surface species*

Separation of ‘C’ and ‘M’ in CMP

Passive Film Formation ***Mechanical Removal***

$$\mathrm{Cu + OX} \xrightarrow{k_1} \mathrm{CuOX^*} \xrightarrow{k_2} \mathrm{CuOX}$$

$$\mathrm{CuOX^*} \xrightarrow[\textit{Dissolution}]{k_3} \mathrm{CuOX}$$

- If k_1 and k_3 can be experimentally determined *a priori*, k_2 comprises mechanical processes only and can be extracted from CMP experiments

- The chemical and mechanical contributions can be quantified separately

In this study, characteristics of Steps 1 and 3 are investigated

Cation Migration

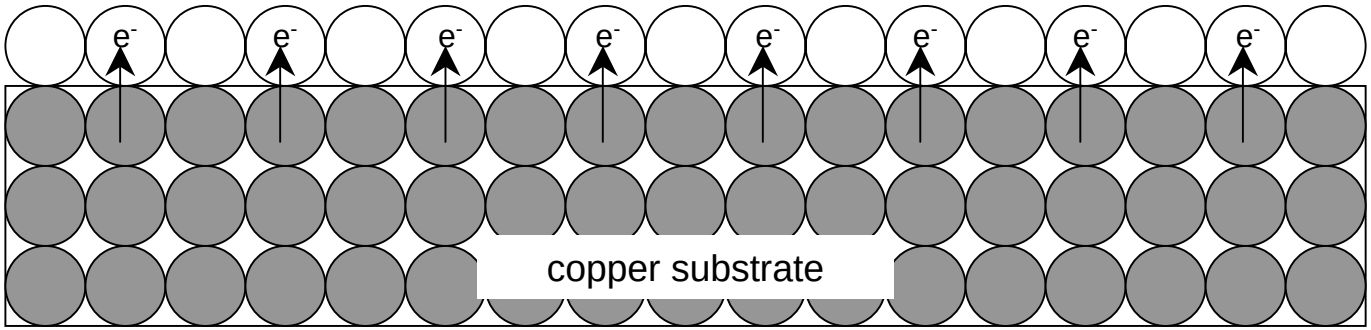

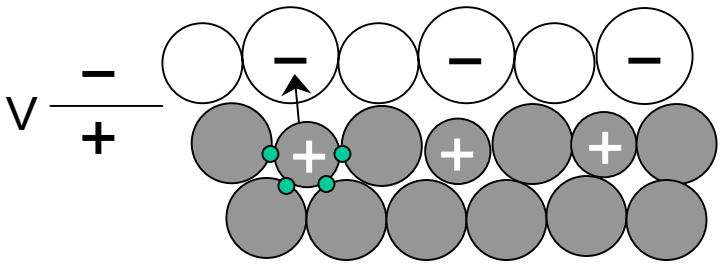

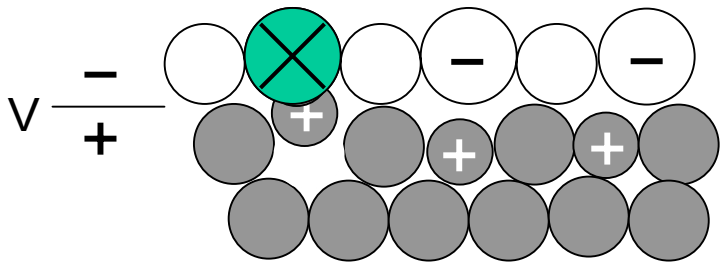

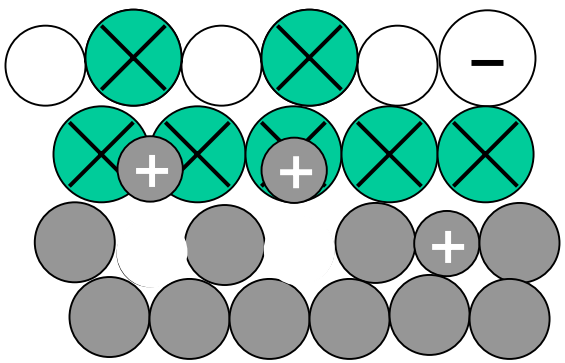

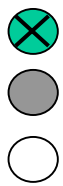

= Cu_2O

= Cu

= oxidant (H_2O_2, O_2, O, etc.)

$$\frac{dx}{dt} = N\Omega f \exp\left(\frac{-W}{kT}\right)\exp\left(\frac{qa}{2kTx}V\right)$$

Model Basis: Drift Velocity

$$\nu = \mu_B E$$

υ = drift velocity

μ_B = ionic mobility

E = electric field

However, for very thin films (10^{-6} cm) the field is so strong that ν is no longer proportional to it.

The probability per unit time that an ion will move from one site (A) to another (B) is:

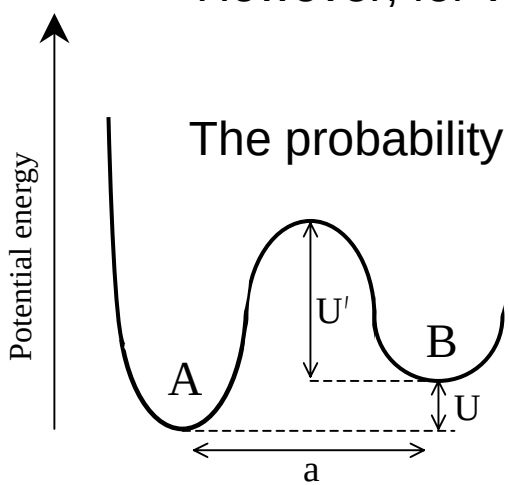

$$p = f \exp\left\{-\left(\frac{W}{kT} - \frac{qaE}{2kT}\right)\right\}$$

$$\nu = ap$$

Rate of oxide growth = (volume of oxide per cation) (# cations per area) (p)

Model Evaluation

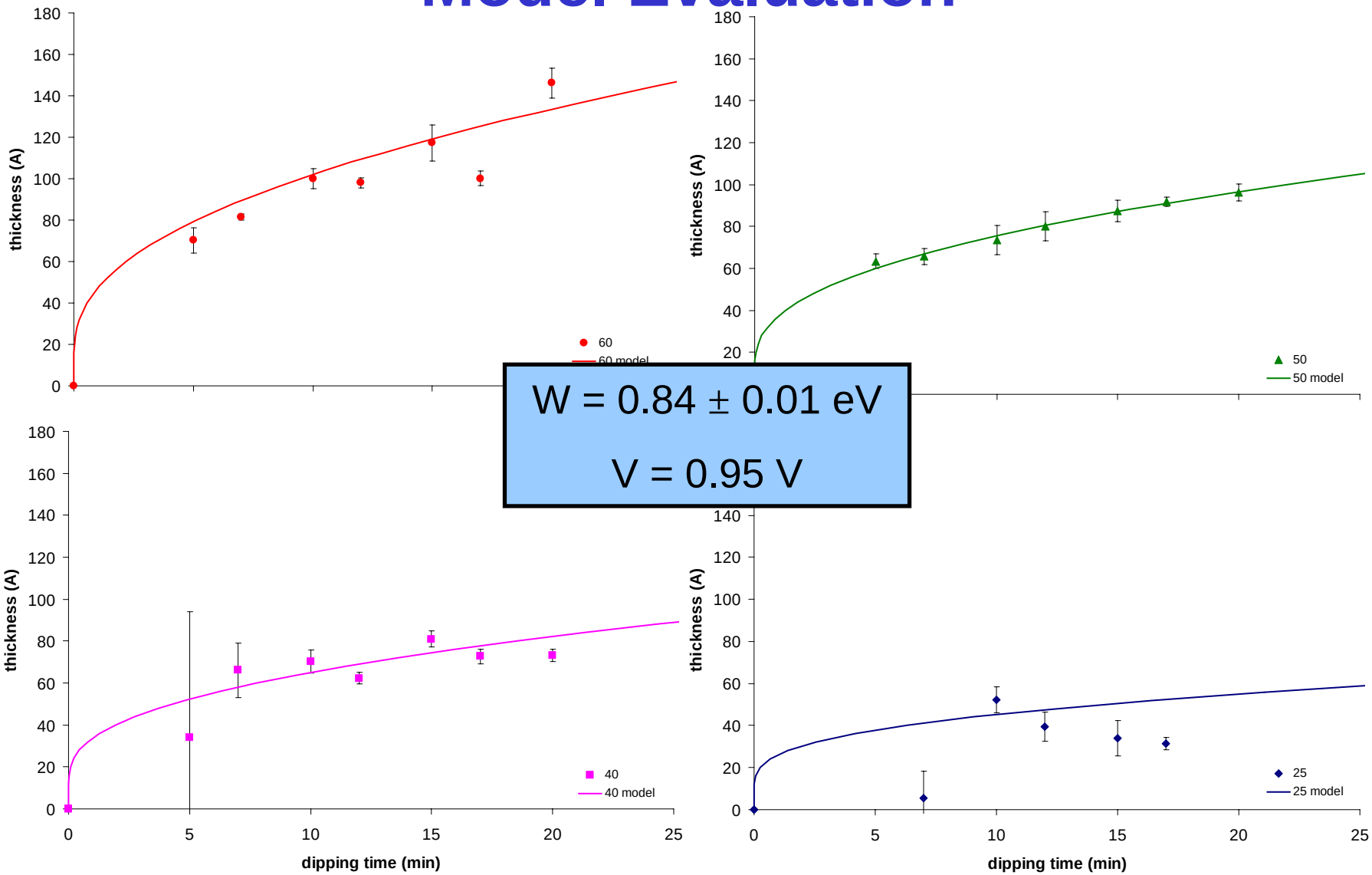

$W = 0.84 \pm 0.01$ eV

$V = 0.95$ V

Oxidation Rates

	oxidant		T(^{o}C) = 8	25	30	40	50	60
Cabrera and Mott*	$O_{2(g)}$	W (eV)		1.0				
1949		V (V)		1.0				
Krishnamoorthy, *et al.*	$O_{2(g)}$	W (eV)	0.9		0.965		1.05	
1970		V (V)	0.5		0.5		0.5	
Current Study	$H_2O_{2(aq)}$	W (eV)		0.851		0.849	0.837	0.831
		V (V)		0.95		0.95	0.25	0.95

** = based on theortical calculations*

$$\frac{dx}{dt} = N\Omega f \exp\left(\frac{-W}{kT}\right)\exp\left(\frac{qa}{2kTx}V\right)$$

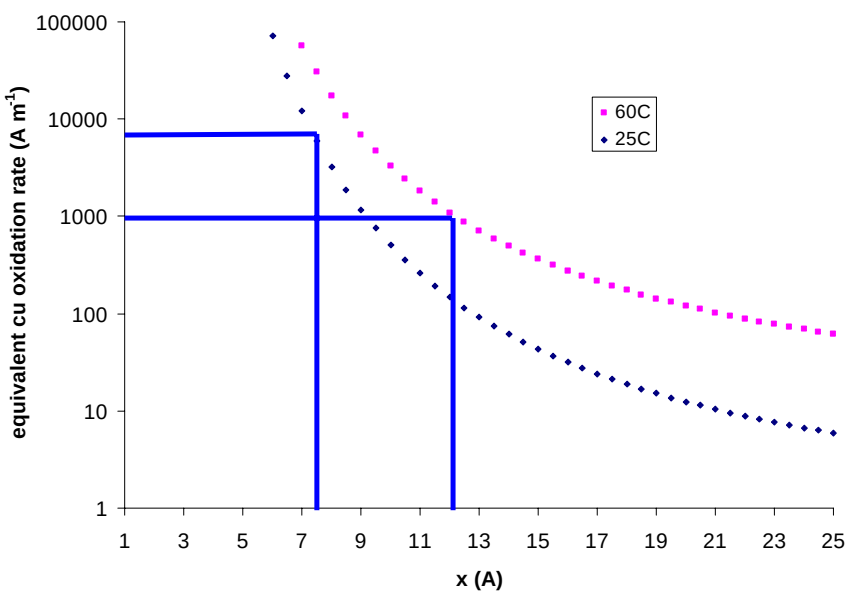

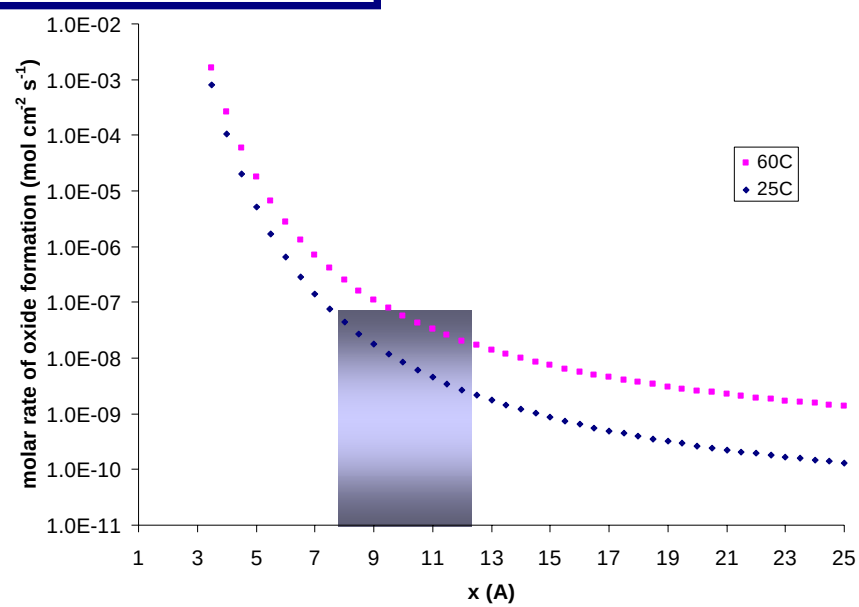

Copper Oxide Dissolution Profiles

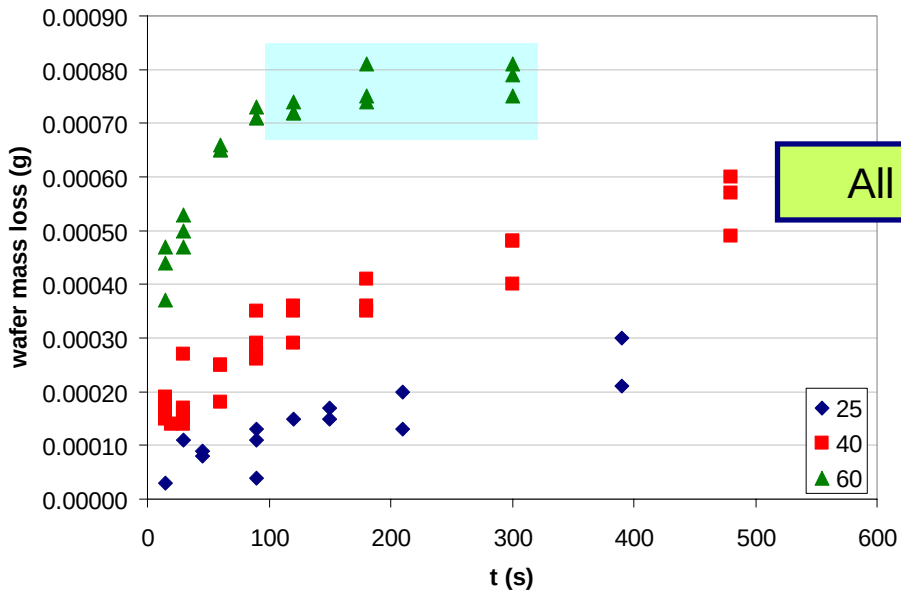

All etchable oxide reacts in 90s for 60ºC

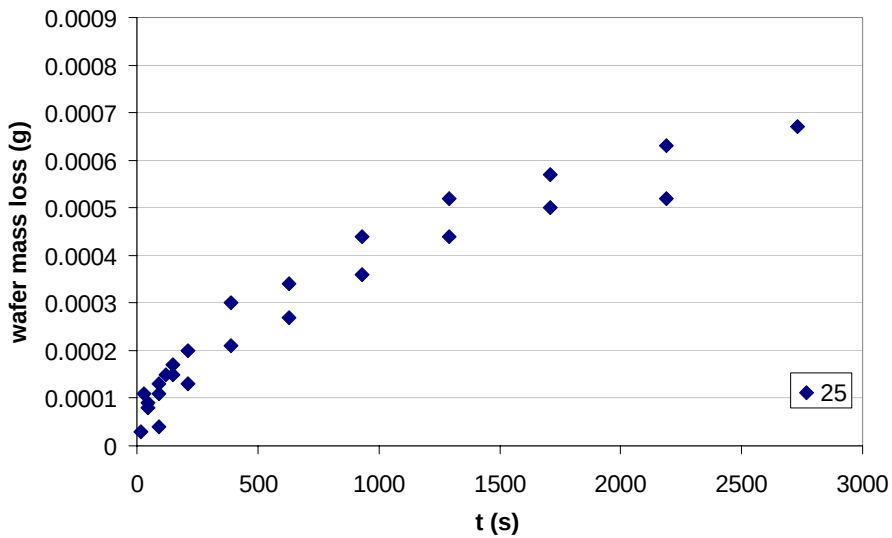

At long times low T profiles approach saturation

Dissolution Process

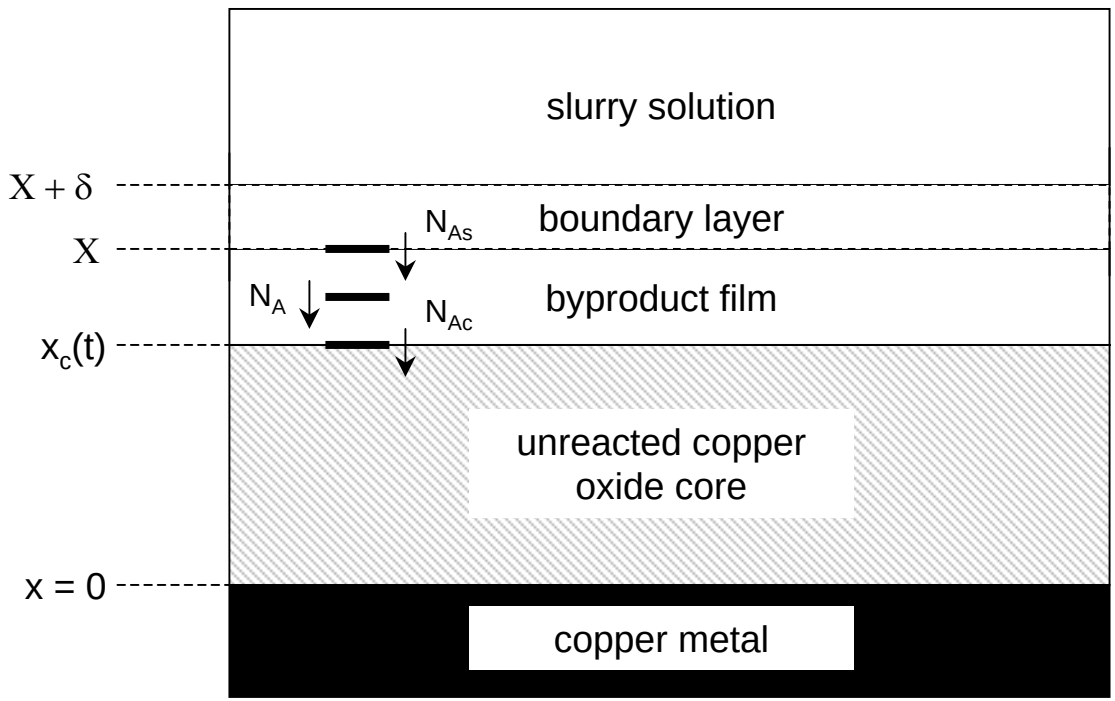

$$RL_{(aq)} + CuO_{(s)} \rightarrow RX_{(s)} + Cu(L)_i^{2+}{}_{(aq)}$$

$$A_{(aq)} + B_{(s)} \rightarrow C_{(s)} + P_{(aq)}$$

- A soft byproduct film was observed on wafer surface
- Film was present after long times
- Controlling Mechanisms
  - Surface reaction
    - Linear profile
  - Diffusion through BL
    - Reported that profiles are not a function of stirring speed
  - **Diffusion through byproduct**

Model Development

QSS Assumption:

Diffusion of A through the byproduct layer is fast compared to dx/dt

Flux of A at any x: $N_A = -D\frac{dC_A}{dx}$

$$\frac{dn_A}{dt} = \frac{\pi d^2}{4}N_A$$

General mol balance: $dn_B = dn_A = \rho_B dV = \frac{\rho_B \pi d^2}{4}dx_C$

Dissolution time: $$t = \frac{\rho_B X^2}{2DC_{AS}}\left(\frac{x_C}{X} - 1\right)^2$$

$$\tau = \frac{\rho_B X^2}{2DC_{AS}}$$

$$DC_{AS} = A\exp\left(-\frac{E_a}{RT}\right)$$

$$m_{wi} - m_{wf} \cong m_X - m_C = m_X\left(\frac{t}{\tau}\right)^{0.5}$$

$$t = \tau\left(\frac{m_C}{m_X} - 1\right)^2$$

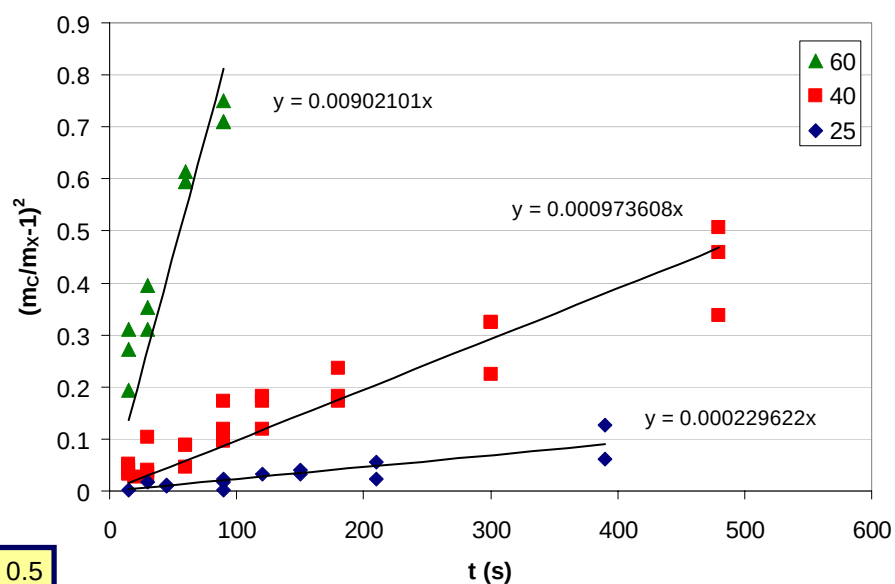

Model Comparison

T (^oC)	$1/\tau$ (s^{-1})	τ (s)	D C_{As} (mol cm^{-1} s^{-1})
25	2.30E-04	4.35E+03	2.63E-17
40	9.74E-04	1.03E+03	1.12E-16
60	9.02E-03	1.11E+02	1.03E-15

Model Parameters:

Ea = 86.9 kJ mol^{-1}

A = 4.12 x 10^{-2} mol cm^{-1} s^{-1}

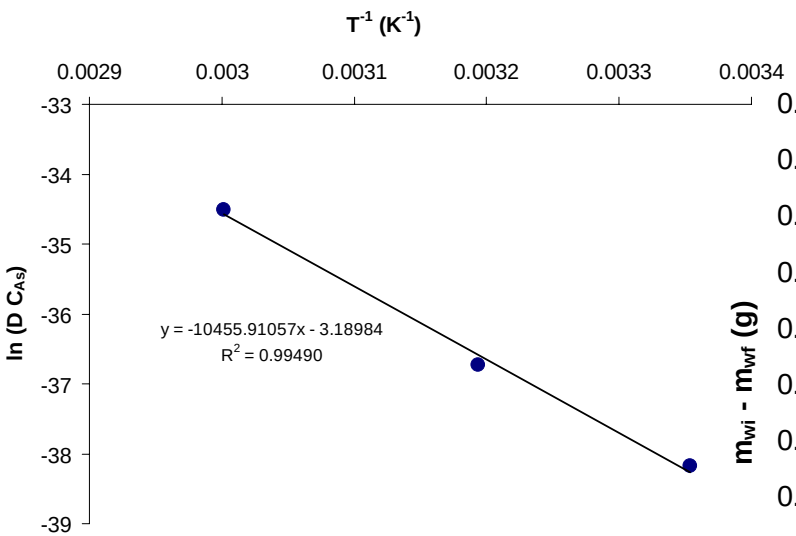

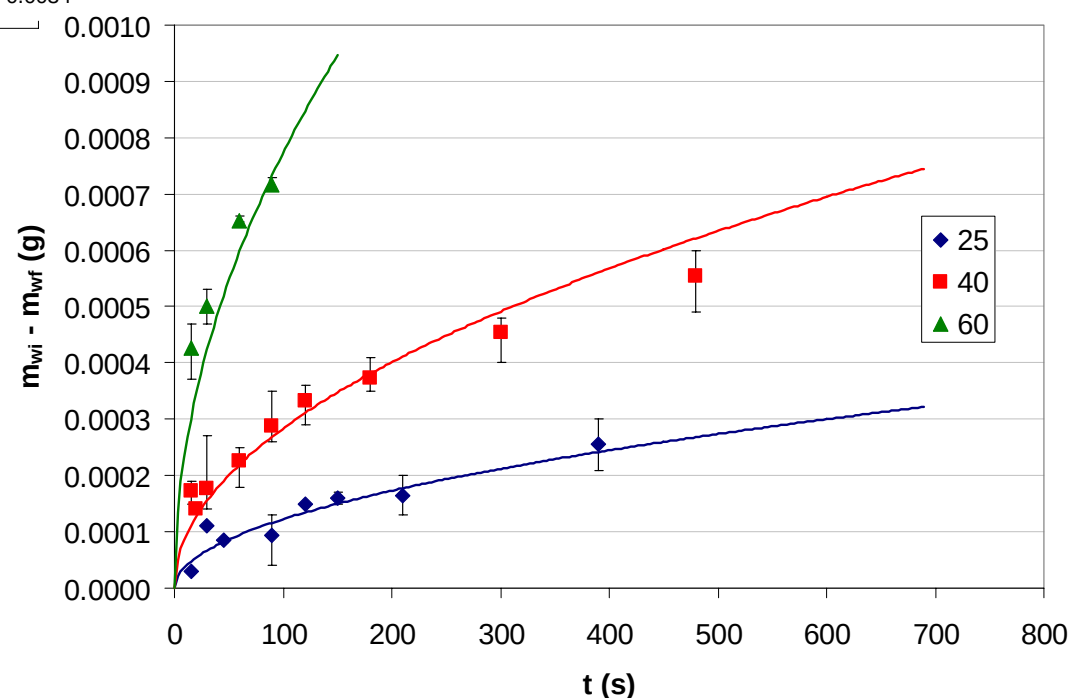

Conclusions

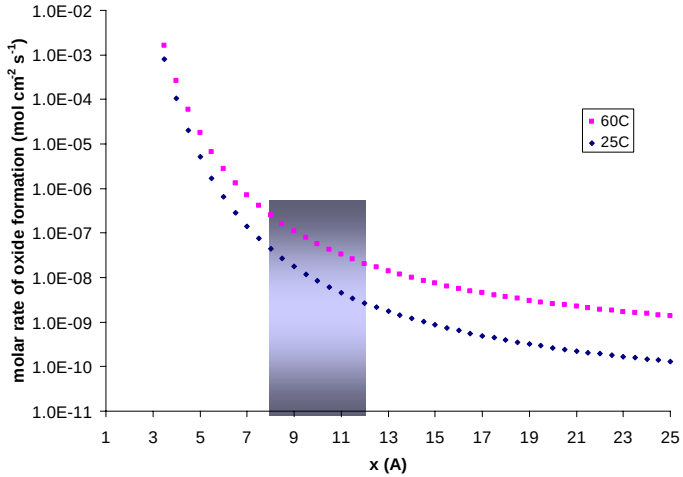

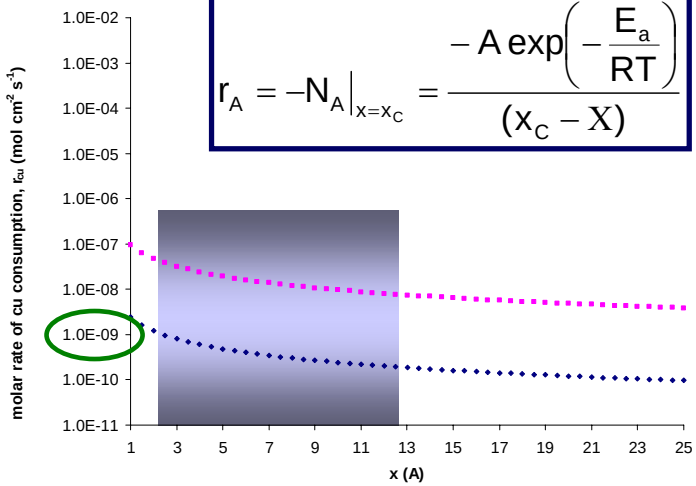

$$r_A = -N_A\big|_{x=x_C} = \frac{-A\exp\left(-\frac{E_a}{RT}\right)}{(x_C - X)}$$

- A 3 – step RR mechanism has been developed which separates chemical and mechanical contributions to removal
- Oxidation is faster than dissolution for thicknesses of interest
- With Steps 1 and 3 characterized, the only parameters that need to be extracted from RR data are those associated with Step 2 (mechanical removal)
- Oxidation model suggests that passivation layers formed during CMP are 2 to 6 A thick to facilitate removal rates on the order of 1000 – 9000 A min^{-1}
- The novel method outlined here for separately determining chemical contributions to the CMP process is crucial in slurry development and commercial slurry evaluation

Study of Inhibition Characteristics of Slurry Additives in Copper CMP Using Force Spectroscopy

(Subtask A-4-2)

H. Lee, Y. Zhuang and A. Philipossian (University of Arizona, Tucson, AZ, USA)

S. V. Babu, U. Patri and Y. Hong (Clarkson University, Potsdam, NY, USA)

L. Borucki (Intelligent Planar, Mesa, AZ, USA)

L. Economikos (IBM Corporation, Hopewell Junction, NY, USA)

M. Goldstein (Intel Corporation, Santa Clara, CA, USA)

NSF/SRC Engineering Research Center for Environmentally Benign Semiconductor Manufacturing

Motivation and Goal

- **Selection of an appropriate corrosion inhibitor is difficult as commonly used corrosion protective organics often produce unavoidable debris, wafer-level scratches, and defects during polishing.***

- **Formation of BTA-copper complex film results in significantly high interfacial friction causing delamination problems in CMP. Surfactants, on the other hand, due to their inherent characteristics are known for tribological benefits.**

- **Determine whether spectral analysis based on raw shear force data obtained during polishing can be used to elucidate the adsorption, lubrication and inhibition characteristics of additives in slurries in CMP.**

* Y. Hong, D. Roy & S. Babu. Electrochemical and Solid-State Letters, 8 (11) G297-G300 (2005).

Experimental Conditions

- **Experimental Apparatus**
  - Fujikoshi Machinery Corporation turntable, University of Arizona conditioner and friction table, and robotics, and Ebara Technologies head
- **Slurry**
  - Reference slurry (3 weight percent fumed silica + 1 weight percent glycine + 5 weight percent H_2O_2 at pH = 4)
  - Ref. + 3 mM BTA at pH = 4
  - Ref. + 3 mM ADS at pH = 4
  - 200 ml/min
- **Pad**
  - Rohm and Haas IC1000 K-groove pad
- **Wafer**
  - 200-mm blanket wafer with electroplated copper film (15,000 A) on Ta on SiO_2 on Si
- **Polishing**
  - Polishing pressure 2 PSI
  - Sliding velocity 0.31 & 0.93 m/s
  - Polishing time 1 minute
- **Pad Conditioning**
  - In-situ conditioning
  - 100 grit TBW perforated diamond disc rotating at 30 RPM and sweeping at 20 times/min
  - Conditioning force 5 lbf

Experimental Results

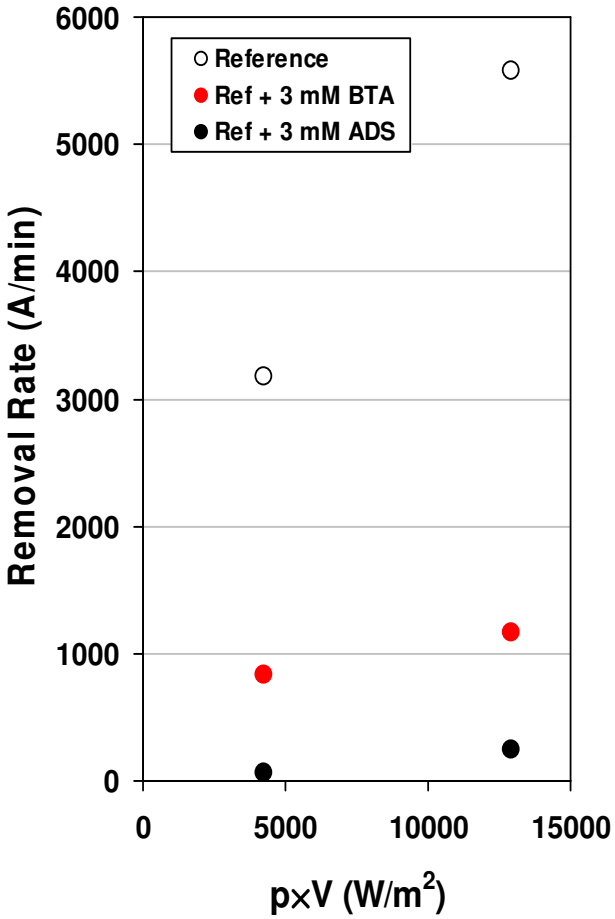

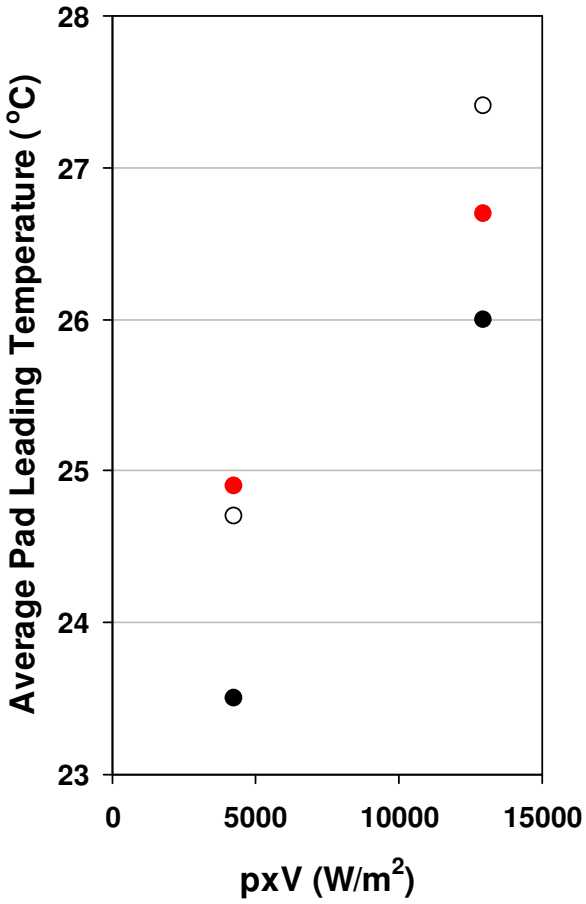

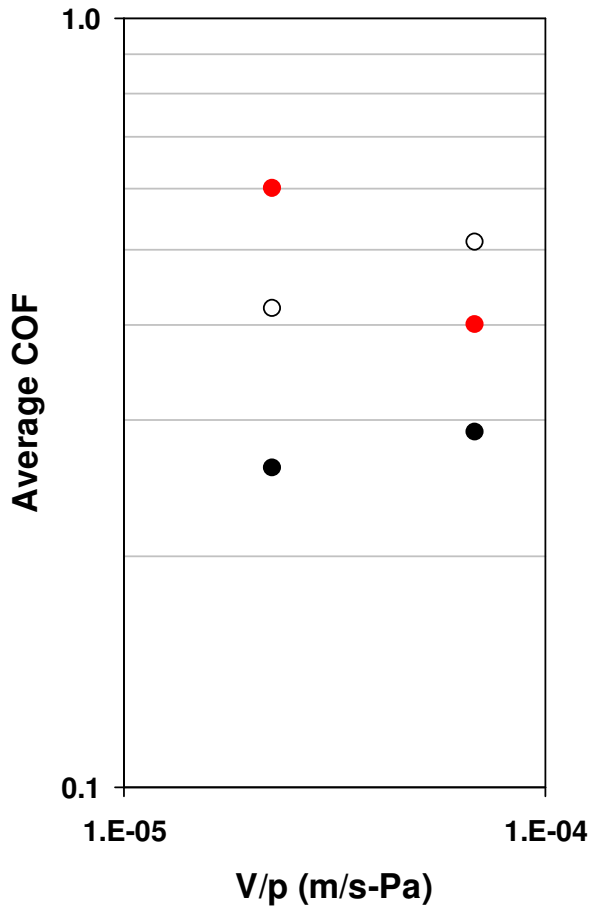

Adsorption Characteristics

Complete Coverage and Closed Packed Structure

ADS

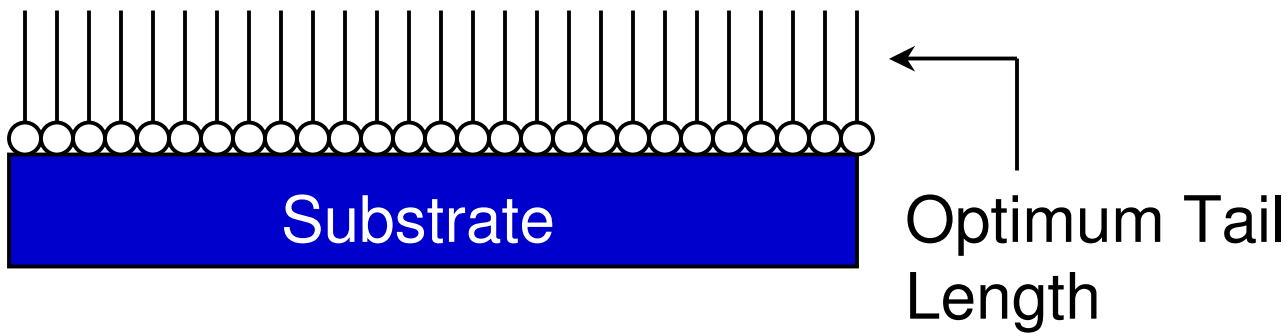

Non-Linear Structure

BTA

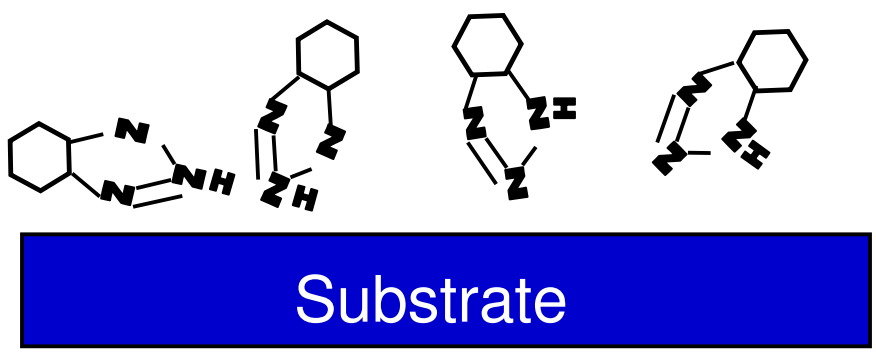

Interaction Zone

Linear molecules like ADS

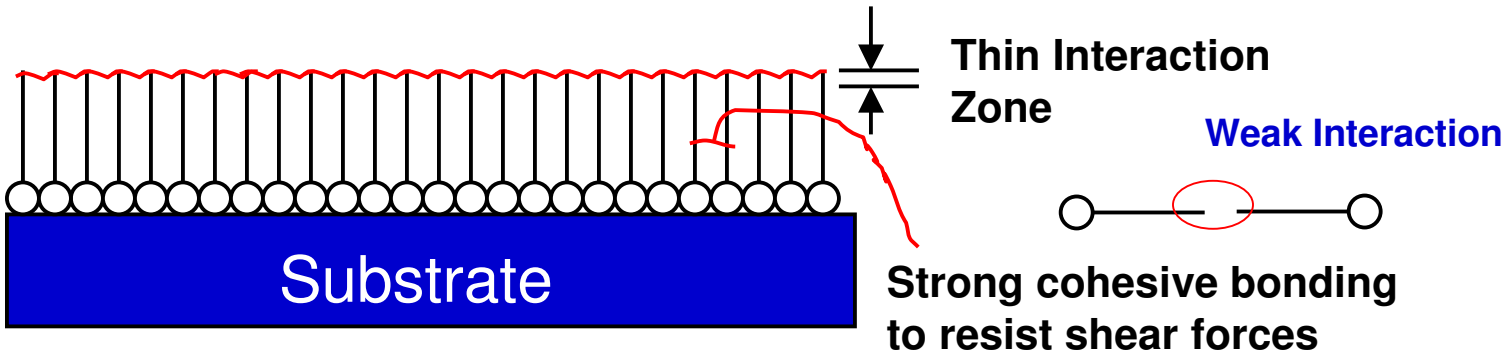

Non-linear molecules like BTA

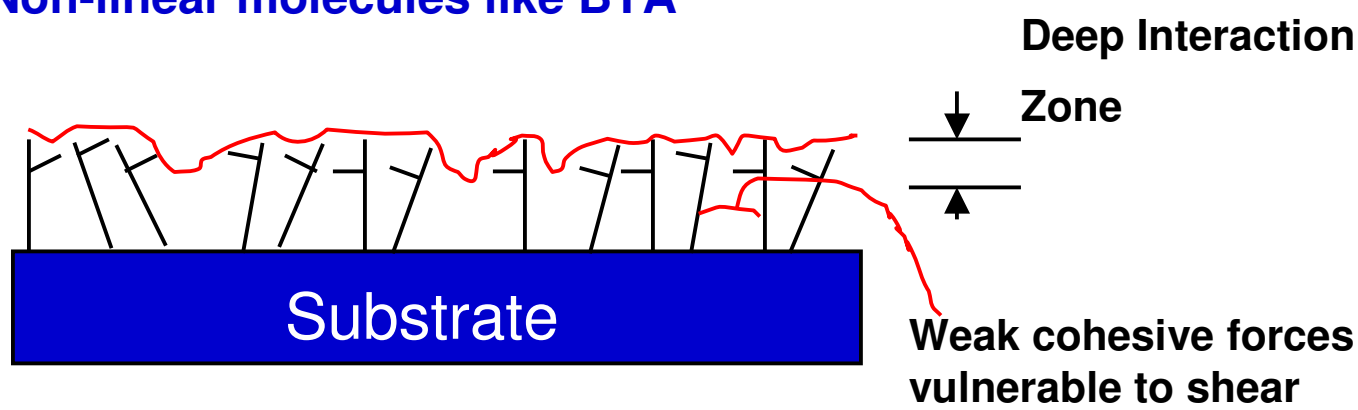

Dynamics of ADS Adsorption in CMP

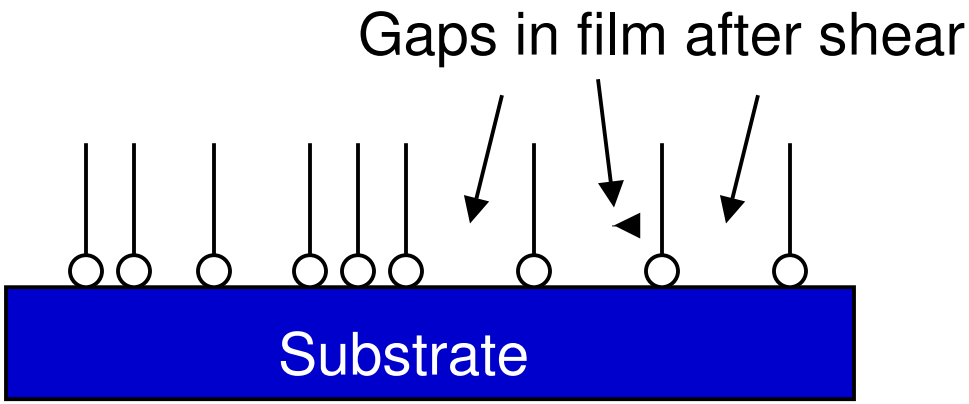

Rate Limiting Process

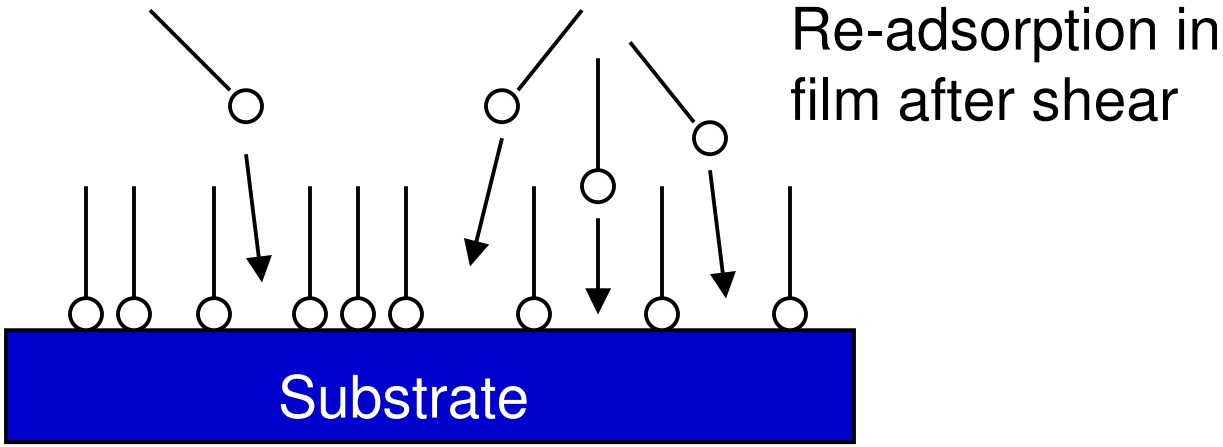

Viscous Component of COF

- **Increasing sliding velocity increases COF for 'Reference' & ADS containing slurry.**

- **Increasing sliding velocity decreases COF for BTA containing slurry.**

$$\mu_{visc} \approx 0.9(\mu_o V(1-\nu^2)/E)^{0.36} R^{-0.19} \lambda^{-0.17}$$

$$\mu_{visc} \propto \mu_o V / E^{0.36}$$

L. Borucki, A. Philipossian and Y. Zhuang, "Physics and Modeling of Fundamental CMP Phenomena", 22nd International VLSI Multilevel Interconnection Conference Proceedings, 175-180 (2005).

Raw Shear Force Data

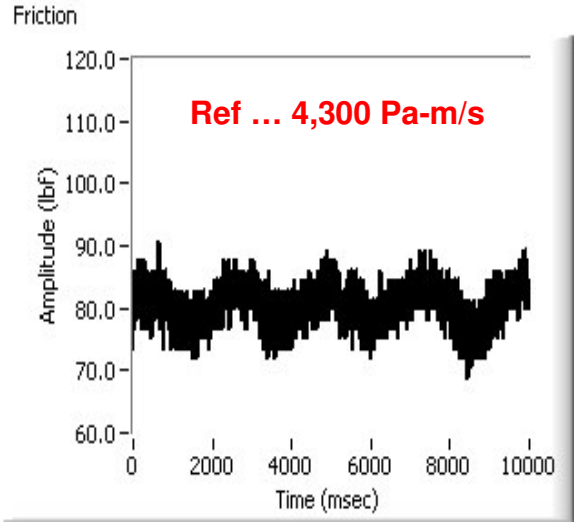

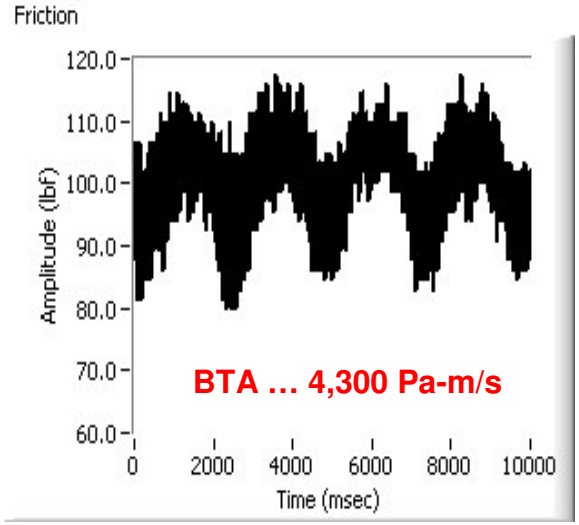

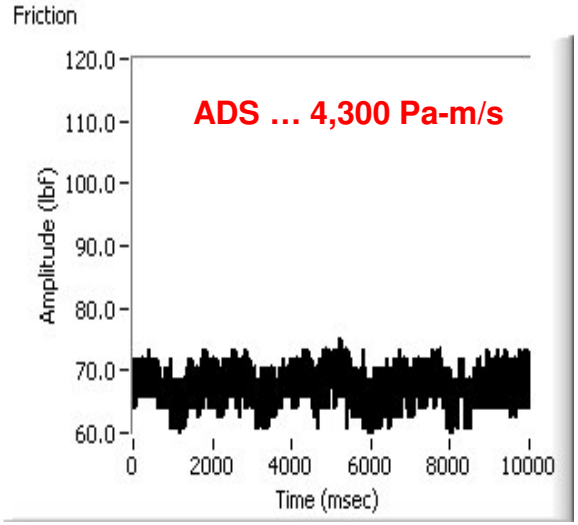

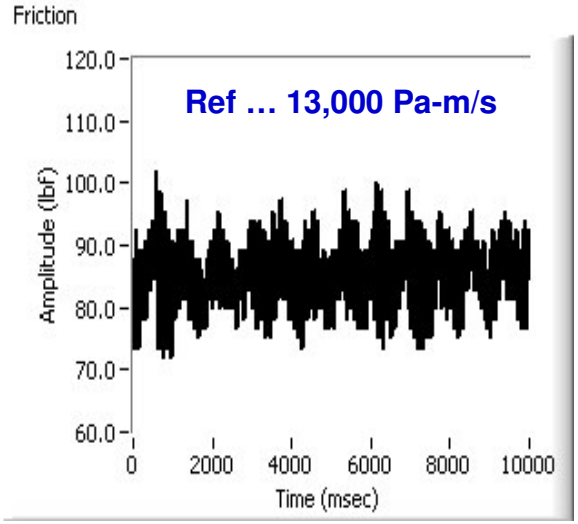

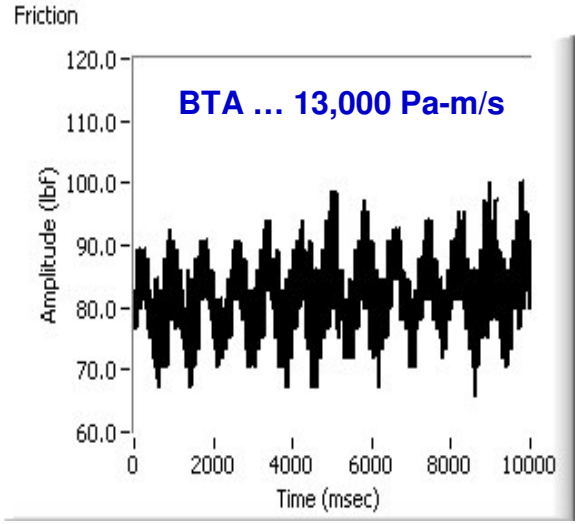

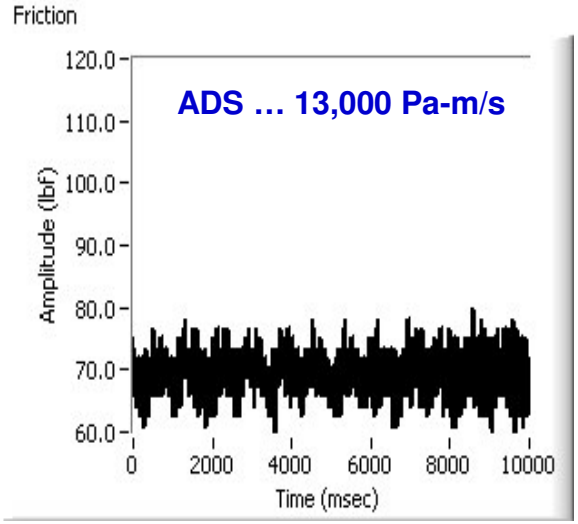

Variance of Shear Force

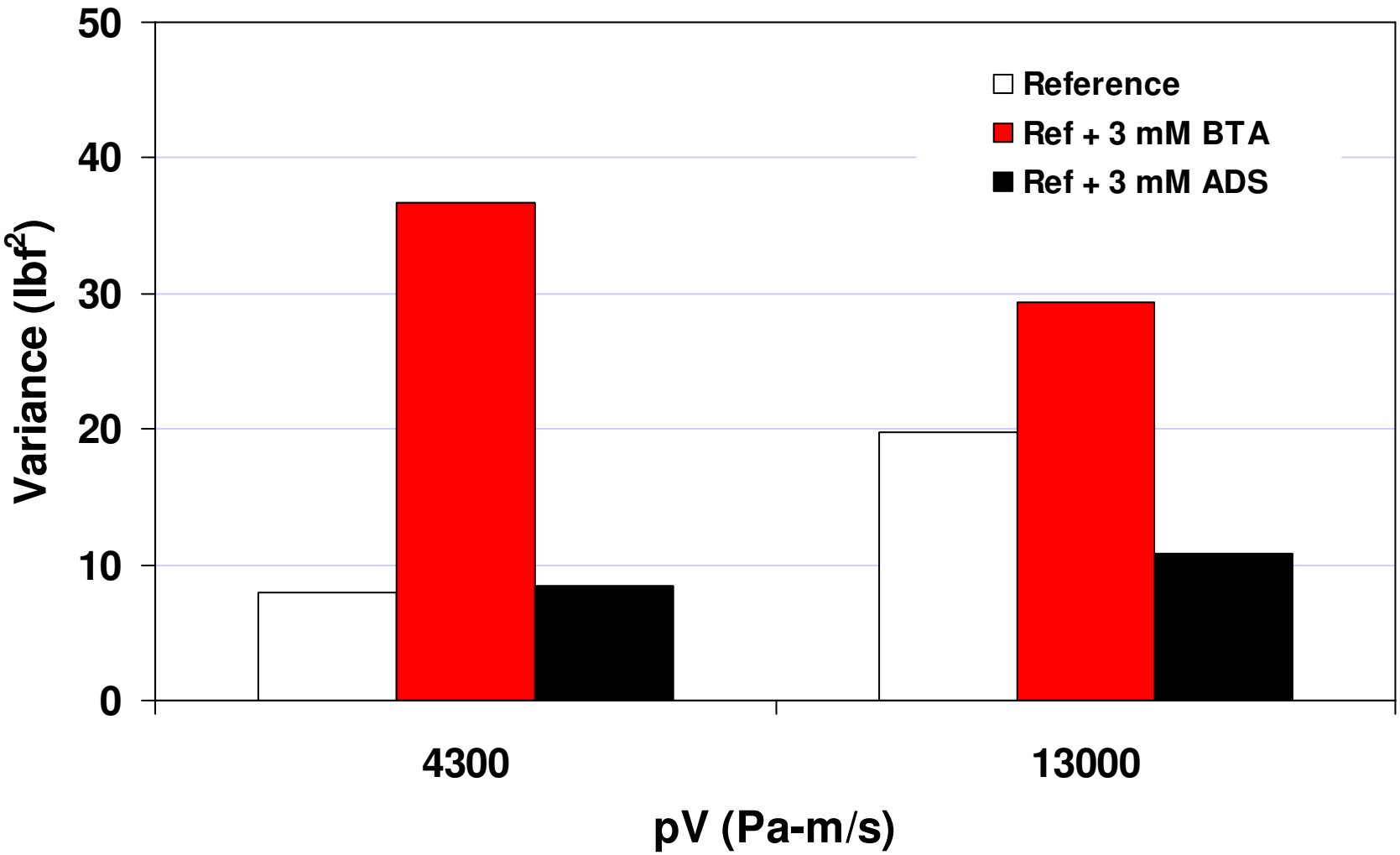

Shear Force Spectral Analysis

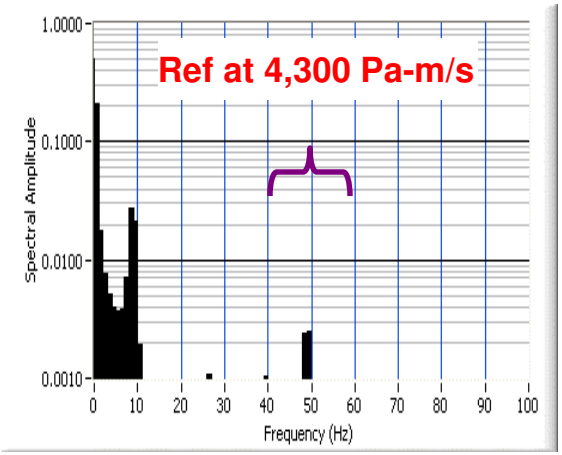

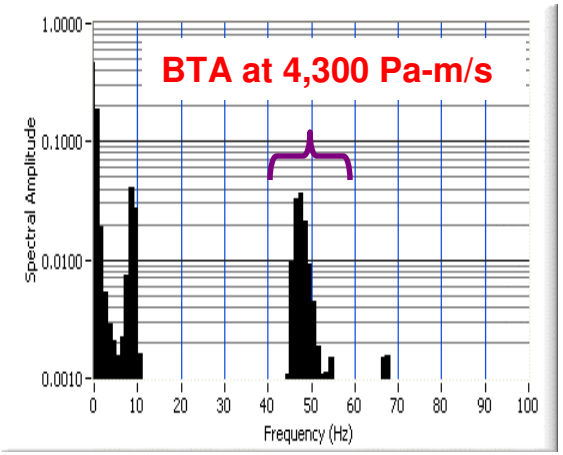

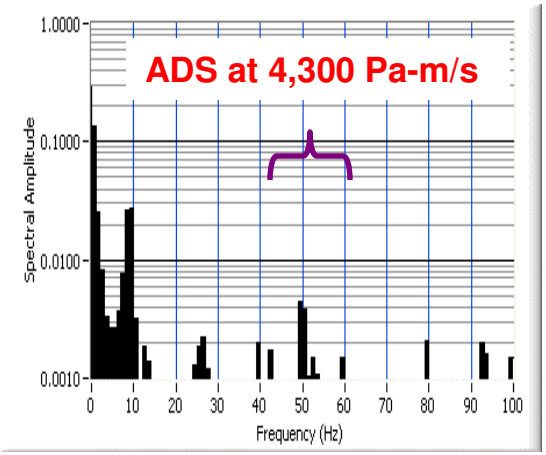

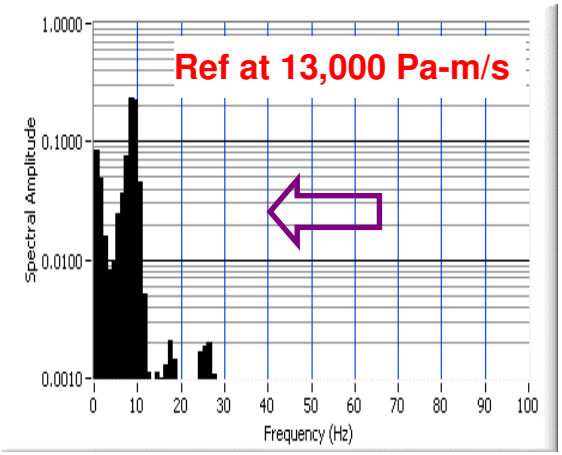

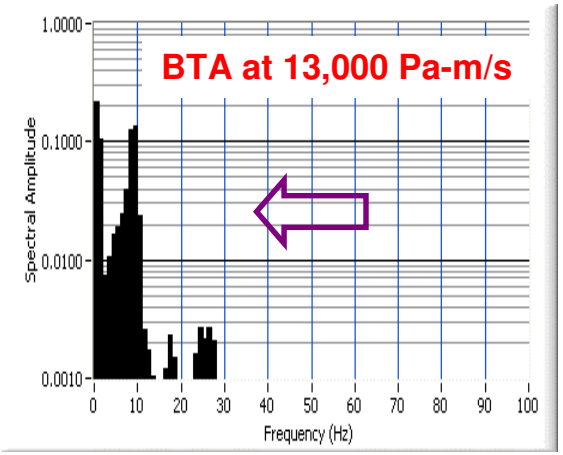

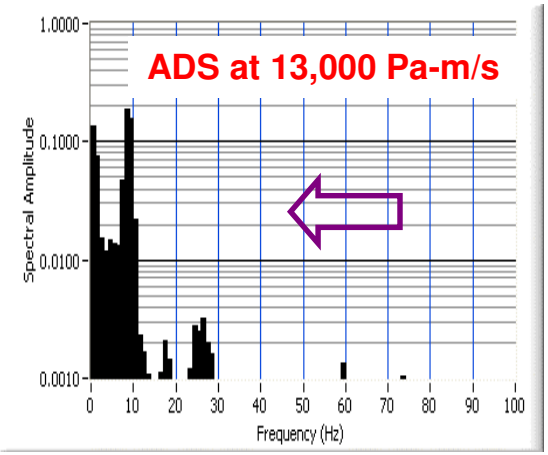

Conclusions

- The inhibition characteristics of ADS are superior to that of BTA
- COF and temperature are lowest with ADS-containing slurry
- Stick-slip phenomena are lowest with ADS-containing slurry
- Dynamics of adsorption in CMP and formation of nano-lubrication layer explain the increase in COF with increasing sliding velocity
- Spectral analysis illustrates the emergence of high intensity peak in BTA containing slurry at lower velocity - an effect exhibited due to high variance of the shear force

Experimental and Theoretical Investigation of Slurry Chemical and Mechanical Characteristics in Copper CMP

(Subtask A-4-2)

Y. Zhuang, R. Zhuang and A. Philipossian
University of Arizona, Tucson, AZ USA

M. Lacy and C. Spiro
Cabot Microelectronics Corporation, Aurora, IL USA

L. Borucki
Intelligent Planar, Mesa, AZ USA

NSF/SRC Engineering Research Center for Environmentally Benign Semiconductor Manufacturing

Objectives

- **Investigate the tribological, thermal and kinetic attributes of two novel Cabot Microelectronics Corporation copper CMP slurries under different slurry flow rates**

- **Simulate wafer surface reaction temperature, chemical and mechanical rate constants, and chemical and mechanical dominance for two novel Cabot Microelectronics Corporation copper CMP slurries under different slurry flow rates**

Experimental Conditions

- **Polisher**
  - Fujikoshi Machinery Corporation turntable
  - University of Arizona conditioner and friction table, and robotics
  - Ebara Technologies head
- **Slurry**
  - iCue 600Y75
  - iCue EP-C7092
  - 120 & 200 ml/min
- **Pad**
  - Rohm and Haas IC1000 K-groove pad
- **Wafer**
  - 200-mm blanket wafer with electroplated copper film
- **Polishing**
  - Polishing pressure = 1, 2 & 3 PSI
  - Sliding velocity = 0.3, 0.75 & 1.2 m/s
  - Polishing time = 1 minute
- **Pad Conditioning**
  - In-situ pad conditioning
  - Mitsubishi Materials Corporation 100-grit Mosaic diamond disc rotating at 30 RPM and sweeping at 20 times/min
  - Conditioning force 6.28 lbf

Coefficient of Friction

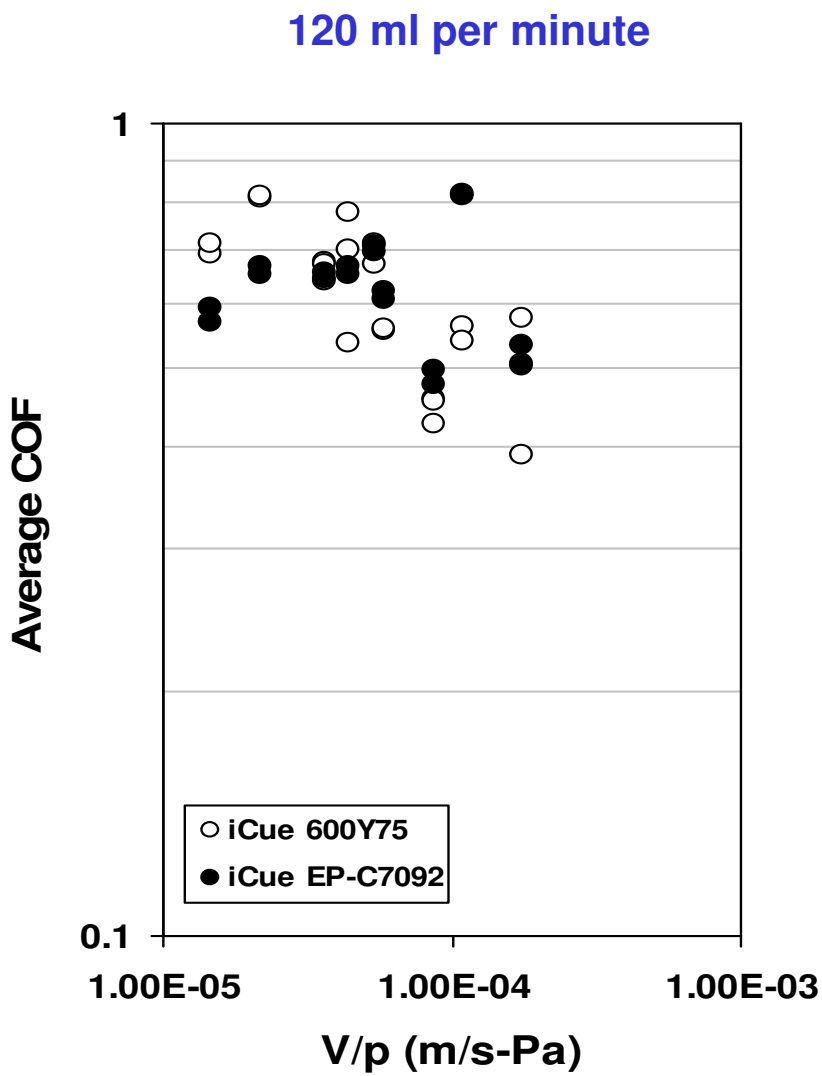

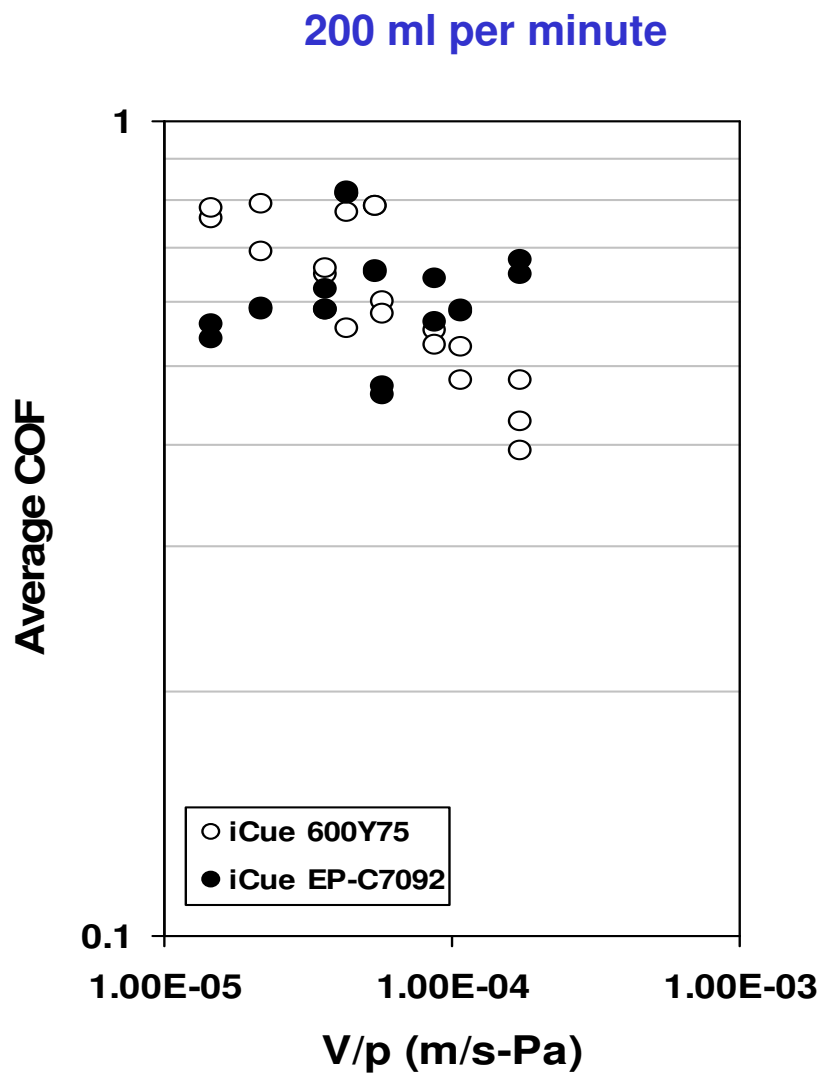

Experimental Removal Rate

120 ml per minute

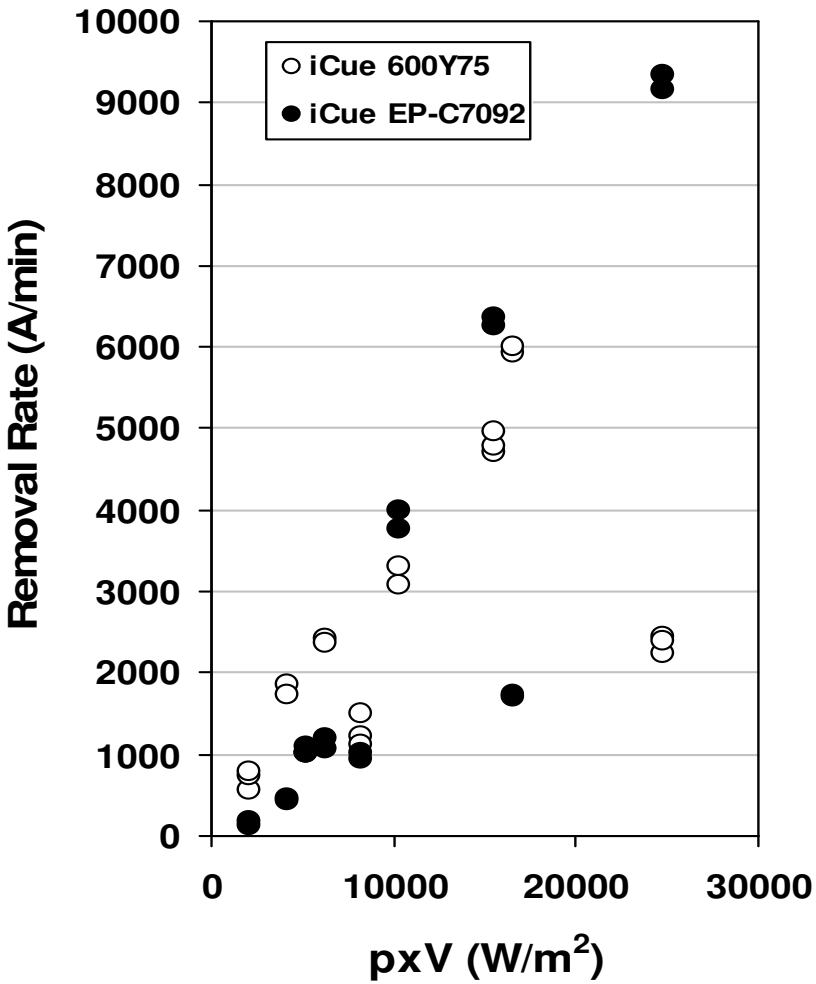

200 ml per minute

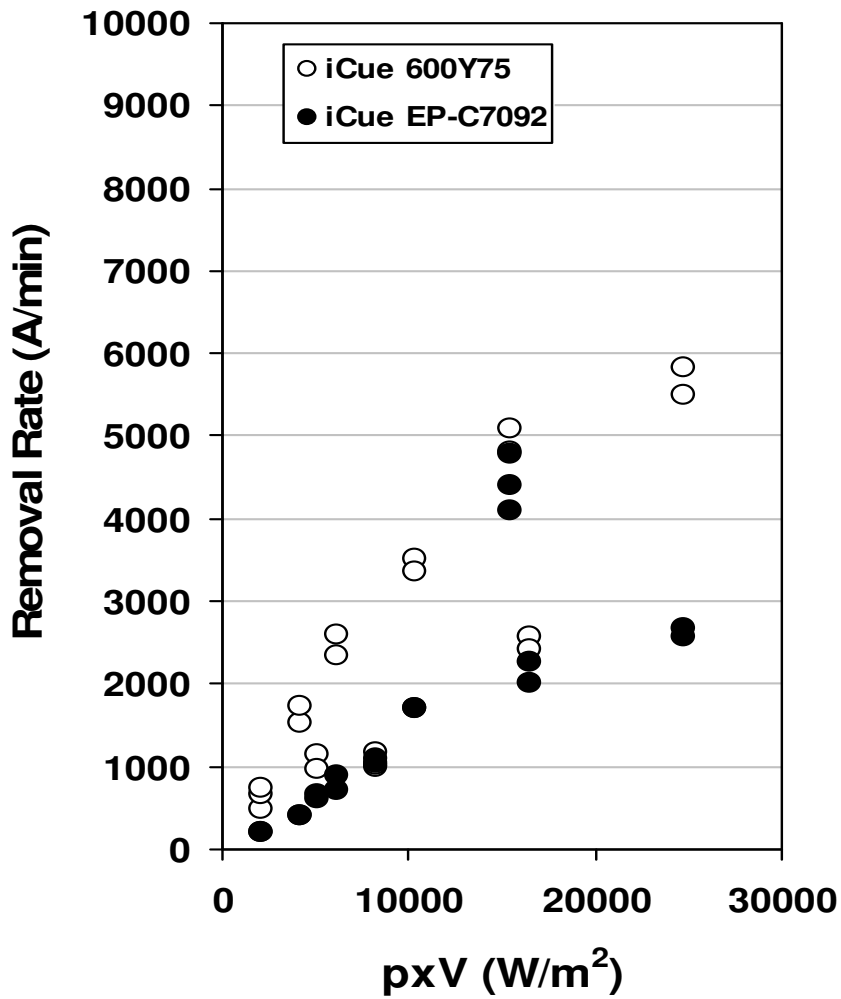

Chemical-Mechanical Rate Model

See J. Tribology 127(3), pp. 639-651 for details

Two step model (oxidation and mechanical removal):

$$RR = \frac{M_w}{\rho} \frac{k_2 k_1}{k_2 + k_1}$$

$$k_1 = A e^{-E/kT}$$ Chemical Rate

$$k_2 = c_p \mu_k p V$$ Mechanical Rate

Mean reaction temperature model:

$$\overline{T} \approx \overline{T}_p + \frac{\beta}{V^{1/2+e}} \mu_k p V$$

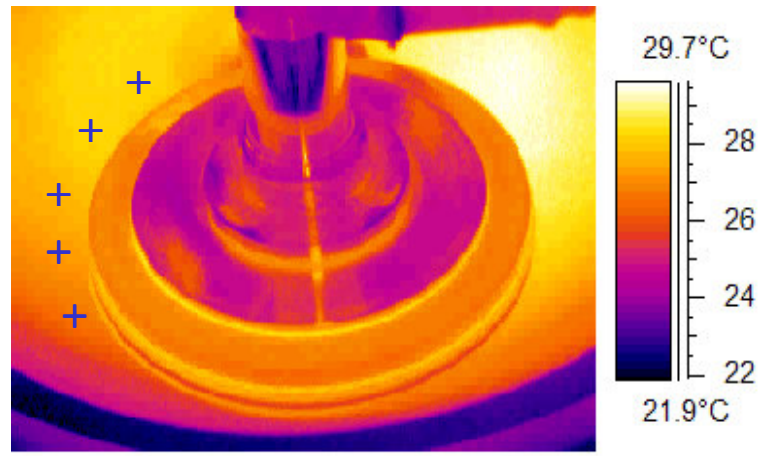

Leading edge temperature T_p

A, c_p, β and e are fitting parameters. A should be chemistry-specific, β and e are predicted by theory to depend on the pad thermal and mechanical properties and on conditioning.

Simulated Removal Rate

iCue 600Y75

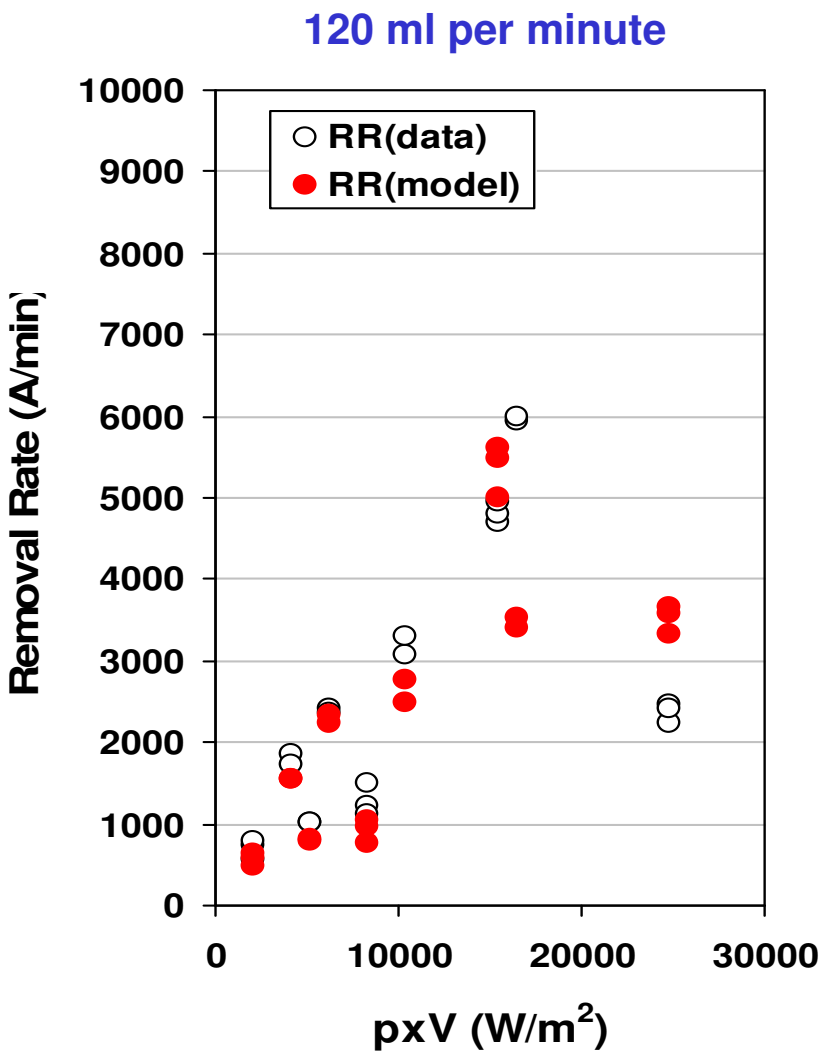

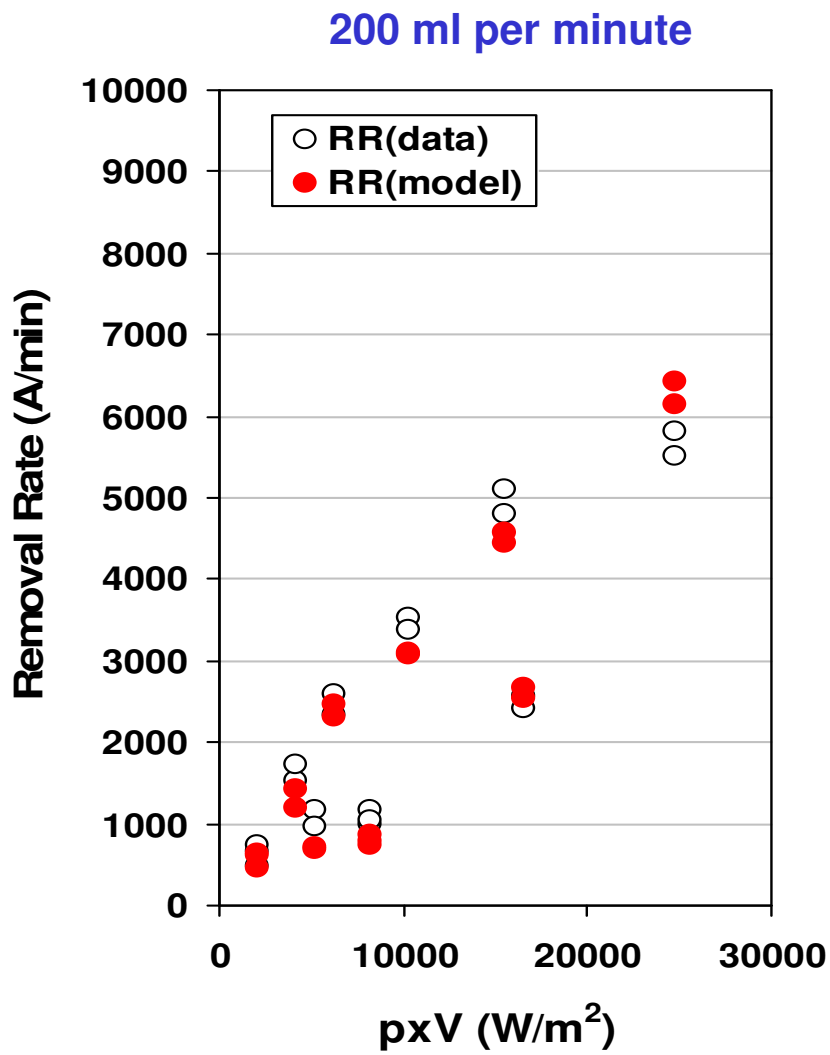

Simulated Removal Rate

iCue EP-C7092

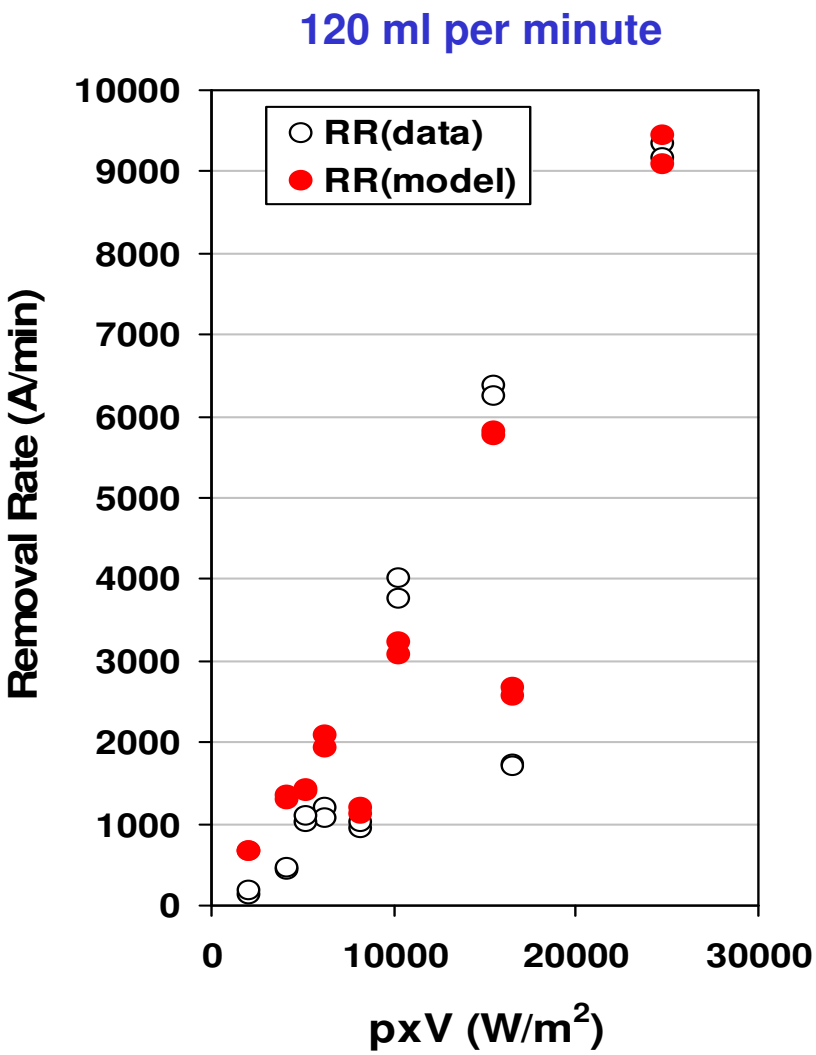

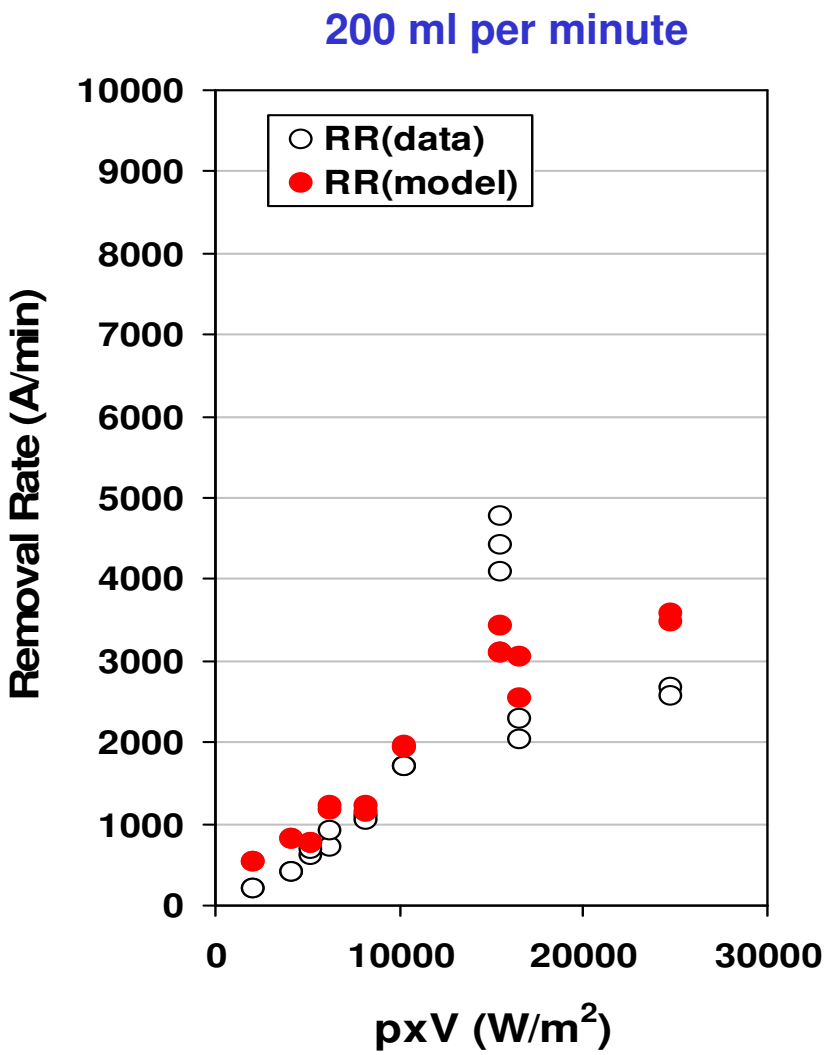

Simulated Chemical Rate Constant K_1

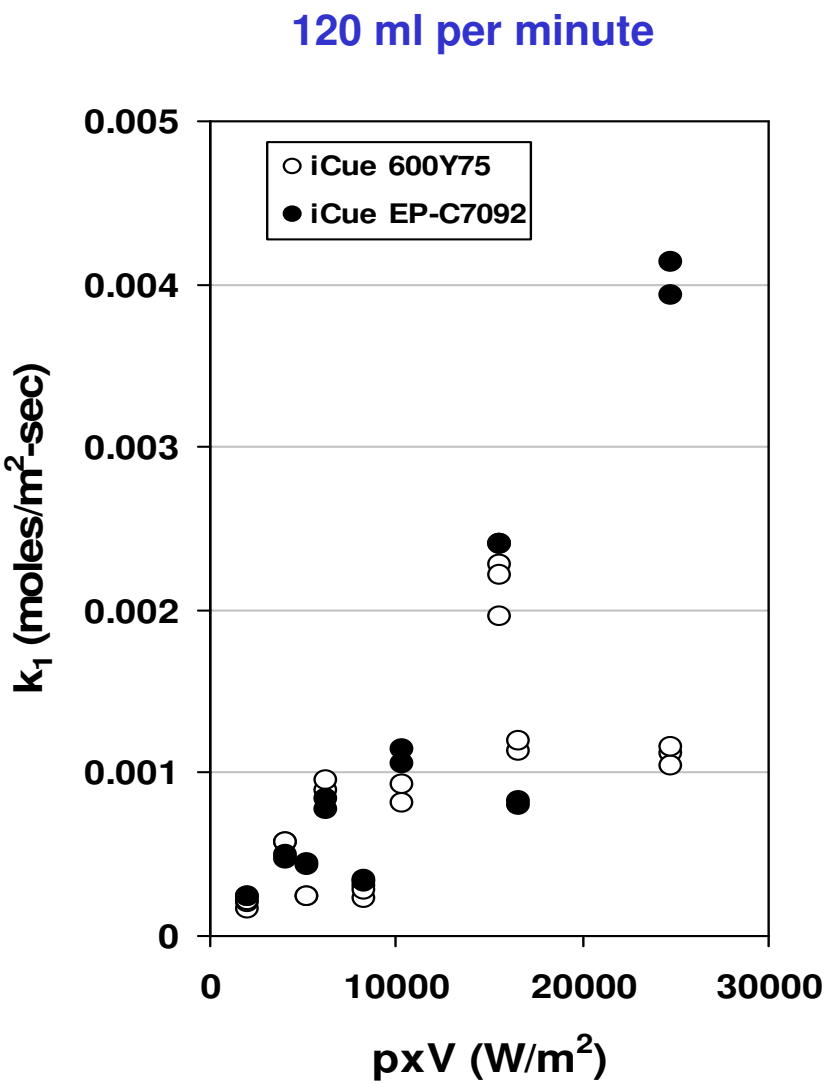

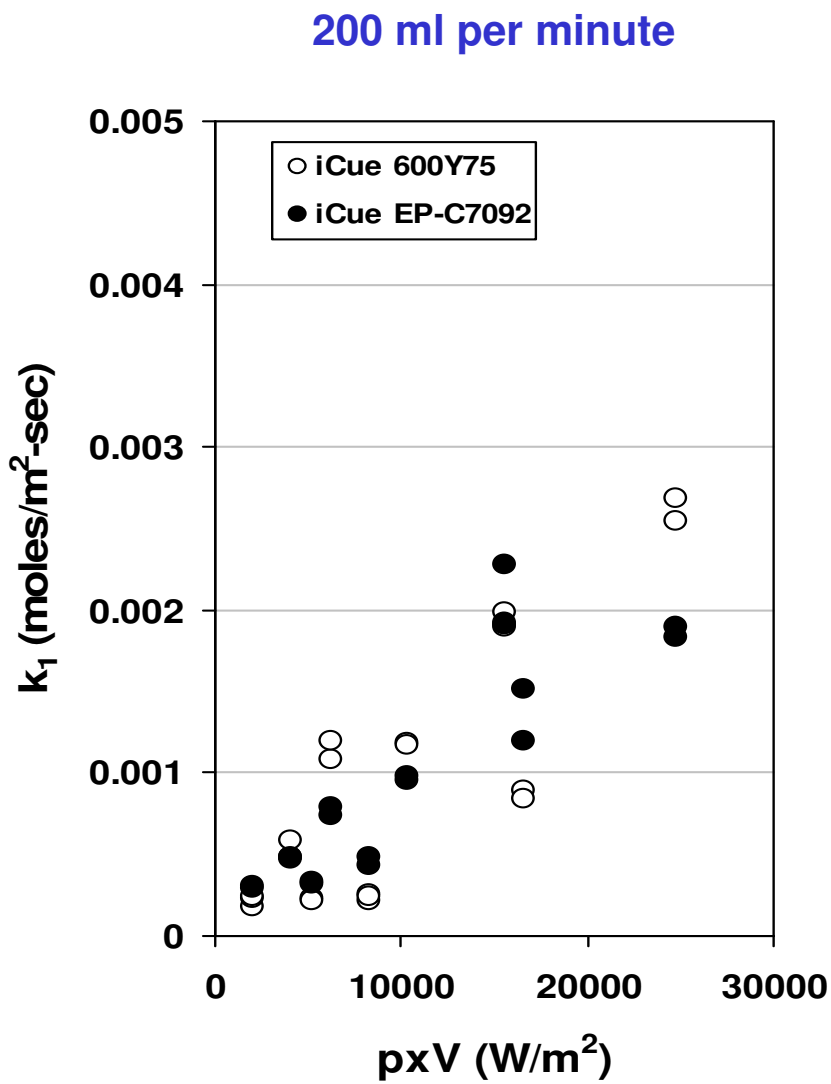

Simulated Mechanical Rate Constant K_2

120 ml per minute

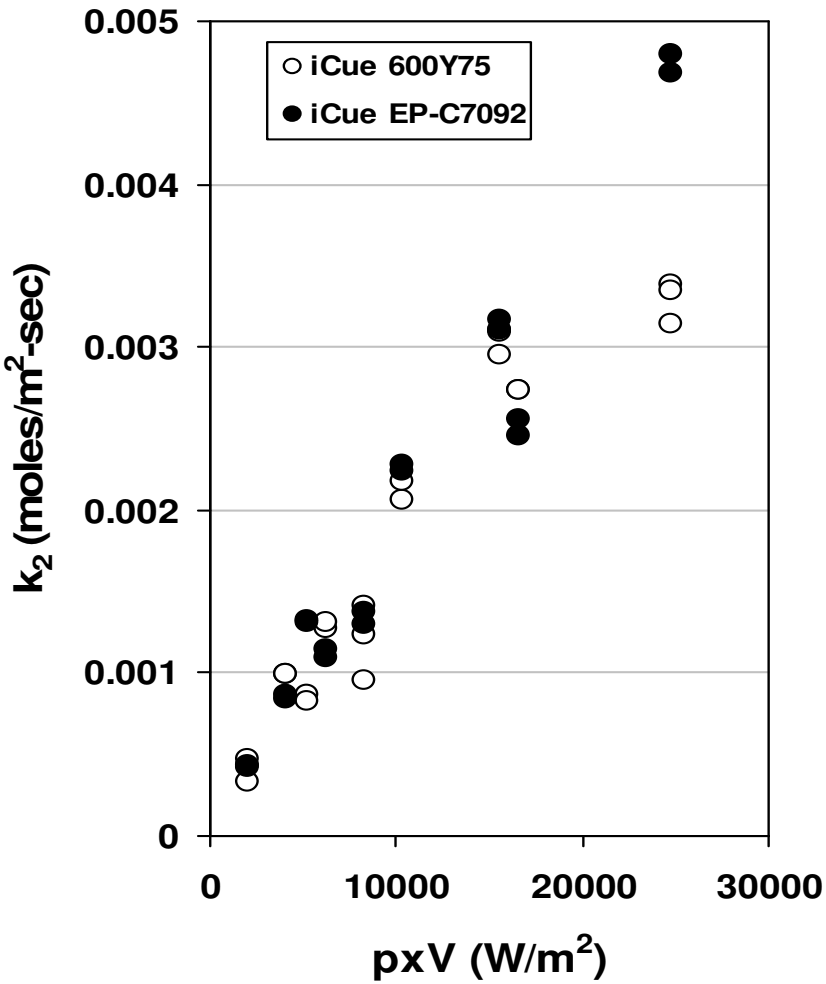

200 ml per minute

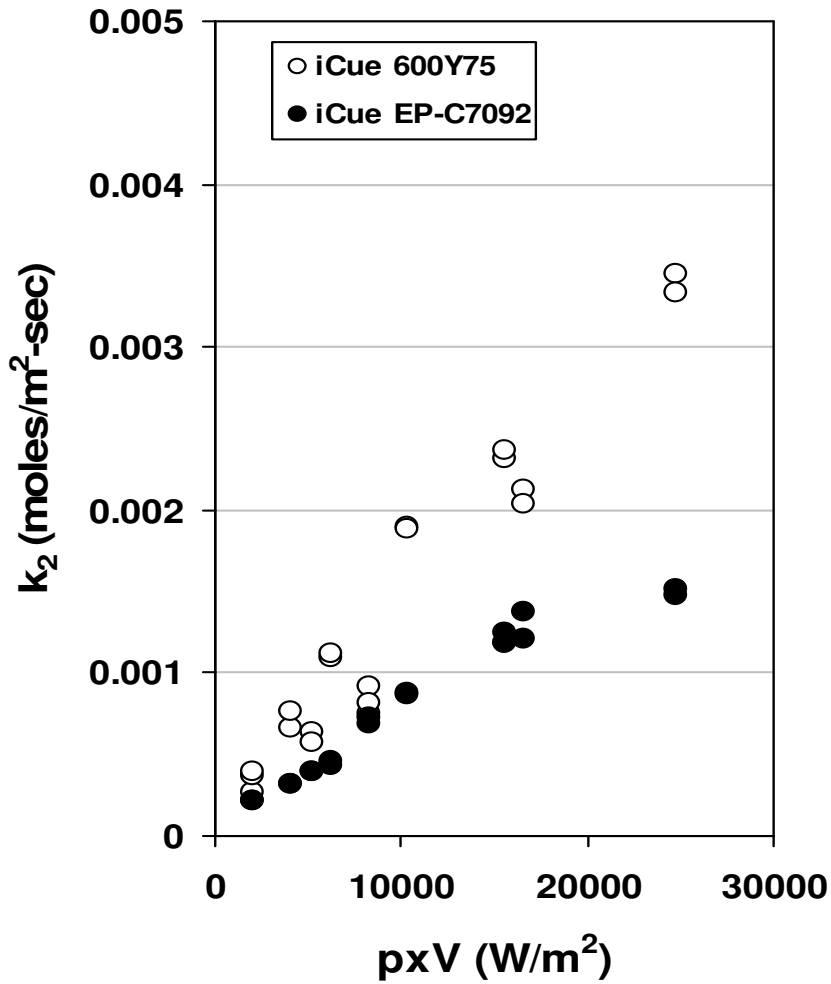

Simulated K_1/K_2

120 ml per minute

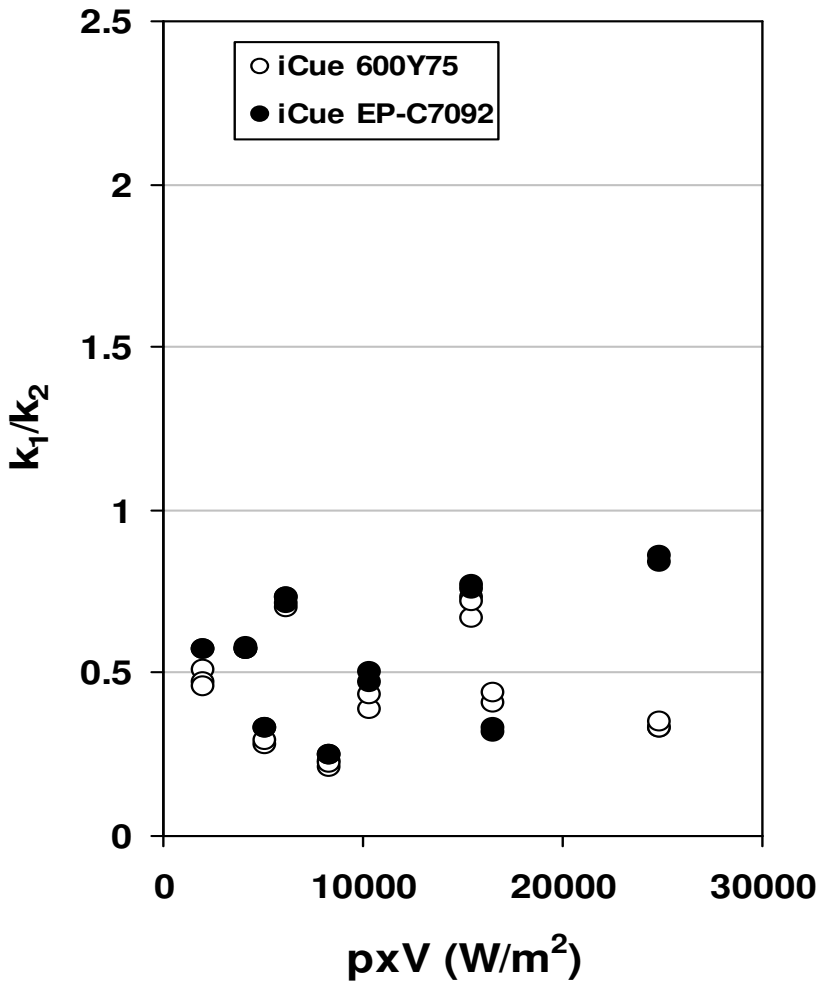

200 ml per minute

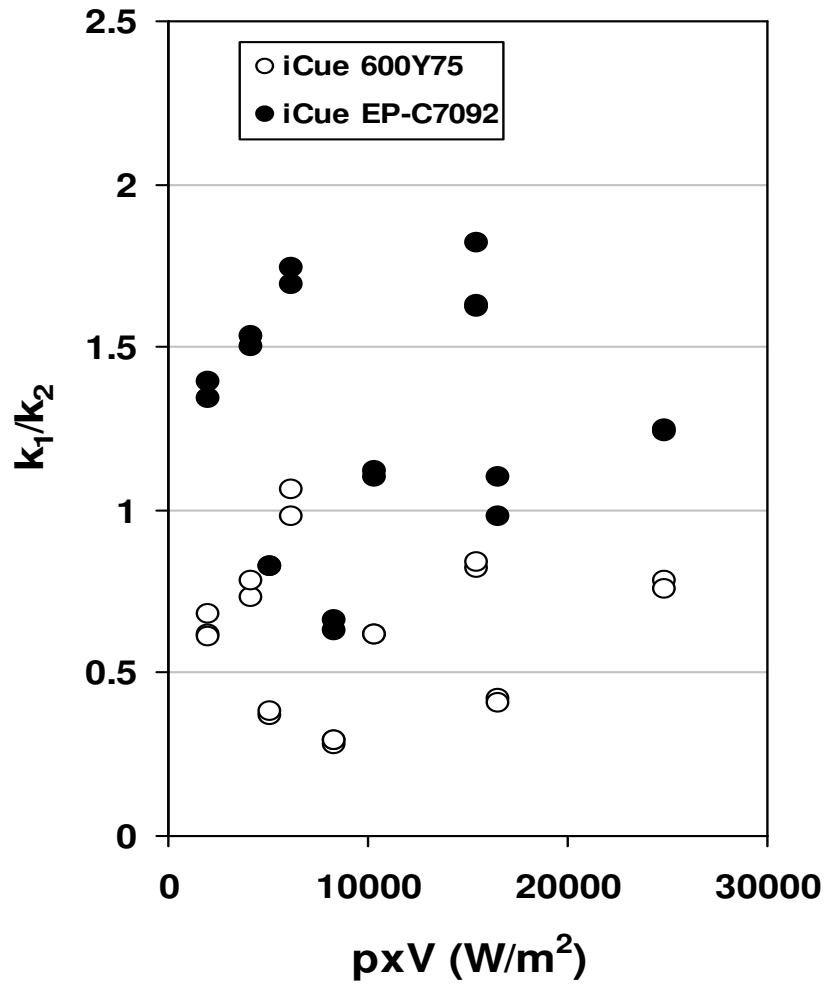

Conclusions

- The tribological study shows a transition for the iCue 600Y75 slurry, suggesting a pressure or lubrication layer dependence of the slurry viscosity. The dominant tribological mechanism for the iCue EP-C7092 slurry is boundary lubrication.

- Both the iCue 600Y75 and iCue EP-C7092 slurries exhibit highly non-Prestonian removal rate behavior, which is successfully captured by the two step chemical-mechanical rate model.

- Simulated chemical rate constants for the iCue 600Y75 and iCue EP-C7092 slurries are similar, suggesting that these two slurries have similar oxidation chemistry during polishing.

- Simulated mechanical rate constants for the iCue 600Y75 slurry are higher than those of the iCue EP-C7092 slurry at 200 ml/min, suggesting the iCue 600Y75 slurry is more mechanically active under this slurry flow rate.

- For both the iCue 600Y75 and iCue EP-C7092 slurries, chemical and mechanical actions are relatively balanced in the studied polishing region. Simulated k_1/k_2 for the iCue 600Y75 slurry are lower than those of the iCue EP-C7092 slurry at 200 ml/min due to its larger mechanical rate constants.

Fundamental Pad Characterization and Modeling: Design and Evaluation of Novel Pad Grooves for Copper CMP Optimization

Subtask A-5-1

D. Rosales-Yeomans, D. DeNardis and A. Philipossian
(University of Arizona, Tucson, AZ, USA)

L. Borucki
(Intelligent Planar, Mesa, AZ, USA)

Driving Force

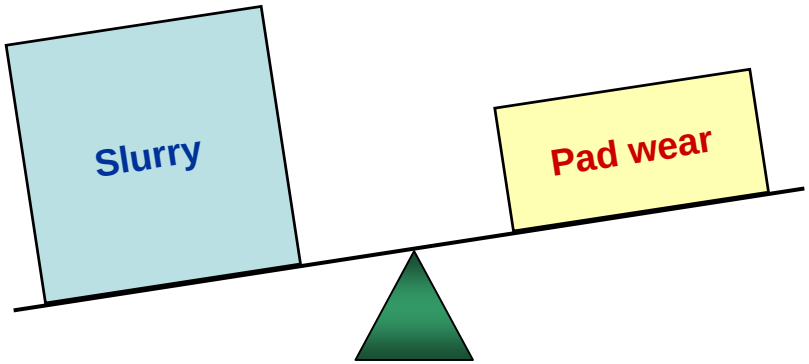

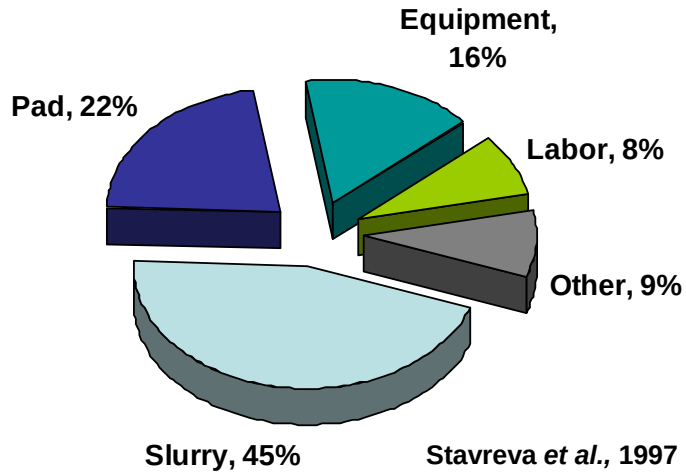

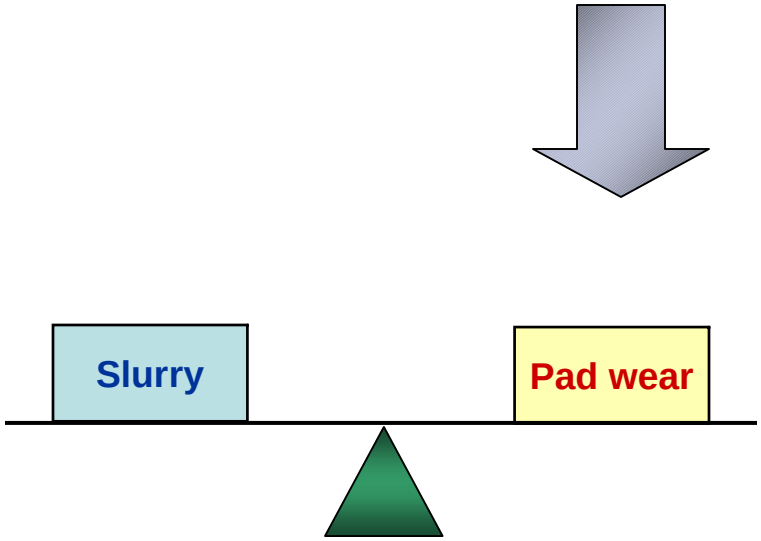

CMP optimization through "smart" pad design could yield higher removal rates, reduction of slurry consumption and/or increase in pad life

Grooved Pads in CMP

IC-1000 K Groove

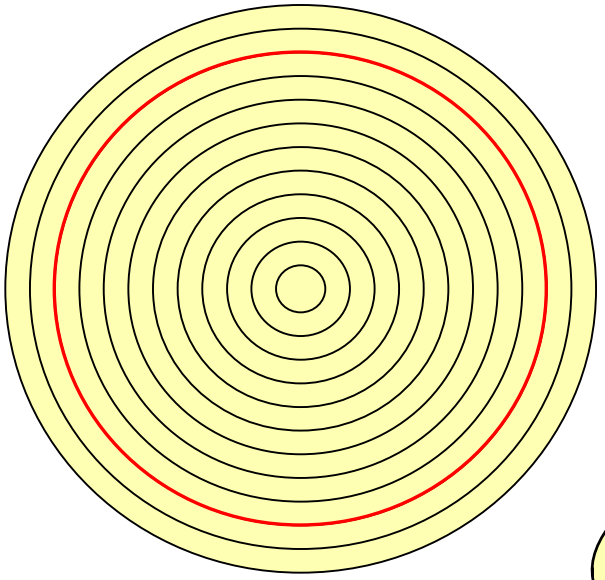

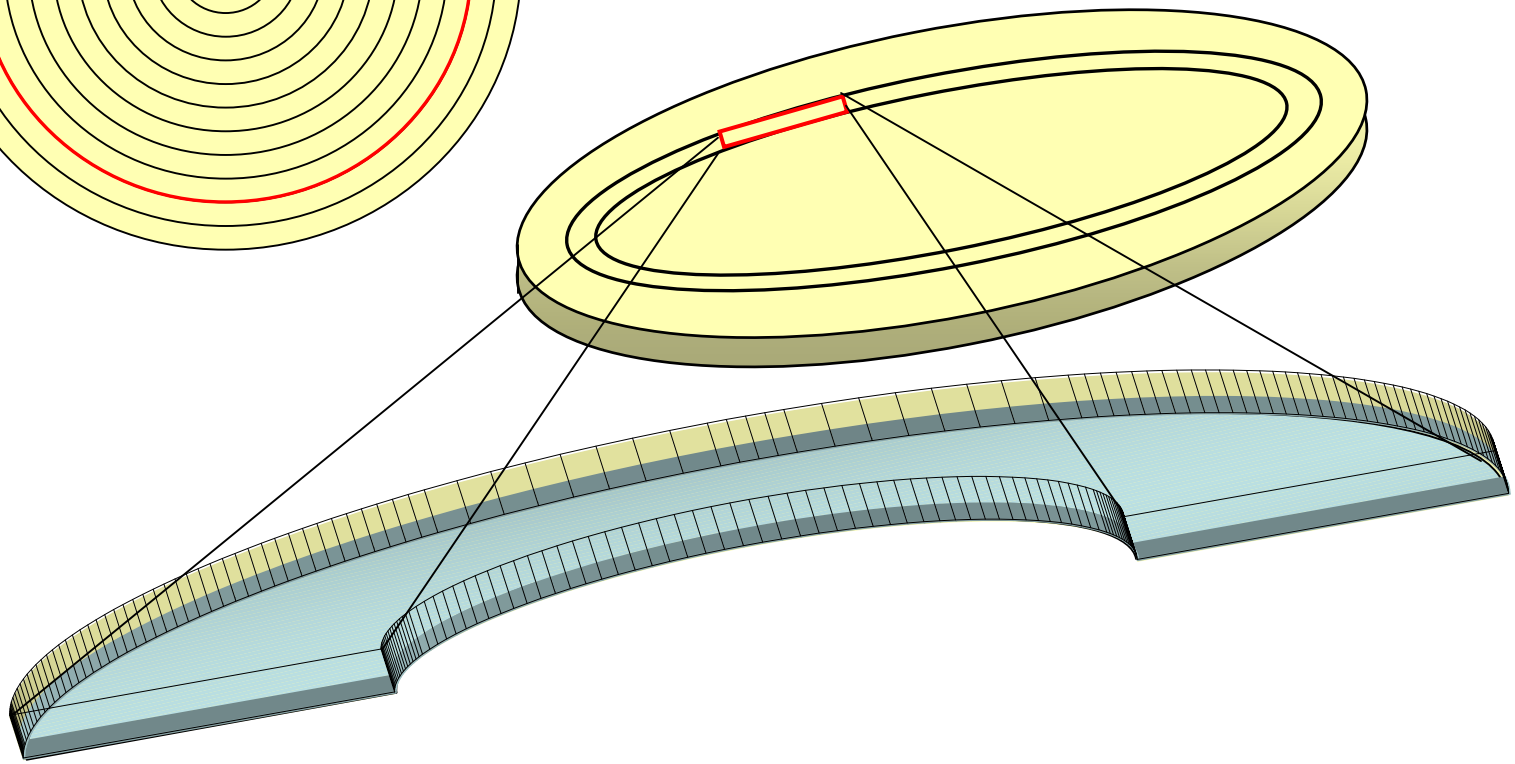

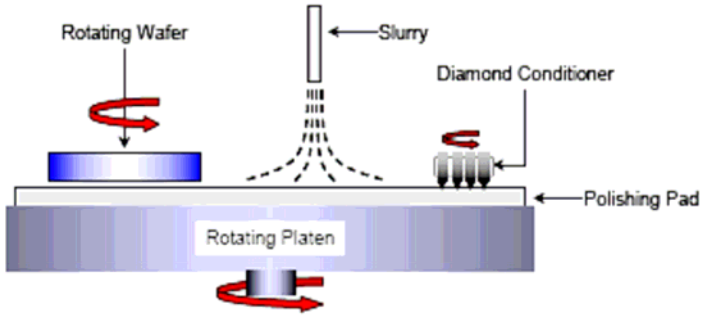

Novel Pads Logarithmic-Spiral Grooves

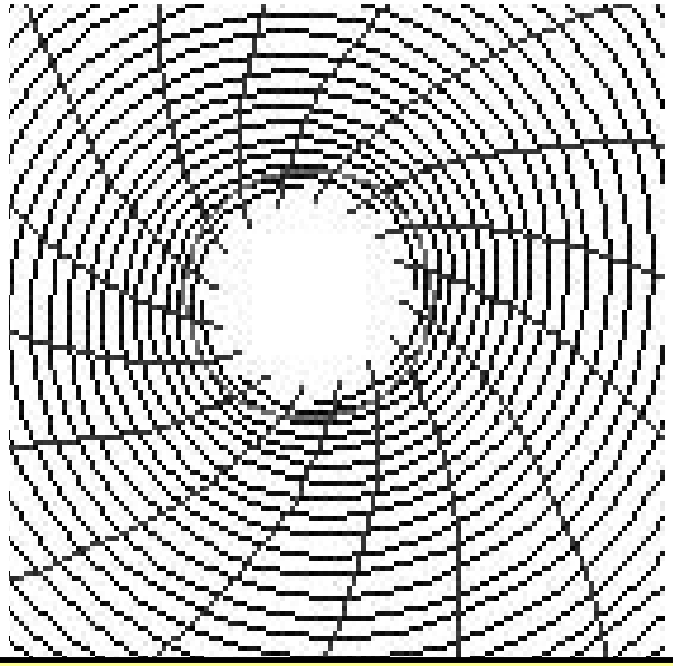

Floral groove design

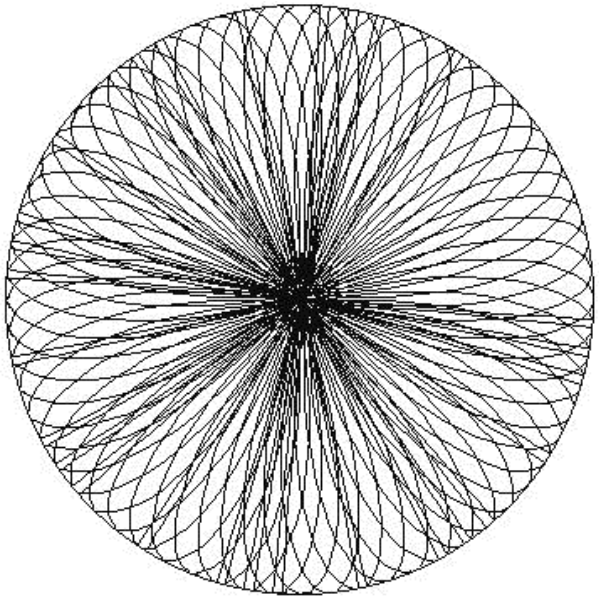

Basic Idea …

Positive Log. and Spiral Grooves

Transport fresh slurry into the pad – wafer interface

Negative Log. and Spiral Grooves

Discharge spent slurry and by – products away from the pad – wafer interface

Wafer and pad (i.e grooves) rotate in the counter-clockwise direction

3 Step Model

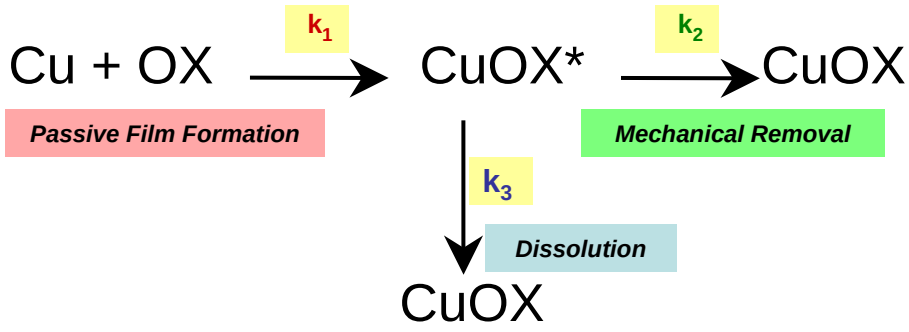

$$k_1 = \frac{\rho_{ox}}{MW_{ox}} N\Omega f \exp\left(\frac{-W}{kT}\right)\exp\left(\frac{qa}{2kTx}V\right)$$

$$RR = \frac{M_w}{\rho}\frac{k_1(k_2+k_3)}{k_1+k_2+k_3}$$

$$k_2 = c_p \mu_k pV$$

$$k_3 = \frac{-A\exp\left(-\frac{E_a}{RT}\right)}{(x_C - X)}$$

Dissolution rate (k_3) was found to be negligible for Fujimi PL-7102 system at the *pressure* and *velocity* conditions used in this study

However it becomes more important as *pressure x velocity* approaches zero

Experimental Conditions

- **Constants:**
  - **Conditioning**
    - **100 grit diamond disc (TBW)**
    - **30 min with UPW at 30 rpm disc speed and 20 per min sweep frequency**
  - **Break-in**
    - **5 dummy Discs (Cu) with Fujimi PL-7102**
  - **Slurry**
    - **Fujimi PL-7102**
    - **220 cc per minute**
  - **Wafers**
    - **200-mm in diameter**
    - **15000 A PVD Cu on 1000 Å Ta on 1000 Å SiO_2 on silicon**
  - **Pad Material**
    - **Rohm & Haas IC-1000**
- **Variables:**
  - **Relative pad-wafer velocity (m/s)**
    - **0.30**
    - **0.75**
    - **1.20**
  - **Wafer pressure (PSI)**
    - **1.0 (6894 Pa)**
    - **1.5 (10300 Pa)**
    - **2.0 (13780 Pa)**
    - **2.5 (17200 Pa)**
  - **Pad surface texture**
    - **K Groove**
    - **Logarithmic (+) Spiral (+)**
    - **Logarithmic (+) Spiral (-)**
    - **Logarithmic (-) Spiral (-)**
    - **Logarithmic (-) Spiral (+)**
    - **Floral**

Removal Rate Results Logarithmic and Spiral Grooves

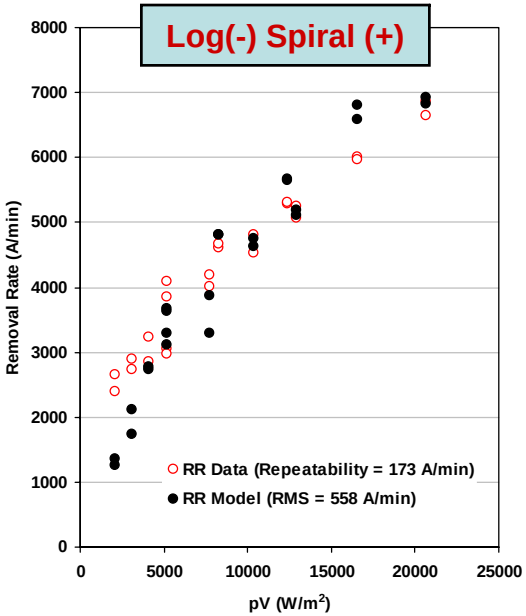

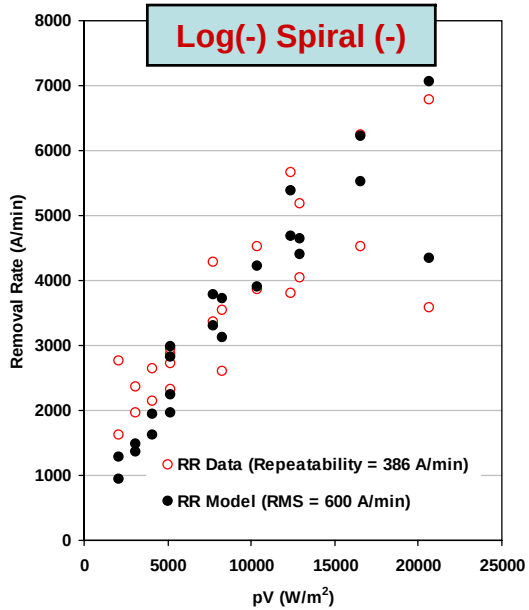

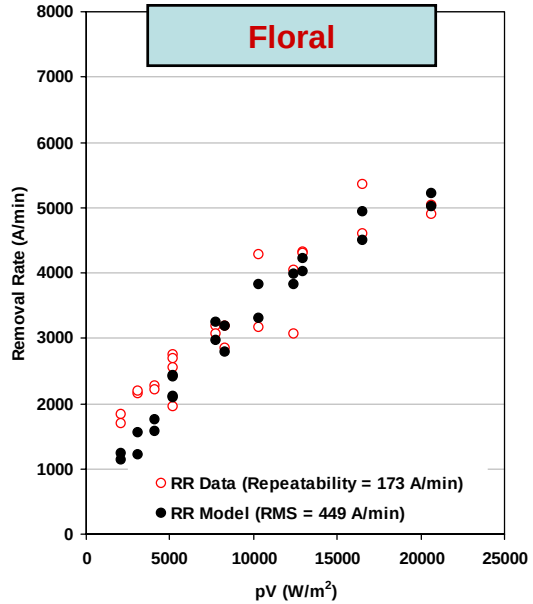

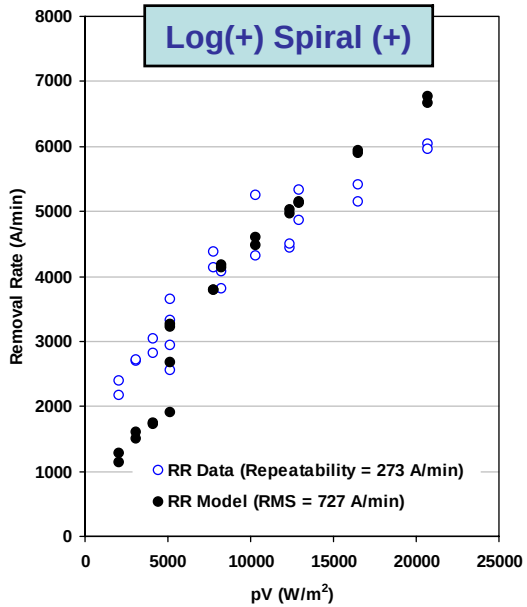

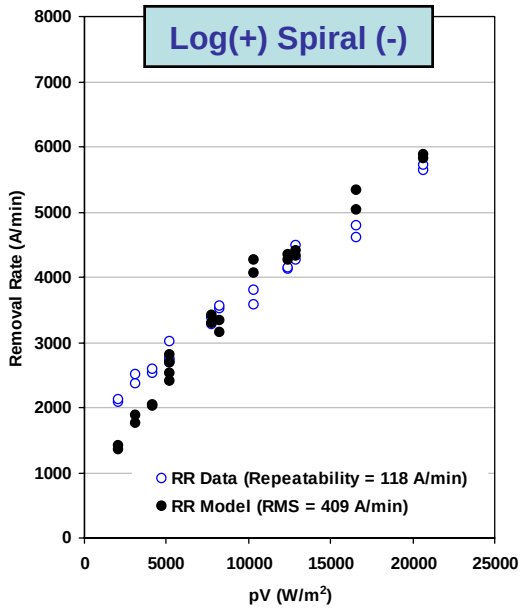

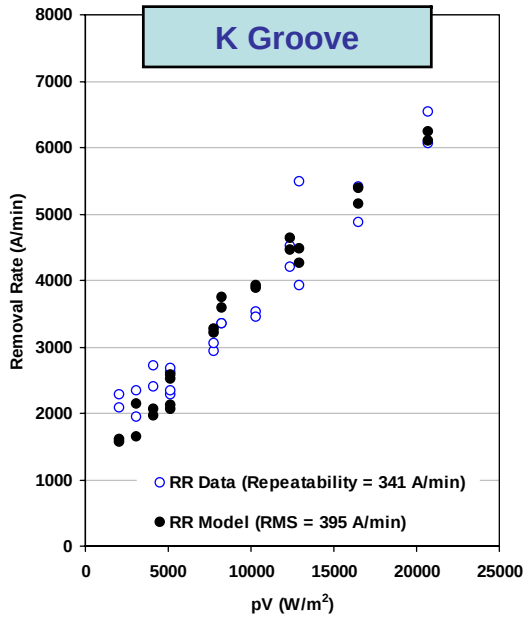

Temperature Results Logarithmic and Spiral Grooves

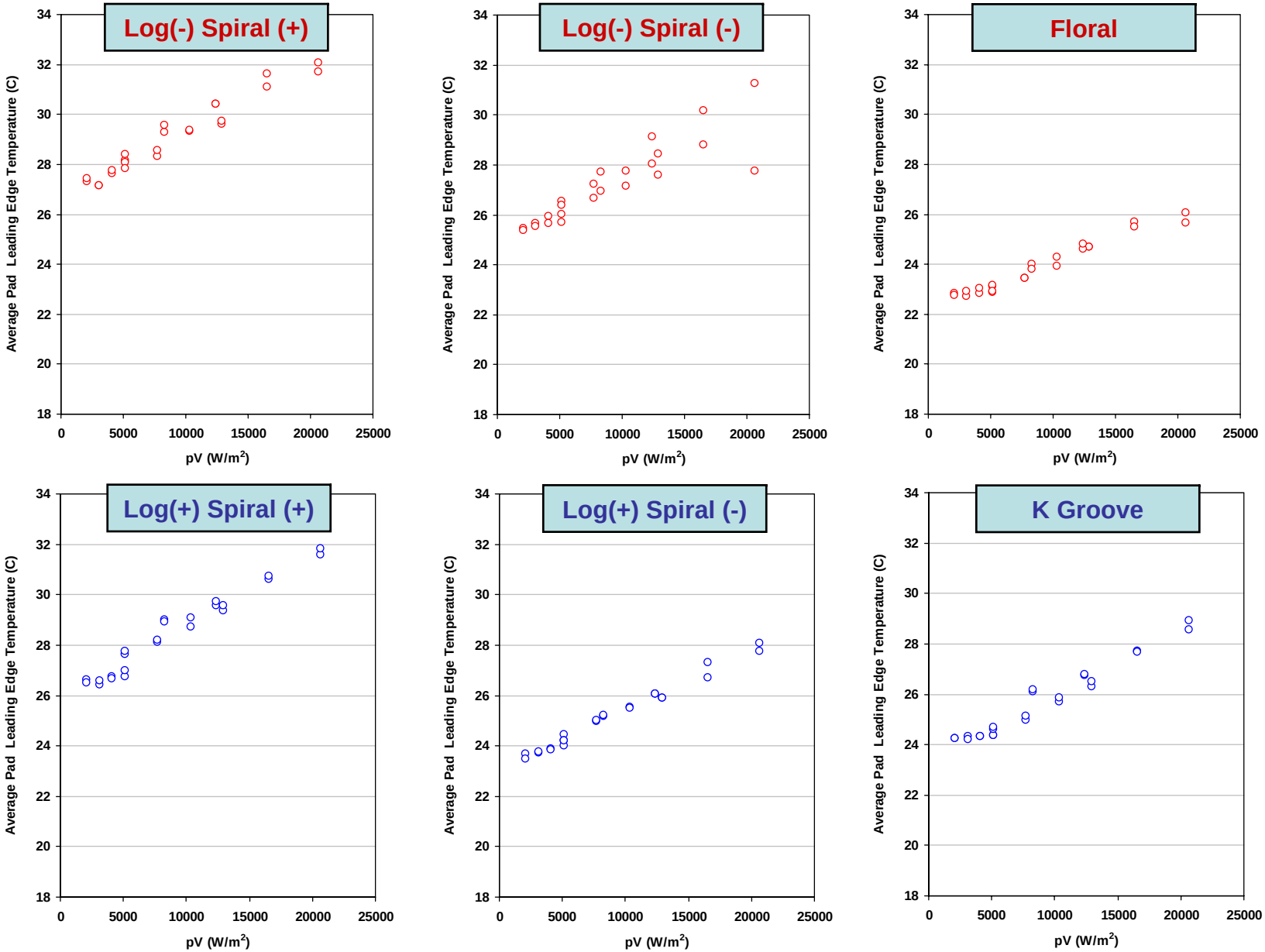

Summary of Frictional Data

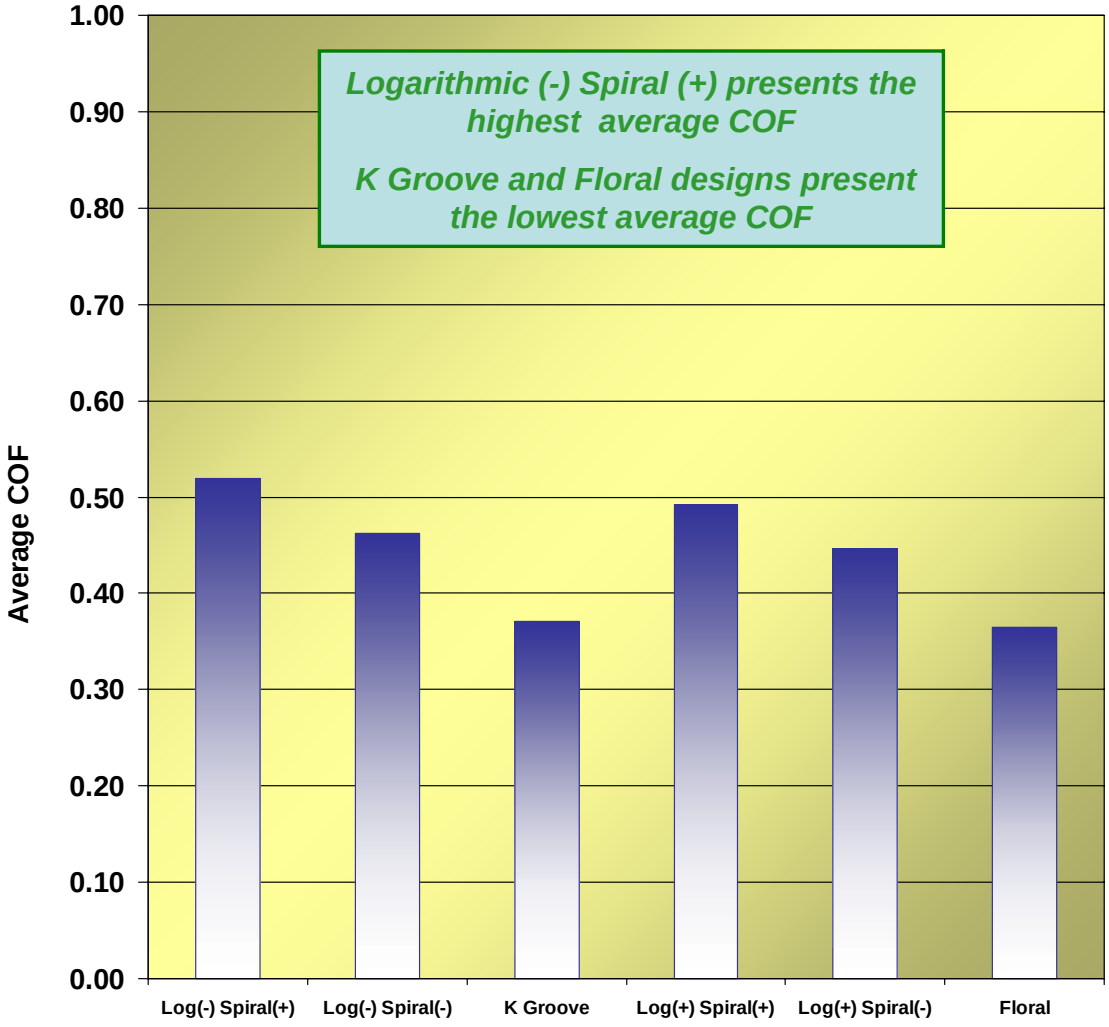

Wilcoxon Signed-Rank Test Results

Pad Type	Removal Rate	Avg. COF	Avg. Leading Pad Temp.	% Confidence
Log (-) Spiral (+)	1	1	1	95.00
Log (-) Spiral (-)	2	2	2	95.00
Log (+) Spiral (+)	2	1	2	95.00
Log (+) Spiral (-)	3	2	3	95.00
K Groove	3	3	3	95.00
Floral	3	3	3	95.00

Rank of 1 represents the highest Rank

Relative Values of k_1 and k_2 for Log and Spiral Grooves

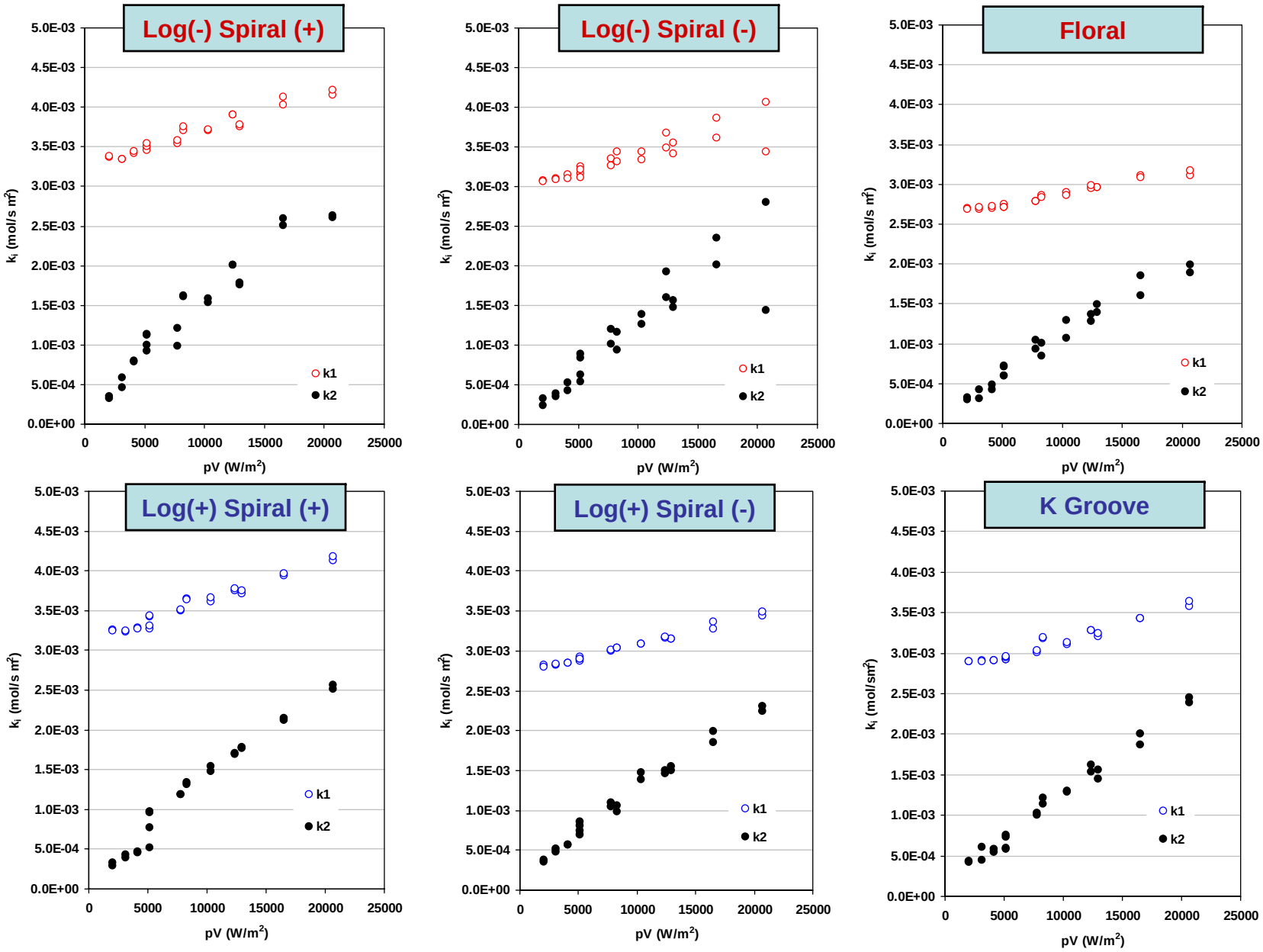

Conclusions

- In order to achieve an optimum process, different types of pad groove design were analyzed and compared to a commercial pad to establish if the flow of slurry to the wafer-pad interface could be effectively controlled during copper CMP.

- When the novel pads where compared, the effect of the logarithmic groove seems to dominate that of the spiral groove. For a fixed spiral groove direction, changing the direction of the logarithmic grooves affects removal rate significantly.

- After statistical analysis, Logarithmic (-) Spiral (+) shows higher removal rate, pad leading edge temperature and COF.

- Theoretical analysis of copper polish rates shows:

  – The 3 step model including the new expression to characterize the rate of oxide growth predicts very well the behavior of the removal rate for different types of pads used in copper CMP. The RMS falls in the range of 400 to 700 A/min in all cases.

  – The dissolution rate (i.e. k_3) does not play an important role for Fujimi PL-7102 under the pressure and velocity conditions evaluated in this study. However this third step will become more and more significant as *pV* approaches zero.

  – The relative values of k1 and k2 as a function of *pV* shows that the process is more limited by film removal through mechanical abrasion, especially at low values of *pV*. However, as pV increase this limitation is reduced and there is a transition to a more balanced process.

Fundamental Pad Characterization and Modeling: Effect of Slanted Groove Designs on Copper CMP

Subtask A-5-2

D. Rosales-Yeomans, D. DeNardis and A. Philipossian
(University of Arizona, Tucson, AZ, USA)

L. Borucki
(Intelligent Planar, Mesa, AZ, USA)

Driving Force

- Design and evaluation of novel pad grooves are critical in the development of an optimal CMP process in terms of slurry and pad consumption, as well as, uniform slurry flow under the wafer.

- Analyzing the role slanted grooves play in the effective transport of fresh slurry into and the discharged of used slurry and unwanted by-products from the wafer pad interface during copper CMP.

- Optimization of CMP consumables (pad and slurry) in order to reduce COO and achieve a more environmentally friendly process.

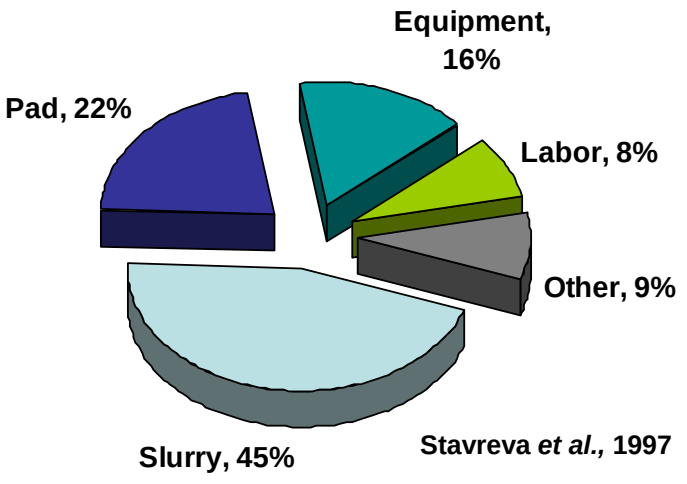

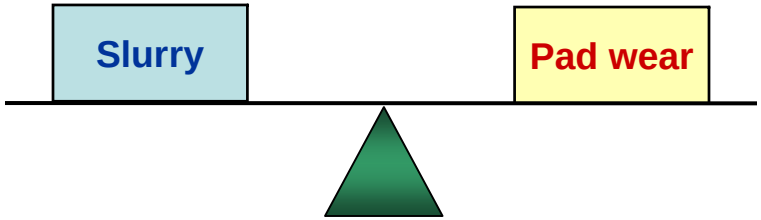

CMP Process

200 mm Polisher at the University of Arizona

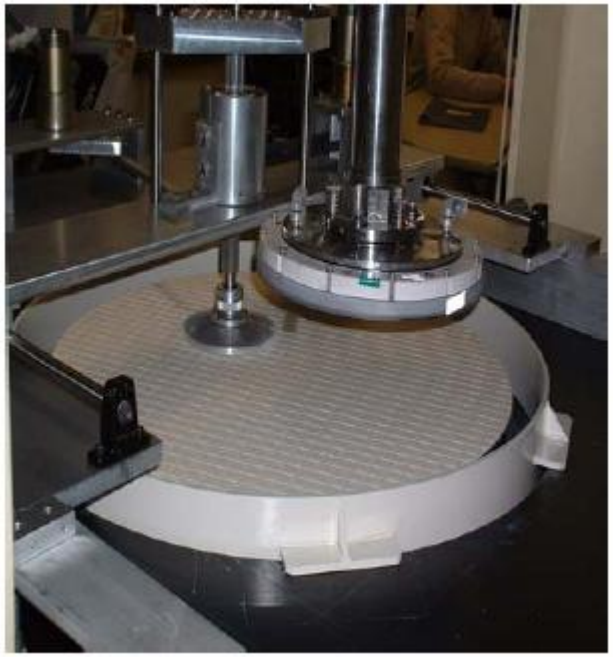

Slanted Concentric Grooves

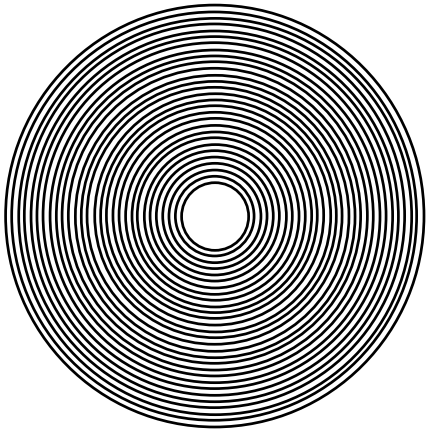

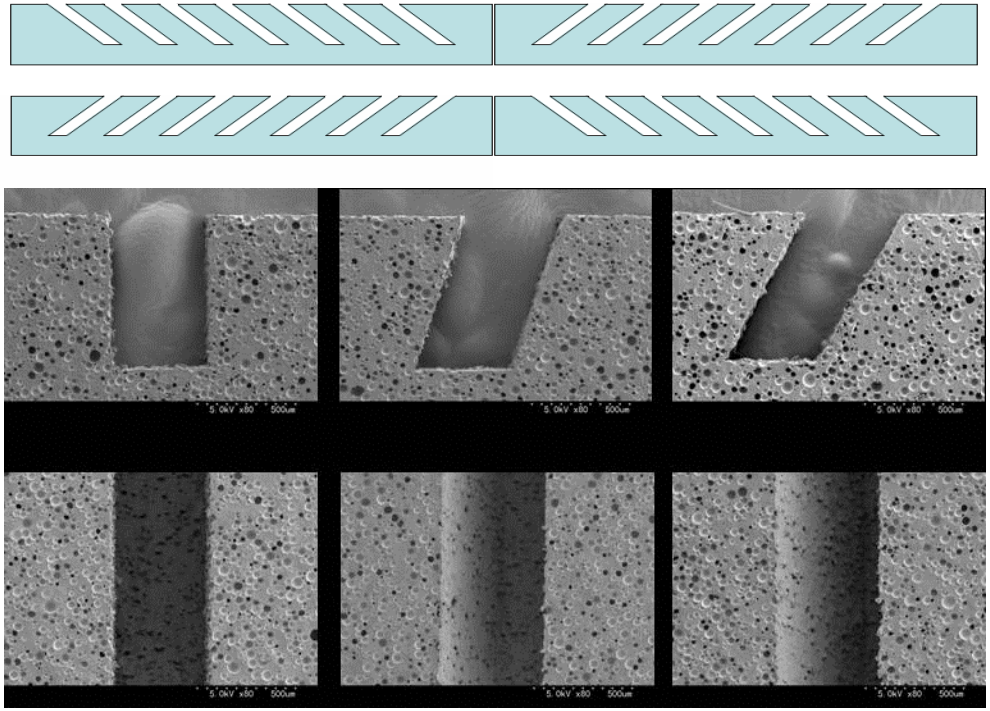

Positive Direction

Negative Direction

3 Step Model

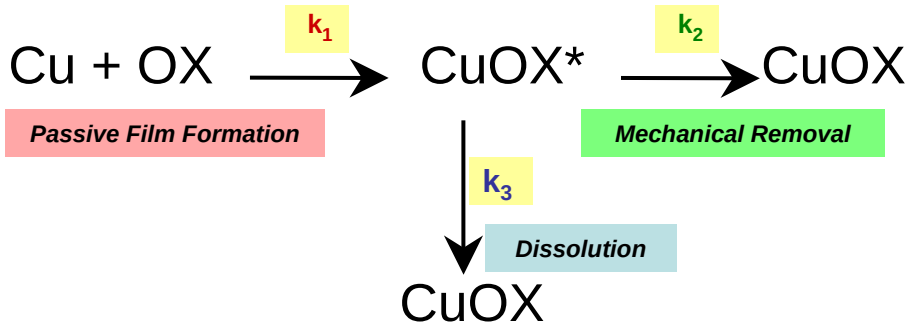

$$k_1 = \frac{\rho_{ox}}{MW_{ox}} N\Omega f \exp\left(\frac{-W}{kT}\right)\exp\left(\frac{qa}{2kTx}V\right)$$

$$RR = \frac{M_w}{\rho}\frac{k_1(k_2+k_3)}{k_1+k_2+k_3}$$

$$k_2 = c_p \mu_k pV$$

$$k_3 = \frac{-A\exp\left(-\frac{E_a}{RT}\right)}{(x_C - X)}$$

Dissolution rate (k_3) was found to be negligible for Fujimi PL-7102 system at the *pressure* and *velocity* conditions used in this study

However it becomes more important as *pressure x velocity* approaches zero

Experimental Conditions

- **Constants:**
  - Conditioning
    - 100 grit diamond disc
    - 30 min with UPW at 30 RPM disc speed and 20 per min sweep frequency
  - Break-in
    - 5 copper discs with Fujimi PL – 7102
  - Slurry
    - Fujimi PL – 7102
    - 220 cc per minute
  - Wafers
    - 200 – mm in diameter
    - 1,500 nm PVD copper on 100 nm Ta on 100 nm SiO2 on Si
  - Pad surface texture
    - Concentrically Grooved (Pitch = Depth = 1000 µm ; Width = 500 µm)
- **Variables:**
  - Relative pad-wafer velocity (m/s)
    - 0.30
    - 0.75
    - 1.20
  - Wafer pressure (PSI)
    - 1.0 (6,900 Pa)
    - 2.0 (13,800 Pa)
    - 3.0 (20,700 Pa)
  - Pad surface texture
    - Plus and Minus 20 degrees
    - Plus and minus 30 degrees
    - Zero
    - Flat

Removal Rate Results Slanted Grooves

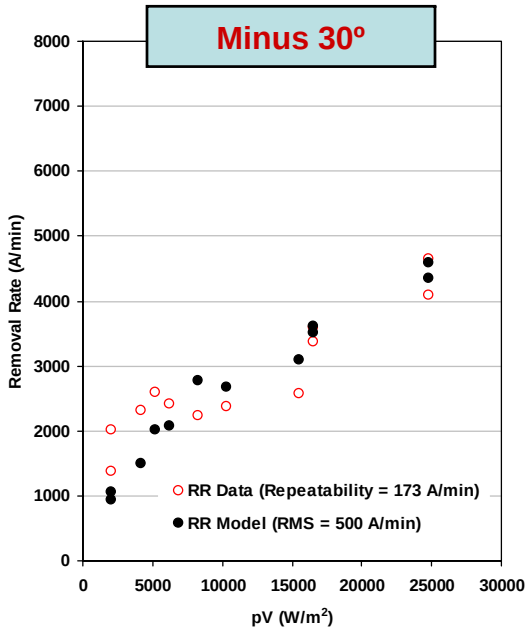

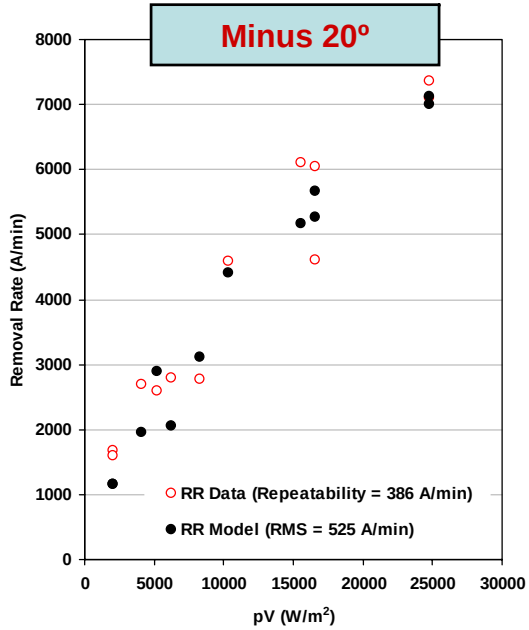

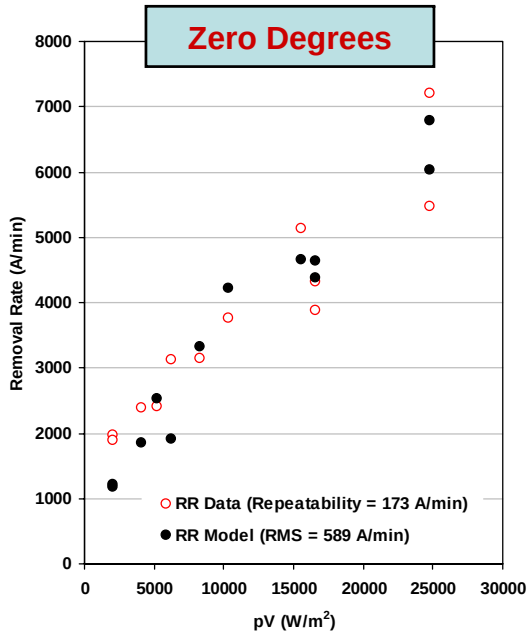

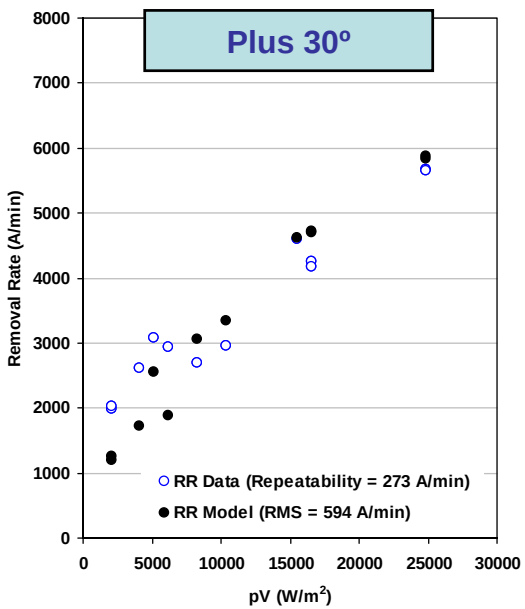

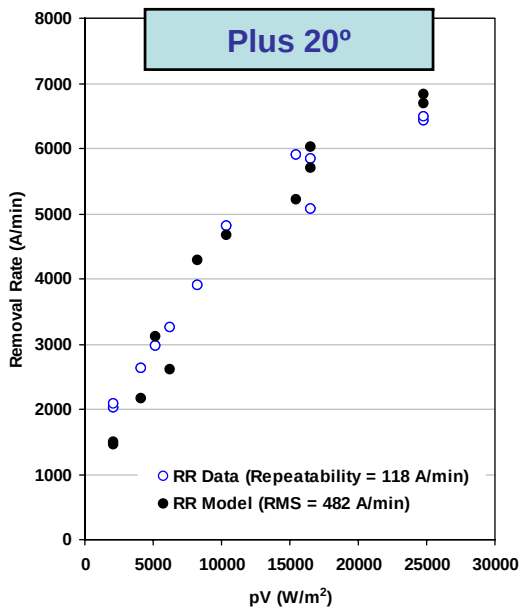

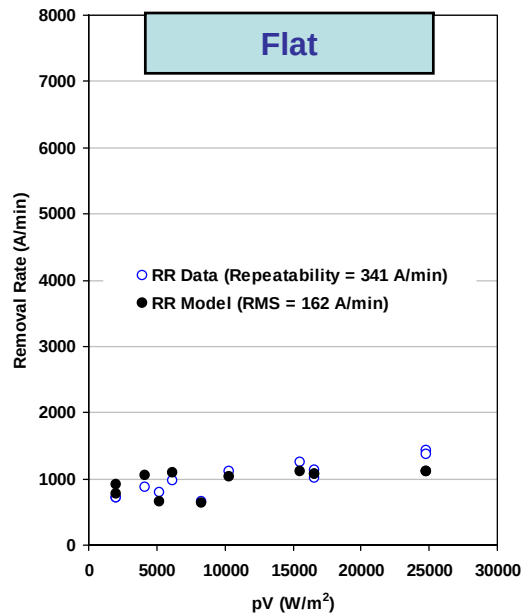

Temperature Results Slanted Grooves

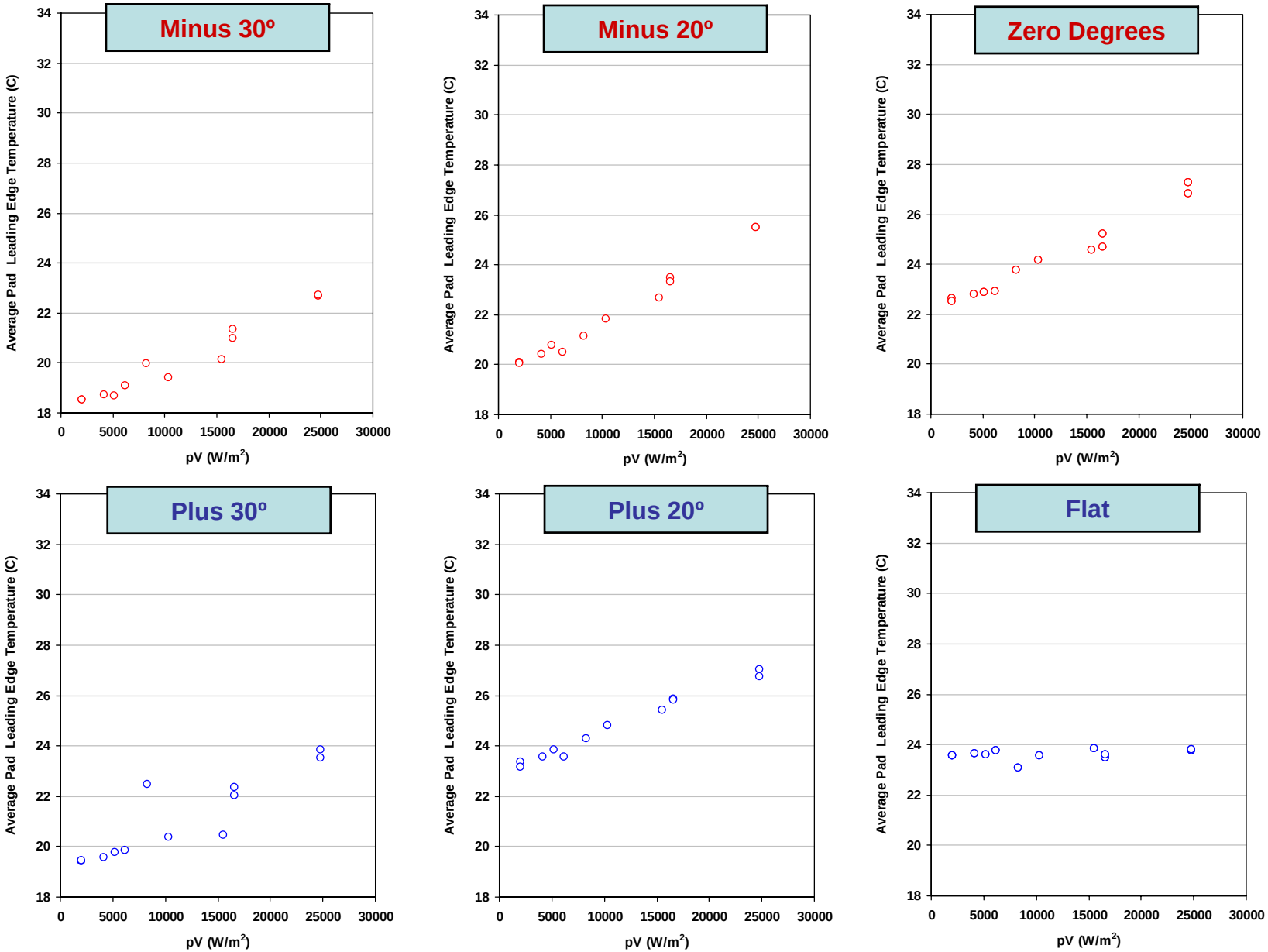

Summary of Frictional Data

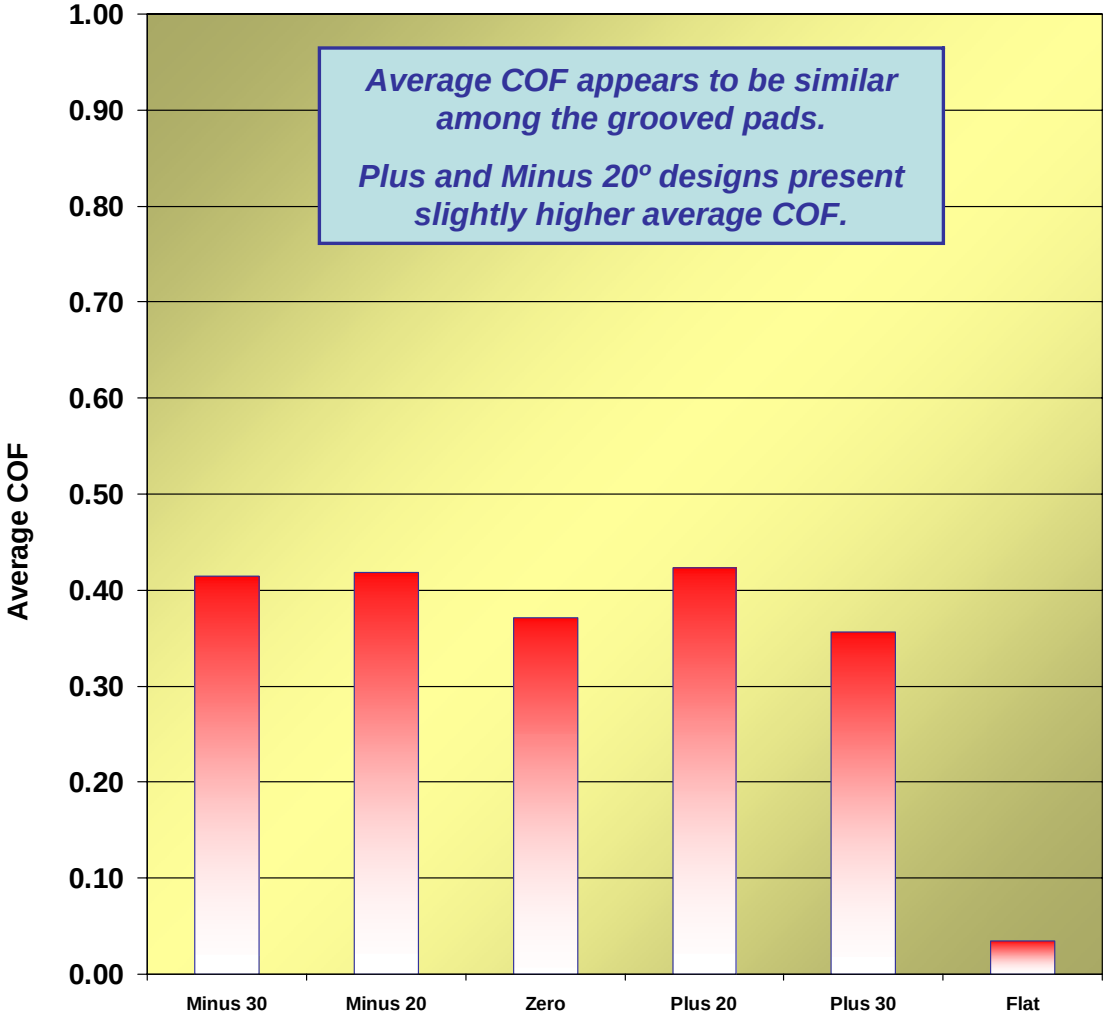

Wilcoxon Signed-Rank Test Results

Pad Type	Removal Rate	Avg. COF	Avg. Leading Pad Temp.	% Confidence
Minus 30°	3	2	3	95.00
Minus 20°	2	1	2	95.00
Zero	2	3	2	95.00
Plus 20°	1	1	1	95.00
Plus 30°	3	3	3	95.00
Flat	4	4	3	95.00

Rank of 1 represents the highest Rank

Relative Values of k_1 and k_2 for Log and Spiral Grooves

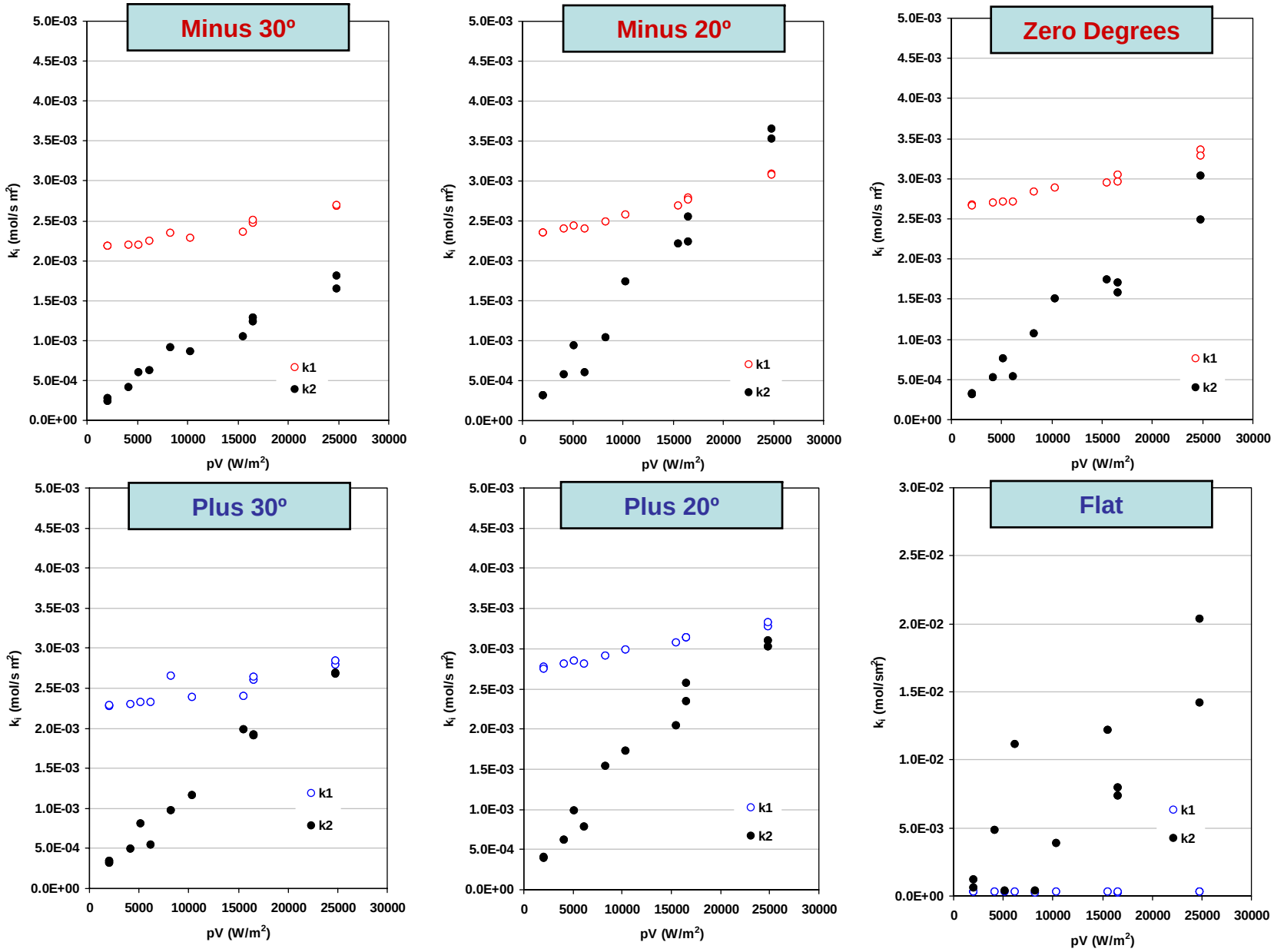

Conclusions

- **Slanted grooves (positive and negative) can be used to modify the removal rate behavior without significantly affecting COF**

- **Experimental results indicate that slanting the grooves at 20º regardless of the direction results in higher removal rates during copper CMP.**

  - **After statistical analysis, Plus 20º shows higher removal rate, pad leading edge temperature and slightly higher average COF. Suggesting a possible path to change the balance between slurry consumption and pad wear.**

  - **When the degree of slant is 30, the grooves apparently give-up and collapse producing lower removal rates.**

- **Theoretical analysis of copper polish rates shows:**

  - **The 3 step model including the new expression for the oxide growth rate predicts very well the behavior of the removal rate for the slanted grooves pads. The RMS falls in the range of 480 to 595 A/min for all grooved pads, and 162 A/min in the case of the Flat pad.**

  - **The dissolution rate (i.e. k_3) does not play an important role ($k_3 << k_1$ and $k_3 << k_2$) for this system.**

  - **The relative values of k1 and k2 as a function of *pV* for all grooved pads shows that the process is more limited by film removal through mechanical abrasion, especially at low values of *pV*. However, as pV increase this limitation is reduced and there is a transition to a more balanced process.**

  - **The model predicts that as pV increase to values higher than tested the removal rate will saturate in terms of mechanical abrasion (i.e. the rate of mechanical abrasion will approach and exceed the rate of film growth).**

Alternative Planarization Technologies - Electrochemical Mechanical Planarization (ECMP) of Copper

Task ID : A-6-1

Srini Raghavan (PI)

Graduate students:

Viral Lowalekar

Ashok Muthukumaran

Department of Materials Science and Engineering

The University of Arizona

ESH Metrics for Task A-6

- **Basis of comparison**:
  - Conventional slurry based Copper CMP
    - Requires slurries with higher solid content
    - Higher polishing pressure
    - Higher polish time during bulk copper removal
- **Manufacturing Metrics**:
  - The use of ECMP will reduce the polish time, polishing pressure and the amount of waste generated by a typical slurry based CMP
- **ESH Metrics:**

	Usage Reduction		Waste Reduction	
Goals	Chemicals	Abrasives	Solid	Liquid
Using ECMP	N/A	80% reduction	<0.01%	N/A

ECMP for Bulk Copper Removal

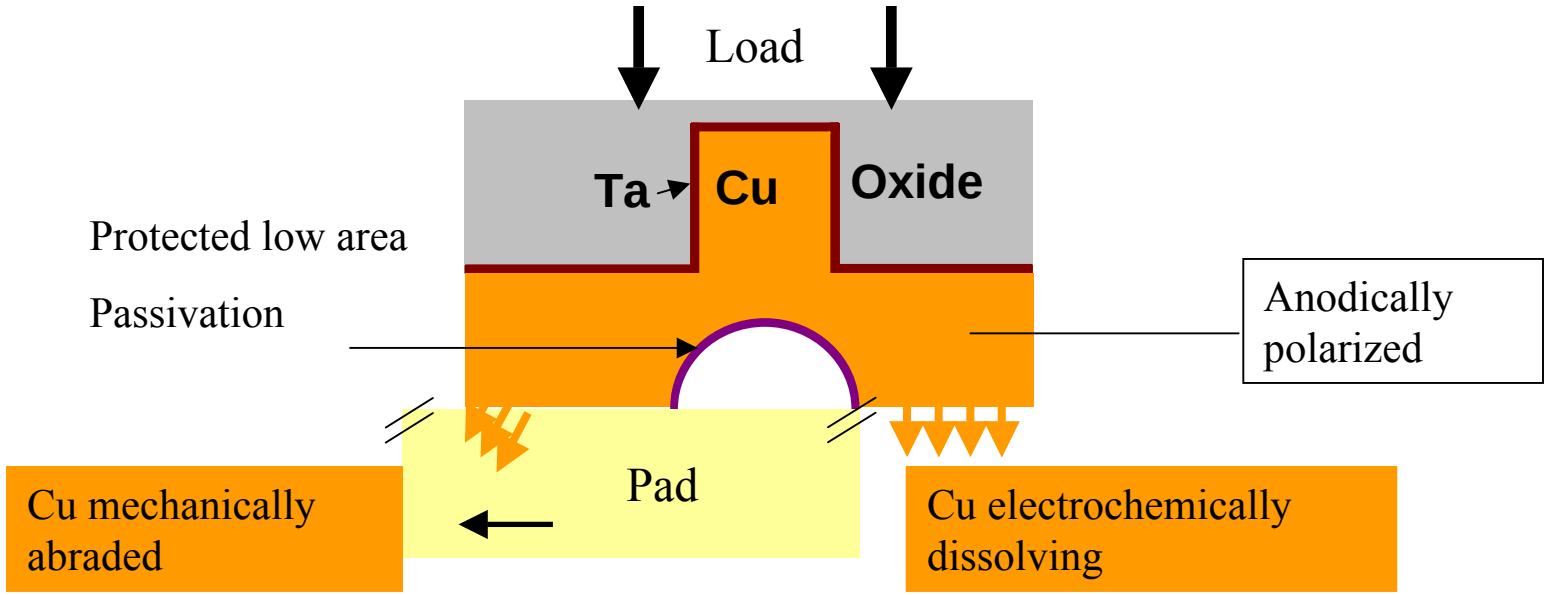

- Wafer is anodically biased during polishing in a solution at very low (~0.5 psi) pressure
- Passivating agent/corrosion inhibitor is added to protect low lying areas while higher areas are polished.
- Inhibitors must be stable at anodic overpotentials; efficiency of the most commonly used inhibitor BTA decreases with applied anodic potential

Objective

- To develop chemical systems suitable for ECMP of copper through electrochemical investigations. Special attention has been paid to the identification of inhibitors that can function effectively under anodic potential conditions used in ECMP.

Accomplishments During the Current Contract Year

- Developed oxalic acid based chemical system containing a redox inhibitor (TSA) that is suitable for copper ECMP.

- Characterized the mechanism of inhibition by electrochemical investigations.

Setup for Electro Chemical Mechanical Polishing

Polishing Area = 4 cm^2

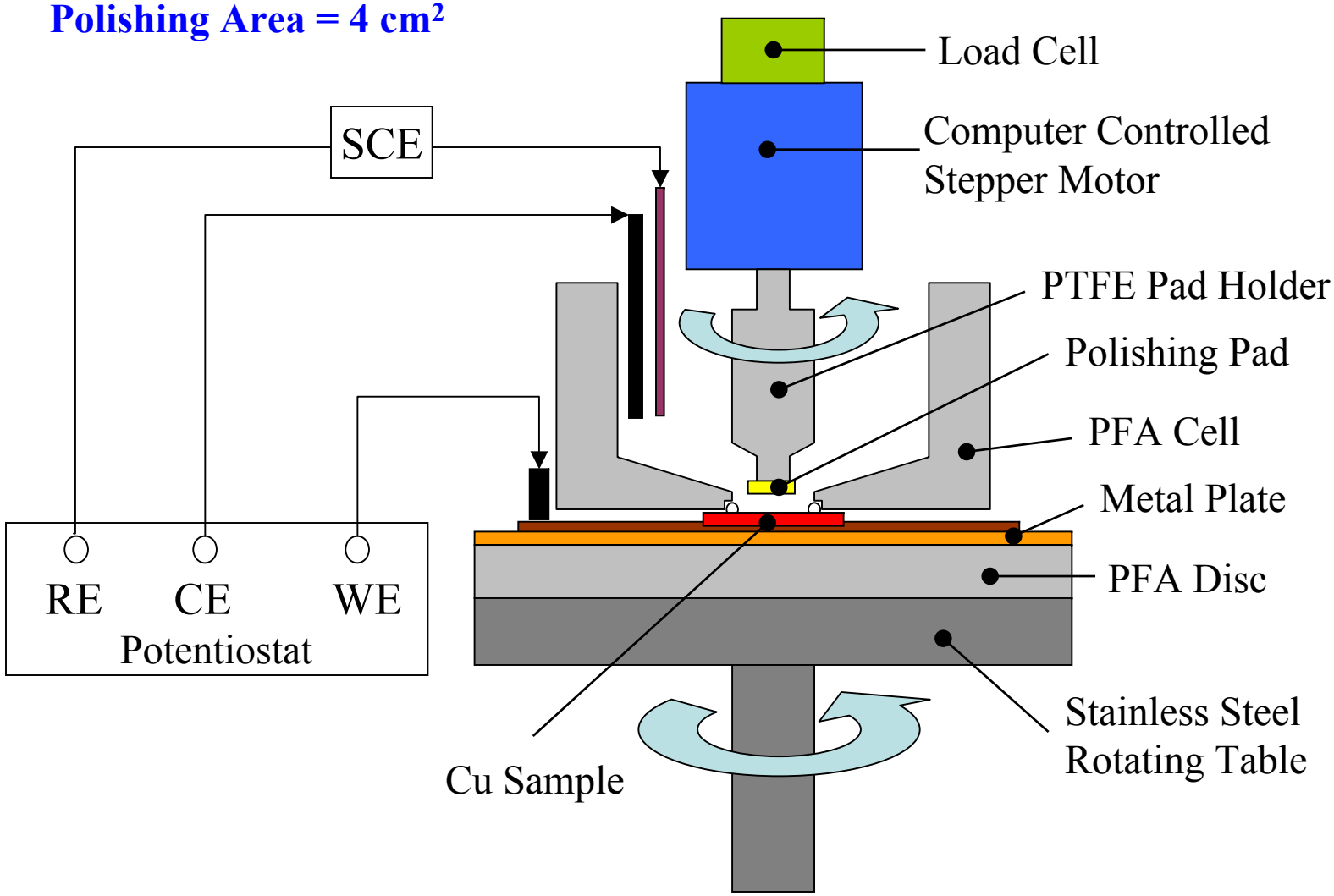

ECMP of Copper in Oxalic Acid System - Comparison of TSA and BTA as Inhibitor

Removal rates determined by profilometry

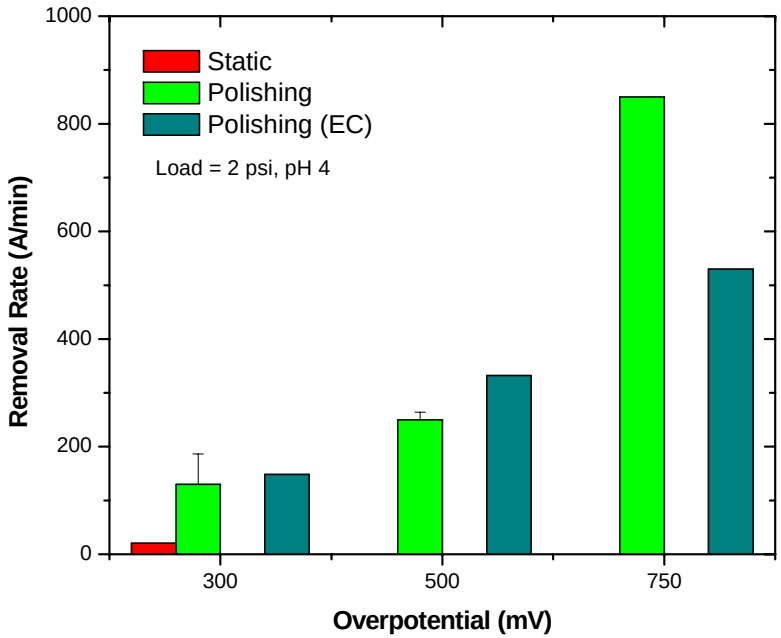

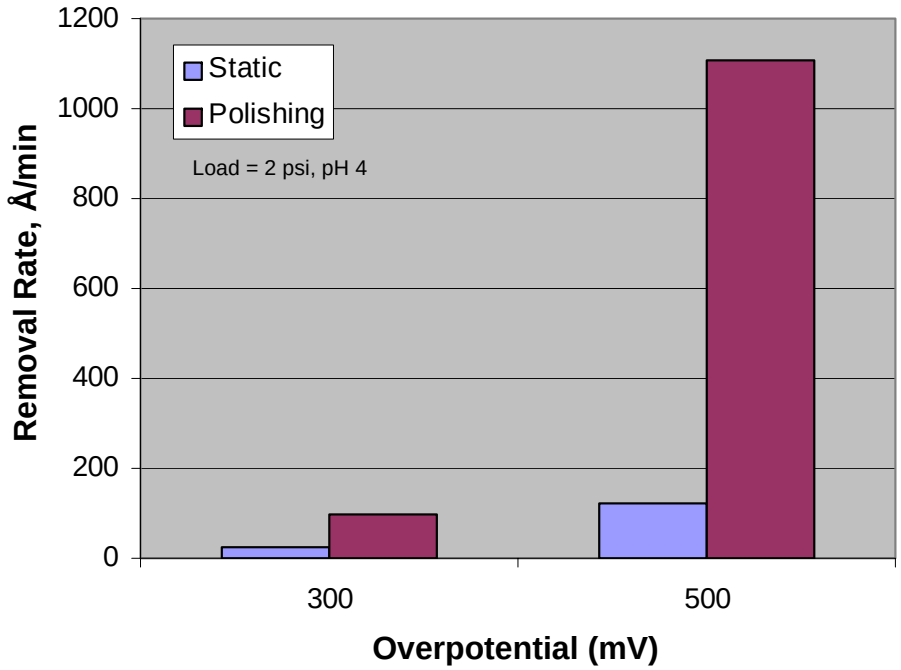

- 0.1 M Oxalic + 0.01 M TSA + 1% SiO_2
- Increase in overpotential increases Cu removal rates.
- *Unlike BTA*, no static removal seen at higher overpotentials.

- 0.1 M Oxalic + 0.001M BTA + 1%SiO_2
- Higher polishing and static removal rates with higher overpotential.

Effect of Current Density on Copper Removal in Oxalic Acid - TSA System - Galvanostatic Study

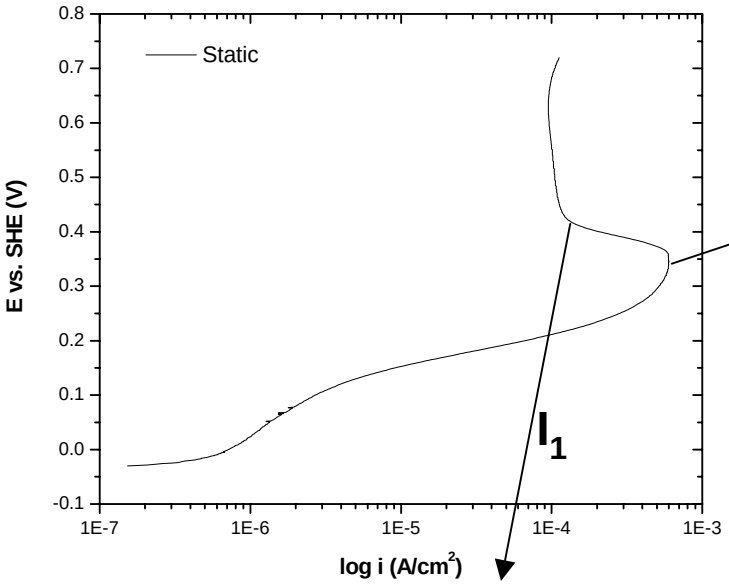

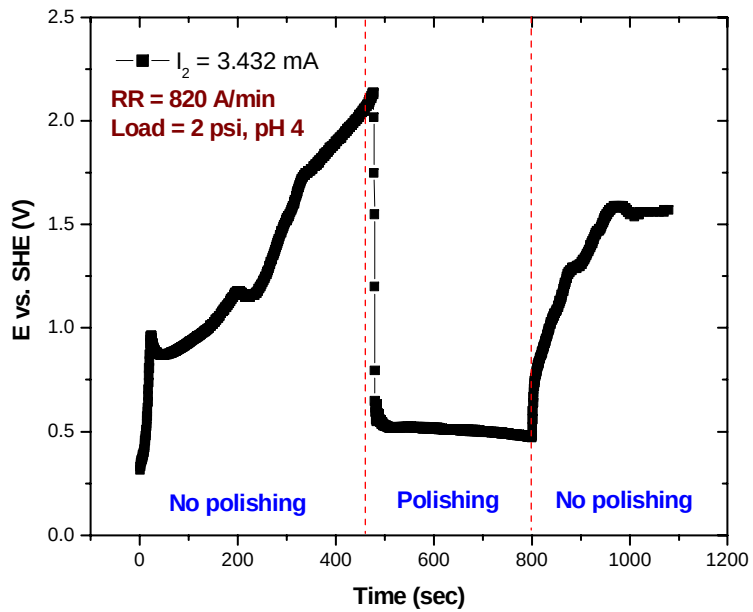

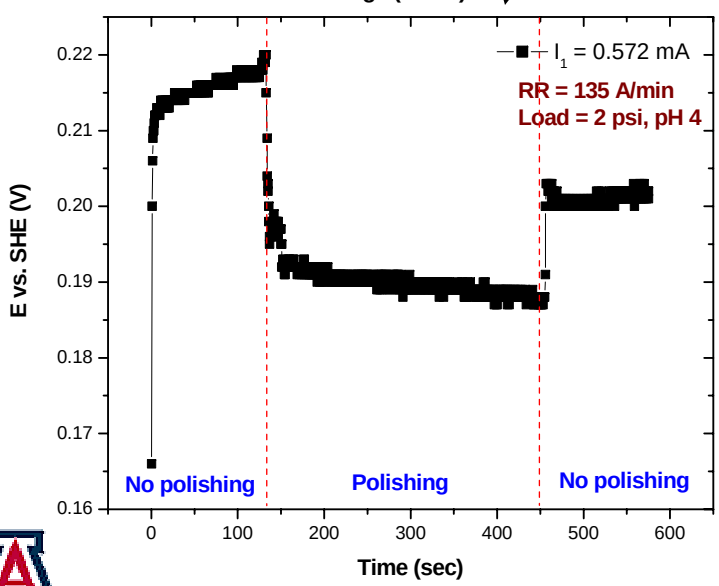

- 0.1 M Oxalic + 0.01 M TSA + 1% SiO_2.
- When sample is held at low current value, potential quickly reaches to a steady state value (220 mV).
- Abrasion decreases this potential value by 30 mV.
- At high current value, potential keeps increasing upto 2 V and no plateau is observed. This indicates resistive film formation.
- Abrasion dramatically drops the potential.

ECMP of Copper in Oxalic Acid System

Polishing Results

Removal rates determined by four point probe

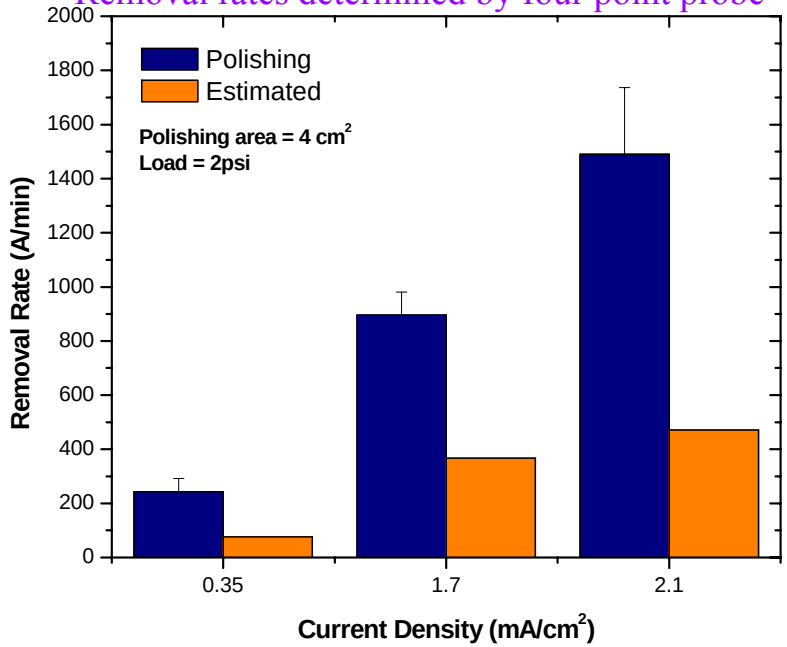

- 0.3 M Oxalic Acid + 0.01 M TSA, pH 4
- Applied current densities of 0.35, 1.7 and 2.1mA/cm^2 correspond to overpotentials of 300, 650 and 750 mV, respectively.
- Removal rate increases with current density but is more than that calculated from applied charge
- Under OCP conditions, the removal rate during polishing in 0.3 M oxalic acid is 6 Å/min.

❖ **Estimated removal rate was calculated from current vs. time profiles.**

QCM Results

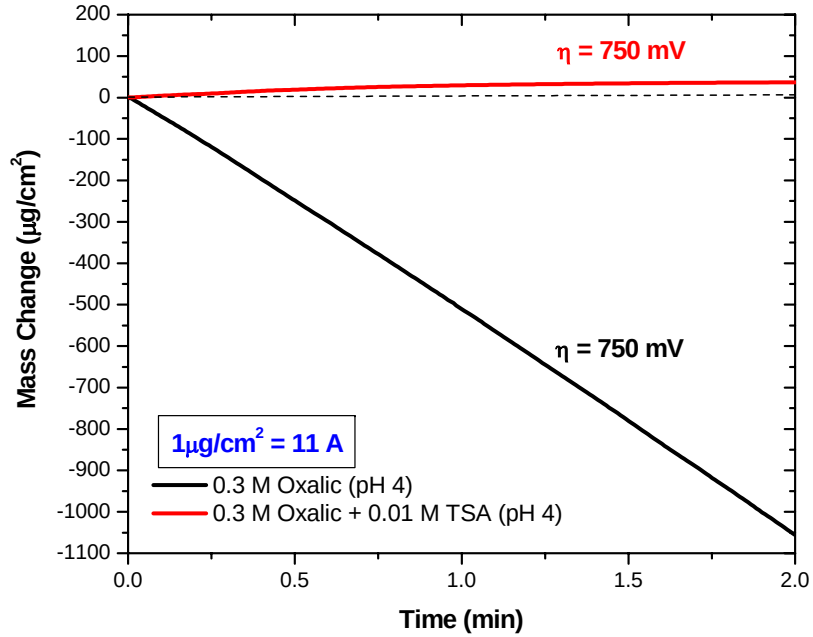

- QCM is an extremely sensitive sensor capable of measuring mass change in ng/cm^2 range.
  - Mass decrease indicates dissolution
  - Mass increase indicates surface layer formation/inhibition
- High dissolution rate of copper (5600 Å/min) in 0.3 M oxalic acid without inhibitor
- Addition of 0.01 M TSA *inhibits* copper dissolution at an anodic overpotential (η) of 750 mV.

Cyclic Voltammetry Studies on TSA

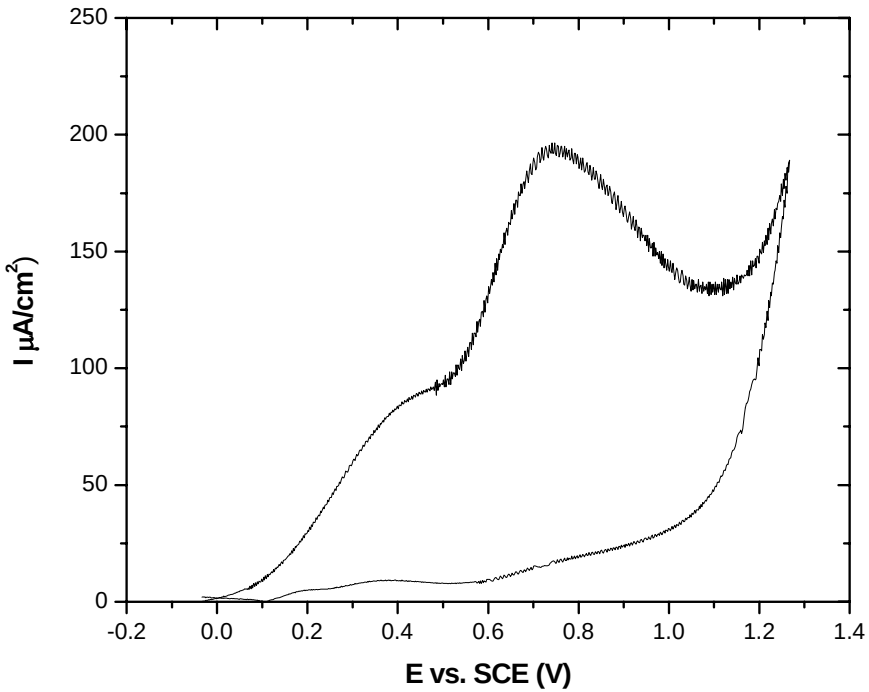

- 0.01 M TSA (pH 4)
- CV carried out under N_2 atmosphere with Pt as working electrode.
- Potential scanned:
  OCP to 1.2 vs. OCP
- Scan rate of 10 mV/sec.

- **TSA get oxidized at ~ 800 mV vs. SCE.**

Effect of Potential on Copper Dissolution - QCM Studies

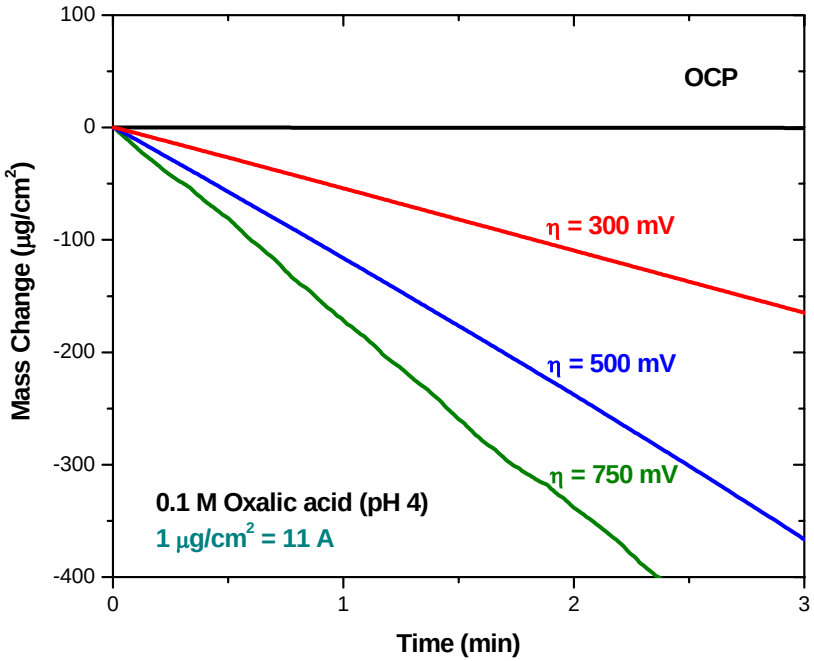

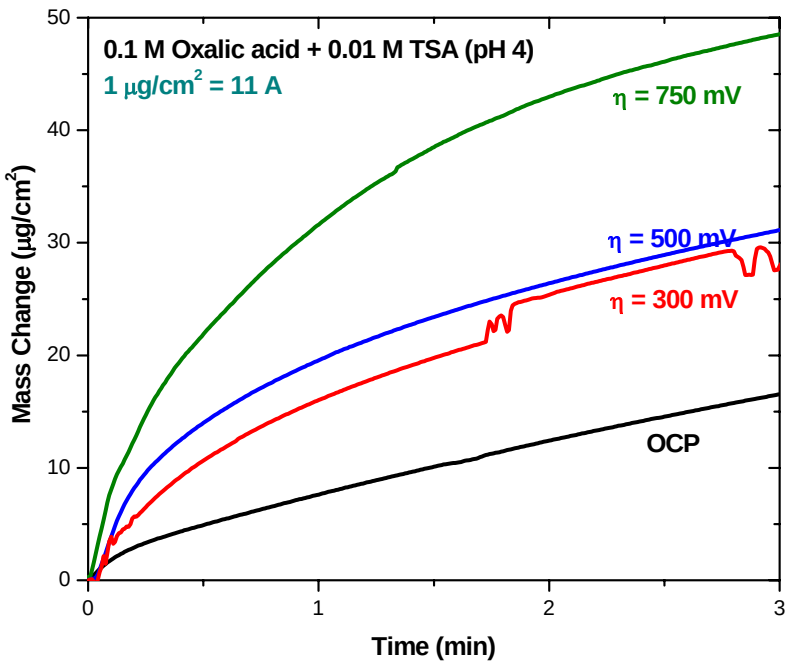

- Copper dissolution increases with overpotential.
- Dissolution rate of 1800 Å/min at η = 750 mV.
- Increase in mass recorded for all overpotentials in presence of 0.01 M TSA.

Cyclic Voltammetry and QCM Studies in Cu/TSA System (No Oxalic Acid)

❖ Mass change was recorded simultaneously with the potential sweep.

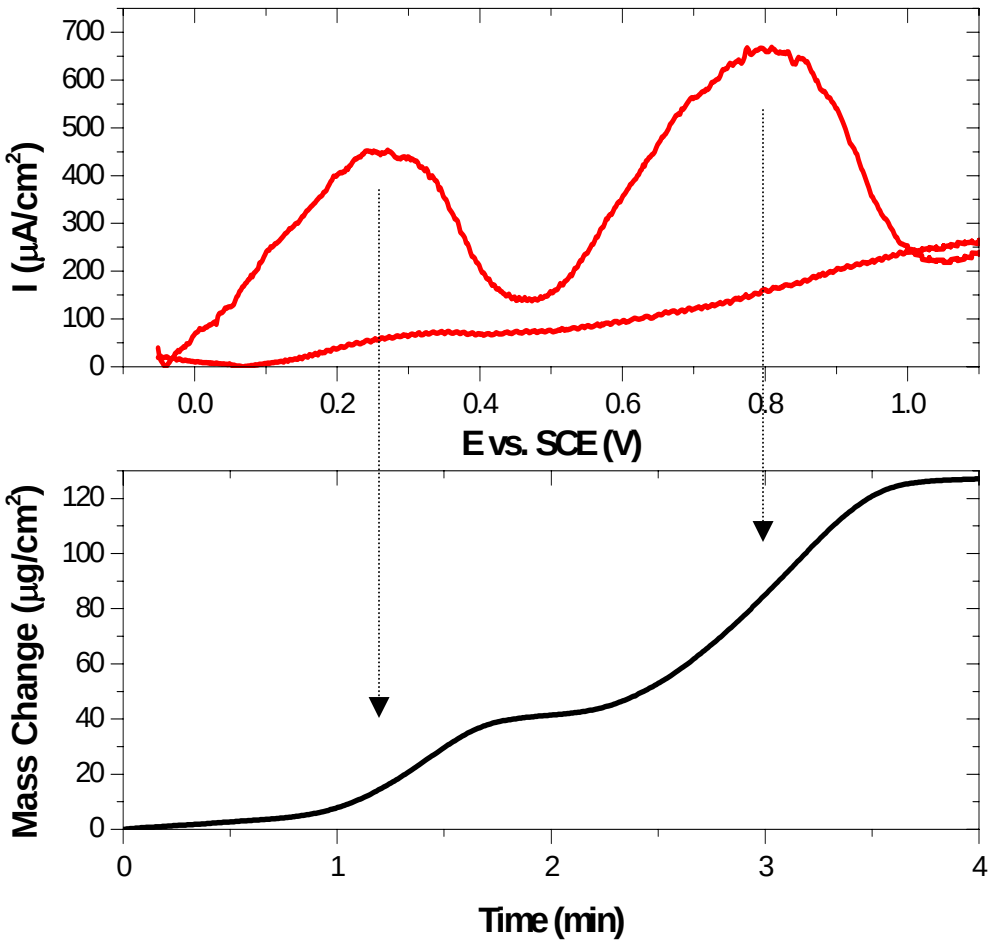

- 0.01 M TSA (pH 4)
- Experiments carried out under N_2 atmosphere with copper as working electrode.
- Cyclic Voltammetry:
  - Potential Sweep: OCP to 1.2 V vs. OCP
  - Scan rate: 5 mV/sec
- Copper oxidation (Cu(I)TSA ?) peak observed at ~ 300 mV vs. SCE.
- **TSA oxidation peak at ~ 800 mV vs. SCE.**
- QCM results show sharp increase in mass at peak potential values

Proposed Inhibition Mechanism for BTA and TSA

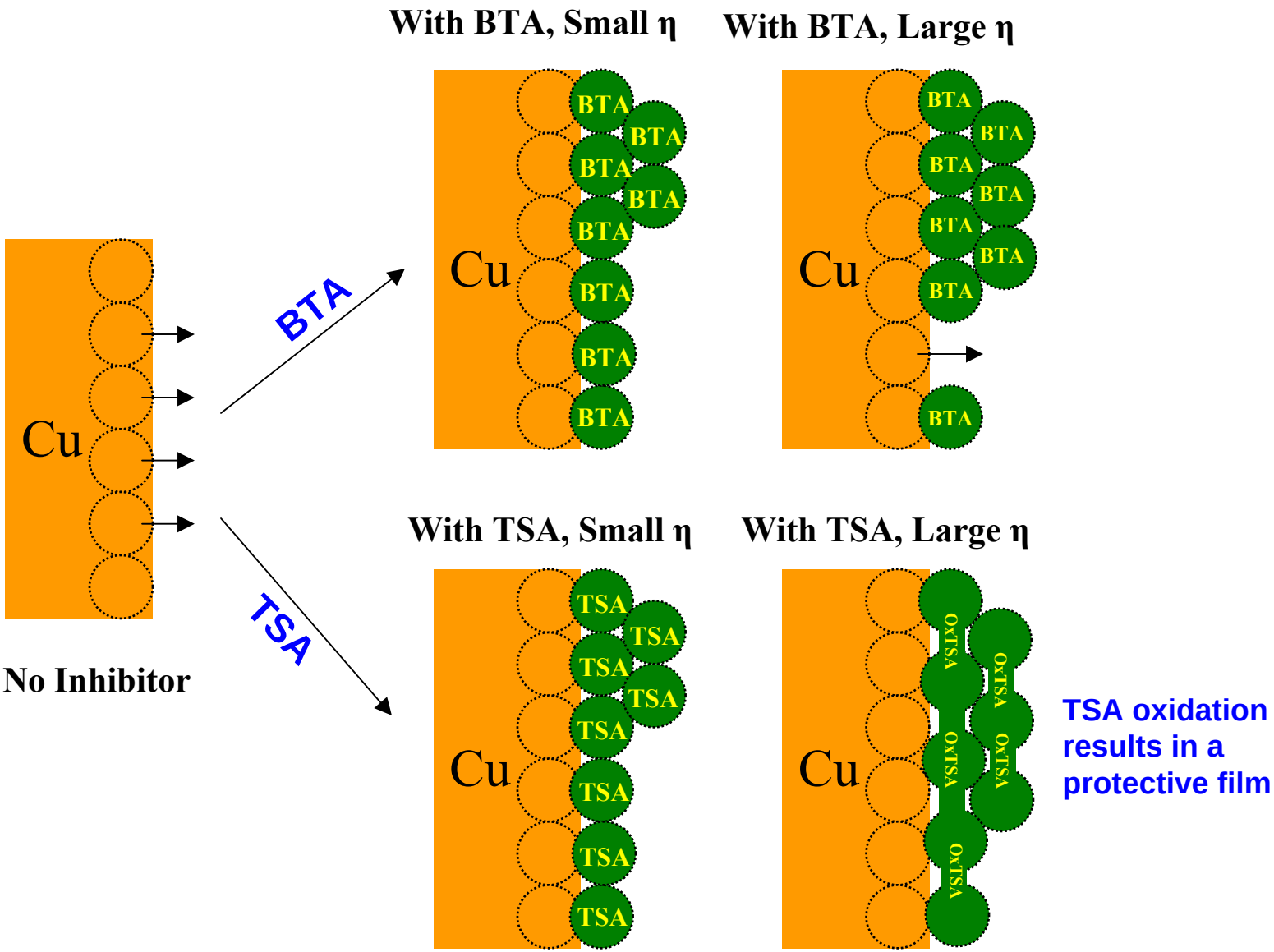

Future Directions

- Continue work with redox inhibitors and study rate – planarity relationship
- Investigate the feasibility of removal of barrier layers (Ta, TaN, Ru) using ECMP technique.
  - 1:1 selectivity between Cu and barrier layer

Subtask A9
Copper Planarization for Integrated Circuit Manufacturing

Principal Investigator: **Steve Beaudoin, Chemical Engineering, Purdue University**

Graduate Student: **Bum Soo Kim, Chemical Engineering, Purdue University**
Caitlin Kilroy, Chemical Engineering, Purdue University

NSF/SRC Engineering Research Center for Environmentally Benign Semiconductor Manufacturing

ESH Impact

- Optimization of Cu CMP Protocols
  - Minimize cleaning load
  - Minimize rework
  - Optimize polish rates and consumables use
- Metrics
  - Basis of Comparison
    - ✓ Existing Cu CMP processes
  - Manufacturing Metrics
    - ✓ Validated polishing model provides predictive tool to identify promising configurations
- ESH Metrics

Goals/ Possibilities	Energy	Water	Chemicals	PFCs	VOCs	HAPs	Other Hazardous Wastes
Optimal post CMP cleaning	up to 30%	up to 15%	up to 15%	N/A	N/A	N/A	N/A

Interpretation: Pad Elastic Modulus Studies

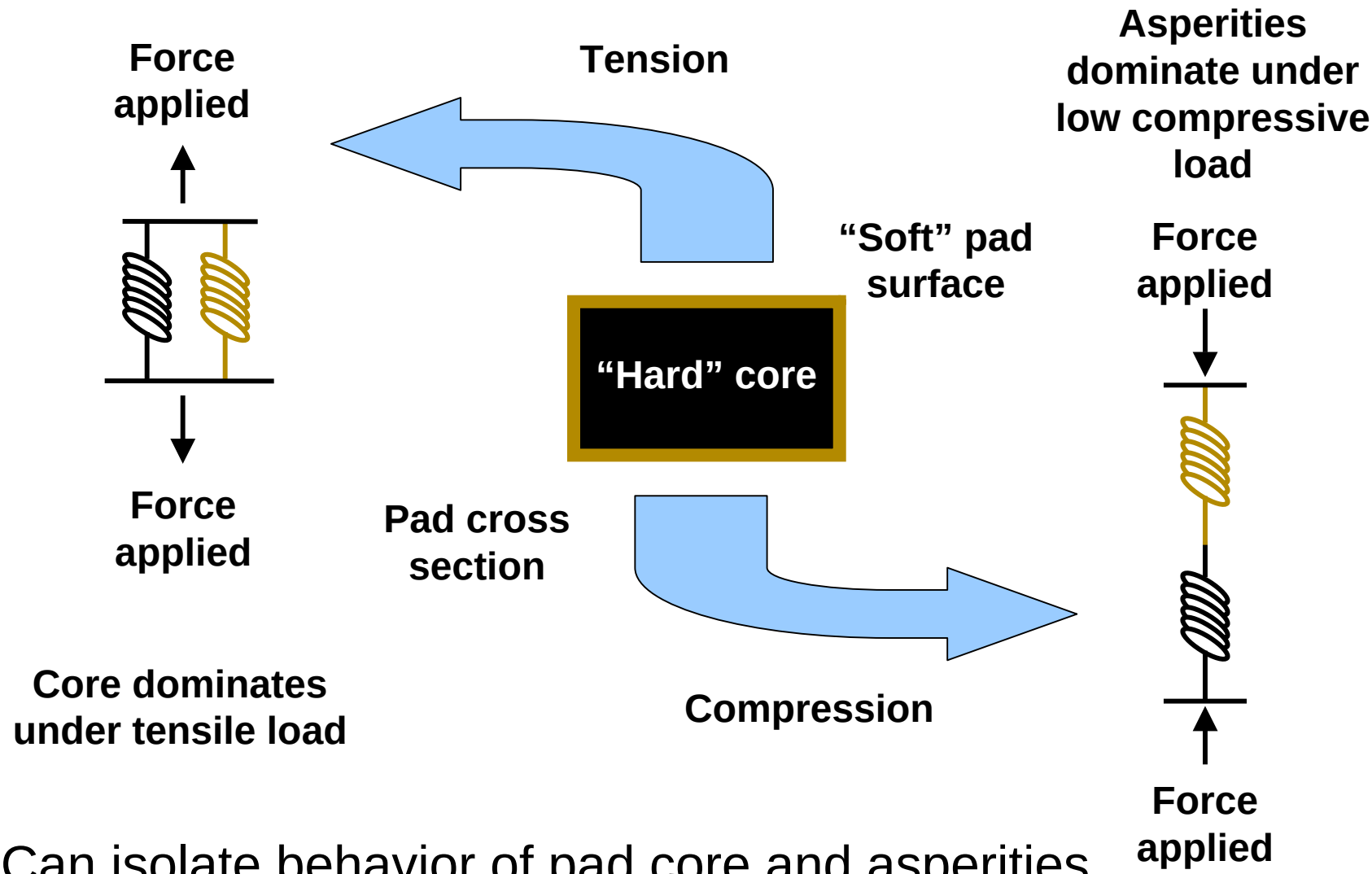

Can isolate behavior of pad core and asperities

Measured Pad Moduli

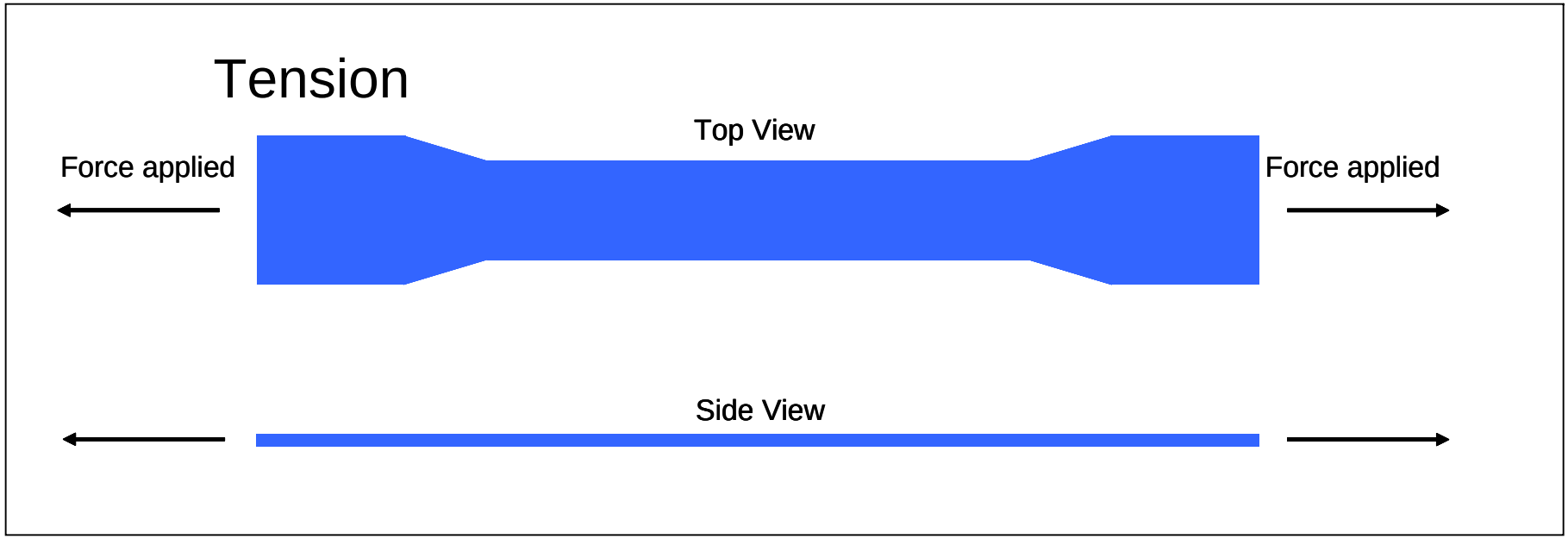

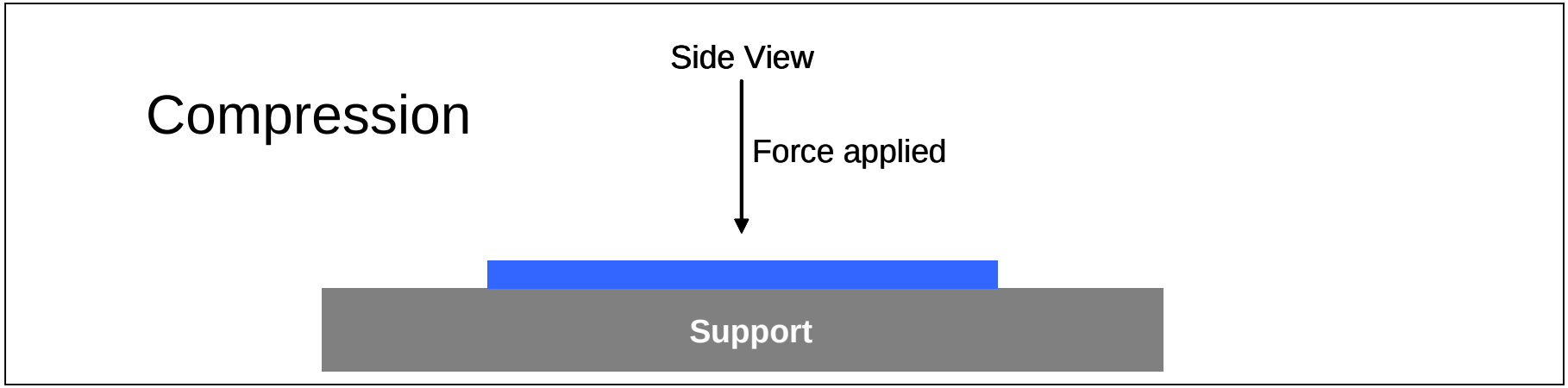

Measured Elastic Modulus in Tension

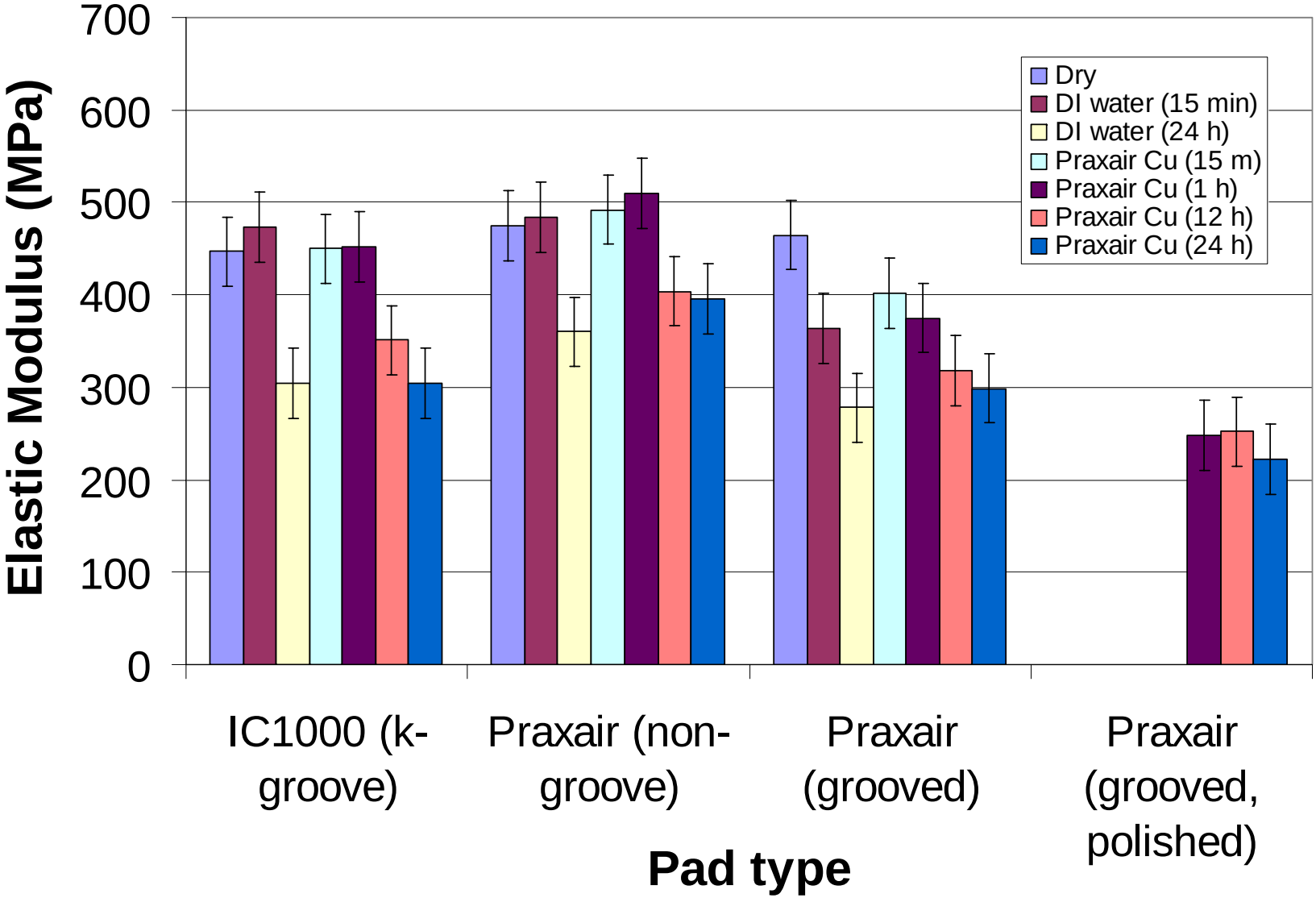

Reproducibility: Elastic Modulus in Tension

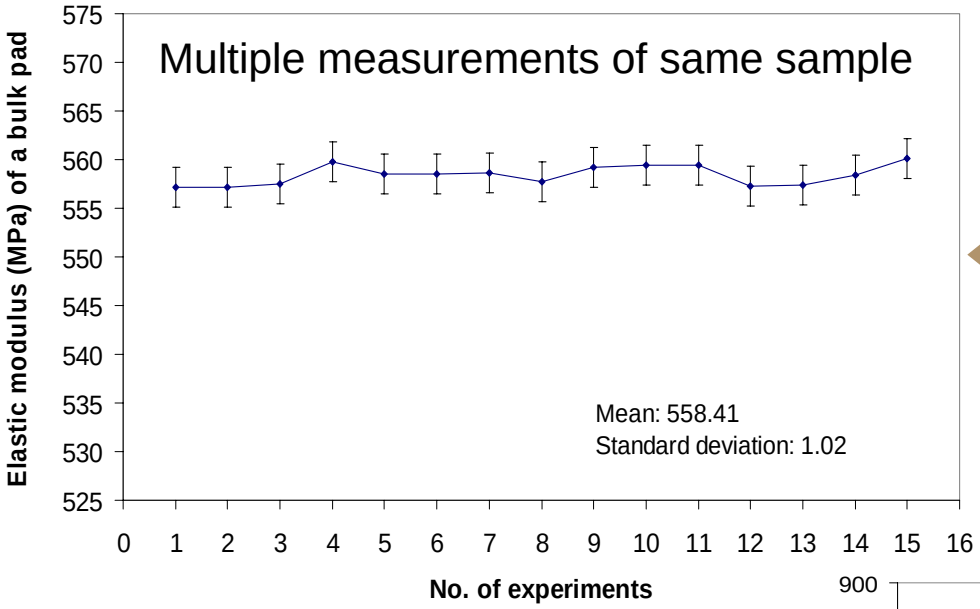

Variations in modulus of bulk pad not affected by number of measurements

Variations in modulus of bulk pad not affected by sample

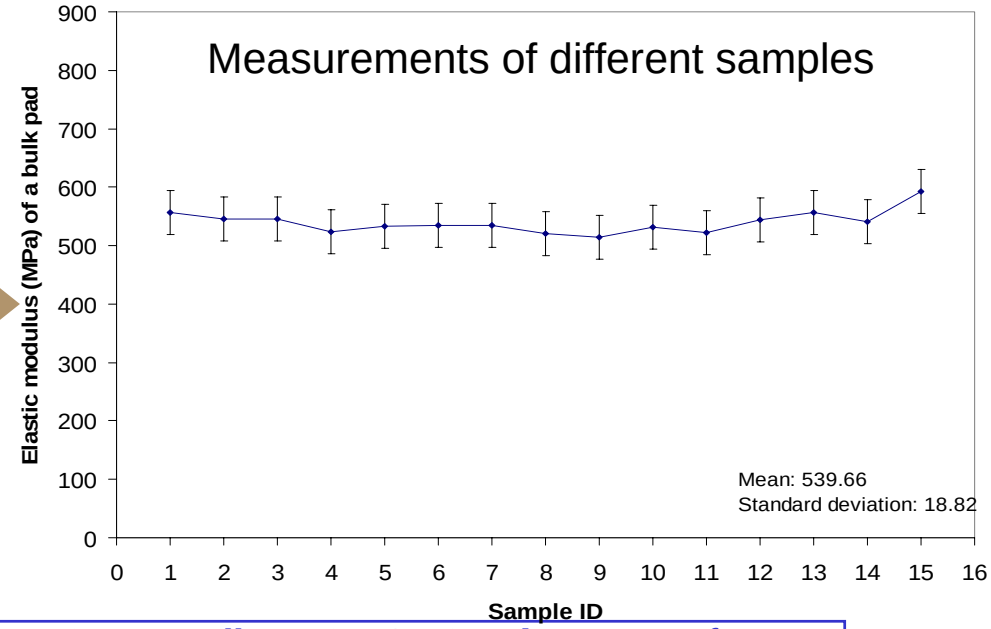

Measured Elastic Modulus in Compression

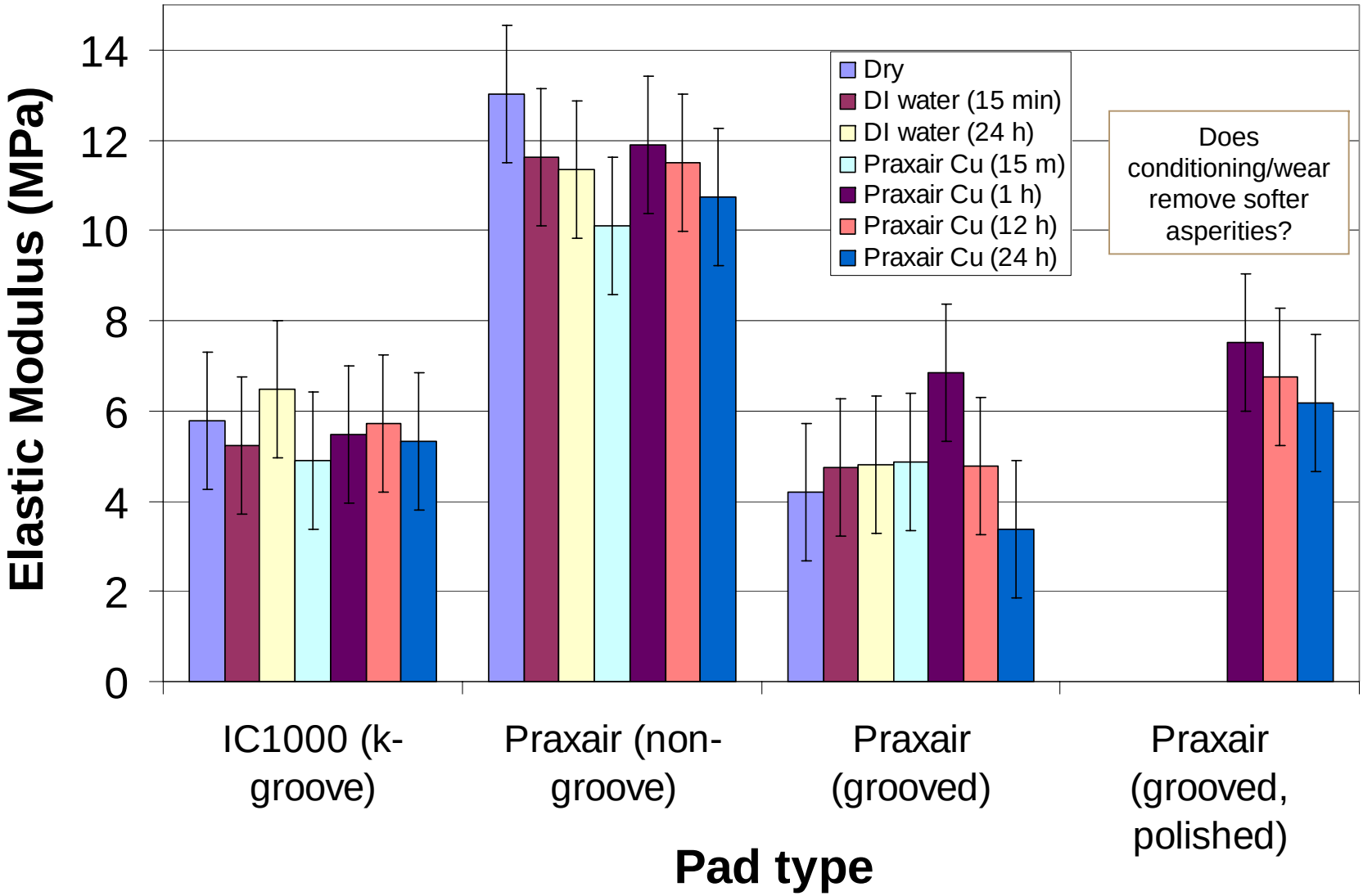

Reproducibility: Elastic Modulus in Compression

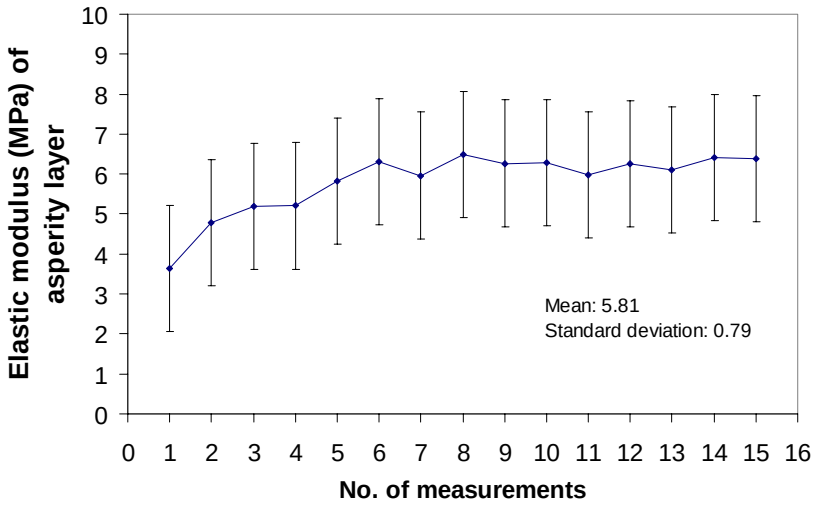

Variations in modulus of asperities not significantly affected by number of measurements

Variations in modulus of asperities not affected by sample

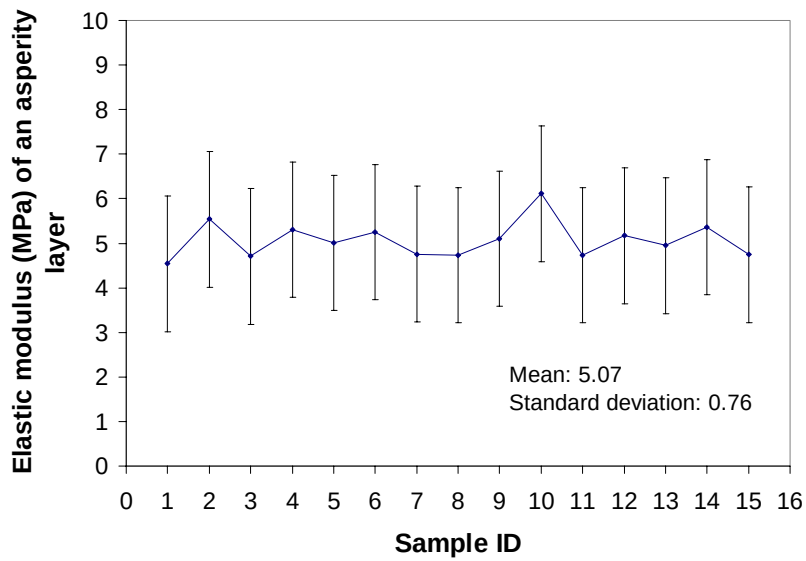

Interpretation: Pad Behavior

- Asperity layer and bulk pad studied
  - Effects of cyclical loading during CMP, soaking in slurries, and soaking in aqueous solutions studied
  - Asperity layer
    - ✓ Pad asperities undergo minor changes
    - ✓ Conditioning/polishing wear may increase effective modulus slightly
  - Bulk pad
    - ✓ Core region of pad becomes softer (lower modulus) with increased exposure to slurry, aqueous solution, or polishing
    - ✓ Polishing accelerates reduction in modulus
- Implications
  - Pad conditioning may influence load/asperity, but may not influence mechanical properties of individual asperities
  - Pad break-in periods may reflect combined evolution of pad bulk modulus and pad asperity contact area

Ongoing Work, Interactions, Acknowledgements

- Ongoing work
  - ➢ Studies of electrochemistry on Cu surfaces during CMP
    - Rotating disk electrode
    - Impedance spectroscopy
      - Higher resolution at shorter time scales
      - Describe local electric field effects during CMP
  - Measure mechanical properties of surface of wafer
    - Copper and Black Diamond
    - Roughness and mechanical properties
- Industrial Collaboration
  - Praxair Microelectronics, Rohm and Haas
- Acknowledgments
  - NSF/SRC Engineering Research Center for Environmentally Benign Semiconductor Manufacturing
  - State of Indiana 21st Century Fund
  - Praxair Electronics

Thrust B1: Surface Chemistry of High-k Barrier Layer Formation

Adam Thorsness, Shariq Siddiqui, and Anthony Muscat

Department of Chemical and Environmental Engineering

University of Arizona, Tucson, AZ 85721

agt@u.arizona.edu

NSF/SRC ERC EBSM Annual Review

Feb. 2006

Outline

- Motivation and ESH Impact
- Research Cluster Apparatus and Process Flow
- UV-Cl_2 Process to create a Cl-terminated Si(100) surface from SiH and SiH_2 terminated surfaces.
- Water reactivity with activated Cl-terminated Si(100) surface
- Detailed surface analysis of the silicon oxides resulting from H_2O(g) + SiCl(a) reaction.

Gate-Last MOSFET Process with Additive Patterning

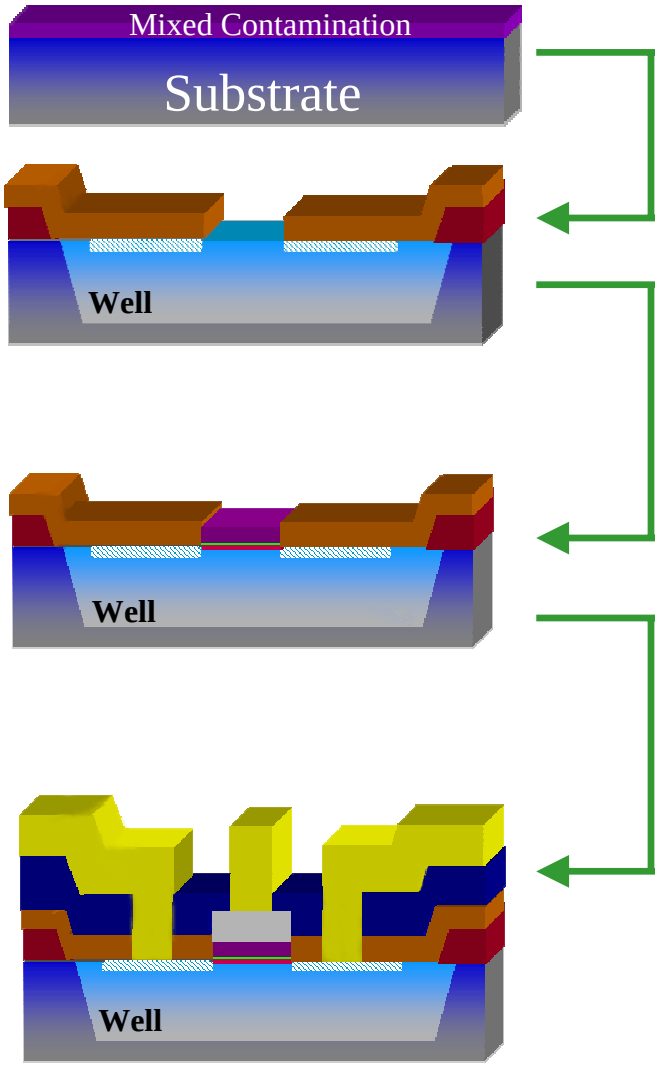

Clean, grow field oxide, pattern device area (Mask 1), ion implant (M2), deposit spacer oxide, pattern gate area (M3)

Selectively deposit barrier layer, high-k seed layer, and high-k dielectric layer

Deposit gate metal, pattern (M4), deposit metal isolation dielectric, pattern (M5), deposit metal 1 layer, pattern (M6)

ESH Impact

- Gas phase processing requires less chemical usage than liquid processes by several orders of magnitude.
- Integrate process into a single vacuum cluster tool.
- Low temperature method of forming a single silicon oxide layer means lower energy usage.

Research Cluster Apparatus

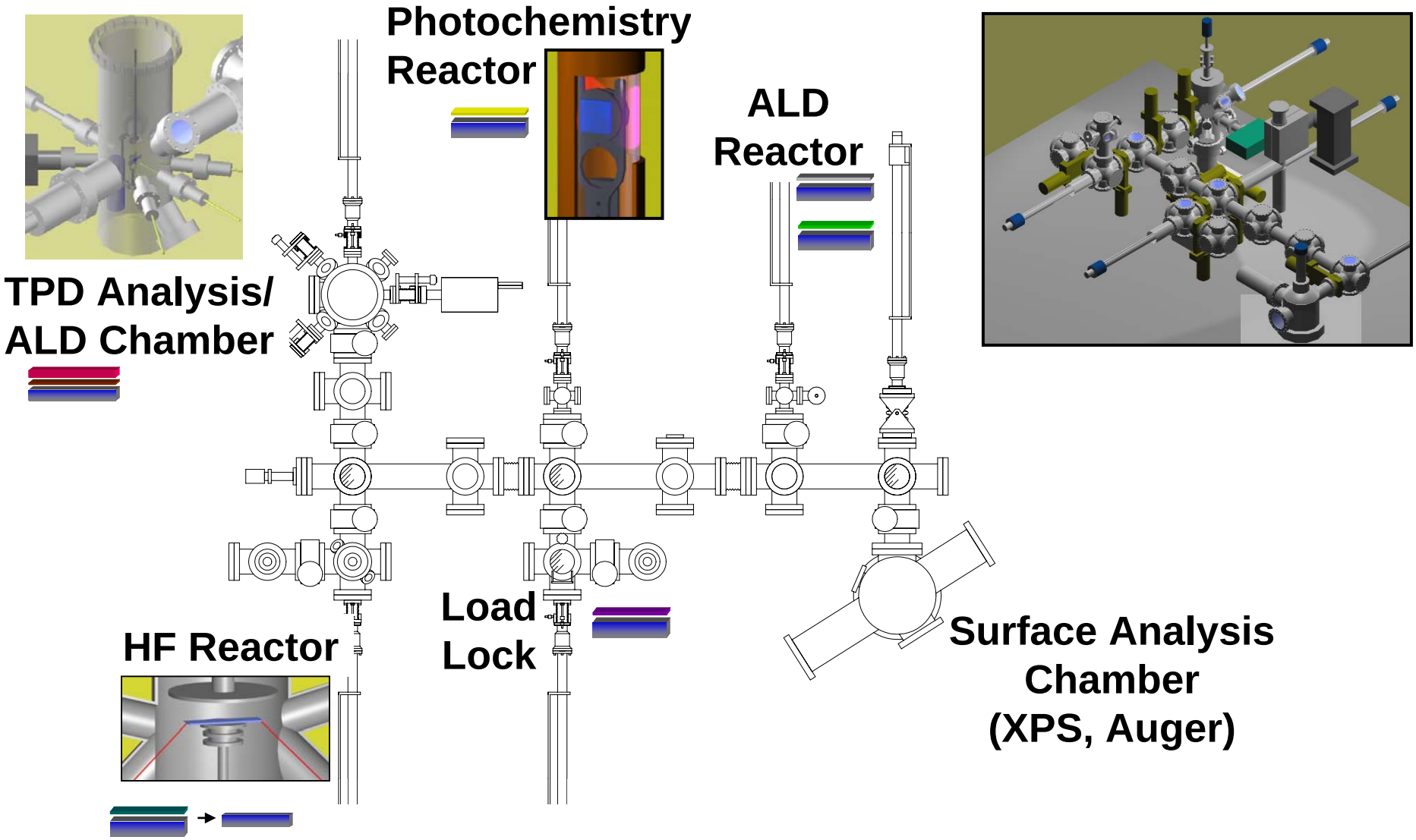

Example of Controlled Starting Surface for ALD

- Focus of this presentation
  - UV/Cl_2 to create a Cl-terminated Si surface
  - H_2O exposure to create SiOH groups or a silicon oxide surface
- Advantages
  - Low temperature process
  - Self-limiting/Controllable formation a uniform oxide and OH-termination

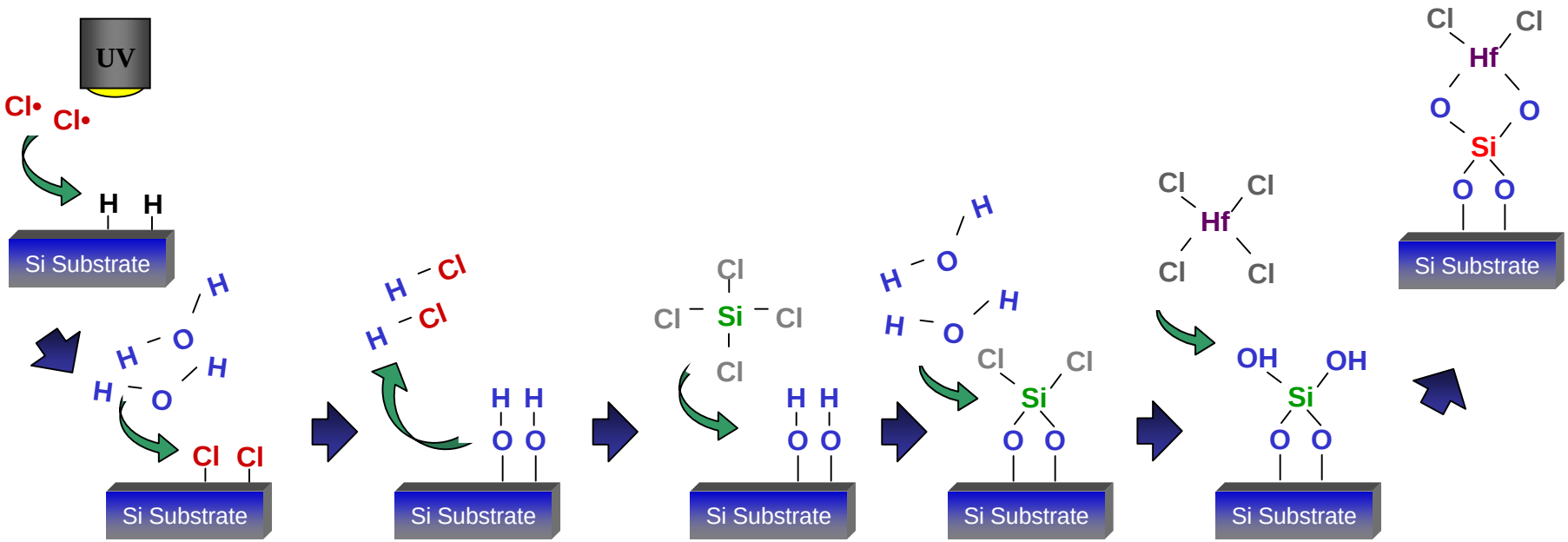

A UV/Cl_2 Process Replaced All Surface H With Cl Atoms

- H_2 desorbs from SiH and SiH_2 surface species after a **dilute HF clean** from an Si(100) surface
- H_2 desorbed from Si(100) surface exposed to **Dark/Cl_2 process**
  - *T = 300 K, 10% Cl_2 at 100 Torr, 5 min*
- No H_2 desorbed after **UV/Cl_2 process** indicating that all H atoms were replaced by Cl atoms.
  - *T = 300 K, 10% Cl_2 at 10 Torr,* 40 sec

Si(100): H_2-TPD

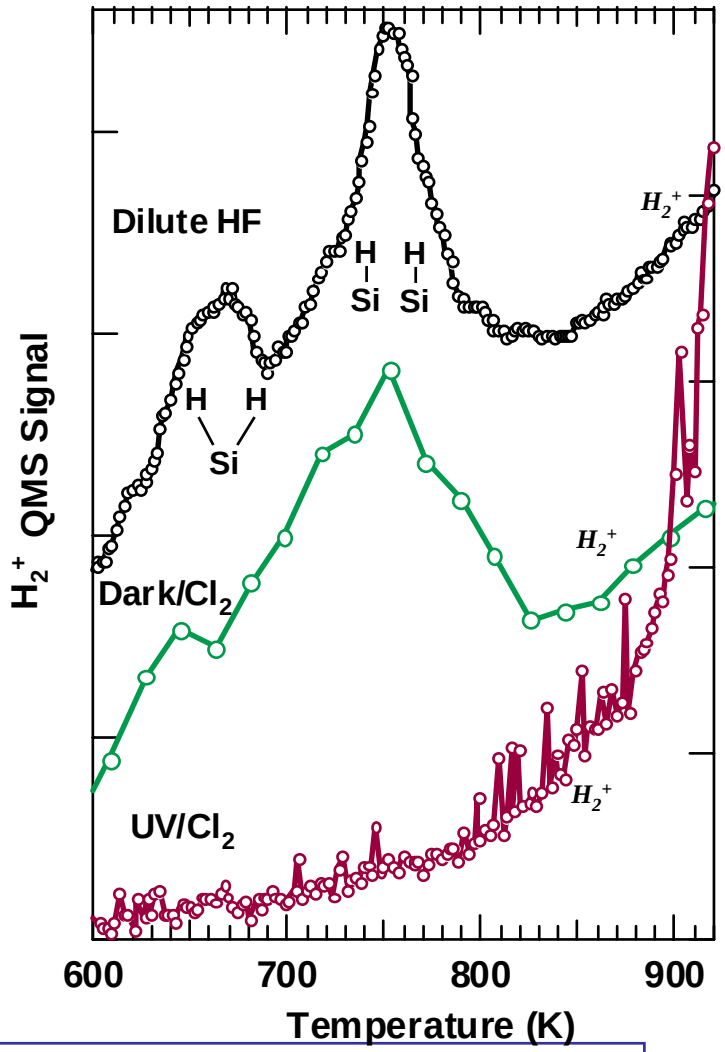

Only Silicon Monochloride on the Surface

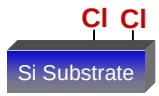

- **No $SiCl_2$ or $SiCl_3$**
- **Cl 2p shift between SiCl**
- **and $SiCl_2$ is 1 eV**
- **Symmetric decrease in the Cl 2p Peak**

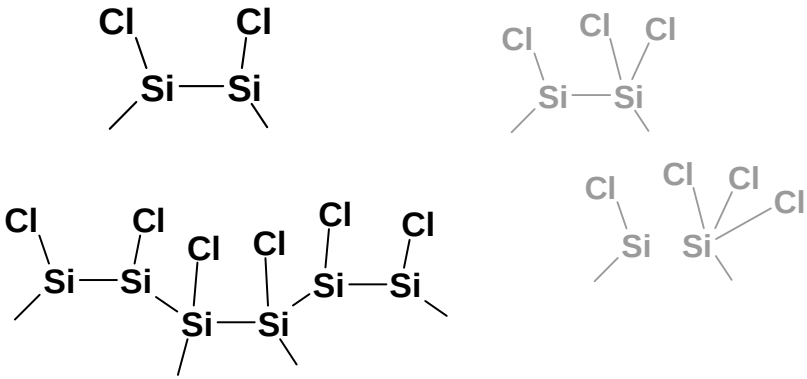

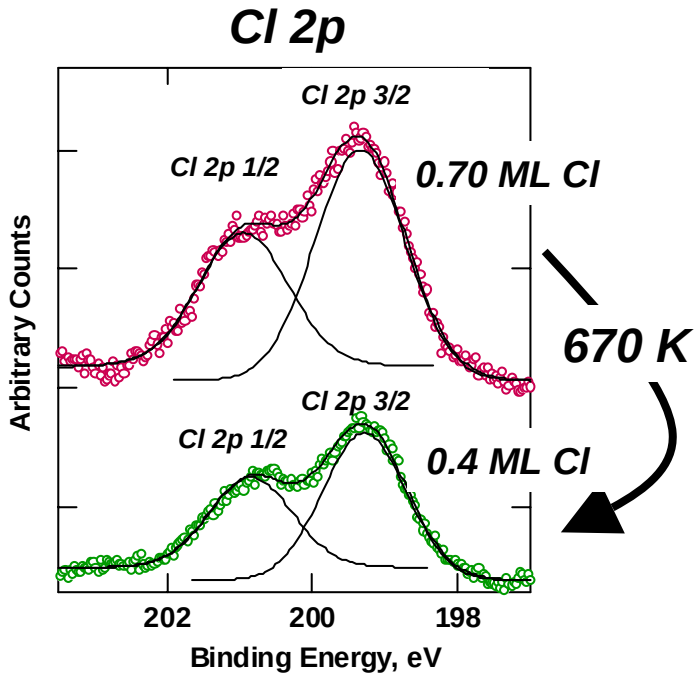

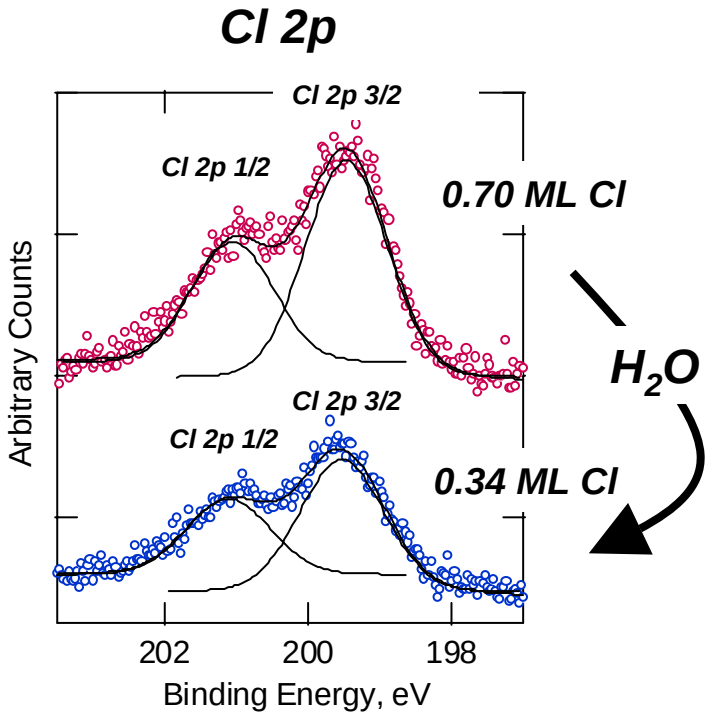

Flash-UV-Cl_2 Exposure

- 0 – 1 second of UV exposure results in H_2 desorption.
- Need at least 2 seconds of UV to displace all Si-H.

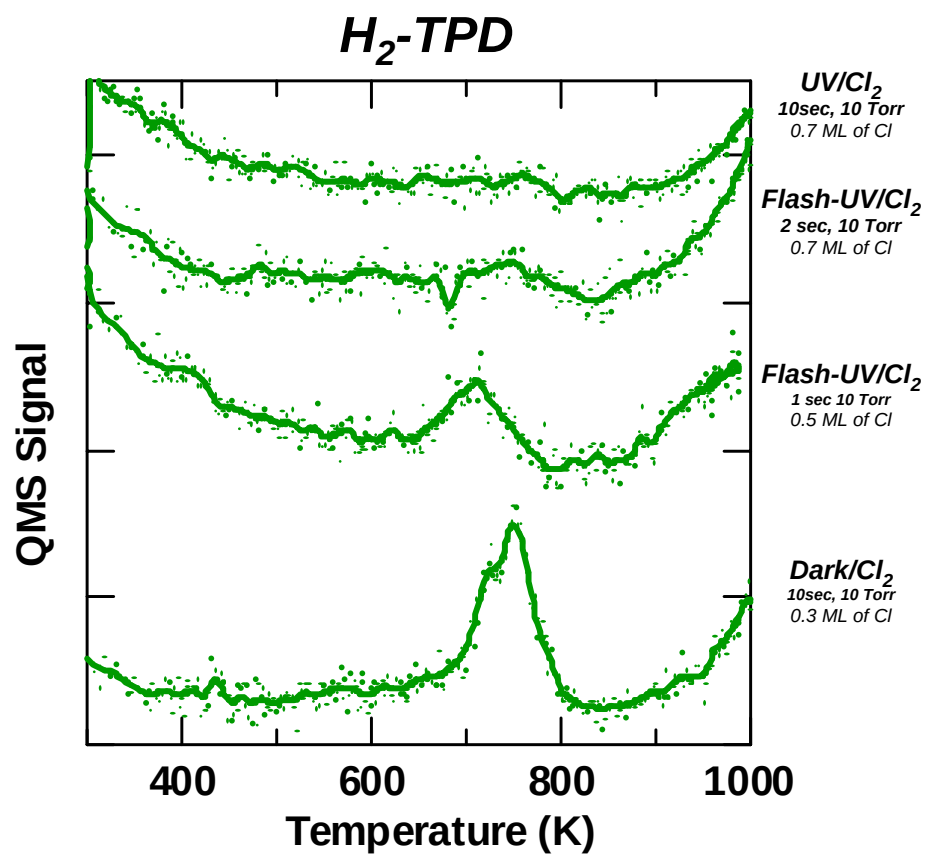

Process: 10%Cl2 in N2 gas at 10 Torr and 25°C for 10 seconds.

More O on a Cl/Si(100) Activated Surface

- H_2O exposure of non-activated surface results in only 0.2 ML O added.
- Cl activates surface for reaction with H_2O gas.
  - 0.83 ML – 1.2 ML added

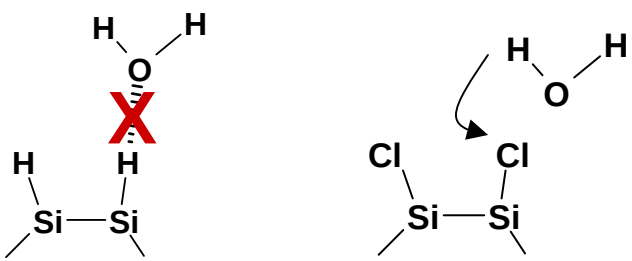

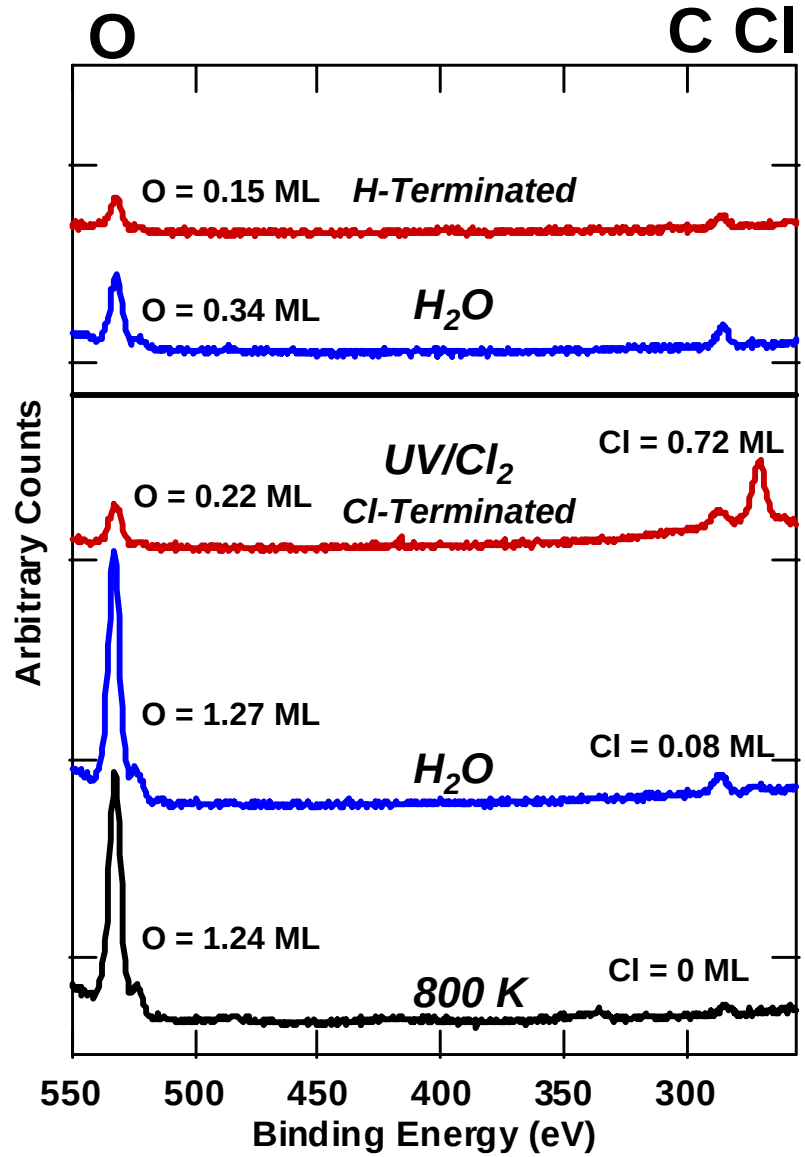

No Increase in O After Cl is Removed

- O addition in the short term is determined by the presence of Cl on the surface.
- No increase in O after Cl is removed.

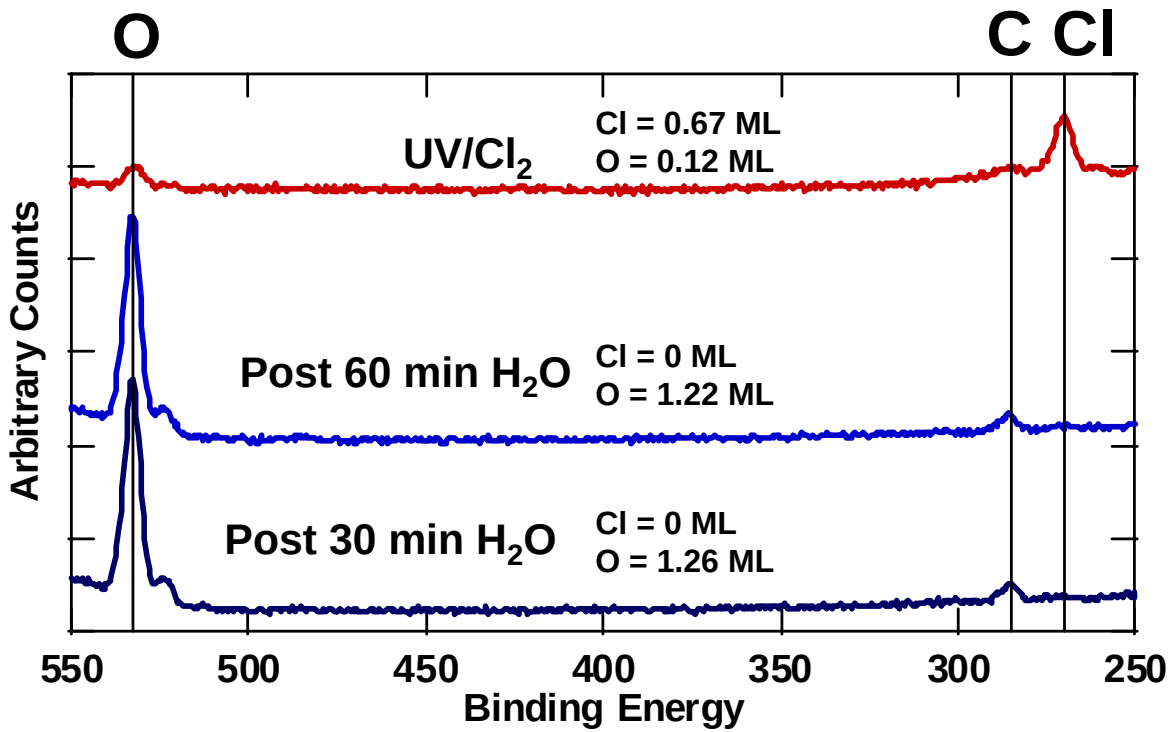

Addition of O and Removal of Cl

- 1.5 O added to 1 Cl removed

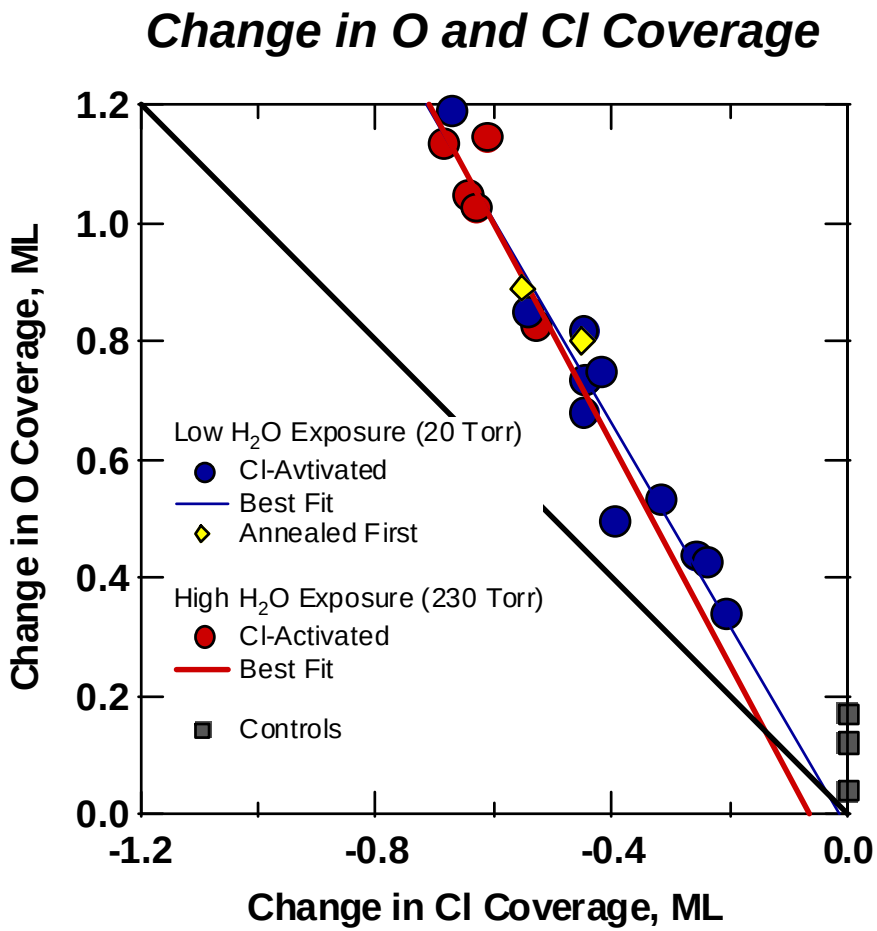

- Stable in atmosphere
  - Only a 0.2 ML increase in O after 14 hours.

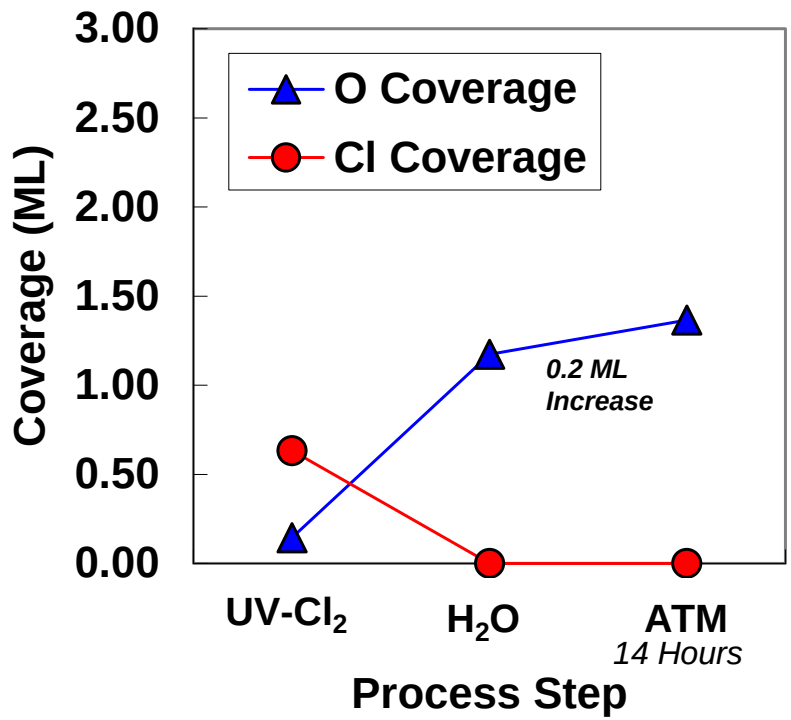

Oxygen in Si Backbonds and Different Suboxides Created

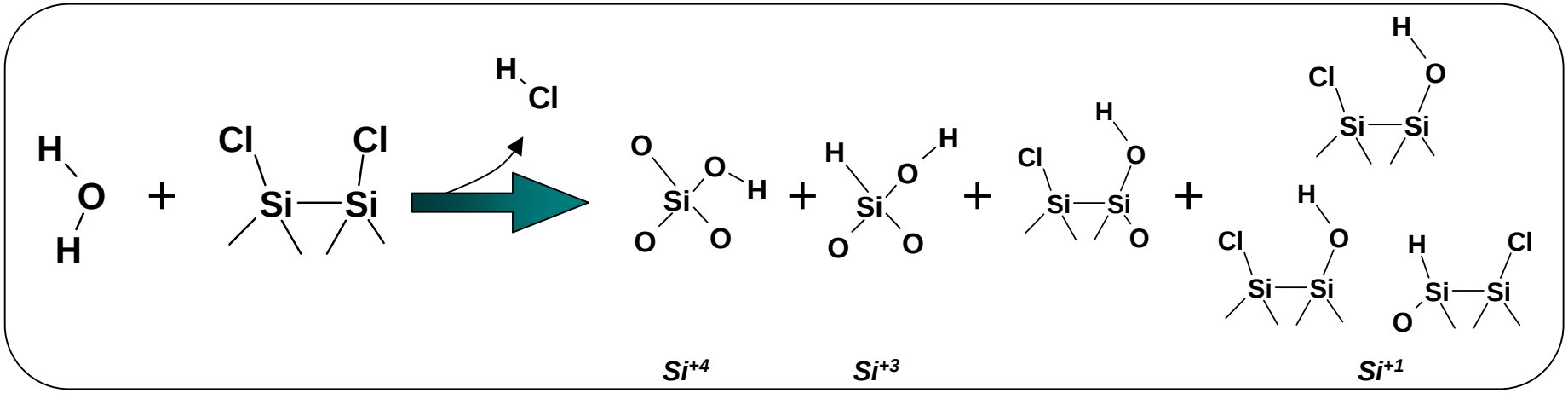

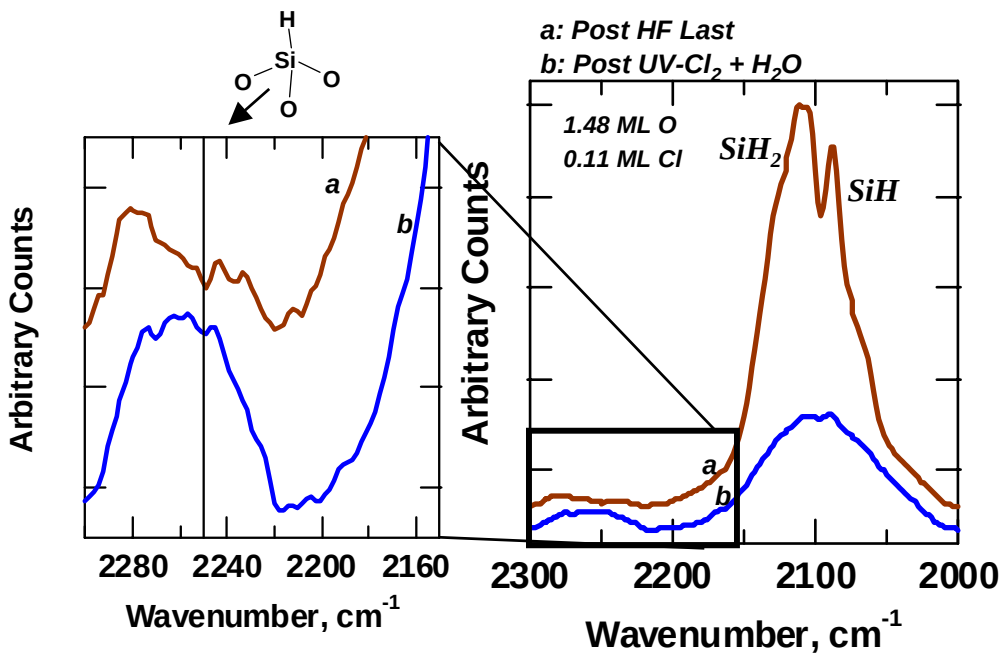

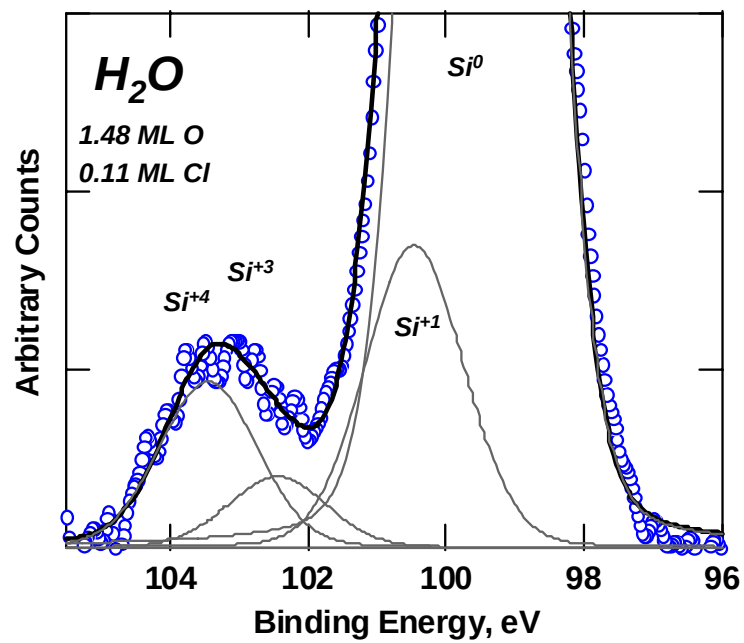

Summary/Conclusions

- Activated surface with halogen for low T interface growth
  - Obtained Cl-terminated Si surface from a UV-Cl_2 process
  - Cl interacted with all Si-H and SiH_2 on the Si(100) surface.
  - Only monochloride formed on the Si(100) surface during UV-Cl_2 process.
  - No H remaining on surface.

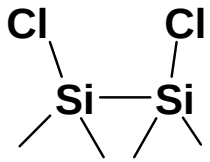

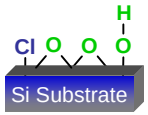

- Deposited single layer of silicon oxide
  - O atoms detected on the surface after water exposure stable up to 800 K. (no decrease in O coverage)
  - Ratio of 1.5 O atoms were added for every 1 Cl removed.
  - O in the Si backbonds
  - SiO_x where x = 1 – 4 exist after water exposure.

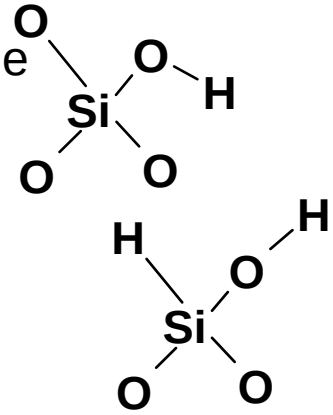

Future Plans

- Investigate parameters for manipulating Si^{+1} and SiO_2 (Si^{+4}) formation.
  - More ideal Cl-terminated surface combined with low H_2O partial pressures.

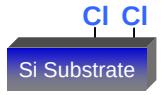

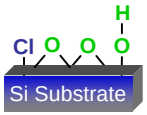

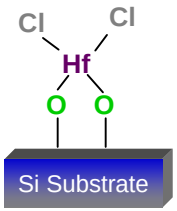

- Deposit high-*k* on thin oxide and perform electrical (CV) measurements on MIS capacitors.

- Activate high mobility substrates

Acknowledgments

- NSF/SRC Engineering Research Center for Environmentally Benign Semiconductor Manufacturing Funding

Improvement of NBTI of High-*k* by Incorporation of Fluorine

Kang-ill Seo

Raghavasimhan Sreenivasan

Paul. C. McIntyre

Materials Science & Engineering, Stanford University

Krishna. C. Saraswat

Electrical Engineering, Stanford University

Task B-2

Selective Surface Preparation and Templated Atomic Layer Film Deposition: Novel Processes for Environmentally Benign Transistor Gate Stack Manufacturing

NSF/SRC Engineering Research Center for Environmentally Benign Semiconductor Manufacturing

NBTI in MOS devices

- What is Negative Bias Temperature Instability (NBTI) ?

➔ Generation of interface traps (ΔD_{it}) and positive charges (ΔQ_f) under negative gate bias especially in elevated temperature.

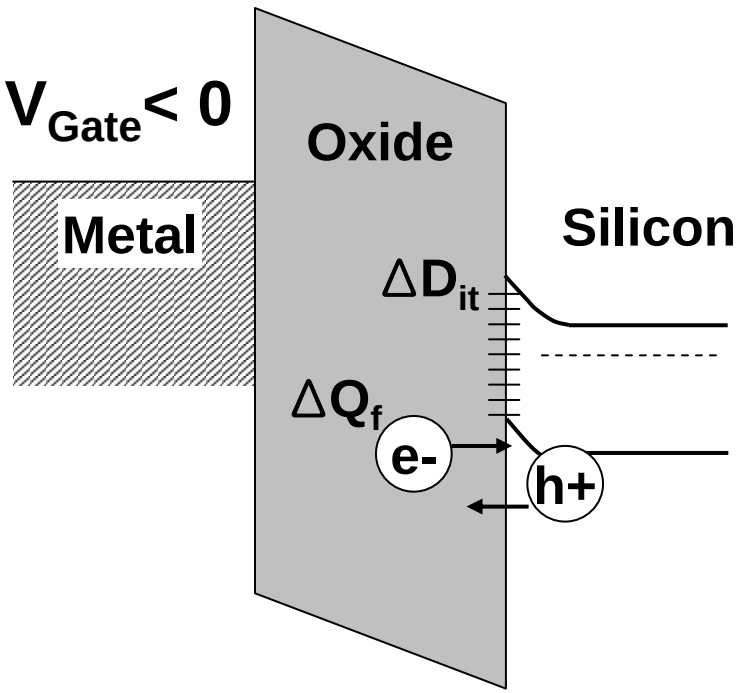

➔ $V_T \uparrow$, $I_{off} \uparrow$, $I_{Dsat} \downarrow$, $g_m \downarrow$ in p-channel MOS with time

$$\Delta V_T = q\,(\Delta Q_{it} + \Delta Q_f)\,/\,C_{ox}$$

R-D model for ΔD_{it} & ΔN_P in SiO_2/Si(001)

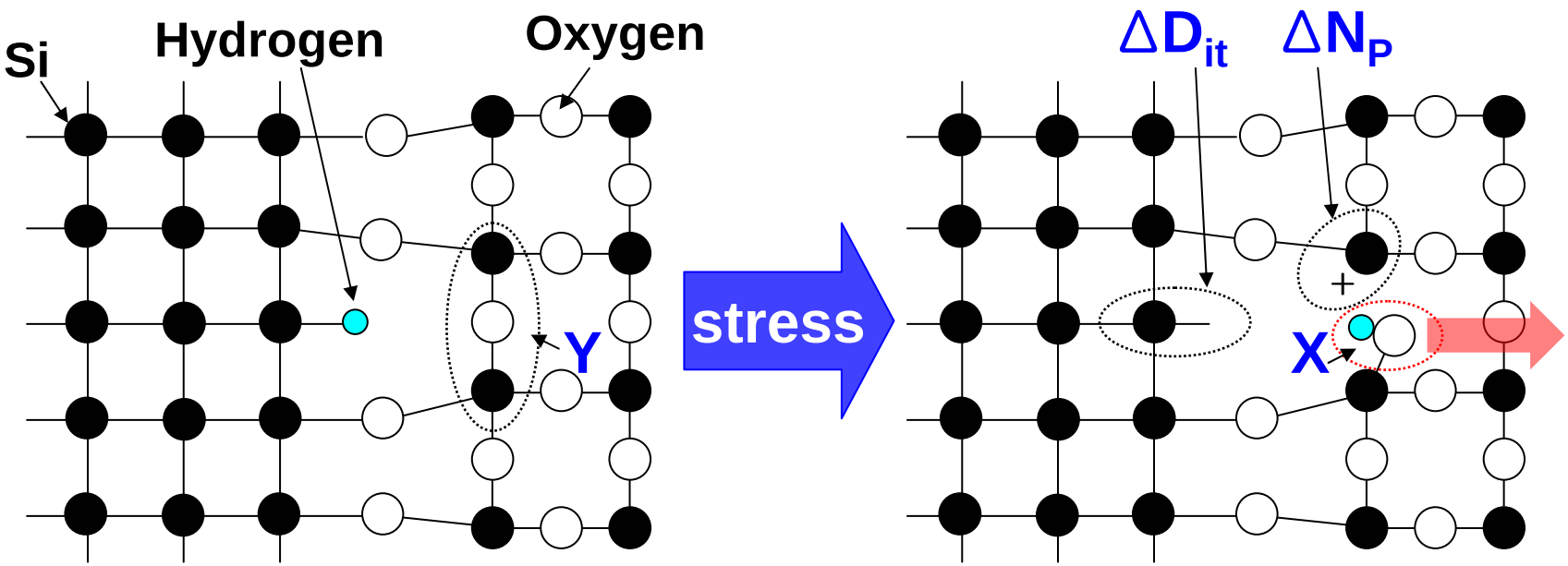

- Reaction; $\underbrace{Si_3{\equiv}Si\text{-}H}_{\text{H passivated defect}} + Y \rightarrow \underbrace{Si_3{\equiv}Si\bullet}_{D_{it}} + \underbrace{O_3{\equiv}Si^+}_{Q_f} + X_{interface}$
- Diffusion; $X_{interface} \leftrightarrow X_{bulk}$
- Y = (Si-O-Si + h^+), (H_2O + h^+), h^+, H^+
- X = Si-OH, H_3O^+, H^+, H_2

K. O. Jeppson and C. M. Svensson, *J. Appl. Phys.*, vol. 48, p 2004 (1977)
D. K. Schroder and J. A. Babcock, *J. Appl. Phys.*, vol. 94, p 1 (2003)

Why "F" is attractive in high-*k* ?

- "F" at the SiO_2/Si interface improves NBTI by forming Si-F (5.73 eV) bonds which are more stable against hot carrier stressing than Si-H bonds (3.18 eV).
  (Peter J. Wright and Krishna C. Saraswat, IEEE Trans. Elect. Dev. Vol. 36, p 879, 1989, and many more reports….)

- However (from many previous reports),
  - "F" enhance boron penetration through SiO_2 from p-type poly-Si gate.
  - Excess "F" increases physical thickness of SiO_2.

- "F" in "high-*k* / metal gate" system ?
  - No boron penetration problem.
  - May not suffer from increasing thickness of high-*k*.

“F” profile engineering in HfO_2/SiO_2

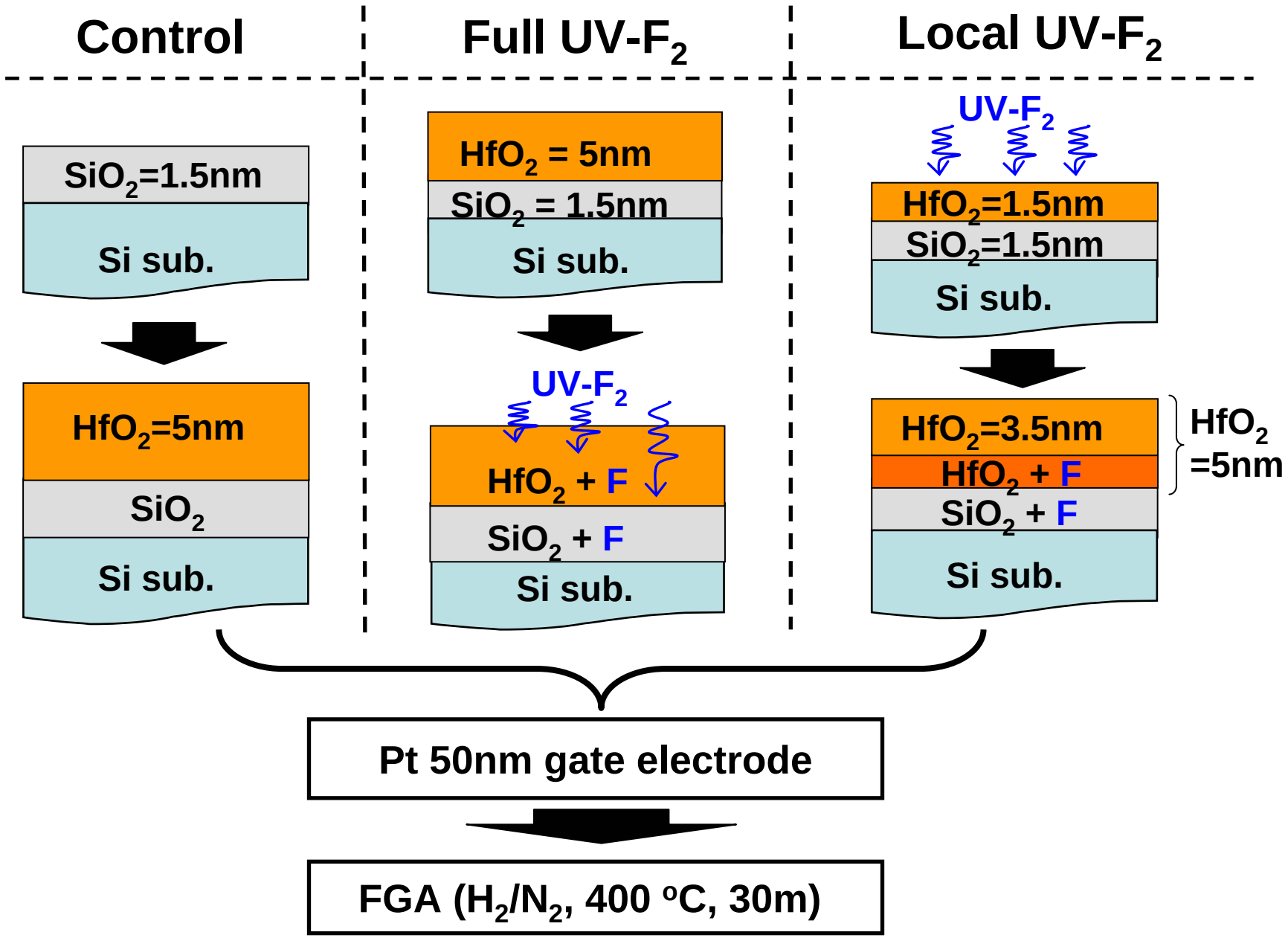

Sample structure & TEM

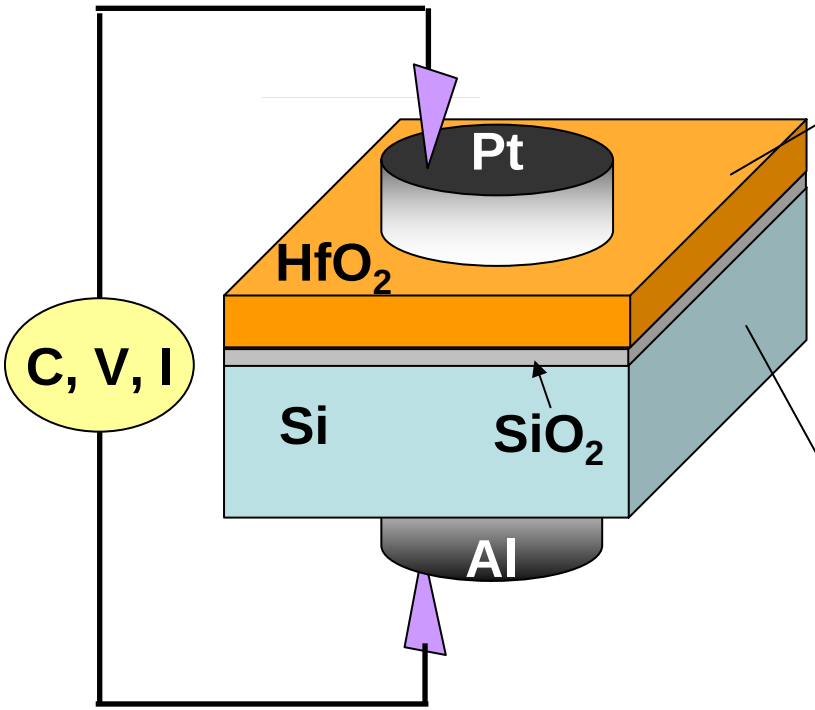

- **Cross sectional TEM (Control sample)**

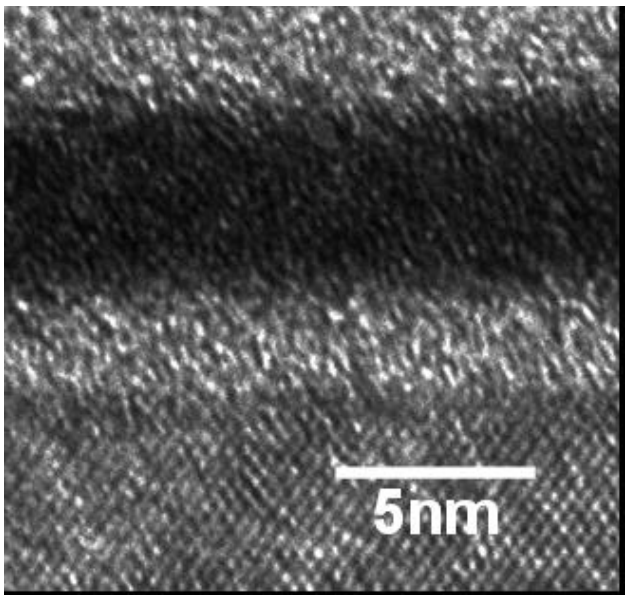

Glue

ALD-HfO_2 = ~5nm

SiO_2 = ~2nm

Si (001)

➔ **Amorphous HfO_2**
Smooth interfaces

"F" incorporation in HfO_2/SiO_2 by UV-F_2

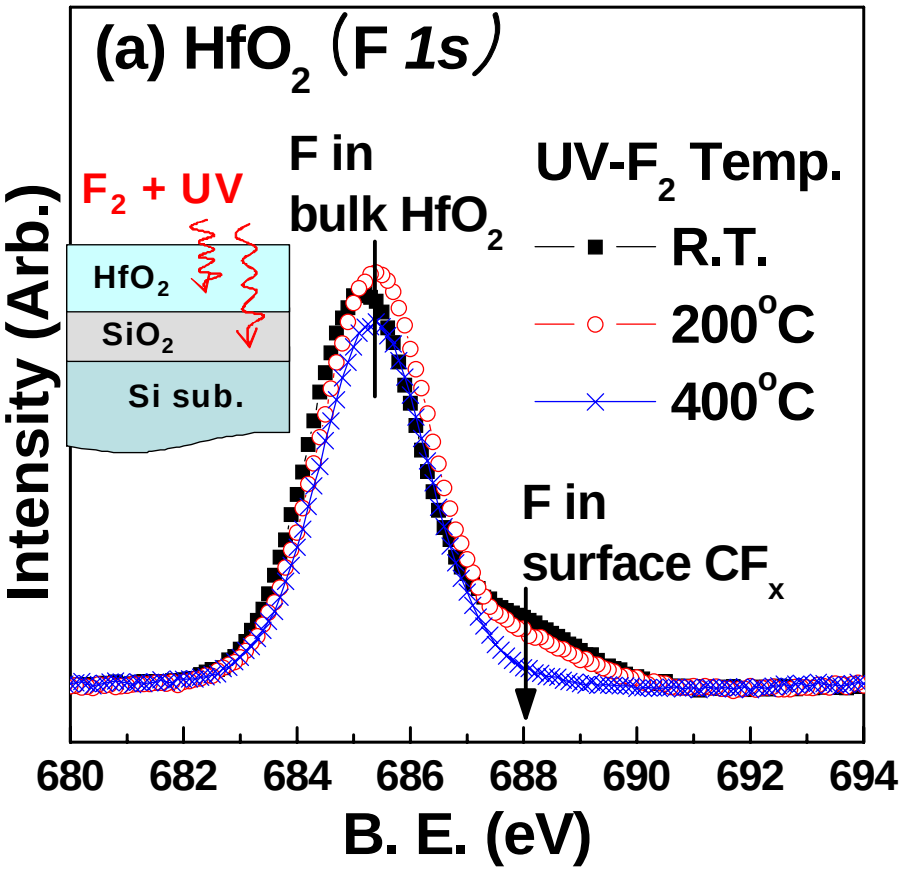

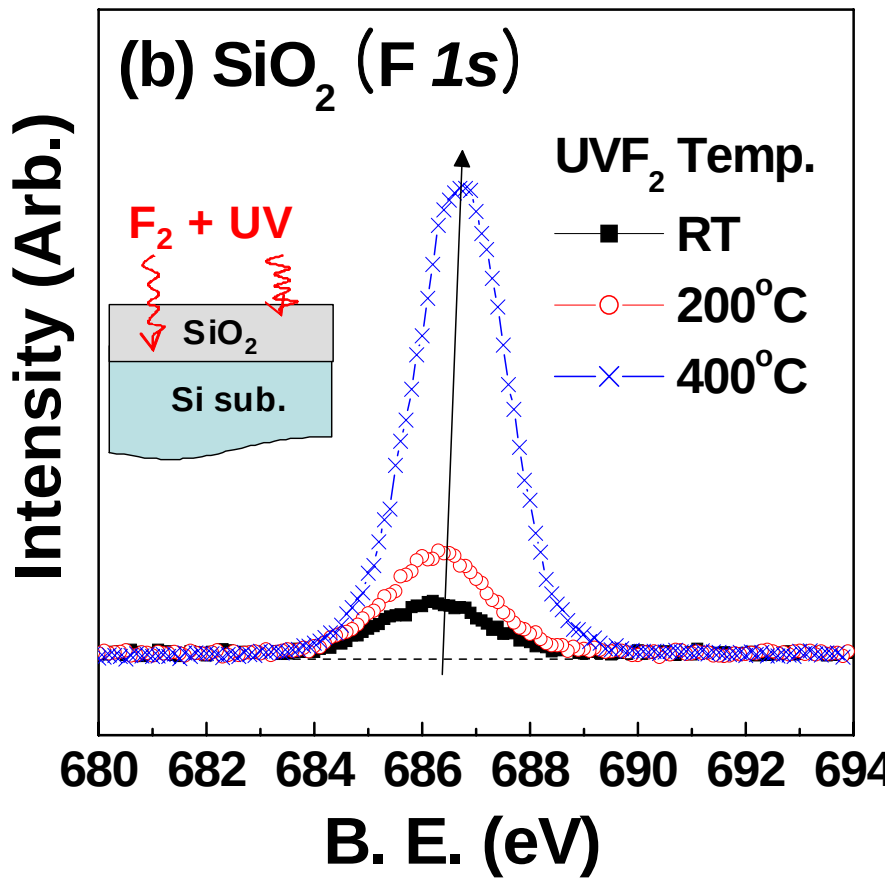

➔ "F" is easily incorporated in HfO_2 even at R.T. (~12%) and surface F species (CF_x) are suppressed as temp. ↑

NBTI of SiO_2 vs. high-*k*(HfO_2/SiO_2)

SiO_2

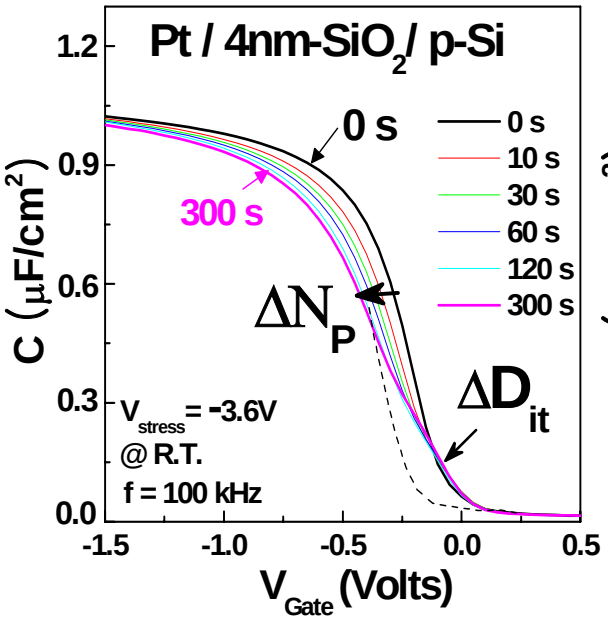

HfO_2/SiO_2

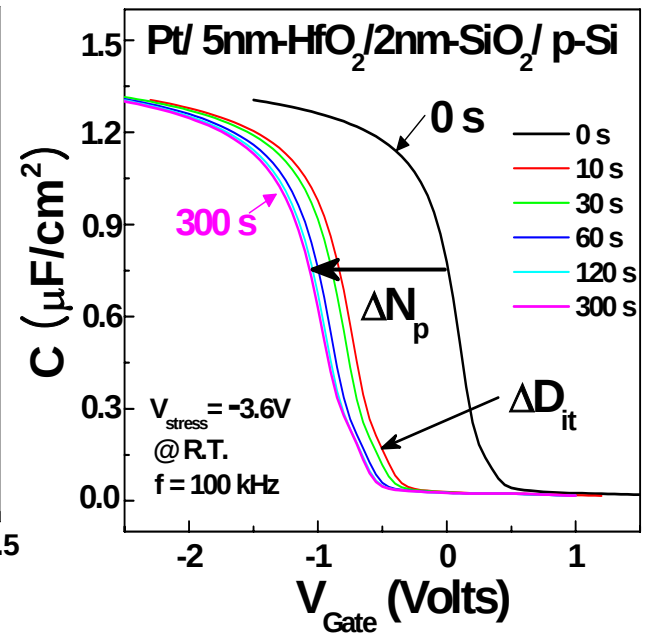

HfO_2/SiO_2 + F

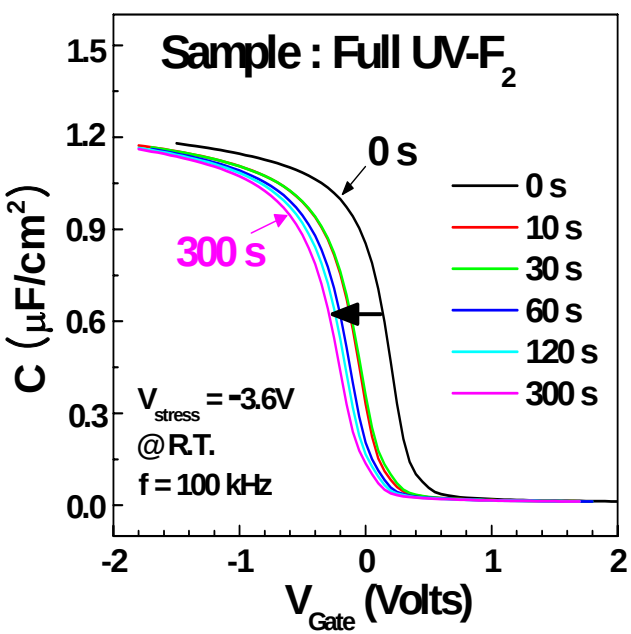

➔Larger C-V shift (ΔN_P) in HfO_2/SiO_2 compared to SiO_2 after same stress, indicating oxide charge trap sites exist either in the HfO_2 bulk or at the HfO_2/SiO_2 interface.

➔HfO_2/SiO_2 with F shows a significant reduction in ΔV_{FB} compared to the control sample.

"F" effect on ΔD_{it}

- **Conductance method for D_{it} measurement**

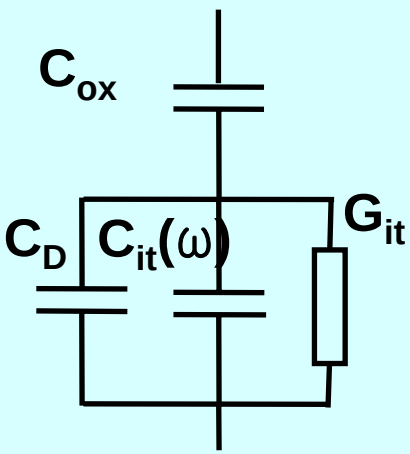

$$\frac{G_{it}}{\omega} = C_{it}\frac{\omega\tau}{1+(\omega\tau)^2} \approx qD_{it}\frac{\omega\tau}{1+(\omega\tau)^2}$$

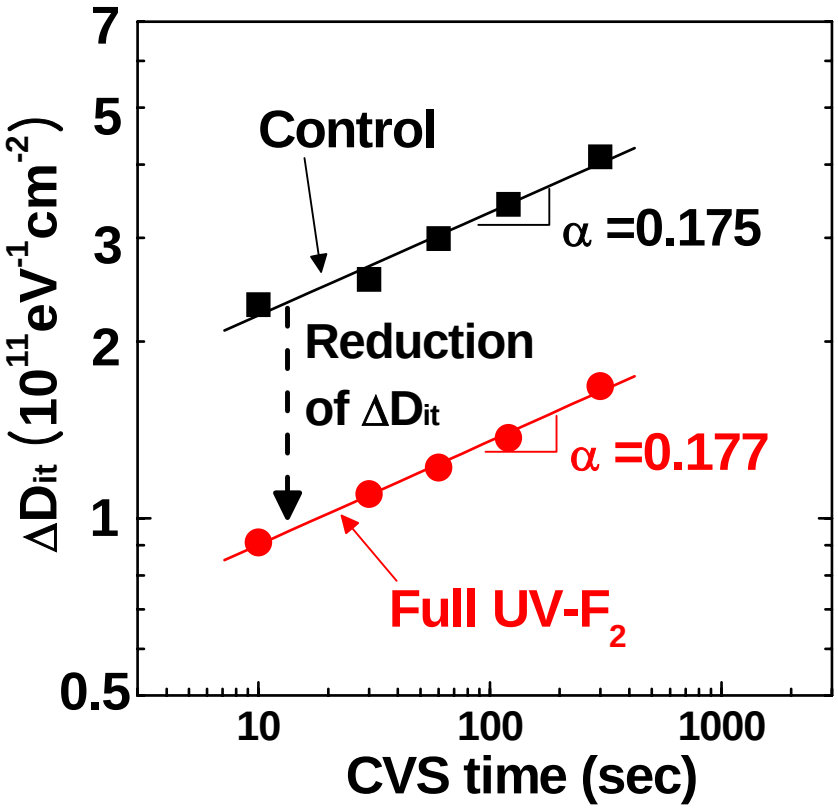

➔ **From R-D model, $\Delta D_{it} \sim t^{\alpha}$**

$$^{*}\ \Delta D_{it} = CE_{OX}{}^{s}\exp(-E_a/k_BT)t^{\alpha} \quad (\alpha = 0.25 \text{ for ideal R-D})$$

*** Shigeo Ogawa and Noboru Shiono, Physical Review B, vol. 51 p 4218, 1995**

"F" effect on ΔN_P

- $\Delta N_p = -C_{ox}\Delta V_{FB}/q$

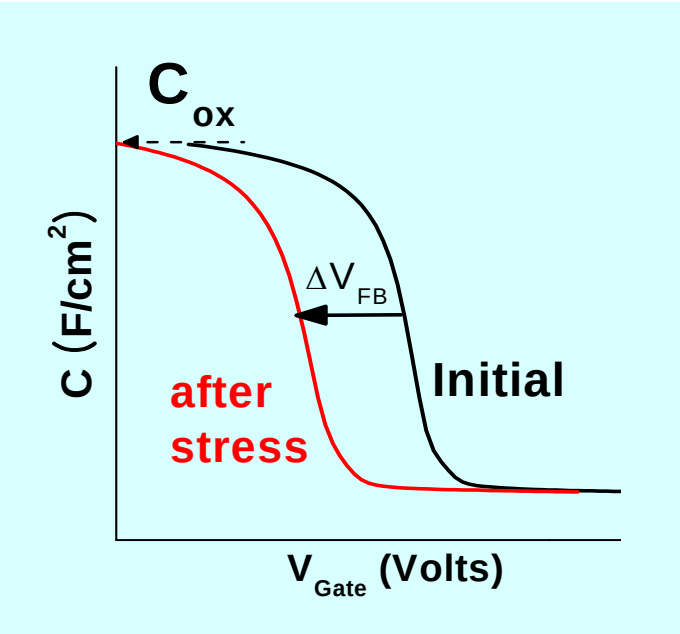

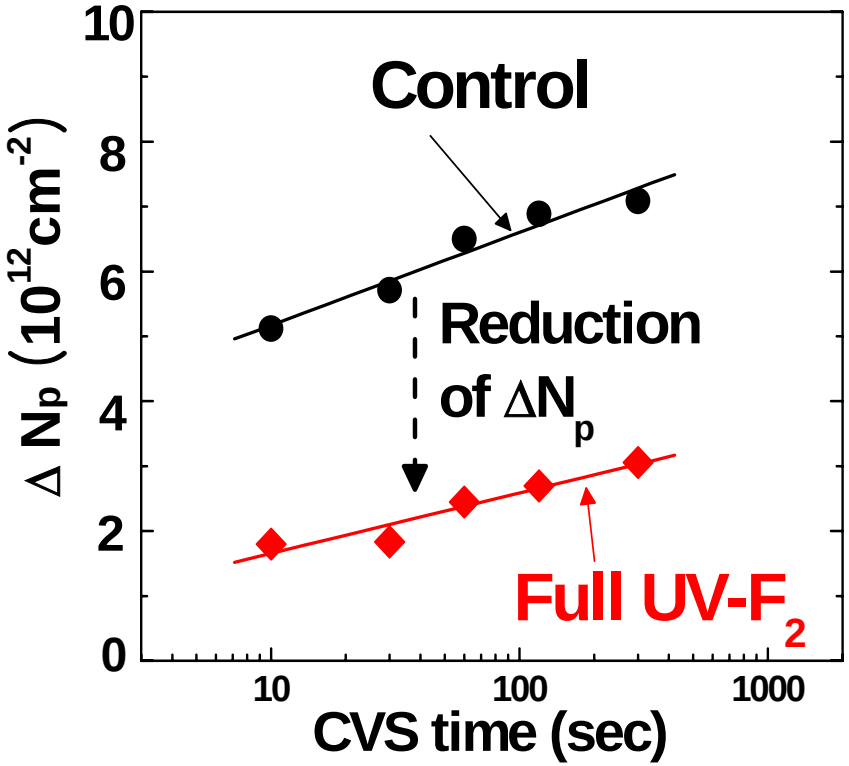

➔ $\Delta N_p \sim \log(t/t_o)^*$ & $\Delta N_p >> \Delta D_{it}$, implies that hole trapping in the oxide traps is the dominant mechanism for ΔN_P.

$$(\text{oxide defect}) + h^+ \rightarrow (\text{oxide defect})^+$$

* A. Shanware, et al, IEEE 41st Ann. Inter. Reliability and Phys. Symp., 2003

"F" SIMS profile of "Local UV-F_2"

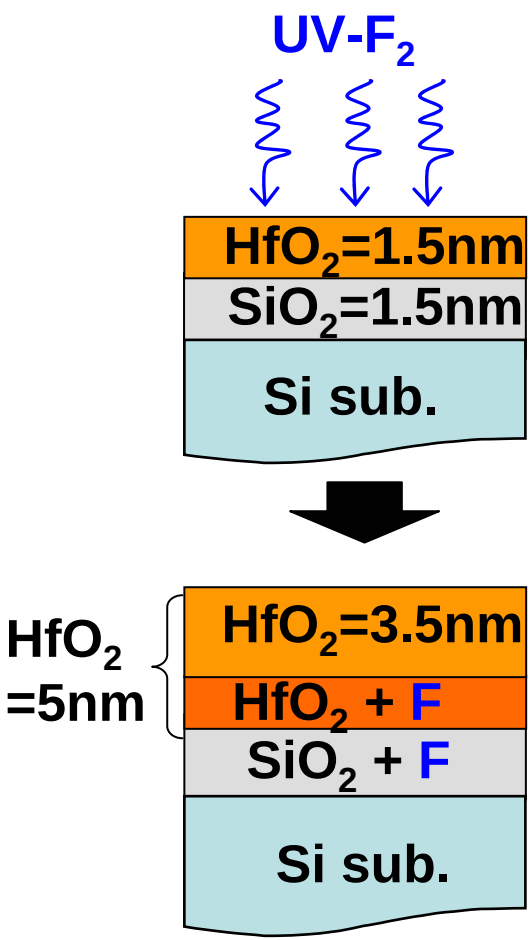

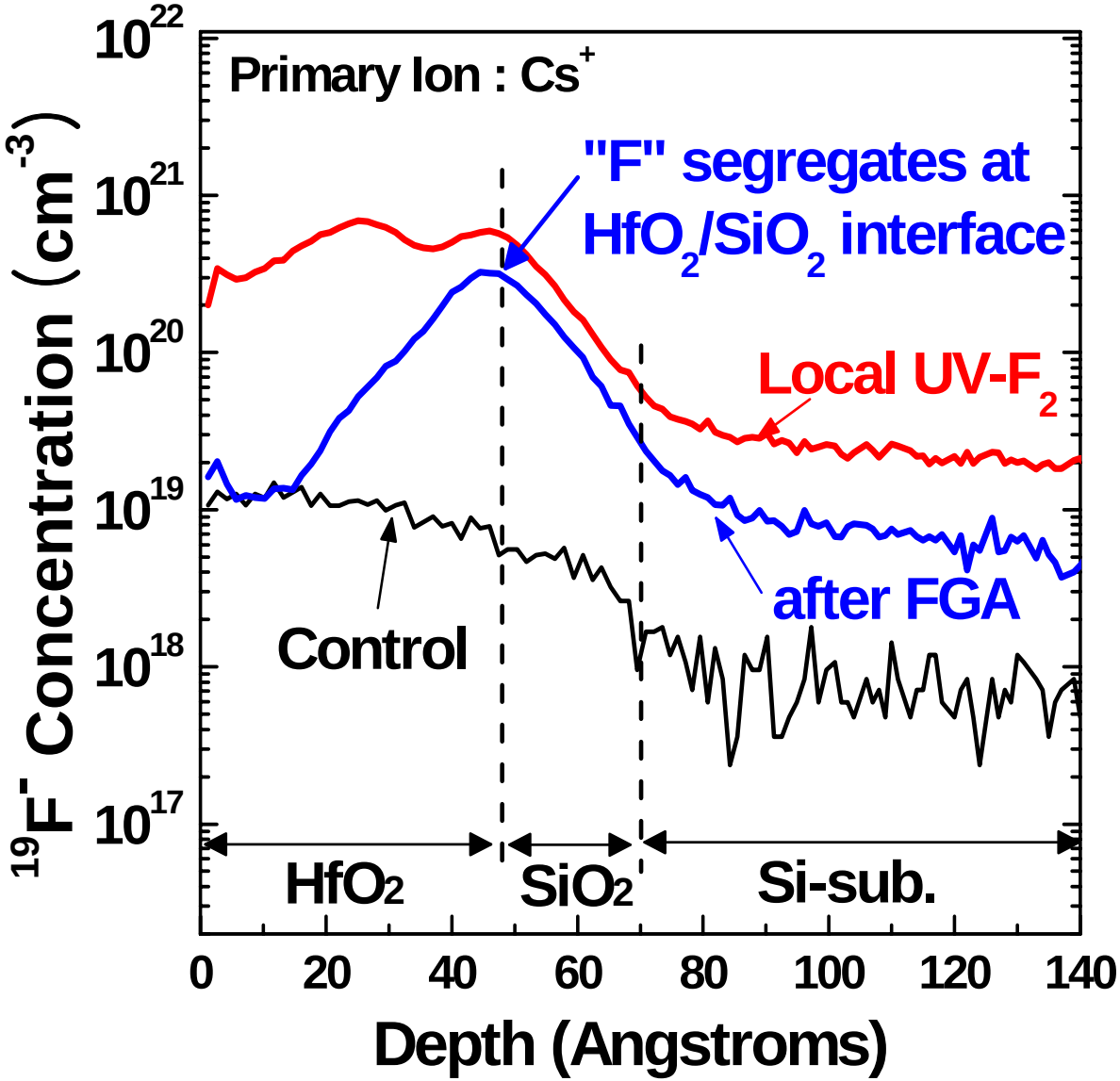

Temperature dependent ΔN_P

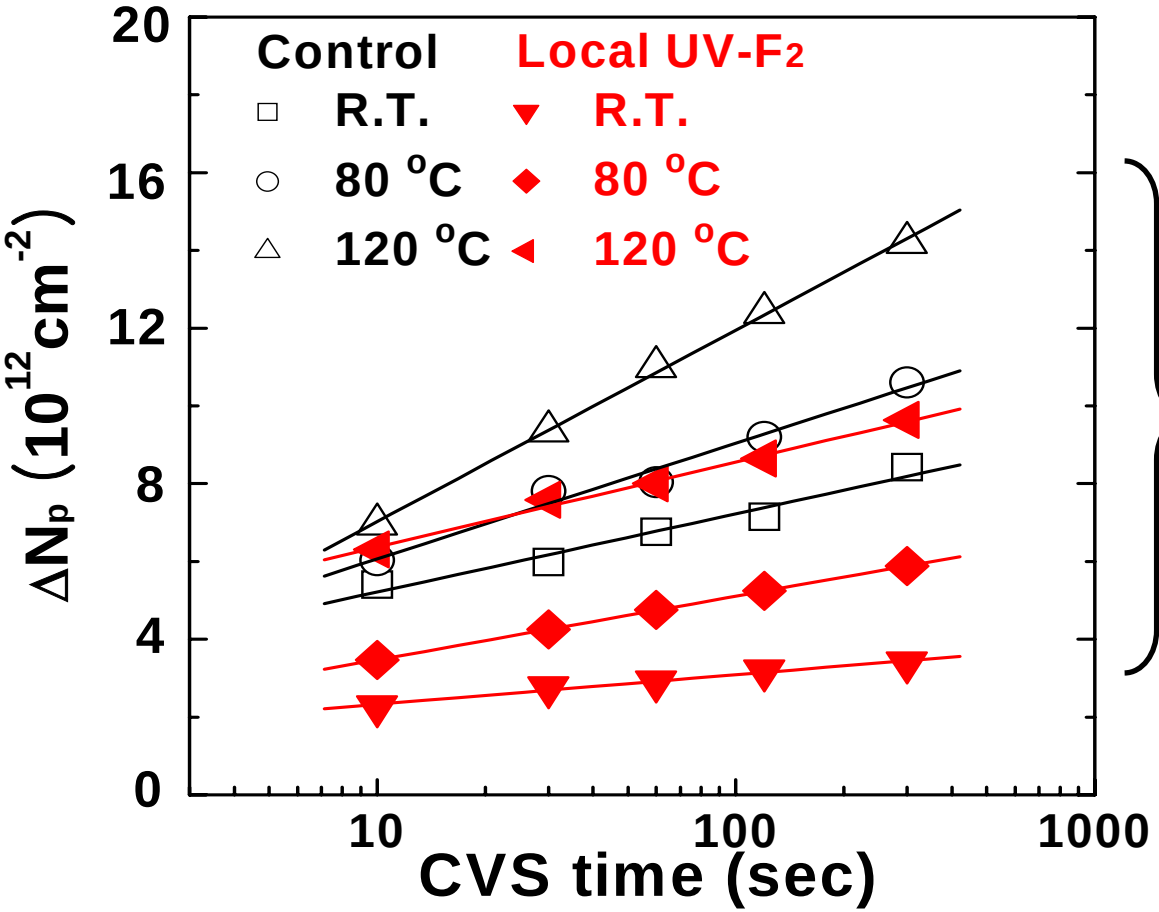

ΔN_P of the Local UV-F_2 are smaller than the Control in all temperatures measured.

$\Delta N_p \sim \log(t/t_o)$

➔ ΔN_P of the Local UV-F_2 is similar to the Full UV-F_2, suggesting charge trapping sites primarily exist at HfO_2/SiO_2 interface.

Suggested Mechanism "F" Effects

Strong Hf-F, Si-F bonds at interfaces improves reliability

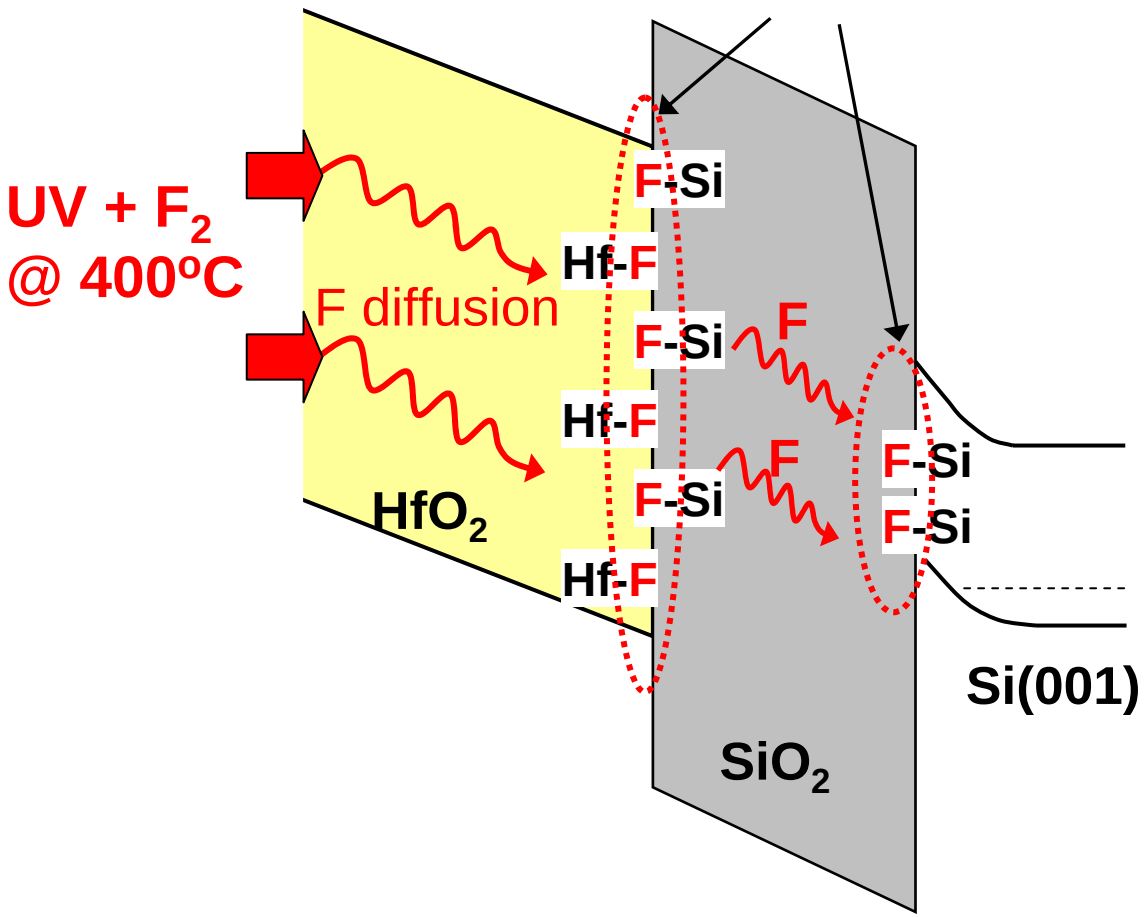

***Bond Enthalpy (KJ/mole)**

Si-H	299
Si-O	800
Si-F	553
Hf-H	?
Hf-O	802
Hf-F	650
Ti-H	205
Ti-O	672
Ti-F	569

***www.webelements.com**
J. A. Kerr, "CRC Handbook of chemistry and physics 1999-2000"

Conclusion

- **Demonstrate that "F" incorporation reduces NBTI significantly in "high-*k*(HfO_2) / metal gate" system (<50%) ; $\Delta D_{it} \downarrow$, $\Delta N_P \downarrow$, and $\Delta V_{hys} \downarrow$.**
- **Demonstrate engineering of "F" profile to segregate at HfO_2/SiO_2 and SiO_2/Si interfaces is effective in reducing NBTI without deteriorating leakage current.**

Acknowledgements

- **Prof. Yoshio Nishi and Prof. Baylor B. Triplett for helpful discussions on electrical data. Prof. Mike Kelly for helping XPS analysis.**
- **Funding: NSF/SRC Center for Environmentally Benign Semiconductor Manufacturing, MARCO Center for Materials Structures and Devices, INMP program (Stanford)**

Gate Stack Engineering by Atomic Layer Deposition

R. Sreenivasan[1], P.C. McIntyre[1], K.C. Saraswat[2]

[1] Department of Materials Science Eng., Stanford University
[2] Department of Electrical Eng., Stanford University

Thrust B, Project 2

NSF/SRC Engineering Research Center for Environmentally Benign Semiconductor Manufacturing

Ultimate Goal

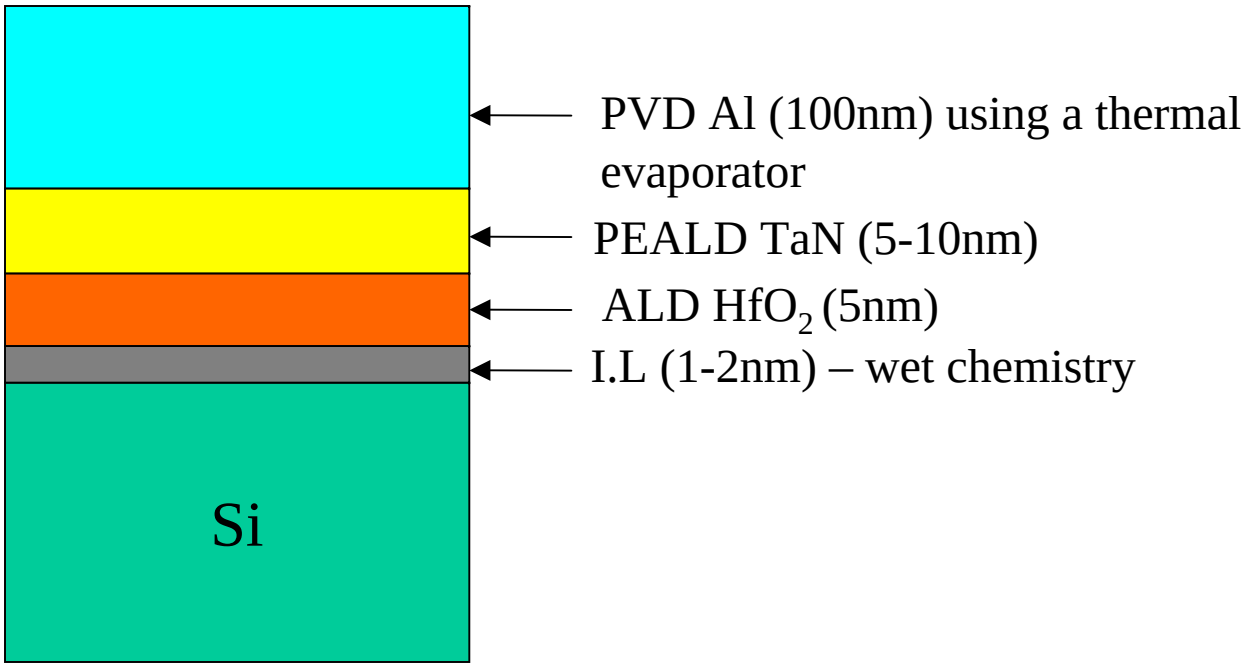

Our goal is to be able to fabricate the entire gate stack without exposure to the ambient. This process has the promise of preventing I.L growth during post processing.

Atomic Layer Deposition

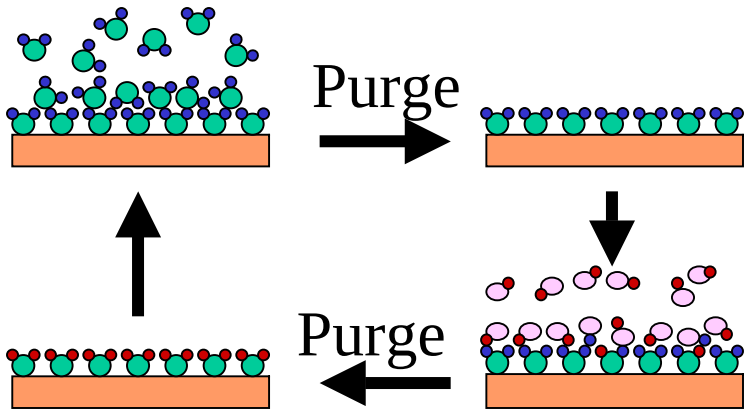

Schematic of the ALD process

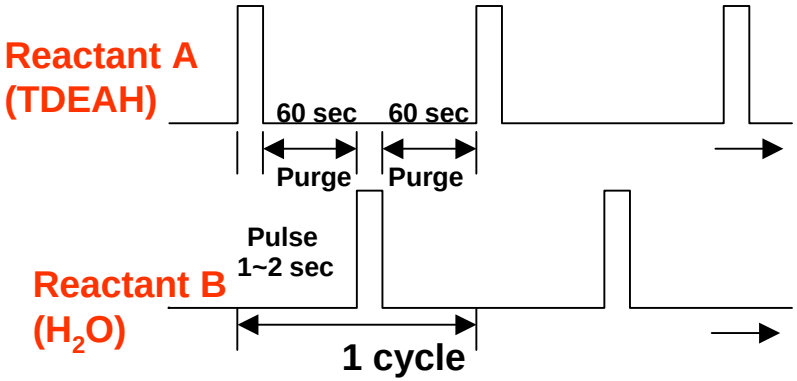

- Self-limiting growth
- Highly conformal, low defect thin films
- Very good step coverage
- Low temperature deposition
- Excellent control over film thickness
- Uniform thickness over large areas
- Good control of stoichiometry
- Abrupt interface to the substrate

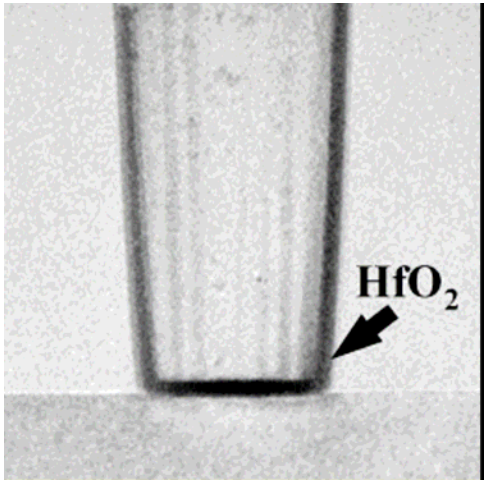

(courtesy Hyoungsub Kim)

ALD Chamber Layout

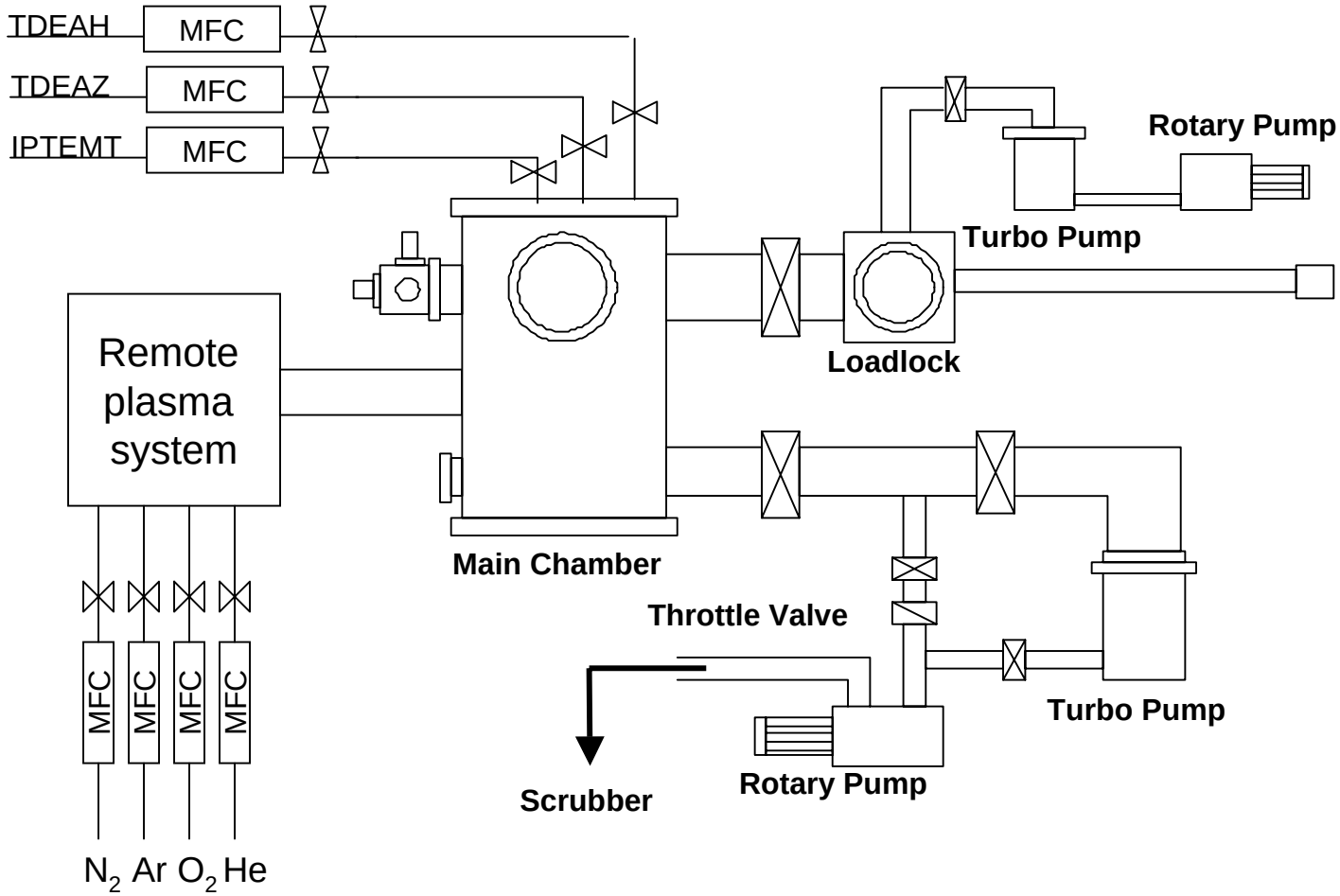

ALD Process Parameters

	$HfCl_4$	TDEAH
Substrate temp	300 °C	**140°C**
Bubbler temp	150 °C	**65°C**
Pulsing	1-60-1-60	1-50-1-50
Dep rate	0.5Å/cycle	**0.75Å/cycle**
Chamber wall	R.T	**75°C**
Oxidizer	H_2O	H_2O
N_2(carrier gas)	20 sccm	2.5 sccm
Process Pr	0.5 Torr	0.5 Torr

C-V Hysteresis

Chloride

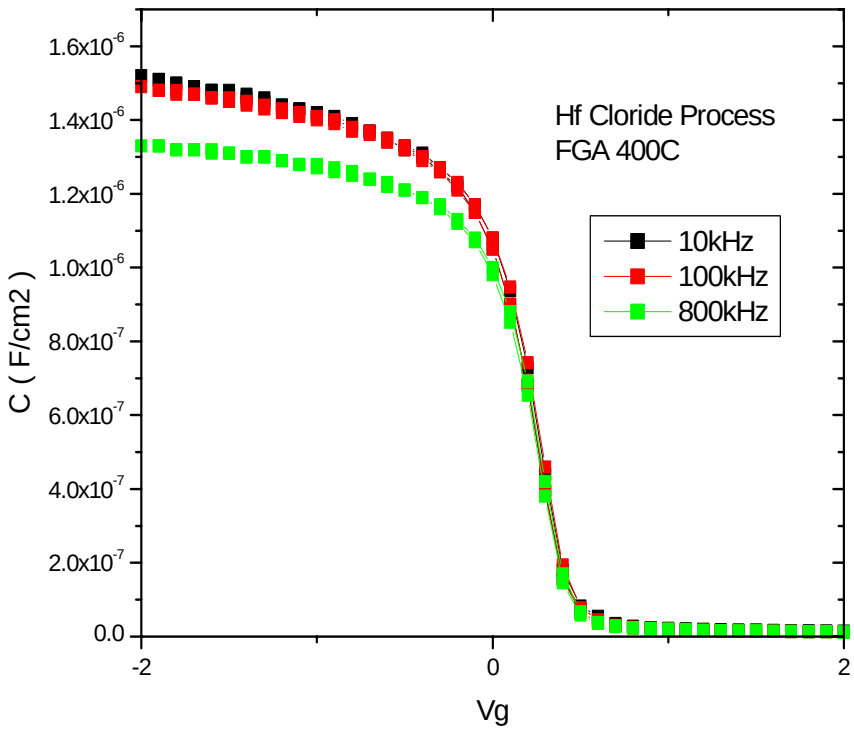

t_{HfO2} = 45Å, I.L = 15Å
Cap derived EOT = 23.1Å
Hysteresis ~ 20 mV

Alkylamide

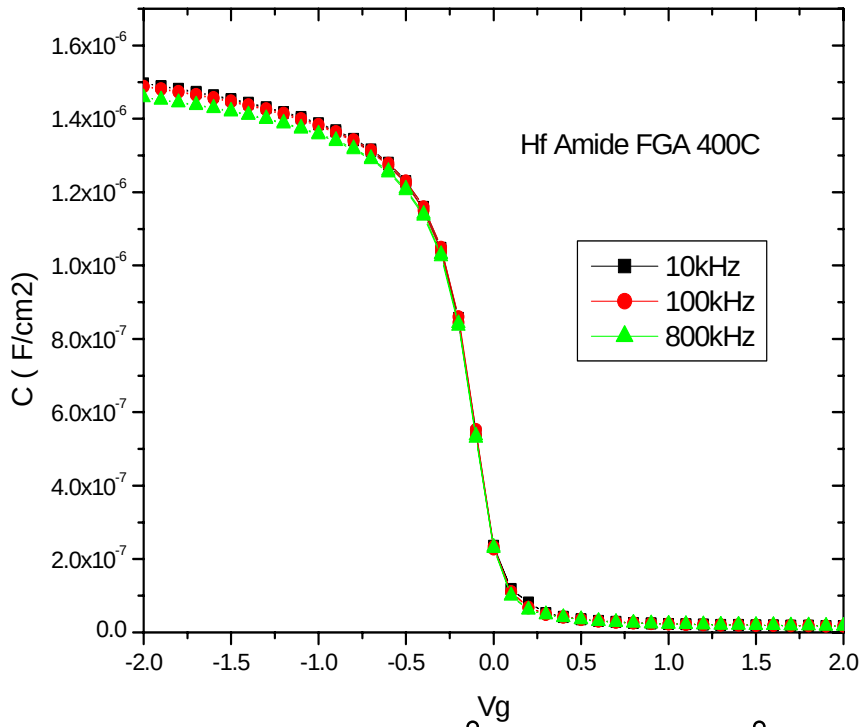

t_{HfO2} = 50Å, I.L = 15Å
Cap derived EOT = 23.2Å
Hysteresis ~ 5 mV

HfO_2 Characteristics

Gate Leakage Current

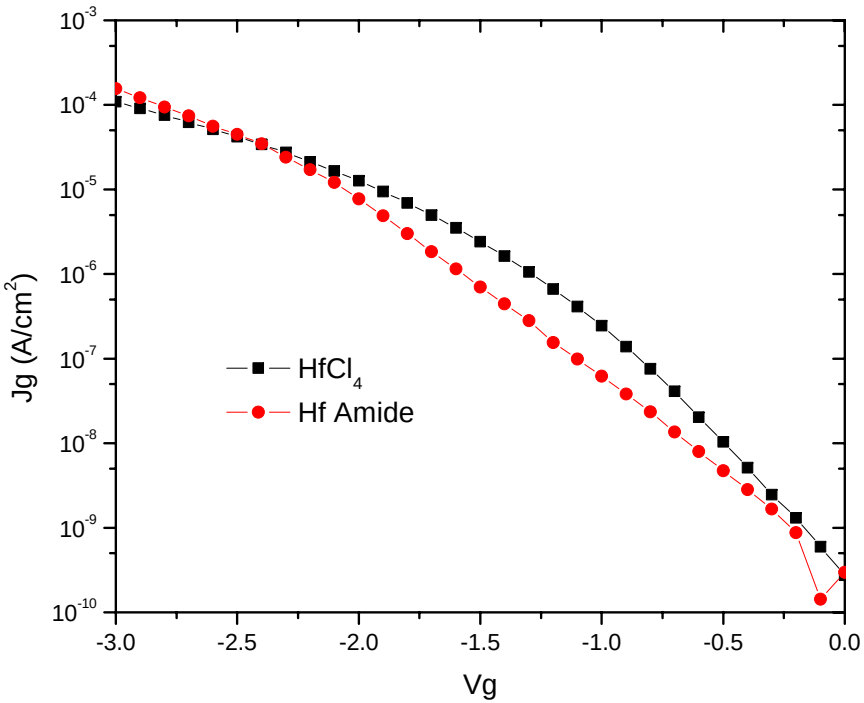

X-section TEM

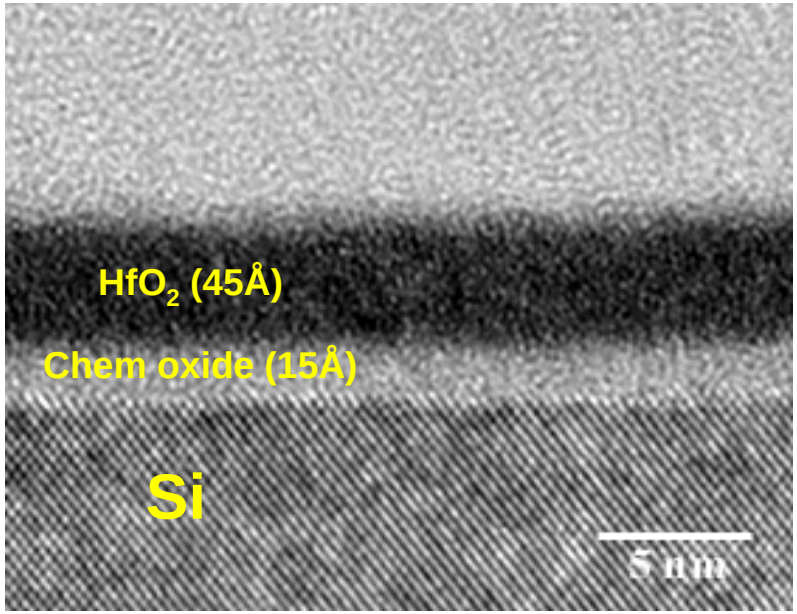

Comparable leakage currents were observed on MOSCAP structures on HfO_2 grown using $HfCl_4$ and TDEAH (**EOT = 23Å)**

Precursor Effect on V_{FB}

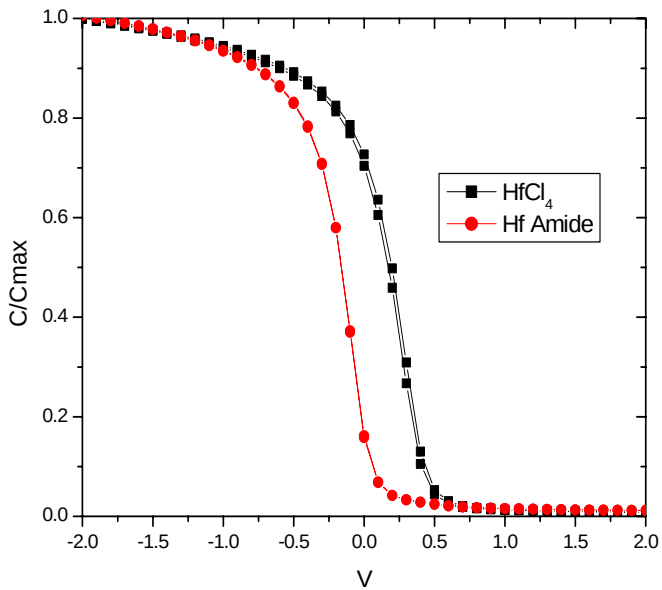

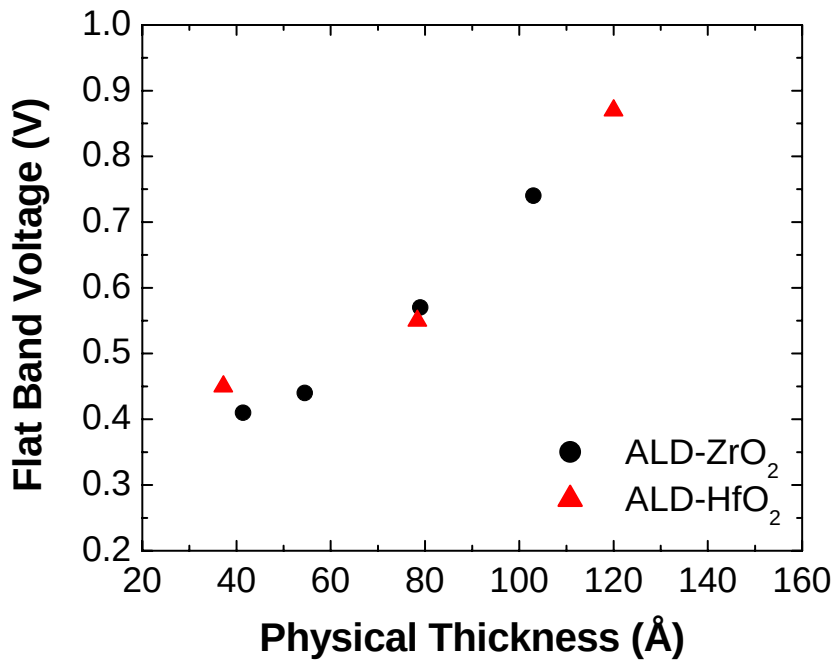

V_{FB} (alkylamide) = 0.09V
V_{FB} (chloride) = 0.49V
ϕ_{Pt} = 5.25 eV on HfO_2
"Ideal" V_{FB} = 0.35V

Q_F (alkylamide) = + 2.4E12
Q_F (chloride) = -1.29E12

Small curvature of V_{FB} vs. thickness suggests fixed charge located mainly at high-*k*/SiO_2 interface with a small "bulk" contribution as well

Plasma Enhanced ALD of TaN

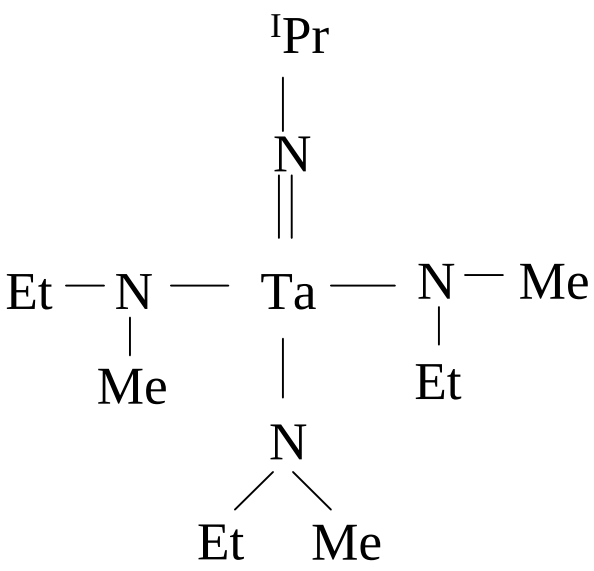

Isopropylimido tris(ethylmethylamino) tantalum (IPTEMT)

Plasma Gas Mixture:
Ar(1000sccm) /N_2 (80sccm)/ H_2(5sccm)

Plasma RF Power: 780W

Process Pr: 1.5Torr

Substrate Temp: 250 - 400°C

Ta precursor: IPTEMT (liq at R.T)

Pulse Times: 10-50-2-50 sec

Growth Rate: 0.45Å/cyl

XPS Spectra

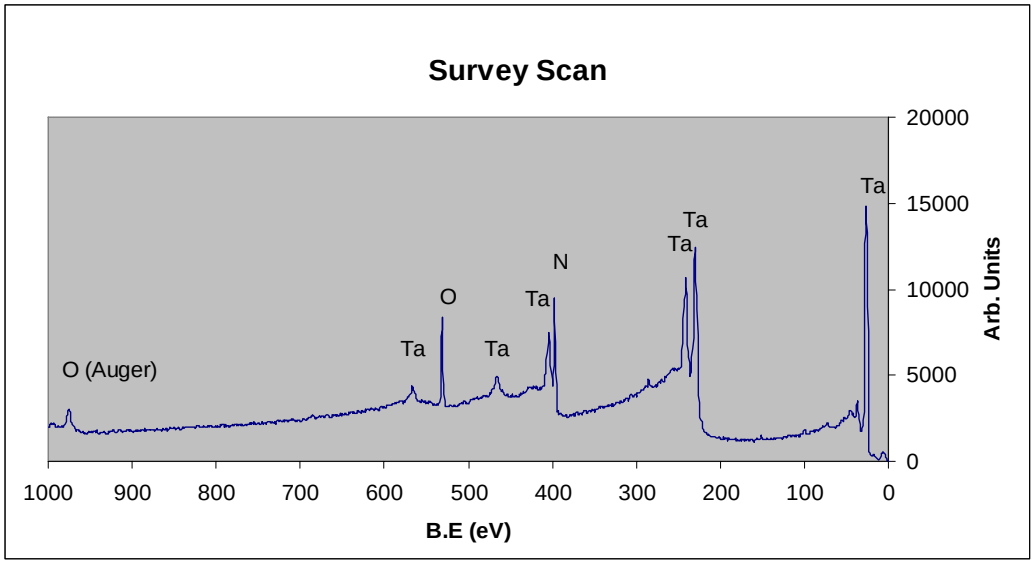

TaxNy deposited @ 400°C showed 35% [N] and 25% [O] in the as-deposited sample. Carbon impurities in the bulk of the film were below the detection limits of the XPS.

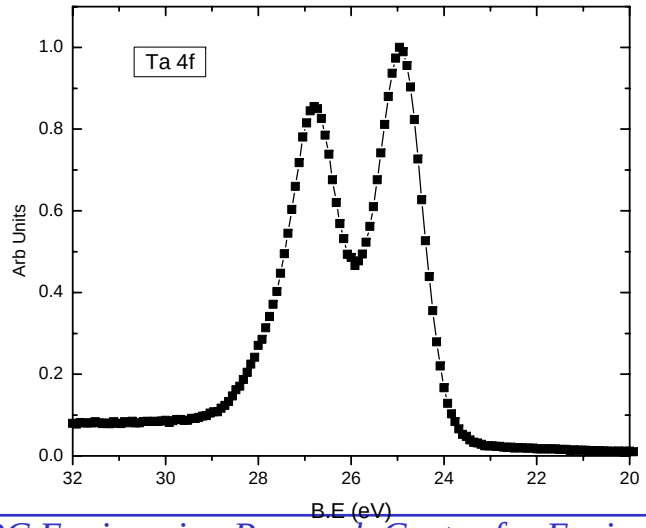

The Ta $4f_{5/2}$ and $4f_{7/2}$ located at 26.7 eV and 24.8 eV resp indicates the as-deposited film to be stoichiometric Ta_3N_5.

In-situ TEM Annealing

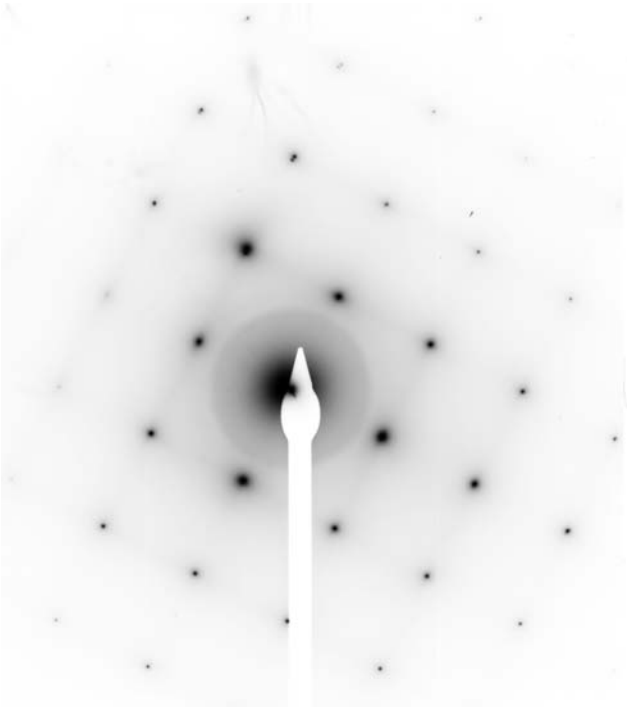

700°C

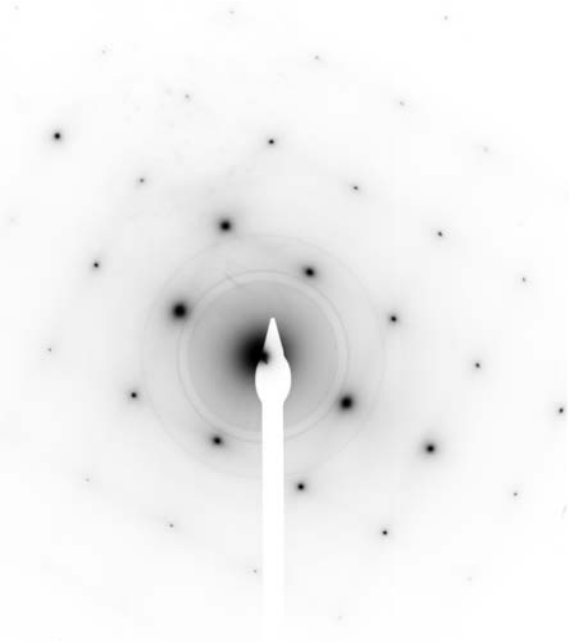

800°C

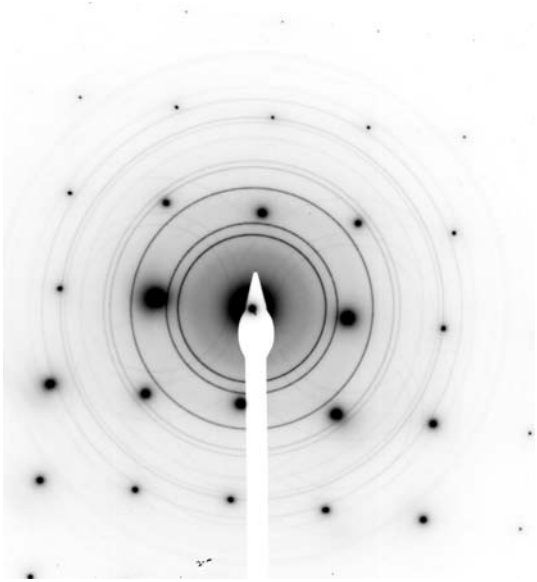

850°C

The Ta_xN_y film deposited on Si/SiO_2 surface crystallized completely at 850°C to form cubic TaN. The observed spot pattern is that of (100) Si substrate.

Stoichiometric TaN

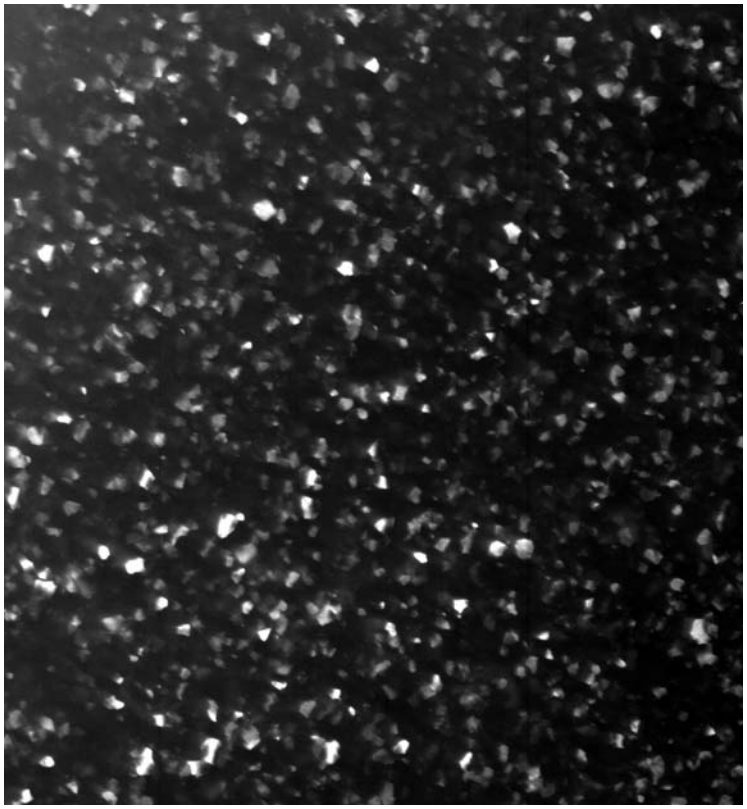

DF image showing TaN crystals after 850°C vacuum anneal

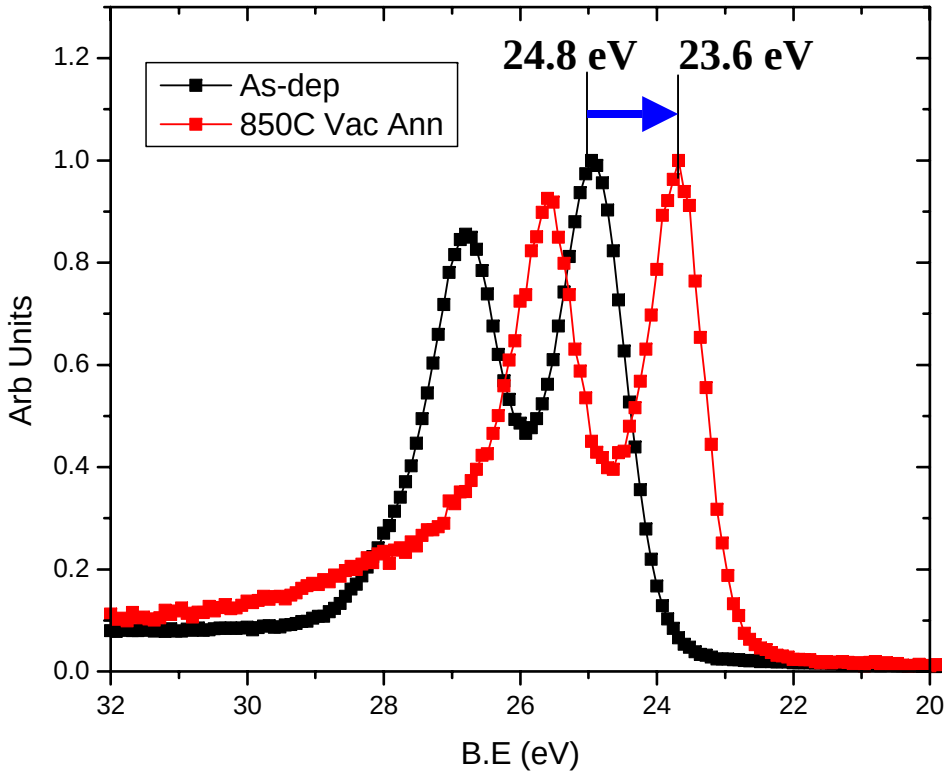

Ta 4f peak shift consistent with the phase change from Ta_3N_5 to cubic TaN

Summary and Future Work

- We have successfully grown high quality HfO_2 thin films on silicon substrates using the ALD process. The electrical characteristics of the HfO_2 films grown using TDEAH are far superior to those obtained using the chlorides.

- We have also optimized a plasma enhanced ALD process to deposit Ta_xN_y at 400 °C which crystallized into stoichiometric cubic TaN when annealed in vacuum at 850°C.

- We are currently working on integrating the two different processes to fabricate capacitors with HfO2 dielectric and TaN metal gate.

- The ESH implications of the Hafnium and the Tantalum precursors have been analyzed.

Task B2: Selective Surface Preparation and Templated Atomic Layer Film Deposition

Rong Chen, Junsic Hong, David W. Porter, Stacey F. Bent
Department of Chemistry; Department of Chemical Engineering

Hyoungsub Kim, Raghavasimhan Sreenivasan, Paul C. McIntyre
Department of Materials Science and Engineering

Hemanth Jagannathan, Yoshio Nishi
Department of Electrical Engineering

Stanford University

NSF/SRC EBSM ERC Review 2006-02-23

Area Selective ALD of Gate Stack

Goal:

- ❖**Self-aligned deposition process for gate dielectrics and gate metal**
- ❖**Avoid tuning etching for different high-κ gate dielectrics and gate metals**

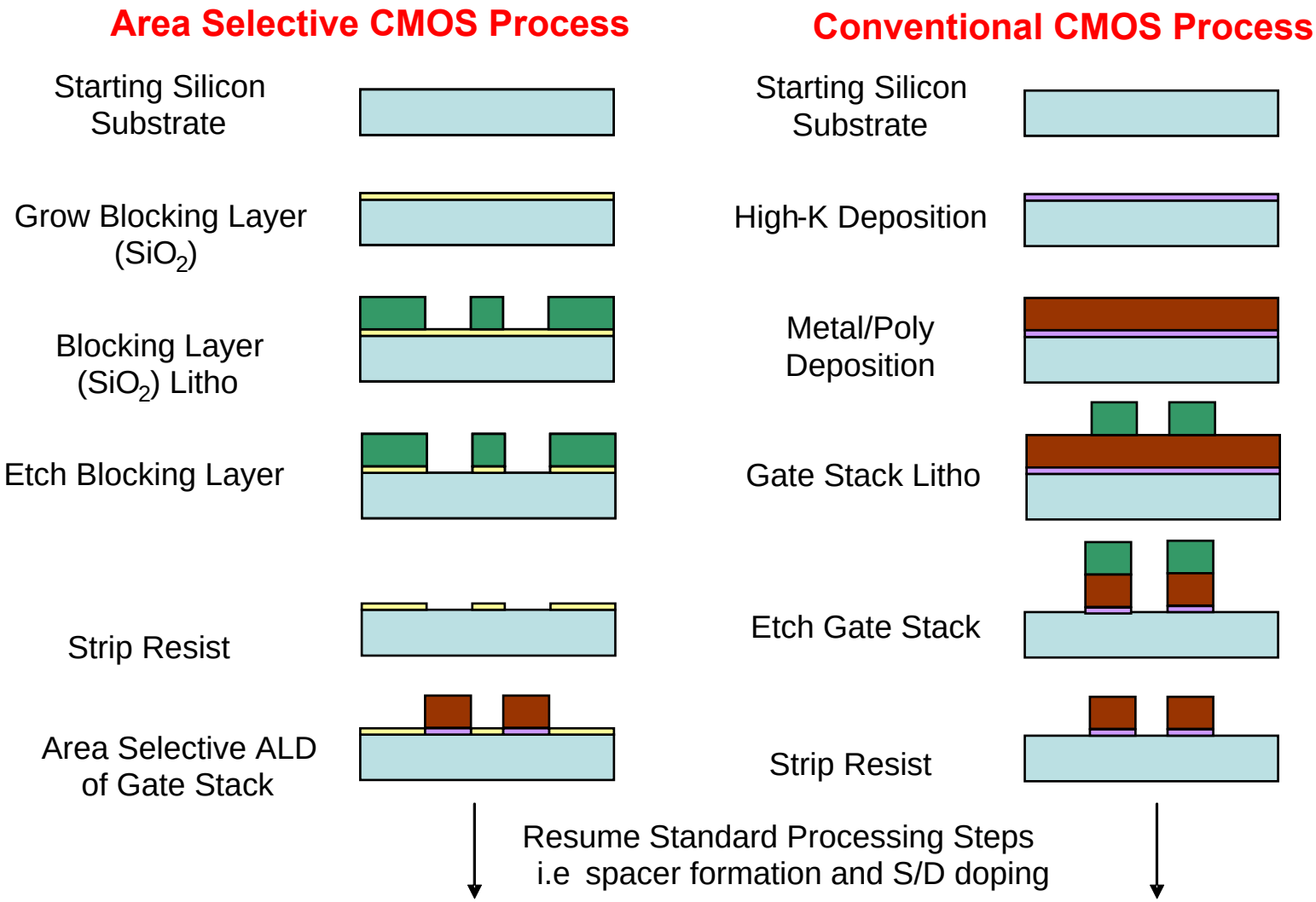

Atomic Layer Deposition

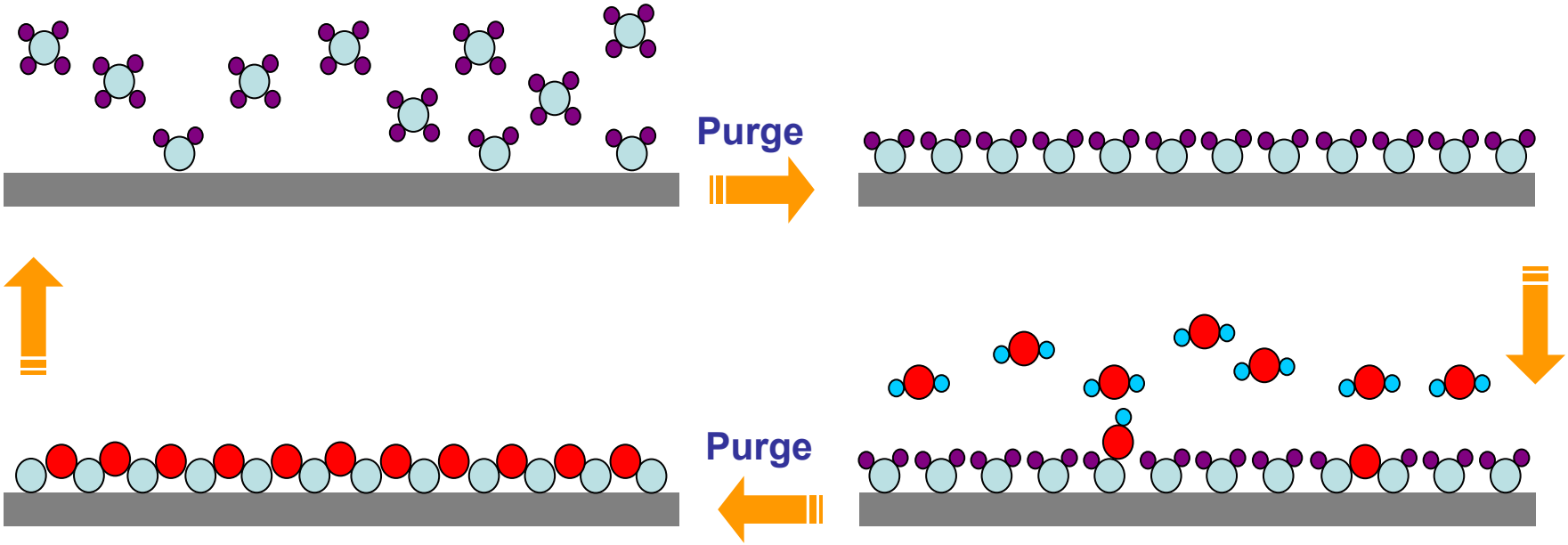

- Layer saturation reactions form conformal film and excellent step-coverage.
- ALD process is based upon chemical reactions between the precursors and the film surface.
- Surface saturation controls deposition.
- Reactions depend on the specific reactive functional groups present at the surface.

➡ Manipulate surface groups before deposition to control the ALD process.

Experimental Setup

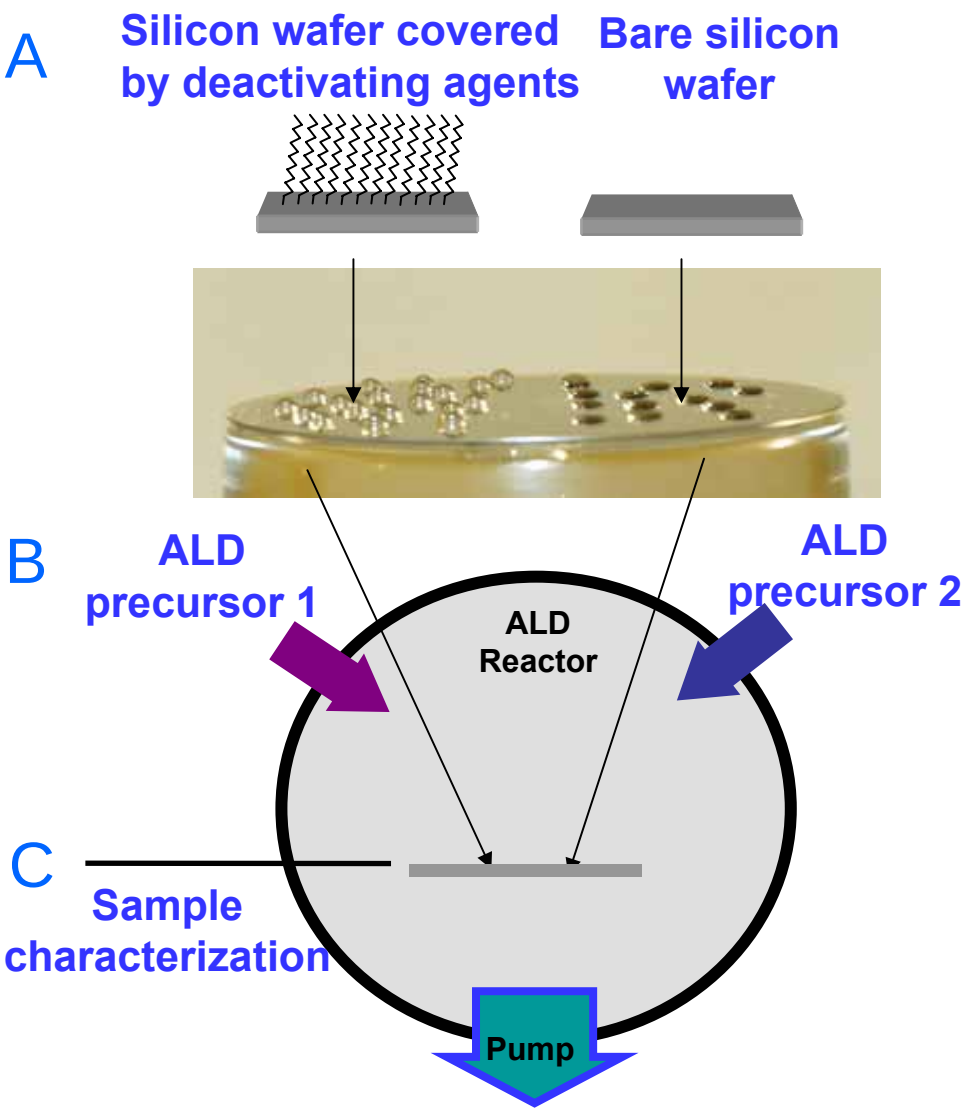

HfO_2 ALD Precursors:

- Hafnium chloride ($HfCl_4$) or hafnium alkylamido $Hf(NMe_2)_4$)
- Water

process temperature: 300°C for $HfCl_4$ and 250°C $Hf(NMe_2)_4$

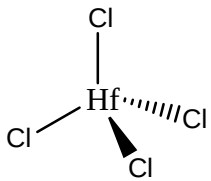

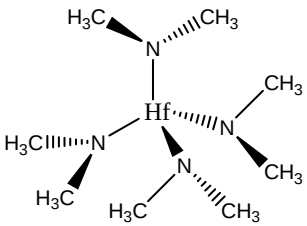

Pt ALD Precursors:

- (Methylcyclopentadienyl)trimethyl platinum ($MeCpPtMe_3$)
- Oxygen

process temperature: 325°C

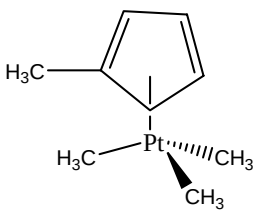

Top View of ALD Reactor

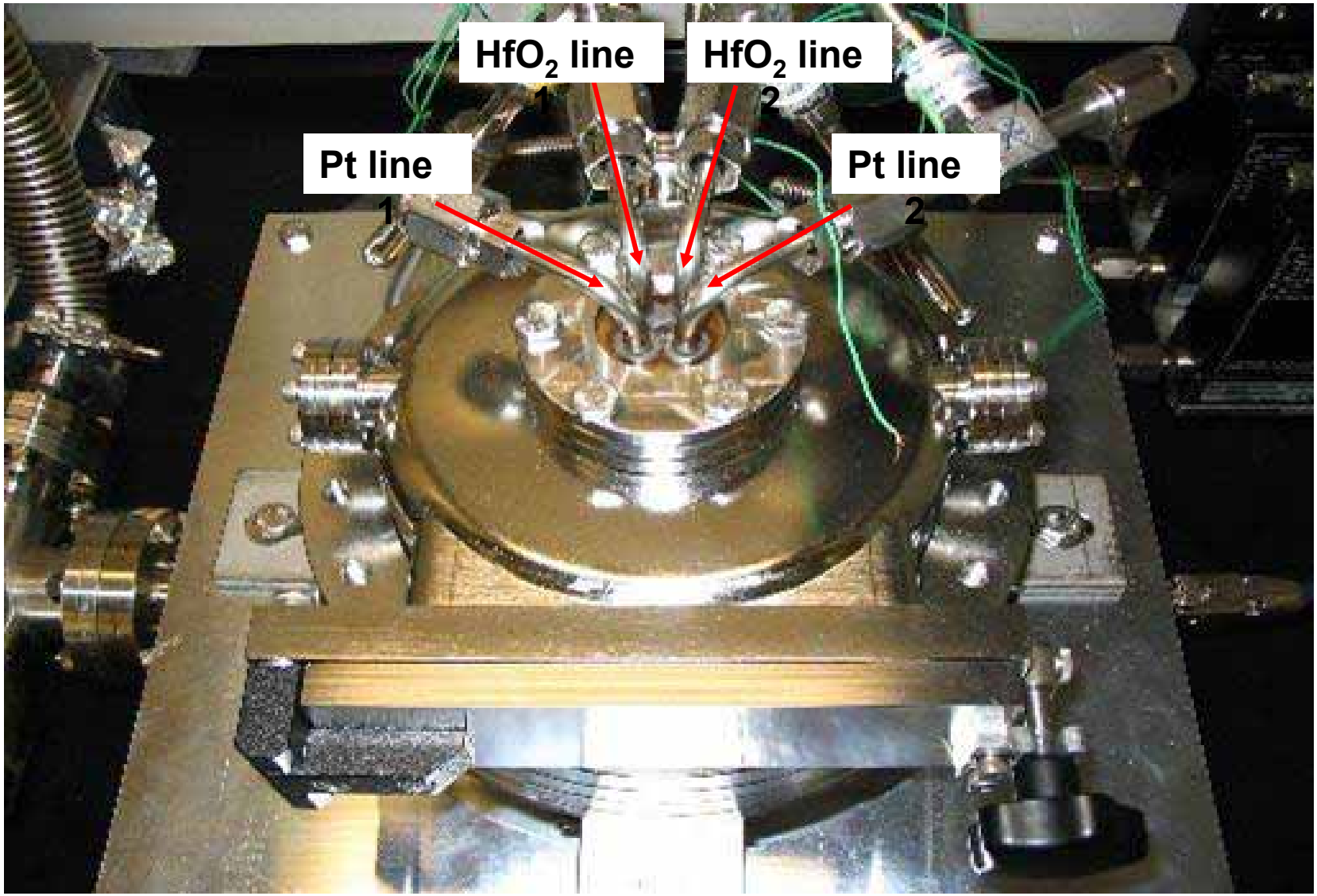

Deactivating Agents on Oxide Surface

silylating reactions

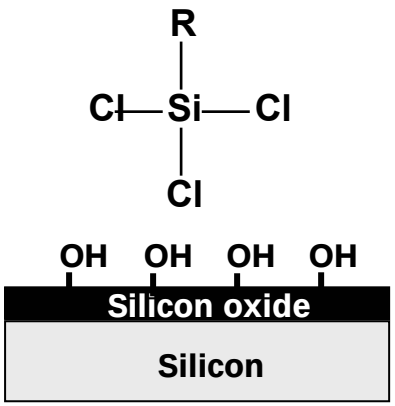

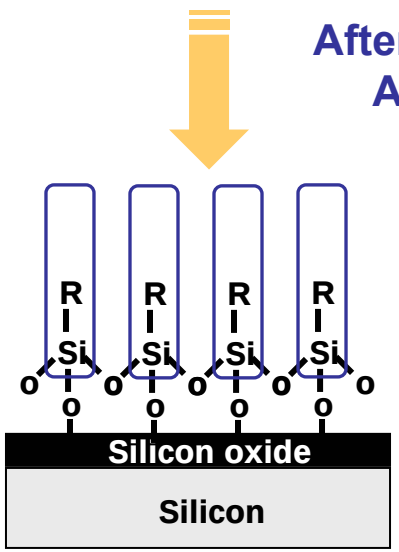

After HfO_2 ALD

native silicon oxide surface

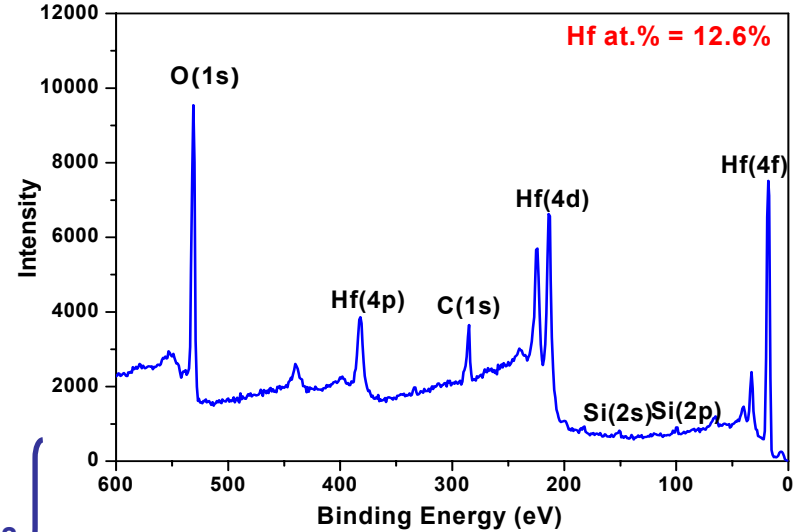

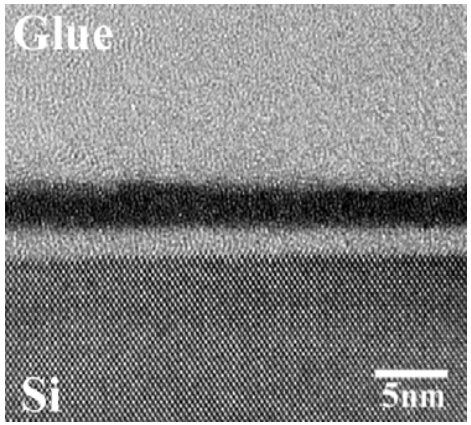

n-octadecyltrichlorosilane (ODTS) deactivated surface

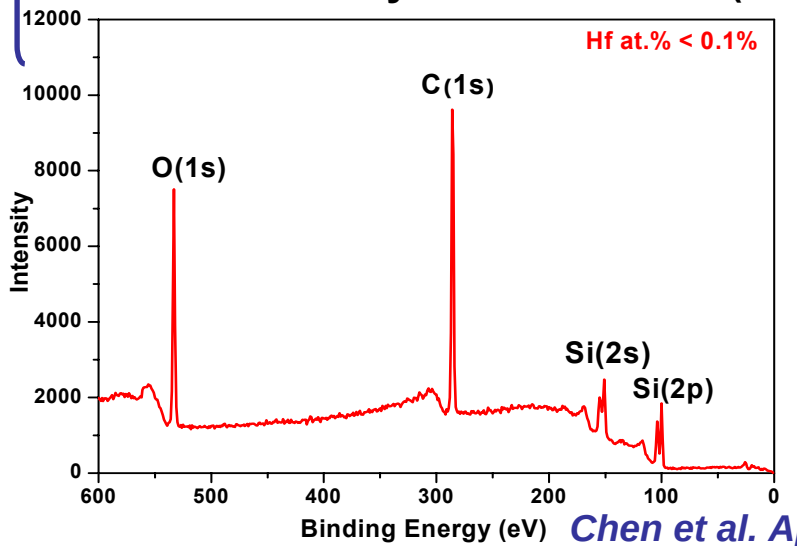

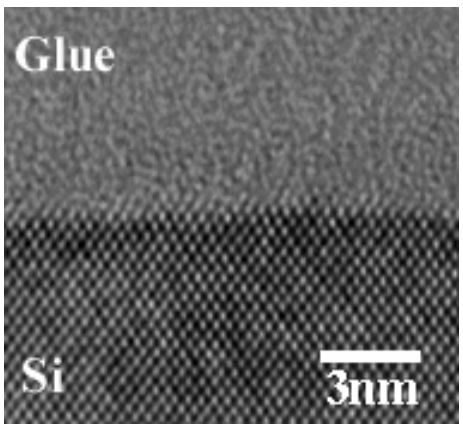

Chen et al. Appl. Phys. Lett. 2004, 84, 4017

- **It is also effective for other high-k dielectrics (eg. ZrO_2) and metals (eg. Pt) ALD**

SAMs Formatiom through Vapor Phase Delivery

Preparation of SAMs by CVD

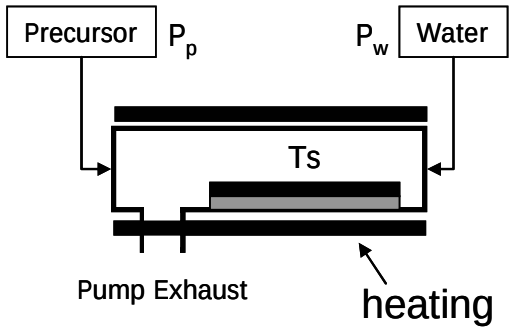

In ALD reactor

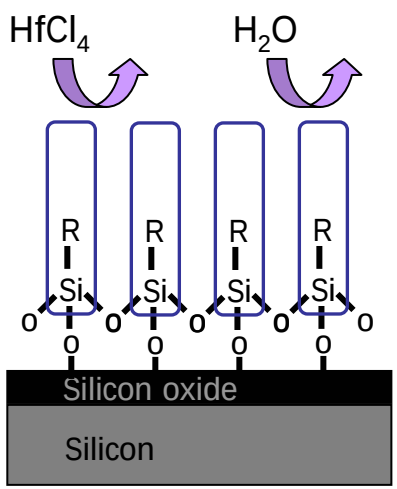

Experimental Condition:

Precursors (ODTS and water)

Ts=170°C

Goals:

- Avoid solvent usage – Environmental friendly
- Compatible to ALD process – Easy scale up to wafers used in IC industry (CVD, vacuum systems)

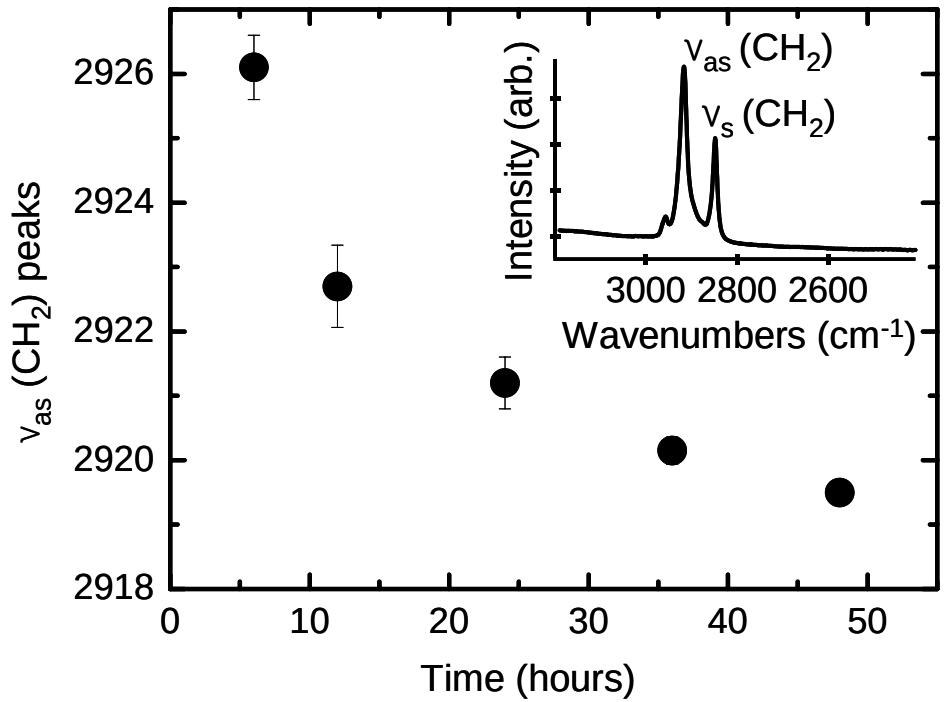

Long reaction time are necessary for SAMs crystallization and complete deactivation

QCM Study of SAMs through Vapor Phase Delivery

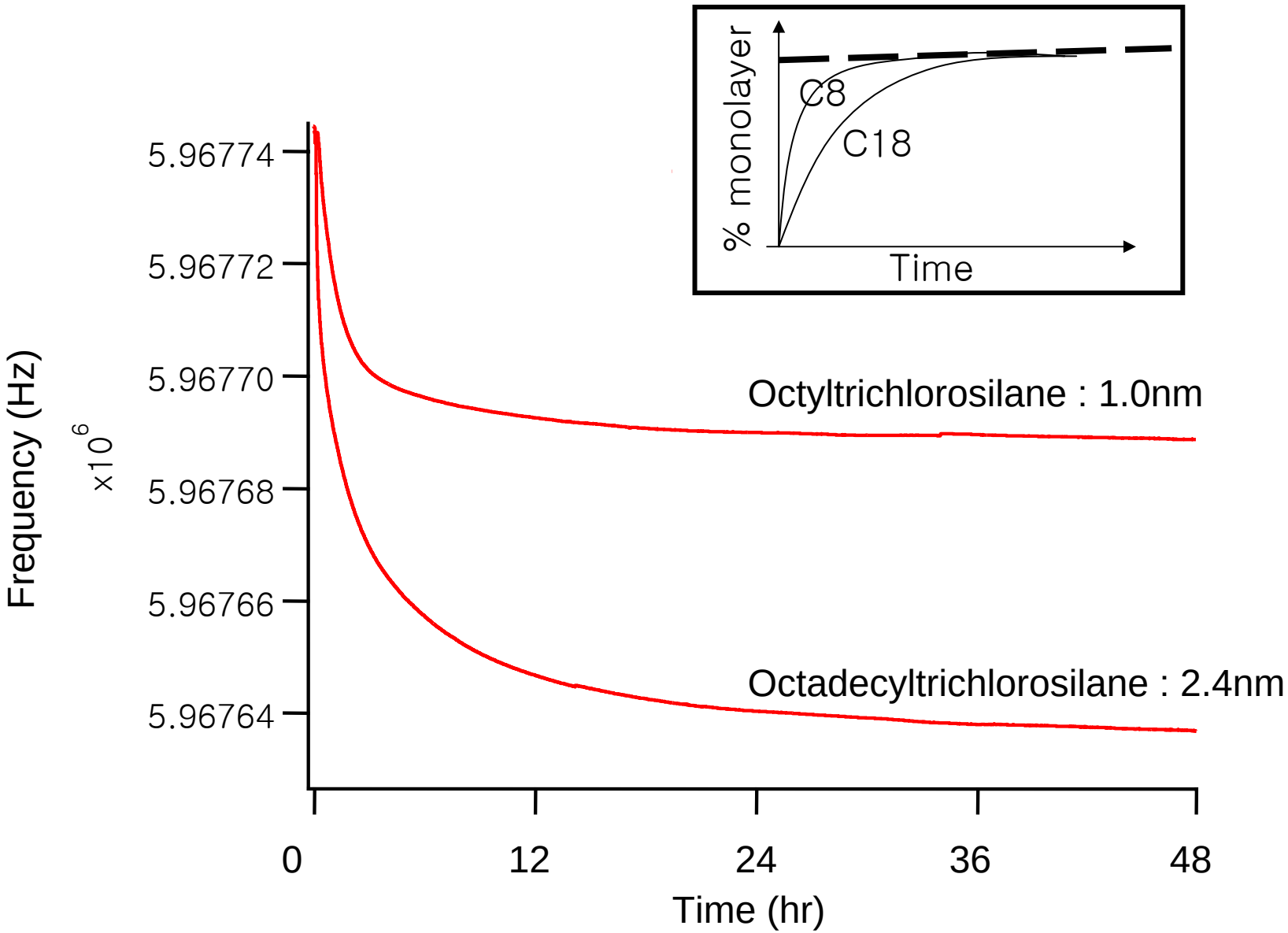

Deactivating Agents Studied

1. Tail group chain length dependence

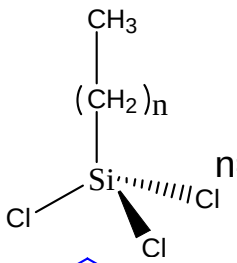

n=0,1,3,5,7,9,11,17

2. Tail group structures

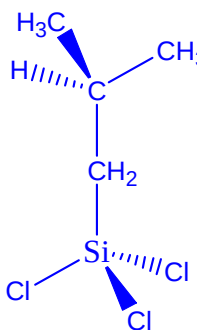

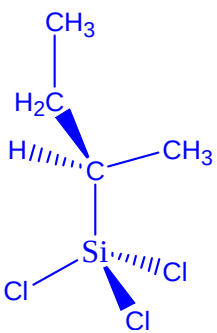

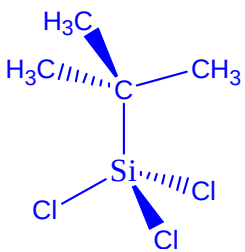

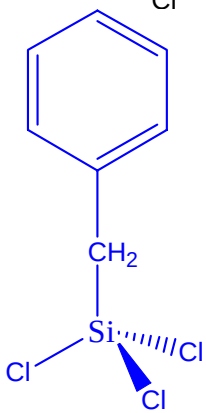

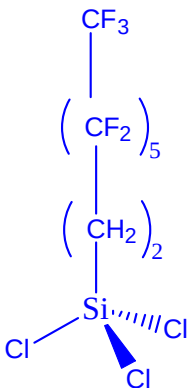

3. Reactive head group dependence

a. number of chlorine substituents

$Si(CH_3)_nCl_{4-n}$ n=1,2,3

b. other reactive groups

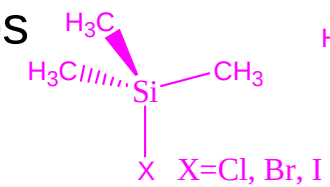

X=Cl, Br, I

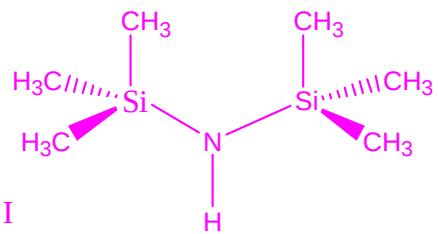

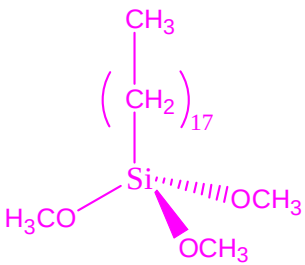

Chen et al. Chem. Mater. 2005, 17, 536

Correlation between Deactivation & Hydrophobicity

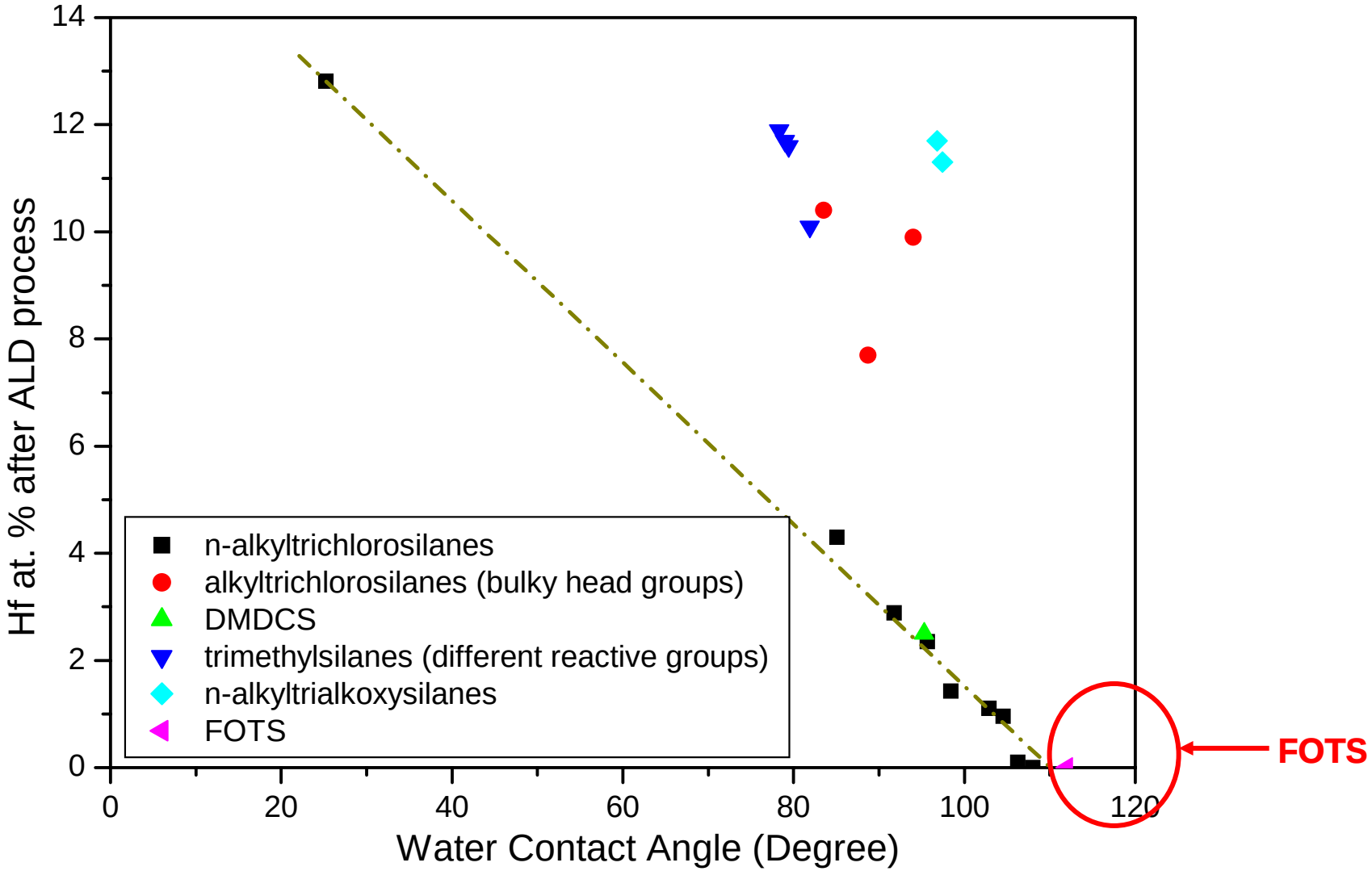

QCM Study of FOTS through Vapor Phase Delivery

Fluorinated compounds exhibit higher hydrophobicity, which may block the water diffusion more efficiently.

Higher vapor pressure than ODTS

High reactivity

Low surface tension

Shorter chain

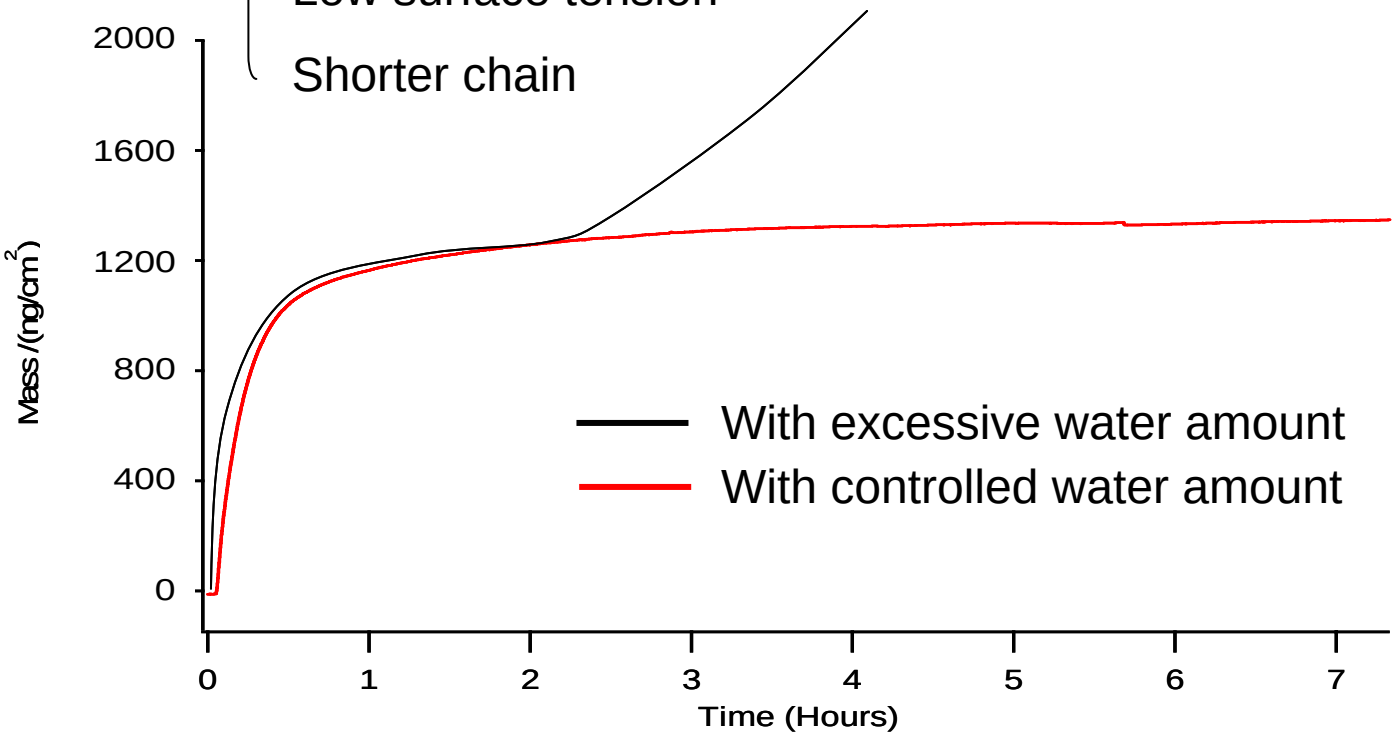

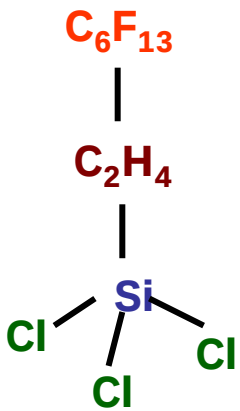

Tridecafluoro-1,1,2,2-tetrahydrooctyl-trichlorosilane (FOTS)

FOTS is more reactive and very sensitive to water amount, it is crucial to control the amount of water to avoid multilayer formation

Deactivation of Ge and Si Semiconductors

Direct Attachment

hydrogermylation
or hydrosilylation

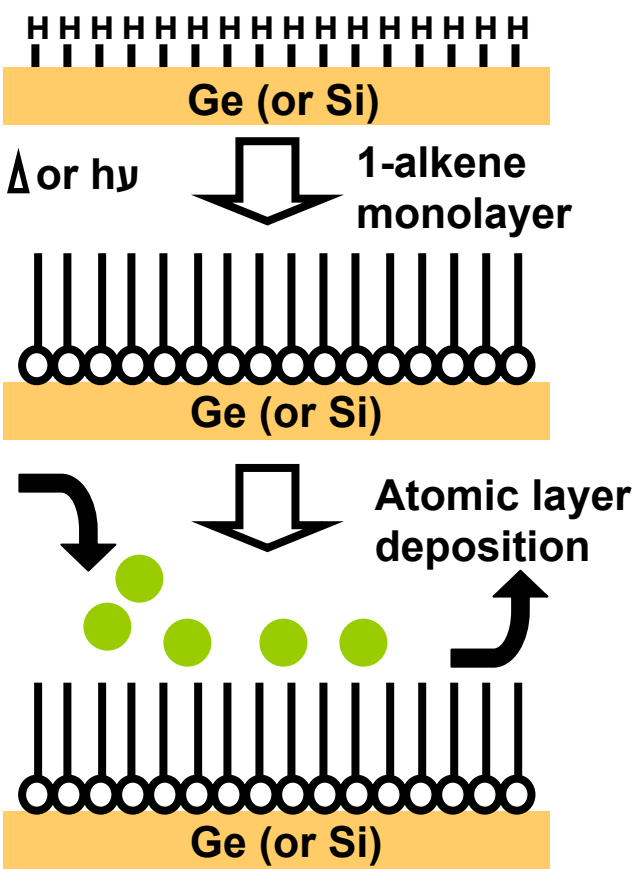

Fresh Ge(100)-H surface
after HfO_2 ALD

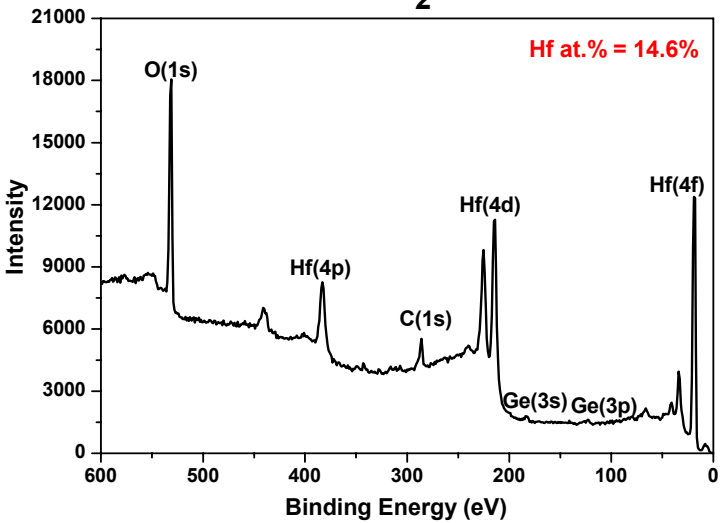

1-octadecene deactivated Ge(100)-H
surface after HfO_2 ALD

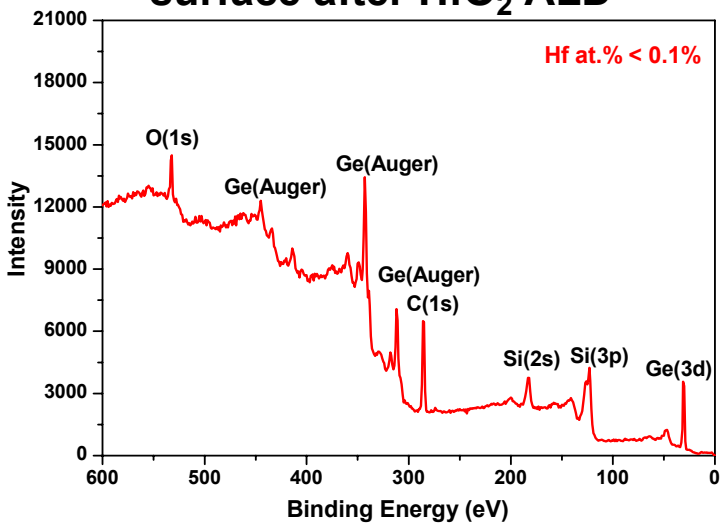

Positive and Negative Pattern Transfers

Negative Patterning

Positive Patterning

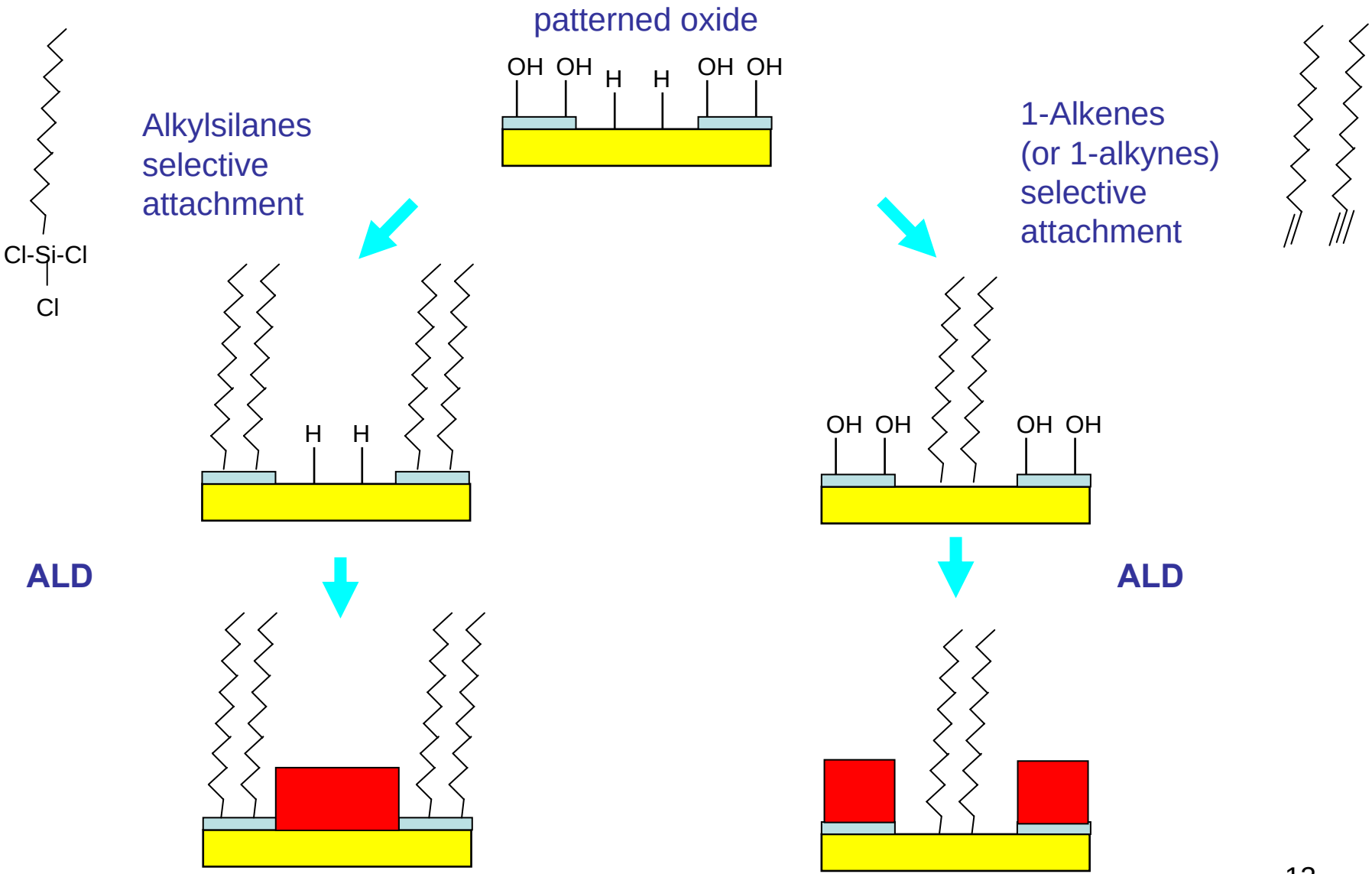

Area-Selective ALD of HfO_2 by Negative Patterning

Area #1, Octadecyltrichlorosilane deactivated oxide surface; Area #2, non-deactivated Si-H surface

SEM Image

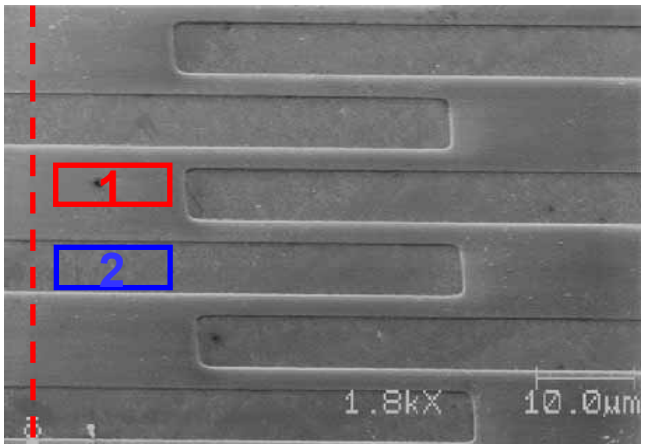

Hf Auger Mapping

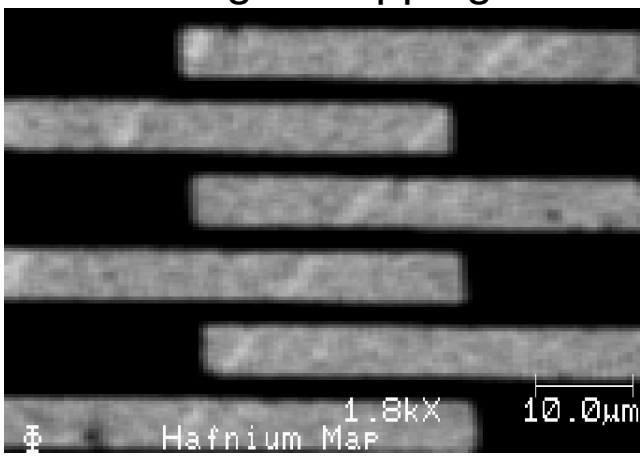

Survey Scan

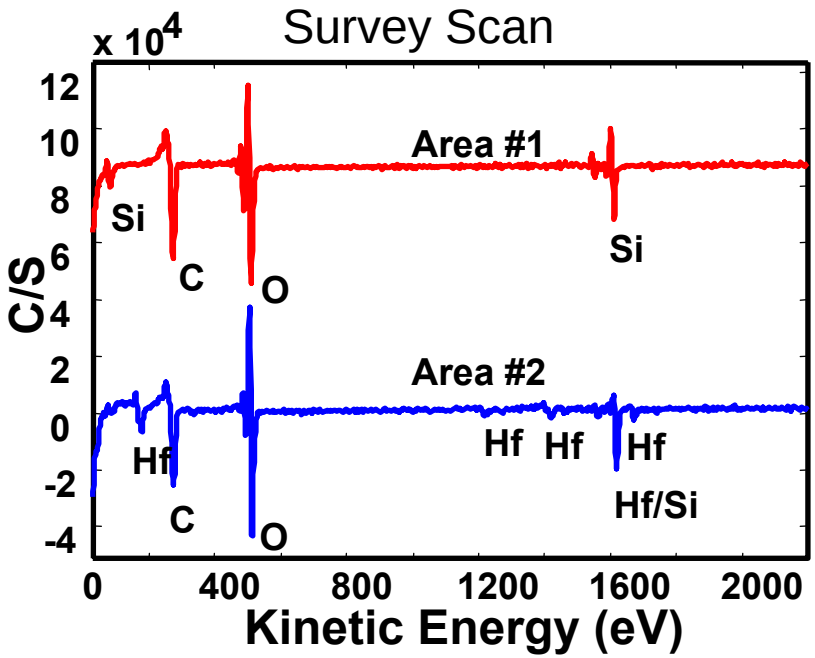

Line Scan

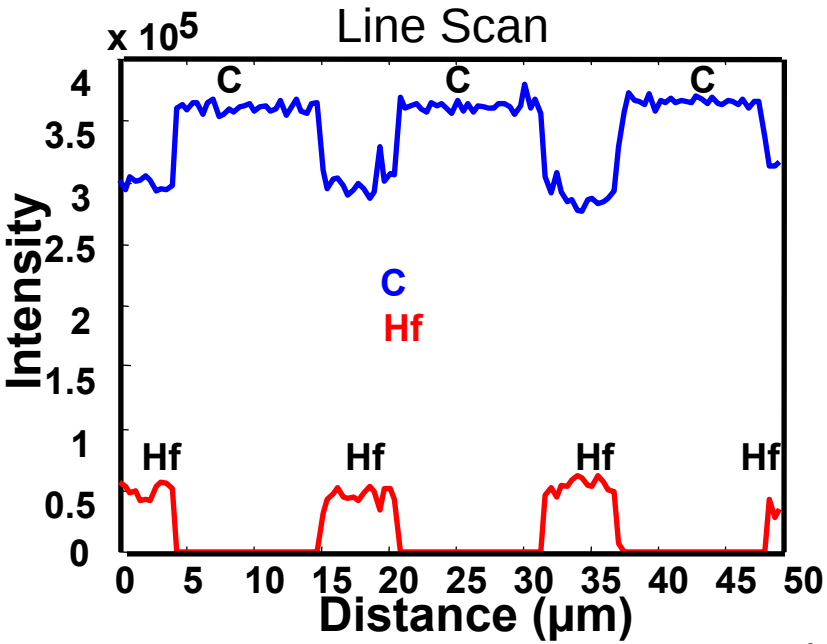

Chen et al. Appl. Phys. Lett. 2005, 86, 191910

Area-Selective ALD of Pt by Positive Patterning

Area #1, non-deactivated oxide surface; Area #2, 1-octadecene deactivated hydride surface

SEM Image

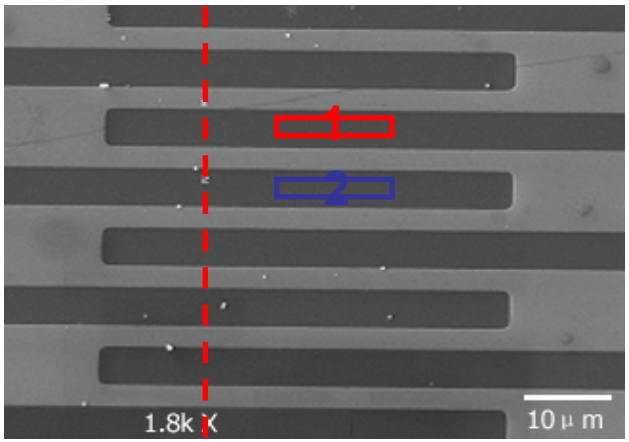

Pt Auger Mapping

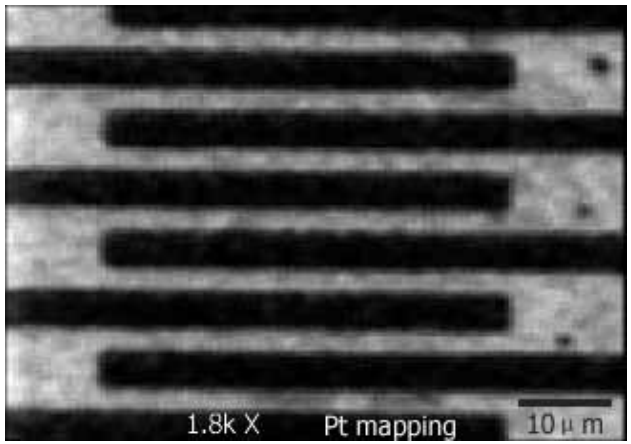

Survey Scan

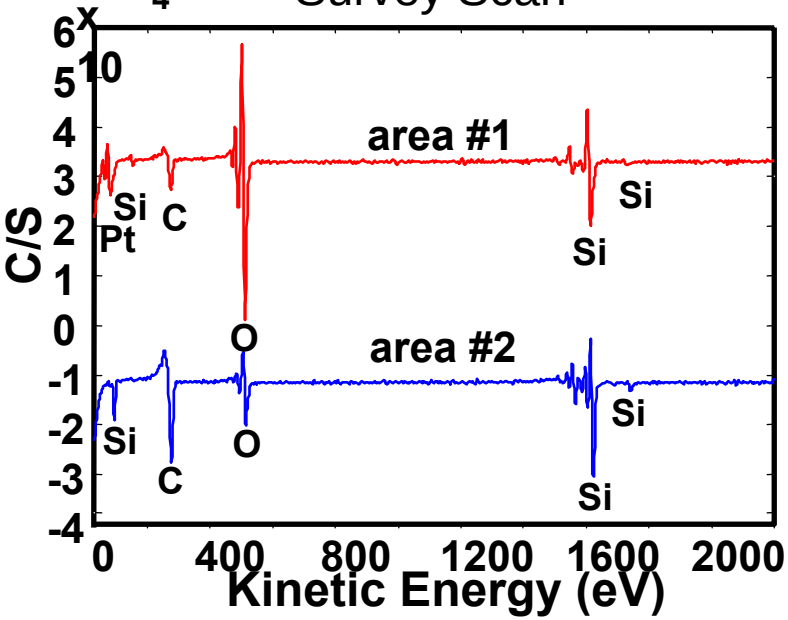

Line Scan

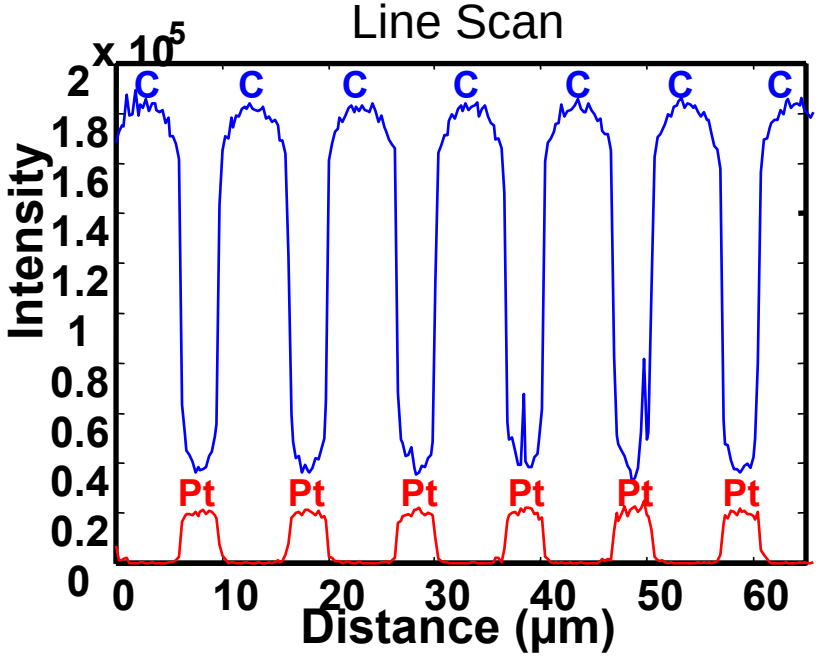

Chen et al. to be published in Adv. Mater. 2006

Selective Adsorption and ALD on Other Surfaces

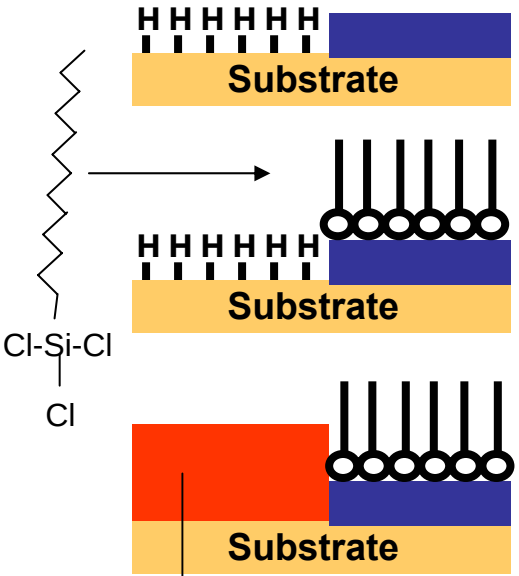

- Blue layer is oxide (e.g. HfO_2) or nitride (e.g. Si_3N_4), red ALD film is HfO_2 or Pt
- Similar results are found for positive patterning samples
- Negative patterning method works better for films that are easy to nucleate but hard to deactivate, while positive patterning works better for films that are difficult to nucleate but relatively easy to deactivate

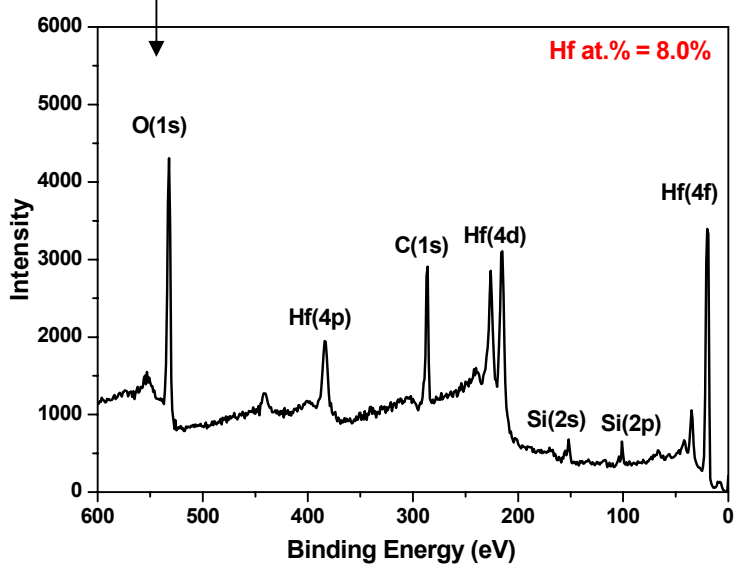

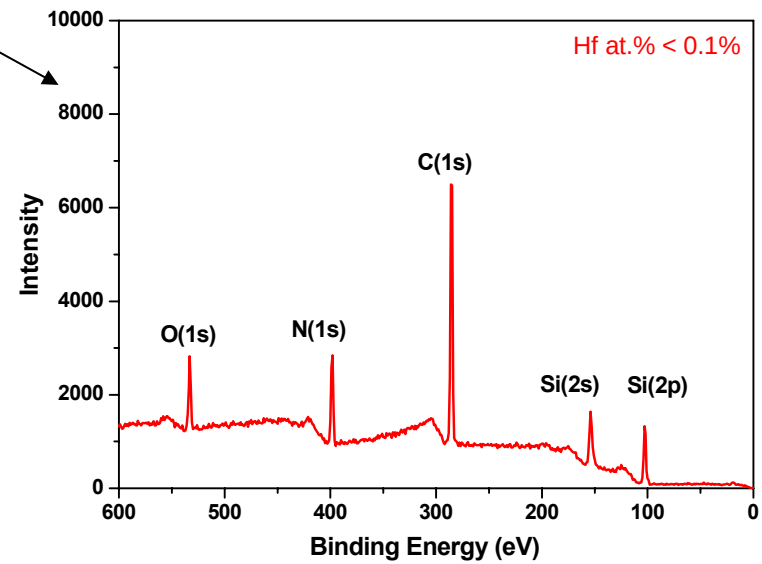

Initial Capacitor Structure and Characterization

Capacitor Cross-Section

top electrode: Pt

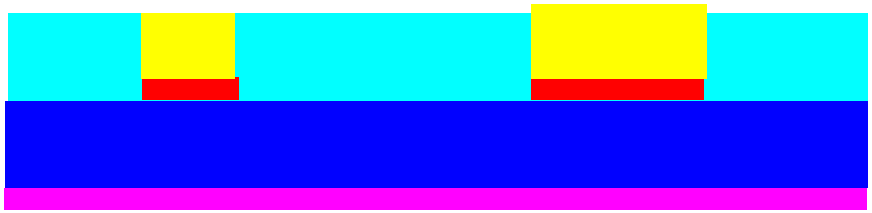

back electrode: Al

Area-Selective ALD Capacitors

- SiO_2 deactivated with ODTS
- Area-selective ALD of HfO_2 and evaporated Pt electrode
- Al back-electrode deposition
- Interfaces: Si/Si:H/HfO_2/Pt

Area-Selective ALD Capacitors

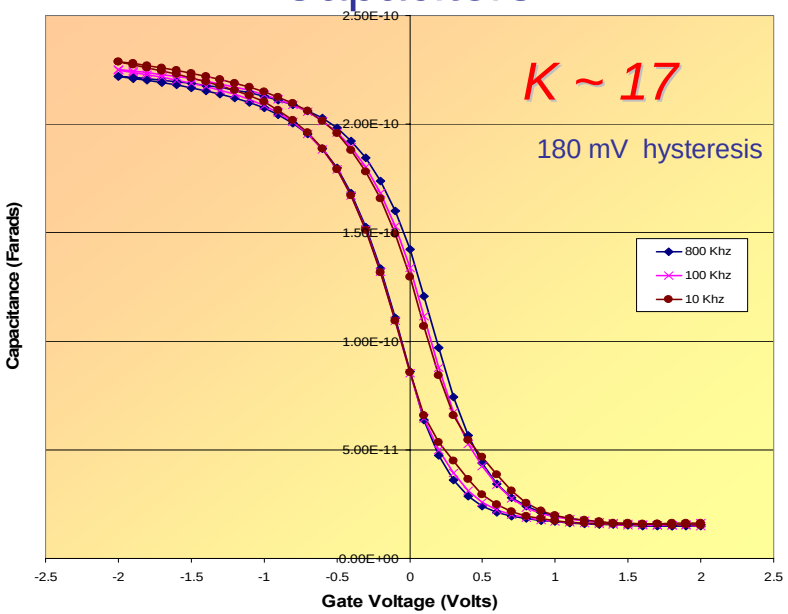

Interface property is poor

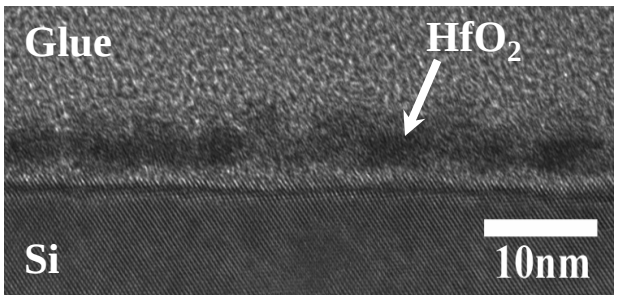

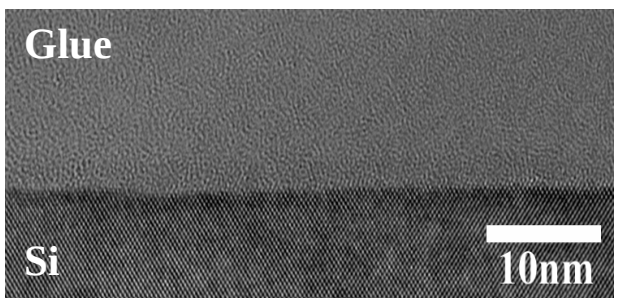

need activation step to achieve better interface property

Summary

- Deactivation study on SiO_2 by siloxane-based SAMs
- Deactivation study on Ge-H and Si-H by 1-alkenes/1-alkynes and alkanethiols
- Vapor phase SAMs formation and deactivation mechanism study
- Pattern transfer investigation by selective attachment and soft lithography
- Area selective ALD on other dielectrics/semiconductor, e.g. medium-k Si_3N_4/Si and high-k HfO_2/Si
- Electrical characterization on Capacitors fabricated by area-selective ALD

Future Work

- Surface activation and cleaning strategies to achieve better electrical performance
- Integration of vapor phase delivery system into ALD reactor
- Transistors and other devices fabrication by area-selective gate stack deposition on both Si and Ge
- Exploration of high resolution, direct patterning methods
- Development of other types of ALD monolayer resists

Acknowledgements

People:

Bent group members
Prof. Michael A. Kelly
Dr. Peter B. Griffin
Prof. Krishna Saraswat
Prof. Chris E. D. Chidsey
Prof. Charles B. Musgrave

Funding:

- **NSF/SRC Engineering Research Center for Environmentally Benign Semiconductor Manufacturing**
- **Initiative for Nanoscale Materials and Processes (INMP)**
- **Stanford Center for Integrated Systems (CIS)**
- **Honda**
- **Texas Instruments Graduate Fellowship**

Facilities:

Task B-3: Evaluating EHS Impacts of New Dielectric and Conductor Materials Etch Processes

Modeling of Inductively Coupled Plasmas

Cheng-Che Hsu, Dr. Mark A. Nierode and
Prof. David B. Graves
Department of Chemical Engineering
University of California, Berkeley

Feb. 23-24, 2006
ERC Review
Tucson, Arizona

ESH Impact and Project Objectives

By-products formation and transport have both process and **ESH significance**.

- **Etching processes**
  - **Large set of chemistries**
  - **Potential toxic by-products.**
  - **Process is complicated, (through gas phase or surface reactions) but very little is known.**
- **ESH significance of by-products:**
  - **A: Wall re-deposition: potential threaten the worker.**
  - **B: Effluent: ESH Impact**
- **Goal**
  - **Understand mechanism**
  - **Identify/Predict the condition with minimum emission**

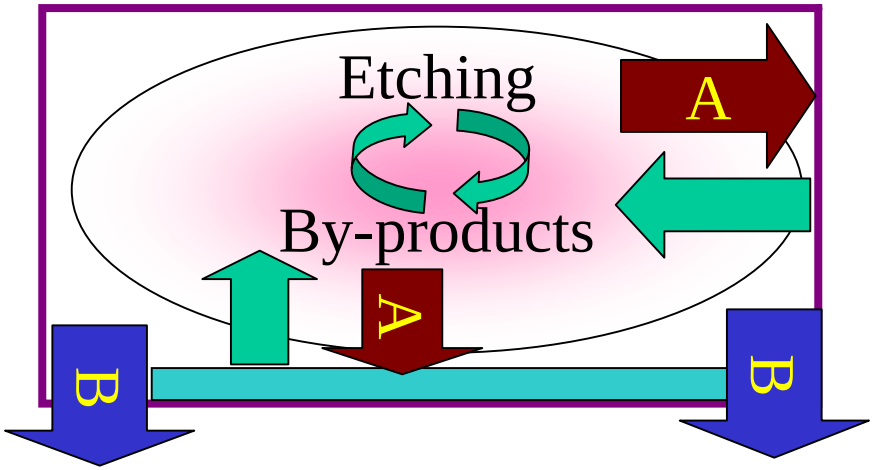

- **Methodology**
  - **Predictive model development**
    - **Validation: Exp. Testbed at UCB (Ar/O_2 plasmas)**
  - **Extend the model capability to different chemistries and reactors.**
  - **Assess process ESH impact.**

ESH metrics

	Usage Reduction			Emission Reduction			
Goals / Possibilities	**Energy**	**Water**	**Chemical**	**PFCs**	**VOCs**	**HAPs**	**Other Hazardous Wastes**
Identify toxic etch by-products	N/A	N/A	N/A	Could replace existing PFC use for chamber wall clean	Some by-products may be VOCs	Most by-products classi-fied as HAPs	Identify toxic materials on tool walls
Reduce toxic etch by-products	N/A	N/A	N/A	N/A	Reduce VOC emission	Reduce HAPs emission	Reduce cost of toxic waste disposal

System

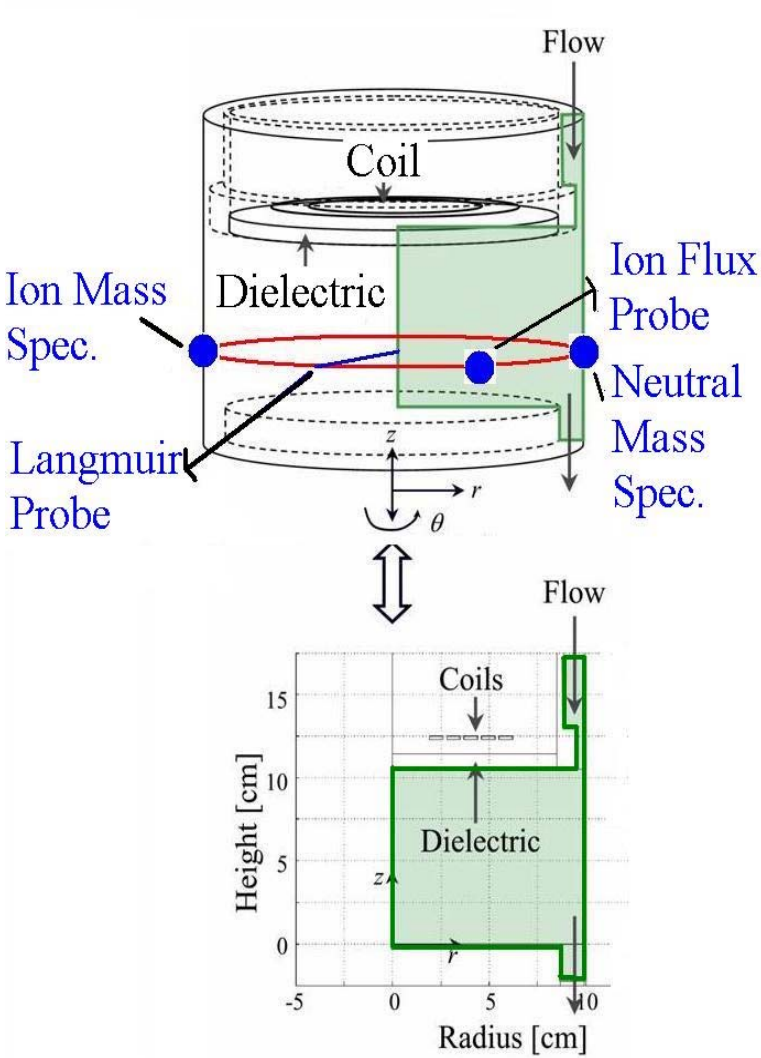

Experimental System*

- Diagnostic ICP
  - Multiple Diagnostics
  - Fits 6-in wafer
  - Well-defined boundaries
  - Axisymmetric

Model

- 2D, Fluid Model
- Ar/O_2 ICP as the preliminary test
- Femlab™ and Matlab™
  - Coupled neutral and plasma model
  - Easy to share / access
  - Easy to extend to different chemistries/systems

*H. Singh, et. al, J. Vac. Sci. Technol. **19**, 718 (2001),

Model Formulation: Equation System

Fluid Model; Ambipolar, quasineutral, isothermal ions, Maxwellian electrons.

Overall Neutral Continuity (p)	$\nabla \cdot \left(\rho \vec{v}\right) = R_n$
Neutral Species j mass balance (wj)	$\nabla \cdot \left(w_j \rho \vec{v} - \rho \mathrm{D_j} \nabla wj\right) = r_j$
Neutral Momentum Balance (u,v)	$\left[\nabla \cdot \bar{\bar{\boldsymbol{\tau}}}\right] = -\nabla p - \nabla \cdot \left(\rho \vec{v} \vec{v}\right)$
Neutral Energy Balance (T)	$\left(\nabla \cdot \vec{q}\right) = -\nabla \cdot \left(\rho \vec{v} C_v T\right) - p\left(\nabla \cdot \vec{v}\right) + S_n$
Ion Continuity ($n_{i,j}$, $n_{ineg,j}$)	$\frac{\partial n_{ij}}{\partial t} + \nabla \cdot (-D_{ij} * (\nabla n_{ij} \pm \frac{\mathrm{T}e}{\mathrm{T}i} n_{ij} \frac{\nabla n_e}{n_e})) = r_{ij}$
Electron Energy (Te)	$\frac{\partial}{\partial t}\left(\frac{3}{2} n_e e \mathrm{T}_e\right) + \nabla \cdot \vec{\mathbf{Q}}_e = -e\vec{\mathbf{E}} \cdot \vec{\boldsymbol{\Gamma}}_e - Ee + P_{abs}$
Holmholtz Wave Equation (E_θ)	$(\nabla^2 E)_\theta = \frac{\omega^2}{c^2} K \cdot E_\theta - i\omega\mu_0 J_{ext,\theta}$

Model Formulation: Numerical Scheme

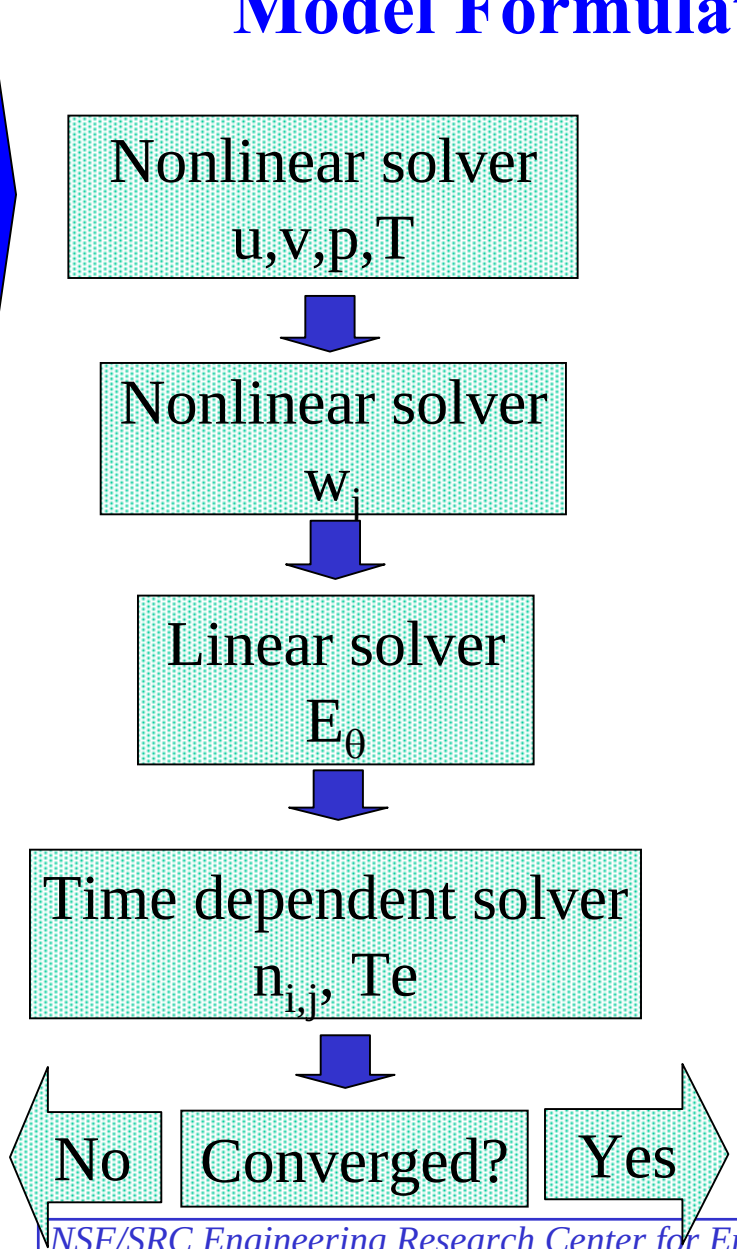

- Able to handle over 9 neutral species, and 8 charged species (totally 22 equations) with PC (~1GB memory).
  - 6 neutral ,4 ions species and 15 equations in current Ar/O_2 model.
- Convergence:
  - one iteration < 20min. Need < 10 iterations.
  - Robust, and easy to converge.

Model Formulation: Ar/O_2 ICP Details

- Chemistries
  - Neutral Species: ground state Ar, O_2, O, and metastable $O_2(a^1\Delta, b^1\Sigma)$ and $O(^1D)$
  - Ion Species: Ar^+, O_2^+, O^+, O^-
  - Major reactions: Ionization, excitation, dissociation, electron impact attachment, charge exchange. All cross sections and rate coefficients were taken from the literature.
- Model and Experiment Comparison
  - ne profile, center ne, and Te,
  - n_O , total ion flux and composition at the wall.

Results: ne and Te: Ar Plasmas

Reasonable Profile Prediction

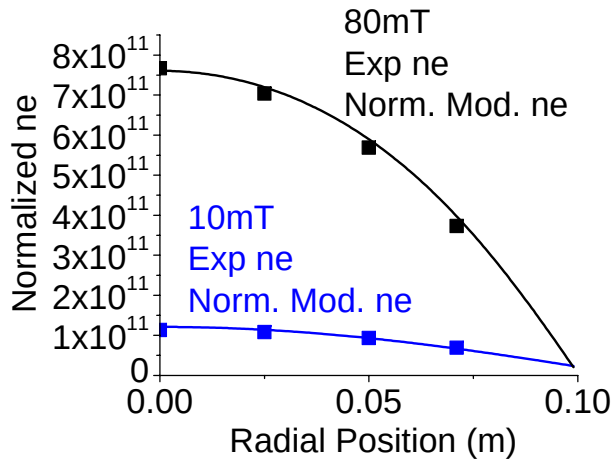

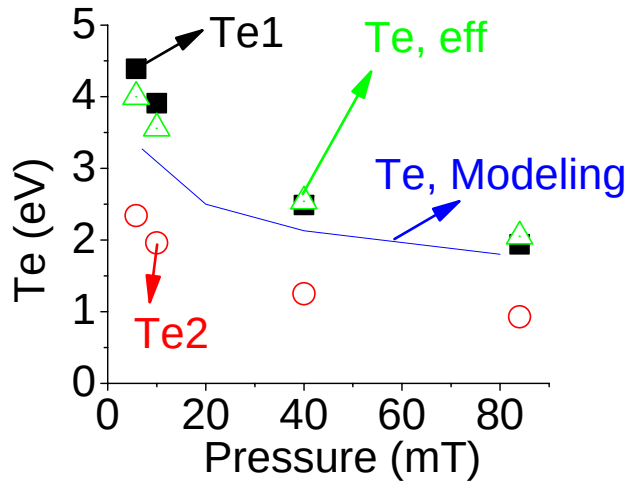

In pure Ar, not accurate ne and Te prediction is caused by non-Maxwellian EEPF.

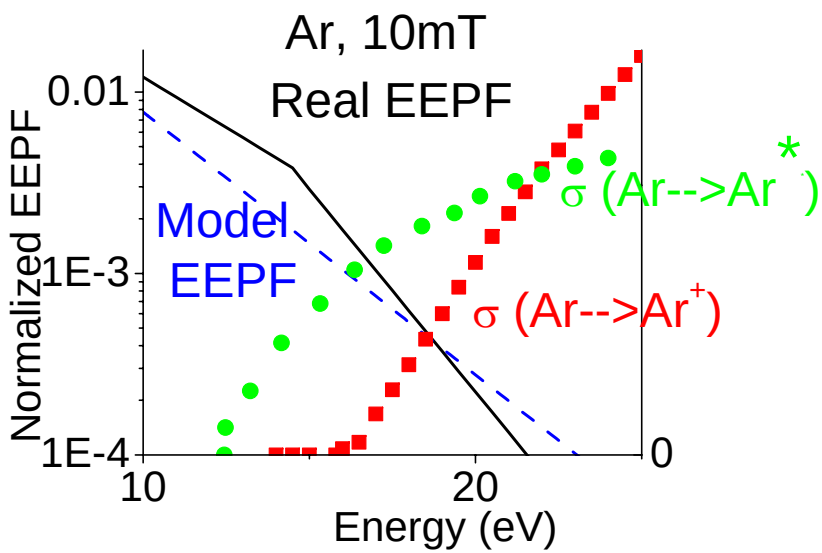

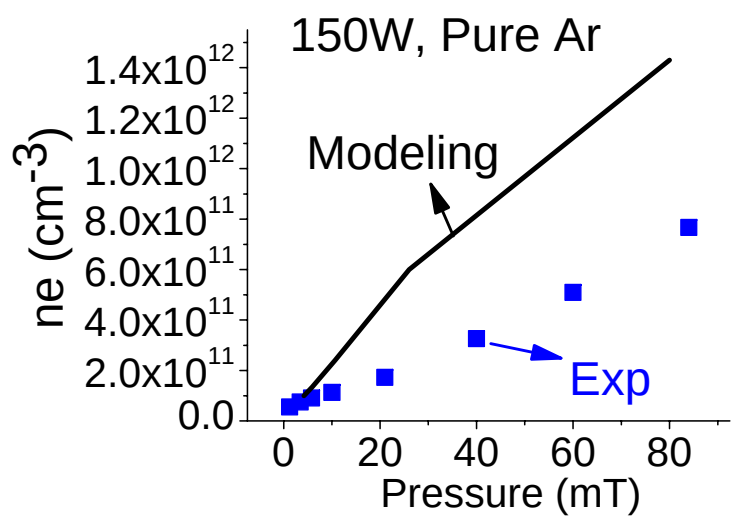

Results: ne and Te: Ar/O_2 Plasmas

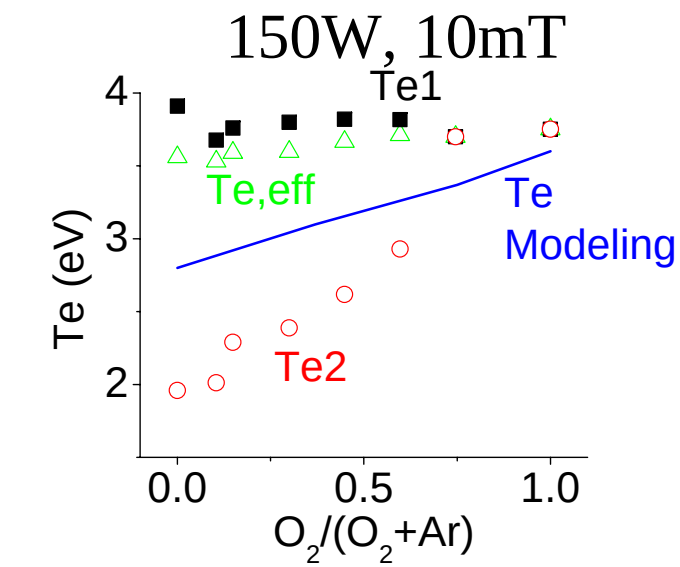

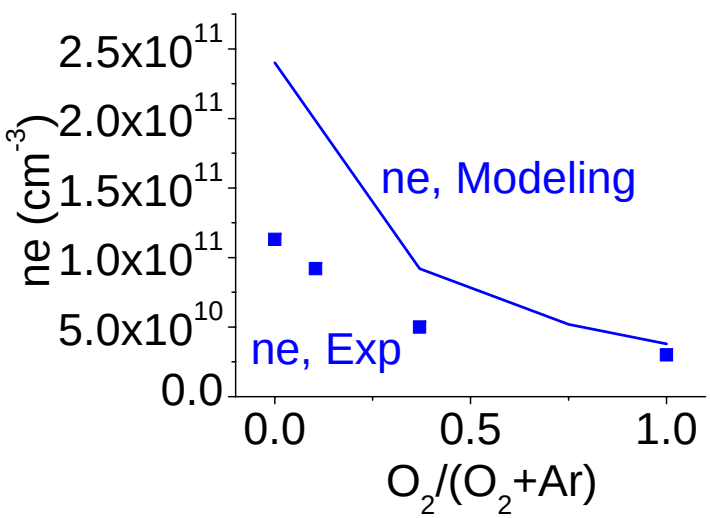

- Maxwellian EEPF at $O_2/(O_2+Ar) > 0.75$*.
  - Better Te prediction
  - Better ne prediction

Good prediction in pure O_2 plasmas.

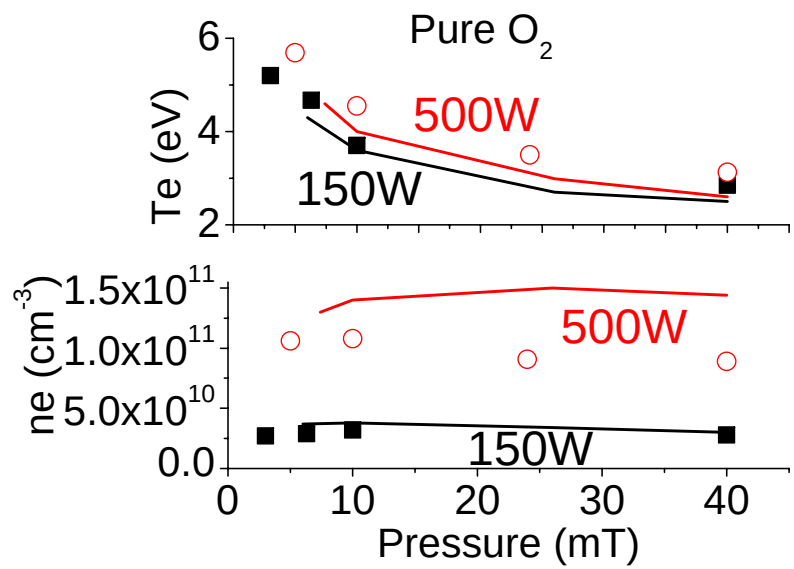

*H. Singh, et. al., J. Appl. Phys. **88**, 3889 (2000)

Result: O radical density

γ=0.3, and Cosby's O_2 disso. cross-sections

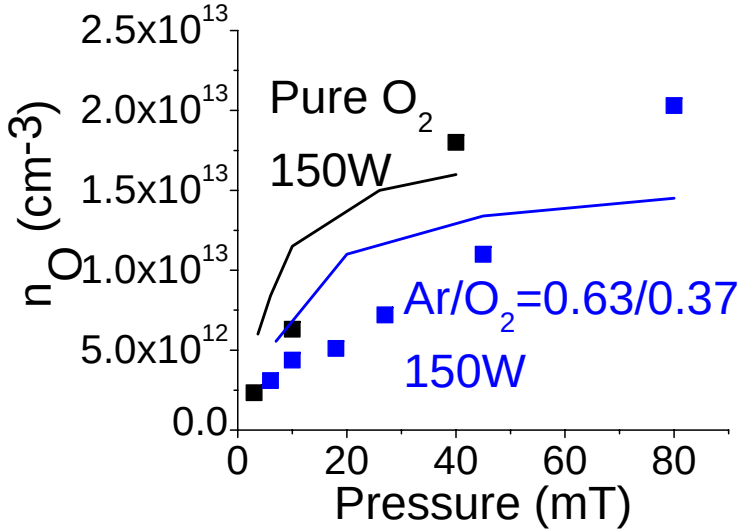

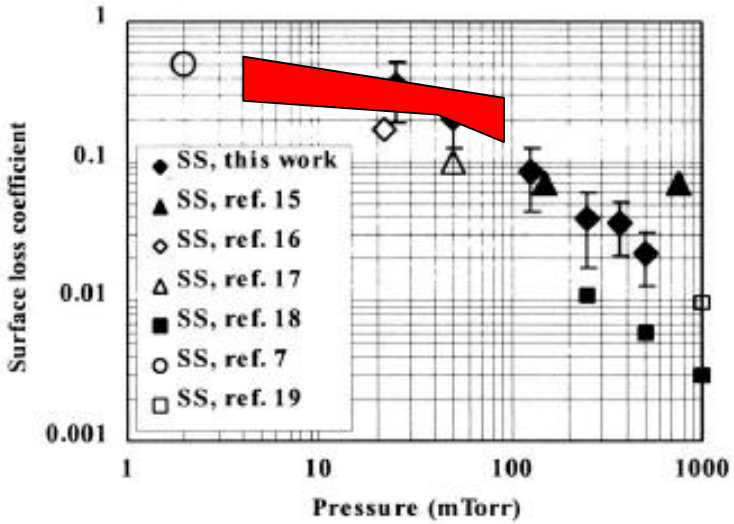

S Gomez, W. Graham et. al. J. Appl. Phys. **81**, 19 (2002)

- Estimate higher n_O at lower pressure, and vise versa.

- Good agreement can be made by using
  - Cosby's dissociation cross section
  - $\gamma = \gamma(p)$

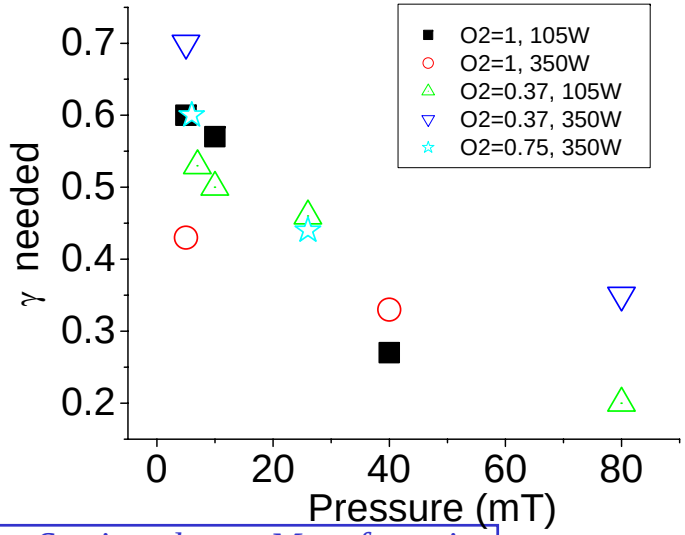

Result: Ion fluxes and Ion Composition

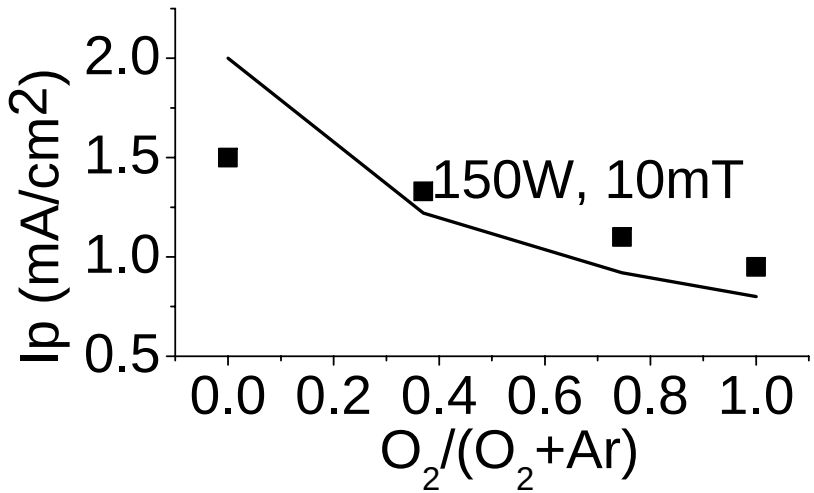

- **Model captures Ip and ion composition to the wall.**
  - **Ip is more controlled by u_b(Te).**
  - **Charge exchange (Ar^++ O_2/O→ O_2^+/O^+ + Ar) are significant at pressure > 10mT.**

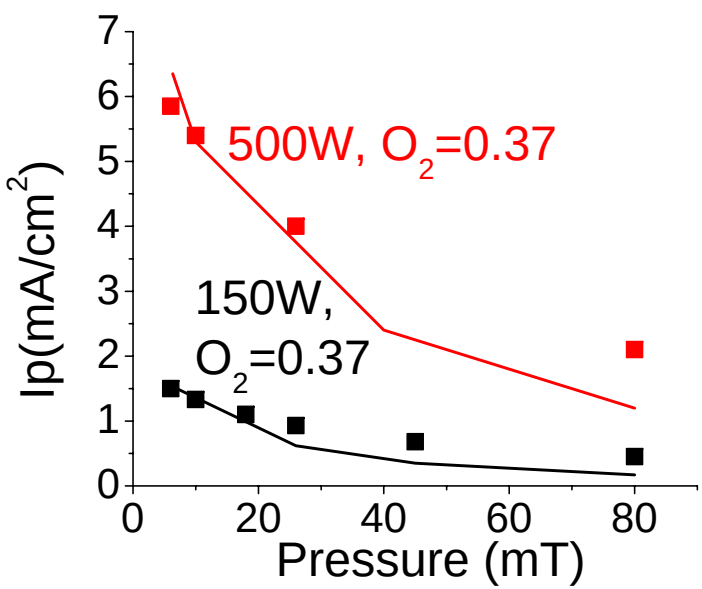

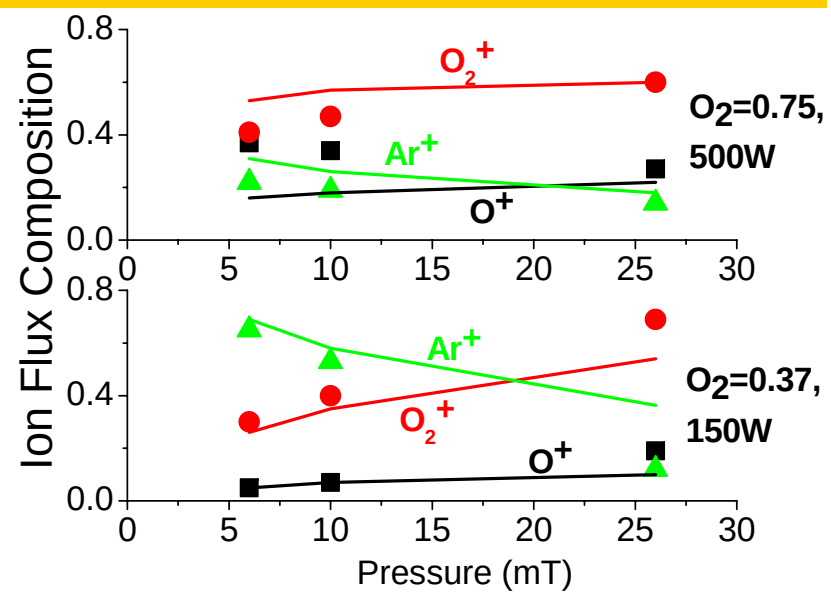

Conclusions and Future Plans

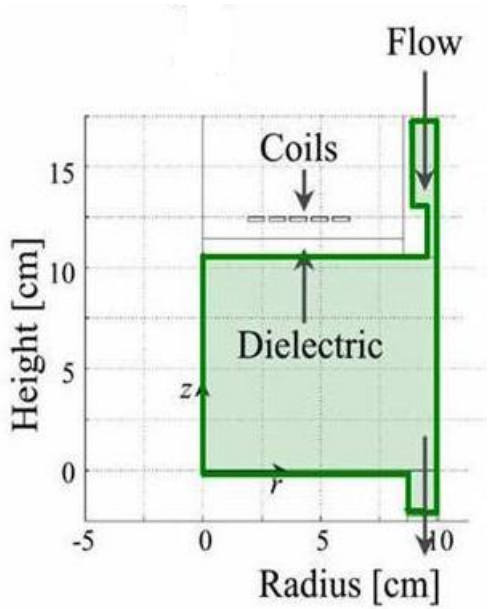

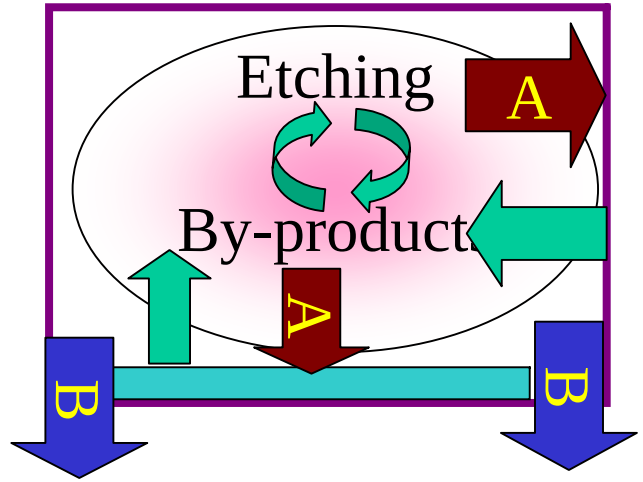

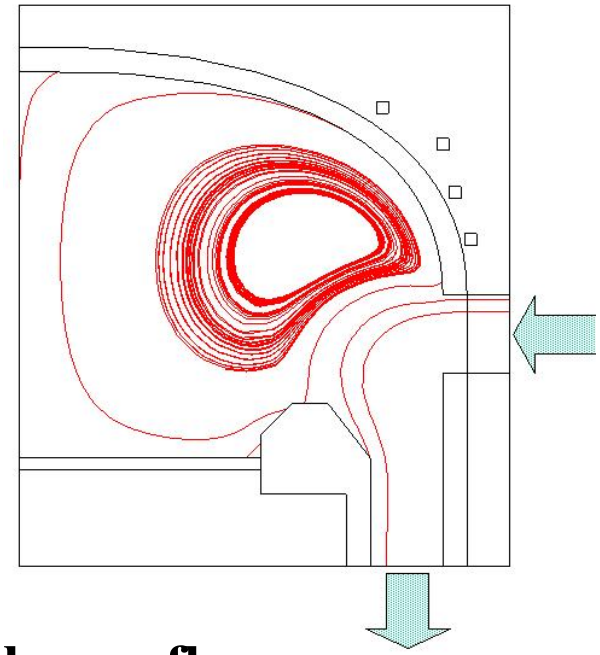

- **An ICP predictive model, couples neutral and plasma flow**
  - **Easy to converge, to share, and flexible (chemistries and systems).**
  - **Validated by a diagnostic ICP in Ar/O_2 plasmas.**
- **ESH significance: for commercial tools, e.g. AMAT Al etcher**
  - **Predicting pollutant flux to the wall and to the emission.**
  - **Predicting the condition that minimizes pollutant emission.**

Acknowledgement

- NSF/SRC ERC for Environmentally Benign Semiconductor Manufacturing
- University of California Discovery Grant through the Feature Level Compensation and Control Project
- Victor Vartanian, Brian Goolsby, Peter Ventzek, Da Zhang, Shahid Rauf, and Laurie Beu, Motorola APRDL
- Krishna Saraswat and Jim McVittie, Stanford (materials, device, profile)
- Rafael Reif and Ajay Somani, MIT (experiment)
- Bing Ji, Air Products (etch gases, plasma characterization)
- John Daugherty and Harmeet Singh, Lam Research (tool, wall interactions)

Low-Energy Hybrid (LEH) Water Purification Technology

A Novel Method for Removal of Recalcitrant Impurities

Subtask C-1-1

Elizabeth Castro, Mike Schmotzer, Kai Chen and Farhang Shadman

Chemical and Environmental Engineering
University of Arizona

NSF/SRC Engineering Research Center for Environmentally Benign Semiconductor Manufacturing

Objectives

- **Develop a novel low-energy hybrid (LEH) purification technique for the removal of organic impurities**
- **Combine the following desirable advantages:**
  - **Improve reliability**
  - **Provide a clear environmental gain**
  - **Improve performance compared to the existing methods**
- **Integrate the new technology with typical fab UPW plant process flow to:**
  - **Promote synergy and efficiency**
  - **Reduce energy usage and waste generation**
- **Resolve long-term technology obstacles against true UPW recycling**

LEH Technology Development Background

Conventional Sequence in Water Purification Systems

→ UV → IX →

Adsorption Sequence for Water Purification System

→ AC → IX →

→ IX → AC →

UV Assisted Adsorption Sequence for Water Purification System

→ UV 185 → AC →

Hybrid Oxidation/Adsorption Purification System

→ UV 185 → AC → IX →

Effect of Organic Impurities on Ion-Exchange Performance

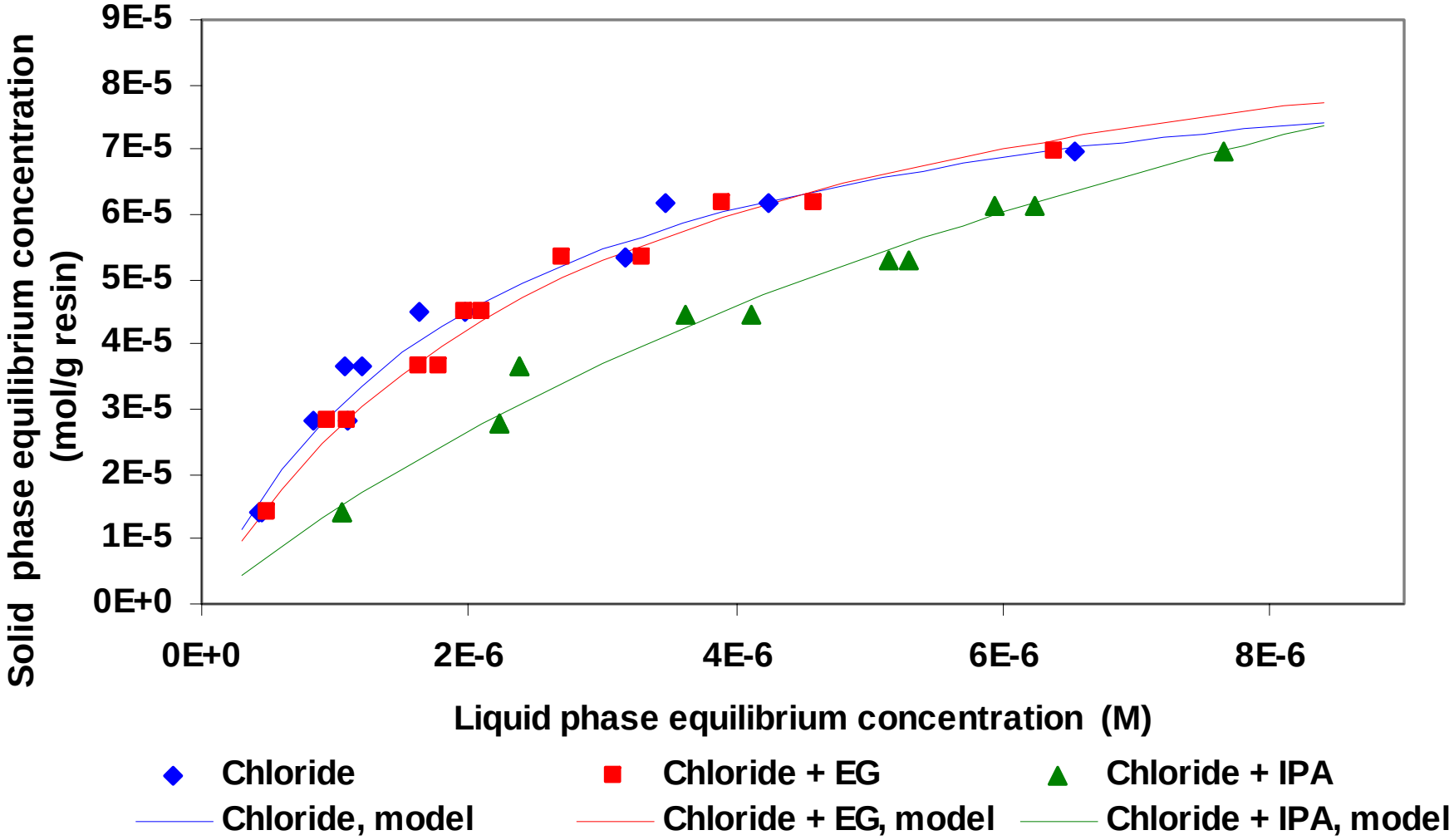

Deactivation Model for Ion-Exchange/Adsorption Processes

- **Exchange reaction**

$$Cl^- + OH^- - X \underset{k_{-1}}{\overset{k_1}{\leftrightarrow}} Cl^- - X + OH^-$$

- **Poisoning reaction:**
  - **Loss of exchange sites due to the presence of organic contaminants**

$$Cl^- - X + Org \underset{k_{-2}}{\overset{k_2}{\leftrightarrow}} OrgCl^- - X$$

$$OH^- - X + Org \underset{k_{-3}}{\overset{k_3}{\leftrightarrow}} OrgOH^- - X$$

- **Adsorption of organic onto inactive sites**

$$Org + Y \overset{k_4}{\rightarrow} OrgY$$

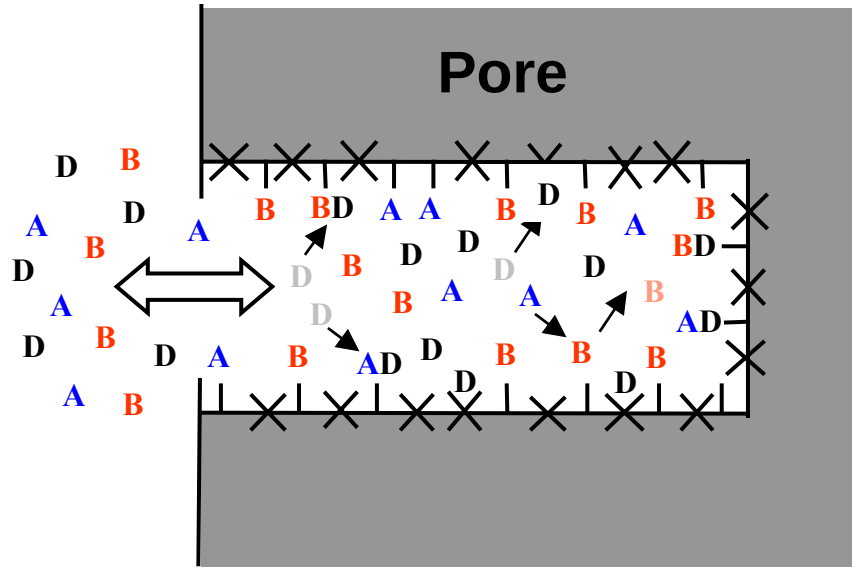

Cl^- = A
OH^- = B
Org = D

Dynamic system

- **Low concentrations**
- **Transient conditions**
- **Multi-component interactions**

Experimental Validation of Process Model

Multi-Component Case

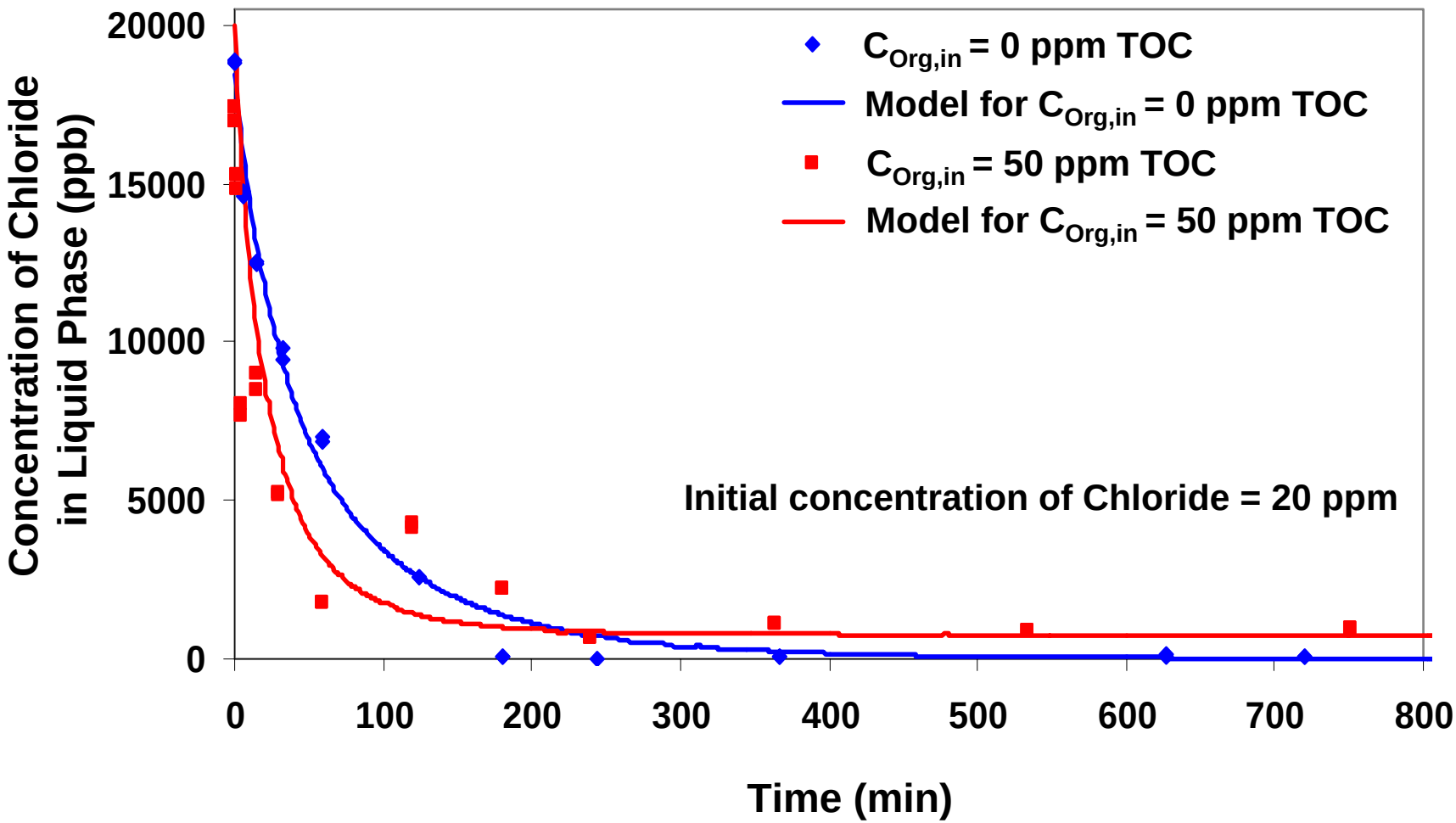

Effect of TOC on the Dynamics of Ion-Exchange Systems

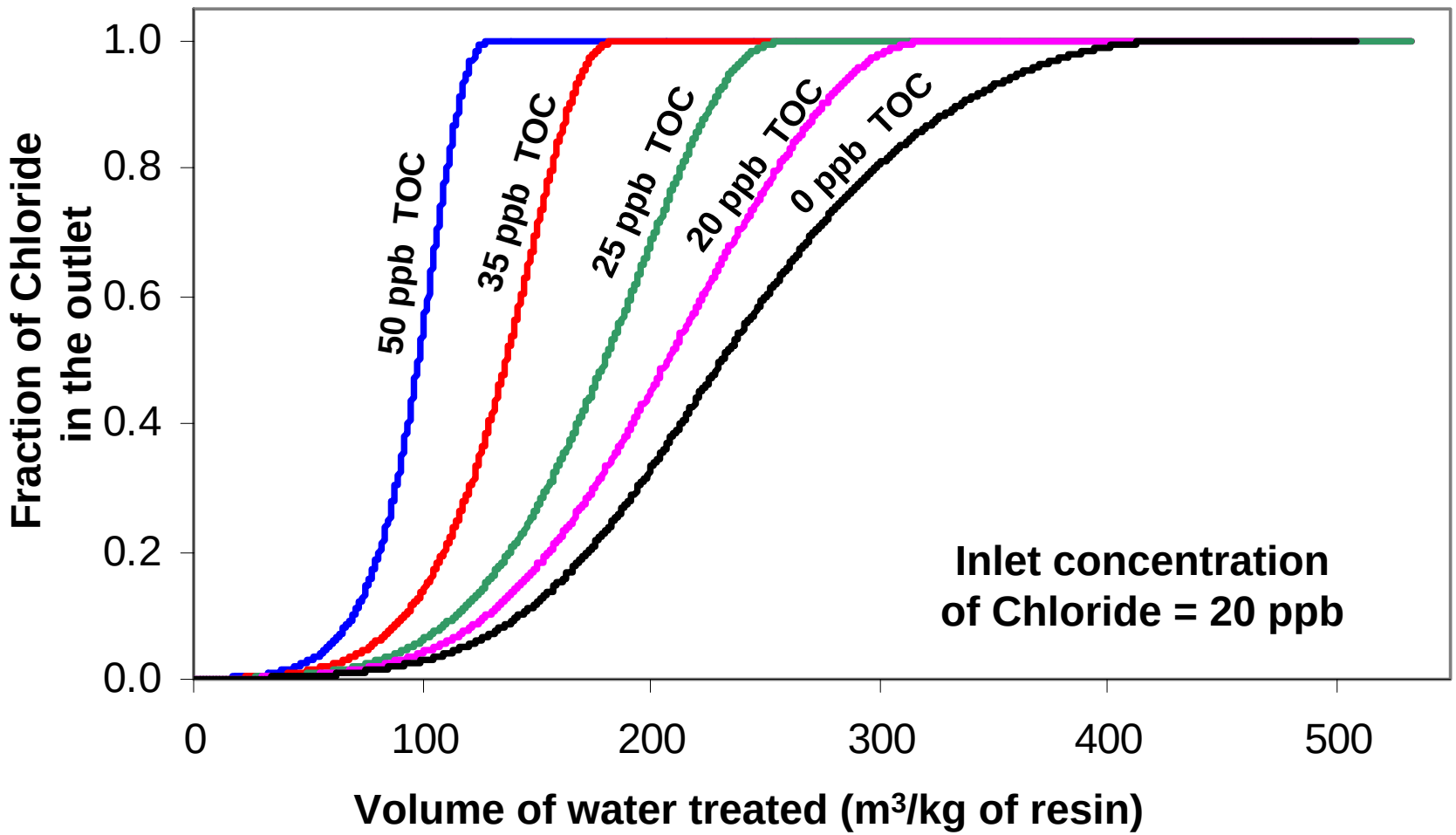

Purification Mechanism in LEH System

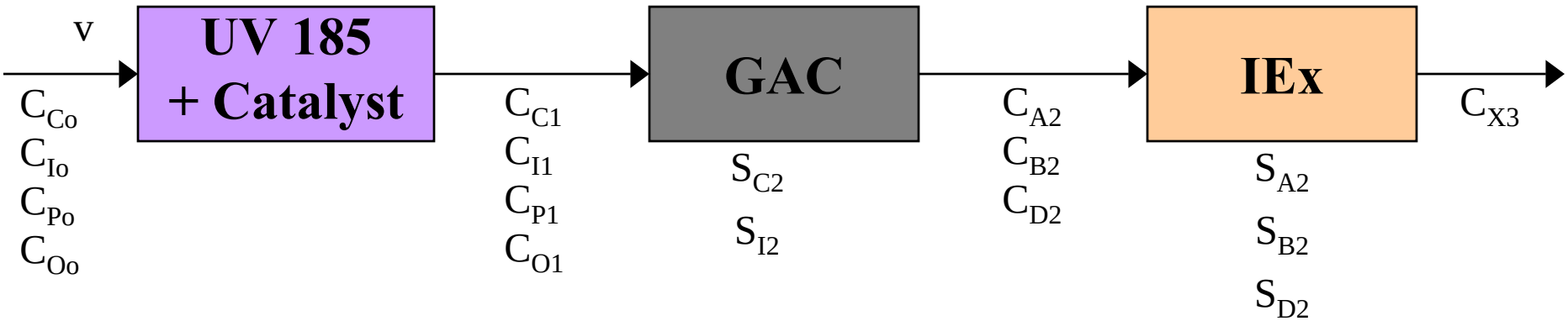

$$H_2O + h\nu \xrightarrow{k_1} O$$
$$C + h\nu \xrightarrow{k_2} I$$
$$C + O \xrightarrow{k_3} I$$
$$I + O \xrightarrow{k_4} P$$

$$C + X_{GAC} \xleftrightarrow{k_{aC_2}, k_{dC_2}} C \bullet X_{GAC}$$
$$I + X_{GAC} \xleftrightarrow{k_{aI_2}, k_{dI_2}} I \bullet X_{GAC}$$
$$C \bullet X_{GAC} + O \xrightarrow{k_5} P$$
$$I \bullet X_{GAC} + O \xrightarrow{k_6} P$$
$$C + O \xrightarrow{k_7} I$$
$$I + O \xrightarrow{k_8} P$$
$$O + GAC \xrightarrow{k_9} \text{products}$$

$$A + B \bullet X \xleftrightarrow{k_{10}, k_{-10}} A \bullet X + B$$
$$A \bullet X + D \xleftrightarrow{k_{11}, k_{-11}} A \bullet X \bullet D$$
$$B \bullet X + D \xleftrightarrow{k_{12}, k_{-12}} B \bullet X \bullet D$$
$$D + Y \xrightarrow{k_{13}} D \bullet Y$$

Model for Photocatalytic Reaction

$TiO_2 + h\nu \xrightarrow{k_1} e^- + h^+$	1. Electron/hole formation
$e^- + h^+ \xrightarrow{k_{-1}} TiO_2 + (heat)$	2. Electron/hole recombination
$h^+ + H_2O \xrightarrow{k_2} OH\bullet + H^+$	3. Radical formation
$OH\bullet + TOC \xrightarrow{k_3} CO_2 + H_2O$	4. Oxidation of organics
$OH\bullet + X \xrightarrow{k_4} products$	5. Radical combining with X (anything other than TOC)
$M + e^- \xrightarrow{k_m} M(e^-)$	6. Metal attracts electron = 0 not metal present.

$$\frac{d(h^+)}{dt} = k_1 S - k_{-1}(e^-)(h^+) - k_2(h^+)$$

$$\frac{d(e^-)}{dt} = k_1 S - k_{-1}(e^-)(h^+) - k_m(e^-)$$

$$\frac{d(OH\bullet)}{dt} = k_2(h^+) - k_3(OH\bullet)(TOC) - k_4(OH\bullet)$$

$$\frac{d(TOC)}{dt} = -k_3(OH\bullet)(TOC) + Cr_{evap}$$

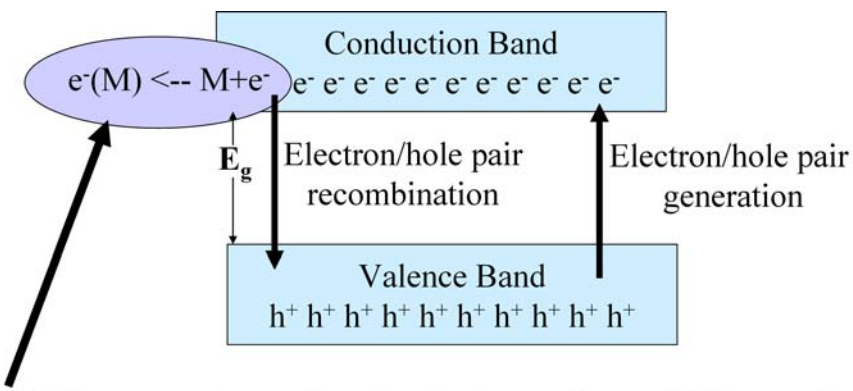

Metallic promoter attracts electrons from TiO_2 conduction band and slows recombination reaction

Photocatalytic Oxidation of Organics

Triton X-100; UV 254nm

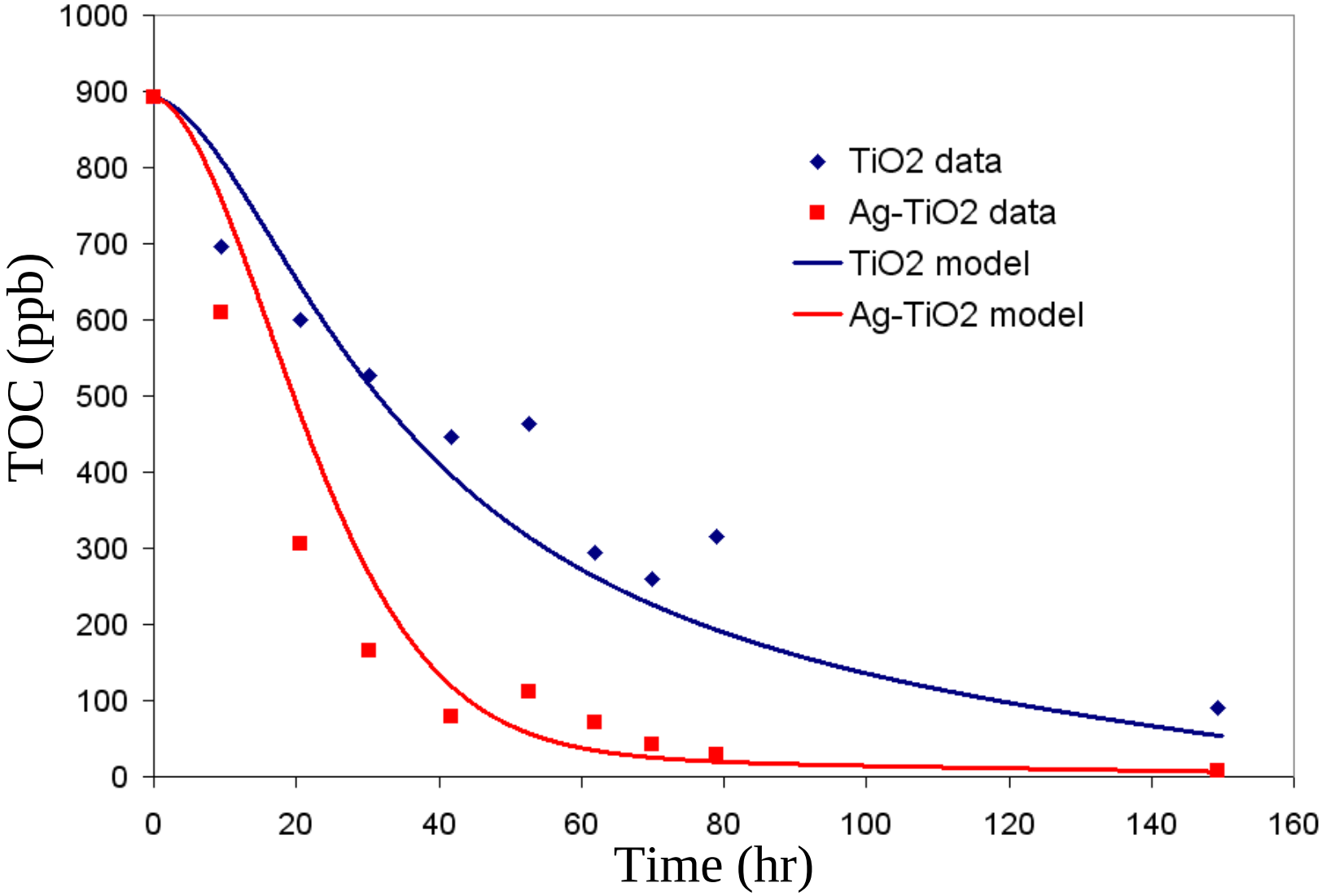

Effects of Nitrogen Doping in TiO_2

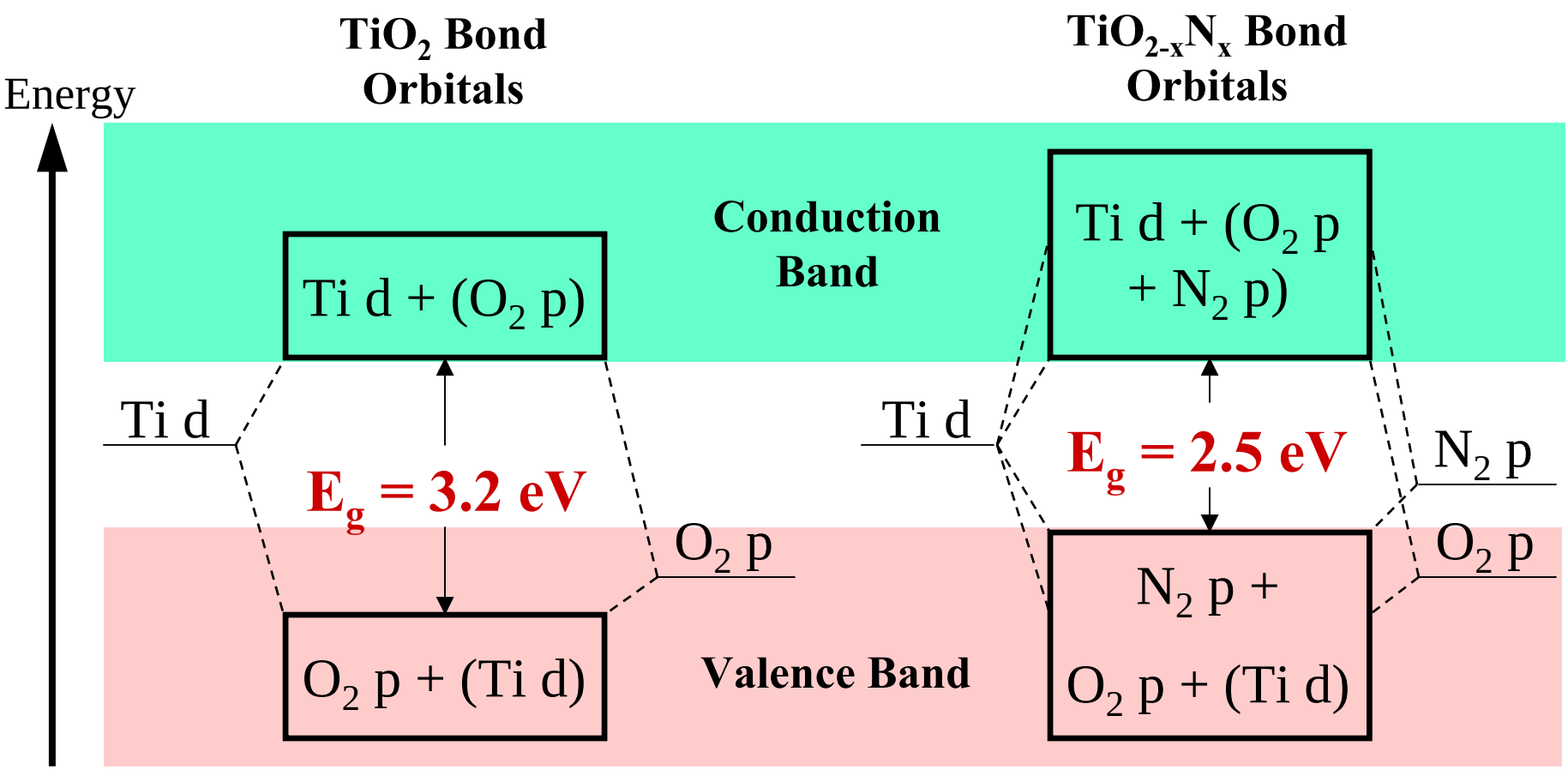

- Addition of nitrogen increases size of bond orbitals, thus **decreasing** the energy band gap.

Sol-gel Method for Preparation of Supported Photo-Catalyst

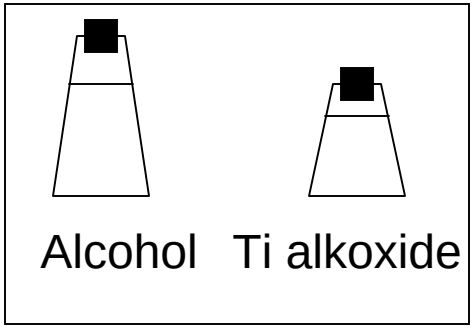

Reagents

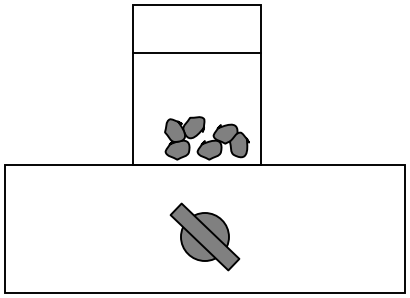

Dip Coating
with Ti alkoxide

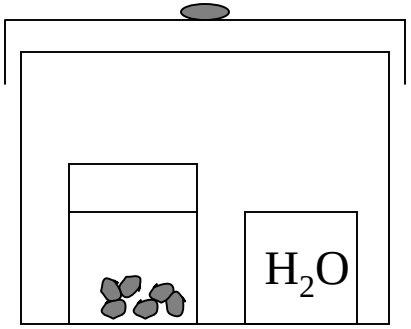

Hydrolysis

$$Ti(\text{-}OC_3H_7)_4 + 2H_2O \longrightarrow TiO_2 + 4C_3H_7OH$$
$$Ti(\text{-}OC_2H_5)_4 + 2H_2O \longrightarrow TiO_2 + 4C_2H_5OH$$

Synthesis of Titanium Oxy-Nitride

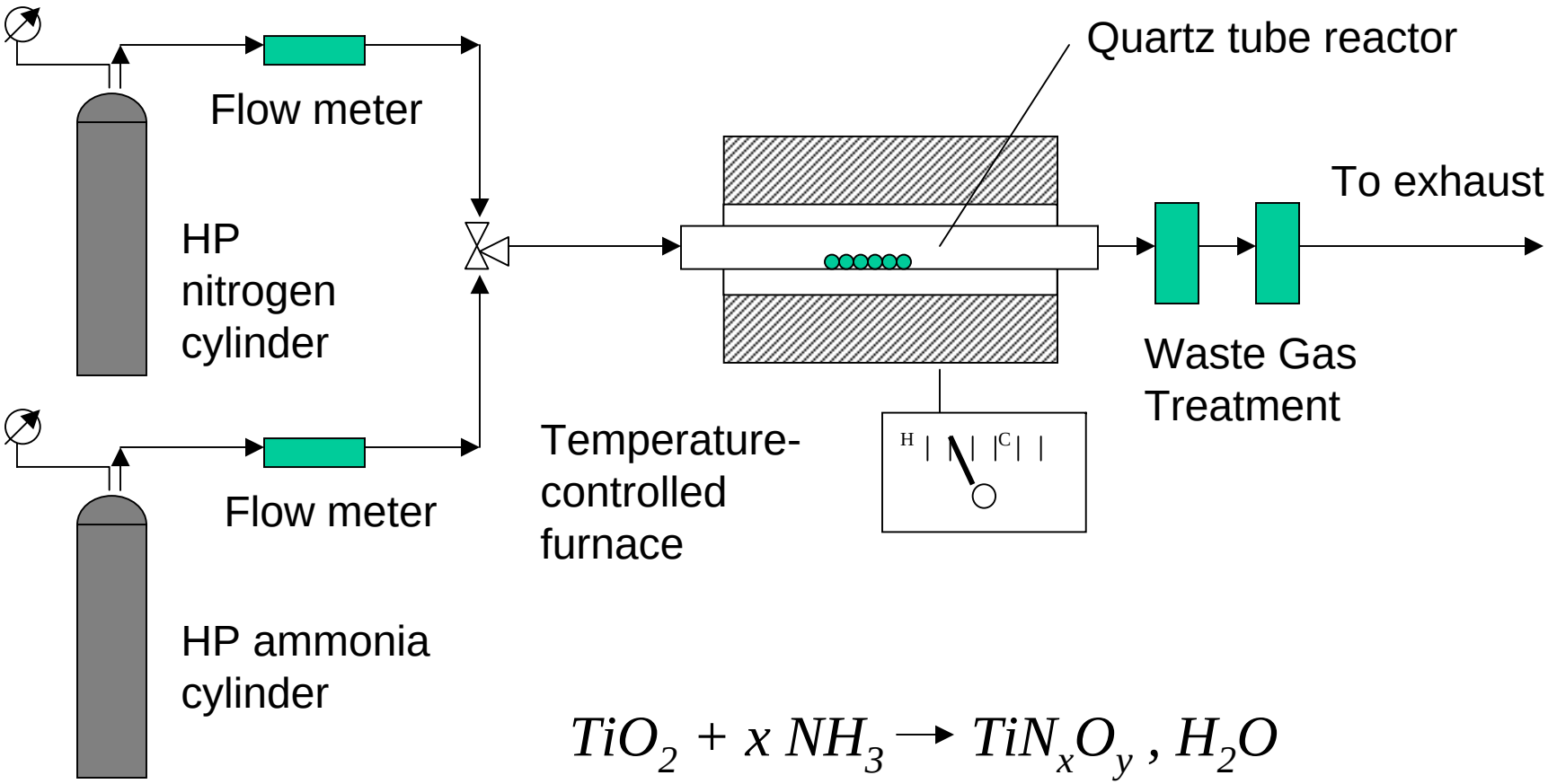

$$TiO_2 + x\,NH_3 \rightarrow TiN_xO_y\,,\,H_2O$$

Photocatalytic Oxidation of TOC

Ethylene Glycol; UV 254nm Illumination

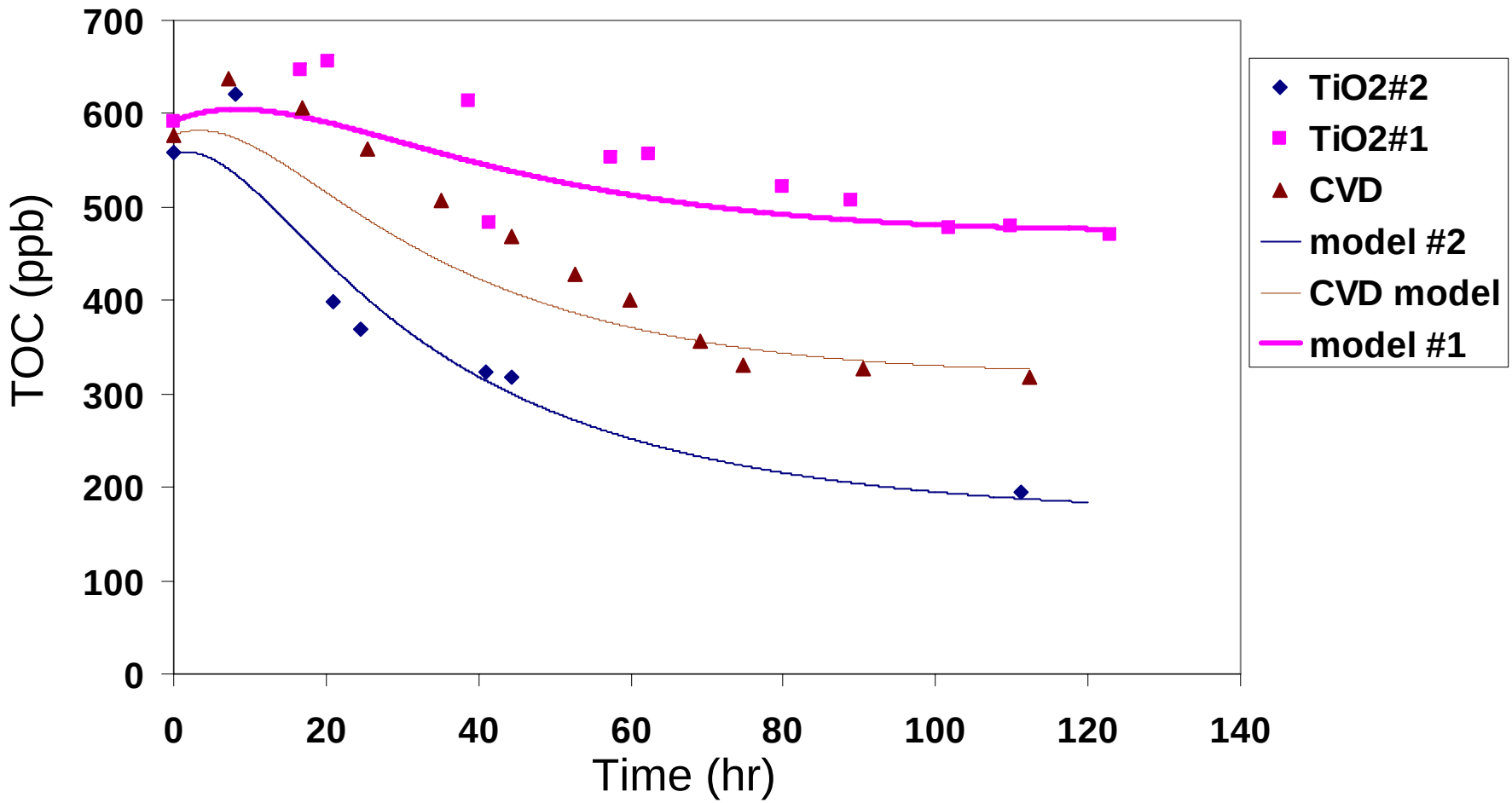

Comparison of Water Purification Systems

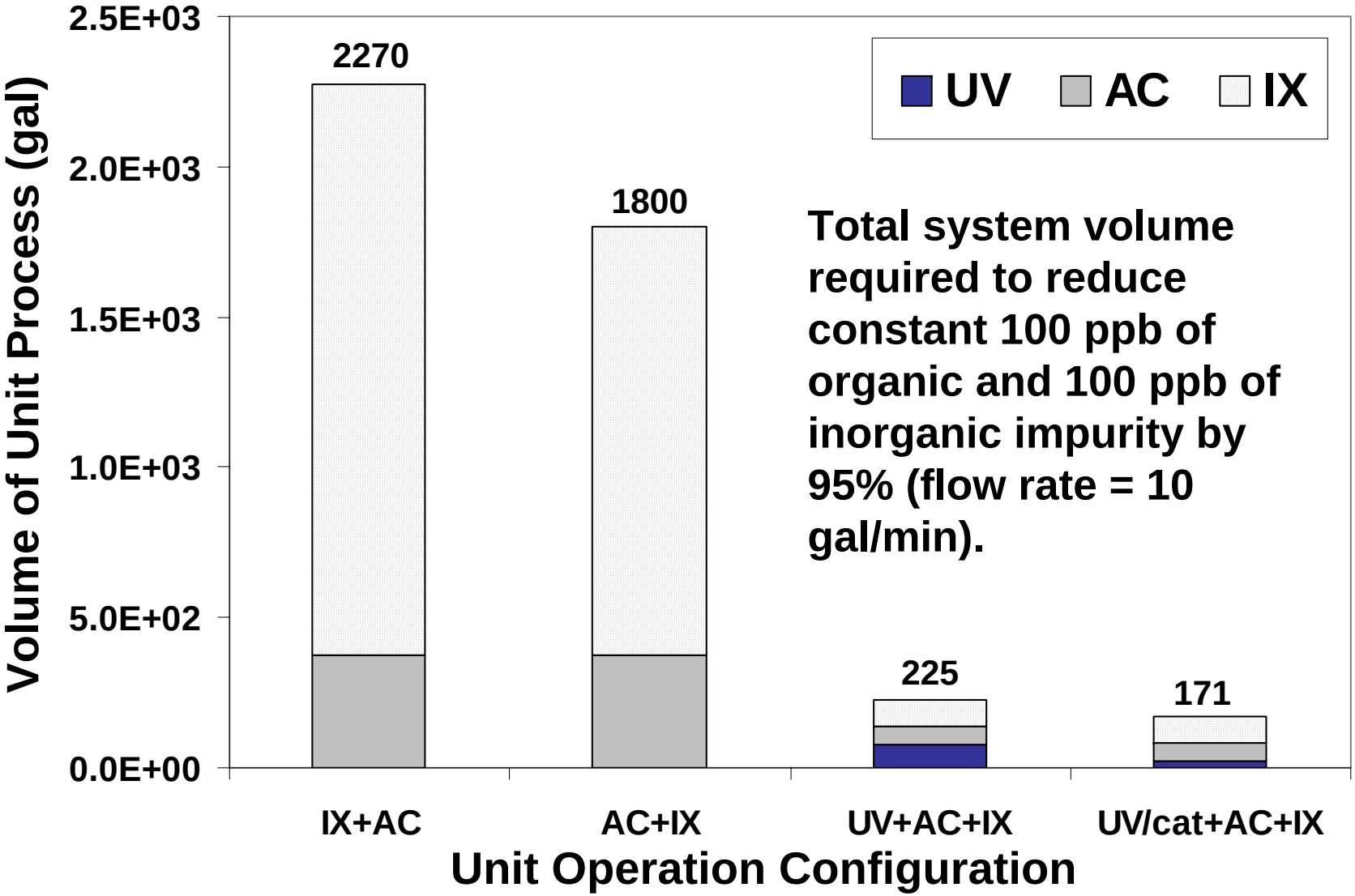

Regeneration/Backwash Requirements of Water Purification Systems

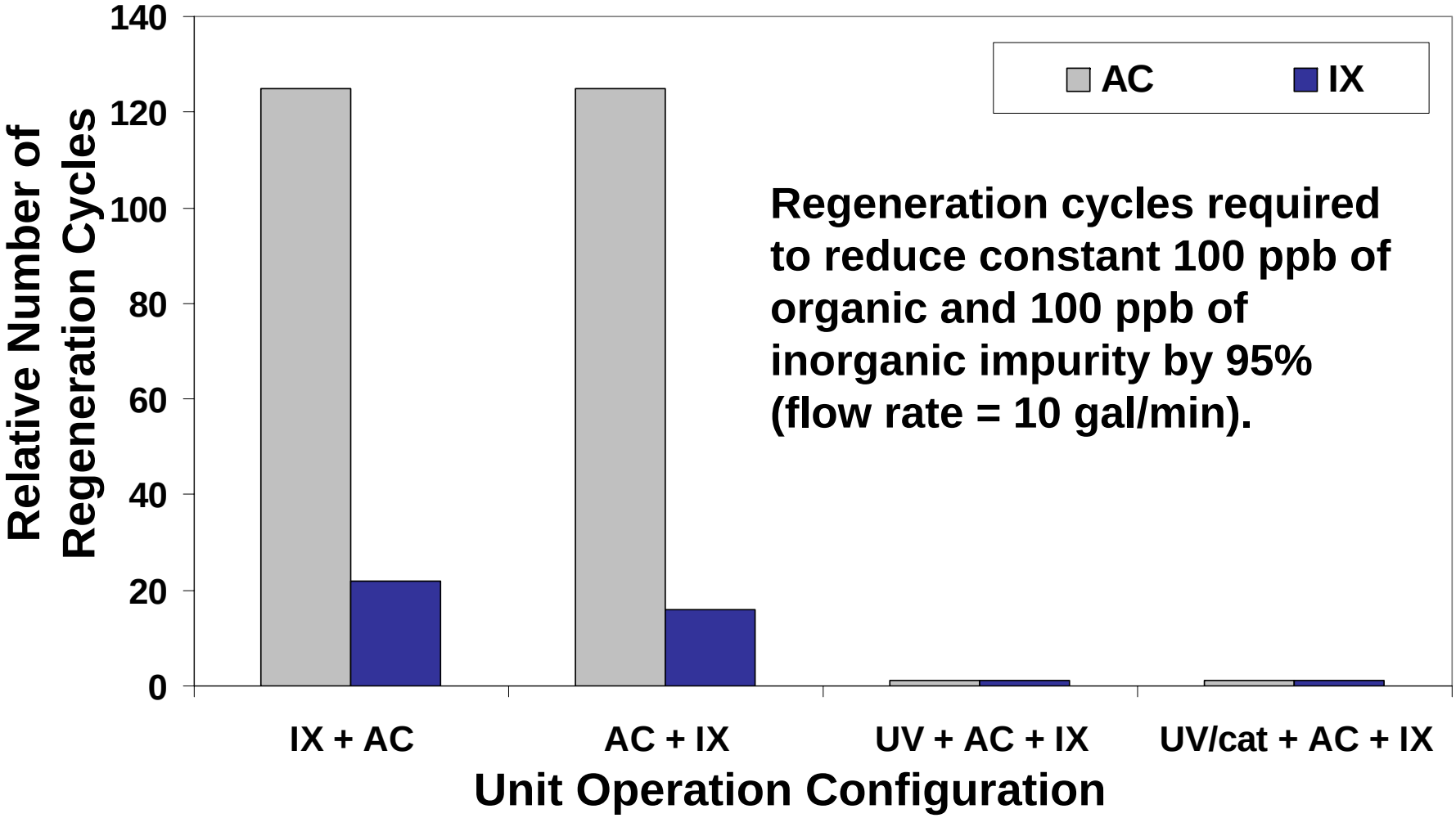

Cost Comparison of Various Water Purification Systems

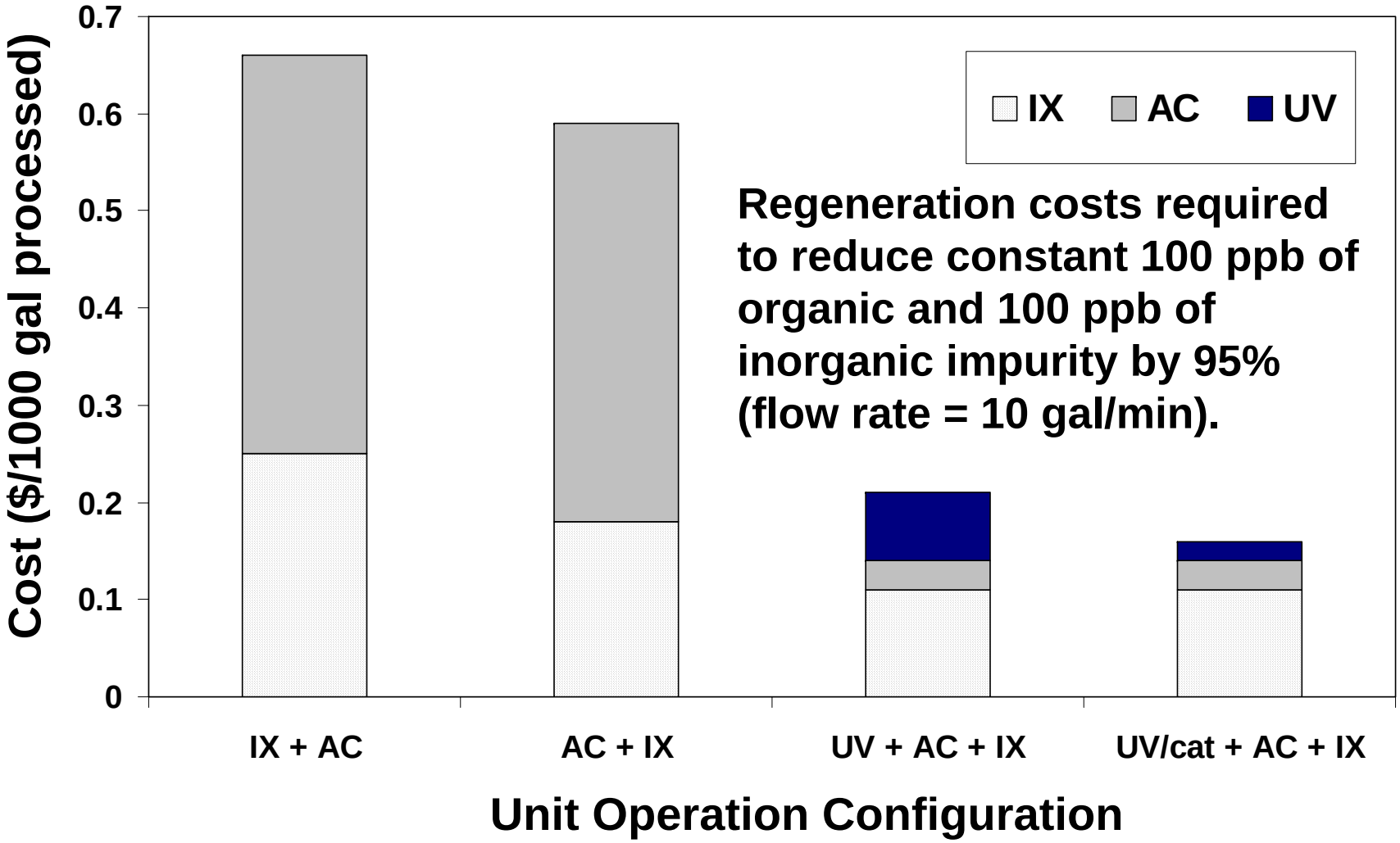

Conclusions and Highlights:

- **The new integrated, hybrid oxidation/adsorption is an effective technique for the removal of recalcitrant organic impurities.**
- **The proposed process reduces waste and chemical usage through prolonging the life of ion-exchange and activated carbon units**
- **The catalyst reduces the energy requirement for oxidation.**

Future Plans:

- **Continue to improve the catalyst deposition methodology; emphasize new promoters, based on the mechanism of promoter action found in this study.**
- **Industrial interactions:**
  - **John Croft (Intel), John DeGenova (TI), Kon-Tsu Kin (ITRI and TSMC)**

ESH Metrics and Impact

I) Basis of Comparison:

Current best technology: Water supply to Ultrapure Water (UPW) treatment facility completely from natural/municipal resource. Spent rinsewaters from wafer fab processes discharged to industrial wastewater system, treated, and sent to the municipal sewer, for sanitary treatment.

II) Manufacturing Metrics

The recycling of previously purified water has been proven to improve the water quality at the point of use and will lower the cost of purification. It also provides for an improved consistency of UPW quality as less maintenance and longer run times between regenerations are necessary. Cost savings are dependent on the region with varying costs of both water supply and wastewater discharge.

An impact on wafer yield has not been determined.

III) *ESH Metrics*

	Usage Reduction			Emission Reduction			
Goals / Possibilities	**Energy**	**Water**	**Chemicals**	**PFCs**	**VOCs**	**HAPs**	**Other Hazardous Wastes**
50% of spent UPW rinsewaters recycled to UPW plant.	Factor of 2	40 % reduction in municipal feed water	50% reduction in regeneration chemicals	N/A	N/A	Some reduction in acid vapors	50% reduction in regeneration waste/ and wastewater
90% of spent UPW rinsewaters recycled to UPW plant.	Factor of 3	70% reduction in municipal feedwater	75% reduction of regeneration chemicals	N/A	N/A	Some reduction in acid vapors	> 80% reduction in regeneration waste/ and wastewater

Treatment of Copper in CMP Waste Streams using Polyethyleneimine (PEI)

(Subtask C-1-2)

Worawan Maketon and Kimberly Ogden

Chemical and Environmental Engineering, University of Arizona

NSF/SRC Engineering Research Center for Environmentally Benign Semiconductor Manufacturing

Objectives

- ***Investigate the removal of copper (II) using Polyethyleneimine (PEI).***
- ***Determine the behavior of a single packed bed column, containing PEI-agarose gel, in treatment process for surrogate Cu-CMP wastes containing copper (II) and organic IPA.***
- ***Investigate the feasibility of chelator binding CMP-pad.***

ESH Metrics for Task C-1-2: Novel Water Purification Technology

I) Basis of Comparison:

Current best technology. Treatment of organic and copper containing effluent by a combination of Carbon Bed, UV, precipitation, membrane filtration, and Ion Exchange.

II) Manufacturing Metrics:

This new treatment method will decrease the water usage by allowing for recycle of contaminated streams. This will improve the quality of water at point of use. However, the precise effect on the manufacturing metrics cannot be assessed at this stage of research.

III) ESH Metrics:

	Usage Reduction			Emission Reduction			
Goals / Possibilities	Energy	Water	Chemical	PFCs	VOCs	HAPs	Other hazardous Wastes
Simultaneous biotreatment of organics and biosorption of copper	~ 90 %	N/A	N/A	N/A	N/A	N/A	Elimination of Ion Exchange Resin disposal

Copper CMP Waste

- ***Copper metal***
- ***Abrasive Particles: Silica, Alumina, Ceria***
- ***Inhibitor: Benzotriazole (BTA)***
- ***Amino Acid: Glycine***
- ***Complexing Agent: EDTA, Citric Acid***
- ***Surfactant: Triton, Sodium dodecyl sulfate***
- ***Microemulsion: Isopropyl Alcohol***

Theory and Method of Approach – Continuous Process

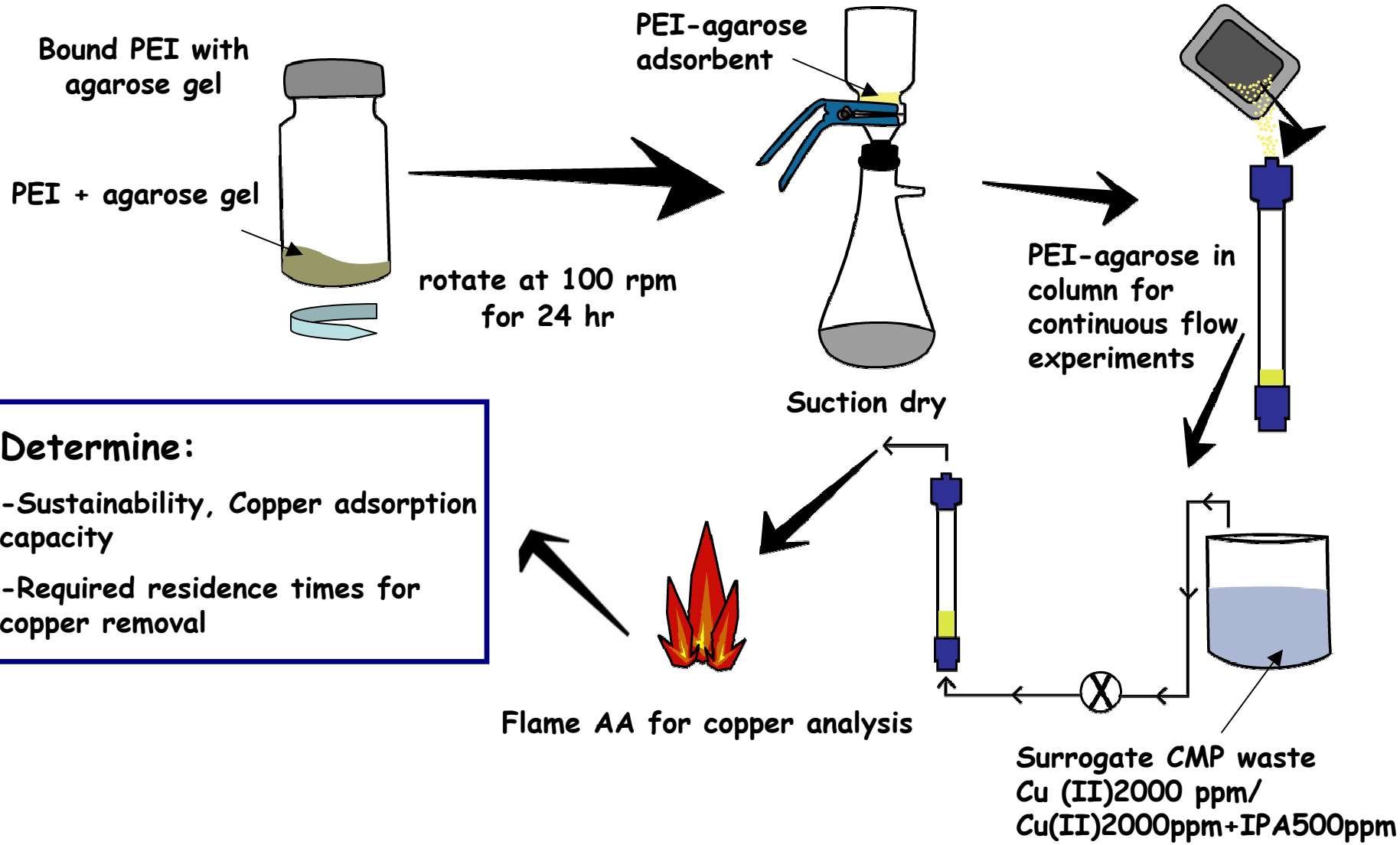

Determine:

-Sustainability, Copper adsorption capacity

-Required residence times for copper removal

Continuous Copper Adsorption to Breakthrough




Breakthrough curves of copper adsorption on PEI

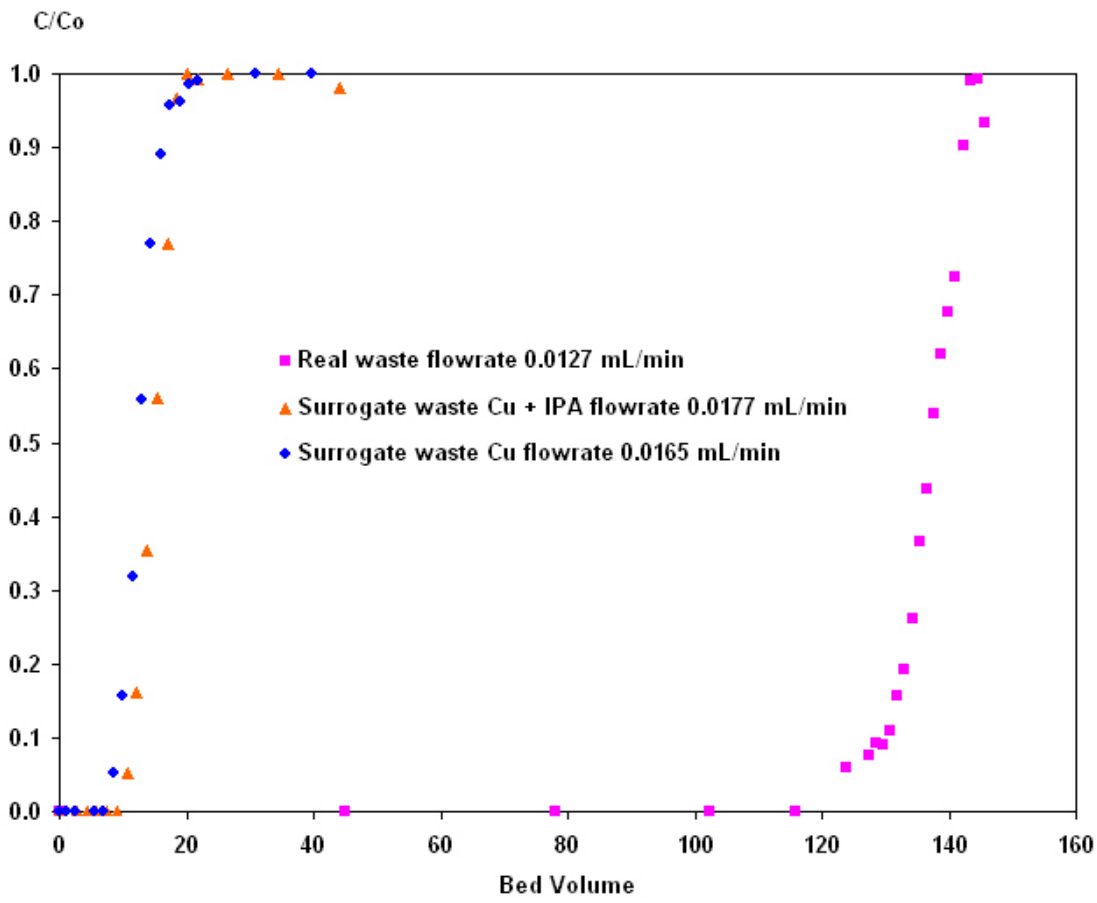

Copper binding capacity in a continuous column (g Cu^{2+}/mL adsorbent):

- ***Surrogate waste***
  - ***w/o IPA 0.027 ± 0.005***
  - ***w/ IPA 0.024 ± 0.005***
- ***Real Waste 0.016 ± 0.005***

Results indicate IPA has no affect in copper adsorption when presents.

Dispersion Coefficient

[Van Genuchten, 1982]

$$\frac{\partial C}{\partial t} = D_z \frac{\partial^2 C}{\partial z^2} - u_z \frac{\partial C}{\partial z} - \cancel{K}$$

Determine D_z by Table Curve Program.

$D_z = 4.28\ cm^2/s \quad r^2 = 0.843$

$$\frac{C(z,t)}{C_o} = \frac{1}{2} erfc\left(\frac{z - u_z t}{\sqrt{4 D_z t}}\right) + \sqrt{\frac{u_z^2 t}{\pi D_z}} \exp\left(\frac{-(z - u_z t)^2}{4 D_z t}\right)$$

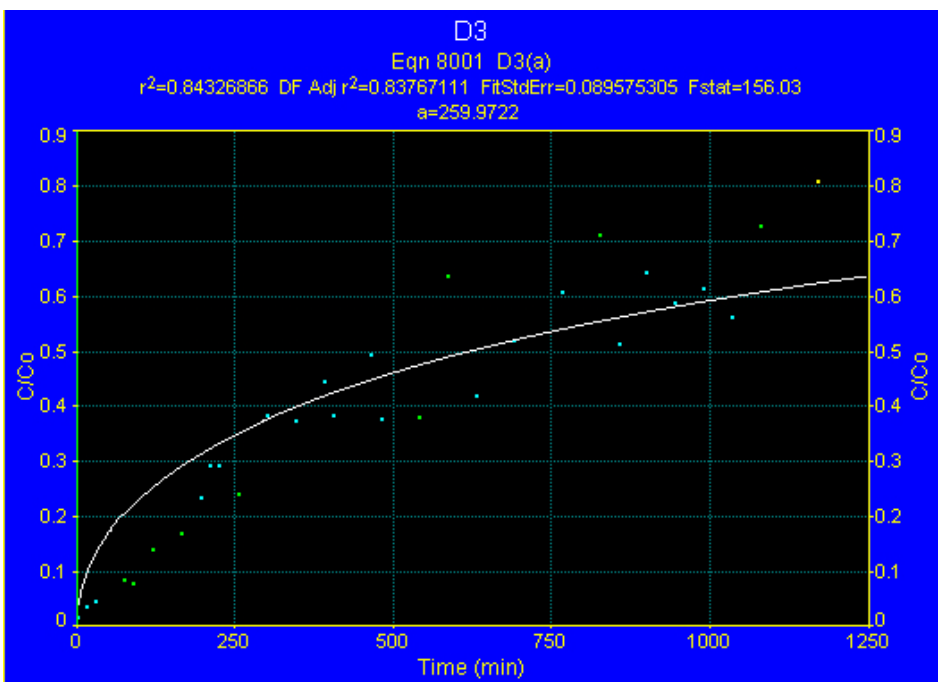

$$-\frac{1}{2}\left(1 + \frac{u_z z}{D_z} + \frac{u_z^2 t}{D_z}\right) \exp\left(\frac{u_z z}{D_z}\right) erfc\left(\frac{z + u_z t}{\sqrt{4 D_z t}}\right)$$

C – Conservative tracer

u_z – Interstitial fluid velocity

K – Source/Sink term

t – Time

D_z – Dispersion coefficient

z – Length of column

Model Formulation

One dimensional Adsorption-Dispersion-Reaction (ADR) equation

$$\frac{\partial C}{\partial t} = D_z \frac{\partial^2 C}{\partial z^2} - u_z \frac{\partial C}{\partial z} - \frac{\rho_s (1-\varepsilon)}{\varepsilon}\left(\frac{\partial q}{\partial t}\right)$$

C – Copper concentration

D_z – Dispersion coefficient = 4.28 cm^2/s

z – Length of column = 1.4 cm

u_z – Interstitial fluid velocity

ρ – Solid density = 0.9 g/cm^3

ε – Bed void volume = 0.0752

q is a function of Langmuir isotherm models: $q = Q^a \frac{bC}{1+bC}$

Q^a – Maximum adsorption capacity of the adsorbent = 27.5 mg Cu^{2+}/mL adsorbent

b – Langmuir constant = 0.14 ppm^{-1}

Conclusion

- ***Initial chelate-agarose adsorbent promising capabilities***
  - ***PEI-agarose showed great affinity of binding copper in batch system***
  - ***Adsorbent's stability is good***
  - ***Performance and reproducibility did not change even after regeneration***
- ***Packed bed column performance***
  - ***Large volumes of copper contaminated solutions can be concentrated down to much smaller volumes for metal recovery***
  - ***A solution containing only copper ions in solution had faster breakthrough than when IPA was present.***
- ***Model for breakthrough curve of copper has been partially developed and still in progress of comparing with experimental data***

Future Plans

- *Continue on developing model of breakthrough curve for copper adsorption on PEI-agarose gel*
- *Investigate the use of chelators directly added to CMP pads*

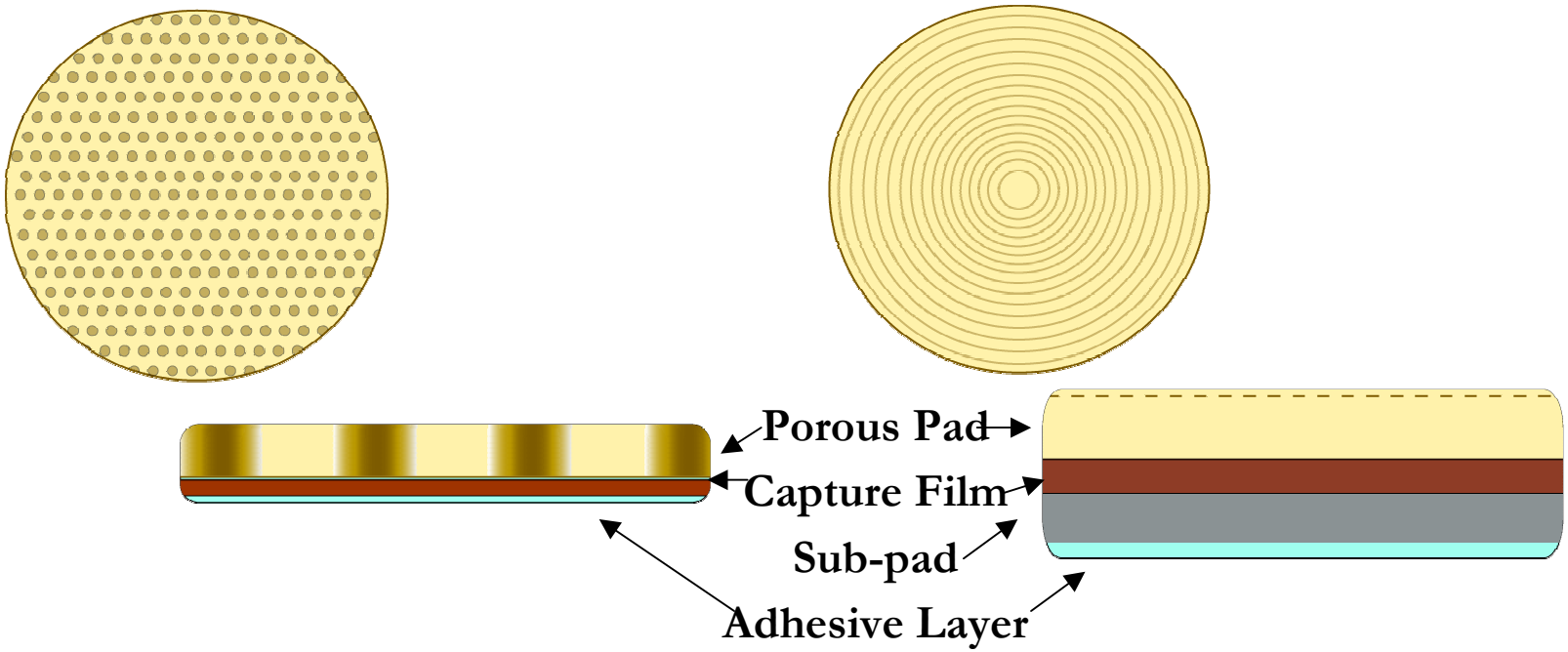

Theory of chelators added to polishing pad

- Target Metal Ion
- Porous and Diffusive Pad
- First binding polymeric adsorbent film
- High capacity polymeric adsorbent film
- Sub-pad
- Adhesive Layer

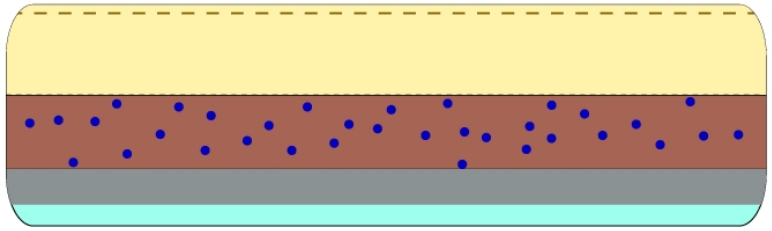

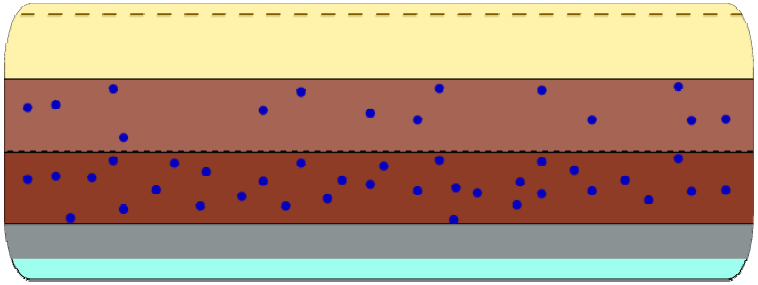

Filtration and Biotreatment Scheme to Recycle CMP Wastewater

Yeira Padilla-Luciano
Chemical Engineering Department
University of Puerto Rico- Mayagüez, PR
Chemical & Environmental Engineering Department
University of Arizona- Tucson, AZ

Goal

- The overall benefit and motivation for this study is to explore the possibility of water reuse in semiconductor and biotechnology industries.

Objectives

- To develop mass-exchanger based on dual function depth filters and bio-treatment to treat wastewater.
- To remove Silica and Alumina nanoparticles, Copper, and IPA from Chemical Mechanical Planarization (CMP) wastewater.

ESH Metrics for Task C-1-2: Novel Water Purification Technology (Biotreatment)

I) *Basis of Comparison:*

Current best technology. Treatment of organic and copper containing effluent by a combination of Carbon Bed, UV, precipitation, membrane filtration, and Ion Exchange.

II) *Manufacturing Metrics:*

This new treatment method will decrease the water usage by allowing for recycle of contaminated streams. This will improve the quality of water at point of use. However, the precise effect on the manufacturing metrics cannot be assessed at this stage of research.

III) *ESH Metrics:*

	Usage Reduction			Emission Reduction			
Goals / Possibilities	Energy	Water	Chemical	PFCs	VOCs	HAPs	Other hazardous Wastes
Simultaneous biotreatment of organics and biosorption of copper	~ 90 %	N/A	N/A	N/A	N/A	N/A	Elimination of Ion Exchange Resin disposal

Research Overview

- Biological Organisms
  - Cu(II) biosorption

    Immobilized *Soil 5Y* cells. 0.14 g Cu^{2+}/g dry biosorbent

    (Stanley and Ogden, 2000)
  - Organics treatment

    IPA4- organics degrading bacteria
- Previous Works
  - Oily Wastewater (Bogere et al. 2004)
  - Biofouling (Zaidi et al. 1996)
  - Behavior of cells to reduce copper and IPA.

    Treatment of Surrogate CMP waste without nanoparticles (Stanley and Ogden 2003; Ruiz and Ogden 2004)

Equipment

- Filter

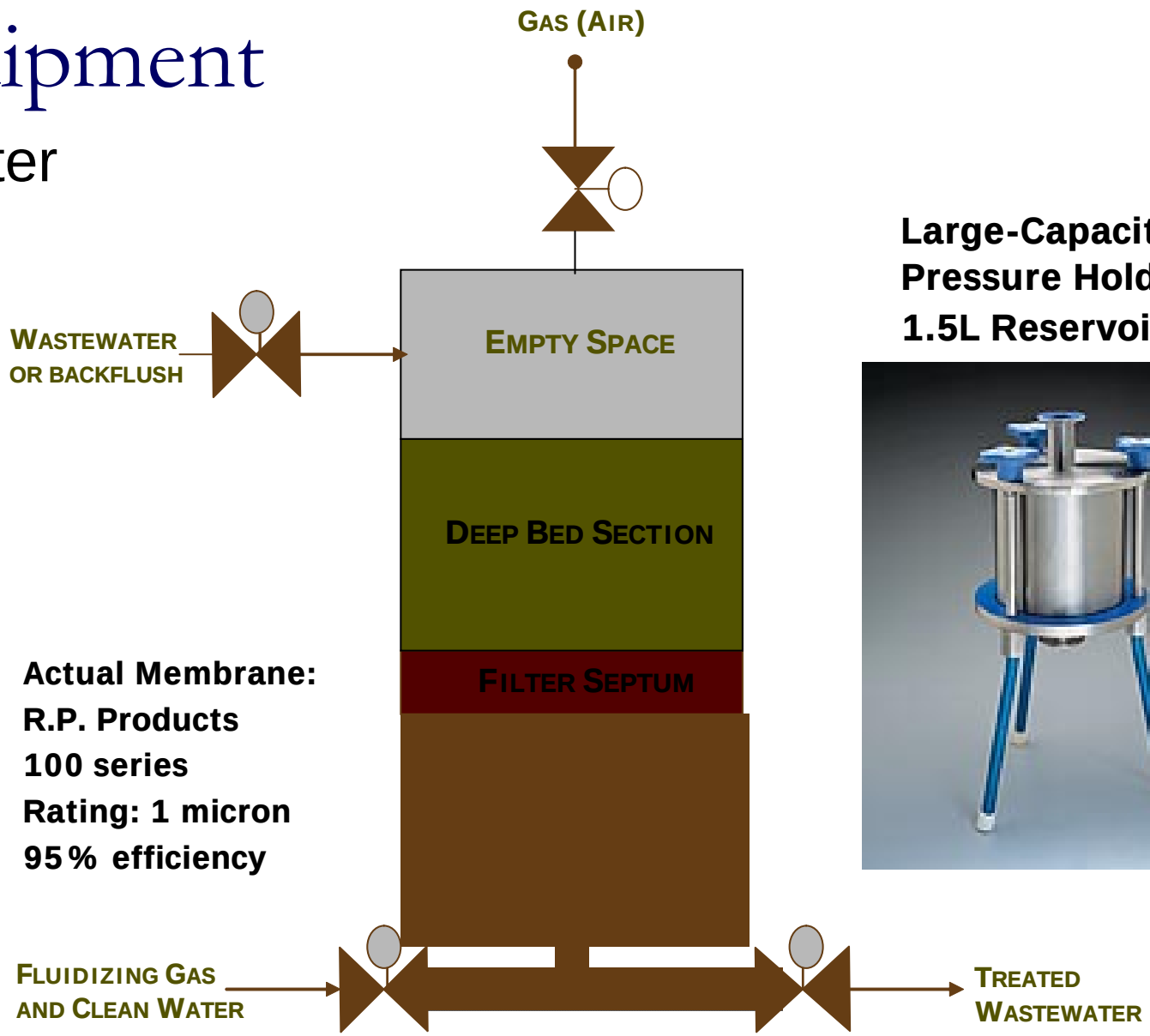

Actual Membrane:
R.P. Products
100 series
Rating: 1 micron
95% efficiency

Large-Capacity Pressure Holder with 1.5L Reservoir

Experimental Methods and Results

- **Filtrated Slurry (100 series filter)**
  - Approximately 500mL of slurry was filtered R.P. Products 100 series (1 micron 95% efficiency).
  - The TSS of each filtered solution was determined using EPA 160.3 Gravimetric method.

Sample	TSS (ppm)	Filtrated TSS (ppm)
1	51280	17250
2	51250	16710
3	51540	17460
Average	51,357	17140

TSS Removal
67%

Results

- **Copper in Particles**

Cabot i-Cue 5001

CMP Slurry. AlO_3 2-5%

pH=4.00 +/- 0.03

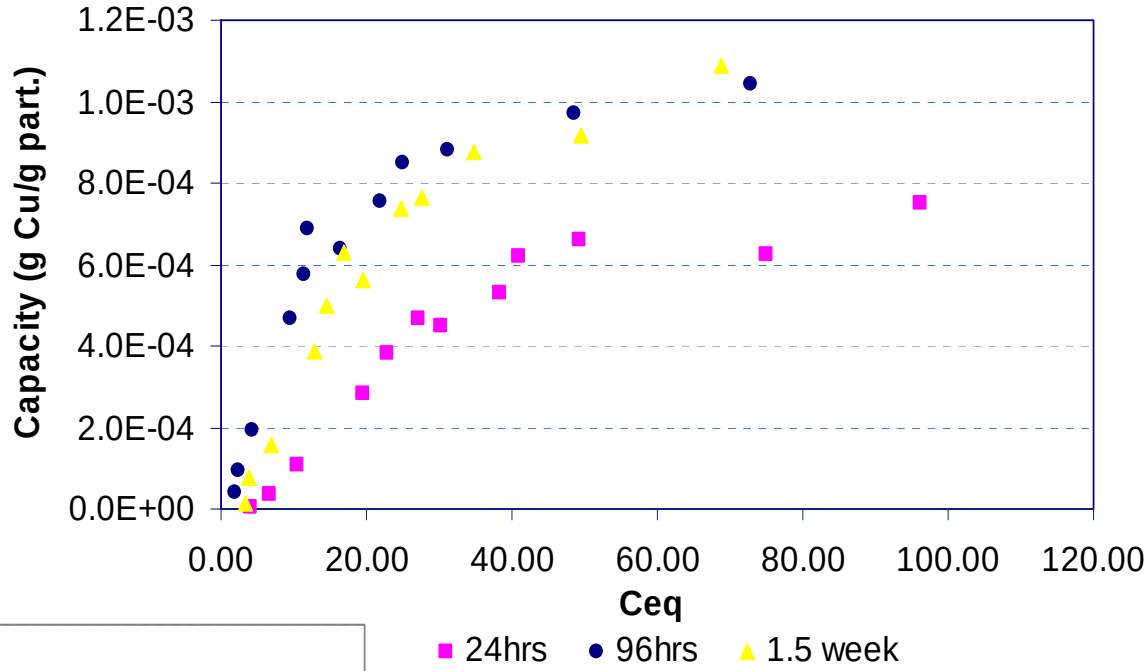

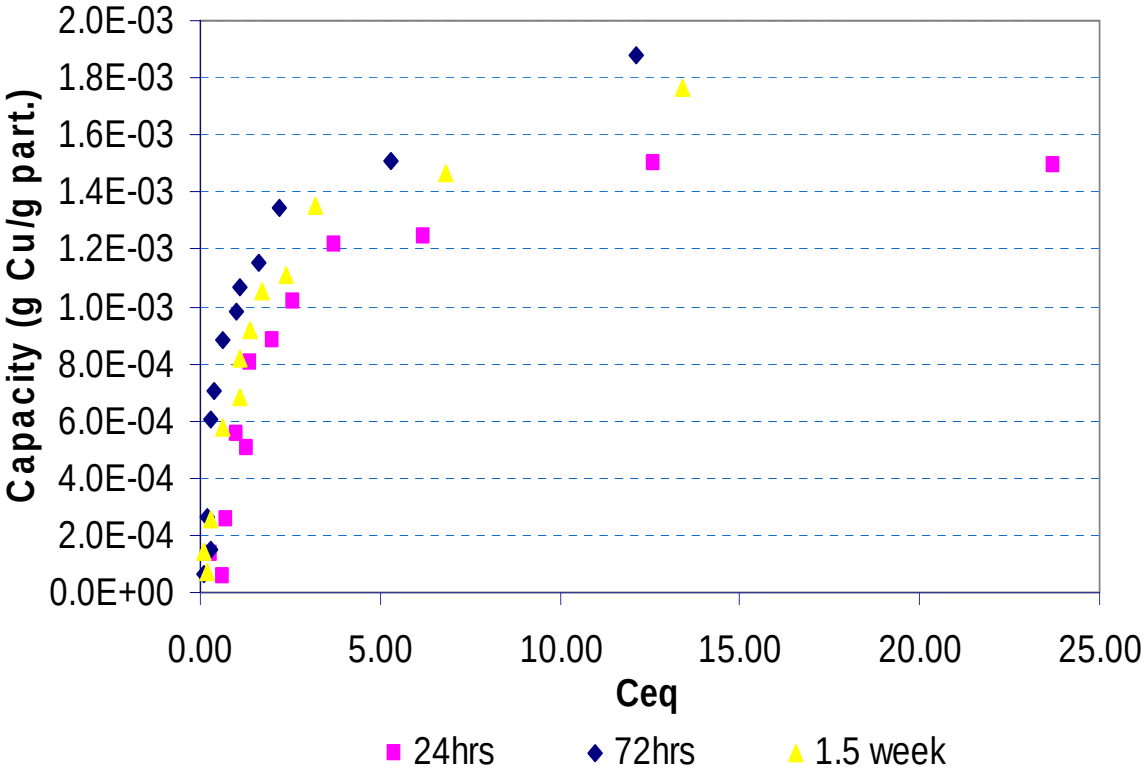

pH=6.00 +/- 0.03

Equipment

- Virtis Omni-Culture Reactor

- Biofilm Carrier Elements

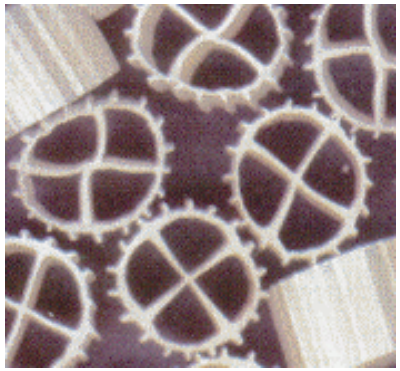

Kaldnes media provides maximum surface area for the bacteria to colonize and produce bio film.

(Source: www.aquamerik.com)

TECHNICAL SPECIFICATIONS	Kaldness
Material	**Polyethylene**
Specific Surface Area	**152 ft2/ft3 (500 m2/m3)**
Maximum Fill	**Up to 65%**
Weight per m3	**152 kg/m3**
Number of units per m3	**1,029,000**
Surface per unit	**4.86 cm2**
Percentage of hollow space	**93 %**
Color	**Natural white**

Experimental Methods and Results

Fermentor with 5Y and biocarriers

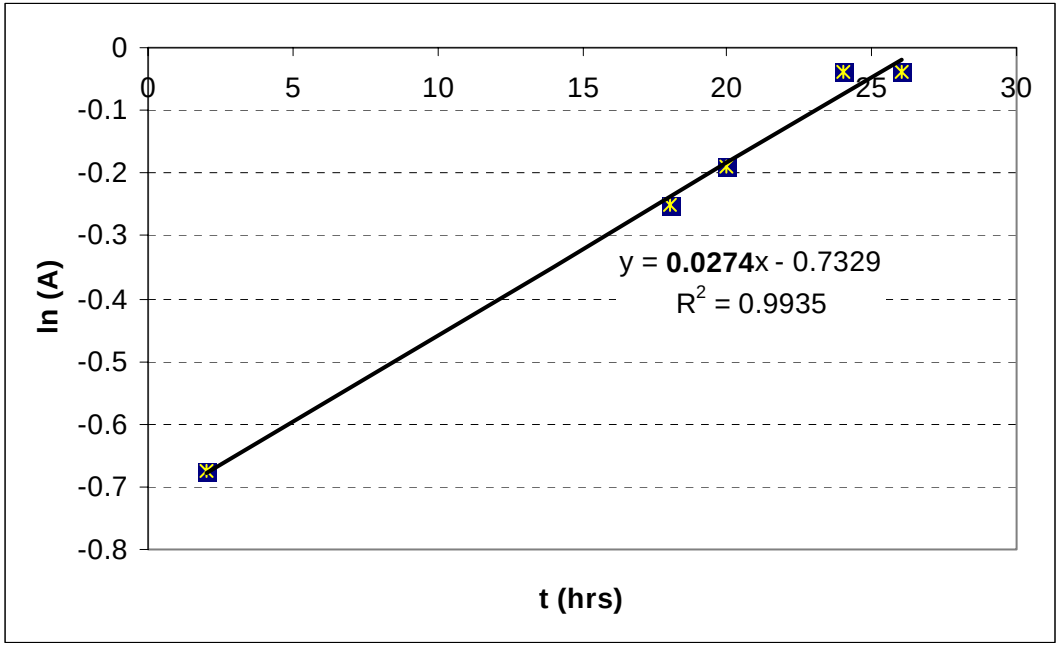

Cell growth in presence of copper :

μ=**0.0274hr^{-1}= 0.658 d^{-1}**

Operation Parameters:

Final Volume Liquid: **1L**

Biocarriers: **0.4L**

5Y - R2A: **0.4L**

Cu (500 ppm stock in 200 nm filtrated slurry): **0.080L**

Expected Cu: 40ppm

less 1% particles

pH = 6.25

Air: 0.5-1 lpm

RPMs: 10-15 rpm

Experimental Methods

- Bacteria Binding Activity (5Y)

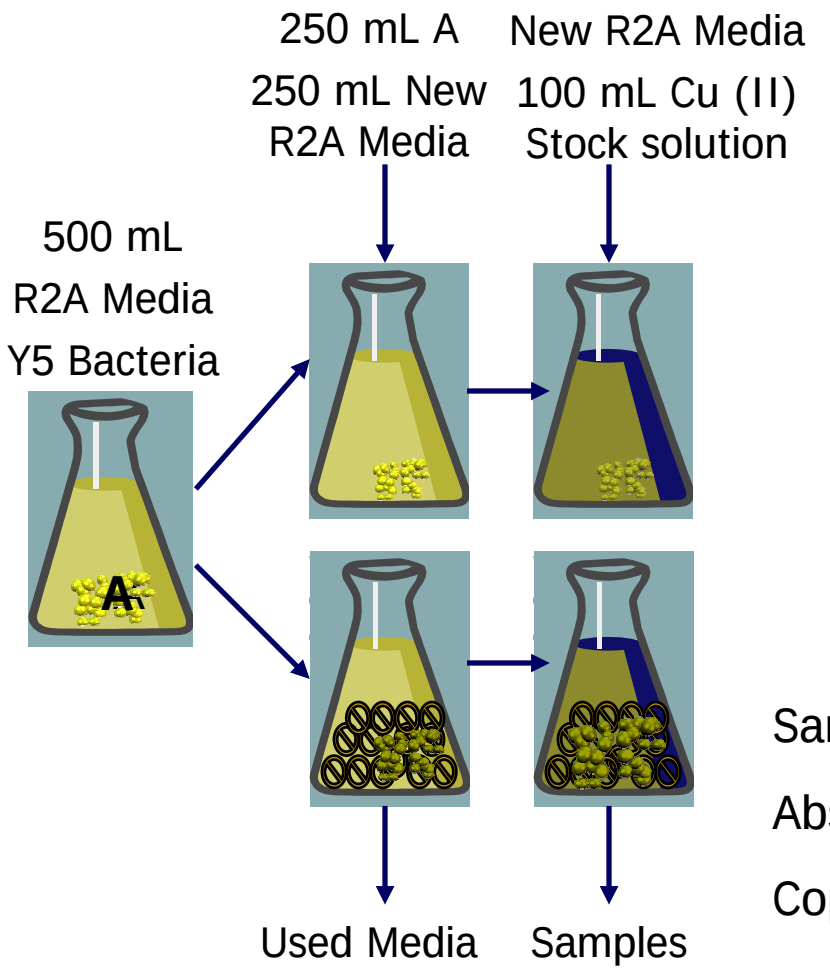

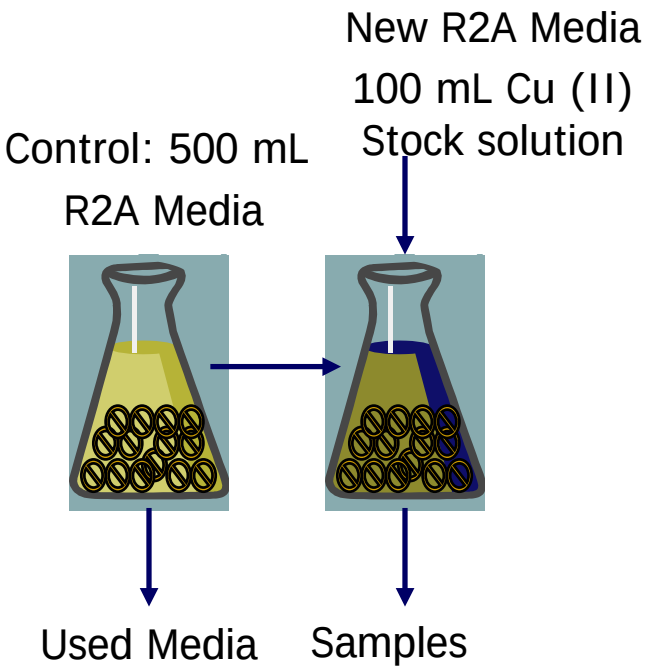

Sampling time: every two hours

Absorbance: Spectrophotometer

Copper concentration: AA

Results

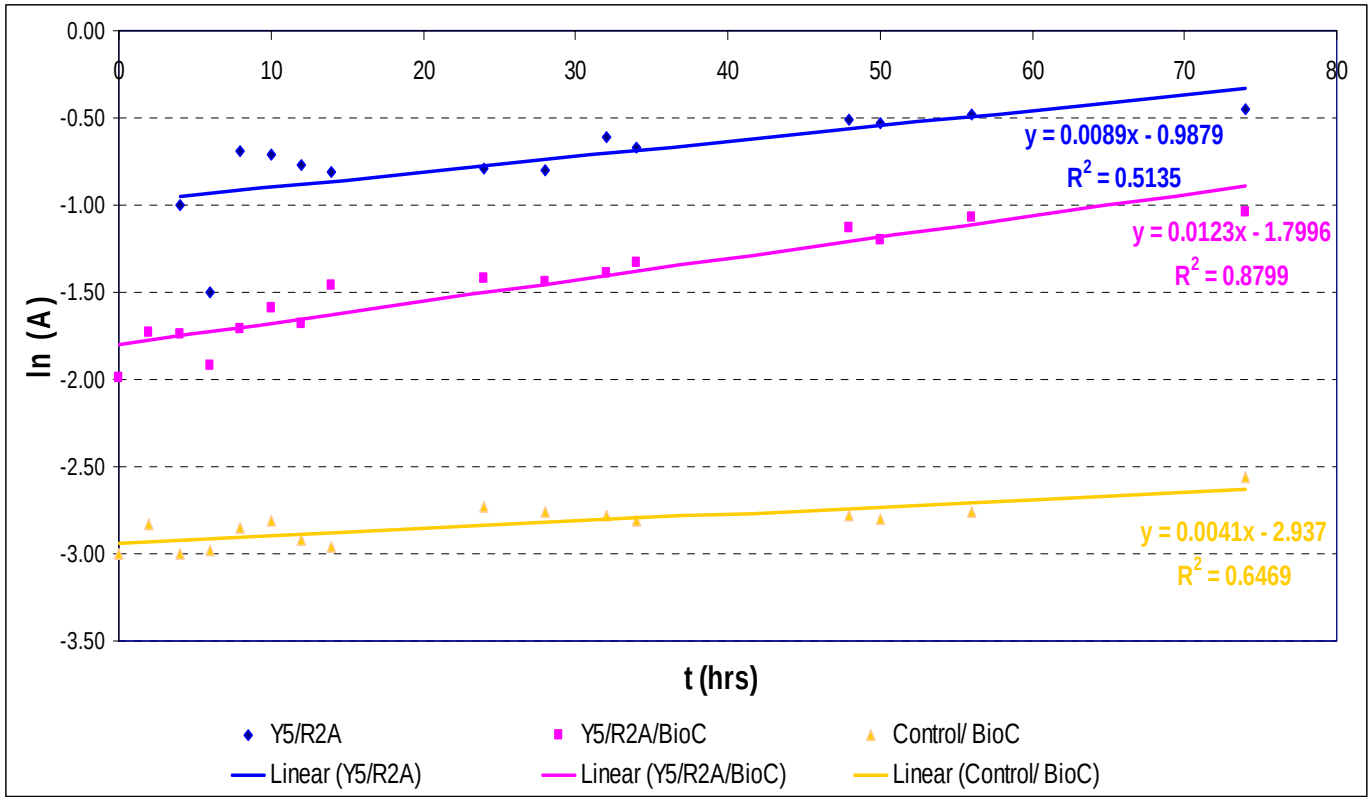
0.00
-0.50
-1.00
-1.50
-2.00
-2.50
-3.00
-3.50
0
10
20
30
40
50
60
70
80
ln (A)
t (hrs)
y = 0.0089x - 0.9879
R2 = 0.5135
y = 0.0123x - 1.7996
R2 = 0.8799
y = 0.0041x - 2.937
R2 = 0.6469
Y5/R2A
Y5/R2A/BioC
Control/ BioC
Linear (Y5/R2A)
Linear (Y5/R2A/BioC)
Linear (Control/ BioC)

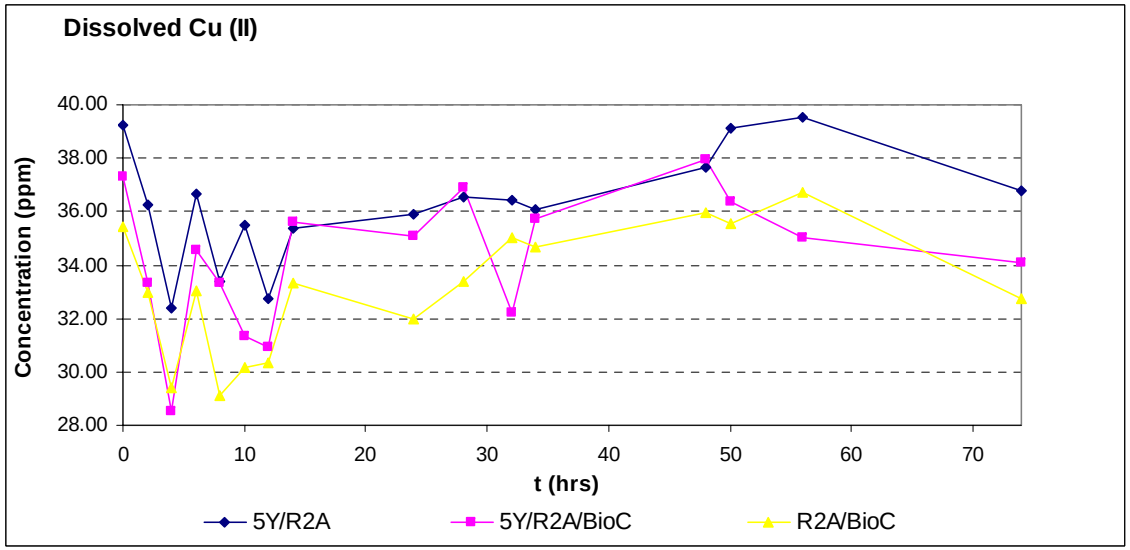
Dissolved Cu (II)
40.00
38.00
36.00
34.00
32.00
30.00
28.00
Concentration (ppm)
0
10
20
30
40
50
60
70
t (hrs)
5Y/R2A
5Y/R2A/BioC
R2A/BioC

Future works

- Perform similar experiments using others surrogate, commercial slurry, and real CMP waste.
- Combine 5Y and IPA-4 previously growth in biocarriers in a Virtis Omni-Culture Bioreactor to treat copper and organics at the same step.
- Study the effect of particle in the biological treatment.
- Assemble a continuous flow system using biocarriers and both bacteria.
- Combine high efficiency filtration and biotreatment in one separation/ reactor step.

Acknowledgments

- Moses N. Bogere, PhD
- Kimberly L. Ogden, PhD
- Worawan (Kay) Maketon and Yi Liu
- University of Arizona Chemical & Environmental Engineering Department
- University of Puerto Rico Chemical Engineering Department
- PR- LSAMP Bridge to Doctorate Program
- NSF/SRC Engineering Research Center for Environmentally Benign Semiconductor Manufacturing

Chemical Engineering Department
University of Puerto Rico at Mayaguez

THE UNIVERSITY OF ARIZONA
TUCSON ARIZONA

Biotreatment of Waste Streams Containing Organic Compounds and Copper

(Subtask C-1-2)

Part II: Anaerobic Treatment

Victor M Gamez, Reyes Sierra, and James Field

Chemical and Environmental Engineering, University of Arizona

NSF/SRC Engineering Research Center for Environmentally Benign Semiconductor Manufacturing

Project Objectives

The goal of this research is to investigate the feasibility of anaerobic treatment for the simultaneous removal of copper and organic contaminants in CMP effluents. Removal of Cu will be stimulated by biogenic sulfides produced by sulfate reducing bacteria. The objective of the work presented here is to assess the anaerobic treatability of CMP effluents, *i.e.*,

- assess the susceptibility of key wastewater components to biodegradation by anaerobic microorganisms under batch and continuous-flow bioreactor conditions
- evaluate the treatment of simulated Cu-CMP effluents in a continuous flow bioreactor in conjunction with a crystallization reactor

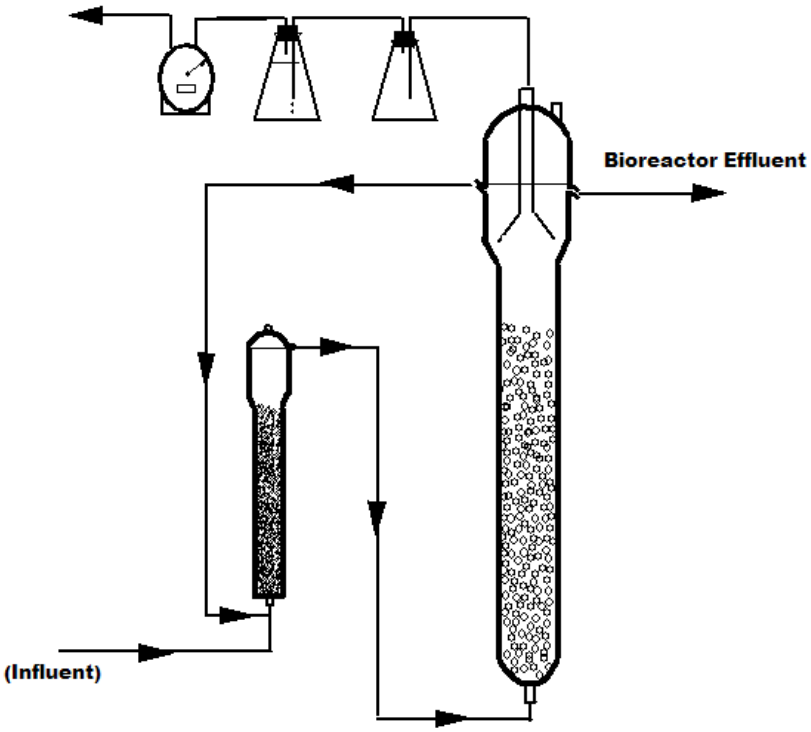

Schematic representation of the anaerobic bioreactor - crystallization reactor utilized in the simultaneous treatment of copper and organics from CMP wastewaters

Our Approach:
Metal Removal by Sulfate Reducing Bacteria

$$SO_4^{2-} + \text{Organics} \longrightarrow HS^- + CO_2$$

(Electron donor)

$$S^{2-} + M^{2+} \longrightarrow MS \downarrow$$

Metal Sulfide

Metal Sulfides: very low solubility products, eg. 10^{-36} for CuS

Examples of Organic Contaminants in CMP are:

- **Citric acid and other complexing agents**
- **Anticorrosion Inhibitors**
- **Surfactants**

Bioreactor Study

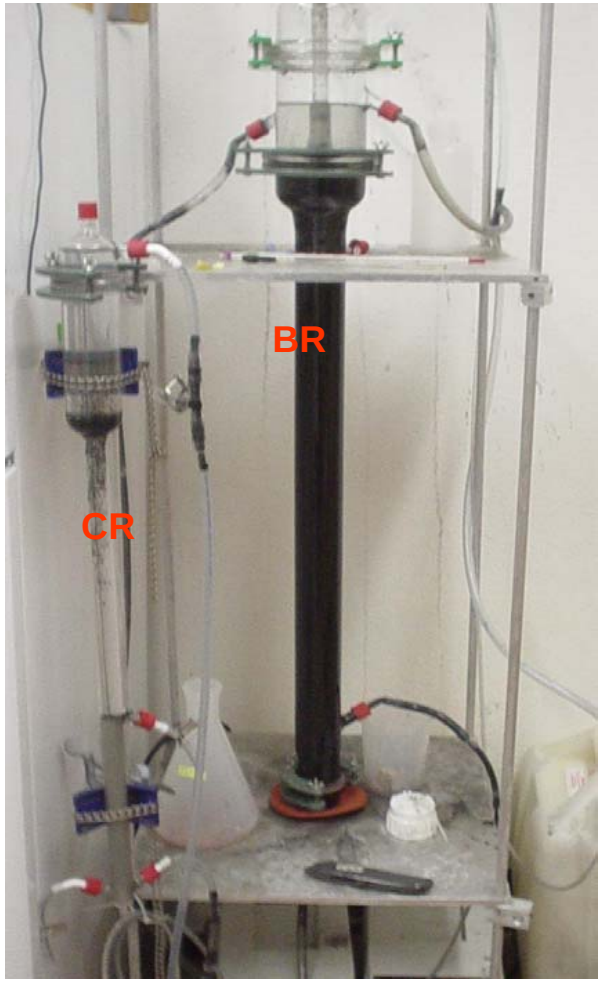

Photograph of the two reactor system used in this research. (BR) Anaerobic bioreactor; (CR) Crystallization reactor packed with sand

Bioreactor (BR) & Crystallization Reactor (CR):

Period I

Ethanol (3000 mg COD/L)

Period II

Simulated Organic CMP Waste [Isopropyl alcohol (IPA)/poly(ethylene glycol) (PEG)/citric acid] (1000 mg COD/L each)

Period III :

Simulated CMP Waste (5 mg Cu/L)

Period IV :

Simulated CMP Waste (25 mg Cu/L)

Period V:

Simulated CMP Waste (65 mg Cu/L)

Period VI:

Simulated CMP Waste (100 mg Cu/L)

System Performance:

Removal of Soluble Copper

Period	Cu^{2+} -in (μg/l)	Cu^{2+} -out (μg/l)	Cu removal (%)	Cu Removal (%) CR only
III	5,000	16 (+/- 19)	99.4 (+/-1.3)	99.3 (+/-0.6)
IV	25,000	162 (+/-84)	99.3 (+/-0.5)	99.3 (+/- 0.2)
V	65,000	104 (+/- 45)	99.9 (+/-0.2)	99.8 (+/- 0.1)
VI	100,000	84 (+/- 47)	99.9 (+/-0.05)	99.9 (+/-0.07)

Bioreactor/CR - EDS Analysis of Sand

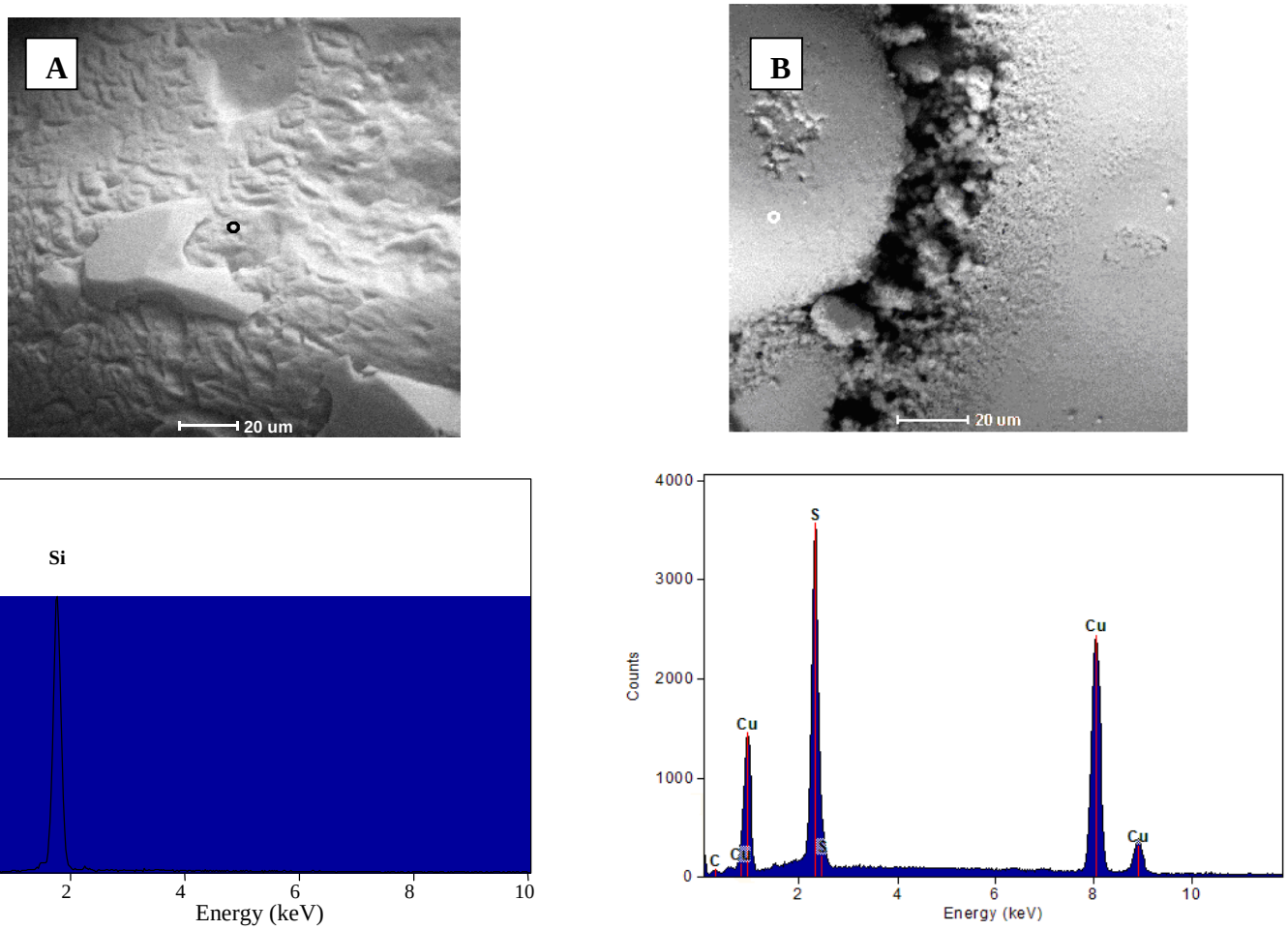

Energy dispersive spectrometry (EDS) results showing (A) the clean sand (B) CuS crystal growth on sand obtained from crystallization following copper (100 mg/l) removal

XRD Analysis of Sand in Crystallization Reactor

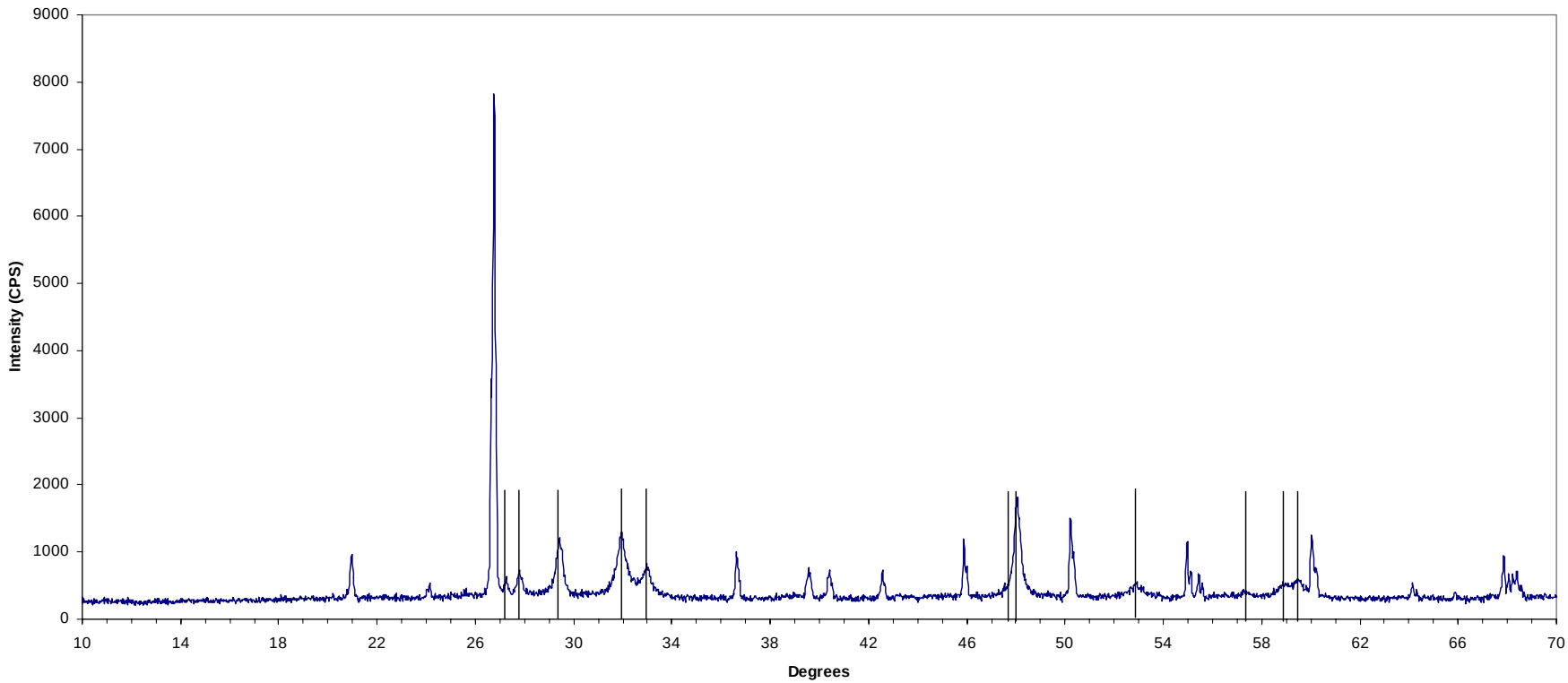

XRD image from sand, the peaks show the presence of ***covellite*** *(CuS)*

Treatment of CMP Wastewaters in Sulfidogenic Bioreactors: Advantages

- Very low effluent Cu concentrations (> 99% removal of soluble Cu)
- Simultaneous removal of organics (>95% BOD removal)
- Selective recovery of Cu (CuS)
- Very low energy input / No chemical additives required
- Robustness and simplicity, low maintenance and operational costs
- Rapid application at the industrial scale due to widespread full-scale experience with core technology

Conclusions

- Soluble Cu was successfully removed (>99% removal) from a simulated CMP wastewater containing 100 mg/L Cu^{2+} by means of precipitation in the combined bioreactor-crystallization reactor system
- Copper has successfully precipitated on sand granules as CuS.
- Further Recovery of Cu from sand should be economically feasible.

Future Work

- Complete the study of the treatment of simulated Cu-CMP effluents in continuous laboratory experiments (anaerobic reactor combined with crystallization reactor) using effluents from a CMP pilot plant
- Evaluate the biodegradability of new compounds found in CMP wastewater
- Develop a feasible and effective biological treatment system for the simultaneous removal of metals and organics in CMP effluents

Acknowledgements. This project is partially supported by the ERC and by an NSF Advance grant (BES 0137368).

Biological and Physico-Chemical Methods for the Removal of Perfluoroctane Sulfonate (PFOS) in Semiconductor Effluents

Substask C-1-5

Valeria Ochoa, Fiona L. Jordan, Jim A Field,
Neil Jacobsen & Reyes Sierra

Dept of Chemical & Environmental Engineering
University of Arizona

NSF/SRC Engineering Research Center for Environmentally Benign Semiconductor Manufacturing

Introduction

- Perfluorinated surfactants are key components in a variety of IC manufacture process steps, including photolithography, wet etch and wafer cleaning, being PFOS the most widely applied perfluorinated surfactant.

- Concern about the ecological impact of perfluorinated surfactants - Increasing evidence that these compounds are toxic and accumulate in biological tissues, and persist in the environment.

- US-EPA and other environmental agencies are considering regulations restricting or banning the use of PFOS and other perfluorinated compounds.

Introduction

Feasible methods for the removal of PFOS and related compounds in semiconductor effluents are needed. The application of conventional treatments for removing PFOS from wastewater streams is restricted by technical and/or economical considerations.

Approaches involving reductive dehalogenation are potentially promising for the degradation of PFOS and related perfluorinated compounds.

I. Microbial Reductive Dehalogenation:

Biodegradation of higher chlorinated aliphatic compounds, such as perchloroethylene (PCE), occurs under anaerobic conditions (1). In this metabolic process, sequential reductive dechlorination occurs by replacing chloro-groups by hydrogen atoms. Although microbial degradation of various organofluorines compounds is well documented (2), reductive defluorination has not yet been considered.

Introduction

II. Biomimetic Dehalogenation

Systems that contain Ti(III) citrate (electron donor) and vitamin B12 (aka cobalamin, catalyst) are very efficient for dehalogenation of highly-halogenated compounds (1). The direct catalysis of dehalogenation by enzyme cofactors is known as *biomimetic dehalogenation*, because it mimics reactions expected in microorganisms.

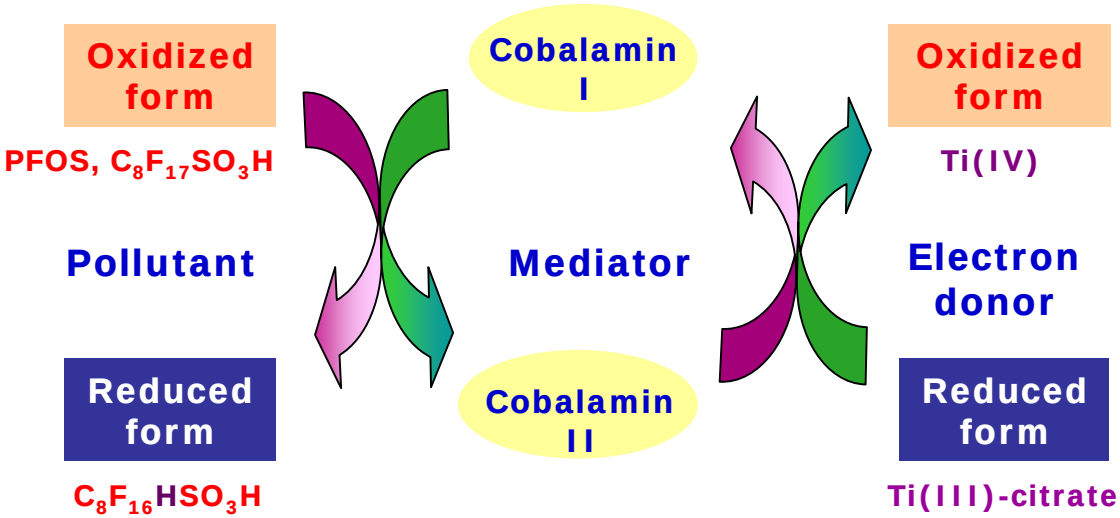

Biomimetic dehalogenation using Ti (III) citrate and vitamin B12

Objectives

To evaluate the effectiveness of four different approaches for the removal of PFOS in semiconductor effluents:

- Anaerobic reductive dehalogenation
- Biomimetic dehalogenation
- Activated carbon adsorption
- Biosorption

Materials and Methods

Analytical Methods *:* PFOS degradation was evaluated by monitoring the release of fluoride using an ion selective electrode. ^{19}F-NMR and MS/MS were used to quantitatively detected and analyzed PFOS and related compounds in environmental samples.

Microbial Toxicity *:*The microbial toxicity of PFOS, PFBS ($CF_3(CF_2)_3SO_3H$), TH-PFOS ($CF_3(CF_2)_5(CH_2)_2$ SO_3H), and TMAH (tetramethyl ammonium hydroxide) was evaluated in batch bioassays inoculated with an anaerobic mixed culture as described elsewhere (3).

Microbial reductive dehalogenation: Standardized batch assays were conducted to evaluate the susceptibility of PFOS and related compounds to microbial degradation. Anaerobic sludges/sediments previously exposed to perfluorinated compounds will be used as inoculum.

Chemical biomimetic degradation*:* The susceptibility of PFOS and related compounds to chemical reductive dehalogenation with vitamin B12/Ti(III) was examined in laboratory assays. Several vitamin B12 and Ti(III) dosage, pH and temperature will be assessed to determine the optimal treatment conditions.

Results

Microbial Toxicity : The inhibitory effects of PFOS, TH-PFOS (a partially defluorinated compound related to PFOS) and TMAH (a common PFOS co-contaminant in semiconductor effluents) towards methanogenic microorganisms in anaerobic wastewater treatment sludge were tested at concentrations ranging from 5 to 500 mg/L. PFOS lead to a small decrease in the methanogenic activity when present at 500 mg/L. None of the other compounds tested were found to cause significant microbial inhibition in these assays.

Microbial reductive dehalogenation: Six different microbial inocula were employed to study the degradation of PFOS, PFBS and THPFOS. No evidence has been obtained yet that the perfluorinated compounds are degraded after 2-4 months.

Chemical biomimetic degradation: We have demonstrated that vitamin B12/Ti(III) can catalyze the reductive defluorination of PFOS (Fig. 1). The evidence is based on fluoride release. Ongoing work aims at the isolation and structural elucidation of defluorinated products of PFOS with MS/MS and F-NMR. This finding is highly significant because it is the first report of reductive dehalogenation of PFOS.

Results

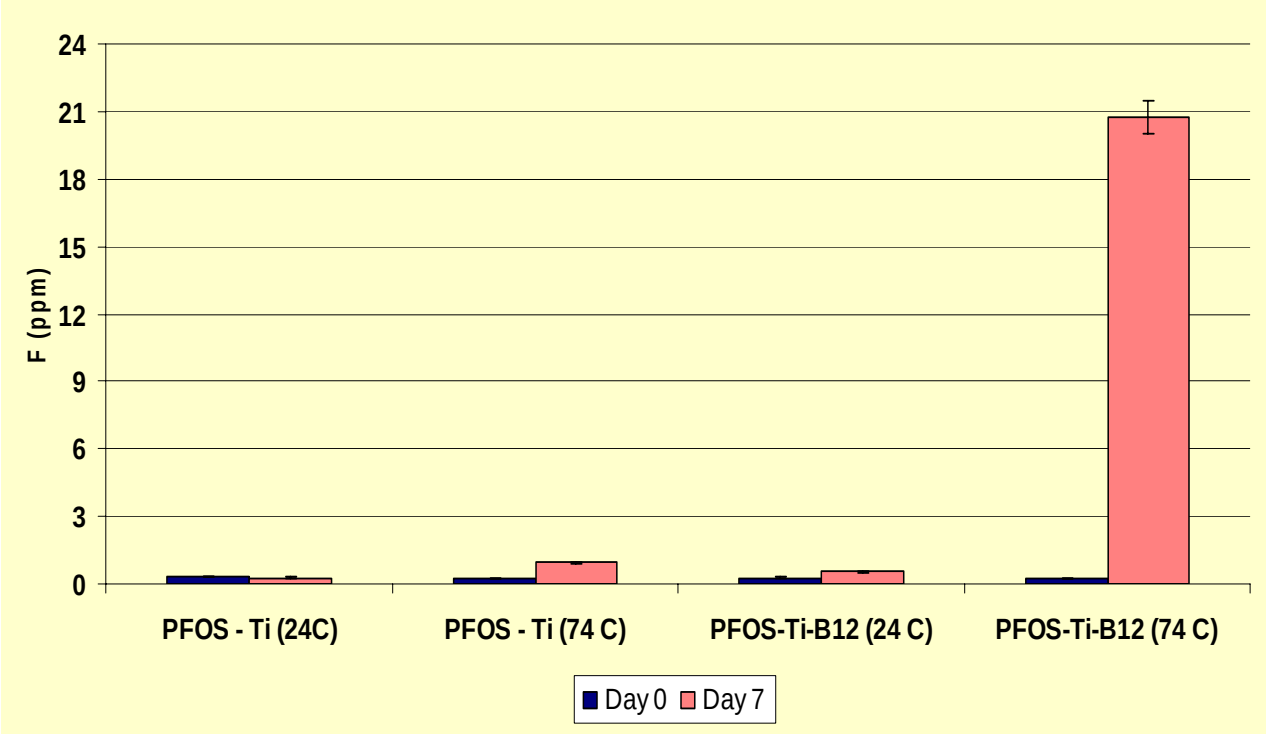

Fig. 1. Fluoride release at 24°C and 74°C based on F- electrode measurements

Conclusions

- PFOS was shown to be susceptible to biomimetic reductive dehalogenation by Ti (III) citrate/vitamin B12.
- These results have important implications for biodegradation since partially defluorinated PFOS derivatives, comparable to the products expected from reductive defluorination are known to be susceptible to biodegradation by aerobic bacteria (4).
- Moreover, the findings suggest that microbial reductive defluorination of PFOS might be possible.

ESH Impact

The replacement of fluorine with hydrogen atoms achieved by reductive dehalogenation is expected to improve the biodegradability of perfluorinated compounds in conventional biological wastewater treatment systems.

The benefits of biodegradation are the following:

- Compounds can be fully mineralized offering an advantage over alternative techniques (e.g. adsorption, membrane processes, ion exchange). These alternative processes generate residuals and brines that contain PFOS, which still need to be dealt with.

- A second advantage is that existing biological treatment infrastructure can be utilized for the proposed process.

Future Work

- Evaluate the removal of PFOS and related compounds by biosorption (using anaerobic and aerobic sludge) and activated carbon adsorption.
- Investigate the microbial degradation of PFOS and selected fluorinated compounds.
- Optimize the biomimetic reductive dehalogenation of PFOS and related compounds
- Investigate the biological removal of the reduced products in the activated sludge process.
- Develop a hybrid process consisting of reductive dehalogenation-biological treatment for the destruction of PFOS and related compounds semiconductor effluents.

Industrial Collaboration

Walter Worth, Sematech

Tim Yeakley, Texas Instruments

Literature:

(1) Field JA & Sierra-Alvarez R. 2004. *Re/Views in Environ. Sci. Bio/Technol.* 3:185 – 254;
(2) Natarajan R *et al.* 2005. *J. Fluorine Chem.*, 126:425-436;
(3) Hollingsworth J, Sierra-Alvarez R *et al*. 2004. *Chemosphere,* 59:1219-1228;
(4) Key BD *et al*. 1998. *Environ. Sci. Technol.*, 32: 2283-2287.

Fundamentals of Cleaning, Rinsing, and Drying

Real-Time and In-Situ Detection of Residual Contaminants in Micro- and Nano- Structures

Subtask C-2-1

Jun Yan[1] , Kedar Dhane[1]

Bert Vermeire[2] and Farhang Shadman[1]

[1]Chemical and Environmental Engineering, UA
[2]Electrical Engineering, ASU

NSF/SRC Engineering Research Center for Environmentally Benign Semiconductor Manufacturing

Objectives

Objectives:

- **Determine the mechanism of residual impurity removal from patterned wafers;**
- **Develop efficient cleaning, rinsing, and drying techniques.**

ESH Impact:

Conserve resources, reduce waste, reduce processing time, reduce cost, and increase productivity.

Mechanism of Chemical Residue Removal

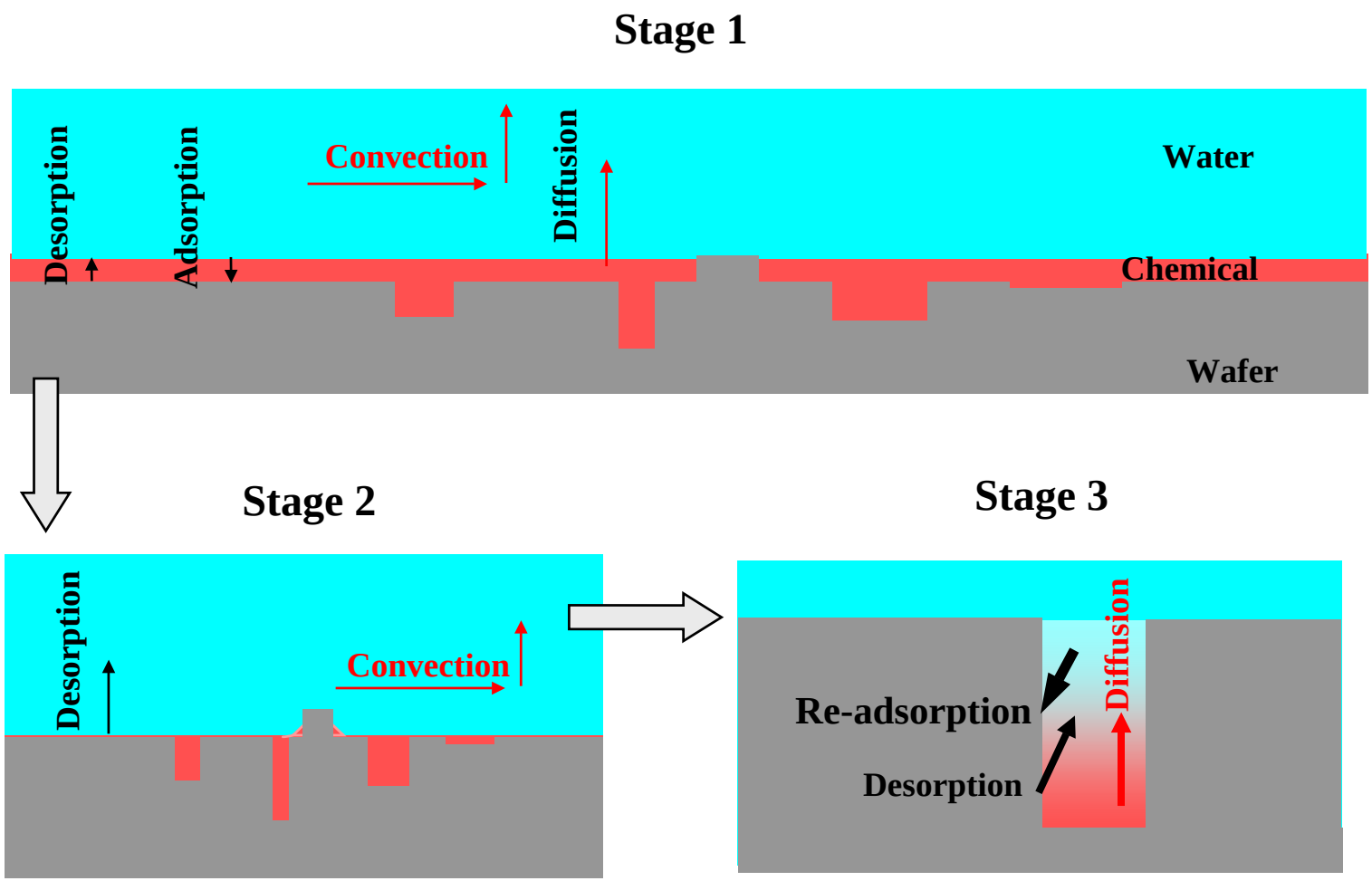

Electro-Chemical Residue Sensor (ECRS)

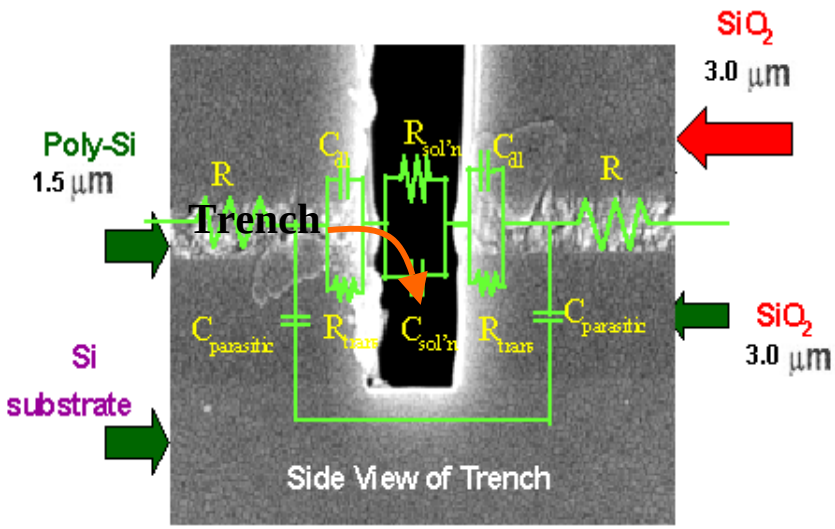

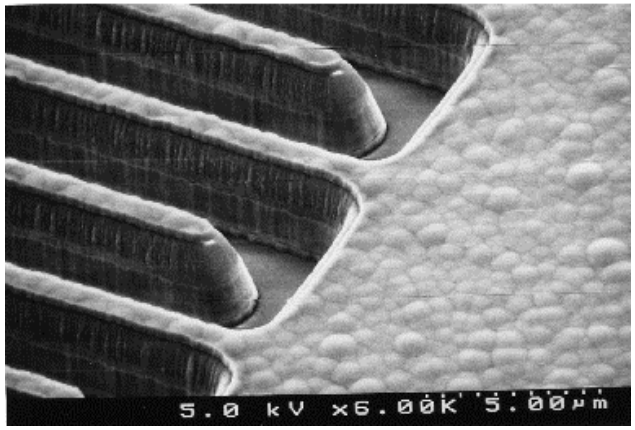

Trench solution impedance

measured trench interface impedance

$$Z_{trench} = \frac{1}{\dfrac{1}{Z_{total} - 2 \times Z_1} - \dfrac{1}{Z_3}} - 2 \times Z_2$$

measured with impedance analyzer

calculated from material properties

Z_{trench} is related to the impurity concentration in the trench during rinsing and drying.

ECRS Sensitivity to Impurity Concentration and Type

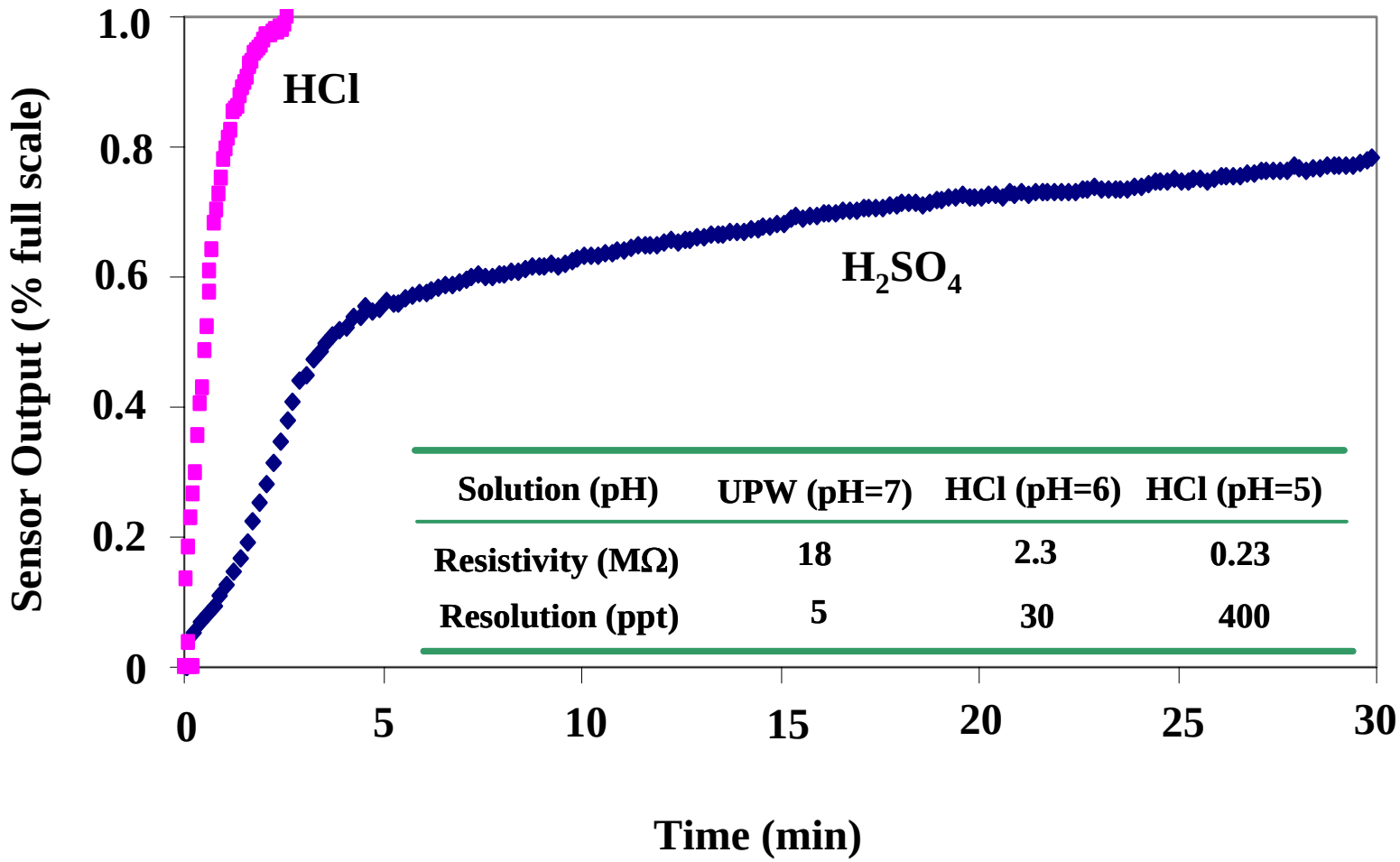

Solution (pH)	UPW (pH=7)	HCl (pH=6)	HCl (pH=5)
Resistivity (MΩ)	18	2.3	0.23
Resolution (ppt)	5	30	400

Dependence of Cleaning Dynamics on Trench Dimensions

$t_{99.99}$ is the time needed for 99.99% clean up

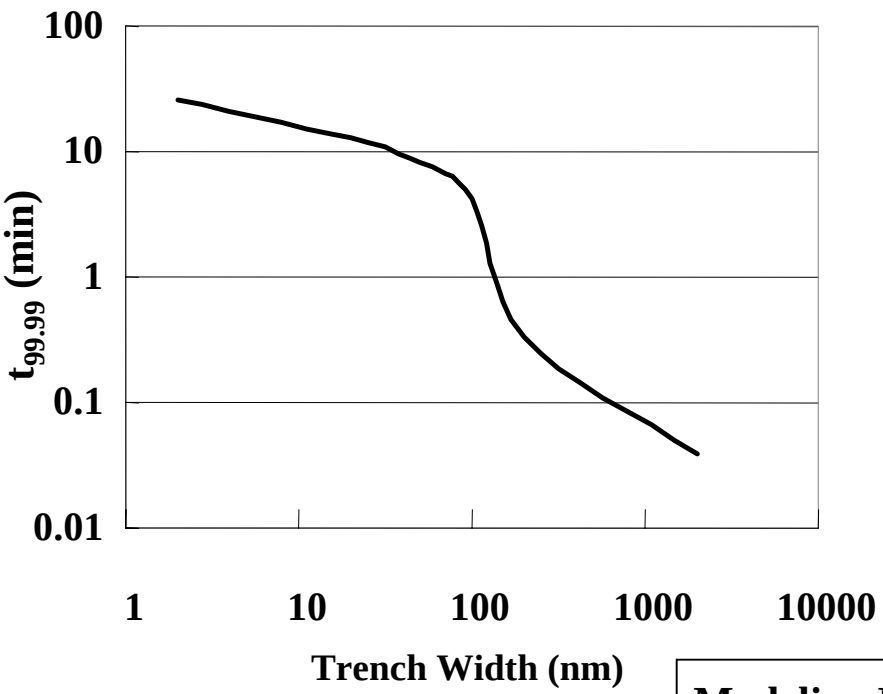

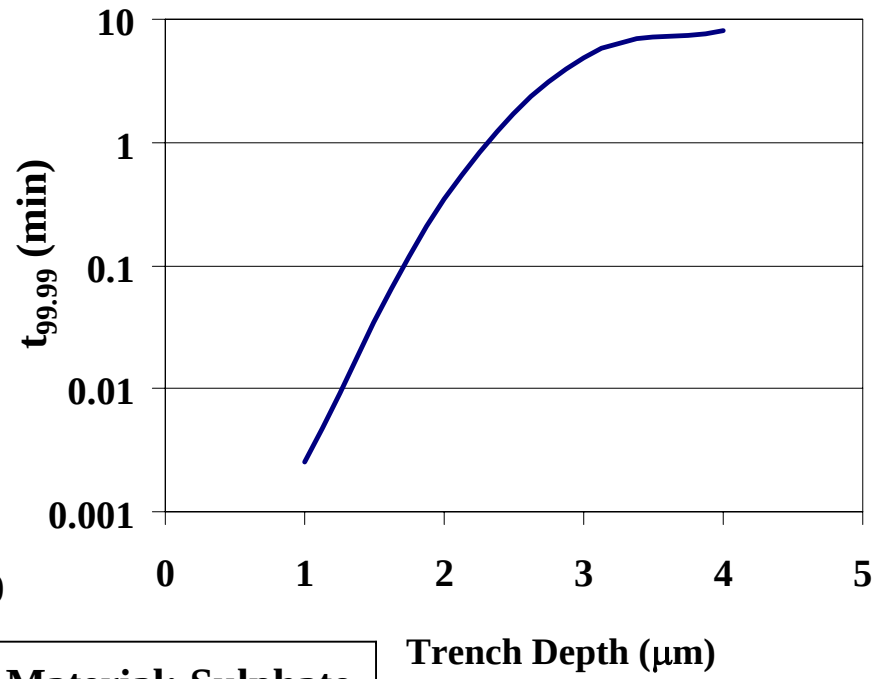

Modeling Material: Sulphate

ESH Impact of Cleaning Time and Resource Usage in Nano-Structures

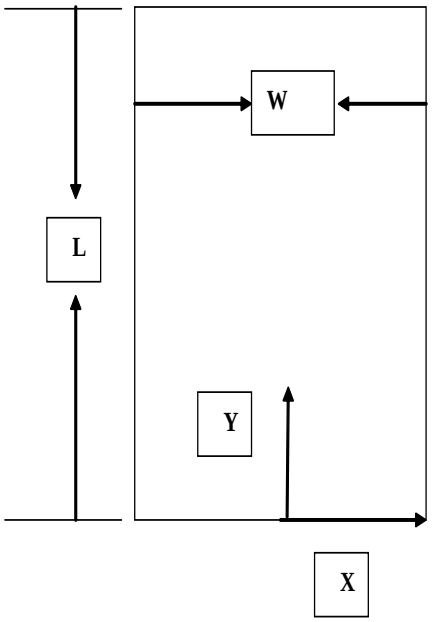

- **Mass balance equations:**

$$\frac{\partial C}{\partial t} = D_{AB}\left(\frac{\partial^2 C}{\partial x^2} + \frac{\partial^2 C}{\partial y^2}\right)$$

$$\frac{\partial C_S}{\partial t} = \left[k_a C(S_0 - C_S) - k_d C_s\right]$$

- **Dimensional analysis:**

$$\frac{\partial \overline{C}}{\partial \tau} = \frac{1}{W^2}\left(\frac{\partial^2 \overline{C}}{\partial \overline{x}^2} + \left(\frac{W^2}{L^2}\right)\cdot\frac{\partial^2 \overline{C}}{\partial \overline{y}^2}\right)$$

- **Accumulation inside the channel is inversely proportional to the square of the trench width. This causes high rate of re-adsorption which leads to the higher cleaning time.**

Sensor Reveals Rinsing Mechanism

1. Overflow Rinsing

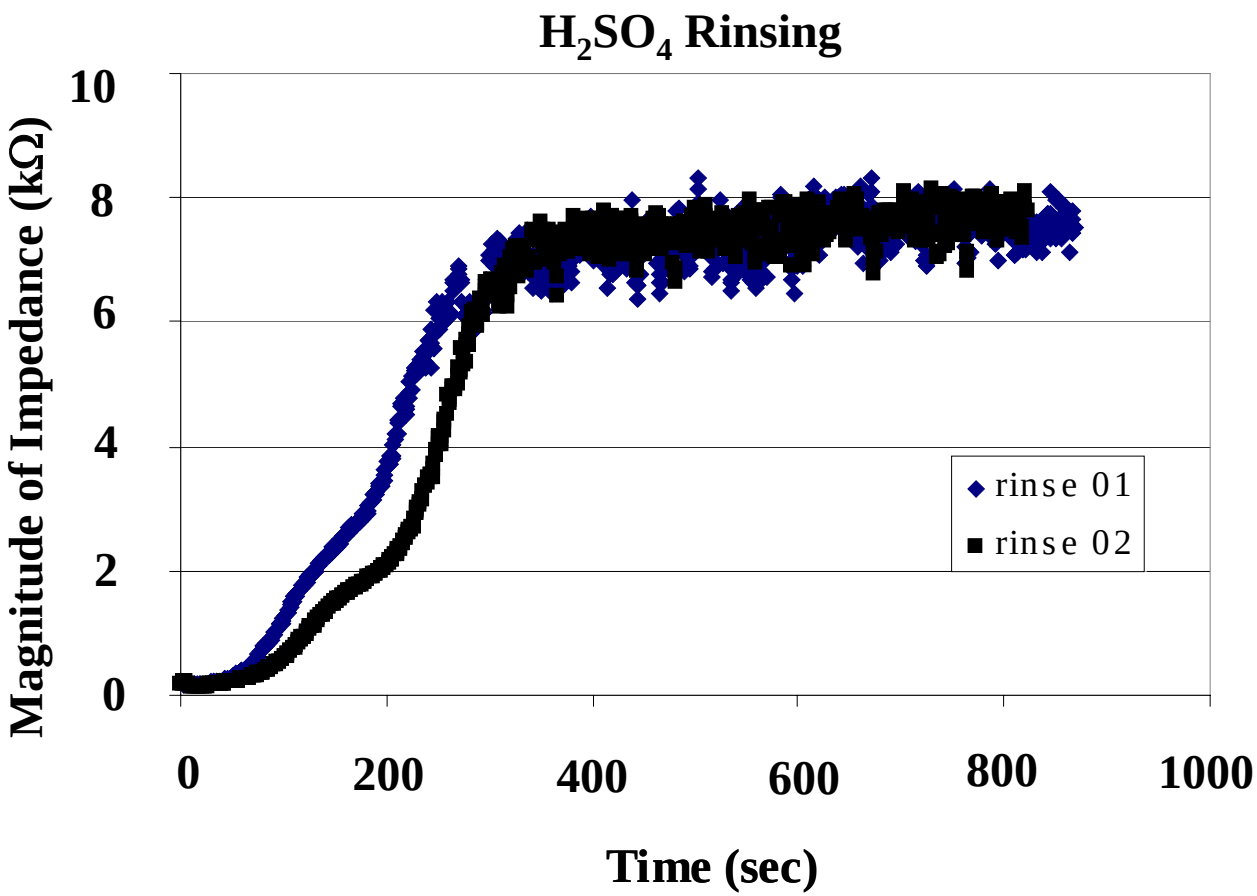

Sensor Reveals Rinsing Mechanism

2. Spray Rinsing

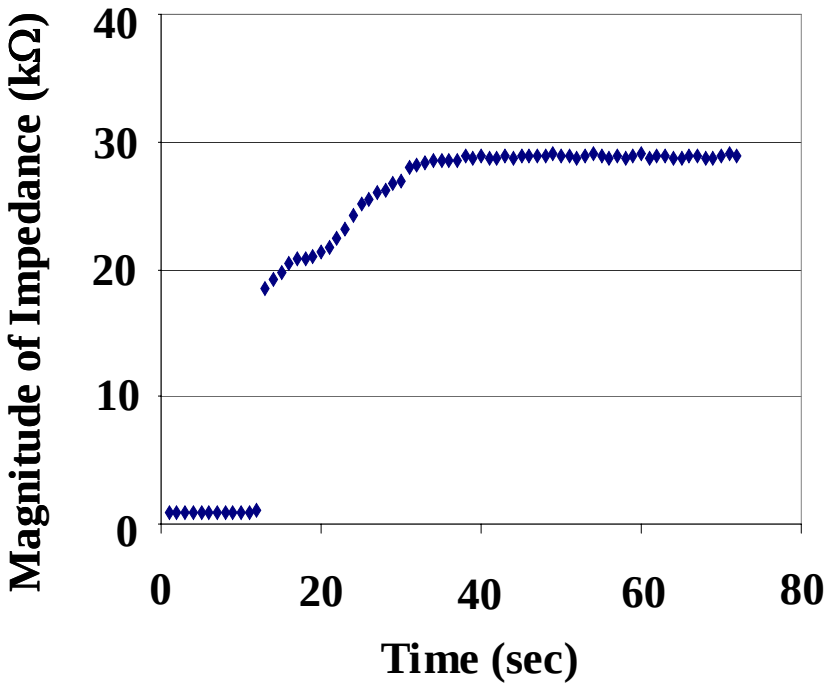

H_2SO_4 Spraying off

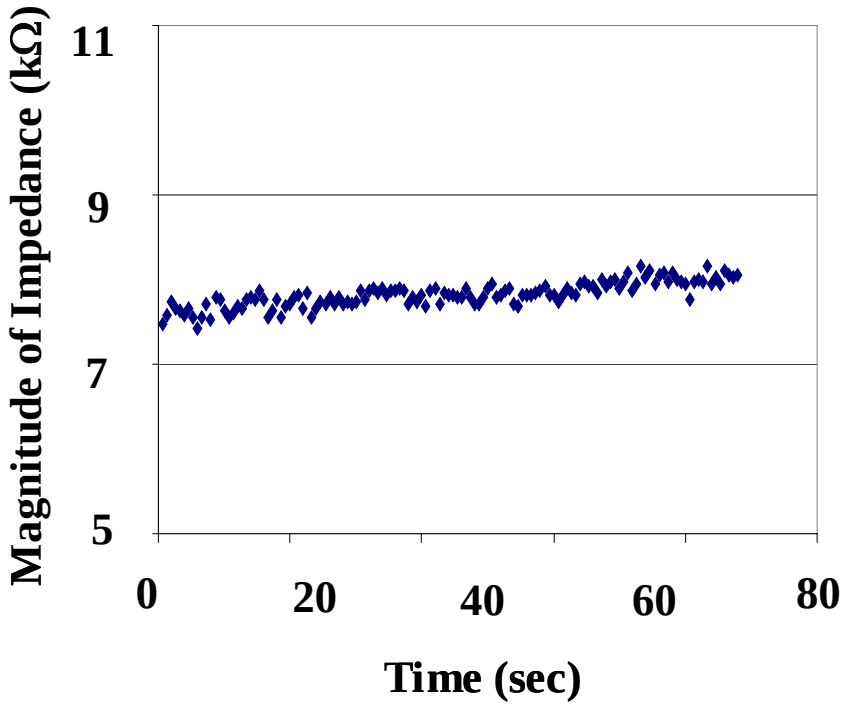

In UPW after Spraying off

Effect of Feature Size on Cleaning Time (at 80°C)

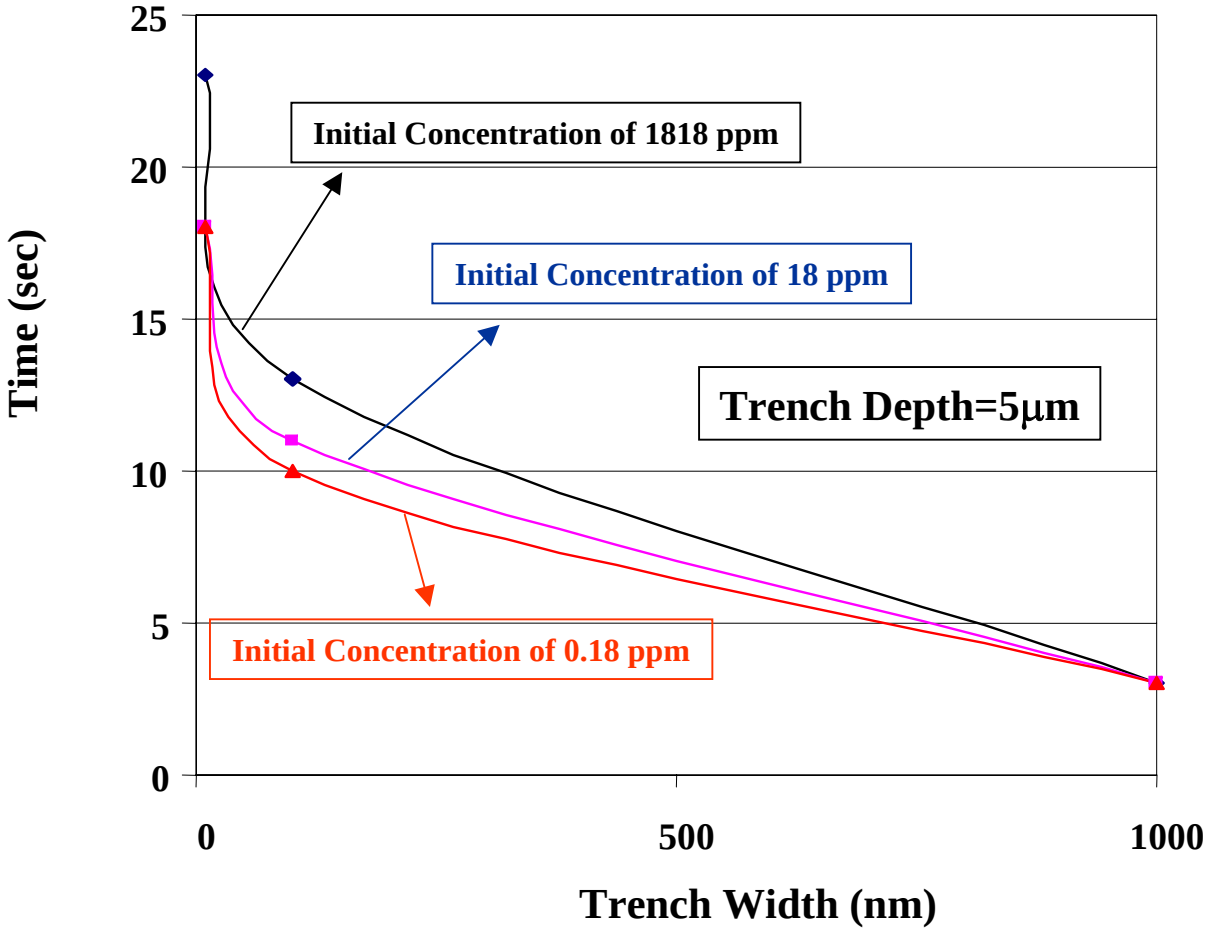

Cleaning time refers to time needed to achieve surface concentration 9.993×10^8 molecules/cm^2 (Modeling material: H_2SO_4)

Effect of Feature Size on End-Point Contamination

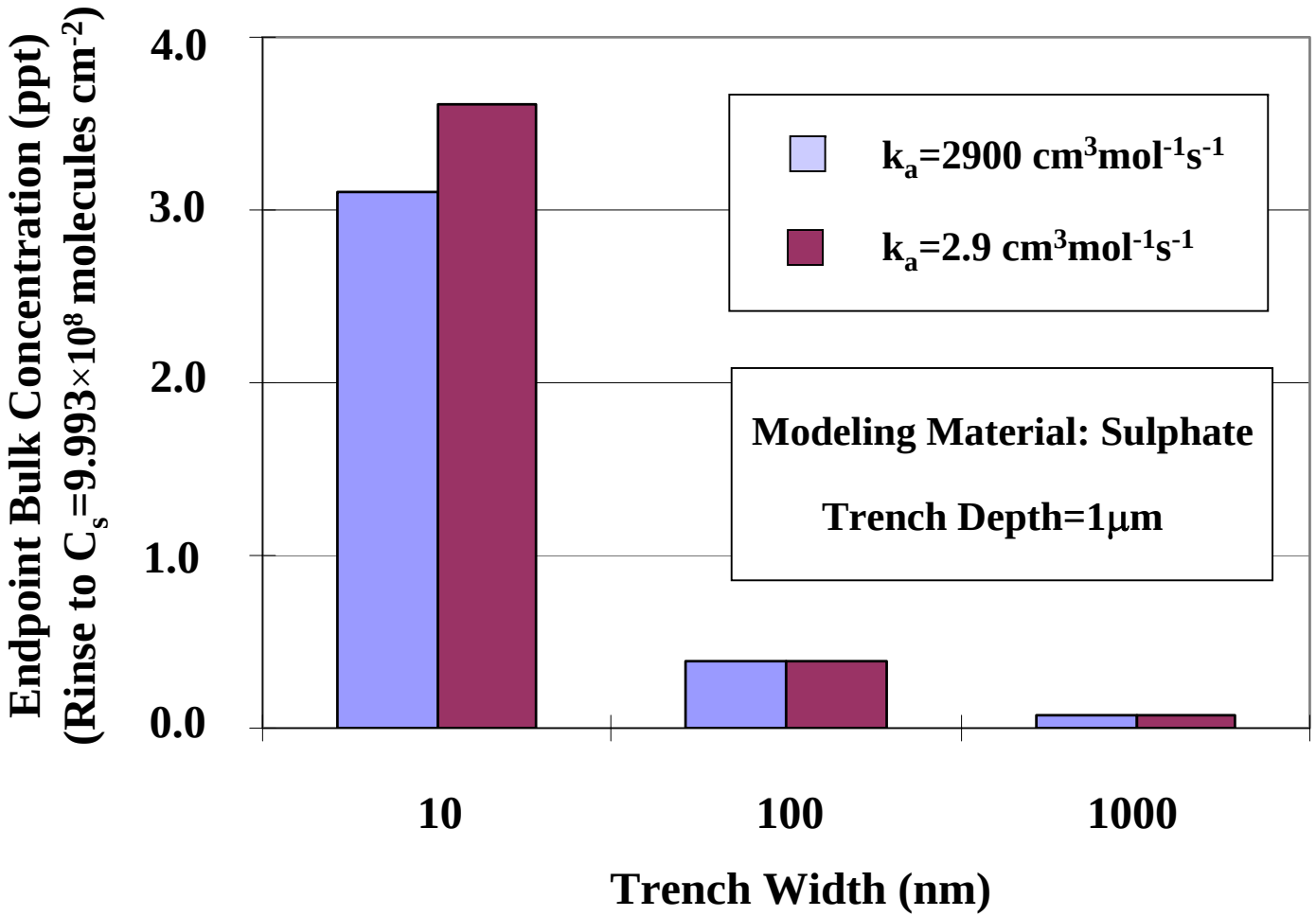

Effect of Contamination Exposure on Cleaning Time

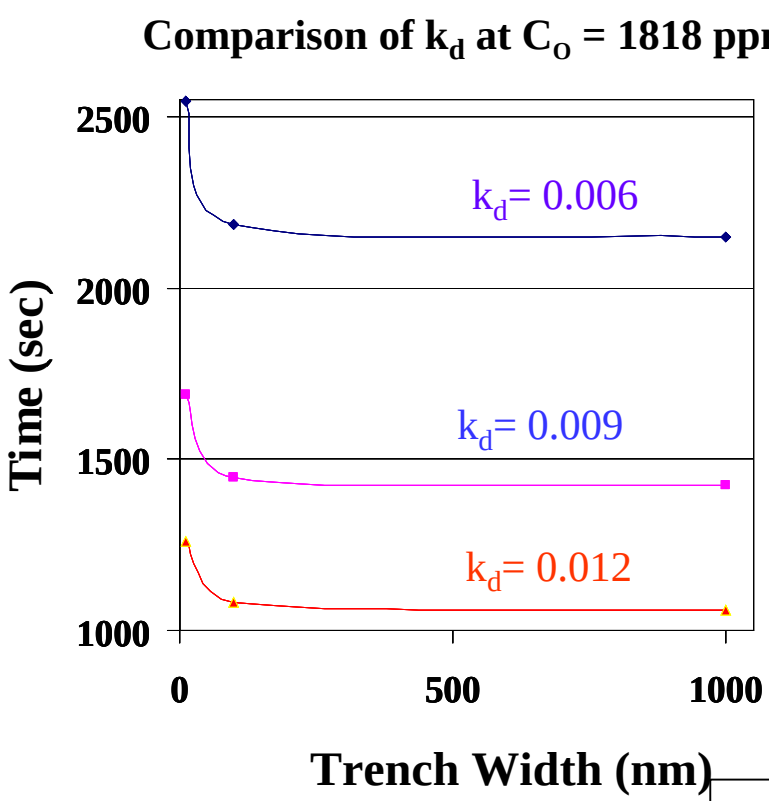

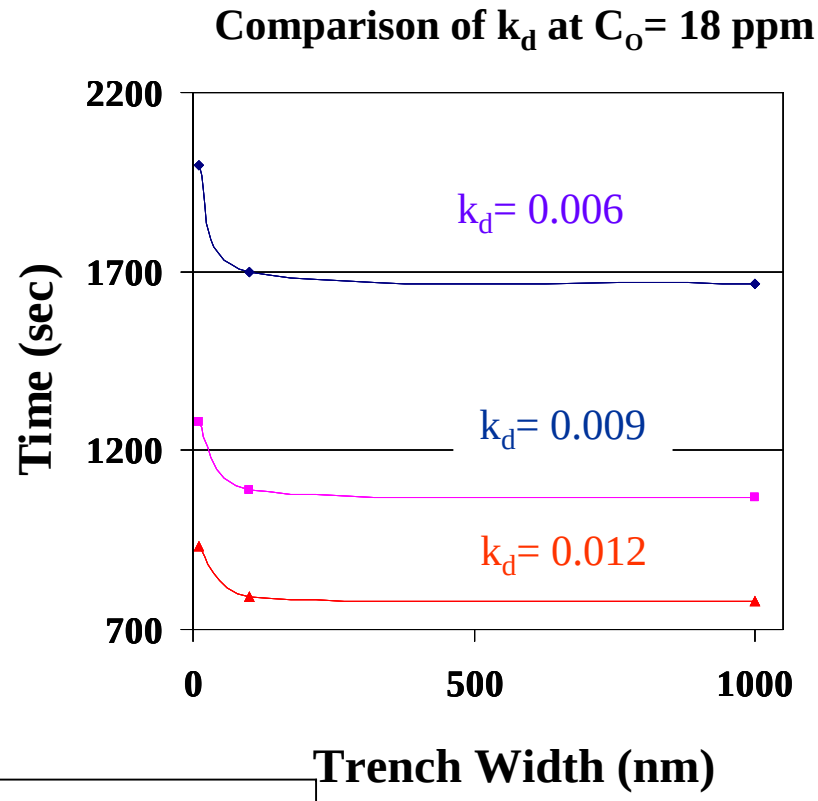

Modeling Material: Sulphate

Trench Depth=5μm

Alternate Applications of ECRS

1. Drying of micro/nano structures

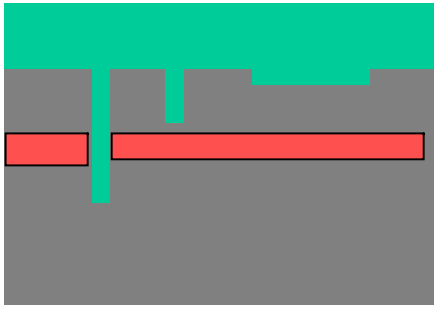

2. Cleaning and drying of porous film

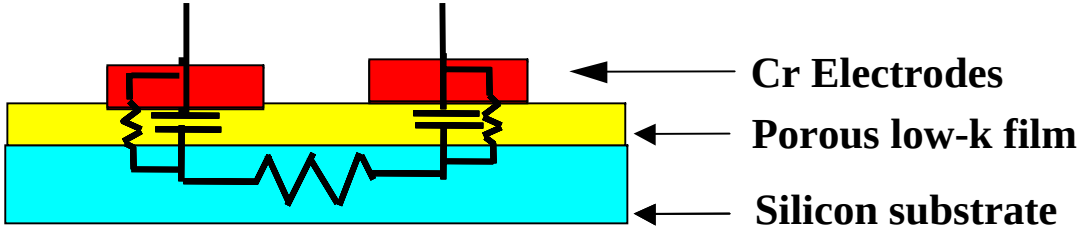

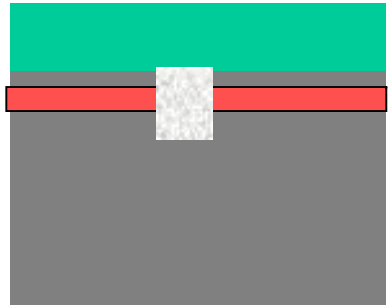

(a) (b)

Sensor Reveals Drying Mechanism

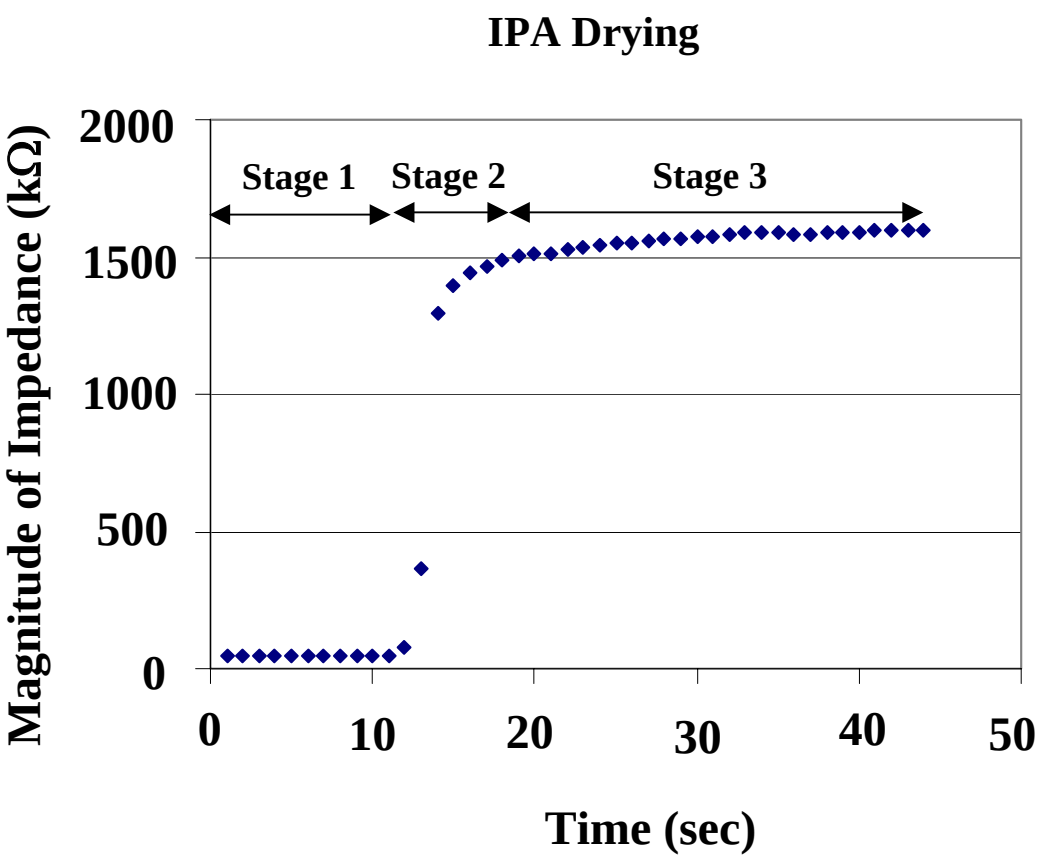

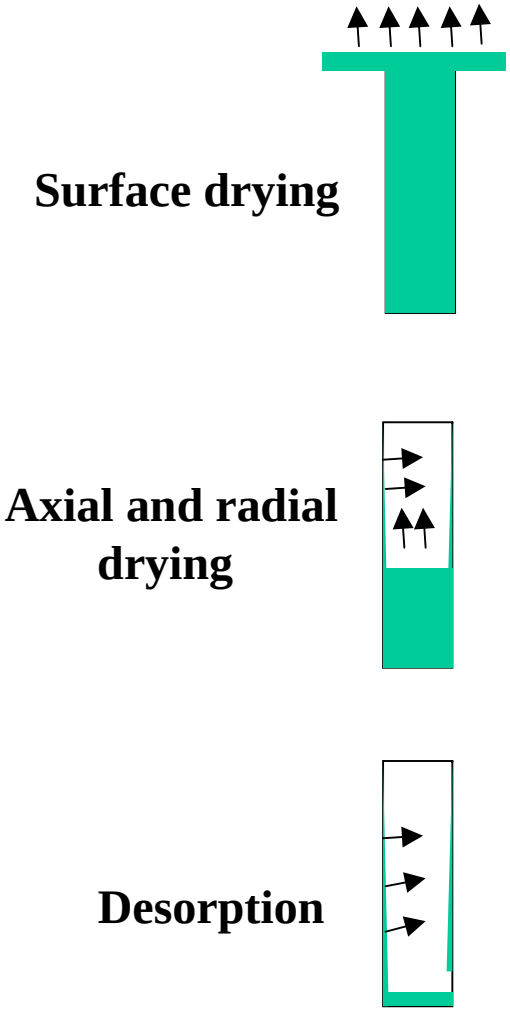

Sensor Response to Drying Processes

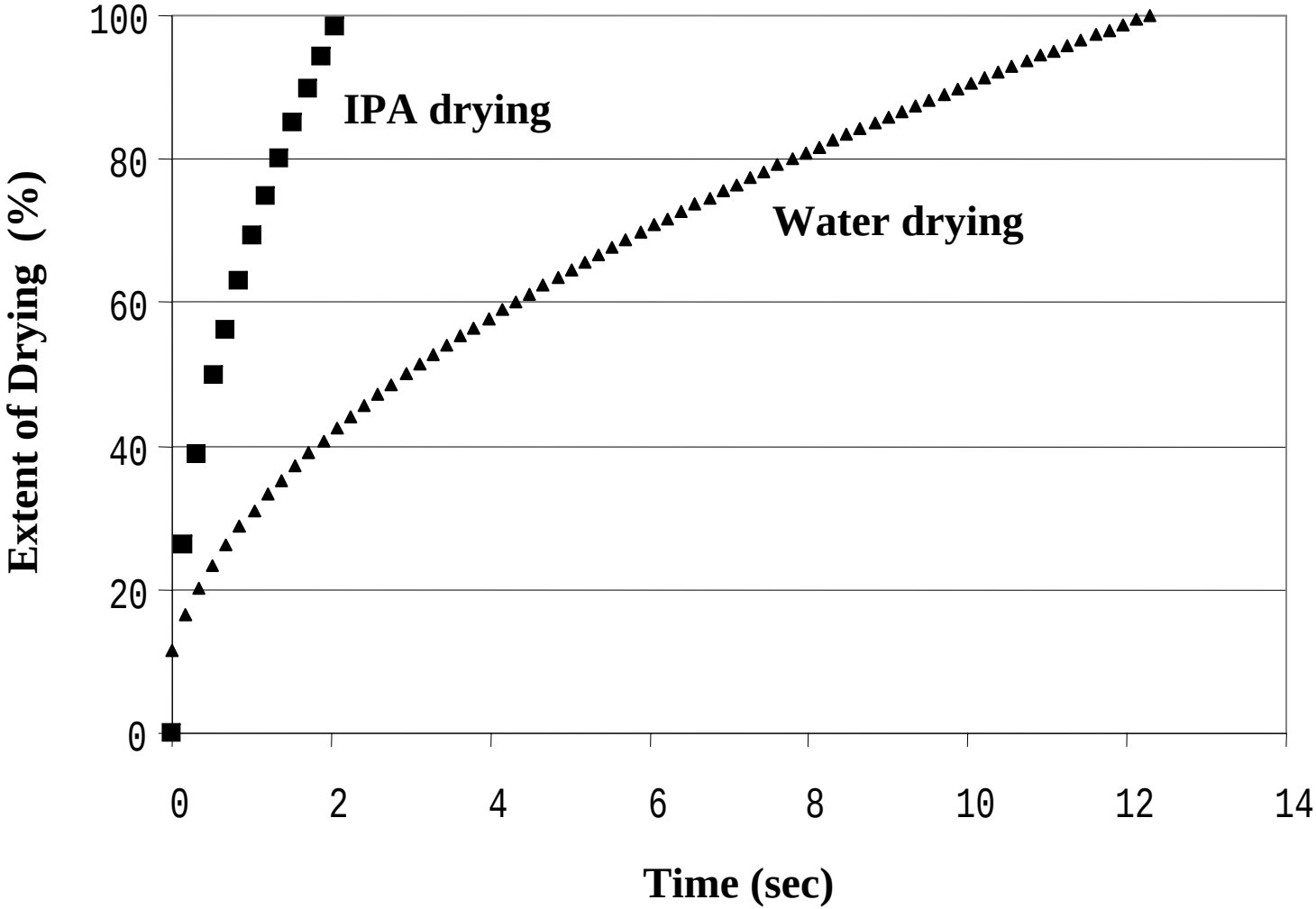

Sensor for Low-k Film Outgassing

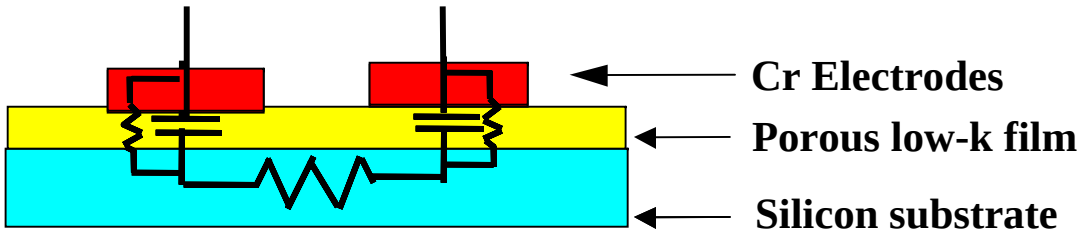

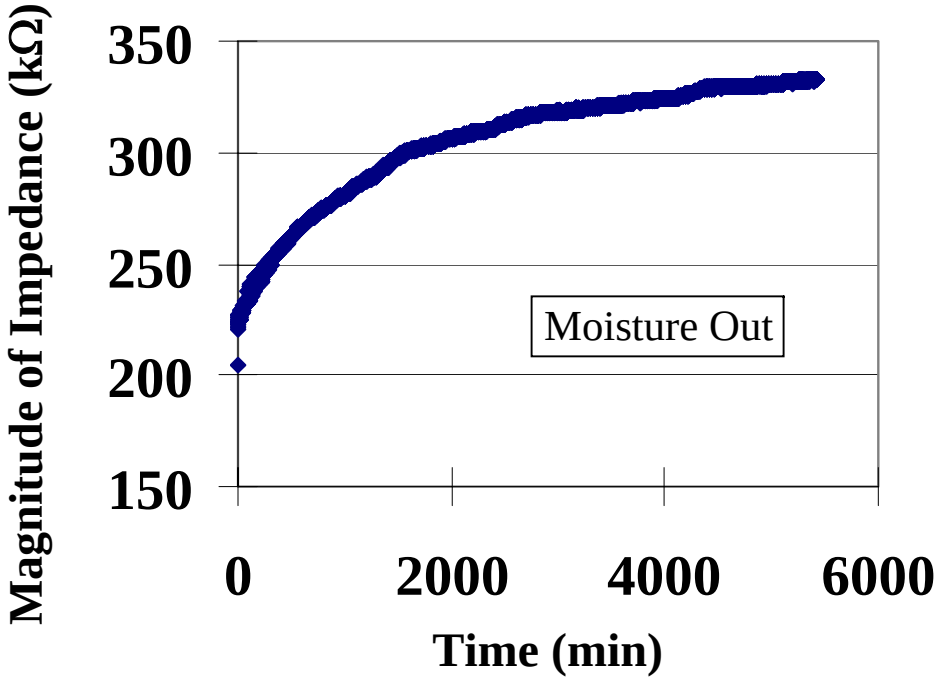

Effect of Temperature and Feature Size on Required Rinse Time

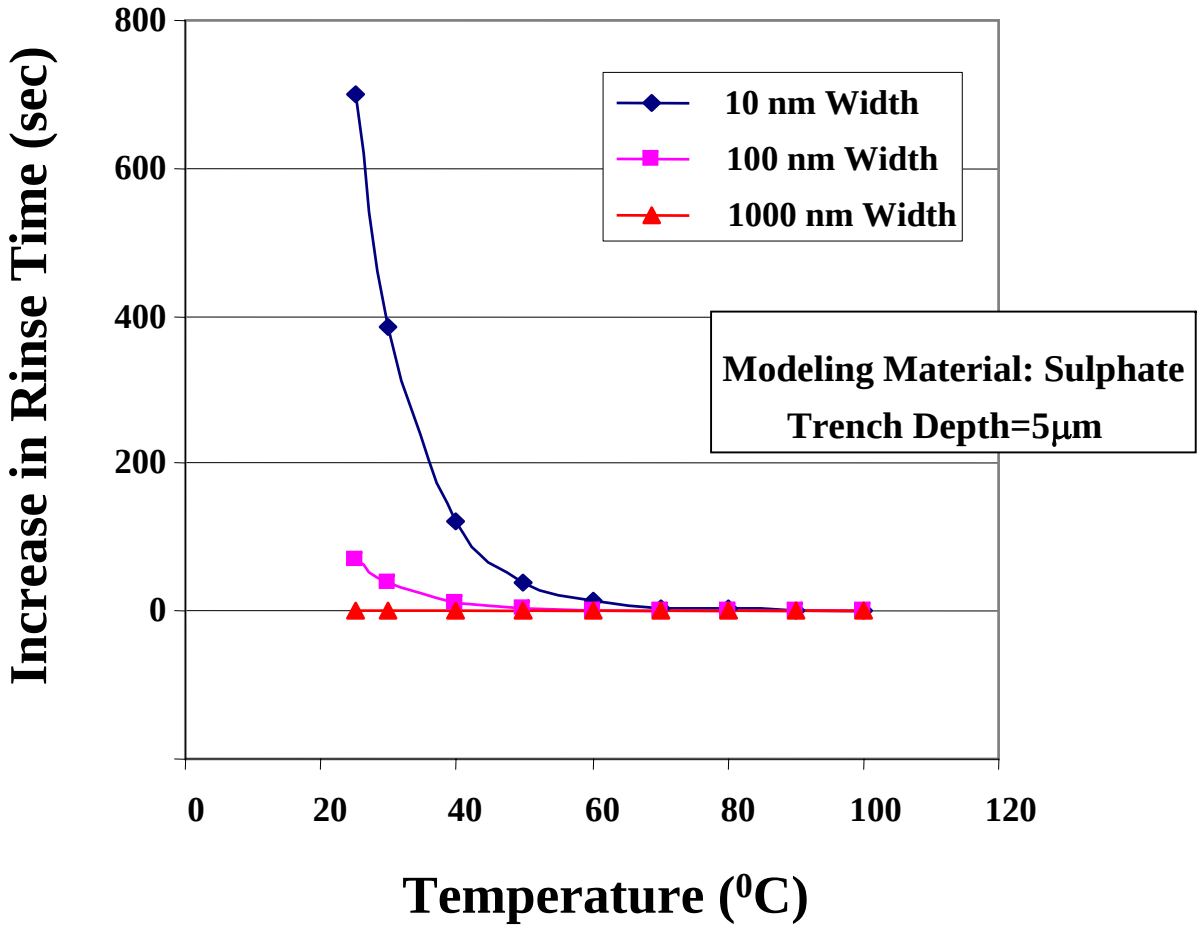

Electrostatic Interactions

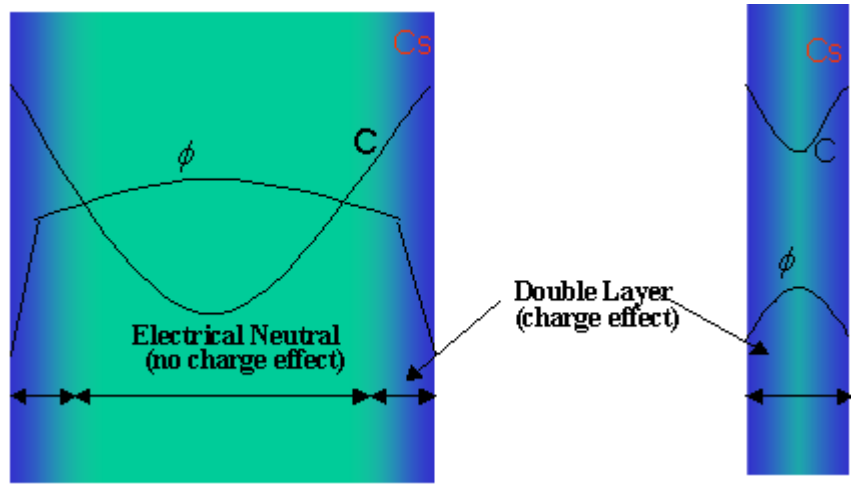

Mass Balance equations:

$$\frac{dC}{dt} = \nabla \cdot (D_{AB} \cdot \nabla C + z \cdot \lambda \cdot F \cdot C \cdot \nabla \phi)$$

$$\frac{\partial C_S}{\partial t} = \left[k_a C(S_0 - C_S) - k_d C_s \right]$$

$$\nabla^2 \phi = -\frac{\rho_e}{\varepsilon\varepsilon_0} = -(\rho_\infty e / \varepsilon\varepsilon_0) * \exp(-z * e * \phi / (k * T))$$

The electrostatic interactions become more significant as feature size decreases and purity requirements increase.

ESH Metrics and Impact

I) Basis of Comparison:

Current best technology: Currently fabs do not have capabilities for on-line and real-time measurement and monitoring of residual contaminants on wafers. Cleaning and rinsing of patterned wafers and porous films are even more complex and in need of new metrology techniques.

II) Manufacturing Metrics

The real-time and on-line metrology tools and techniques for cleaning and rinsing would save water, chemicals, and energy; it will also reduce processing time, increase throughput, and reduce cost. The impact on reliability and yield are expected to be significant but need to be evaluated later.

III) *ESH Metrics*

	Usage Reduction			Emission Reduction			
Goals / Possibilities	**Energy**	**Water**	**Chemicals**	**PFCs**	**VOCs**	**HAPs**	**Other Hazardous Wastes**
Real-time and on-line sensor with 10 ppt or better sensitivity based on H_2SO_4 concentration in rinse water calibration	At least 20%	50 % reduction in water usage	Reduction in chemicals usage; difficult to estimate at this time	N/A	N/A	Some reduction in acid vapors	50% reduction in waste/ and wastewater

Acknowledgement

- **Sematech: providing samples**
- **Freescale: joint work on testing the ECRS in a commercial rinse tool.**
- **American Semiconductor: assistance in fabrication**
- **On Semiconductor: joint work on testing test the ECRS in a commercial drying tool.**
- **Environmental Metrology Corporation (start-up): joint work for commercialization**

Low-Energy and Low-Chemical Cleaning and Drying of Nano-Structures:

Drying of Porous Low-k Films

Subtask C-2-5

Junpin Yao, Asad Iqbal, Harpreet Juneja, and Farhang Shadman
Department of Chemical and Environmental Engineering
University of Arizona

In Collaboration with Sematech Interconnect Group

NSF/SRC Engineering Research Center for Environmentally Benign Semiconductor Manufacturing

Background

- Porous low-k inter-layer dielectrics (ILD) are highly prone to molecular contamination
- Cleaning and drying of porous thin films is a slow and complex process

Objectives

- Study molecular contamination of low-k materials like p-MSQ and compare them with SiO_2
- Determine the adsorption and outgassing dynamics
- Determine the fundamental outgassing properties such as loading, molecular transport, chemical interactions, and removal of moisture in porous low-k films
- Develop process modeling approach for minimizing the chemical and energy usage during purging and cleaning

Experimental Setup

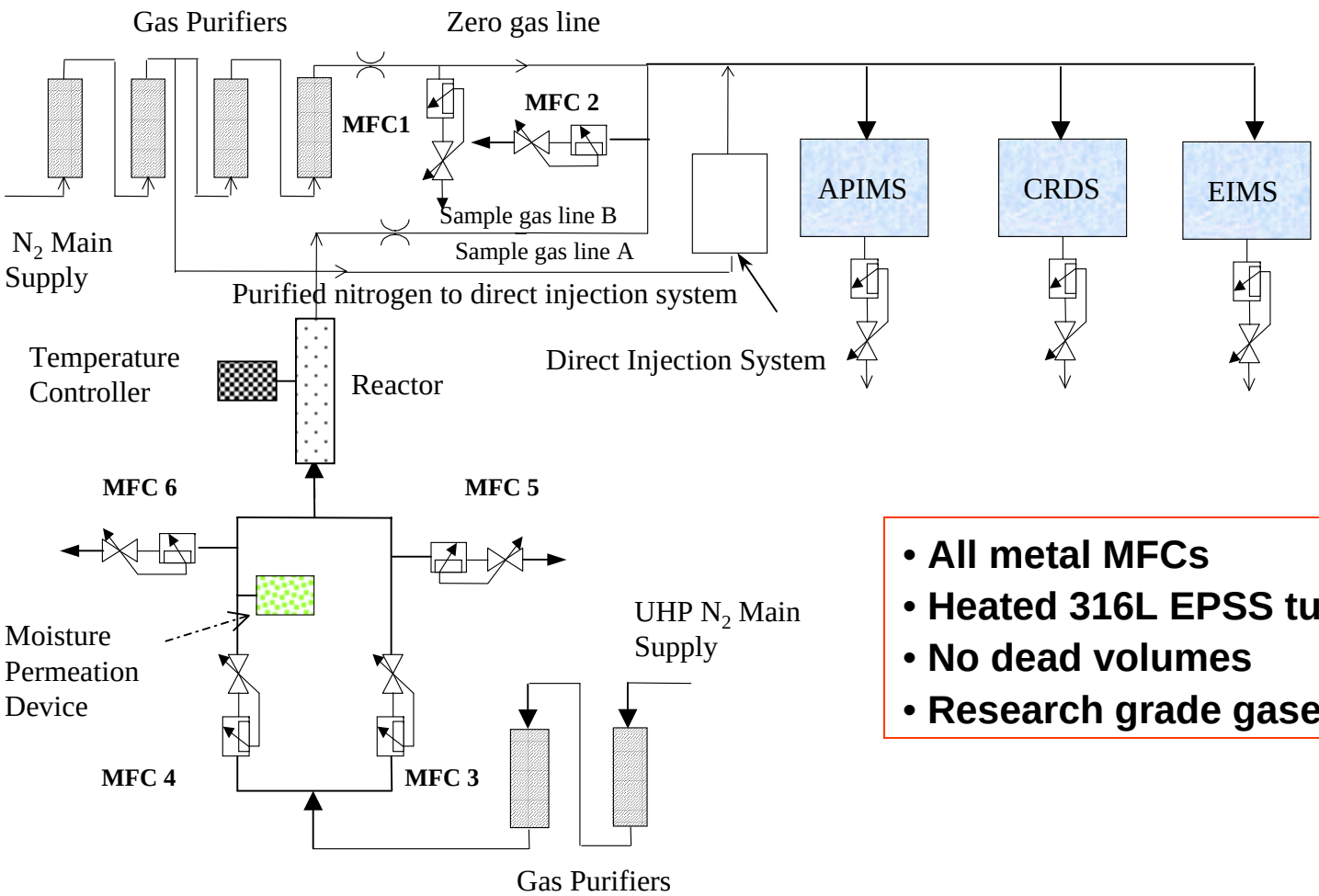

- **All metal MFCs**
- **Heated 316L EPSS tubing**
- **No dead volumes**
- **Research grade gases**

Experimental Procedure

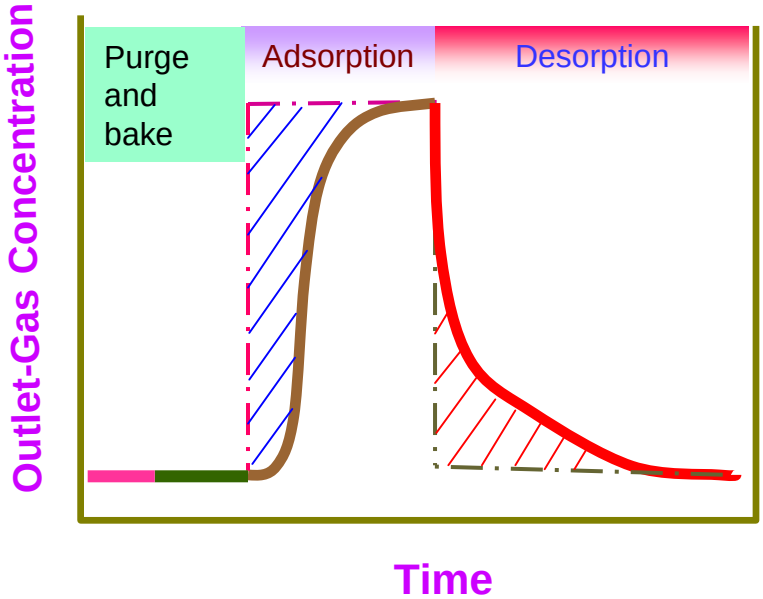

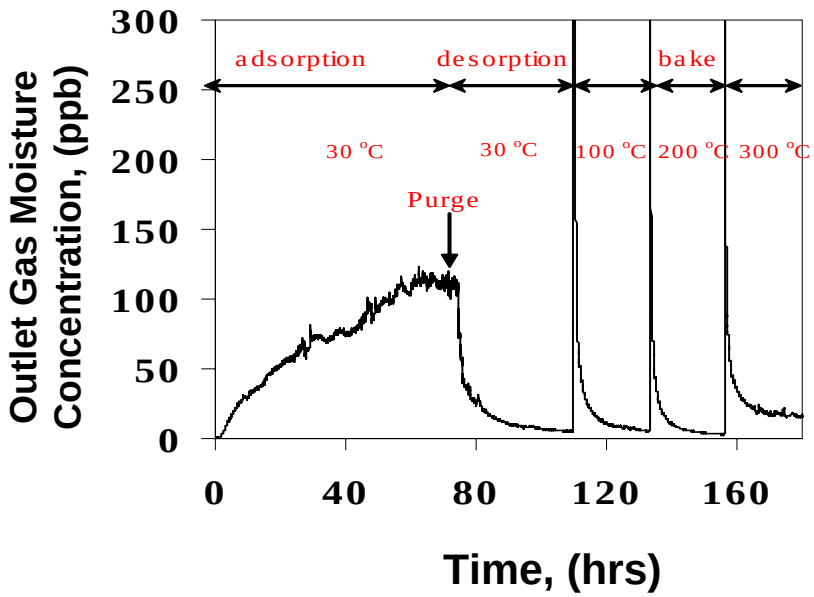

Experimental procedure

Adsorption at 30°C

Desorption at 30°C

Bake-out at 100, 200 & 300°C

Temporal profile of adsorption (challenge 110 ppb moisture), followed by temperature-programmed desorption as measured by mass spectrometer

Test Samples

Wafer	Processing Conditions
A*	Partial etch @ 10s, N_2H_2 ash @ 20s
B*	Partial etch @ 10s, HeO_2 ash @ 20s
C*	Blanket and cure only
D* (JSR 5109)	Standard JSR cure, partial etch and partial ash

*** Samples provided by Sematech**

Comparison of moisture loading and water contact angle

Wafer	Loading (molecules/cm^2)		Contact angle
	25°C	380°C	
A*	5.17E16	3.61E16	102°
B*	5.86E16	5.75E16	50°
C*	6.19E16	6.00E16	105°
SiO_2	4.50E14	-	-

Dynamics of Purge

Experimental Data

Challenge Concentration: 156 ppm; Temperature: 380°C

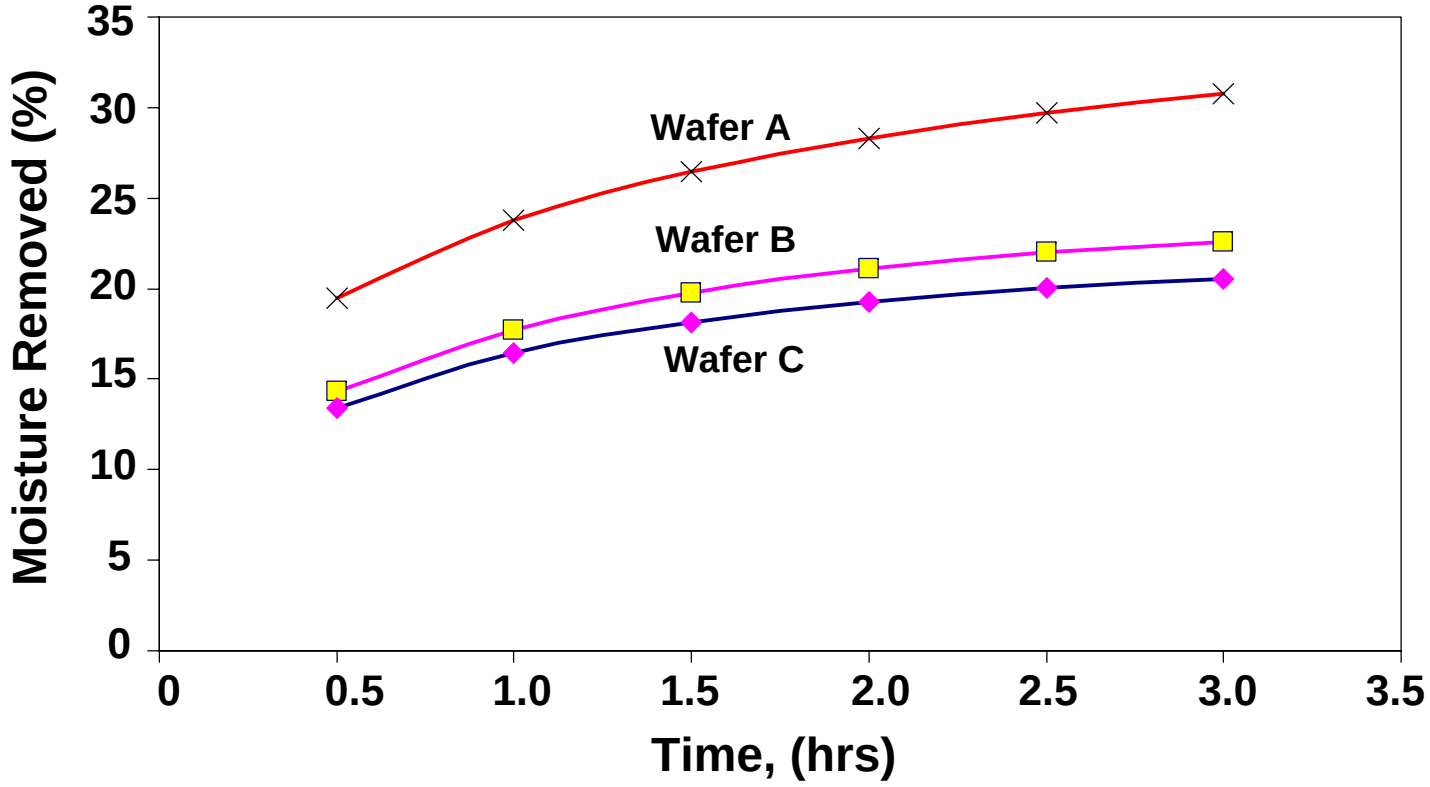

Moisture Adsorption Loading

Challenge Concentration : 56 ppb

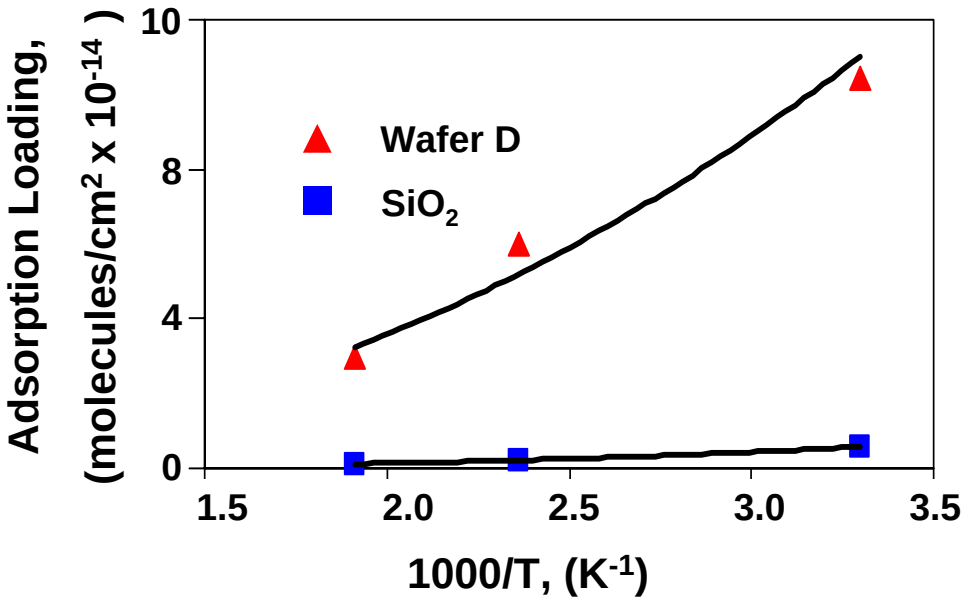

- **Wafer D has much higher sorption loading than SiO_2**

SiO_2

Δ Electronegativity	1.7
-OH site density (#/cm²)	4.6×10^{14}

p-MSQ

$$C_{film0} = C_{gp0}\varepsilon + C_{s0}(1-\varepsilon)$$

$$C_{s0} = C_{gb0} * S$$

C_{gbo} = challenge moisture concentration

C_{gpo} = equilibrium moisture concentration in the pore

C_{so} = equilibrium moisture concentration in the matrix

C_{filmo} = total moisture loading

ε = porosity, *S* = solubility

Moisture Retention after Isothermal Purge

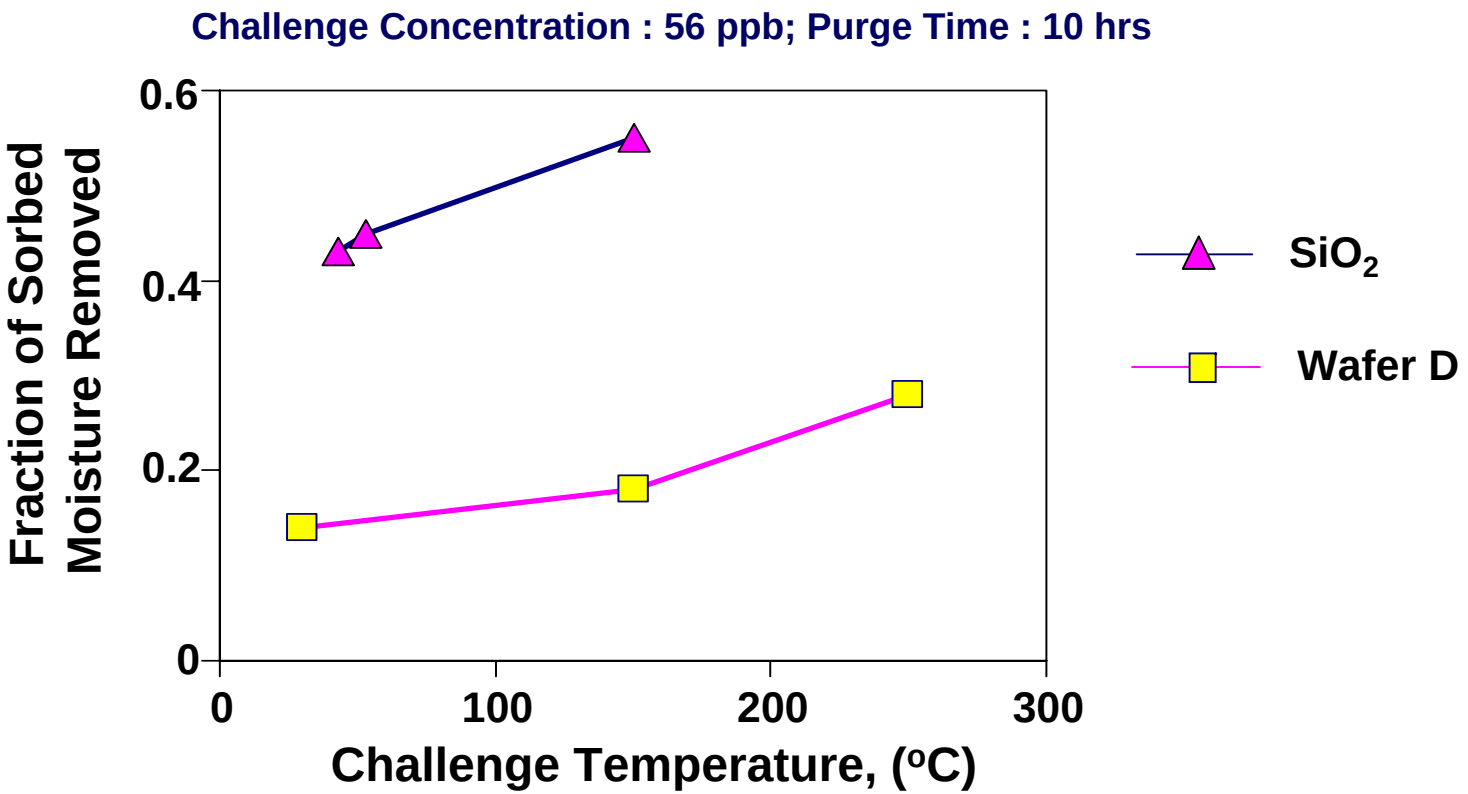

- 45-50 % of adsorbed moisture removed from SiO_2 during isothermal N_2 purge
- Around 15-25 % of absorbed moisture removed from Wafer D

Validation of Model

Desorption

Wafer D; Challenge Conc: 56 ppb; Purge Gas Conc: 1 ppb; Purge Gas Flow Rate: 318 sccm; Porosity: 0.48; Film Thickness: 4000 Å

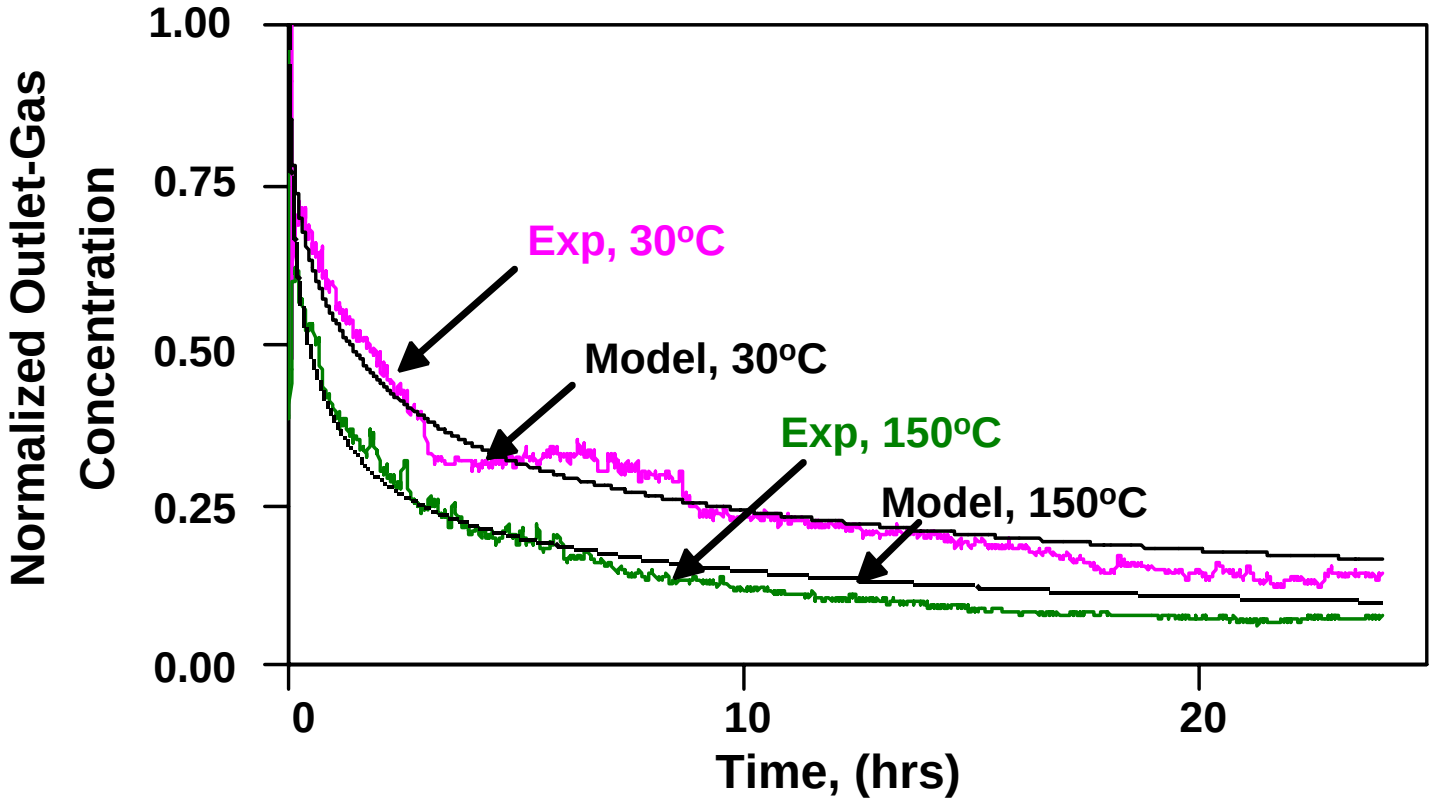

Process Parameters

Parameters	Units	30°C	150°C	250°C
D_s	cm^2/s	1.4e-15	1.7e-15	3.5e-15
D_g	cm^2/s	8.5e-10	1.0e-9	3.0e-9
S	$\frac{\text{molecules/cm}^3\text{ of film}}{\text{molecules/cm}^3\text{ of gas}}$	3.65e7	1.9e7	1.0e7
k_m	cm/s	5.0e-13	5.0e-13	5.0e-13
k_{ms}	cm/s	1.0e-8	1.0e-8	1.0e-8
k_{mg}	cm/s	1.0e-7	1.0e-7	1.0e-7

- **Transport through pores is micro pore diffusion**
- **Diffusion in matrix is primarily through molecular or intra-lattice cavities**
- **Exchange coefficients k_m, k_{ms} and k_{mg} are weak functions of temperature and are constant for all cases**

Effect of Purge Gas Flow Rate

Wafer D; Challenge Conc: 56 ppb; Temperature: 30°C; Film Thickness: 4000 Å; Porosity: 0.48; Purge Gas Conc: 1 ppb

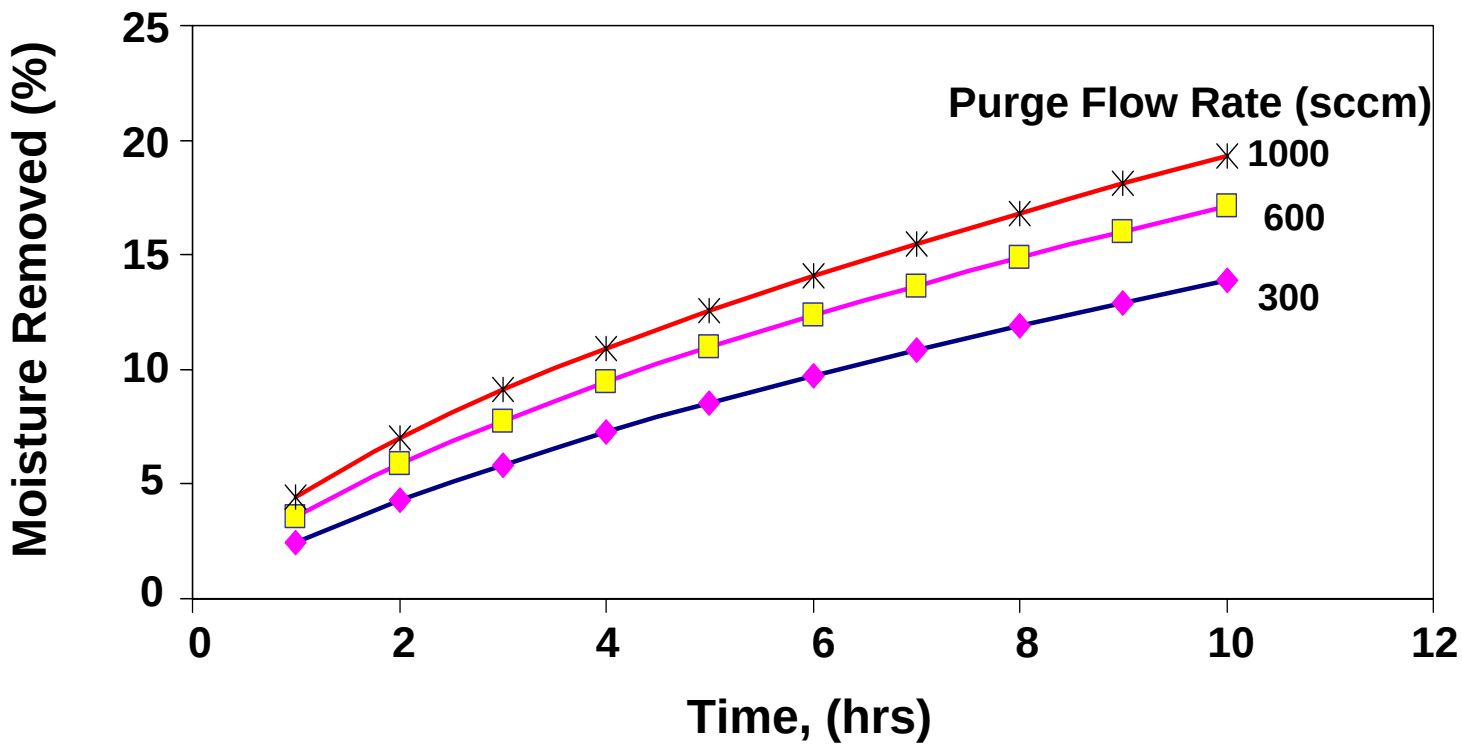

Parametric Study : Effect of Film Porosity

Wafer D; Challenge Conc: 56 ppb; Temperature: 30°C; Film Thickness: 4000 Å; Purge Gas Conc: 1 ppb; Purge Gas Flow Rate: 318 sccm

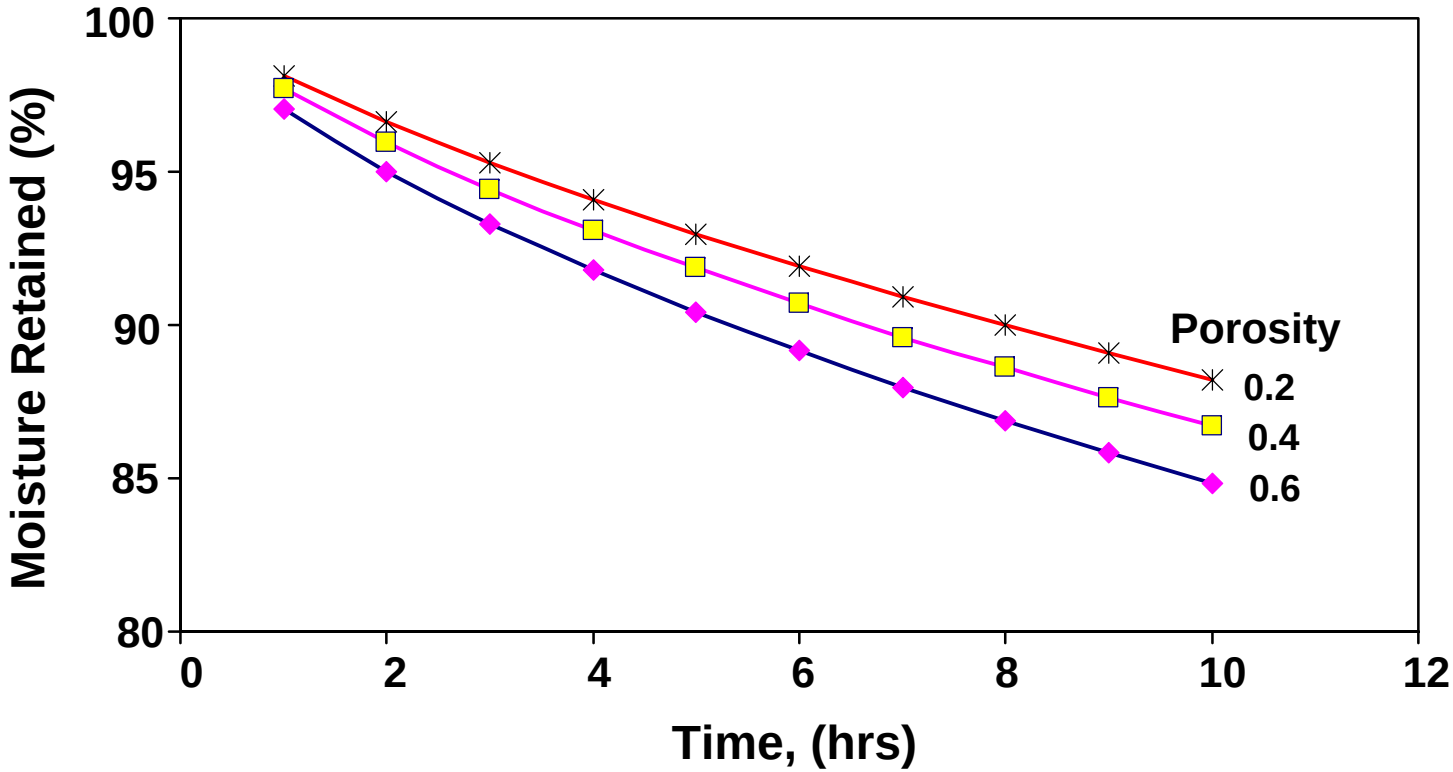

Parametric Study: Effect of Film Thickness

Wafer D; Challenge Conc: 56 ppb; Temperature: 30°C; Porosity: 0.48; Purge Gas Conc: 1 ppb; Purge Gas Flow Rate: 318 sccm

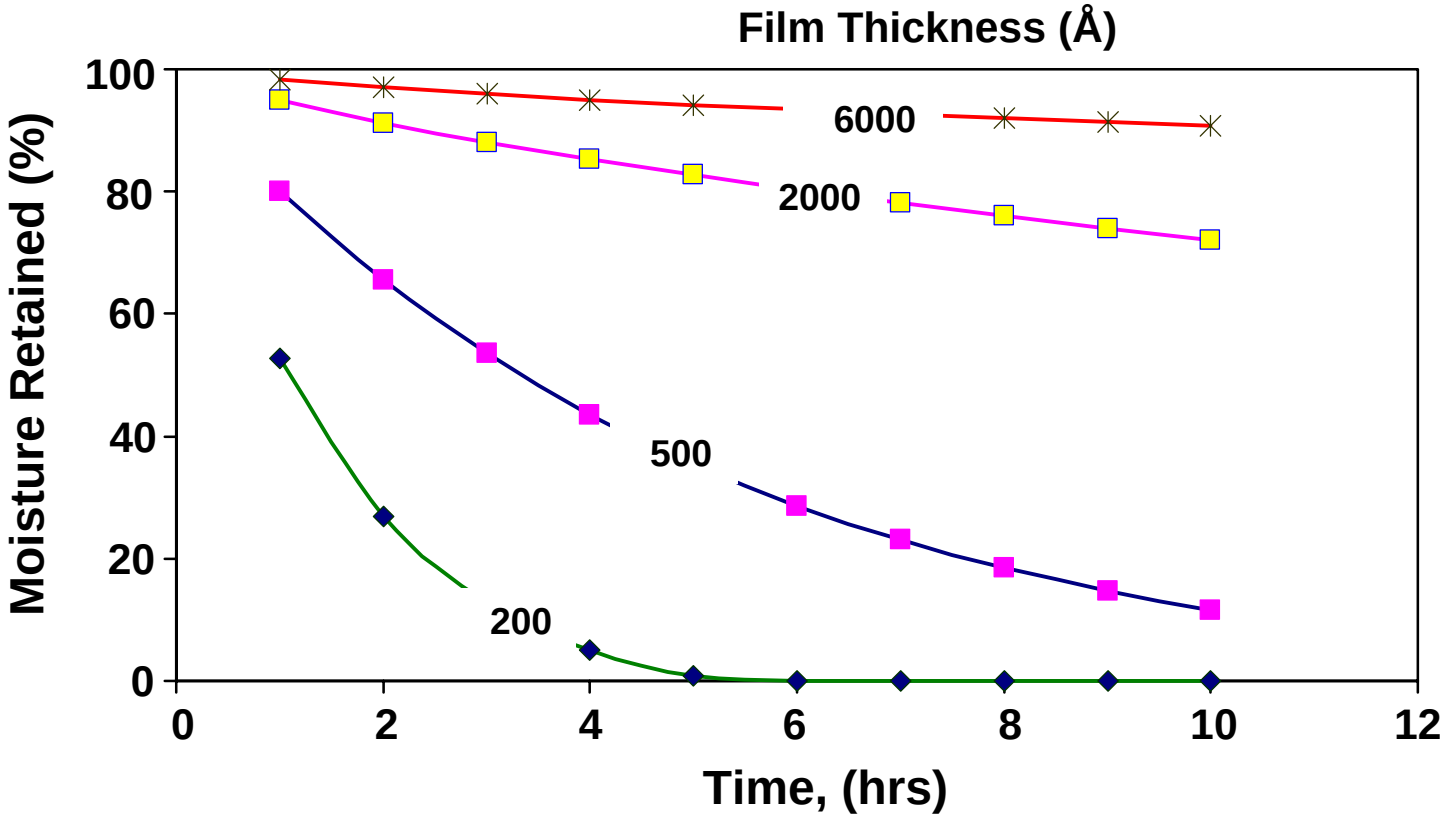

Practical Applications of Model

- **Model describes the interactions among various process steps and helps in explaining the experimental results**
- **It is a practical tool for**

  - estimation of residual contamination and

  - optimization of process conditions to minimize effects of molecular contamination

  - valuable tool for designing a desorption recipes (temperature, gas flow, and gas purity) to assure effective and efficient clean up of the dielectric films

Conclusions

- **Interaction between porous low-k films and moisture cannot be correlated with thermodynamic properties alone (such as conventional application of contact angle measurements).**
- **Moisture removal is a slow and highly activated process**
- **A process model is developed for data analysis and purge optimization.**
- **Interphase transport and the pore diffusion coefficients are smaller that those predicted by bulk or Knudsen diffusion mechanism.**
- **Increase in purge flow rate or temperature (to a much greater degree) enhance the removal of moisture; increase in film thickness and decrease in porosity slow the moisture removal.**
- **Moisture removal efficiency depends on purge gas purity concentration only under certain conditions (important in cost and waste reduction).**

ESH Metrics and Impact

I) Basis of Comparison:

Current best technology. Purge and drying is done by best quality gas available in the fab. Very little is known about the actual dynamics of outgassing and purge requirements for cleaning and drying of porous low-k.

II) Manufacturing Metrics

More effective purge process will lower chemical (mainly pure gas) and energy usage. Purge sequence to lower the drying time leading to ESH gain as well as lower down time, higher throughput, and lower cost.

III) ESH Metrics

	Usage Reduction			Emission Reduction			
Goals/ Possibilities	**Energy**	**Water**	**Chemicals**	**PFCs**	**VOCs**	**HAPs**	**Other Hazardous Wastes**
Purge and outgassing with lower ESH impact	Lower temperature and lower energy	N/A	Lower purge gas	N/A	N/A	N/A	N/A

Future Work

- Study adsorption of other molecular contaminants on other well-characterized and processed low-k films.
- Determine effect of pore sealing on outgassing
- Extend model to multi-component molecular contamination and non-uniform films for application to etched and ashed films.
- Apply experimental data and modeling to develop more efficient purge process for lowering purge gas and energy usage, lowering purge time (increase throughput), and lowering cost.

CMOS Biochips for Rapid Assessment of New Chemicals

Subtask C-4-3

David Mathine[1,2], Joseph J. Bahl[3], and Raymond B. Runyan[4]

[1]Optical Sciences, [2]Electrical Engineering, [3]Sarver Heart Center, and

[4]Cell Biology and Anatomy, University of Arizona, Tucson

Project Objectives

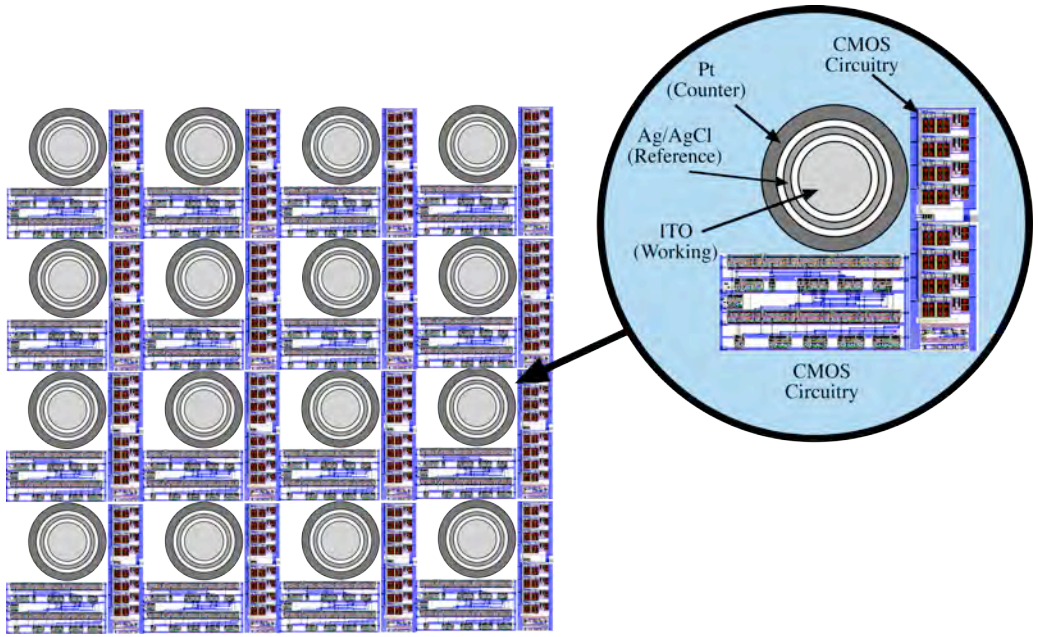

Traditional means of determining chemical toxicity, which typically involve expensive and laborious animal studies, cannot keep pace with the demand for new chemicals by industry. The advent of biochip technology promises to yield a high-throughput means of screening even complex mixtures of chemicals for toxicity. By monitoring the exposure response of reporter cells/tissues, investigators can identify signature reactions that indicate toxic insult.

Cell health will be monitored in real time using a CMOS based sensor where each pixel is capable of optical, chemical, and electrical measurements.

Approach to Toxicity Assay

- **Rapid assessment of chemicals and process chemistries**
- **Important for both chemical suppliers (starting materials) and equipment suppliers/end users (for process-generated by-products, interactions of multiple chemicals, proprietary chemistries in R/D stage, etc.)**
- **A first step towards an on-line ESH monitor.**

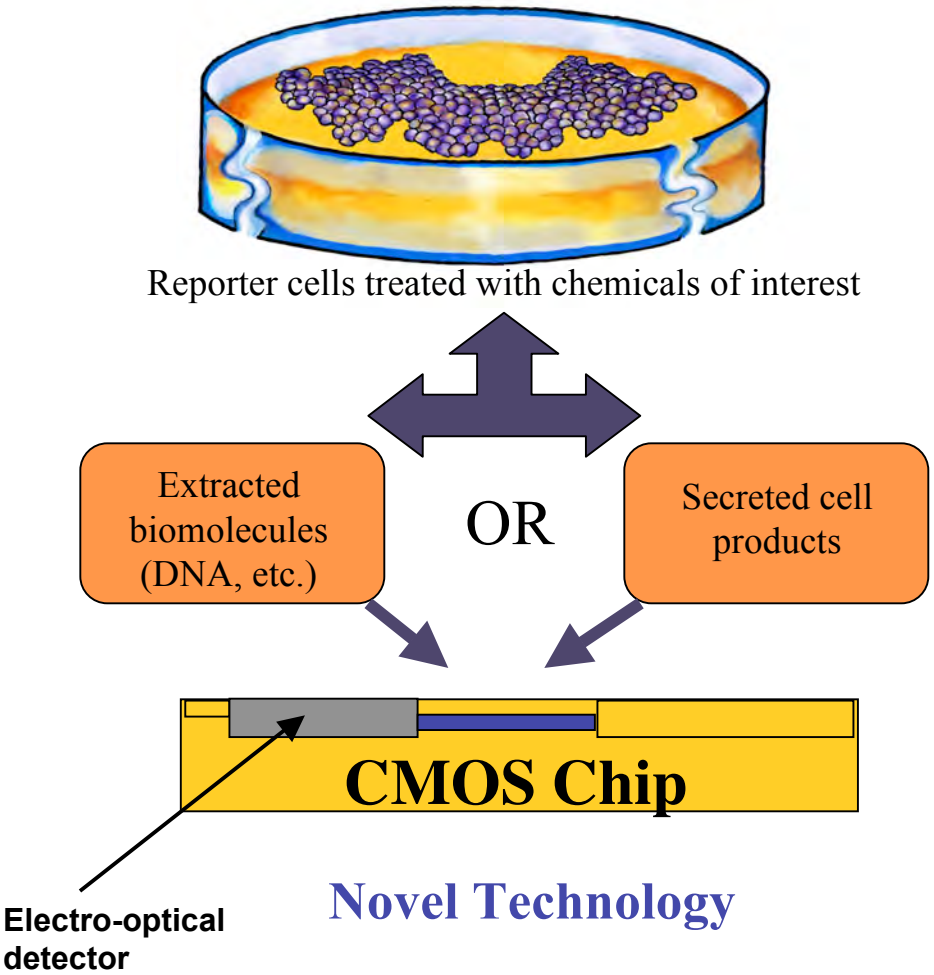

Environmental Control

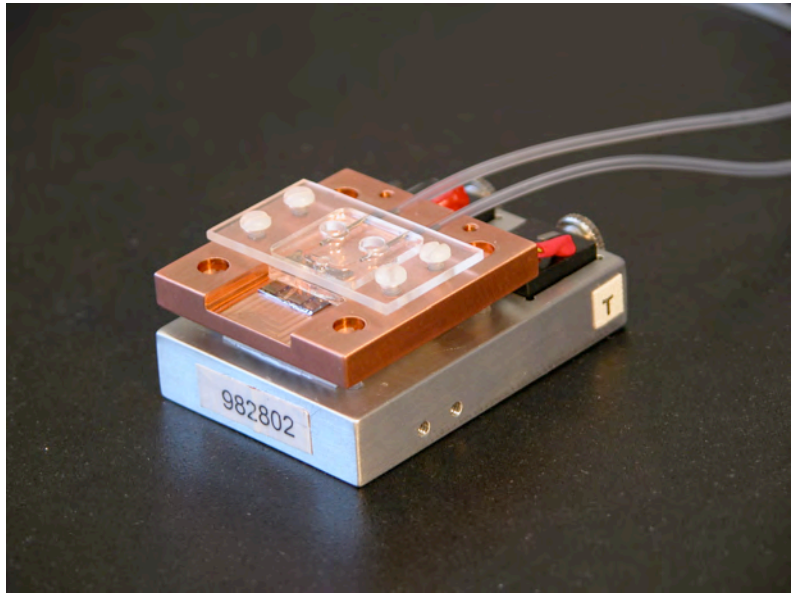

The overall biochamber design is based on controlling the environment for cell growth while providing the means to stimulate the cells chemically, thermally, optically and electrically.

Temperature in the chamber is controlled with a TEC module while a syringe infusion pump is used to control fluid flow through the chamber.

Spectroscopic CMOS Photodetectors

Spectral Response

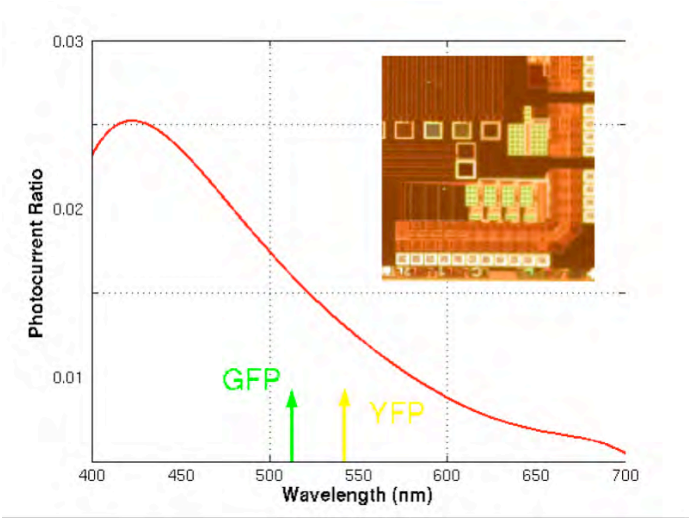

Spectroscopic Photodetectors

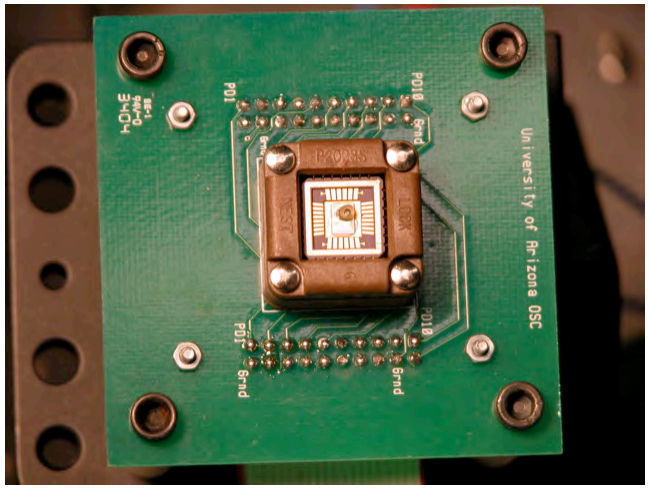

Spectroscopic photodetectors fabricated in a standard CMOS technology can be used to monitor this color change. The spectroscopic photodetectors also have applications in distinguishing fluorescent markers.

Monitoring Pad Capacitance

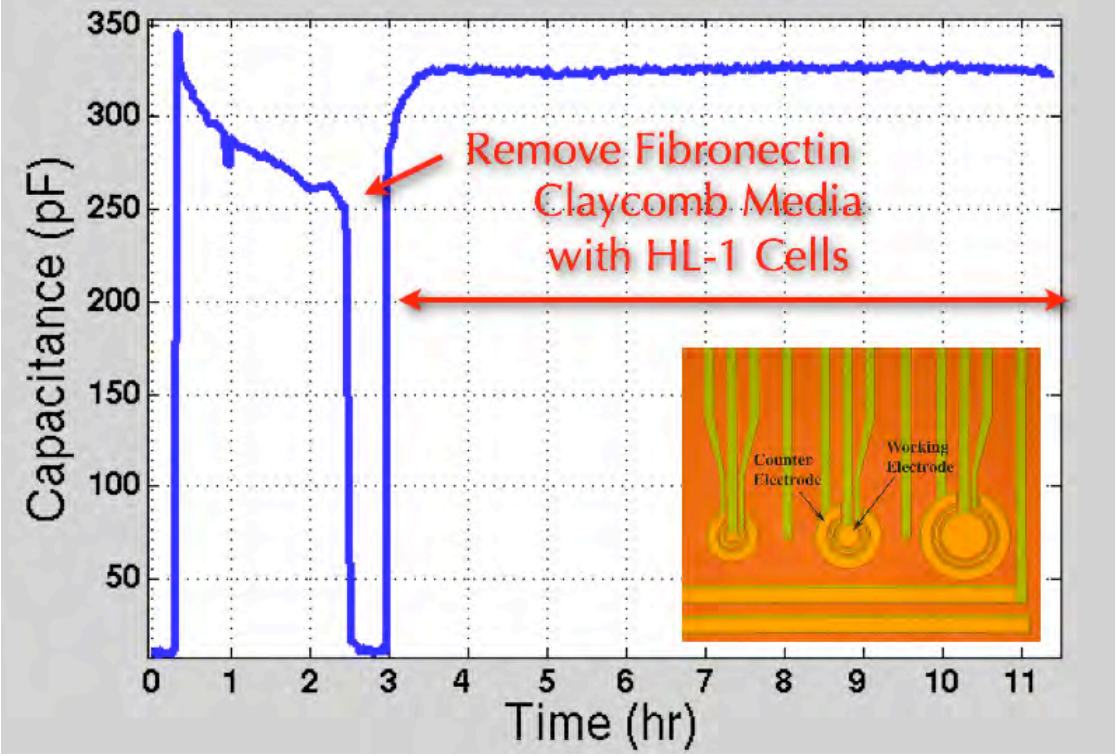

The capacitance from ITO electrodes is monitored in real time to detect protein coating of the electrodes and the induction of HL-1 cells. The HL-1 cells are cardiomyocytes and provide spontaneous beating which can be monitored during chemical exposure.

Characterization of CMOS chips for Chemical Analysis

Design

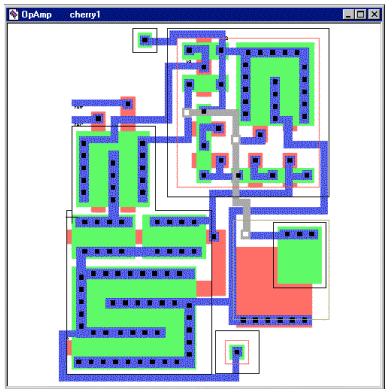

Prototype Custom CMOS Chip

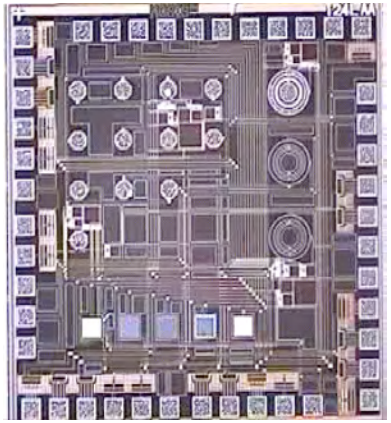

Experimental Test Bed

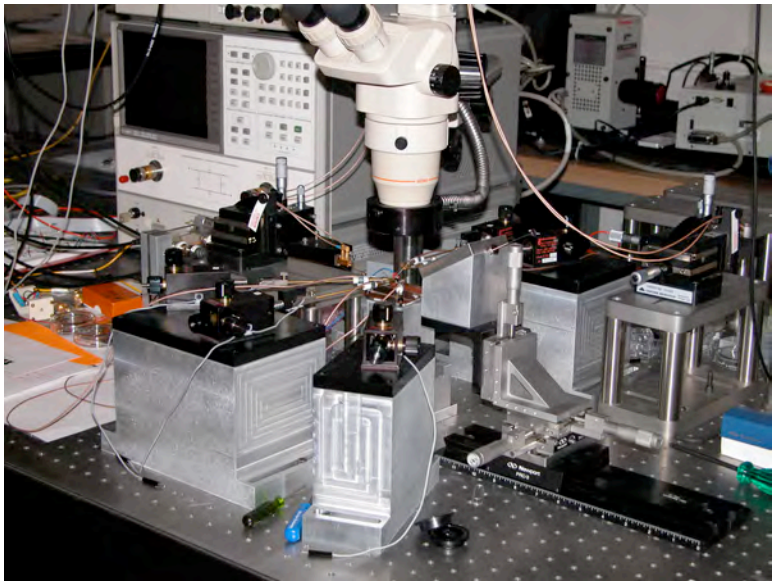

Cell Attachment Studies

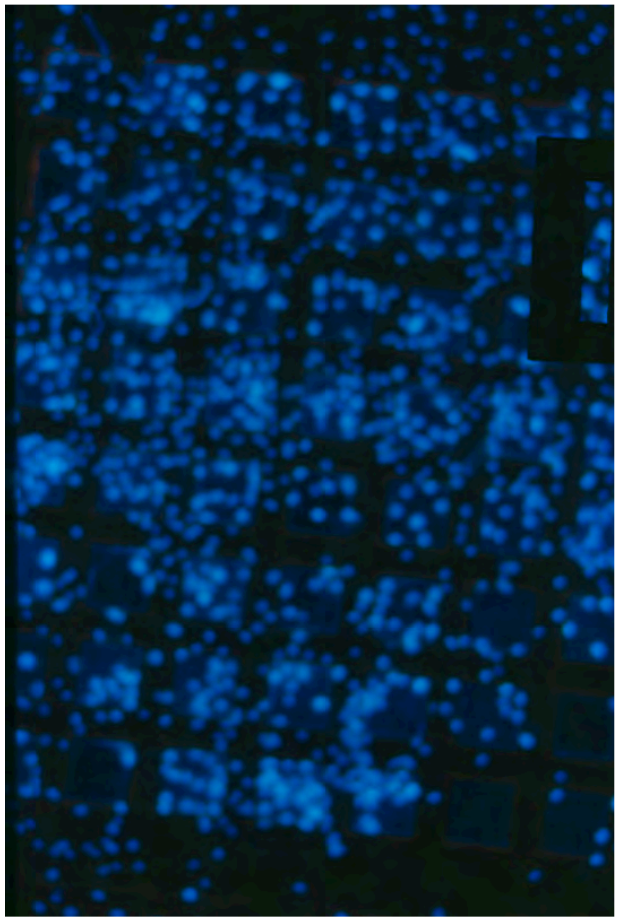

The biosensor surface is foreign to cells. Therefore, the attachment to the SiO_2 and ITO surfaces was studied. We found that COS-7 cells derived from monkey kidney cells, attached and grew well on ITO and SiO_2 coated silicon substrates without patterned biomolecules. COS-7 cells attached better to ITO coated substrates and we were able to obtain confluent cell layers.

The above figure shows DAPI stained COS-7 cells attached to a CMOS chip. An electrode grid pattern can be seen in the image.

EHS Metrics

I) Basis of Comparison - Current best technology involves animal studies to determine toxicity of new chemicals. Approaches to solve this problem center around reduced usage of toxic materials.

II) Manufacturing Metrics - The new approach aims to increase the through put of chemical toxicity testing so that new chemicals will not be introduced into the manufacturing line before the toxicity effects of these chemicals is known.

III) ESH Metrics

The goals of this work are to determine the toxicity of new chemicals. This work hopes to define the standards for toxicity.

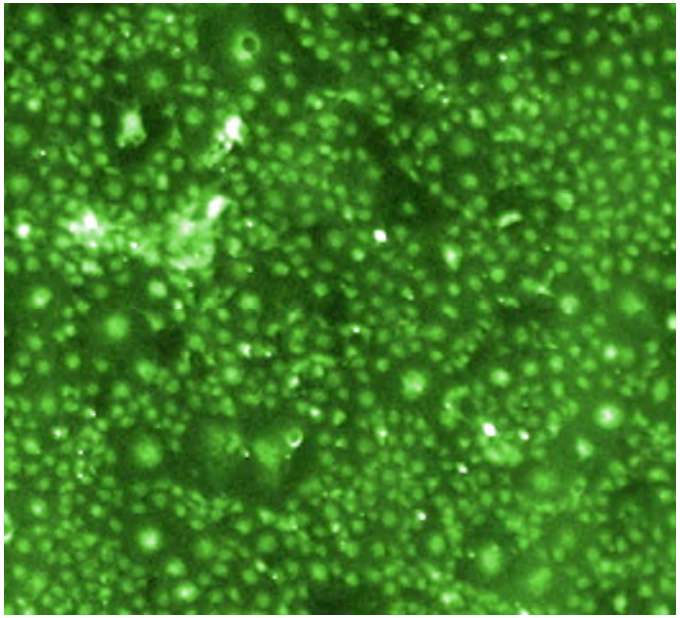

Technology Development and Application

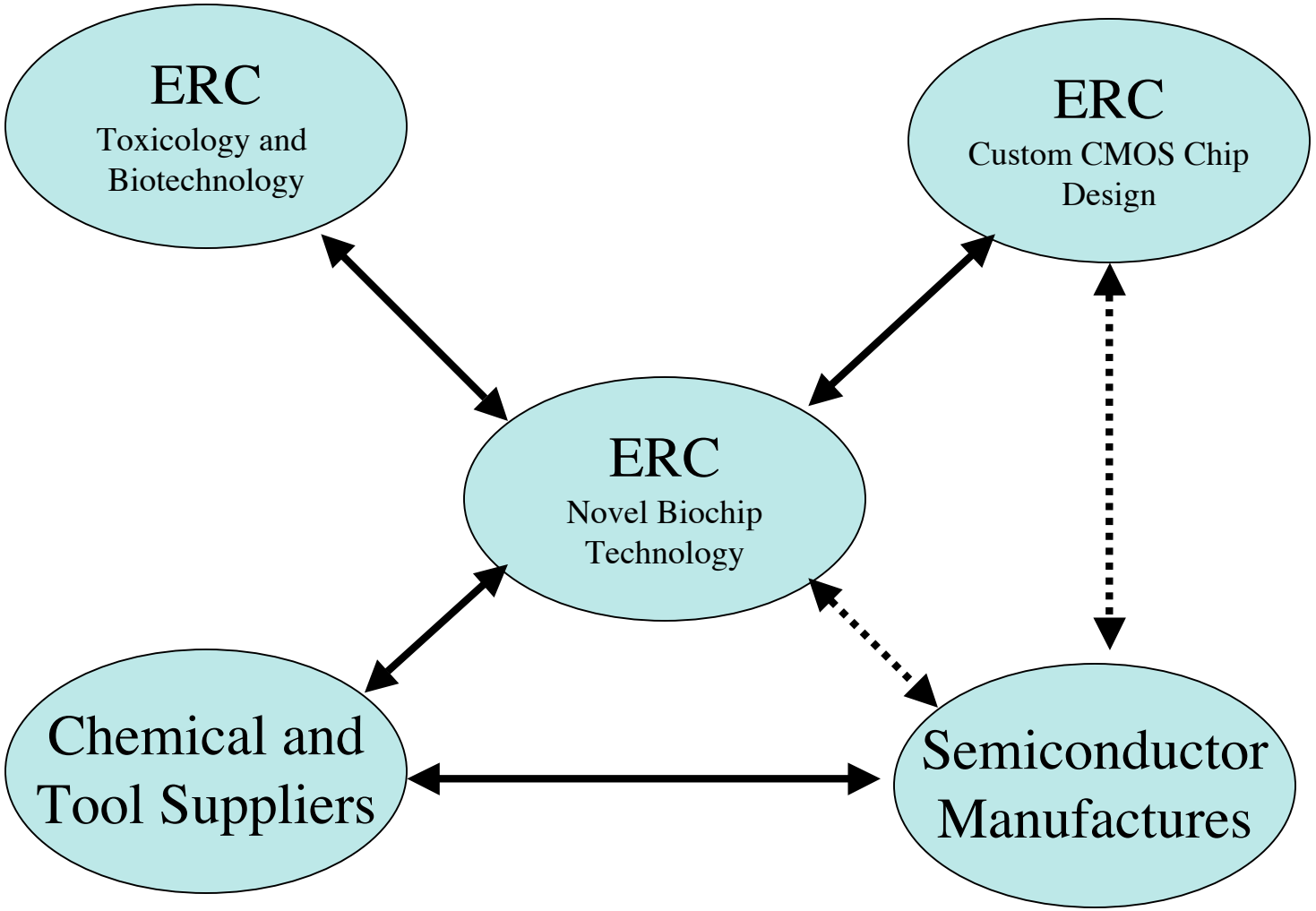

Future Plans

Next year plan:

- **Integrate cells with optical detectors**
- **Test electrochemical sensors within biochamber**
- **Monitor cellular responses to chemicals in real time**

Future Plans:

The CMOS biochip promises to deliver a new generation of highly selective and inexpensive sensors for real-time and online monitoring at the manufacturing site. Future plans include building low-cost sensors for use by chemical suppliers (responsible for starting feed materials) and process engineers and ESH professionals (responsible for evaluation of new chemistries during and after the processing cycle).

Megasonic Cleaning in Semi-aqueous and Non-aqueous media

Task ID C-6-1: Seed Project

Srini Raghavan (PI)
Hrishi Shende (Graduate Student)

Department of Material Science and Engineering
University of Arizona

Mentors

Steven Verhaverbeke, Applied Materials.
Wade Xiong, Texas Instruments.
Mark Beck, Prosys Megasonics.

ERC Annual Review, February 2006

Objectives

- Study cavitation phenomenon in non-aqueous and semi-aqueous liquid systems using a cavitation probe.

- Identify the physical properties of liquid media (e.g. surface tension, viscosity, thermal conductivity) responsible for cleaning without damage in megasonic field.

Motivation

Cleaning of sub-100nm patterns is becoming challenging task. Application of Megasonic energy allows the use of dilute cleaning chemistries, but it also damages the patterns. It is important to find optimum parameters required for megasonic cleaning without damage.

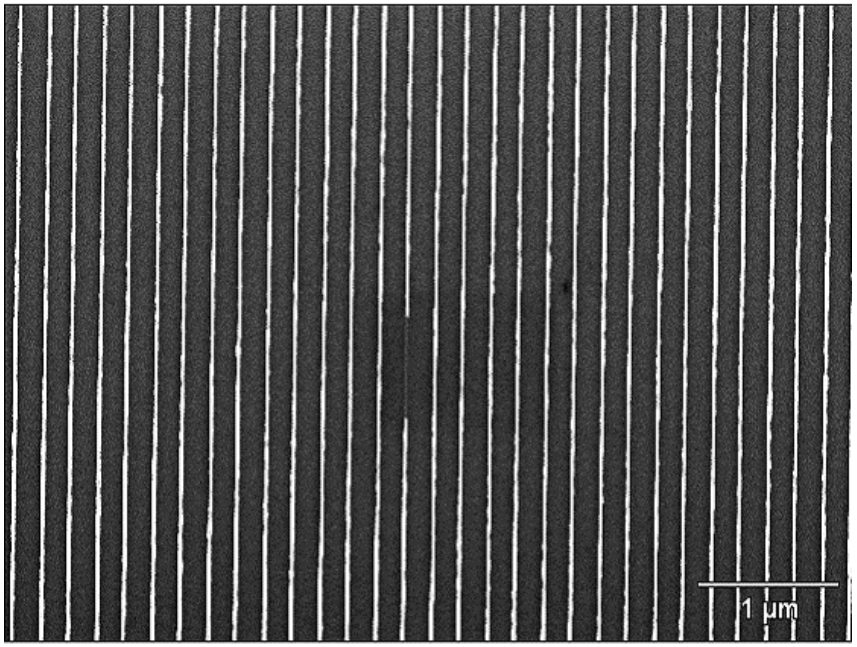

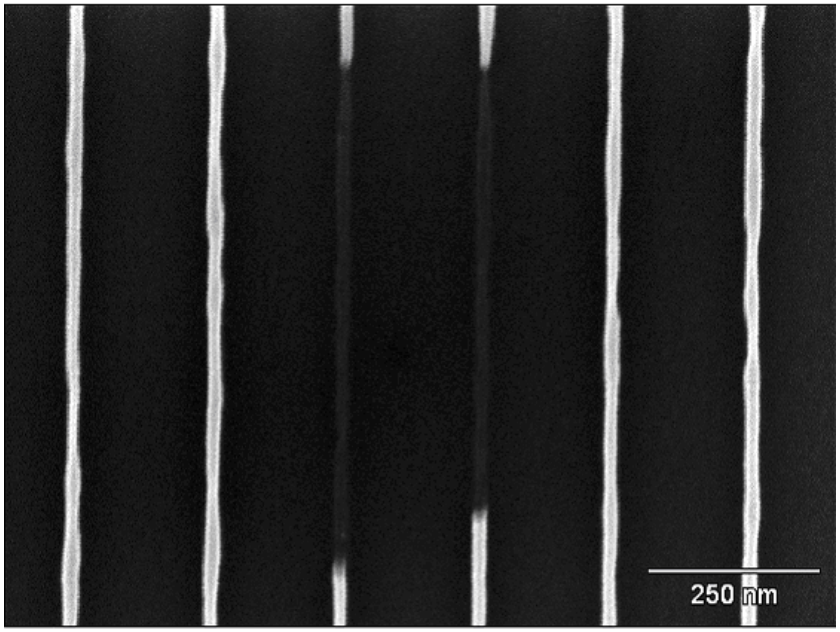

50nm poly-Si lines on SiO2 substrate (SOI), cleaned with DI Water at 2.17W/cm2

Accomplishments During the Current Contract Year

- Investigated the effect of surface tension of the cleaning liquid and megasonic power density on cavitation
- Studied effect of viscosity of the cleaning liquid on cavitation

Setup for Megasonic Cleaning System

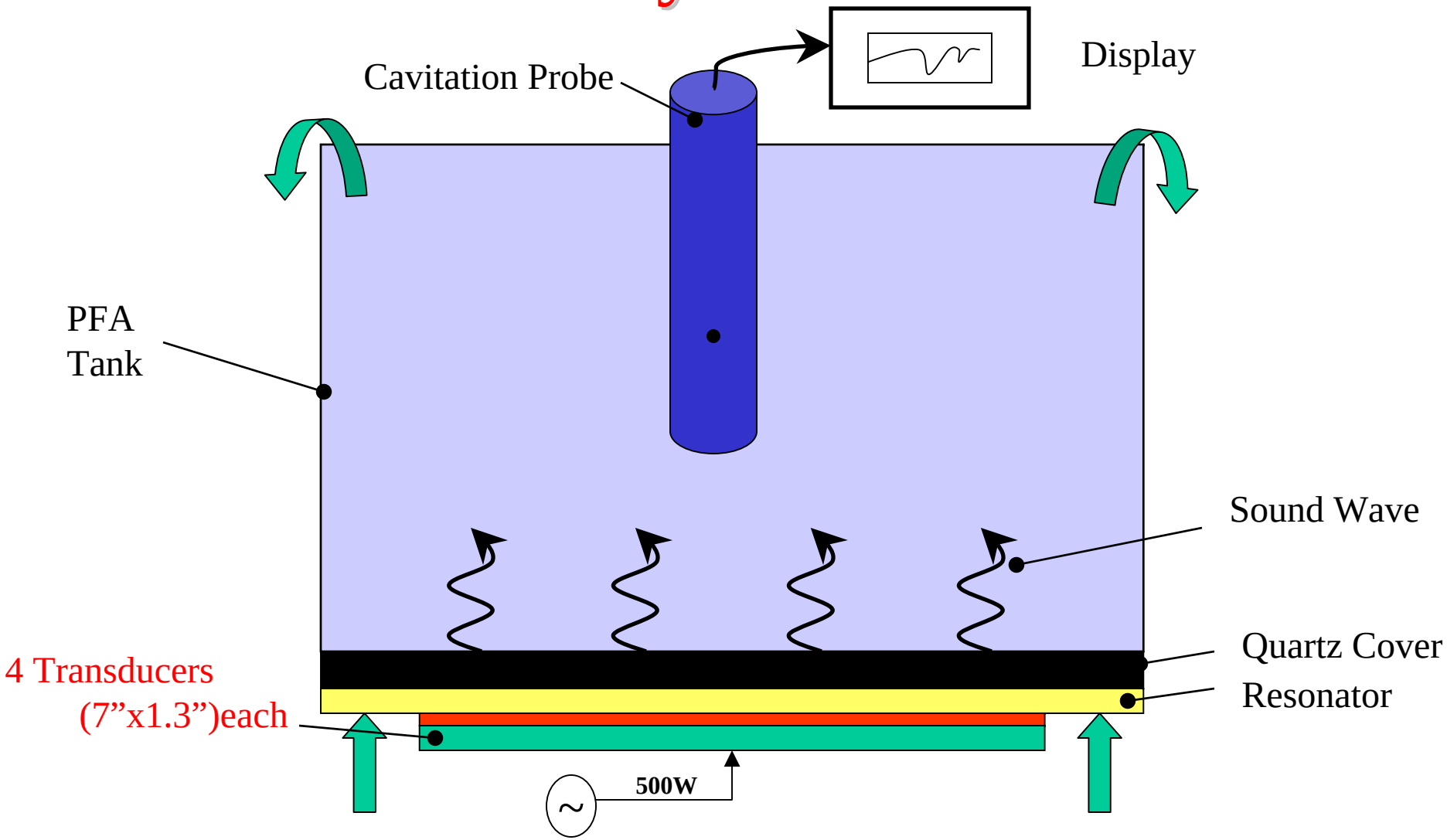

Cavitation Probe

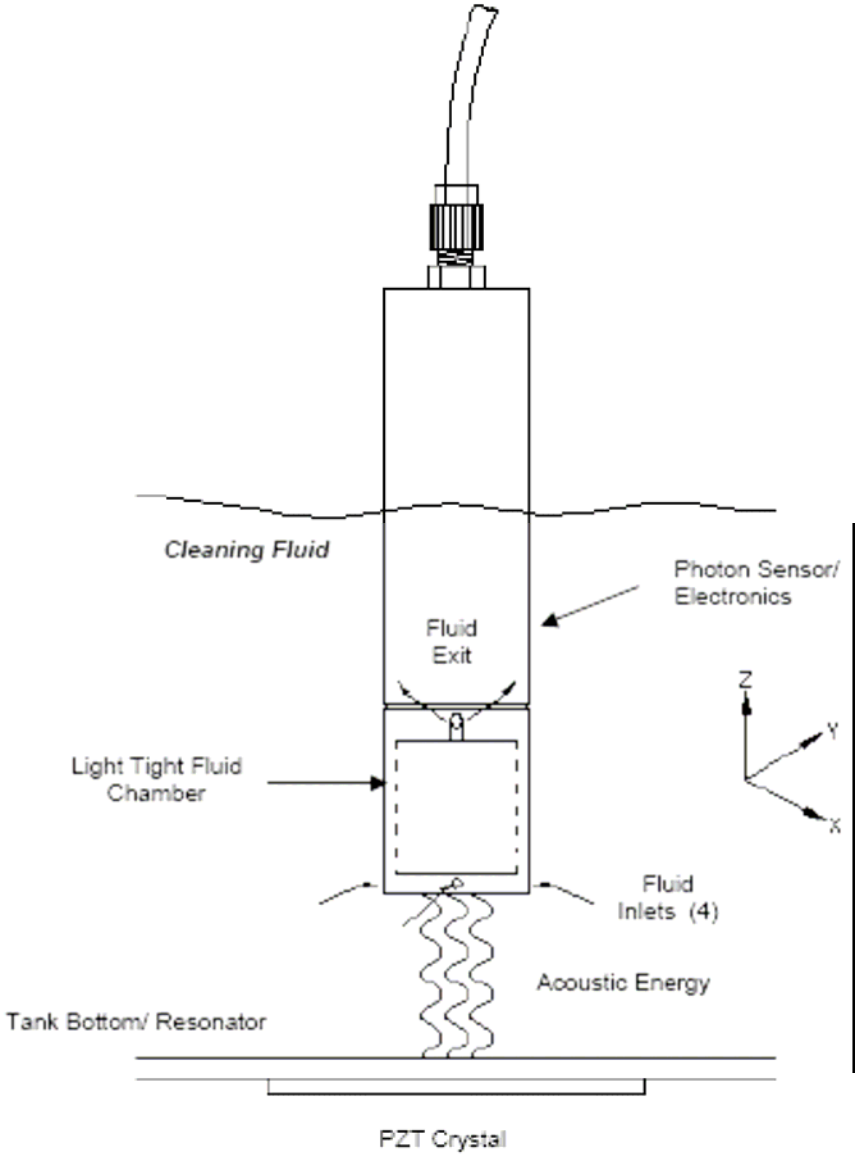

- Sonoluminescence measurements are carried out by a Cavitation probe from PROSYS Megasonics.
- It is a real time monitor for photon count generated due to acoustic cavitation.

Effect of Surface Tension on Cavitation

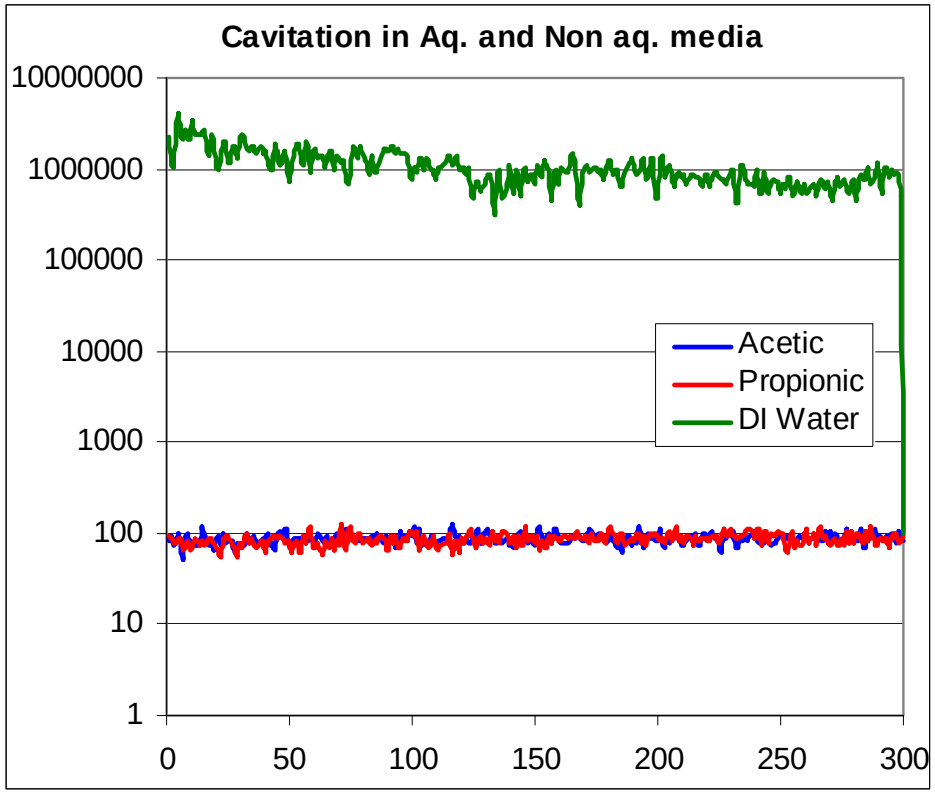

Power density : 2.17 W/cm^2

- In non- aqueous liquids of low surface tension, lower photon counts were measured
- Acetic acid and Propionic acid produced very low photon count compared to DI water at a power density of 2.17 W/cm^2.

Liquid	S. tension (mN/m)	Viscosity (centiPoise)
Propionic acid	25.8	1.03
Acetic acid	26.3	1.056
DI water	71.99	0.855

Cavitation in DI Water-Acetic system

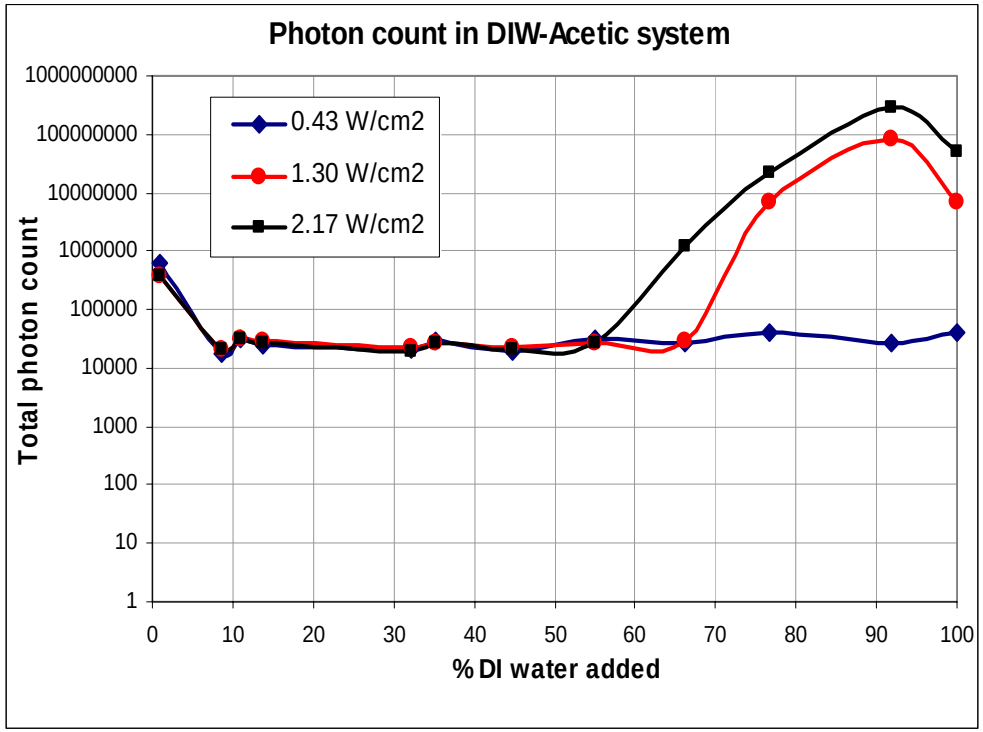

- DI water and Acetic acid have roughly the same viscosity, but different surface tensions.
- Surface tension of acetic acid solutions was altered by adding DI water.

- **No change in photon count was observed at low power density (0.43W/cm2), for different conc. of DIW.**
- **For higher power densities (1.3 & 2.17W/cm^2) photon count started increasing roughly after 55% DIW conc.**

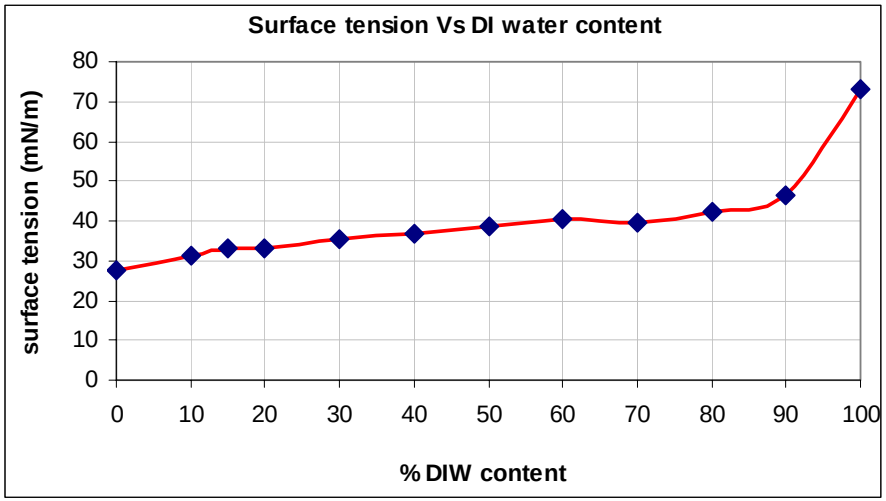

Effect of Viscosity on Cavitation

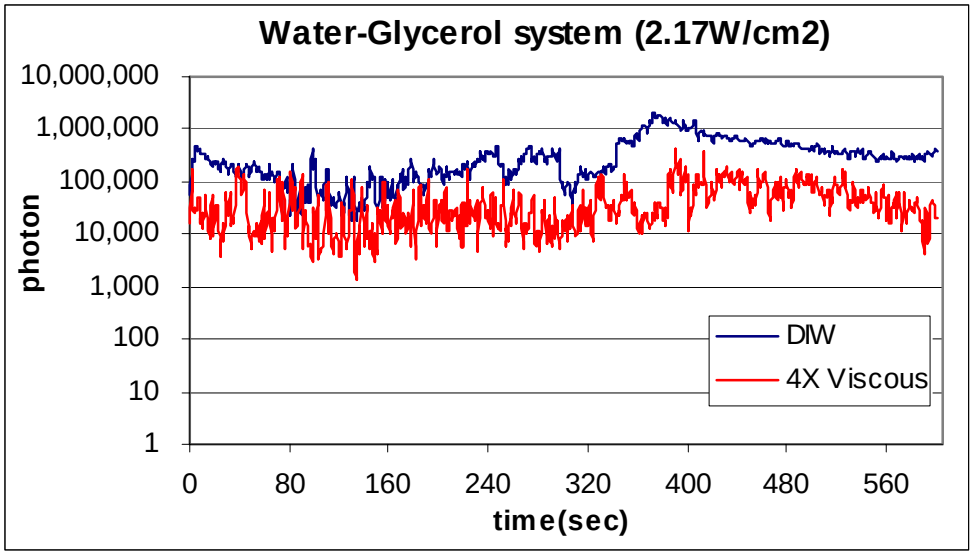

Liquid	S. tension (mN/m)	Viscosity (centiPoise)
DI water	71.99	0.855
Glycerol	62.5	945

Higher the viscosity, lower the photon count.

- Glycerol has ~same surface tension as DI water, but extremely high viscosity.
- The dynamic viscosity (μ) of DI Water- Glycerol is calculated by*,

$$\mu = (1 - X_b)\mu_a + X_b\mu_b + X_b(1 - X_b)[\mu_0 + \mu_1(1 - 2X_b) + \mu_2(1 - 2X_b)^2 + \mu_3(1 - 2X_b)^3 + ...]$$

*Y Marcus, Solvent Mixtures Properties and Selective Solvation, New York, Marcel Dekker, 2002.

Experiments with Test Structures

- Texas Instruments has provided poly-Si fin (SOI) test structures which contain fins of different length (10,20,50,100 μm) and width (50,55,65,80 nm).

- The test structures will be used for the study of pattern damage in different chemistries.

Future Work

- Identify the interrelation between photon count (Cavitation), particle removal efficiency and pattern damage through controlled contamination of bare wafers and test structures

Chemical Vapor Deposition: Direct Patterning and Selective Deposition Thrust D (Task 425.006)

Yu (Jessie) Mao, Hilton Pryce Lewis, Sal Baxamusa, and Karen Gleason
Department of Chemical Engineering, MIT

Nelson Felix, Victor Pham, Gina Weibel, and Chris Ober
Department of Material Science, Cornell

Opportunities for Thrust D

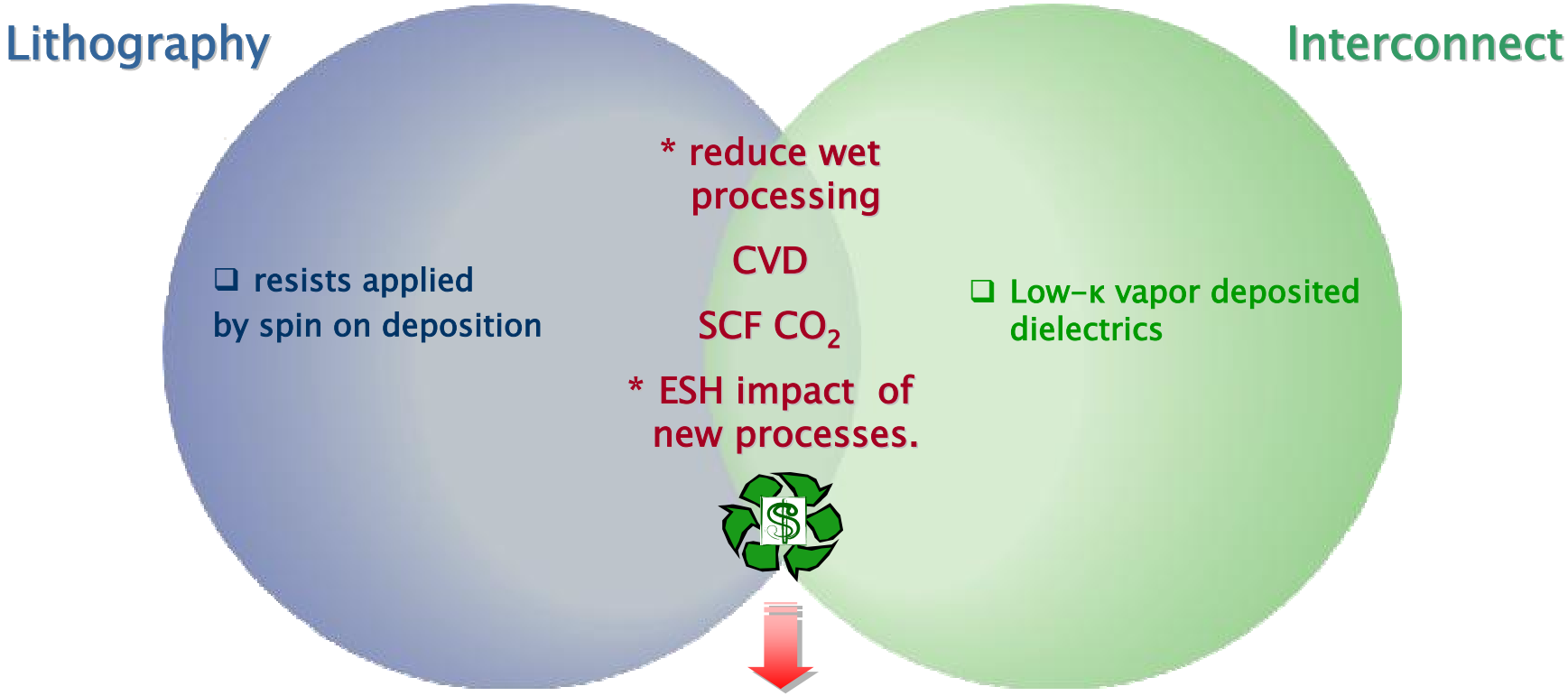

Goal: Superior Performance with Environmental Responsibility

Started October 1998 via extension funding from NSF

Proposed Evolution of Dielectric Patterning

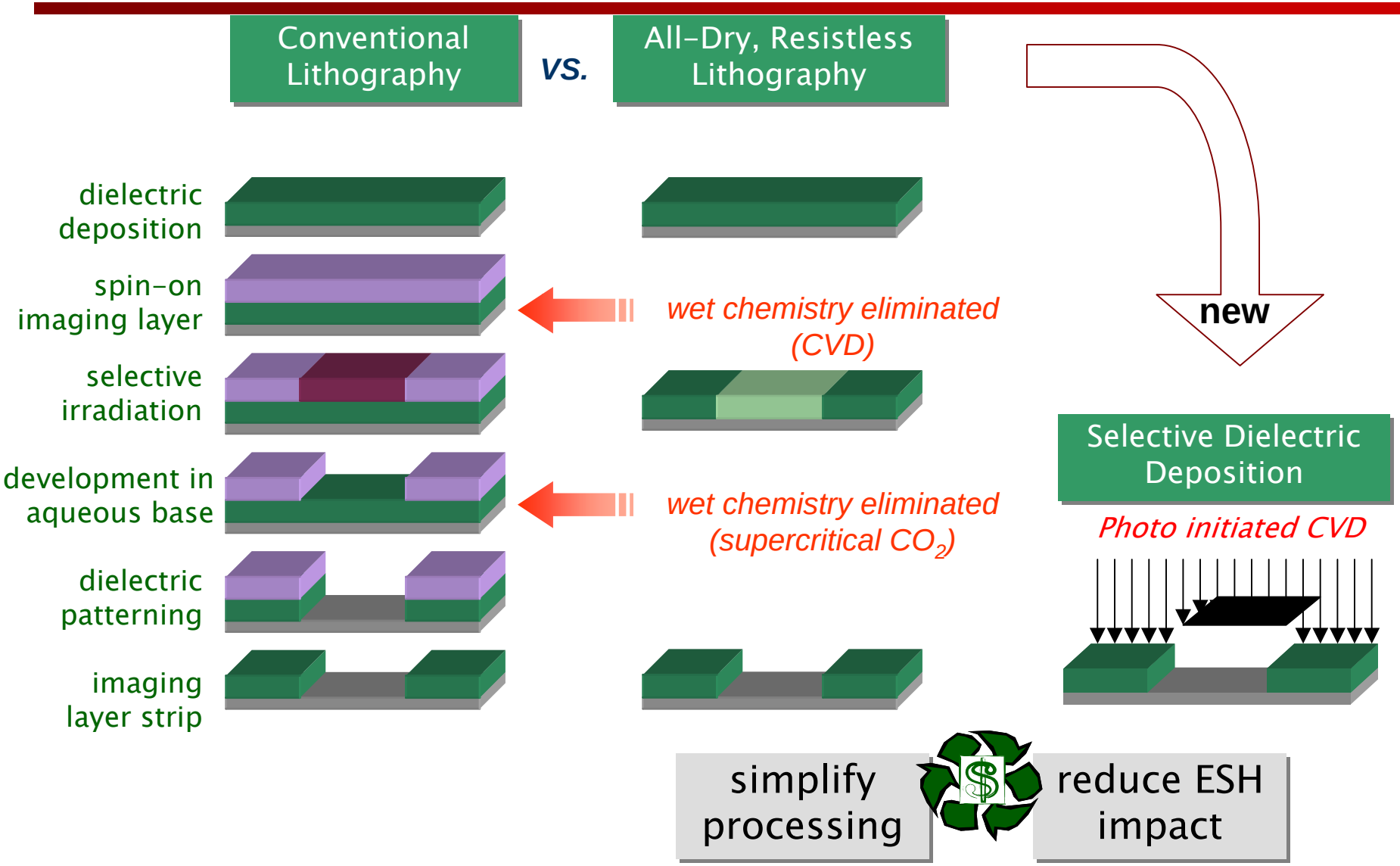

Progress in patterning of CVD Films

30 microns

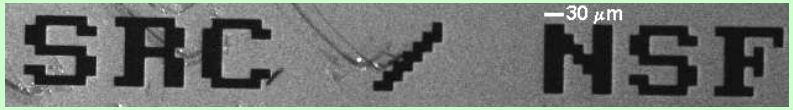

5 microns

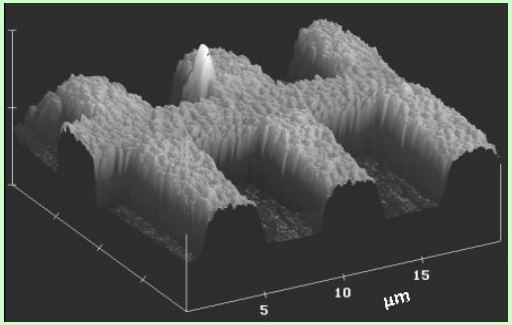

2 microns

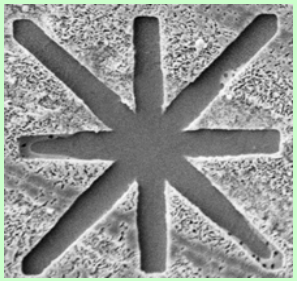

1 micron

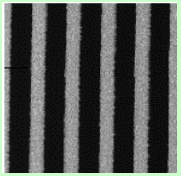

Low k dielectric films

Pryce Lewis HG, Weibel GL, Ober CK, and Gleason KK CVD 7, 195 (2001)

80 nm

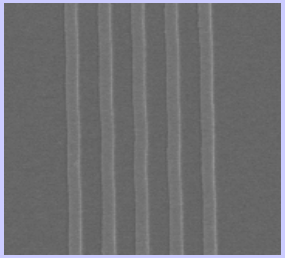

negative tone

60 nm

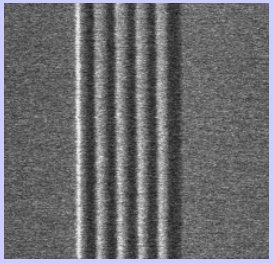

positive tone

iCVD photoresists

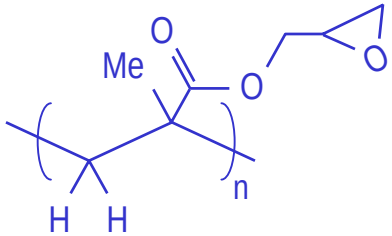

Mao Y, Felix NM, Nguyen PT, Ober CK and Gleason KK JVST B 22, 2473 (2004).

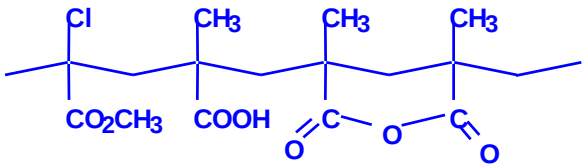

Mao Y and Gleason KK Langmuir (in press).

initiated CVD (iCVD)

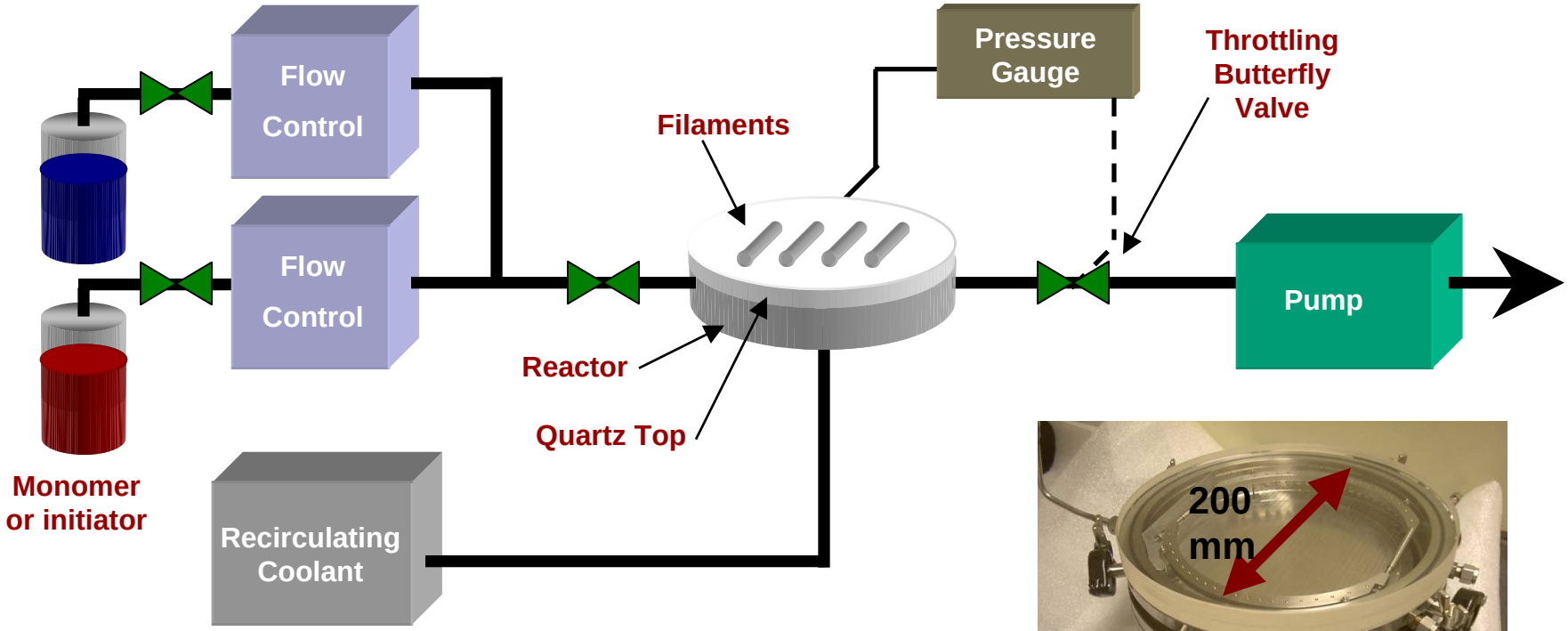

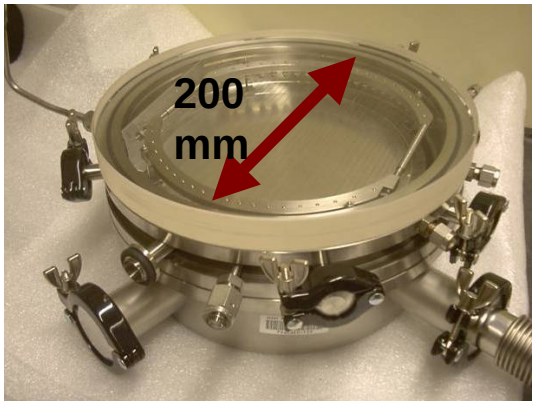

$$I\text{–}I \xrightarrow{\Delta} 2\,R^{\bullet} \quad \textit{initiation}$$

$$R^{\bullet} + n\,M \longrightarrow R\text{–}(M)_n^{\bullet} \quad \textit{propagation}$$

$$R\text{–}(M)_n^{\bullet} + R^{\bullet} \longrightarrow R\text{–}(M)_n\text{–}R \quad \textit{termination}$$

Polyacrylics by iCVD

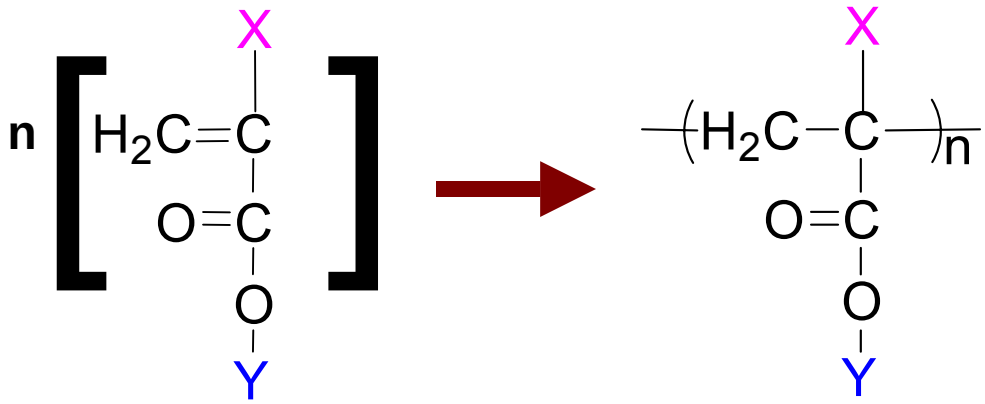

	X	Y	
crosslink under irradiation	$-CH_3$	$-CH_2-CH(O)-CH_2$	poly(glycidyl methacrylate) **PGMA**
chain scission under irradiation	$-Cl$	$-CH_3$	poly(methyl α-chloroacrylate) **PMCA**
	$-CH_3$	$-O-C(=O)-R$	poly(methacrylic anhydride) **PMAH**

iCVD P(MCA-MAA) Copolymer

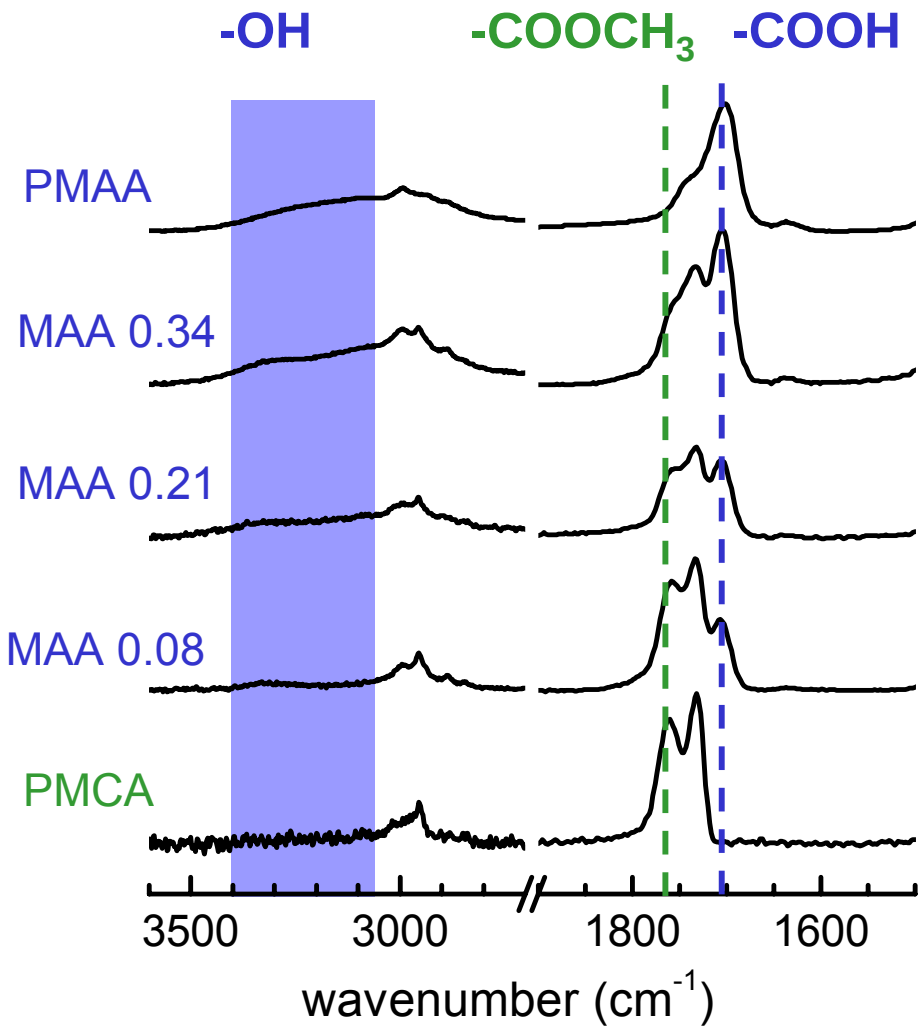

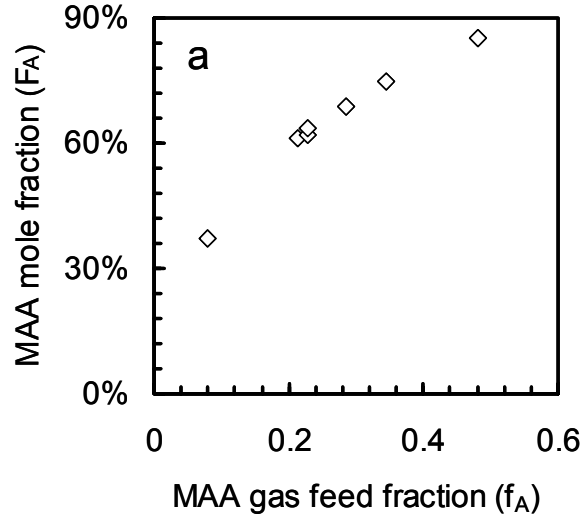

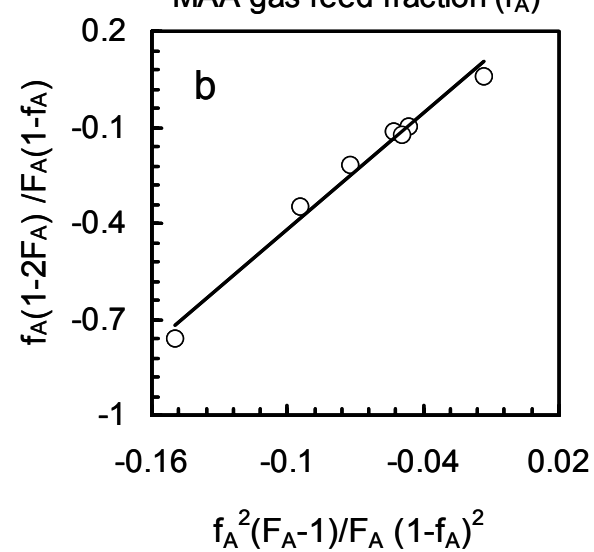

Control of MW and Sensitivity

P(MCA-MAA) iCVD copolymer thin films
with original MAA compositions
75-76 mol% (•) and 40-44 mol% (◊).

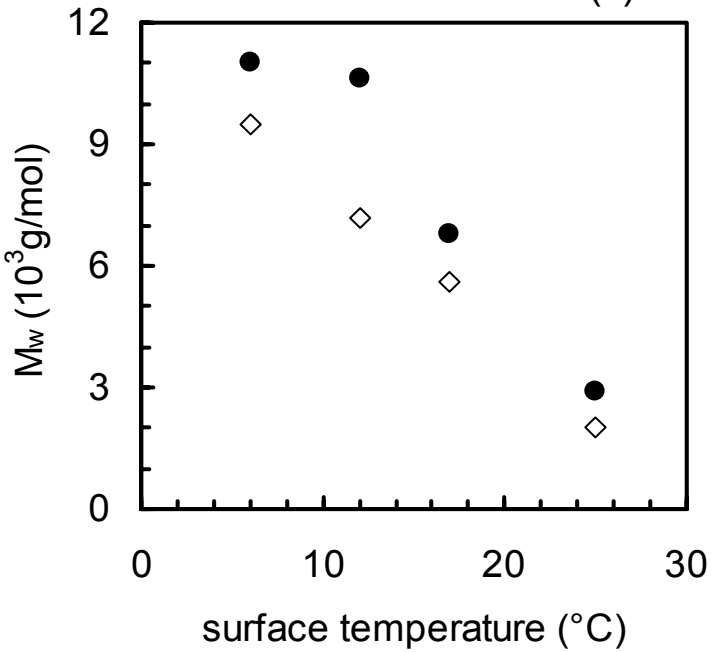

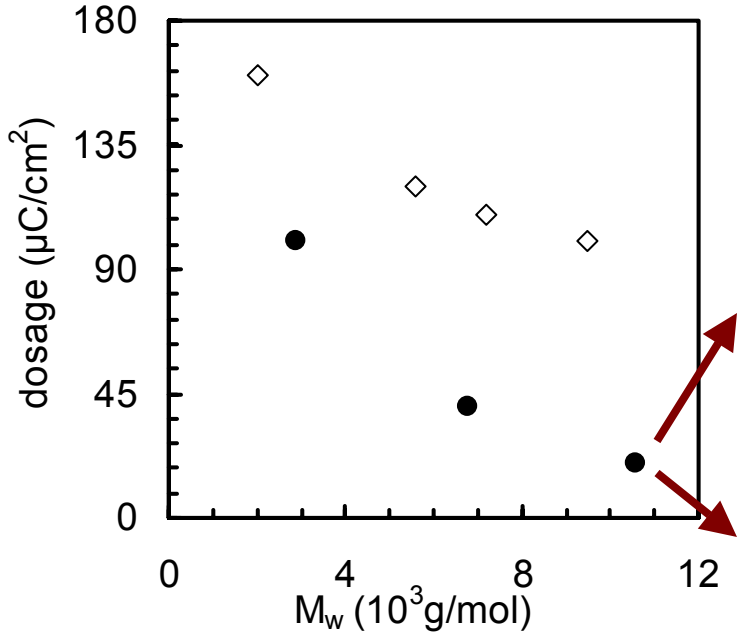

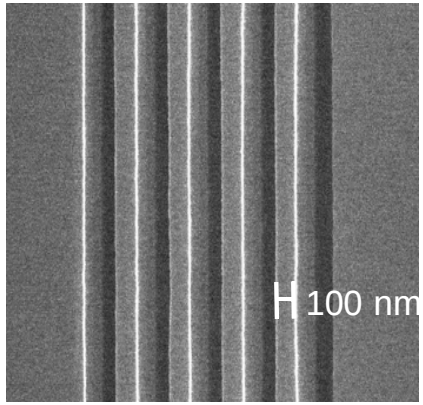

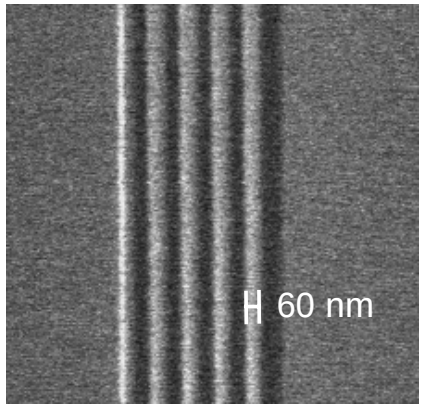

MW decreases with increasing surface temperature, indicating surface propagation.

Minimum dosage for complete removal of post annealed films decreases with MW and increase MAA fraction.

photo-initiated (piCVD) Reactor

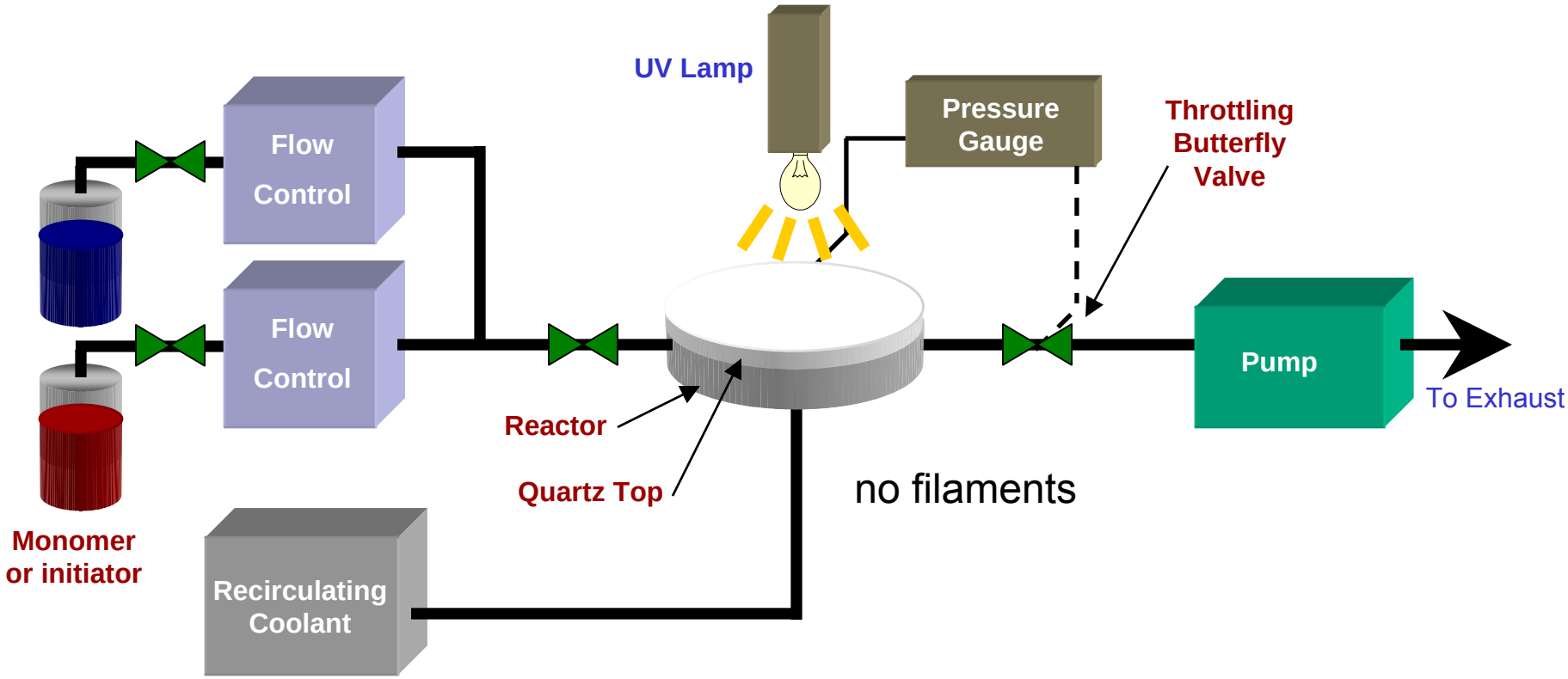

FTIR poly(glycidyl methacrylate) [PGMA]

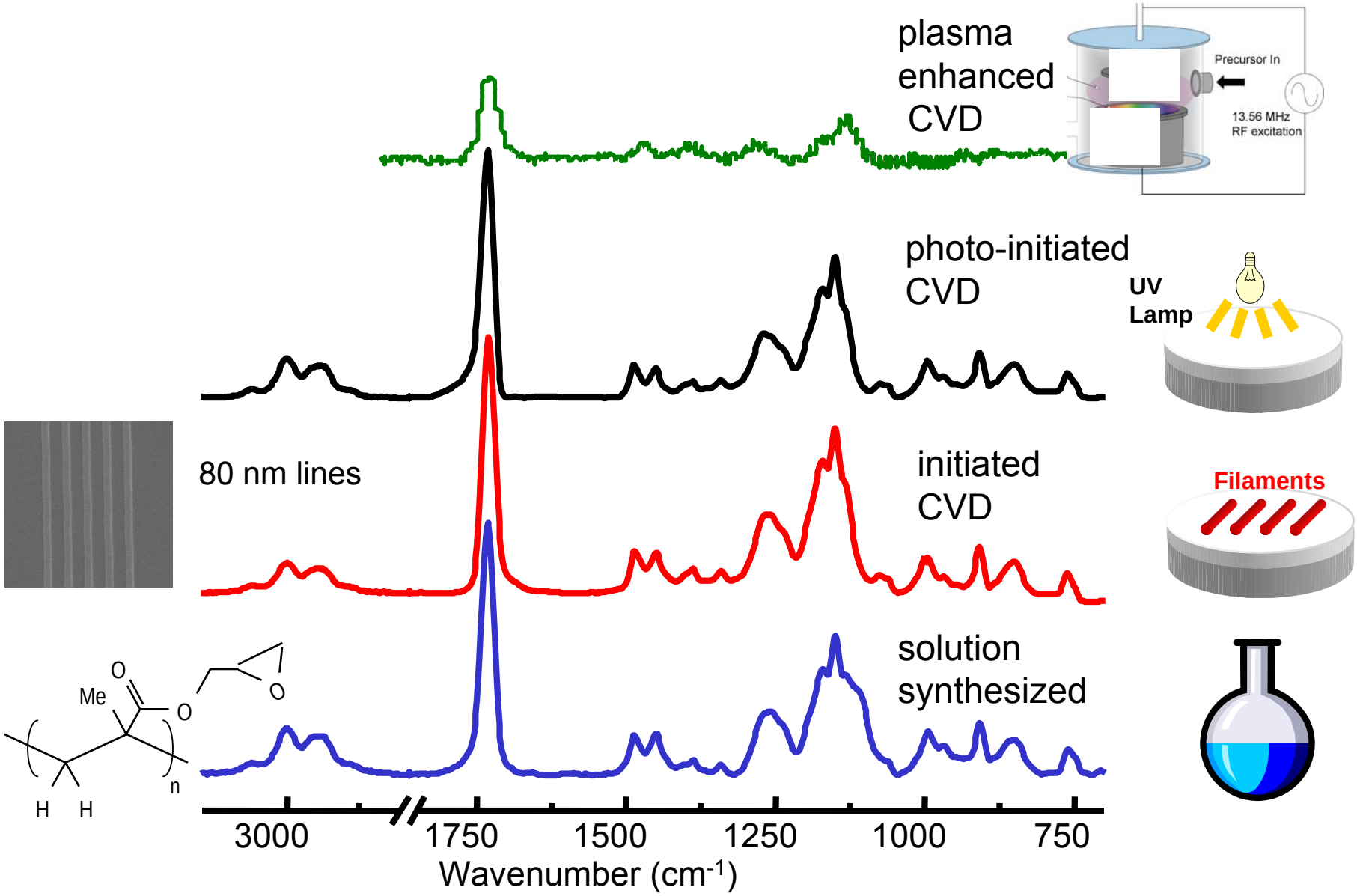

Photo-initiation

Type I (gas phase)

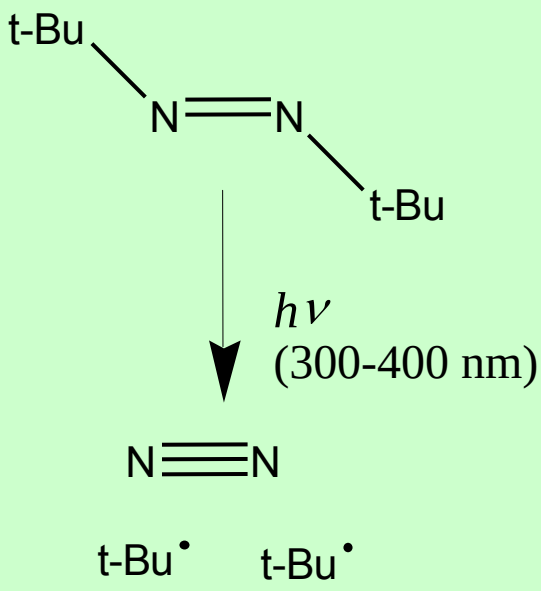

Type II (surface)

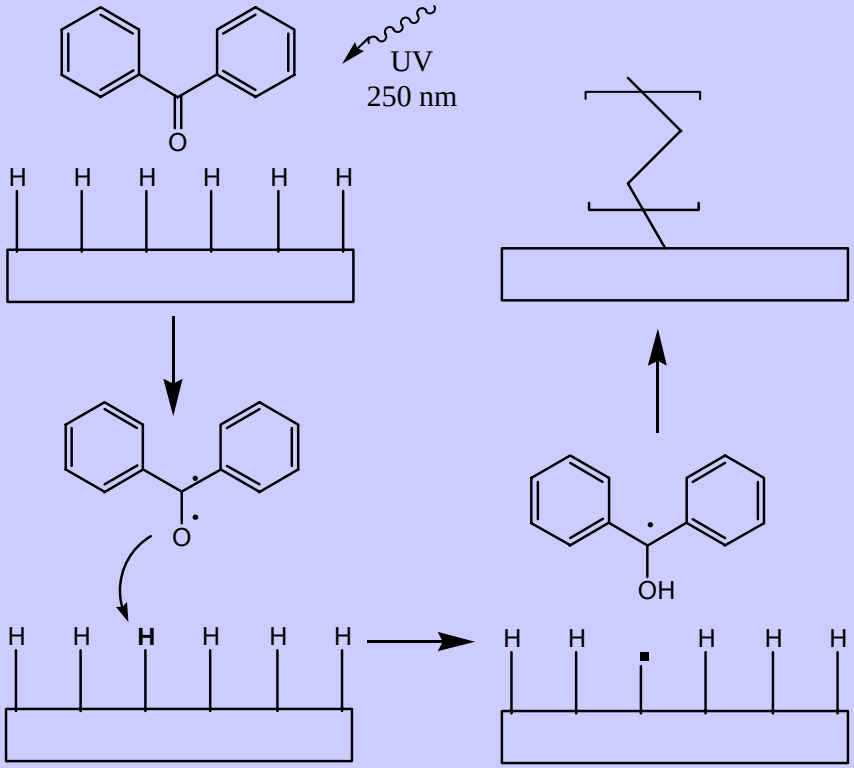

Preliminary Work: Selective Deposition by piCVD

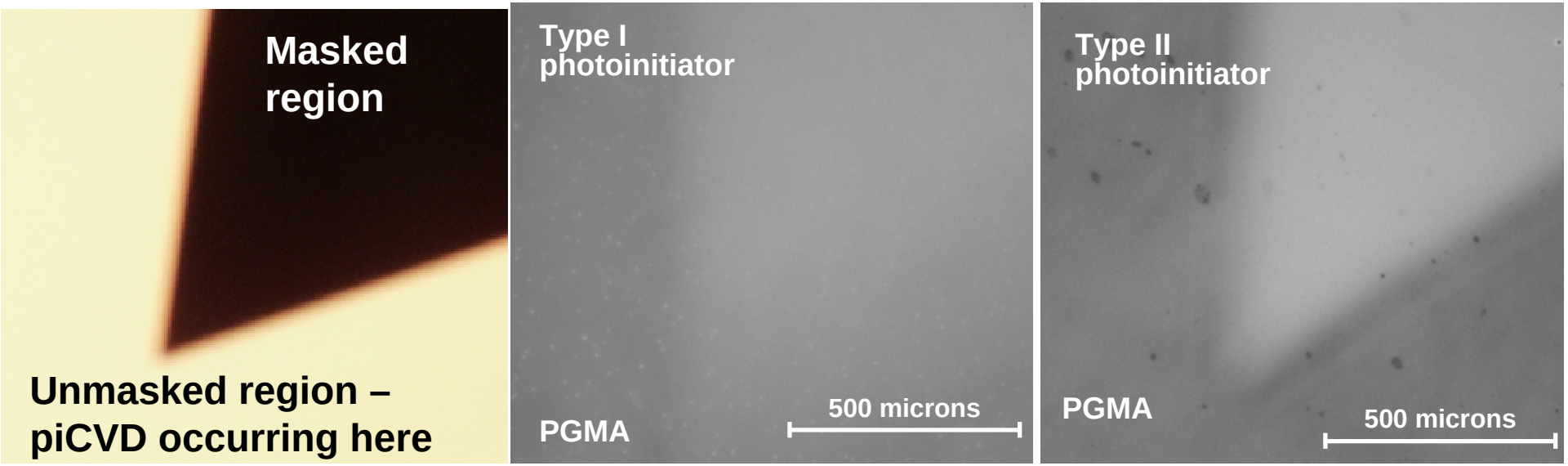

resolutions improvement expected with
•substrate preparation (H terminated wafers instead of PMMA films)
•exposure optics

future work: demonstrate selective piCVD of low k films from commercial precursors and molecular glass precursors synthesized in the Ober group

Solventless Lithography: Lithographic Processing Using Supercritical CO_2

Thrust D, Subtask D-1

Nelson Felix[1], Anthony Spizuoco[2], Yu (Jessie) Mao[3], Karen Gleason[3], James Watkins[4], and Christopher K. Ober[1]

[1]Department of Materials Science, Cornell University
[2]Department of Chemical Engineering, University of Massachusetts, Amherst
[3]Department of Chemical Engineering, Massachusetts Institute of Technology
[4]Polymer Science and Engineering Department, University of Massachusetts, Amherst

D-1 Project Objectives

Objectives:

- Identify key composition **parameters** for environmentally benign supercritical CO_2 development.
- Develop fundamental structure/property **relationships** for patternability and supercritical CO_2 solubility.
- **Optimize** SCF processing parameters for high resolution lithography.
- Investigate **new chemistries** for positive and negative tone e-beam and EUV dry resists developable in $scCO_2$.
- Reduce **ESH** impact by replacing wet chemistry.
- Improve resist and interfacial **quality** through all-dry processing.
- **Evaluate** environmentally benign cosolvents for device cleaning and process enhancement.

ESH Metrics

Metrics for Task
Supercritical Fluid CO2

I) Basis of Comparison:

Organic solvent developers.

II) Manufacturing Metrics:

(Effect on Performance, Yield, and Cost)

Using scCO2 in place of traditional developers can drastically reduce, or even eliminate, the amount of organic solvents that are spent. There are also savings in terms of operating cost associated with using scCO2 as opposed to traditional development methods.

	Usage Reduction			Emission Reduction			
Goals / Possibilities	**Energy**	**Water**	**Chemicals**	**PFCs**	**VOCs**	**HAPs**	**Other Hazardous Wastes**
Reduction of organic solvents used in developing photoresists and cleaning	N/A	Elimination of the need for water.	Up to 100% reduction of organic solvents.	N/A	Minimal use of organic co-solvents	Up to 100% reduction of HAPs.	N/A

Advantages of Supercritical CO_2 Development

Elimination of organic solvents and ultra-pure water during processing

2 gram DRAM chip → 32 kg of water

Williams, et al., *Environ. Sci. Tech.*, **36**, 5504, (2002).

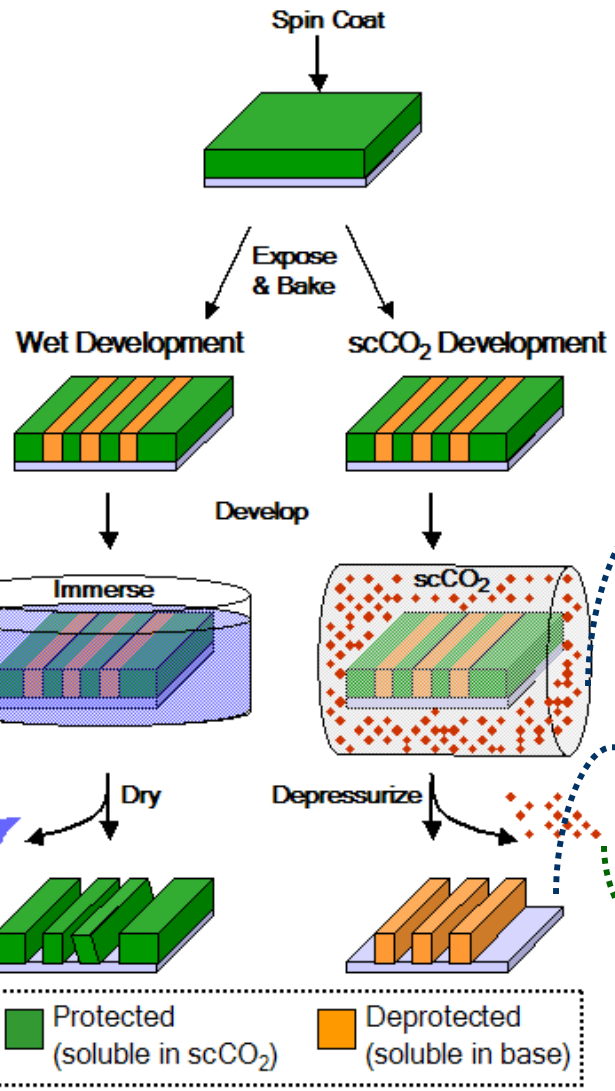

Liquid-like density, Tunable Solvating Power

Gas-like transport

Penetrates crevices, no residue

Harmful solvents are cleanly separated via depressurization

No surface tension, eliminates pattern collapse

Next Generation Lithography: Key Problems

Pattern Variations

< 3nm for 32nm node

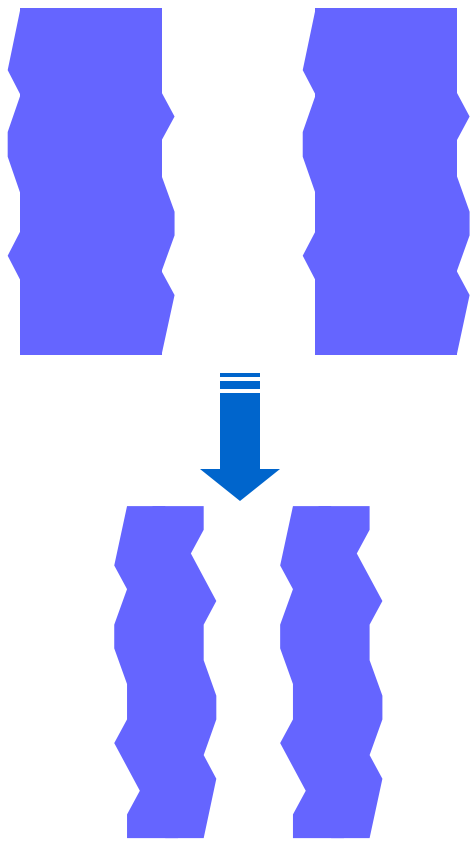

Pattern Collapse

Reduce surface tension

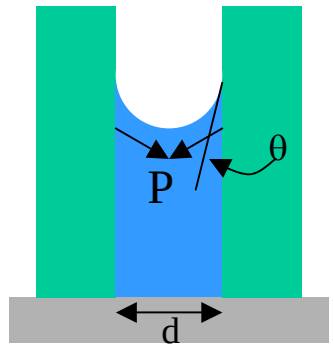

$$P = \frac{\sigma}{R} = \frac{2\sigma\cos\theta}{d}$$

@ 50nm L/S, aspect ratios >2:1 collapse w/water

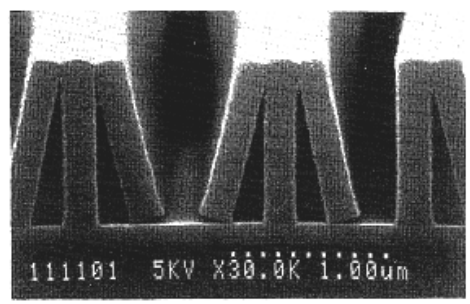

T. Tanaka, M. Morigami, N. Atoda, *JJAP*, **32**(pt1, 12B) 6059 (1993).

Non-polar Materials

Low-κ applications

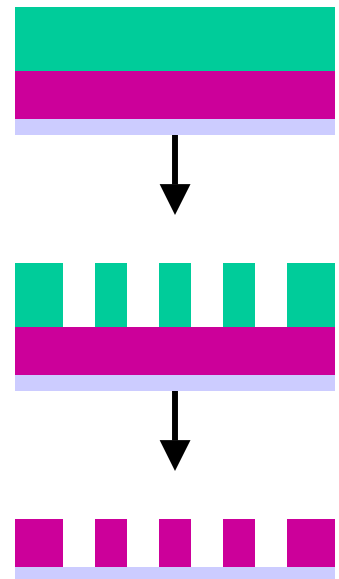

Lack of appropriate non-polar developers → Must use mulitple subtractive steps

Molecular Glasses and $scCO_2$

- Due to their small size, molecular glass resists of all types have **potential for CO_2 solubility…no fluorine needed**!
  - Nonpolar molecules with aromatic rings are most soluble
  - Crosslinking chemistries offer better contrasts, processing windows
- Example:

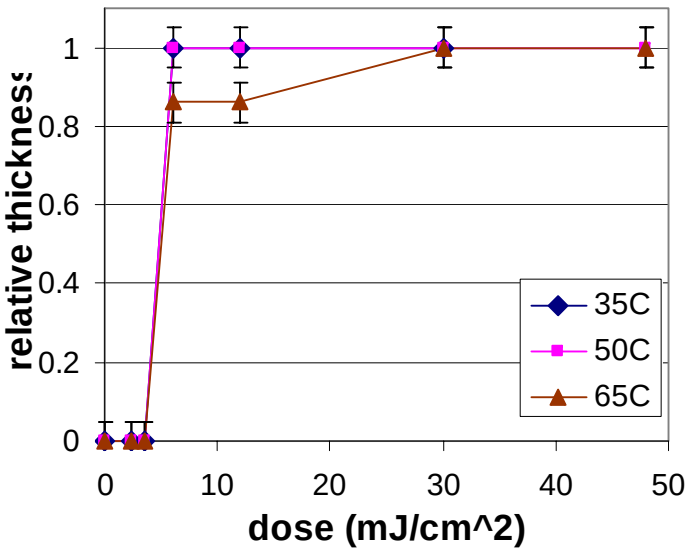

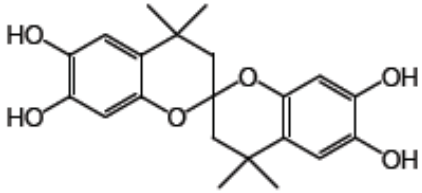

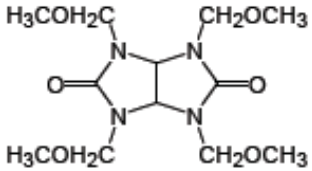

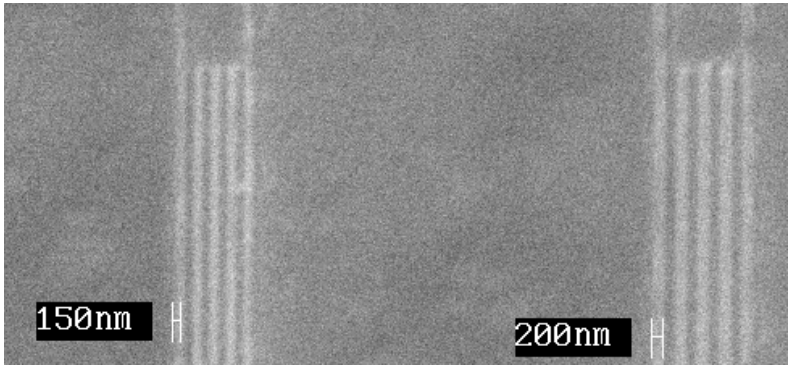

Developed at 50C, 300 bar

Dissolution Rate Monitor

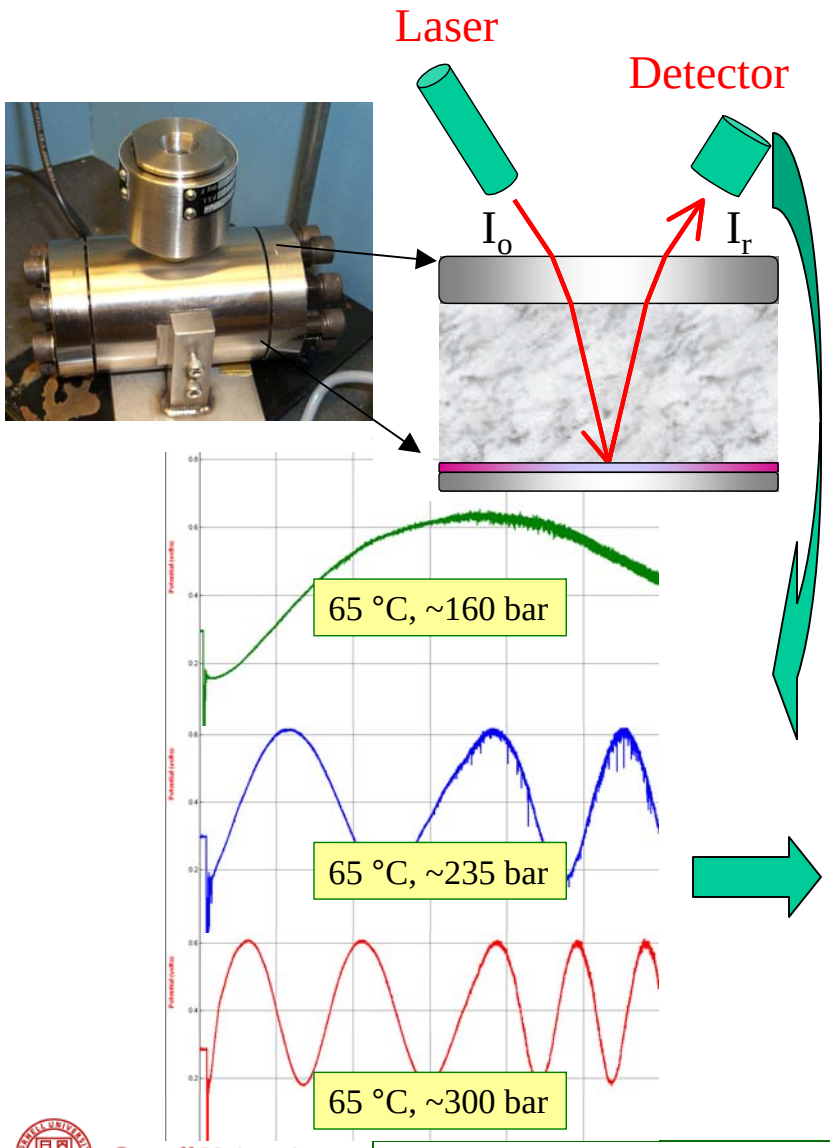

- Using interferometry to probe dissolution rate of thin resist film
- Use data to calculate necessary residence time for development

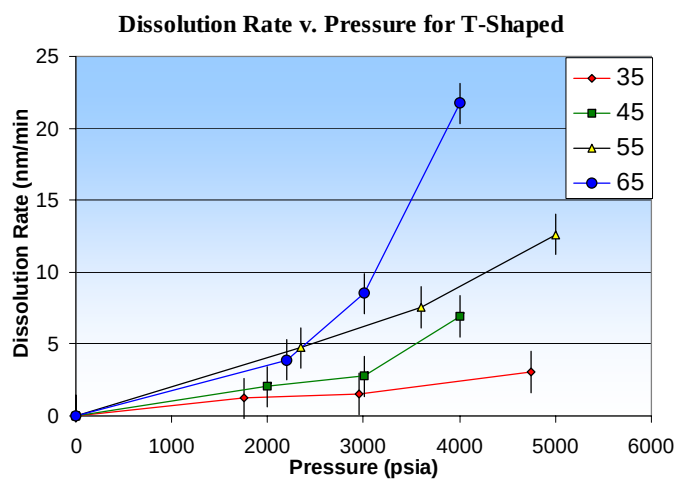

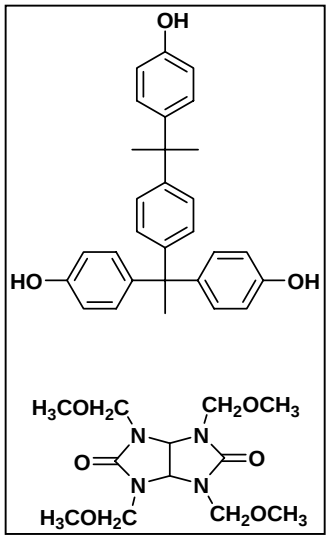

Positive Tone Molecular Glass Resists for $scCO_2$ Development

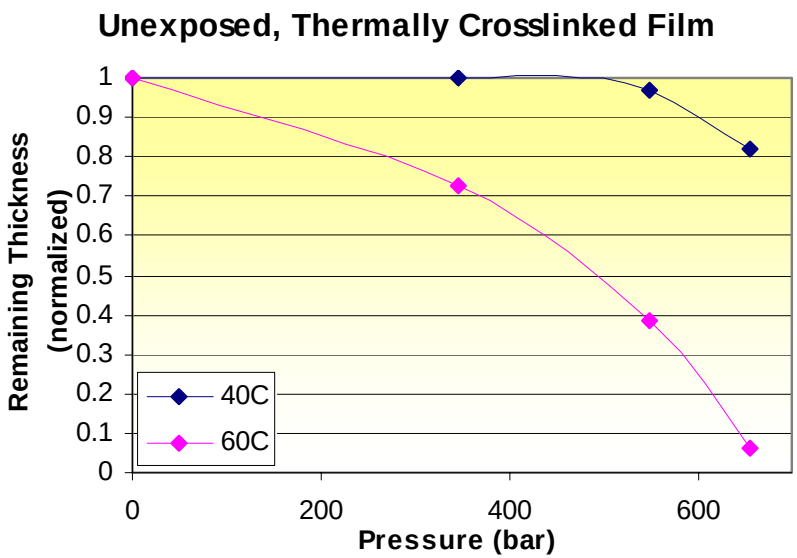

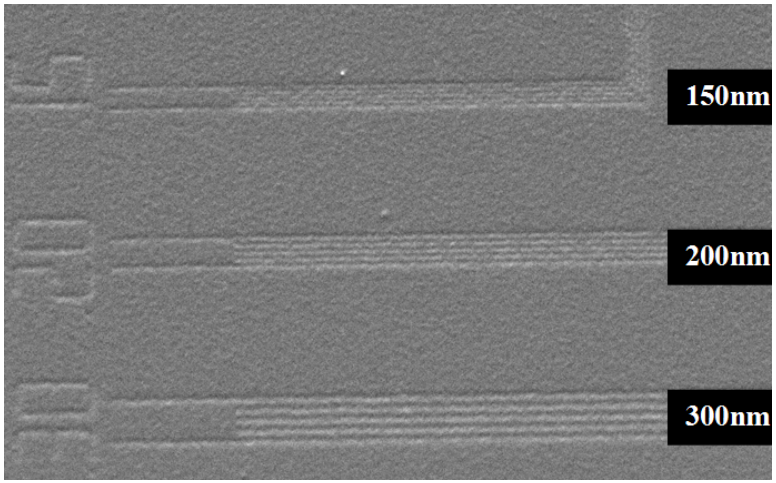

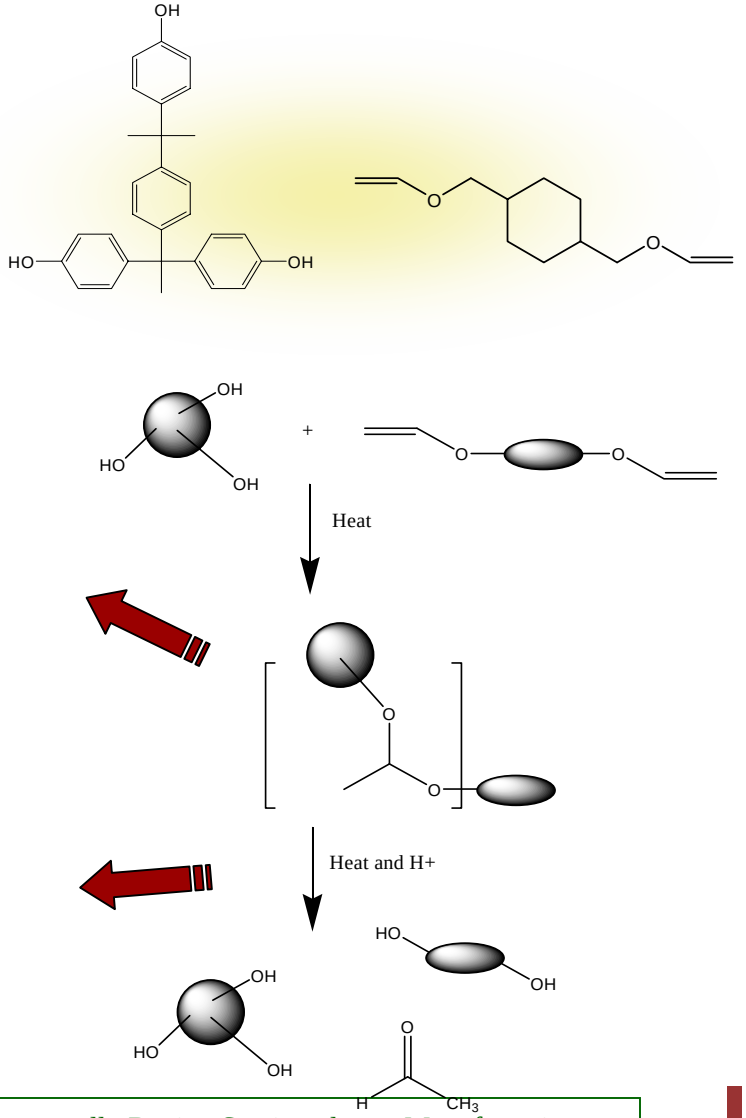

Manuscript under preparation

Molecular Glass Resists for CO_2 Solubility

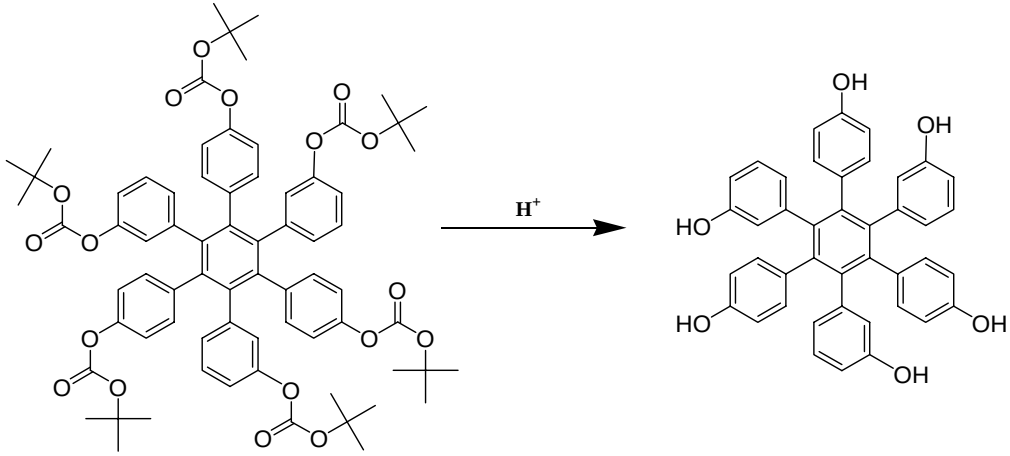

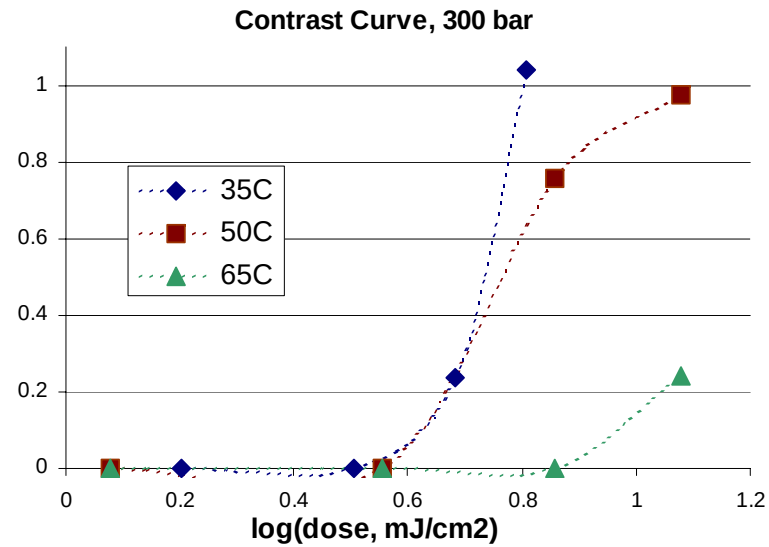

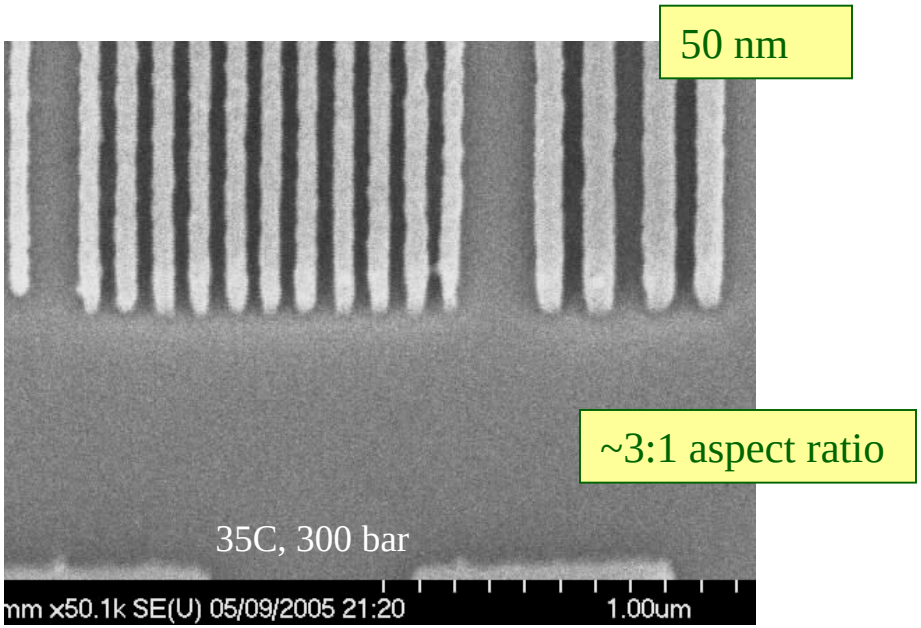

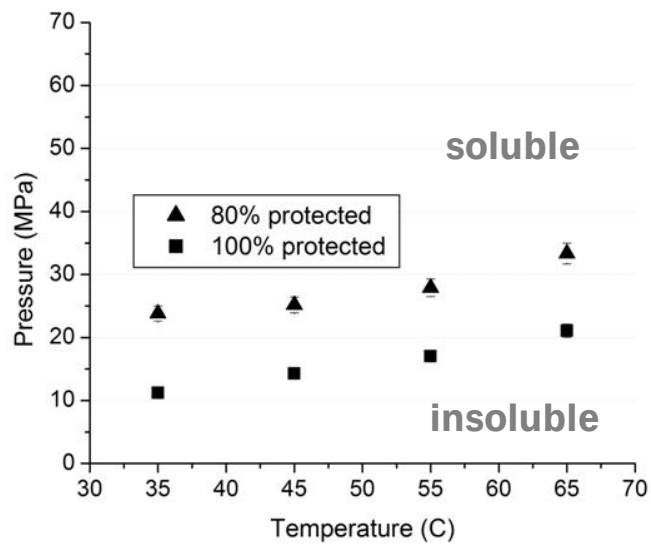

Advanced Materials, **18**(4), 442, (2006).

Future Projects

- Use film-forming precursors based on molecular glass photoresists
  - Comprised of structures similar to current C- and Si-based low-κ materials
- Use $scCO_2$ to develop features and remove sacrificial porogens

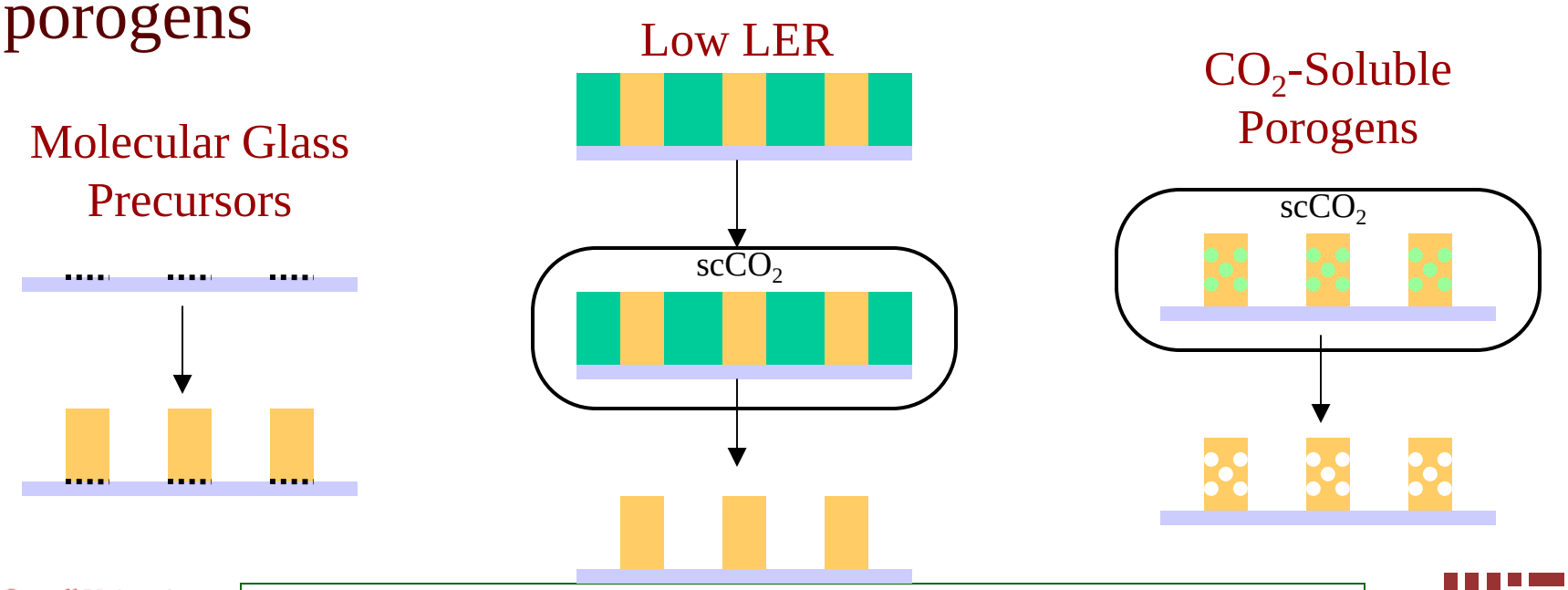

SCF Routes to ULKs and Directly Patterned Dielectrics

ULK Optimization:
2 nm Pores Using Stabilized Template Blends

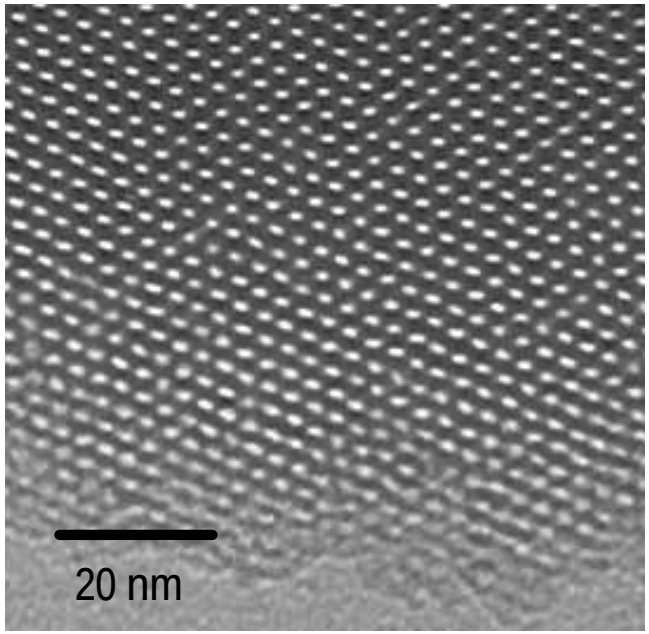

Direct Patterning:
Proof of Concept using Optical Lithography

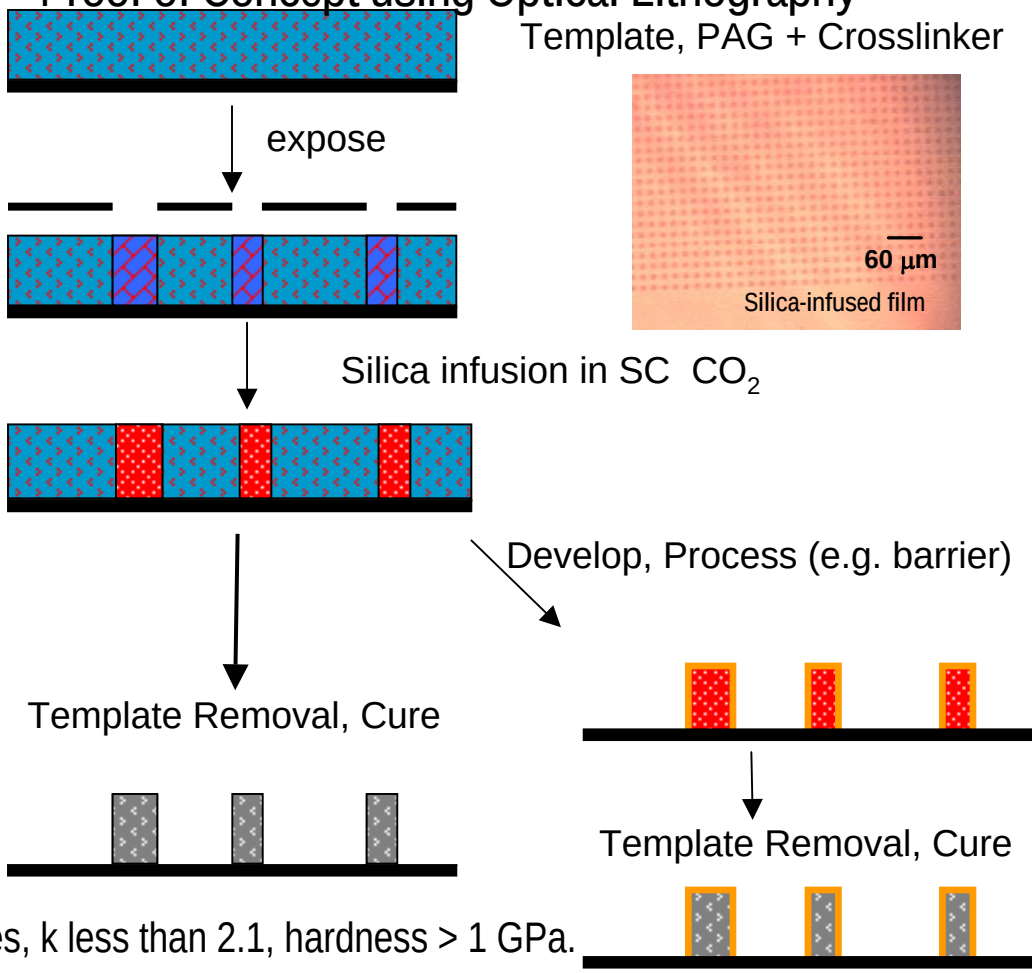

Yr 1. ULK Optimization: Target: Robust film, 2 nm pores, k less than 2.1, hardness > 1 GPa.

Yr 2. Direct Patterning: First Target: Homopolymer template, 20-30% microporosity (micropores< 1 nm)
Second Target: Block copolymer template, 40% porosity, micropores + mesopores (2-3 nm)
Pattering: Nanoimprint or optical

Conclusions / Acknowledgements

- A green process can also be made industrially attractive by optimizing materials and conditions.
  - New materials
  - Inherent performance advantages
- Impressive synergy between molecular resists and $scCO_2$ development.

- Cornell Nanofabrication Facility (CNF)
- Cornell Center for Materials Research (CCMR)
- Semiconductor Research Corporation (SRC)
- IBM; Heidi Cao / Intel; Will Conley / Freescale
- Ober Group members
  - Kosuke Tsuchiya, Camille Luk, Anuja De Silva
  - Dr. Seung Wook Chang, Dr. Da Yang, Dr. Dan Bratton

Solubility of chlorosilanes in $scCO_2$ for the repairing of low-k films

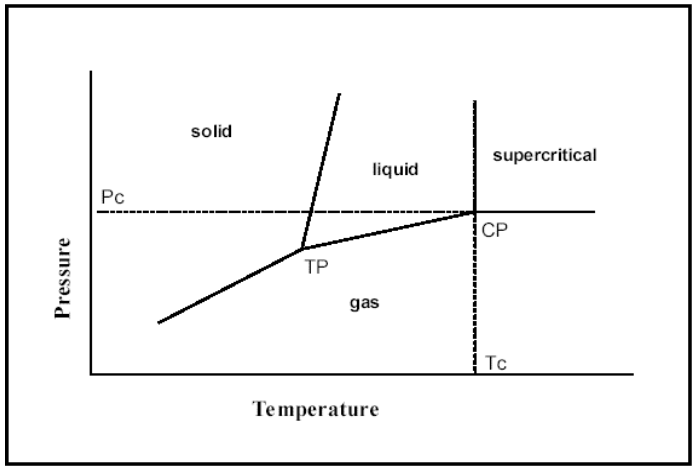

Eduardo Vyhmeister

Advisors: Anthony Muscat[†]. Antonio Estévez[*] and David Suleiman*.

(† Chemical & Environmental Engineering, University of Arizona. * Chemical Engineering. University of Puerto Rico, Mayagüez campus.)

Eduardov@email.arizona.edu

Department of Chemical & Environmental Engineering

University of Arizona, Tucson, AZ 85721

NSF/SRC Engineering Research Center for Environmentally Benign Semiconductor Manufacturing

Introduction

- High performance semiconductor devices require lower power consumption, resistance and capacitance (RC delay) while diminishing cross talk. The introduction of low-*k* films reduces the capacitance of interconnection (figure 1). The incorporation of non polarizable component can reduce even more the *k* value of these films. Air, in the form of pores, is introduced to produce this effect but it add more complexity for it's integration.

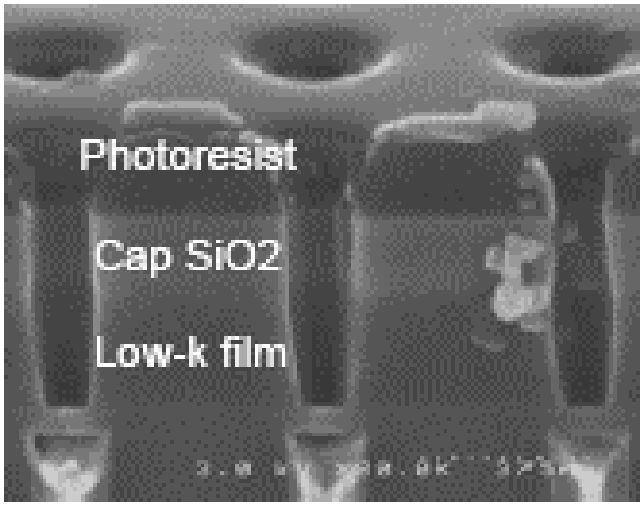

Figure 1, M. B. Korzenski, and T. H. Baum, Chemical Formulations for Stripping Post-Etch Photoresists on a Low-k Film in Supercritical Carbon Dioxide

Introduction

Porous materials are damaged during the pattering (etching and ashing) and the *k* value is increased. Various approaches have been proposed to avoid, protect or repair the films.

The use of chlorosilanes to repair the damaged pores can generate a protective layer to prevent future damage, previous studies have showed the thickness of this protective layers in function of the chemical compound used (figure 7).

Due to enhanced transport properties, low surface tension and solvating power solvents such as scCO2 may find use processing porous materials with features below 50 nm.

The concentration of chemical additives may affect the thickness of the capping layer, an important aspect for the integration of this technology.

ESH Impact and Metrics

- Basis of Comparison
  - Current best technology: organic solvents such as methanol or inorganic acids for backend cleaning

- Manufacturing Metrics
  - Eliminate aqueous cleans and subsequent rinses, reducing consumption of co-solvents and ultra-pure water.
  - Reduce volume of aqueous water requiring treatment
  - Requires recovery and treatment of co-solvent products
  - Reduces worker exposure to vapors
  - Saves energy with ultra-pure water reductions
  - Non-aqueous cleaning techniques more compatible with vacuum processing, encouraging development of a tool to serve multiple functions

	Usage Reduction			Emission Reduction			
Goals / Possibilities	Energy	Water	Chemicals	PFCs	VOCs	HAPs	Other Hazardous Wastes
Backend liquid phase chemistry and drying.	>50%	100%	Replace n-methyl pyrrolidone .	undeterm-ined.	Must capture and treat co-solvents.	CO_2 is non-hazardous. MeOH is on HAPs list.	100% reduction in liquid waste.

Objectives

- Measure solubility and critical point of mixtures of chlorosilane (MTCS, DMDCS and TMCS) dissolved in scCO2 to determinate the optimal temperature and pressure for the repair of damaged low-k films.

- Generate new data for the seldom studied interaction between supercritical fluids and liquid additives.

- Through the knowledge of solubility at different temperatures and pressures, attempt to control thickness of chlorosilanes capping

- Study by in-situ FTIR the chemical reaction of chlorosilanes and water on the surface and pores of damaged low-k films.

Equipment and system setup

- Solubility cell (stainless steel cylinder with sapphire window) and batch reactor (extraction chamber closed to the ambient for 3 hours to reach equilibrium between compounds and CO_2, figure 4) have been used to obtain information on solubility and phase equilibrium.

- Chlorosilanes are corrosive, toxic and volatile compounds.

- A heating blanket and thermocouples were used to control the temperature to ±0.1 ºC in the solubility cell. A syringe pump was used to deliver the CO_2 inside both chambers within the cylinder and control the pressure during experimentation (figure 2). A piston separated the chambers allowing a constant concentration on the front side.

Solubility cell

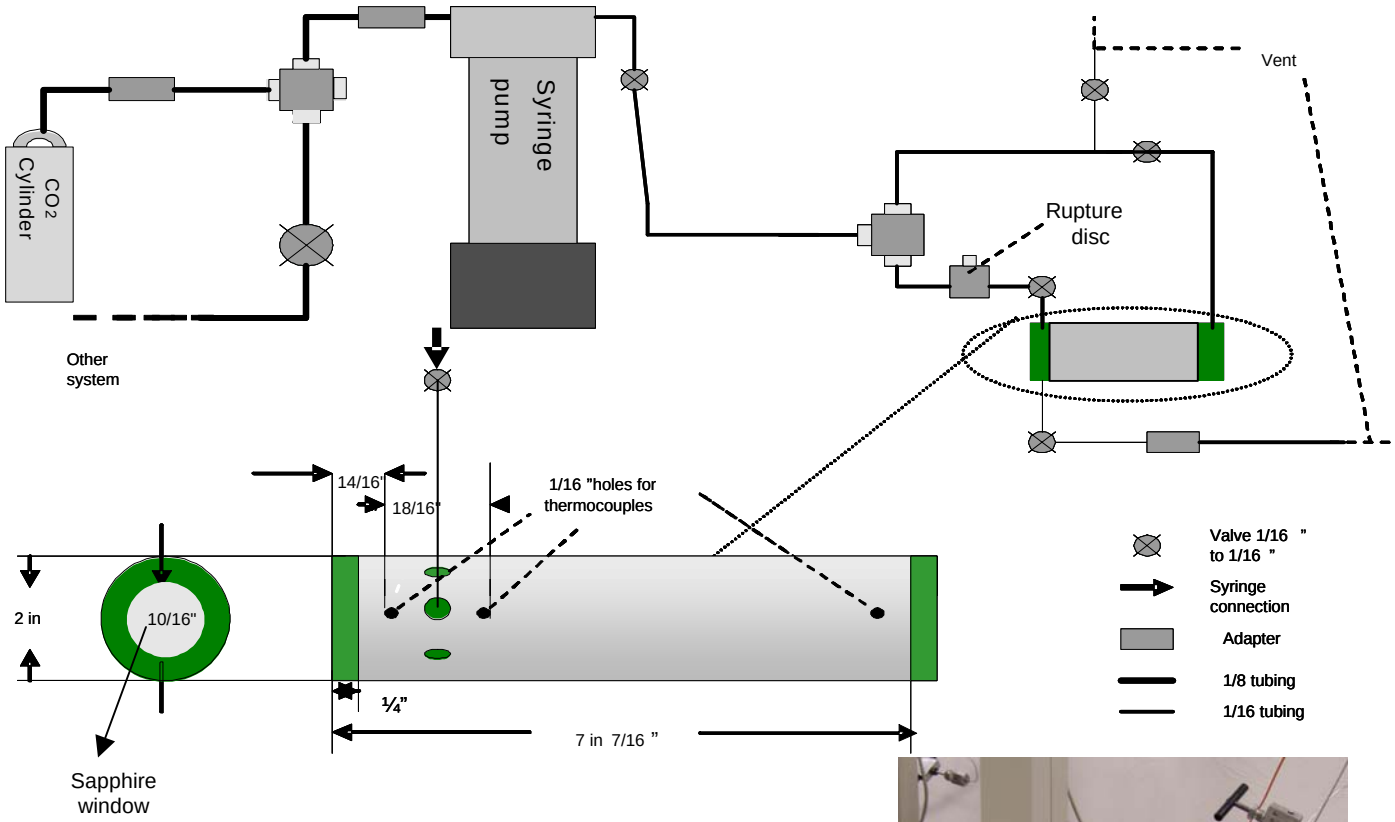

Figure 2 solubility cell configuration.

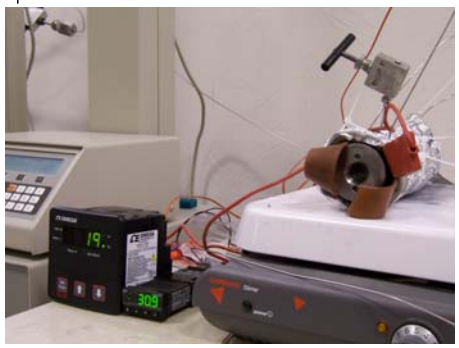

Validation of the solubility cell

Found the C.P. of pure CO2

- Solubility of Naphthalene at a given molar fraction at 36 ºC,120mg producing an error of ~2 bar.

	Critical point found	Critical point of CO_2
Temperature (°C)	30.9 – 32.0	31.1
Pressure (bar)	74.4 – 76.1	73.8

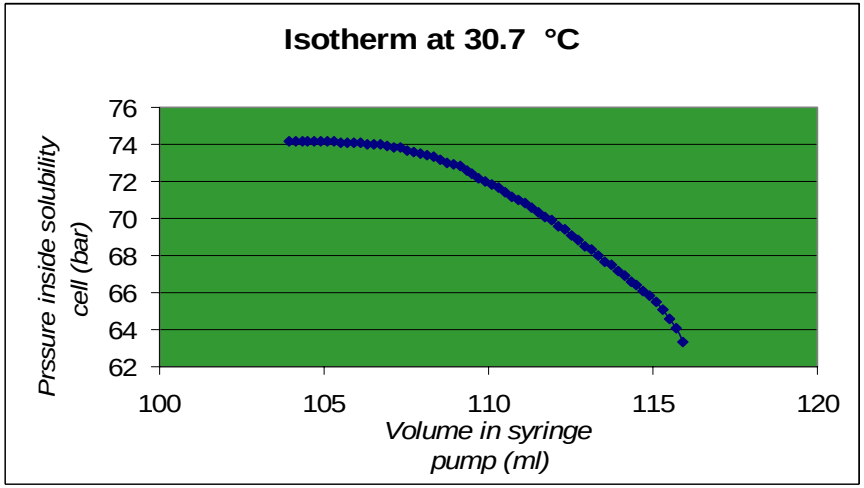

Figure 3 representation of the variation of volume in pump related to the variation in pressure inside the solubility cell at 30.7 °C .

Results

- Due to lack of stirring, lack of knowledge of the diffusion rate and uncontrolled depressurization in the extraction chamber, the results obtained in this system can be viewed as preliminary data of the molecular interaction of these compounds with supercritical CO_2 (figure 4).

- The information gathered in the solubility cell shows the phase equilibrium at high pressures. It represents the mixture's critical point (red dots) and the pressures and temperatures in which at a given concentration the mixture reaches only 1 phase (liquid). (figure 5).

- By finding the mixture's critical point, it is possible to perform a more profound analysis of the chemical reaction than in previous research. Figure 6 shows the time needed to reach and go over the critical temperature of the mixture, in that way the time of reaction can be estimated at supercritical conditions (~7 min). Moreover, a higher control over the thickness of the growing layer could be obtained (figure 7).

Transpiration Technique

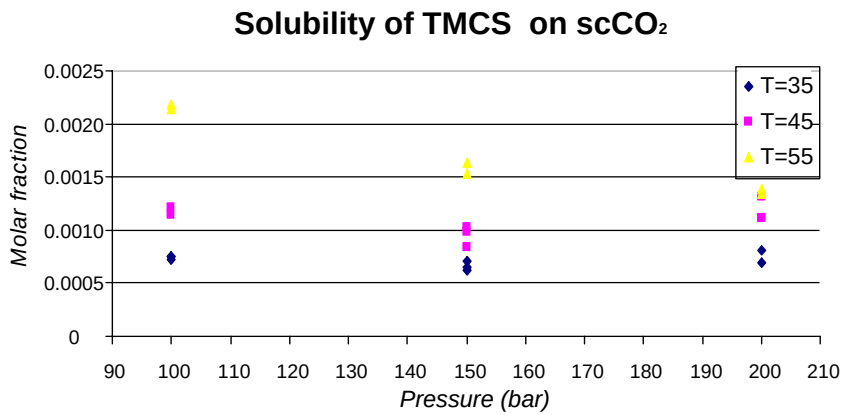

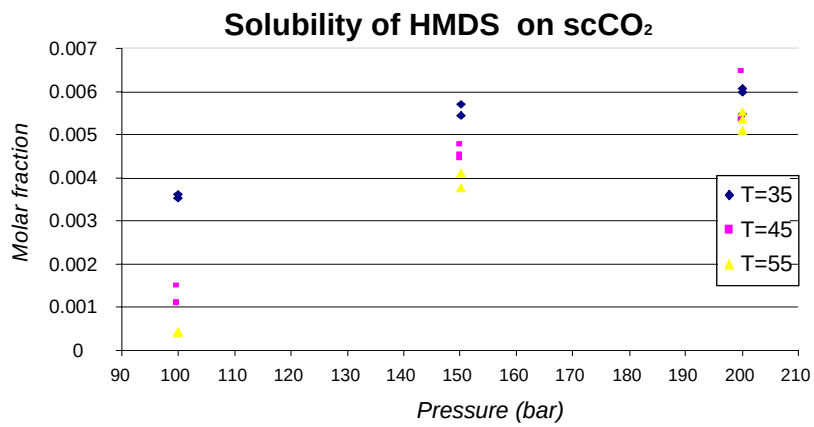

Figure 4, Solubility in scCO2 of HMDS and TMCS by the use of a extraction chamber and allowing equilibrium of 3 hours. Solubility was found by weight differences of previous and final results. Precision is not necessarily accurate because during weighting , contact with air was impossible to be avoided.

Solubility of MTCS and DMDCS in $scCO_2$

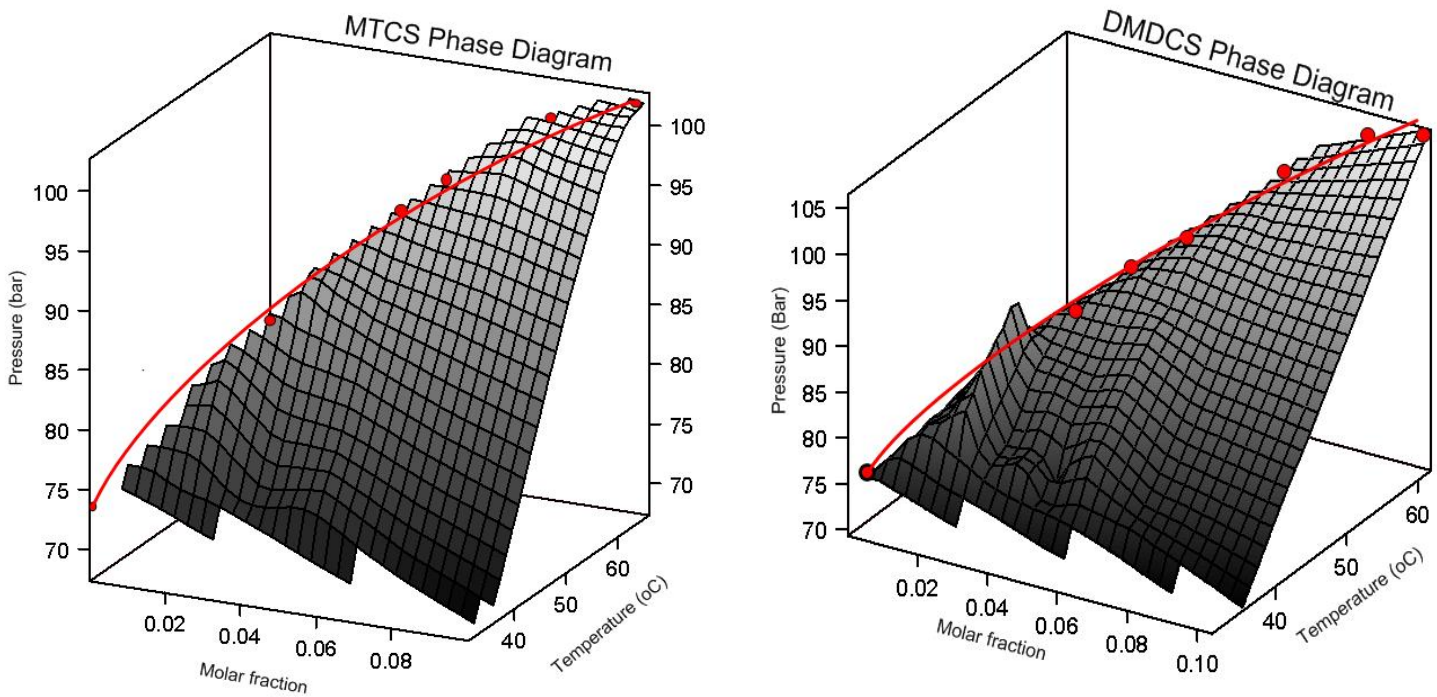

Figure 5 Phase diagram found for MTCS and DMDCS . Red points represent the measured critical point. the shaded surfaces show the phase boundaries between liquid and gas.

Effect of the study in low-k research

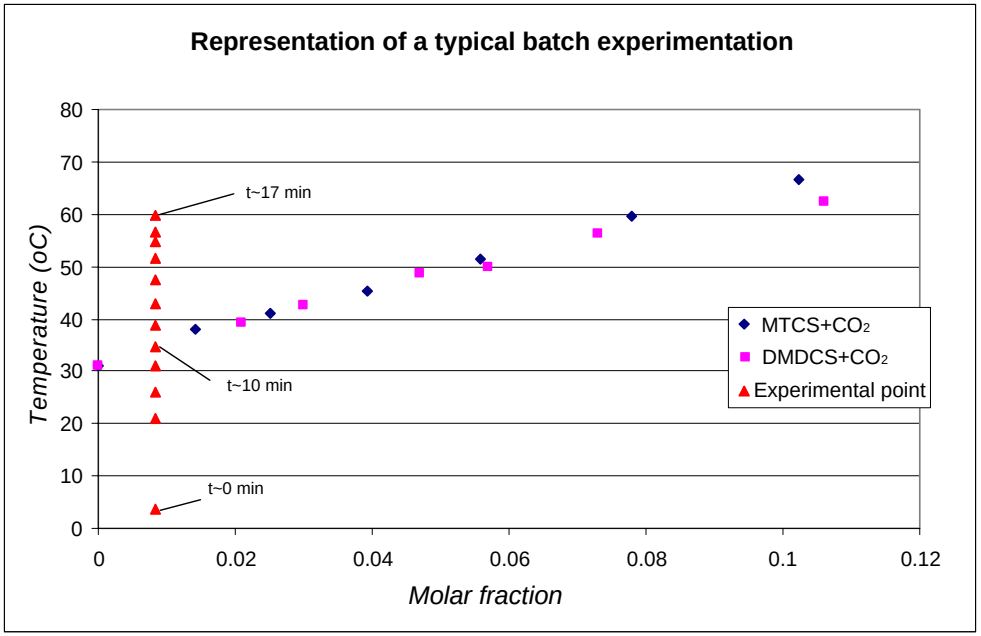

Figure 6 Representation of the layer growing by the reaction in $scCO_2$

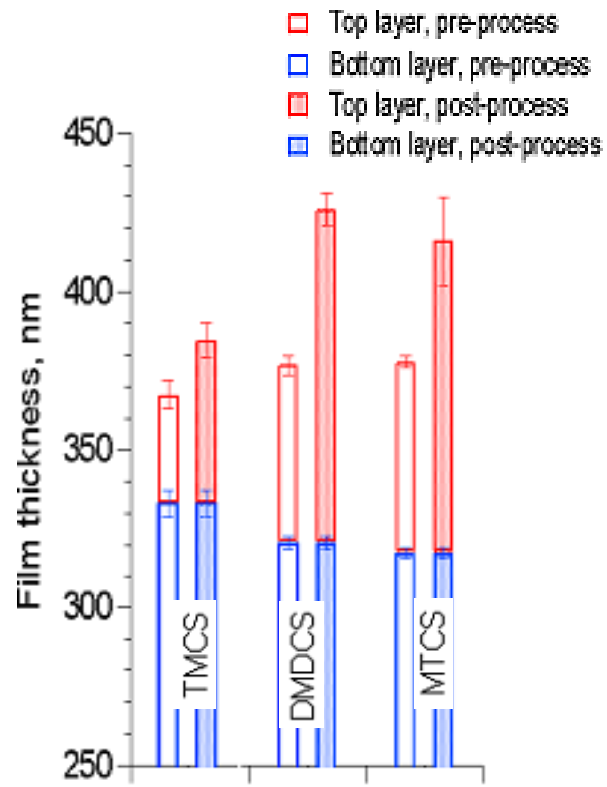

Figure 7 typical path of reaction in batch reactors between chlorosilanes in scCO and damaged layers.

Future Work

- *Finish the phase diagrams for TMCS and produce additional phase diagrams for other compounds that are of interest for semiconductor applications.*

- *Perform a more profound study of the reaction between chlorosilanes, water and damaged films by the use of in-situ FTIR.*

- *Find a method to control the thickness of the capping layer.*

- *Model the solubility by use of E.O.S.*

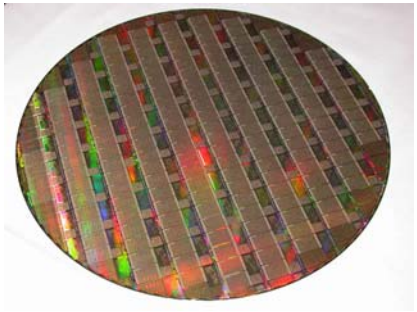

pc.watch.impress.co.jp

Acknowledgements

- *NSF/SRC EBSM Engineering Research Center (EEC-9528813/2001-MC-425)*

- *Bo Xie, Lieschen Choate and all the coworkers of the Muscat research group.*

Ultra Low-*k* Film Repair and Pore Sealing Using Supercritical Fluids (Thrust D-5, Task 425.010)

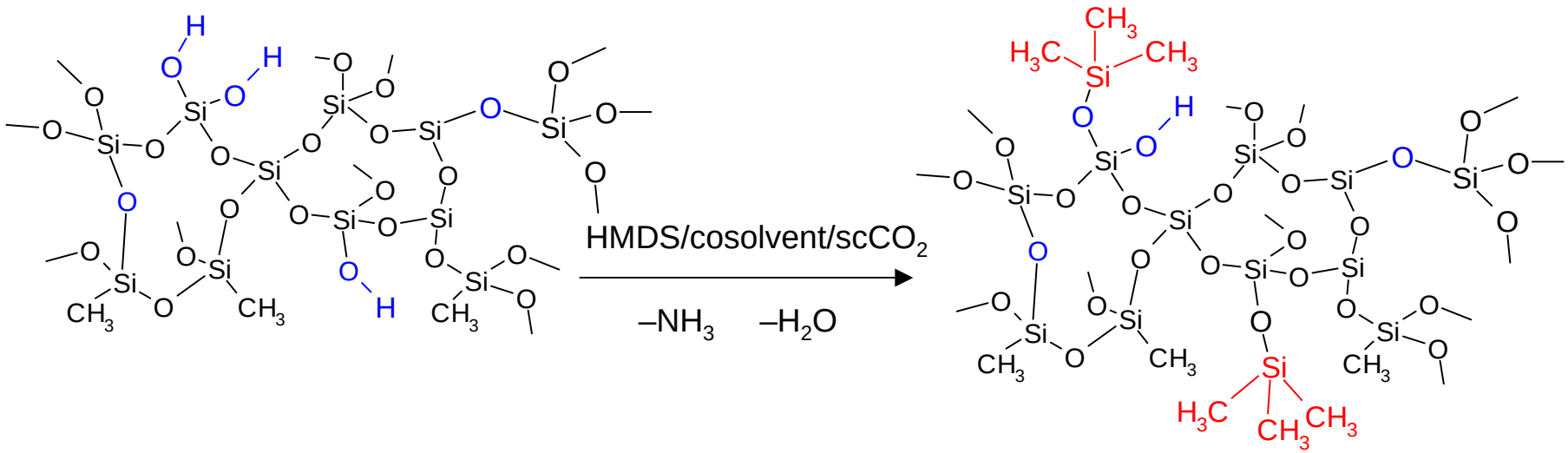

Lieschen Choate

Advisor: Anthony Muscat

lchoate@email.arizona.edu, muscat@erc.arizona.edu

Department of Chemical & Environmental Engineering

University of Arizona, Tucson, AZ 85721

NSF/SRC Engineering Research Center for Environmentally Benign Semiconductor Manufacturing

Project Objectives

Porous Methylsilsesquioxane (pMSQ)

- Remove silanol groups to lower dielectric constant
- Restore hydrophobicity
- Maintain mechanical strength
- Find environmentally benign methods for processing wafers
- Use inert, inexpensive, easily controlled solvents. Ex: supercritical carbon dioxide ($scCO_2$)

ESH Impact and Metrics

Basis of Comparison

Current best technology: organic solvents such as methanol or inorganic acids for backend cleaning

Manufacturing Metrics

Eliminate aqueous cleans and subsequent rinses, reducing consumption of co-solvents and ultra-pure water.

Reduce volume of aqueous water requiring treatment

Requires recovery and treatment of co-solvent products

Reduces worker exposure to vapors

Saves energy with ultra-pure water reductions

Non-aqueous cleaning techniques more compatible with vacuum processing, encouraging development of a tool to serve multiple functions

	Usage Reduction			Emission Reduction			
Goals / Possibilities	Energy	Water	Chemicals	PFCs	VOCs	HAPs	Other Hazardous Wastes
Backend liquid phase chemistry and drying.	>50%	100%	Replace n-methyl pyrrolidone .	undeterm-ined.	Must capture and treat co-solvents.	CO_2 is non-hazardous. MeOH is on HAPs list.	100% reduction in liquid waste.

Chemistry of Chlorosilanes and p-MSQ

When the Silicon wafers are processed by O_2 plasma ashing, silanol (SiO-H) groups form in the low-*k*. These SiO-H groups cause the film to be hydrophilic, increasing the dielectric constant.

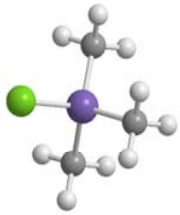

Trimethylchlorosilane
(TMCS, 0.44 nm)

Dimethyldichlorosilane
(DMDCS, 0.44 nm)

Methyltrichlorosilane
(MTCS, 0.43 nm)

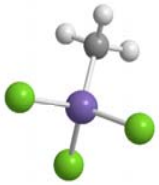

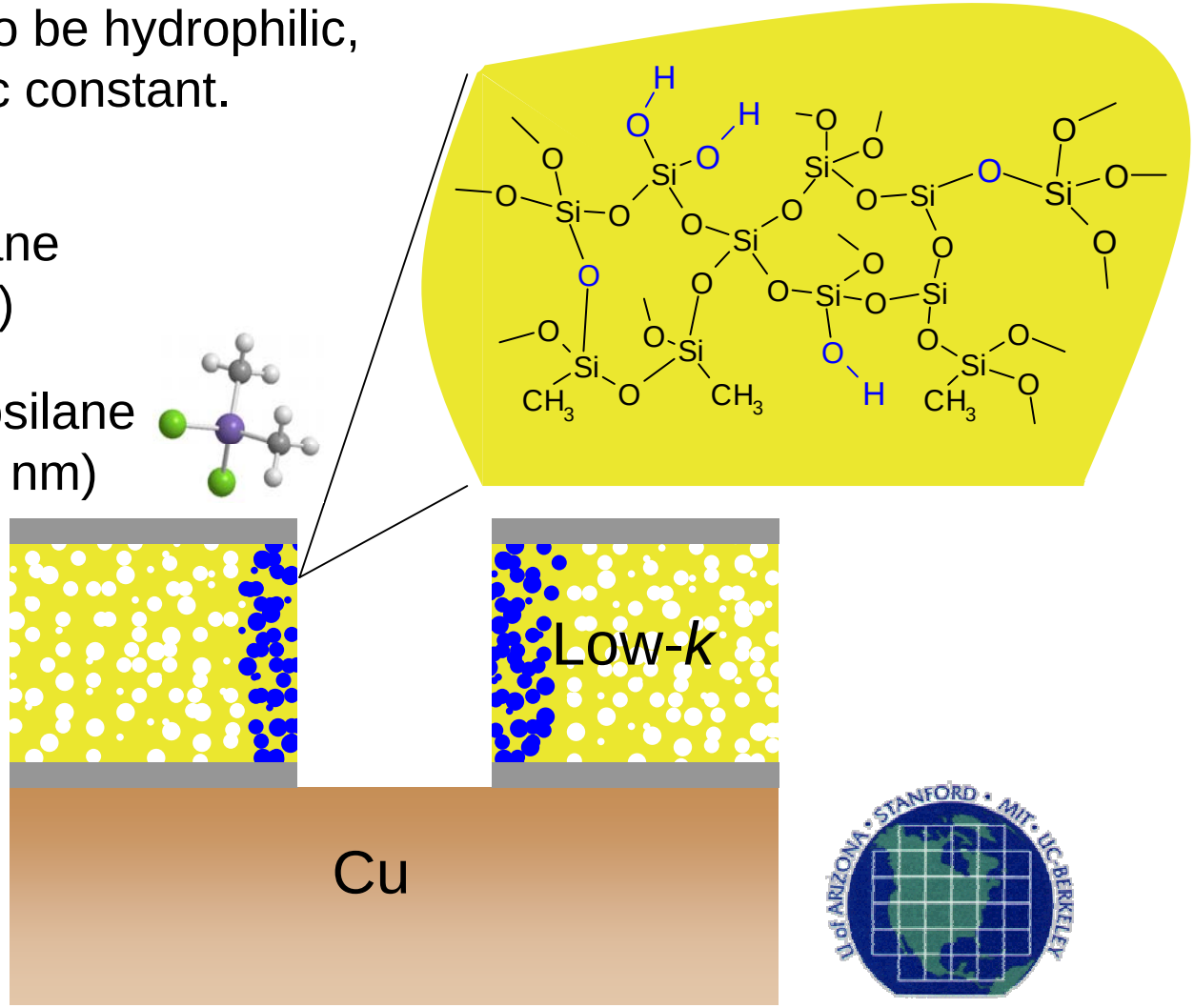

Chemistry of Chlorosilanes and p-MSQ

TMCS reacts with HCl and water (from ambient air in reactor) to form trimethylhydroxylsilane

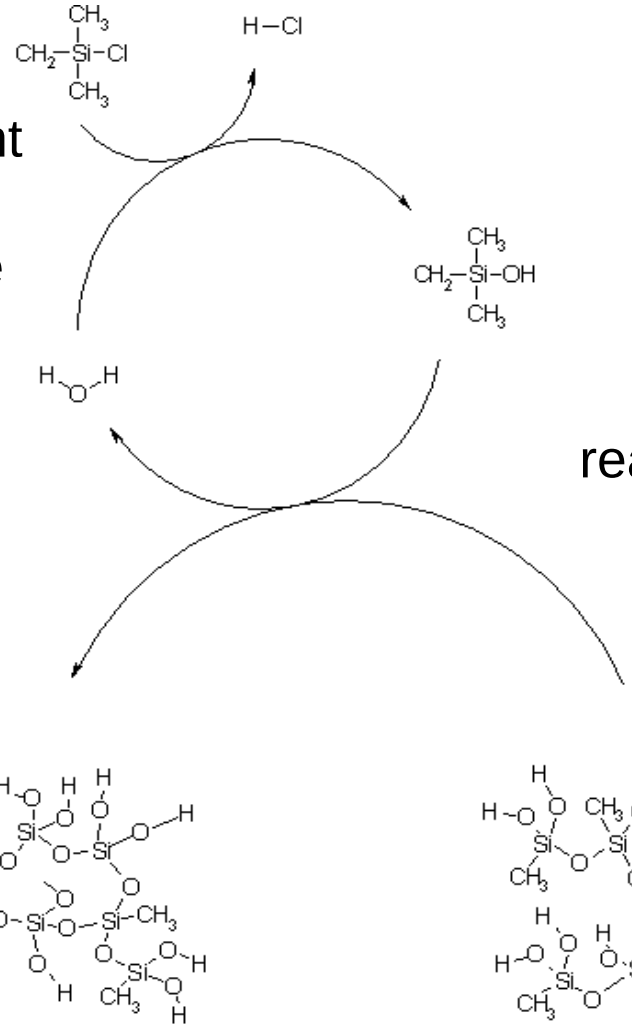

Trimethylhydroxylsilane reacts with a hydroxyl group on the p-MSQ surface

Chemistry of Chlorosilanes and p-MSQ

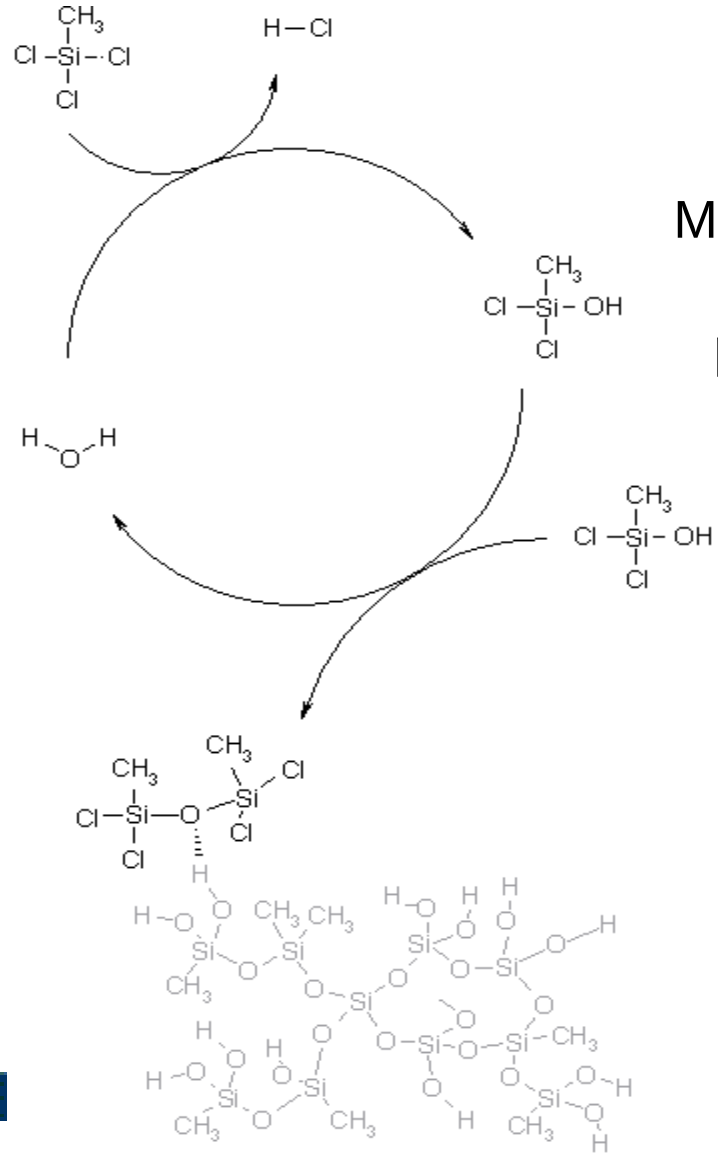

MTCS and DMDCS experience self condensation and physisorption on the p-MSQ surface

Processing Samples

- Samples are loaded into a batch reactor with chlorosilanes
- Reactor is filled with $scCO_2$ and cooled to about 5ºC
- Reactor is heated for 17 minutes and then evacuated
- Final Temperature = 53 ±10ºC
- Final Pressure = 252 ± 50 atm
- CO_2 Critical Temperature = 32ºC
- CO_2 Critical Pressure = 72 atm

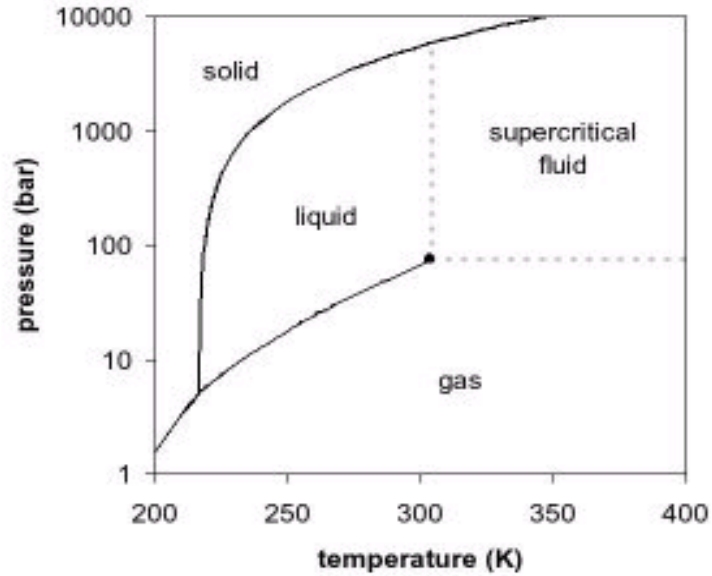

FTIR of p-MSQ Film Repair with MTCS

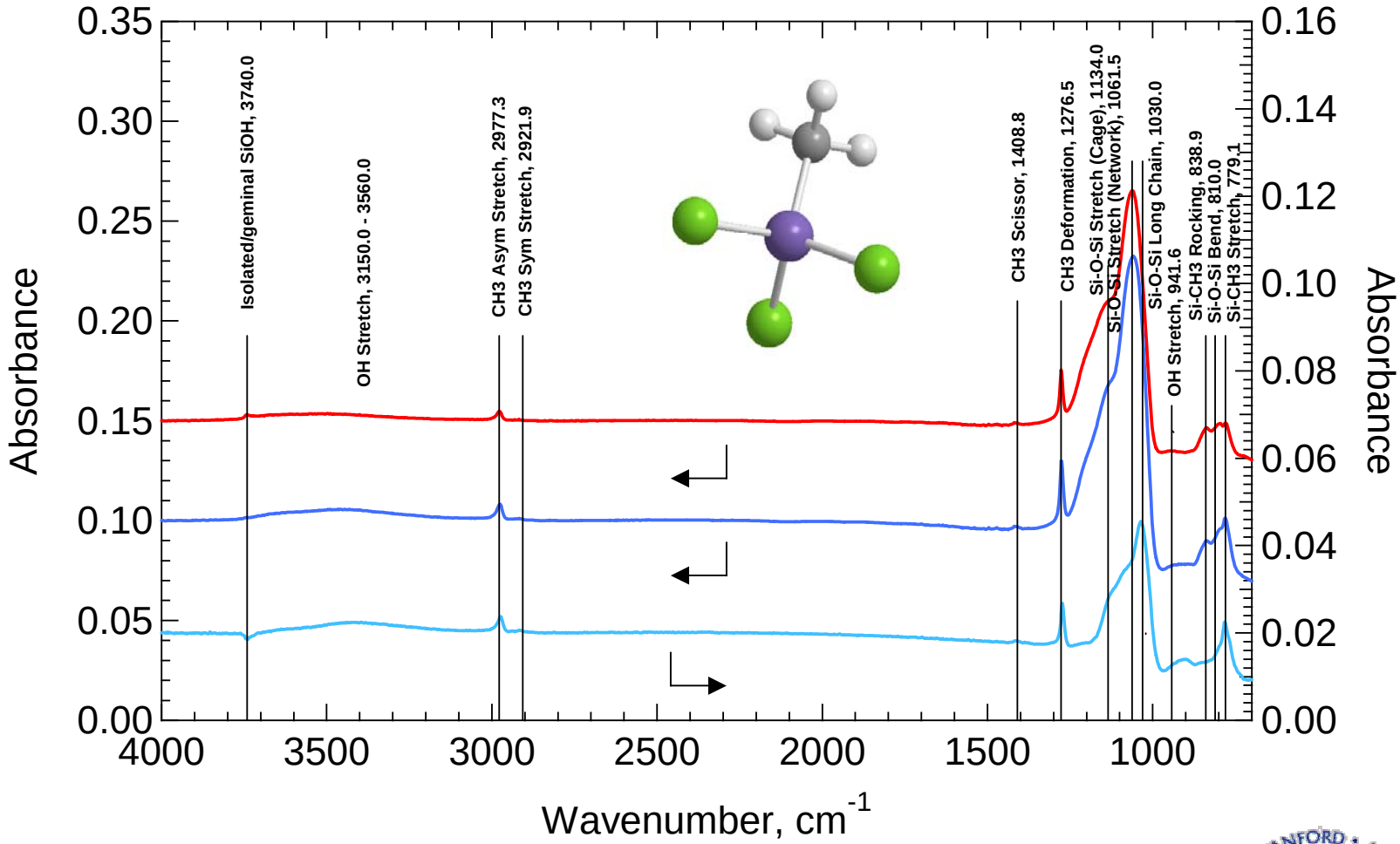

- Isolated/geminal silanol groups reacted but H-bonded silanol groups added
- Si-O-Si band at 1030 cm^{-1}

Contact Angle/Dielectric Constant/ Ellipsometry Measurement

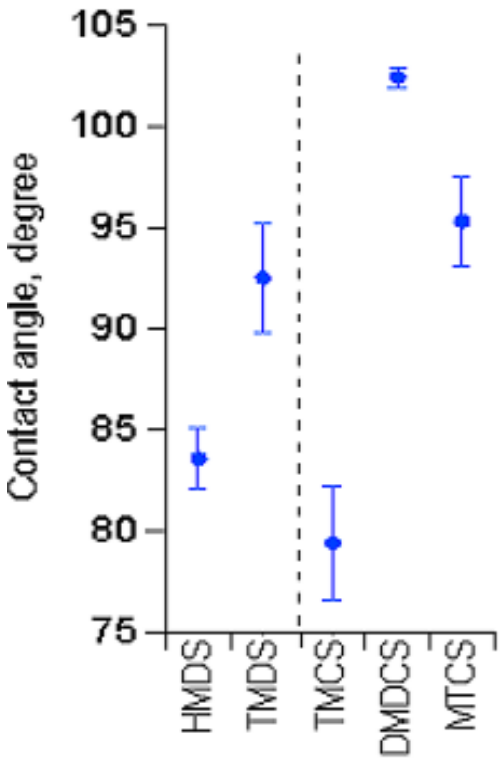

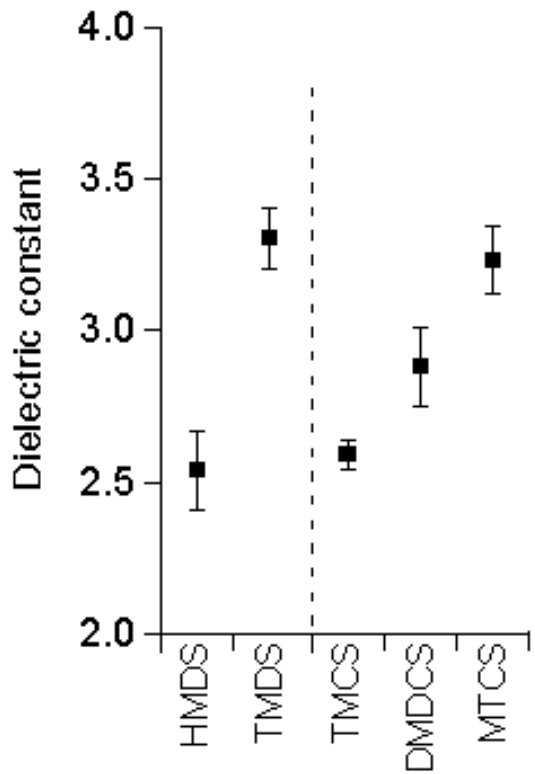

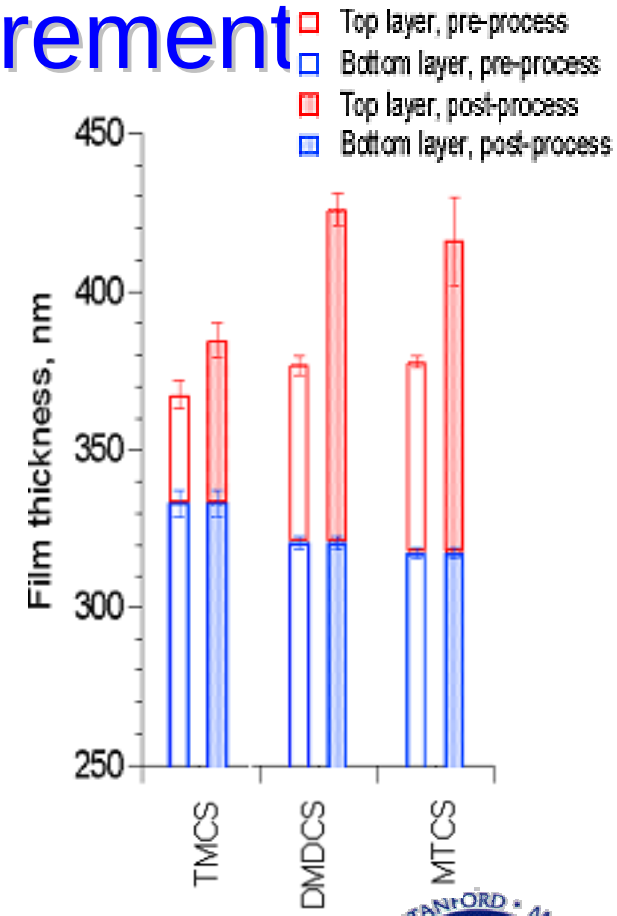

TMCS: 79.4º
DMDCS: 102.4º
MTCS: 95.3º

TMCS: 2.6
DMDCS: 2.8
MTCS: 3.3

TMCS: 8.4 nm
DMDCS: 47.8 nm
MTCS: 32.4 nm

Ellipsometric Porosimetry: Pore Capping

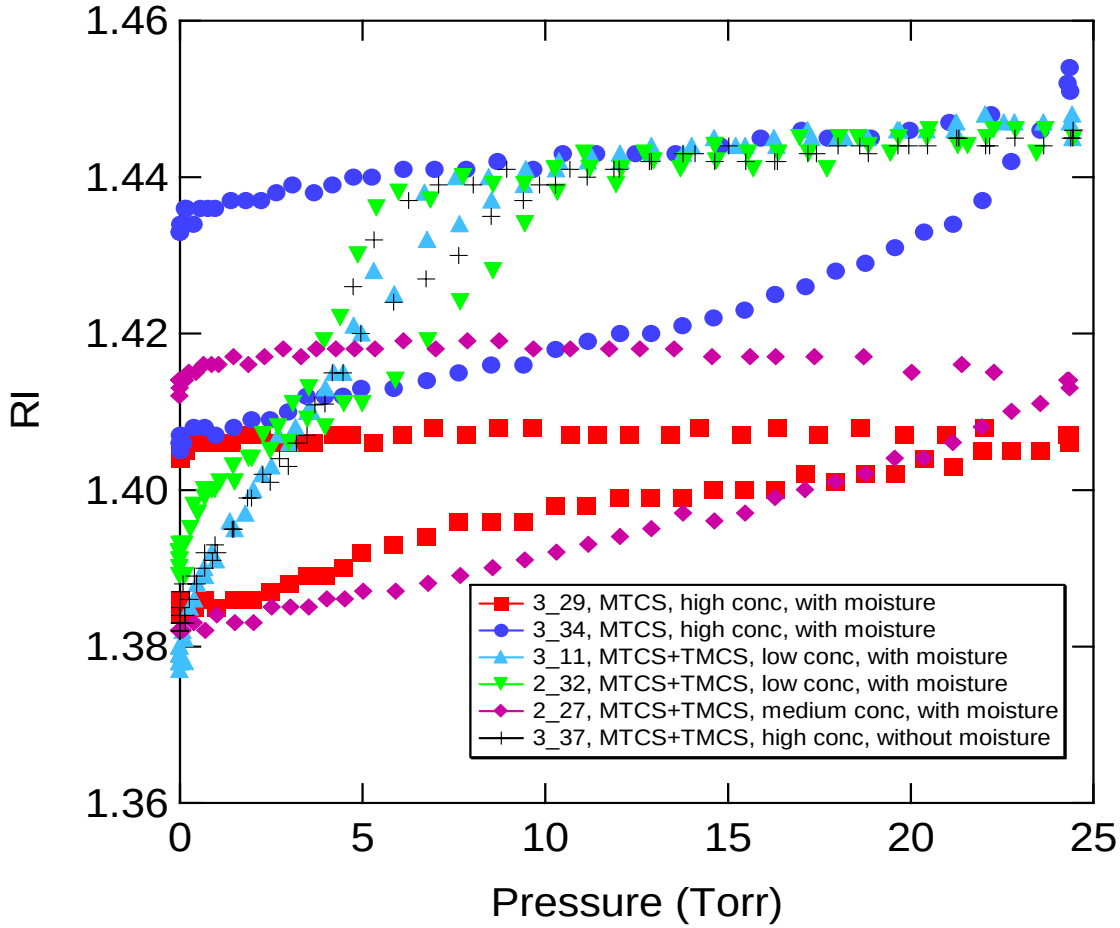

•Pore capping for MTCS and MTCS followed by TMCS requires moisture in the reactor

Conclusions/Future Plans

- Conclusions:
  - TMCS restores the dielectric constant, but not the contact angle
  - MTCS very reactive, adds silyl layer to film's top surface, sealing pores
- Future Plans:
  - Experiment with different pore sizes
  - Build ellipsometric porosimetry capability
  - Patterned/CVD low-*k* samples
  - Use continuous flow reactors
  - Vary experiments by controlling pressure/temperature
  - Investigate successful $scCO_2$ chemistries using gas phase process

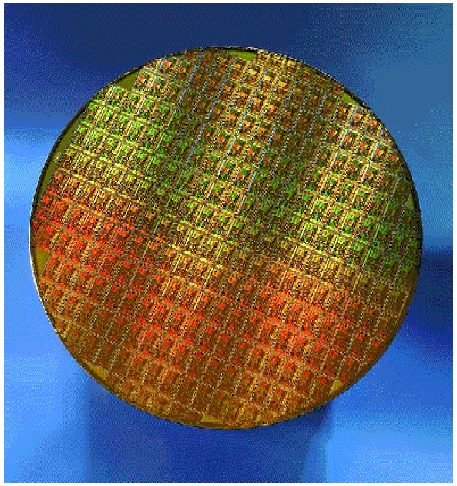

Industrial Collaboration/ Technology Transfer

- Sematech
  - Steve Burnett (ESH Program Manager)
  - Eric Busch (Interconnect Division, AMD Assignee)
  - Frank Weber (Interconnect Division, Infineon Assignee)
- NSF/SRC EBSM Engineering Research Center (EEC-9528813/2001-MC-425)
- Texas Instruments
  - Phil Matz
- University of Arizona
  - Bo Xie, Adam Thorsness, Gerardo Montano

Non-PFOS Photoacid Generators: Environmentally Friendly Candidates for Next Generation Lithography

Christopher K Ober
Department of Materials Science and Engineering
Cornell University, Ithaca, NY 14853 -1501
cober@ccmr.cornell.edu

Reyes Sierra
Department of Chemical and Environmental Engineering,
The University of Arizona, Tucson, AZ 85721- 0011
rsierra@email.arizona.edu

ERC Review, February 2006

Cornell University

Collaborators & Support
- **Ramakrishnan Ayothi and Yi Yi (Cornell University)**
- **Chris Ober Group (Cornell University)**
- **Intel Corporation**
- **Dr. Heidi Cao and Dr. Wang Yueh (Intel)**

Project Objectives

To develop environmentally friendly perfluorooctylsulfonate (PFOS) free photoacid generators (PAG) targeting high quantum yield of acid generation, high boiling point, adequate distribution and diffusion and line width roughness reduction

ESH Metrics

- Metrics for Task - Non-PFOS Photoacid Generators (PAGs)
- Basis of Comparison – Pefluoroalkylsulfonate (PFAS) PAGs
- Manufacturing Metrics – Use of PFOS free PAGs that can address both performance and environmental concern raised by PFOS PAGs
- ESH Metrics – PFOS emission reduction – Environmentally friendlier chemicals

Fundamental Resist Challenges For NGL: Example EUV

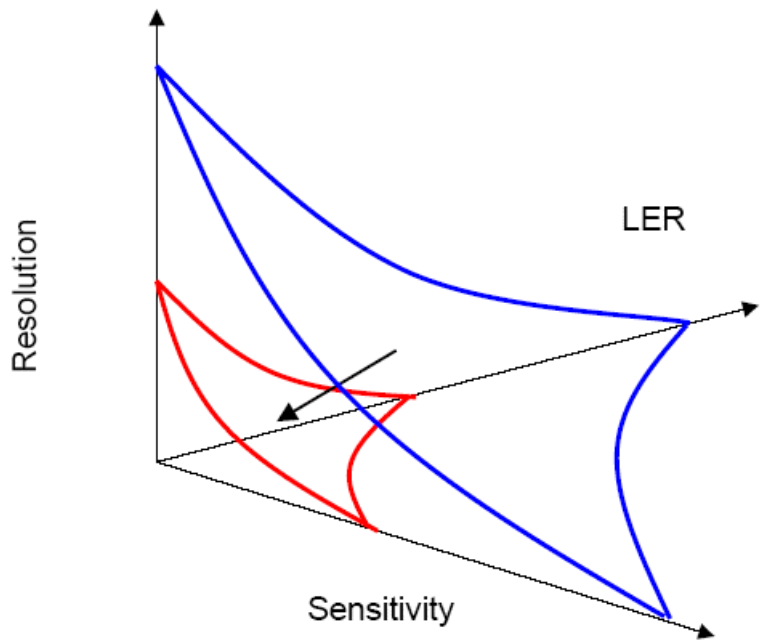

- EUV resist must have higher sensitivity (5 -10 mJ/cm^2), resolution (32 nm) and lower LER (3 σ <1.6 nm)
- Phtoacid Generators generates strong catalyst upon exposure, which increases the resist sensitivity
- The Stronger the acid, the more sensitive the resist but poor LER
- The Weaker the acid, less sensitive the resist but good LER
- **Photoacid Generators Critical Component for Chemically Amplified Resist**

"EUV Resist Performance Trade-Offs" Robert Brainard, Kim Dean, Thomas Koehler

Why PFOS Photoacid Generators?

- Strong acid (pKa ~ -11) – sensitivity & speed
- Non-polar tail – solubility, miscibility, low contamination, defects, thermal and hydrolytic stability
- Optical properties – Uniform exposure/image contrast
- Size (272 cm^3) – low acid volatility/diffusion length

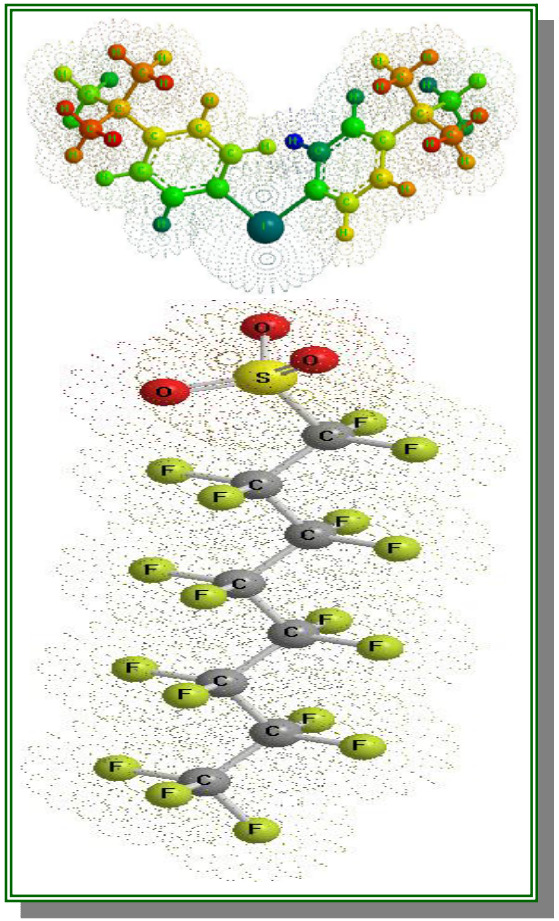

Cornell University

Perfluorooctylsulfonate (PFOS) Issues

PFOS - Environmental, Health and Safety Challenges

Global Distribution (polar bears to EU minister)

Higher P_{OW} (Preference to Aquatic Animals)

Fluorine (Longer Biological Life)

Toxic

PFOS PAG - Lithography/Nanotechnology Challenges

Fluorous self-assembly - Segregation and Leaching

Acid Diffusion – Line Edge Roughness

Fluorine absorption and side reactions

Arctic ringed seals show varying concentrations Perfluoro compounds (Science, 2004)

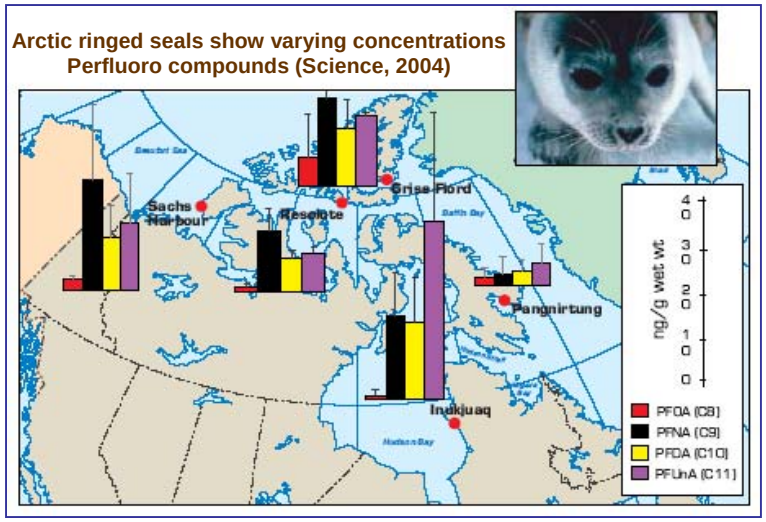

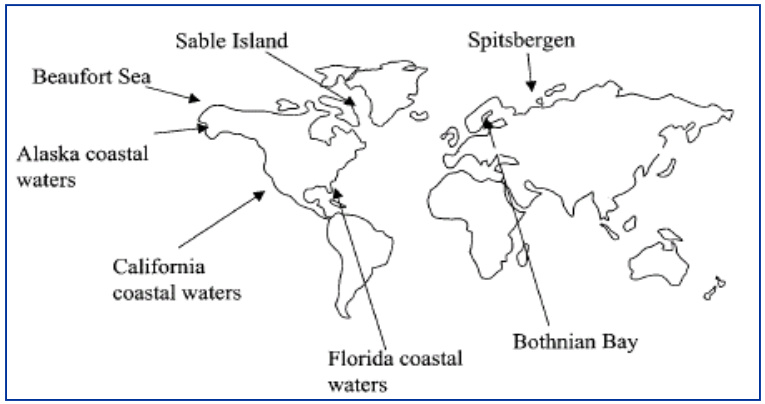

Map showing collection locations for marine mammal samples
Environ. Sci. Technol. 2001

Cornell University

Anatomy of Non-PFOS PAG

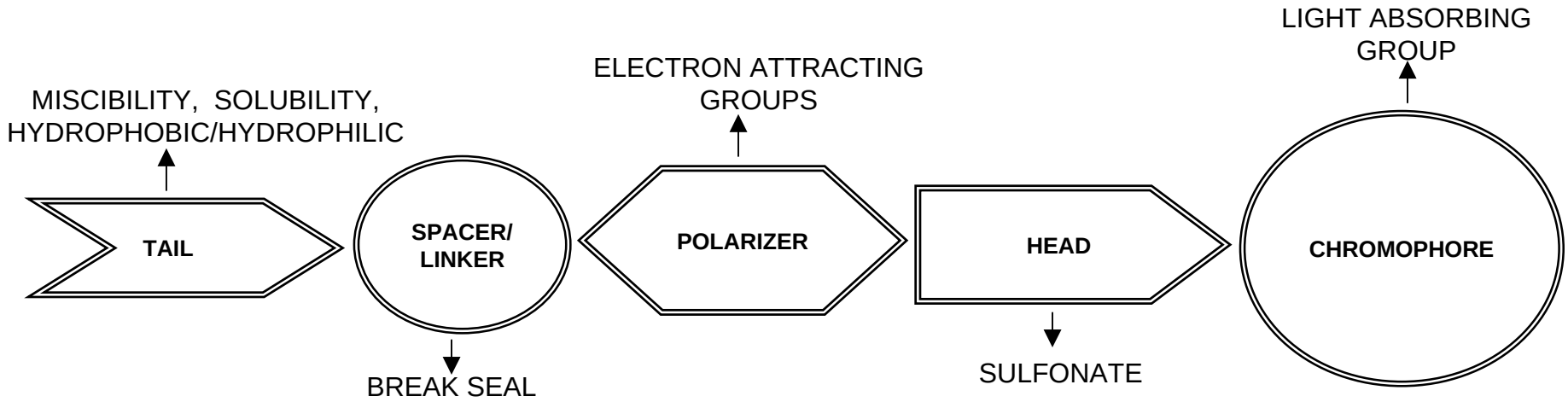

Non-PFOS PAG Design

- Acid strength - Few fluorine atoms or Non-Fluoro electron attracting Group
- Transparency - Aromatic for EUV / Non-aromatic for 193
- Distribution and Diffusion - Functional Groups
- Size/volatility/solubility/Leaching - Variation of R group
- Absorption, outgassing and thermal/formulation stability - Stable Chrmophores

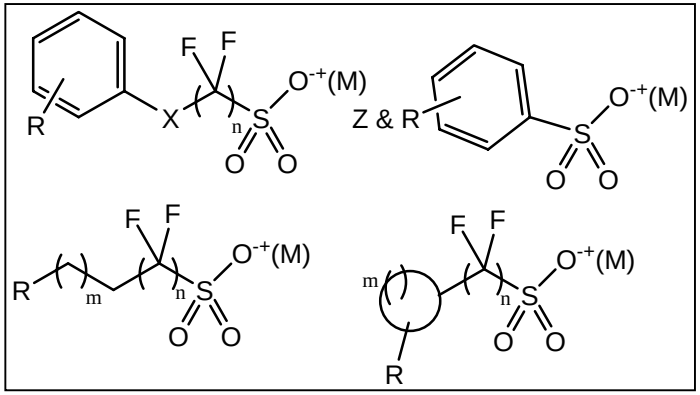

Cornell University

E S H

Synthesis and Characterization

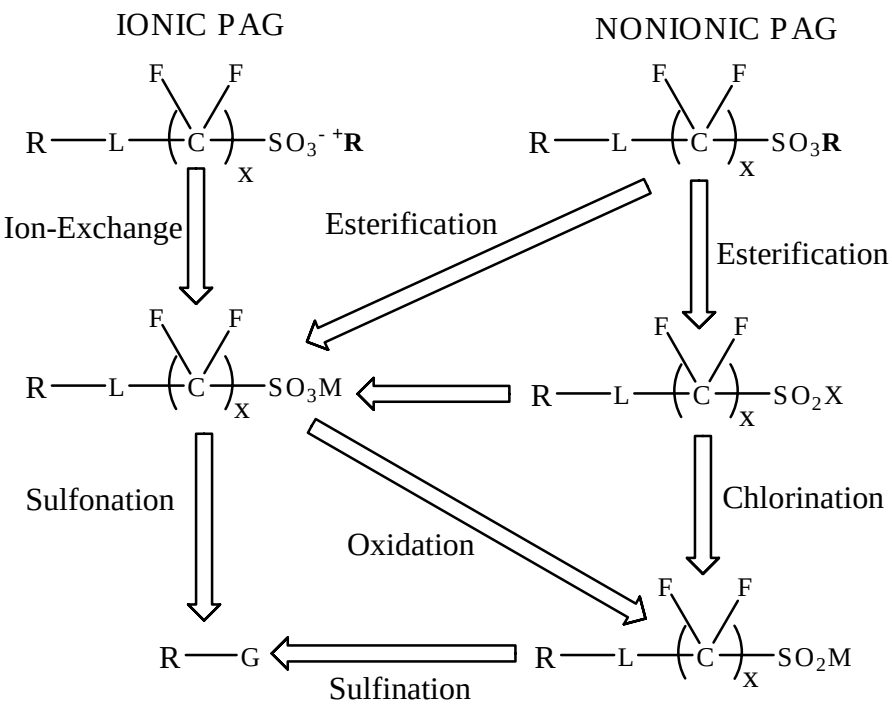

Key steps: Substitution, Hydrogenation, Dehalogenosulfination, Dehalogenosulfonation, Chlorination/Oxidation, Ion-exchange reaction and Esterification.

Analytical Instrument	Information
NMR (H,C,F)	Conversion
MS and Elemental	Purity/Structure
TGA and DSC	Thermal Properties
UV/VIS Spectroscopy	Absorption Characteristics, Residual acid, Solubility
ICP/AAS	Metal content
DUV/e-Beam	Sensitivity

- Standard PAG Fragments outgas from non-PFOS PAGs (Outgassing Experiments Performed at University of Wisconsin)
- Lower Absorption at EUV (Estimated using http://www-cxro.lbl.gov/optical_constants/filter2.html)

Cornell University

Non-PFOS PAG Performance Versus TPS PFBS at EUV

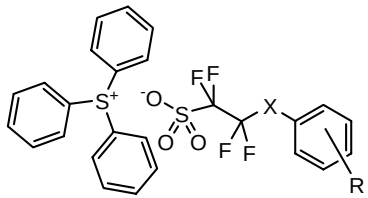

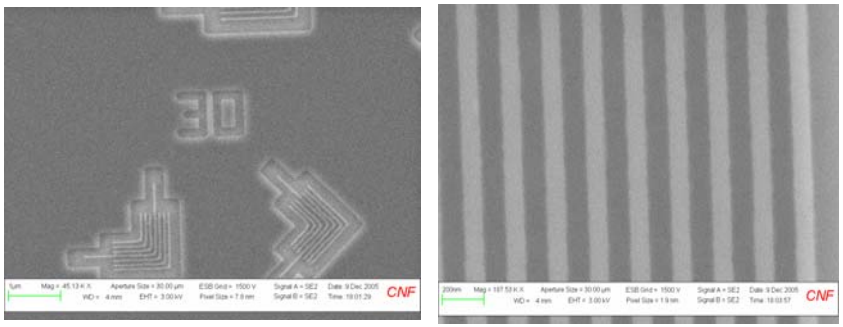

Polymer Resist E_0 (100 nm) < 4.9 mJ/cm^2; E_s = 7.5 mJ/cm^2; LER (100 nm 1:1 lines) = 7.7 ± 0.8 nm

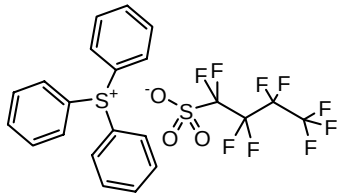

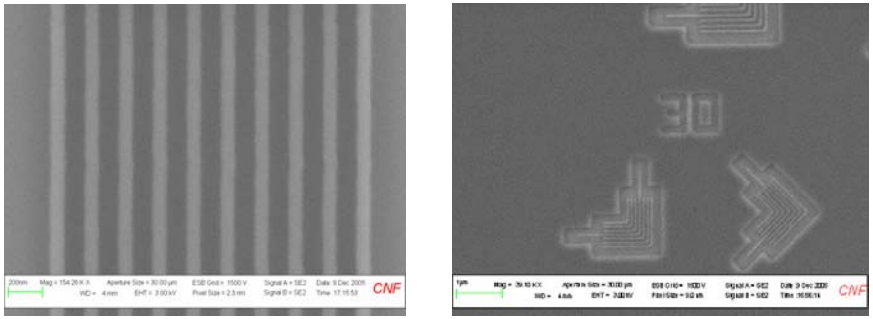

Polymer Resist E_0 (100 nm) < 6.4 mJ/cm^2; E_s = 8.6 mJ/cm^2; LER (100 nm 1:1 lines) = 8.0 ± 0.6 nm

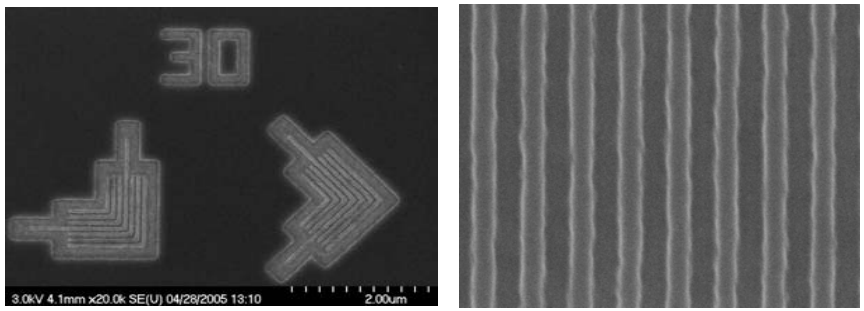

Molecular Glass Resist : E_s = 21.0 mJ/cm^2
R = 25 - 30 nm; LER (60 nm lines) = 5.0 nm

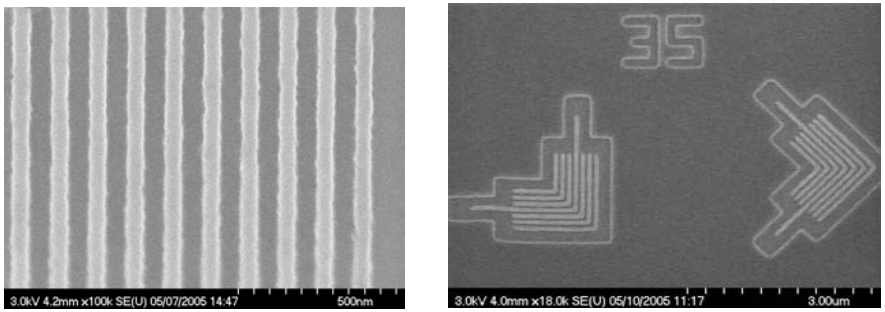

Molecular Glass Resist : E_s = 39.0 mJ/cm^2
R = 30-35 nm; LER (60 nm lines) = 4.3 nm

Cornell University

E S H

- Cornell Nanofabrication Facility (CNF)
- Cornell Centre for Material Characterization (CCMR)
- Lawrence Berkeley National Laboratory (EUV exposure)

Estimation of Environmental Fate of Non-PFOS Photoacids (PGAs)#

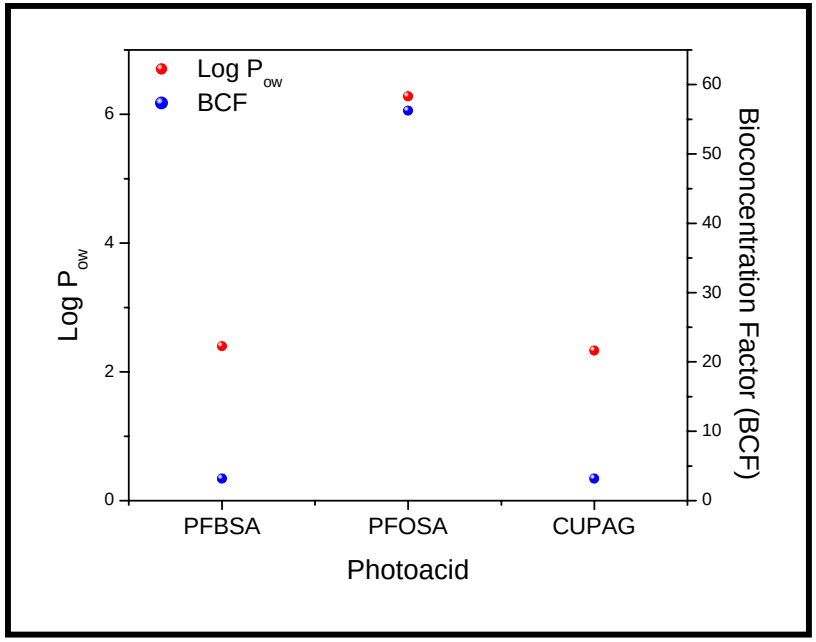

PFBSA - Perfluorobutane Sulfonic Acid
PFOSA - Perfluorooctane Sulfonic Acid
CUPGA - Cornell non-PFOS photoacid

Acid (No. of Fluorine)	Biodegradation Timeframe (Primary)	Biodegradation Timeframe (Ultimate)	Formula Weight
PFBSA (9 F)	Weeks	Recalcitrant	300
PFOSA (17 F)	**Months**	**Recalcitrant**	**500**
CUPGA (4 F)	Days-Weeks	Weeks-Months	274

* Compounds with 9 Fluorine atom and below do not bioaccumulate

#Estimated using EPI Suite - environmental fate estimation models developed by the EPA's Office of Pollution Prevention Toxics and Syracuse Research Corporation (SRC)

"Non-PFOS PGA no/low bioaccumulation"

Cornell University

E S H

Assessment of the Environmental Fate of Non-PFOS PAGs

- **Development of analytical methods for compound detection**
- **Bioaccumulation potential**
- **Inhibitory effects**
  - e.g., Microtox assay, inhibition of aerobic and anaerobic microorganisms in wastewater treatment systems, inhibition of mitochondrial respiration (MTT assay)
- **Fate in wastewater treatment systems**:
  - Sorption to biosolids
  - Susceptibility to microbial degradation:

    - Utilization as carbon/energy source: Aerobic and anaerobic conditions

    - Cooxidation[#] : Aerobic heterotrophic- and nitrifying conditions

[#]The new non-PFOS PAGs are only partially fluorinated. Lower halogenated hydrocarbons are generally susceptible to attack by monooxygenases

Removal of Non-PFOS PAGs from Semiconductor Effluents

Assessment of the treatability of the new non-PFOS PAGS using biological and physico-chemical methods, e.g.,

- Activated sludge treatment
- Activated carbon adsorption
- Ion exchange
- Membrane processes
- Advanced oxidation methods

Cornell University

Research Plan

- Synthesis and Characterization of Non-PFOS PAGs with fewer fluorine atom
- Evaluation of PAGs at 193 nm and EUV Lithography
- Synthesis of the acid or their alkali metal salt of the best performed PAG for obtaining Environmental, Health, Safety, and Regulatory (EHSR) Profile
- EHSR Profile for new Non-PFOS acids or anions